\6

# NASA CONTRACTOR FINAL REPORT

NASA CR-66668

NASA CR-66668

FACILITY FORM 602

N68-34279 (ACCESSION NUMBER)
(THRU)
373 (PAGES)
1 (CODE)
CR-66668 (NASA CR OR TMX OR AD NUMBER)
31 (CATEGORY)

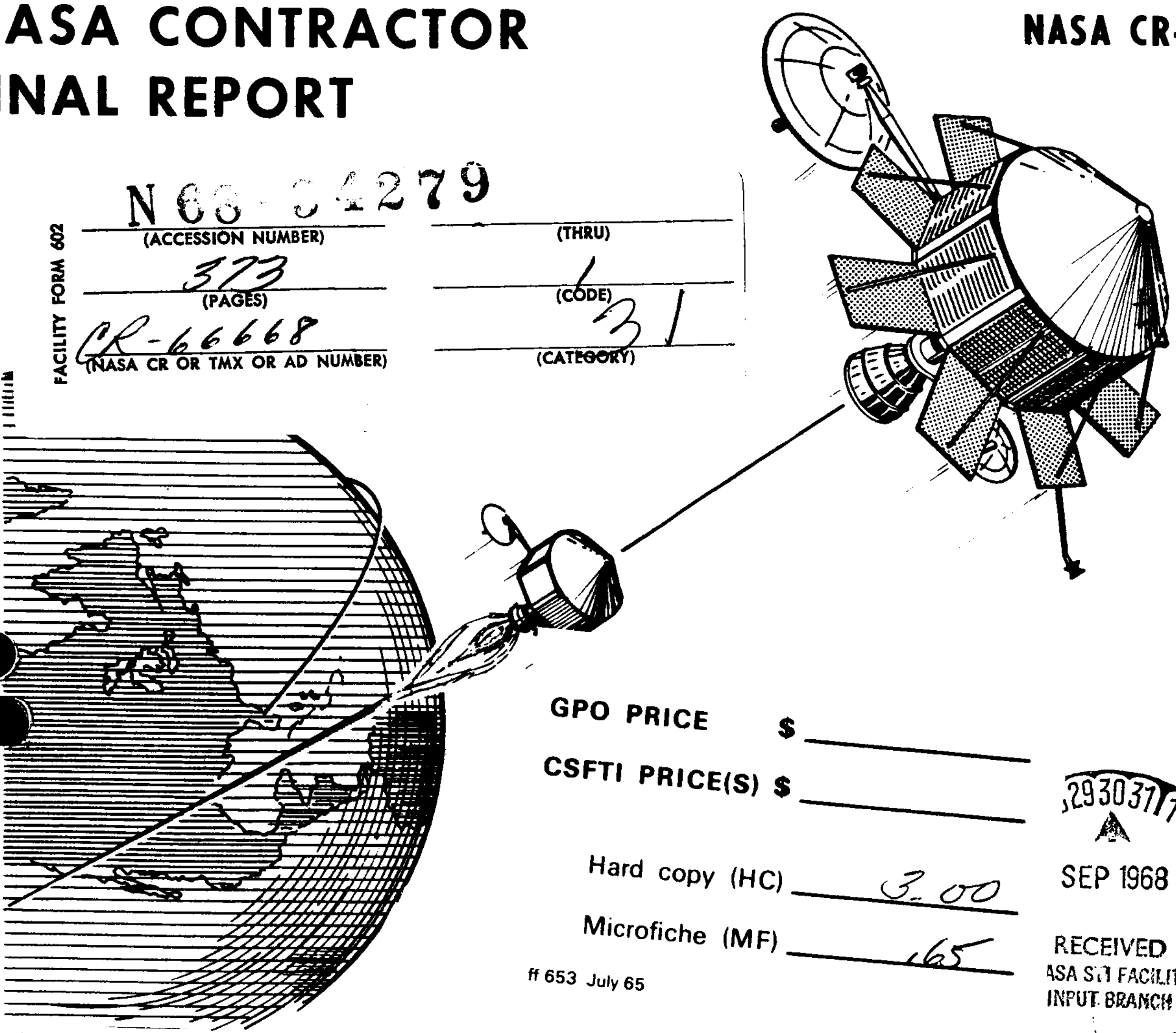

GPO PRICE $
CSFTI PRICE(S) $
Hard copy (HC) 3.00
Microfiche (MF) .65
ff 653 July 65

SEP 1968
RECEIVED
NASA STI FACILITY
INPUT BRANCH

# STUDY OF POWERED SPACECRAFT FOR MARS MISSIONS

## ■ PERFORMANCE, SUBSYSTEMS, AND CONFIGURATIONS ■

*Prepared by*

THE BOEING COMPANY
Seattle, Washington

*for Langley Research Center*

SEPTEMBER 1968

NATIONAL AERONAUTICS AND SPACE ADMINISTRATION ■ WASHINGTION, D.C.

NASA CR-66668

# STUDY OF POWERED SPACECRAFT FOR MARS MISSIONS

## PERFORMANCE, SUBSYSTEMS, AND CONFIGURATIONS

FINAL REPORT
SEPTEMBER, 1968

Distribution of this report is provided in the interest of information exchange. Responsibility for the content resides in the author or organization that prepared it.

Issued by Originator as Boeing Document
D2-140028-5 (Vol.II)

PREPARED UNDER CONTRACT NO. NAS1-7995 BY

THE BOEING COMPANY
SEATTLE, WASHINGTON

FOR LANGLEY RESEARCH CENTER

NATIONAL AERONAUTICS AND SPACE ADMINSTRATION

PRECEDING PAGE BLANK NOT FILMED.

## ABSTRACT

This volume provides parametric performance data, conceptual configuration studies, subsystem definition and trades, and operational data for a Mars exploration powered spacecraft launched by a Titan IIIC or IIID in 1973. In addition, refined mission and preliminary design analyses are provided for two specific cases chosen by NASA-Boeing.

PRECEDING PAGE BLANK NOT FILMED.

# FOREWORD

This study was performed by The Boeing Company for the National Aeronautics and Space Administration, Langley Research Center, under Contract NAS1-7995. "Study of Powered Spacecraft for Mars Missions" was a 4.5 month effort to assess the benefits and penalties associated with using powered spacecraft concepts to increase useful payload in Mars orbit.

The work included analyses and trade studies associated with launch vehicles, spacecraft configurations, subsystems, and operations. From these, mission and trajectory parameters, useful weights in Mars orbit, subsystem definitions, and operational factors were established.

PRECEDING PAGE BLANK NOT FILMED.

## CONVERSION FACTORS

### English to International Units

| Physical Quantity | English Units | International Units | Multiply by |
|---|---|---|---|
| Acceleration | $ft/sec^2$ | $m/sec^2$ | $3.048 \times 10^{-1}$ |
| Area | $ft^2$ | $m^2$ | $9.29 \times 10^{-2}$ |
| | $in.^2$ | $m^2$ | $6.45 \times 10^{-4}$ |
| Density | $lb/ft^3$ | $kg/m^3$ | 16.02 |
| | $lb/in.^3$ | $kg/m^3$ | $2.77 \times 10^4$ |
| Energy | Btu | Joule | $1.055 \times 10^3$ |
| Force | lbf | Newton | 4.448 |
| Length | ft | m | $3.048 \times 10^{-1}$ |
| | n mi | m | $1.852 \times 10^3$ |
| Power | Btu/sec | watt | $1.054 \times 10^3$ |
| | Btu/min | watt | 17.57 |
| | Btu/hr | watt | $2.93 \times 10^{-1}$ |
| Pressure | Atmosphere | $Newton/m^2$ | $1.01 \times 10^5$ |
| | $lbf/in.^2$ | $Newton/m^2$ | $6.89 \times 10^3$ |
| | $lbf/ft^2$ | $Newton/m^2$ | 47.88 |
| Speed | ft/sec (fps) | m/sec | $3.048 \times 10^{-1}$ |
| Volume | $in.^3$ | $m^3$ | $1.64 \times 10^{-5}$ |
| | $ft^3$ | $m^3$ | $2.83 \times 10^{-2}$ |

PRECEDING PAGE BLANK NOT FILMED.

# CONTENTS

Page

1.0 INTRODUCTION 1-1

- 1.1 Background 1-1
- 1.2 Objectives 1-2

2.0 DEFINITIONS, SYMBOLS, AND ABBREVIATIONS 2-1

3.0 SUMMARY 3-1

- 3.1 Objectives 3-1
- 3.2 Scope and Approach 3-1
- 3.3 Conclusions 3-2
- 3.4 Results 3-4
  - 3.4.1 Launch Vehicles 3-5
  - 3.4.2 Parametric Studies 3-10
  - 3.4.3 Subsystems 3-18
  - 3.4.4 Refined Configurations and Mission Analysis 3-21

4.0 TECHNICAL GUIDELINES 4-1

- 4.1 Mission Parameters 4-1
- 4.2 Spacecraft Parameters 4-1
- 4.3 Launch Vehicles 4-2
- 4.4 Range 4-2

5.0 PERFORMANCE AND MISSION ANALYSIS 5-1

- 5.1 Launch Vehicle Analyses 5-2
  - 5.1.1 Performance 5-2
  - 5.1.2 Trajectory Constraints 5-5
  - 5.1.3 Empty Stage Splash Points 5-5
- 5.2 Preliminary Spacecraft and Propulsion Sizing 5-9
  - 5.2.1 Nonuseful Weight 5-9
  - 5.2.2 Data Correlation 5-12
- 5.3 Mission Parameter Effects 5-12
  - 5.3.1 Fixed Arrival Date 5-12
  - 5.3.2 Variable Arrival Date 5-20
- 5.4 Spacecraft Sizing Parameters 5-23
  - 5.4.1 Launch Vehicle Selection 5-23
  - 5.4.2 Spacecraft Thrust Selection 5-23
  - 5.4.3 Post-Injection $\Delta V$ Effects 5-26
  - 5.4.4 $C_3$ Effects 5-26
  - 5.4.5 Spacecraft Weights 5-26
- 5.5 Near-Earth Mission Design 5-31
  - 5.5.1 Titan IIIC 5-31
  - 5.5.2 Titan IIID 5-39
- 5.6 Operational Analyses 5-49
  - 5.6.1 Launch Analysis 5-49
  - 5.6.2 Tracking and Data Acquisition 5-55

## CONTENTS (Cont)

Page

5.6.3 Event-Sequence Analysis 5-61
5.6.4 Guidance Error Analysis 5-65

6.0 PRELIMINARY CONFIGURATIONS 6-1

6.1 Model 971-101 6-2
6.1.1 Configuration Assessment 6-2
6.1.2 Weight Analysis 6-6
6.2 Model 971-102 6-6
6.2.1 Configuration Assessment 6-10
6.2.2 Weight Analysis 6-11
6.3 Model 971-103 6-11
6.3.1 Configuration Assessment 6-11
6.3.2 Weight Analysis 6-15
6.4 Model 971-104 6-15
6.4.1 Configuration Assessment 6-15
6.4.2 Weight Analysis 6-17

7.0 REFINED CONFIGURATION AND MISSION ANALYSIS 7-1

7.1 Performance and Mission Analysis 7-1
7.1.1 Mission Velocity Requirements 7-2
7.1.2 Spacecraft Weights 7-2
7.1.3 Spacecraft Payload Capability 7-8
7.1.4 Launch Analysis 7-11
7.1.5 Tracking and Data Acquisition 7-11
7.1.6 Guidance Analysis 7-19
7.1.7 Mission Summary 7-19
7.2 Configurations 7-25
7.2.1 General Arrangement---Indirect Lander Entry 7-26
7.2.2 General Arrangement---Direct Lander Entry 7-29
7.2.3 Structural Criteria and Design 7-34
7.2.4 Spacecraft Weights 7-40
7.3 Orbiter Subsystems 7-47
7.3.1 Propulsion System 7-47
7.3.2 Guidance and Control System 7-55
7.3.3 Electrical Power Subsystem Studies 7-73
7.3.4 Additional Subsystems 7-88

APPENDIX A---PERFORMANCE AND MISSION ANALYSIS A-1

A1 Aerodynamic Characteristics of Stages A-2
A2 Mission Parameter Effects A-8
A3 Spacecraft Sizing Parameters A-14
A4 Tracking and Data Acquisition A-45
A5 Event Sequence Analysis A-64
A6 Minimum Velocity Bit (MVB) A-71

APPENDIX B---PROPULSION SUBSYSTEM STUDIES B-1

APPENDIX C---GUIDANCE AND CONTROL SUBSYSTEM TRADE STUDIES C-1

REFERENCES R-1

# ILLUSTRATIONS

Page

3.2-1 Space Vehicle Terminology 3-2
3.4-1 Trajectory Description 3-4
3.4-2 Titan IIIC Launch Vehicle 3-5
3.4-3 Launch Vehicle Payload Capabilities 3-6
3.4-4 Empty Stage Splash Points---Titan IIIC 3-7
3.4-5 Off-Perigee Injection 3-7
3.4-6 Injection Velocity Loss With Elliptical Parking Orbits---Long Coast 3-8
3.4-7 Launch-Arrival Date Effects on Injection Velocity Loss 3-9
3.4-8 Daily Launch Windows 3-10
3.4-9 Nonuseful Orbiter Weight 3-11
3.4-10 Titan IIIC Arrival Date Effects 3-11
3.4-11 Titan IIIC Spacecraft Thrust Effects 3-12
3.4-12 Thrust Vectoring System Control Response 3-14
3.4-13 Design Point Choice 3-14
3.4-14 Short and Long Holding Orbit Coast Penalties 3-15
3.4-15 Holding Orbits 3-16
3.4-16 Boost-Assist Sequence---Engine Up 3-16
3.4-17 Boost-Assist Sequence---Engine Down 3-17
3.4-18 Variable Arrival Date Effect on Useful In-Orbit Weight 3-17
3.4-19 Refined Nonuseful Orbiter Weight 3-22
3.4-20 Useful Spacecraft Weight 3-23
3.4-21 Capsule Plus Science Weights---Indirect Entry 3-23
3.4-22 Capsule Plus Science Weights---Direct Entry 3-24
3.4-23 Useful In-Orbit Weight---Indirect Entry 3-25
3.4-24 Event Sequence---Short Holding Orbit 3-26
3.4-25 Tracking Station Coverage---Launch Phase---Short Parking Orbit Coast 3-27
3.4-26 Tracking Station Coverage---Launch Phase---Long Parking Orbit Coast 3-28
3.4-27 Model 971-105 Launch Configuration 3-29
3.4-28 Model 971-105 Space Configuration 3-30
3.4-29 Model 971-106 Launch Configuration 3-31
3.4-30 Model 971-106 Space Configuration 3-32

5.1-1 Launch Vehicle Payload Capabilities 5-3
5.1-2 Burnout Altitude Effect on Burnout Velocity 5-4
5.1-3 Empty Stage Splash Points---Titan IIIC 5-7
5.1-4 Empty Stage Splash Points---Titan IIID 5-8
5.2-1 Nonuseful Orbiter Weight 5-11
5.2-2 Bladder Expulsion Propellant Tank Weight Correlation 5-13
5.2-3 Pressurant Tank Weight Correlation 5-14
5.2-4 Pressurization and Propellant Feed System Weight Correlation 5-15
5.3-1 Arrival Date Effects---Titan IIIC Type I 5-16
5.3-2 Arrival Date Effects---Titan IIIC Type II 5-17
5.3-3 Arrival Date Effects---Titan IIID Type I 5-18
5.3-4 Arrival Date Effects---Titan IIID Type II 5-19
5.3-5 Maximum Useful In-Orbit Weight With Variable Arrival Date 5-21
5.3-6 Variable Arrival Date Effect on Useful In-Orbit Weight 5-22

## ILLUSTRATIONS (Cont)

Page

5.3-7 Effect of Velocity Allowance on Useful In-Orbit Weight 5-24
5.4-1 Launch Vehicle Comparison 5-25
5.4-2 Spacecraft Thrust Effects---Titan IIIC 5-27
5.4-3 Effect of Post-Injection $\Delta V$ on Useful In-Orbit Weight 5-28
5.4-4 $C_3$ Effects on Useful In-Orbit Weight 5-29
5.4-5 Powered Spacecraft Weight 5-30
5.4-6 Effect of Spacecraft Size on Useful In-Orbit Weight---Titan IIIC 5-32
5.5-1 Mission Profile---Circular Parking Orbit (Short Holding Orbit) 5-33
5.5-2 Mission Profile---Circular Parking Orbit (Long Holding Orbit) 5-34
5.5-3 Useful In-Orbit Weight Comparison---Short and Long Holding Orbits 5-36
5.5-4 Useful In-Orbit Weights for Short Holding Orbits 5-37
5.5-5 Useful In-Orbit Weights for Long Holding Orbits 5-38
5.5-6 Steering Profile Definitions 5-40
5.5-7 Holding Orbit Characteristics 5-41
5.5-8a Near-Earth Trajectory Geometry---Perigee Injection 5-42
5.5-8b Near-Earth Trajectory Geometry---Off-Perigee Injection 5-42
5.5-9 Injection Velocity Loss With Elliptical Parking Orbits---Short Coast 5-44
5.5-10 Injection True Anomalies With Elliptical Parking Orbits---Short Coast 5-45
5.5-11 Injection Velocity Loss With Elliptical Parking Orbits---Long Coast 5-46
5.5-12 Injection True Anomalies With Elliptical Parking Orbits---Long Coast 5-47
5.6-1 Launch Time Variation With Launch Azimuth 5-50
5.6-2 Launch Window Durations 5-51
5.6-3 Parking Orbit Coast Time 5-52
5.6-4 Near-Earth Shadow Entry and Exit Time---Short Coast 5-53
5.6-5 Near-Earth Shadow Entry and Exit Time---Long Coast 5-54
5.6-6 Station Tracking Coverage---Launch Phase---Short Parking Orbit Coast 5-56
5.6-7 Station Tracking Coverage---Launch Phase---Long Parking Orbit Coast 5-57
5.6-8 Ship Coverage of Injection Maneuver 5-58
5.6-9 Tracking Station View Periods (Short Coast) 5-59
5.6-10 Tracking Station View Periods (Long Coast) 5-60
5.6-11 Event Sequence---Short Holding Orbit 5-62
5.6-12 Tracking Station View Periods (Short and Long Coast) 5-64
5.6-13 First Midcourse $\Delta V$ 5-67

6.1-1 Model 971-101 Launch Configuration 6-3
6.1-2 Model 971-101 Space Configuration 6-4
6.1-3 Model 971-101 Space Configuration (Isometric) 6-5
6.2-1 Model 971-102 Launch Configuration 6-7
6.2-2 Model 971-102 Space Configuration 6-8
6.2-3 Model 971-102 Space Configuration (Isometric) 6-9
6.3-1 Model 971-103 Launch Configuration 6-12
6.3-2 Model 971-103 Space Configuration 6-13

## ILLUSTRATIONS (Cont)

| | | Page |
|---|---|---|
| 6.3-3 | Model 971-103 Space Configuration (Isometric) | 6-14 |
| 6.4-1 | Model 971-104 Launch Configuration | 6-16 |
| 7.1-1 | Mars Orbit Insertion Velocity Requirements | 7-3 |
| 7.1-2 | Velocity Allowance Requirements | 7-4 |
| 7.1-3 | Refined Nonuseful Orbiter Weight | 7-6 |
| 7.1-4 | Useful Weight Minus Science and Capsule | 7-7 |
| 7.1-5 | Capsule Weights---Indirect Entry | 7-9 |
| 7.1-6 | Capsule Weights---Direct Entry | 7-10 |
| 7.1-7 | Steering Profile Definitions | 7-12 |
| 7.1-8 | Usable Launch Azimuths | 7-13 |
| 7.1-9 | Launch Times | 7-14 |
| 7.1-10 | Daily Launch Windows | 7-15 |
| 7.1-11 | Parking Orbit Coast Times | 7-16 |
| 7.1-12 | Near-Earth Shadow Entry and Exit Times---Short Coasts | 7-17 |
| 7.1-13 | Near-Earth Shadow Entry and Exit Times---Long Coasts | 7-18 |
| 7.1-14 | Station Tracking Coverage---Launch Phase---Short Parking Orbit Coasts | 7-20 |
| 7.1-15 | Station Tracking Coverage---Launch Phase---Long Parking Orbit Coasts | 7-21 |
| 7.1-16 | DSIF Station Coverage---Trans-Mars Phase (Short Coast) | 7-22 |
| 7.1-17 | DSIF Station Coverage---Trans-Mars Phase (Long Coast) | 7-23 |
| 7.2-1 | General Arrangement Drawing---Model 971-105 | 7-27 |
| 7.2-2 | General Arrangement Drawing---Model 971-106 | 7-31 |
| 7.2-3 | Lateral Load Factor Amplification | 7-35 |
| 7.2-4 | Load Factors---Model 971-105 | 7-38 |
| 7.2-5 | Structural Sizing---Model 971-105 | 7-39 |
| 7.2-6 | Load Factors---Model 971-106 | 7-41 |
| 7.2-7 | Structural Sizing---Model 971-106 | 7-42 |
| 7.2-8 | Adapter Weight | 7-45 |
| 7.3-1 | Propulsion System Schematic | 7-49 |
| 7.3-2 | Guidance and Control Block Diagram---Pitch and Yaw Axes | 7-61 |
| 7.3-3 | Guidance and Control Block Diagram---Roll Axis | 7-62 |
| 7.3-4 | Thrust Vector Actuator Block Diagram | 7-66 |
| 7.3-5 | Reaction Control Block Diagram | 7-68 |
| 7.3-6 | Guidance and Control Event Sequence | 7-72 |
| 7.3-7 | Sun-Spacecraft Distance---Mars Orbit | 7-75 |
| 7.3-8 | Electrical Power Block Diagram | 7-78 |
| 7.3-9 | Solar Array Power Output Temperature Effects at Earth at 30.5 Volts on Bus | 7-79 |
| 7.3-10 | Solar Array Power Output | 7-83 |
| 7.3-11 | Battery Loads---Orbit Versus Launch | 7-87 |
| 7.3-12 | Telecommunication Subsystem | 7-89 |
| 7.3-13 | Antenna Weight | 7-90 |
| 7.3-14 | Temperature Control | 7-92 |
| 7.3-15 | Cabling Weight | 7-93 |

# TABLES

| | | Page |
|---|---|---|
| 3.4-1 | Engine Selection | 3-13 |
| 3.4-2 | Propulsion Subsystem Weight | 3-18 |
| 3.4-3 | Guidance and Control Weight, Power, and Volume | 3-19 |
| 3.4-4 | Power Subsystem Weight and Size | 3-20 |
| 3.4-5 | Additional Subsystem Weights | 3-20 |
| 3.4-6 | Mission Velocity Requirements | 3-21 |
| 3.4-7 | Design Parameters | 3-29 |
| 3.4-8 | Model 971-105 Weights | 3-30 |
| 3.4-9 | Model 971-106 Weights | 3-32 |
| 5.1-1 | Launch Vehicle Trajectory Constraints | 5-6 |
| 5.2-1 | Engine Weight---Initial Sizing Study | 5-12 |
| 5.5-1 | Launch-Arrival Date Effects on Injection Velocity Loss | 5-48 |
| 6.4-1 | General Design Parameters | 6-18 |
| 6.4-2 | Group Weight Statement | 6-20 |
| 7.0-1 | Design Conditions | 7-1 |
| 7.1-1 | Mission Velocity Requirements | 7-5 |
| 7.1-2 | Typical Mission Event Sequence | 7-24 |
| 7.2-1 | Design Parameters | 7-25 |
| 7.2-2 | Limit Design Load Factors | 7-34 |
| 7.2-3 | Factors of Safety | 7-36 |
| 7.2-4 | Summary Weight Statement---Model 971-105 (Indirect Lander Entry) | 7-44 |
| 7.2-5 | Summary Weight Statement---Model 971-106 (Direct Lander Entry) | 7-46 |
| 7.3-1 | Powered Spacecraft Propulsion System Description | 7-51 |
| 7.3-2 | Propulsion System Weight Breakdown | 7-55 |
| 7.3-3 | Propulsion System Components | 7-56 |
| 7.3-4 | Propulsion System Performance Summary | 7-57 |
| 7.3-5 | Guidance and Control Design Conditions and Constraints | 7-58 |
| 7.3-6 | Guidance and Control Component Characteristics---Inertial Reference Unit | 7-63 |
| 7.3-7 | Guidance and Control Component Characteristics---Canopus Tracker | 7-64 |
| 7.3-8 | Guidance and Control Component Characteristics---Sun Sensor | 7-65 |
| 7.3-9 | Guidance and Control Component Characteristics---Gimbal Actuator | 7-65 |
| 7.3-10 | Guidance and Control Component Characteristics---Reaction Control | 7-67 |
| 7.3-11 | Guidance and Control Component Characteristics---Computer Sequencer | 7-70 |
| 7.3-12 | Guidance and Control---Weight Power Volume | 7-71 |
| 7.3-13 | Mission Parameters Applicable to Power Subsystem Design | 7-74 |
| 7.3-14 | Electrical Load on Power Subsystem Components (Watts) | 7-77 |
| 7.3-15 | Choice of Battery Type (Ni-Cd Versus Ag-Zn) | 7-81 |
| 7.3-16 | Point Design---Power Subsystem Weight and Size Estimates | 7-84 |
| 7.3-17 | Power Subsystem Component Characteristics | 7-85 |

# 1.0 INTRODUCTION

Landing an unmanned scientific data package on the surface of Mars, to obtain information for understanding the origin of life and the evolution of our solar system, is a recognized goal of the United States space program. Present schedules for accomplishing this task call for a 1973 launch date for a space vehicle capable of placing on the Martian surface a meaningful experimental package along with associated utility equipment. In addition, many studies (including the present one) have had a requirement to place an orbiter around Mars for further scientific and engineering data gathering and to serve as a communications relay for lander data. Preliminary studies have shown that from the present launch vehicle stable only the Saturn V is capable of injecting spacecraft of acceptable mass toward Mars. However, the costs of a Saturn V launch and the Saturn's greater-than-necessary payload capability lead to studies aimed at defining space vehicles that can provide adequate capability in a cost-effective and timely manner. One obvious approach is to create a new launch vehicle from existing stages (Titan-Centaur, S-IC/S-IVB, etc.) of sufficient payload capability. Another approach that provides an attractive alternative to a new launch vehicle is one called a powered spacecraft.

By definition, the powered spacecraft is a concept that uses the spacecraft propulsion system(s) and guidance and control system(s) to provide that additional ascent performance necessary to inject heavier payloads to the planets. Thus, at one limit, it represents typical present-day unmanned spacecraft ($\Delta V$ assist = 0) that are injected into transplanet trajectories solely by the launch vehicle, while at the other limit it represents a vehicle that provides all the velocity increment ($\Delta V$ assist = $V_{inj} - V_{park}$) needed to attain a transplanet trajectory from a parking orbit established with the launch vehicle.

To provide quantitative data for a realistic judgment of this type of spacecraft for a Mars lander-orbiter mission, an examination and optimization study was needed; the study has been performed and is documented in this report.

## 1.1 BACKGROUND

Preliminary studies have indicated that up to 2,000 pounds of useful payload in planetary orbit will be required to satisfy the objectives of Mars missions for the next several launch opportunities. To provide this useful in-orbit weight, and additional flexibility, the launch vehicle payload injection capability must be in excess of 3,000 pounds, which is somewhat beyond the capability of the Titan IIIC. However, it may be desirable from a cost standpoint to use the existing Titan IIIC class of launch vehicles.

Spacecraft planned for planetary missions will carry on-board propulsion and guidance systems for normal functions such as midcourse corrections, planetary braking, and orbit maneuvers. Preliminary studies have shown that significant performance gains can be achieved by increasing the propellant capacity of such a spacecraft and using its propulsion system in the ascent mode to complement that of the launch vehicle. In this document these launch-assist, multiburn vehicles will be designated powered spacecraft.

## 1.2 OBJECTIVES

The primary objective of this study is to define and investigate the problems, and to determine the technical feasibility, of using a spacecraft propulsion system to supplement the performance of the Titan III class of launch vehicles to gain the additional velocity necessary to inject heavier payloads to Mars. A secondary objective is to determine the maximum useful payloads that can be inserted into Mars orbit by employment of the powered spacecraft concept. A final, but equally important objective, is to accomplish more refined mission analyses and preliminary design analyses for spacecraft weights to be selected by NASA during the course of the study.

# 2.0 DEFINITIONS, SYMBOLS, AND ABBREVIATIONS

The space vehicle terminology, graphically shown below, was used for the study.

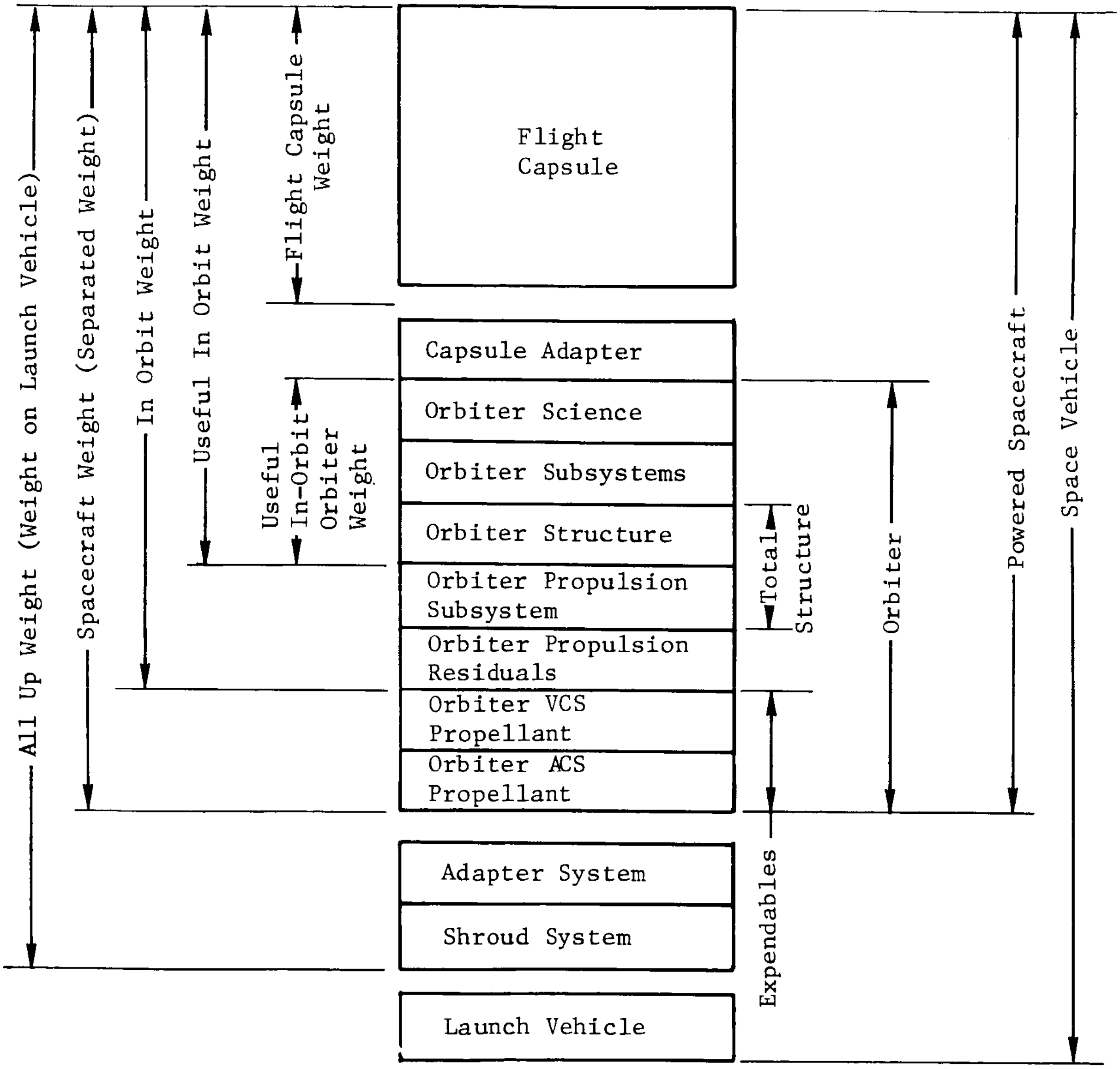
All Up Weight (Weight on Launch Vehicle)
Spacecraft Weight (Separated Weight)
In Orbit Weight
Useful In Orbit Weight
Flight Capsule Weight
Useful In-Orbit Orbiter Weight
Flight Capsule
Capsule Adapter
Orbiter Science
Orbiter Subsystems
Orbiter Structure
Orbiter Propulsion Subsystem
Orbiter Propulsion Residuals
Orbiter VCS Propellant
Orbiter ACS Propellant
Adapter System
Shroud System
Launch Vehicle
Total Structure
Expendables
Orbiter
Powered Spacecraft
Space Vehicle

Two more terms used in this document, but not shown above, are useful spacecraft weight and nonuseful weight. Useful spacecraft weight includes the orbiter structure and subsystems. Nonuseful weight includes the orbiter propulsion subsystem, propulsion residuals, and VCS and ACS propellants.

The following symbols and abbreviations were used throughout the study.

ACS = attitude control system

AFETR = Air Force Eastern Test Range

AU = astronomical unit

$\vec{B}\cdot\vec{T}$, $\vec{B}\cdot\vec{R}\cdot$ = direction cosines at Mars

CG = center of gravity

DLA = departure launch asymptote

DSIF = deep space instrumentation facility

DSN = deep space network

$C_D$ = drag coefficient

$C_3$ = twice the specific total energy referenced to Earth

DOD = Department of Defense

ETR = Eastern Test Range

G&CS = guidance and control system

Isp = specific impulse

IMU = inertial measuring unit

IRU = inertial reference unit

O/F = oxidizer to fuel ratio

PBPS = Post-Boost Propulsion System

RCS = reaction control system

RTC = real-time command

RSS = root sum square

RMS = root mean square

SRM = solid rocket motor

"S" vector = vector from Earth center parallel to departure asymptote

TWTA = traveling wave tube amplifier

$N_2O_4$-A50 = nitrogen tetraoxide-aerozine 50

MMH = monomethylhydrazine

UDMH = unsymmetrical dimethyl hydrazine

MSFN = manned space flight network

MVB - minimum velocity bit

TVC = thrust vector control

VCS = velocity control system

$V_\infty$, $V_{HP}$ = hyperbolic excess velocity

$V_{inj}$ = injection velocity

$V_{park}$ = parking orbit velocity

$\Delta V$ = velocity increment

♂ = Mars

$\sigma$ = Stephan Boltzmann constant or measure of dispersion

$\alpha$ = solar absorptivity

$\tau$ = time

finite burn loss = losses due to nonimpulsive engine burn and thrust vector orientation

true anomaly = angle in orbit plane measured from perifocus to object in plane in its direction of motion

holding orbit = orbit after second burn of transtage and before spacecraft engine ignition.

parking orbit = orbit after first burn of transtage

# 3.0 SUMMARY

Studies have shown that up to 2000 pounds of useful in-orbit weight are required to satisfy Mars mission objectives for near future launch opportunities. This requires a launch vehicle capability in excess of 3000 pounds. The Titan IIIC class of launch vehicles, though lacking this capability, appear attractive enough from a cost standpoint to warrant investigations aimed at augmenting payload injection capability. One such technique, the subject of this study, is to increase the propellant capacity of the spacecraft's propulsion system and use it to assist the launch vehicle in providing the required transplanet injection velocity. These launch-assist vehicles have been designated powered spacecraft.

## 3.1 OBJECTIVES

The objectives of the "Study of Powered Spacecraft for Mars Missions" were:

- To investigate the practicality of using a powered spacecraft for supplementing Titan IIIC and Titan IIID performance so that heavier payloads can be injected to Mars.
- To determine the maximum useful payloads that can be inserted into Mars orbit using the powered spacecraft concept.
- To accomplish refined mission analysis and preliminary design analysis for spacecraft weights and design conditions selected by NASA.

## 3.2 SCOPE AND APPROACH

The primary initial guidelines for the study as supplied by NASA were:

| | |
|---|---|
| Mission Year | 1973 |
| Launch Vehicle | Titan IIIC and Titan IIID |
| Mission Type | I and II |
| Launch Window | 10, 20, and 30 days |
| DLA | ± 36 degrees |
| Configuration | Spacecraft designed with modular propulsion system |
| Spacecraft Propulsion | Developed or in-development engines |
| Guidance and Control | G&C concepts must be compatible with no boost assist |
| Range | ETR launch--NASA ranging facilities preferred |

A final condition for design necessary for more effective analysis was subsequently added:

| | |
|---|---|
| Mars Orbit | 1,000-kilometer periapsis x 33,000-kilometer apoapsis altitude. |

The study approach consisted of: (1) establishing launch vehicle capability and compatibility with a powered spacecraft concept; (2) defining parametrically the preliminary performance of the powered spacecraft; (3) conducting detail subsystem studies of propulsion, guidance and control, and electrical power, and establishing the weights of additional subsystems; (4) performing refined configuration and mission analyses; and (5) establishing the orbiter costs associated with nonpowered (no boost assist) and powered (boost assist) spacecraft.*

Powered spacecraft element weights were defined for the study in accordance with the standard space vehicle terminology of Figure 3.2-1.

## 3.3 CONCLUSIONS

Significant conclusions that follow from an evaluation of the study results are:

a) The powered spacecraft is compatible with both the Titan IIIC and Titan IIID in that no launch vehicle constraints are violated, and no stage impact problem on a major land mass exists for spacecraft weights exceeding 6,000 pounds (Titan IIIC).

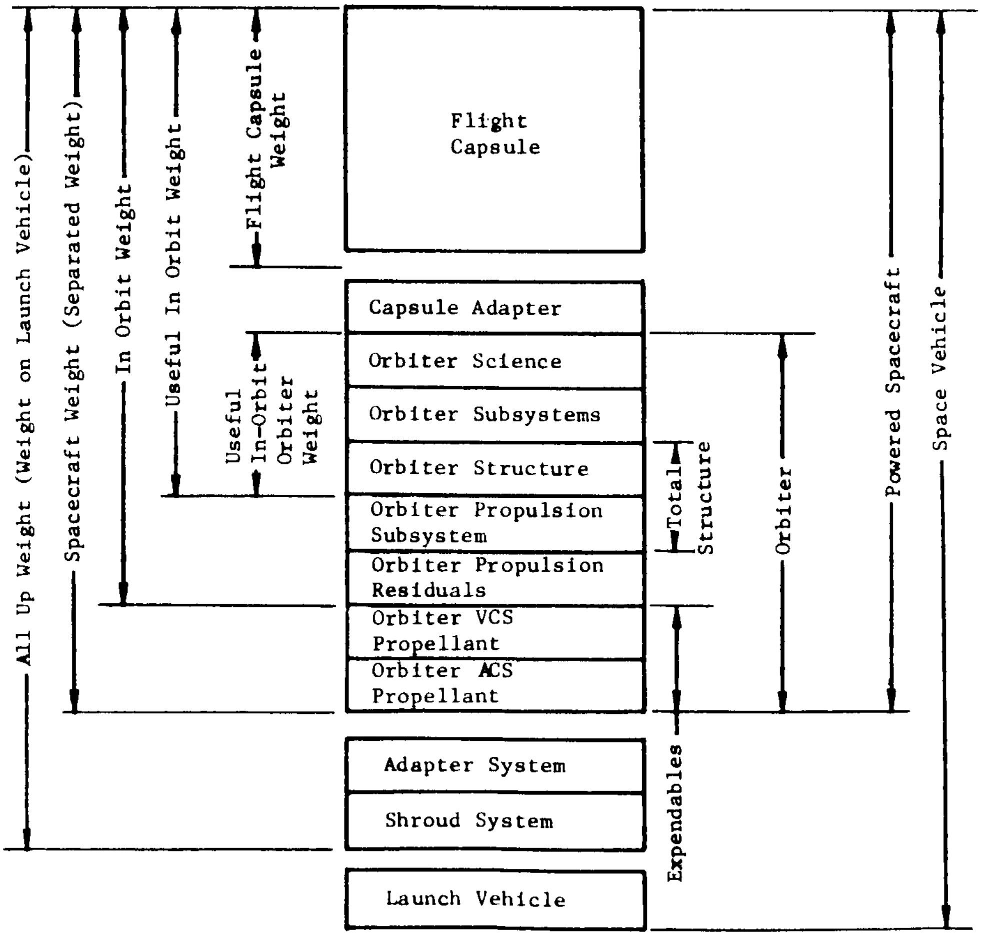
All Up Weight (Weight on Launch Vehicle)
Spacecraft Weight (Separated Weight)
In Orbit Weight
Useful In Orbit Weight
Flight Capsule Weight
Useful In-Orbit Orbiter Weight
Flight Capsule
Capsule Adapter
Orbiter Science
Orbiter Subsystems
Orbiter Structure
Orbiter Propulsion Subsystem
Orbiter Propulsion Residuals
Orbiter VCS Propellant
Orbiter ACS Propellant
Adapter System
Shroud System
Launch Vehicle
Total Structure
Expendables
Orbiter
Powered Spacecraft
Space Vehicle

Figure 3.2-1: SPACE VEHICLE TERMINOLOGY

*This information available from NASA-Langley.

b) The Titan IIIC is the preferred launch vehicle because the useful in-orbit weight penalties resulting from the additional ΔV penalties (>1,000 m/sec) incurred by the Titan IIID due to its nonrestartable (Core 2) characteristics are unacceptable.

c) Based on a minimum energy-fixed arrival date analysis with the Titan IIIC, a Type I trajectory provides approximately 400 pounds more useful in-orbit weight than does a Type II trajectory.

d) Based on useful in-orbit weight, the 2,200-pound Apollo Subscale and 3,500-pound LEM Ascent engines are competitive. The 300-pound and 900-pound (cluster of three 300-pound) PBPS engines are not competitive.

e) The 3,500-pound LEM Ascent engine is preferred for the powered spacecraft because it represents a developed and qualified flight-type engine that is in production and being funded. This is not true for the 2,200-pound Apollo Subscale engine.

f) With the 3,500-pound LEM Ascent engine, propellant migration must be eliminated, and unsymmetrical depletion of propellants must be minimized if the required minimum velocity bits are to be achieved without either undue ΔV penalties or operational complexity. These conditions were satisfied by using check valves and trimming orifices in propellant tank outlet lines.

g) A separated spacecraft weight of 7,000 pounds represents a good design point because it achieves nearly peak useful in-orbit weight and further small increases in useful in-orbit weight are associated with large increases in separated spacecraft weight (mostly propellant).

h) An analysis of fixed versus variable arrival date trajectories for a 20-day launch period shows a useful in-orbit weight increase of 150 pounds for a variable versus fixed arrival date approach.

i) A 7,000-pound powered spacecraft, with the Titan IIIC, can provide approximately 1,350 pounds of flight capsule plus orbiter science in Mars orbit when an indirect lander mode (out of orbit) with a variable arrival date and 20-day launch period is used. Comparable flight capsule plus orbiter science weight for a nonpowered spacecraft (no boost assist) is approximately 800 pounds.

j) A 7,000-pound spacecraft, with the Titan IIIC, can provide 200 pounds of orbiter science in Mars orbit and approximately 1,700 pounds of flight capsule, when a direct lander mode (lander jettisoned before orbiter injection into Mars orbit) with a variable arrival date and 20-day launch period are used. Comparable science and flight capsule weights for a nonpowered spacecraft (no boost assist) are 200 and 750 pounds, respectively.

k) Application of spacecraft boost-assist ΔV shortly after separation from the transtage is feasible and preferred. A once-around holding orbit involves additional operational complexities and probably additional guidance and control hardware.

l) Real-time telemetry during the powered spacecraft (transtage second burn followed by spacecraft-assist burn) injection maneuver requires one or two tracking ships and TWTA operation. These requirements are similar to those for a nonpowered interplanetary spacecraft.

m) Powered spacecraft designs (configurations and subsystems) are, except for the increased size and thrust of the modular propulsion module, similar to nonpowered (no boost assist) spacecraft designs.

n) It can be concluded, based on a fairly detailed cost study, that a powered spacecraft provides significant payload gains over a nonpowered spacecraft for only moderate cost increases.*

## 3.4 RESULTS

Study results will be presented by considering six major categories of technical information:

Launch Vehicles
Parametric Performance and Mission Analysis
Refined Performance and Mission Analysis
Configurations
Subsystems

The powered spacecraft mission originates with space vehicle launching along the Eastern Test Range between launch azimuth limits of 66 to 114 degrees. This is followed by insertion of the transtage-spacecraft into a 100 n mi circular parking orbit (Titan IIIC) or the spacecraft into an elliptical parking (or holding) orbit with a 100-n mi perigee (Titan IIID). After coasting in the parking orbit to the required injection point, there occurs either transtage ignition, followed by spacecraft ignition to provide the required boost assist $\Delta V$ (Titan IIIC), or spacecraft ignition to provide all the injection $\Delta V$ (Titan IIID). Figure 3.4-1 depicts the other major mission events: the injection $\Delta V$ maneuver from Earth onto a trans-Mars trajectory consisting of three midcourse maneuvers

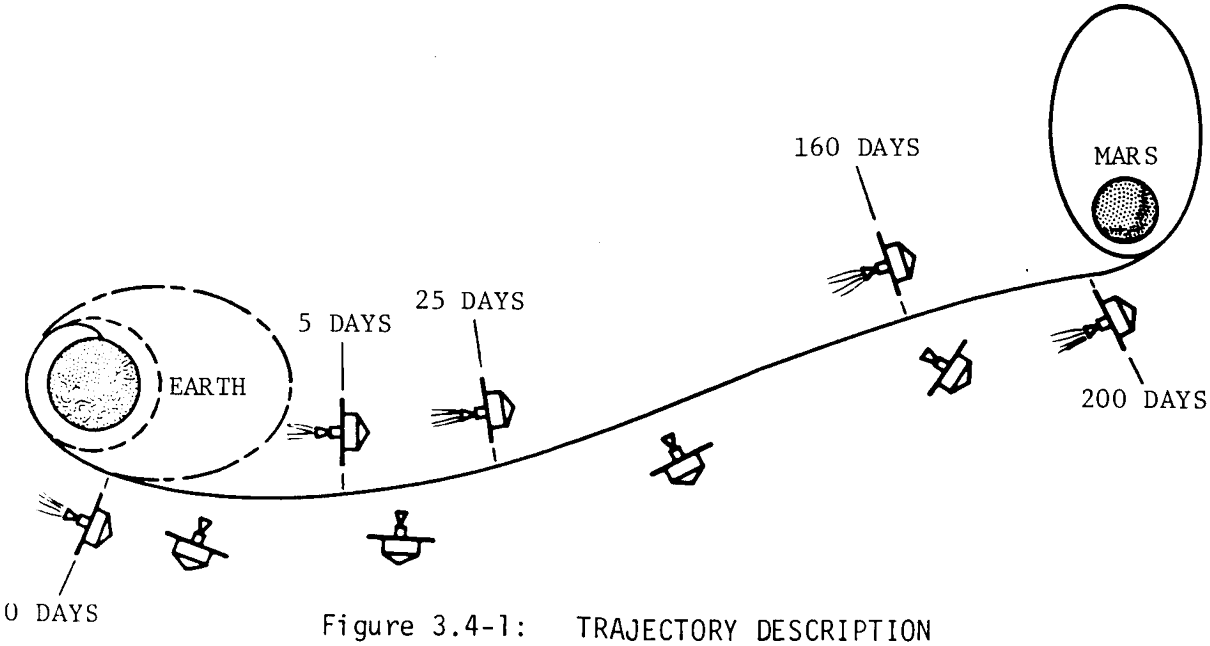

Figure 3.4-1: TRAJECTORY DESCRIPTION

---

*This information available from NASA-Langley.

nominally occurring at 5 and 25 days after injection and about 40 days before Mars arrival, and a Mars orbit insertion maneuver into a 1,000-kilometer periapsis by approximately 33,000-kilometer apoapsis altitude, 24.6-hour orbit.

From this orbit, after suitable surveillance, the lander is sent to the Martian surface. This preferred lander mode has been designated the "out of orbit" or indirect lander. Another, less preferred, lander mode is one in which the lander is sent to the Martian surface before orbiter injection into Mars orbit; this has been designated the direct lander.

### 3.4.1 Launch Vehicles

The gross configuration of the Titan IIIC is shown in Figure 3.4-2. As indicated, the Titan IIID has been defined for this study as the Titan IIIC minus transtage. Launch vehicle payload capability versus inertial velocity is shown in Figure 3.4-3 for both the Titan IIIC and IIID. The data was generated from NASA-supplied weight and thrust characteristics by employing a trajectory simulation in which the vehicle rises vertically for 20 seconds, then instantaneously

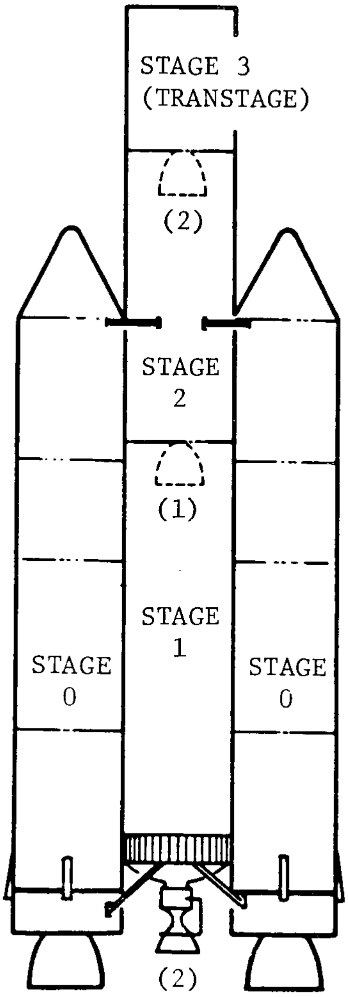

TITAN IIID = TITAN IIIC - TRANSTAGE

LIFTOFF WEIGHT = $1.4 \times 10^6$ $LB_M$

LIFTOFF THRUST = $2.4 \times 10^6$ $LB_F$

Figure 3.4-2: TITAN IIIC LAUNCH VEHICLE

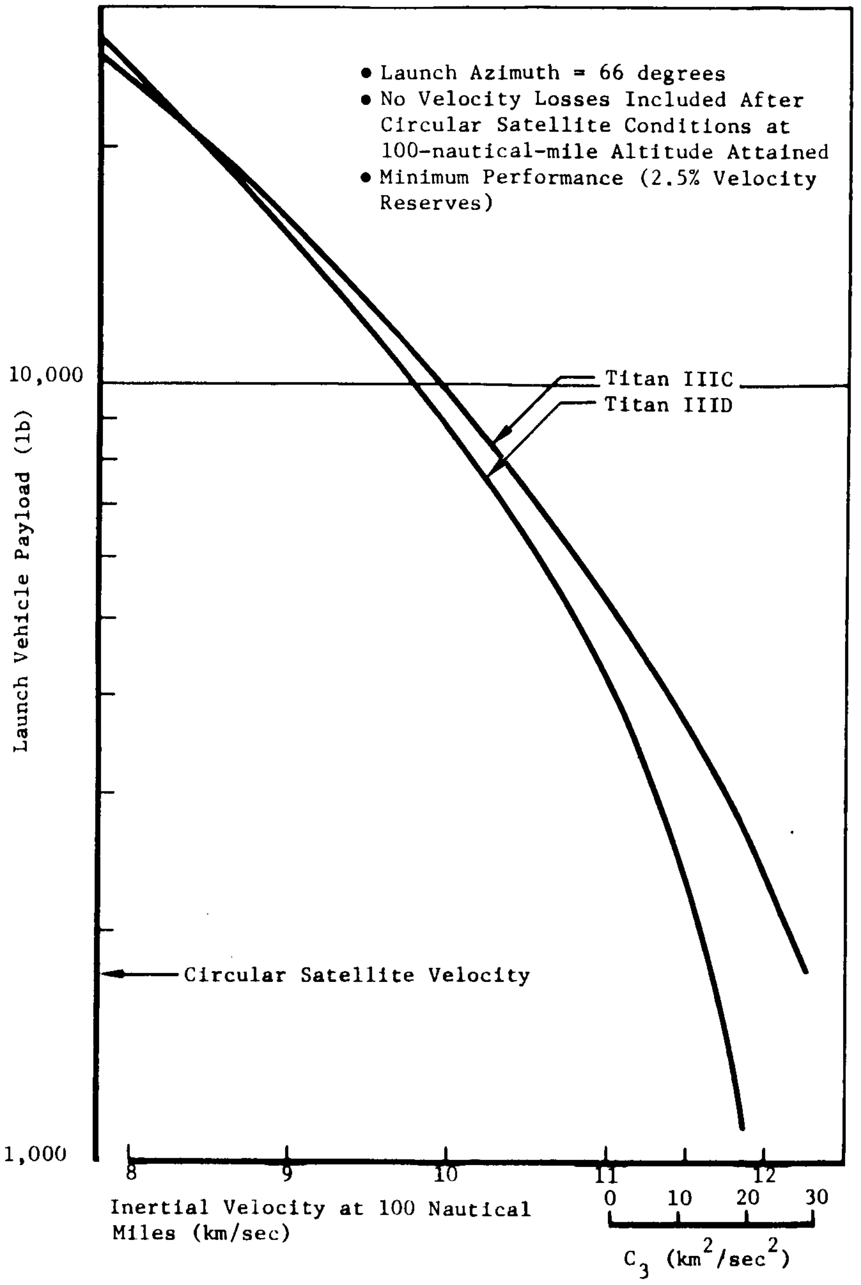

Figure 3.4-3: LAUNCH VEHICLE PAYLOAD CAPABILITIES

tilts into a gravity turn until the dynamic pressure is 10 lb/ft$^2$. This is followed by a constant angle of attack until burnout. The expected result is clearly shown: as inertial velocity (or $C_3$) is increased, the payload difference between the launch vehicles increases with the four-stage Titan IIIC being superior to the three-stage Titan IIID.

However, before using either of these launch vehicles for a powered spacecraft mission, both launch vehicle trajectory constraints and stage impact point constraints (no impact on a major land mass) must be met. The launch vehicle trajectory simulation for payloads of 5,000 to 24,000 pounds with both the

Titan IIIC and IIID gave results that were compatible with all trajectory constraints. Stage impact point calculations were not germane to the Titan IIID because Core 2 (third stage) goes into orbit and Core 1 and the payload fairing present no new problem. For Titan IIIC, Core 2 does not go into orbit. Therefore, its impact point is of concern and, as shown in Figure 3.4-4, is a function of payload weight. For launch azimuths between 66 and 90 degrees, payload weights in excess of 6,000 pounds are required to ensure that no impact of the African mainland by Core 2 occurs.

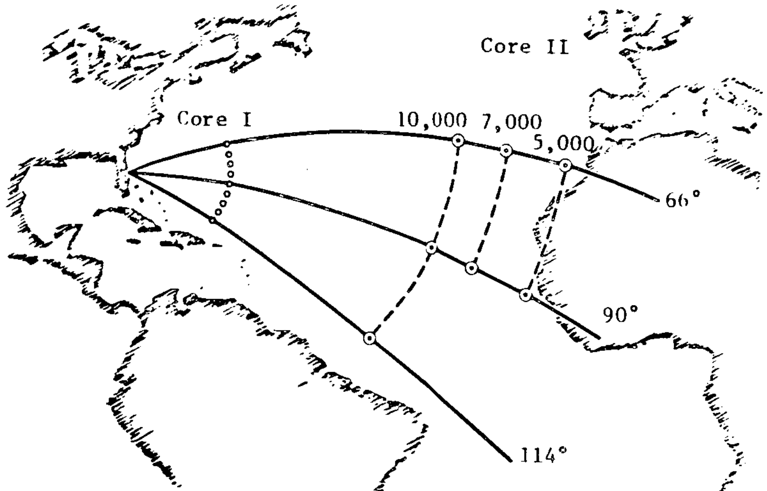

Figure 3.4-4: EMPTY STAGE SPLASH POINTS---TITAN IIIC

It would appear from the preceding discussion that both the Titan IIIC and IIID are acceptable for a powered spacecraft mission; however, this is not true. The Titan IIID is not acceptable because its use involves additional excessive ΔV losses throughout the launch period due to off-perigee injection. This results because of the nonrestartable Titan IIID Core 2, the launch azimuth constraints, the launch site, and the orientation of the required outgoing asymptote, which combine to create the situation shown in Figure 3.4-5 for a 1973 launch.

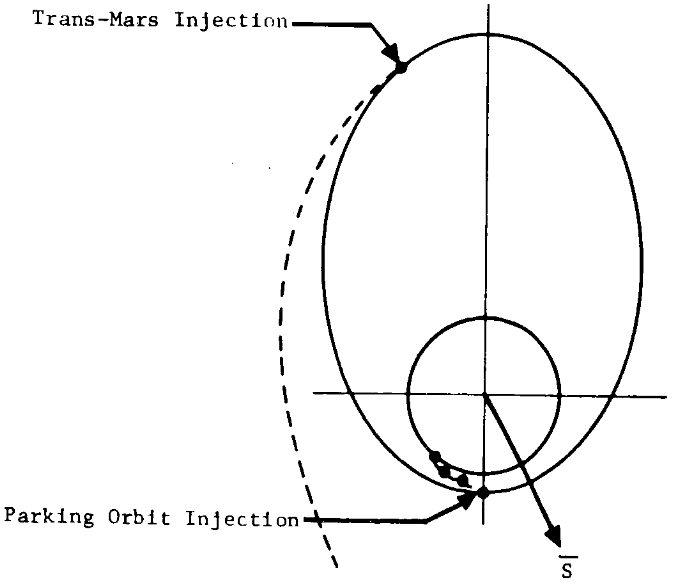

Figure 3.4-5: OFF-PERIGEE INJECTION

Here the true anomaly of the trans-Mars injection point lies considerably off the perigee of the elliptical orbit resulting from a Titan IIID launch with reasonable payloads. The minimum velocity losses associated with an August 11, 1973 launch date and the Titan IIID are shown in Figure 3.4-6.

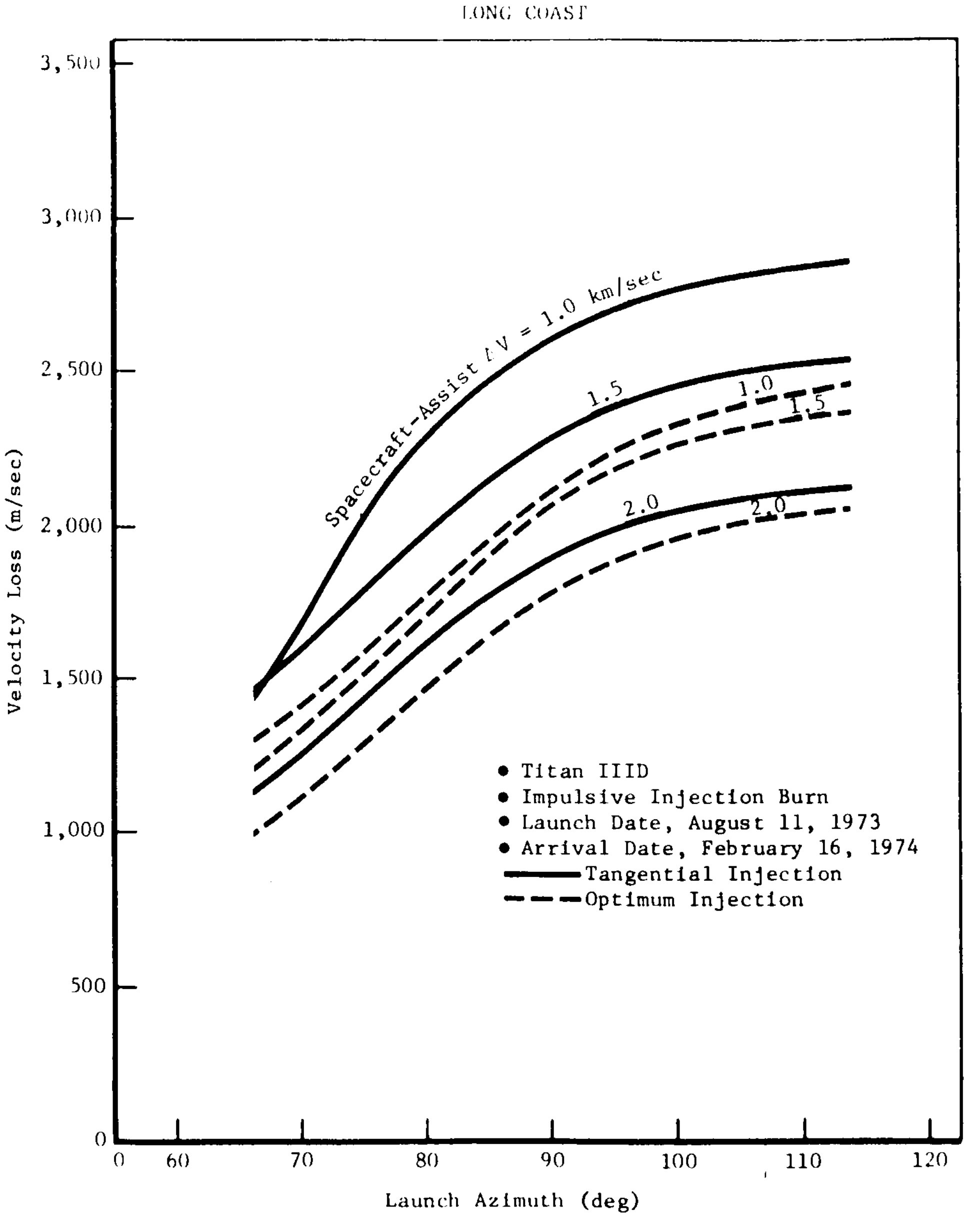

Figure 3.4-6: INJECTION VELOCITY LOSS WITH ELLIPTICAL PARKING ORBITS---LONG COAST

Figure 3.4-7 provides similar data for other launch and arrival dates that surround the conditions of Figure 3.4-6. Note that a velocity loss of 1,000 m/sec is approximately equivalent to a useful in-orbit weight reduction of 1,000 pounds.

Finally, the results of a launch-on-time investigation for a Type I trajectory, variable arrival dates, and the best 20-day launch period in 1973 are shown in Figure 3.4-8. The daily launch time constraints exist because the Earth parking orbit must contain within its plane the launch site vector and the departure trans-Mars asymptote vector, and yet not violate launch azimuth constraints. No launch-on-time problem exists because more than 2.5 hours are available twice a day for the daily launch window (throughout the launch period) in contrast to a minimum requirement of 0.5 hour per Titan IIIC launch.

| | | | Short Coast | | | Long Coast | | |
|---|---|---|---|---|---|---|---|---|
| Trajectory Number | Launch Day 1973 | Arrival Day 1974 | Launch Azimuth For Minimum Loss (deg) | Minimum Velocity Loss (m/sec) | Injection True Anomaly (deg) | Launch Azimuth For Minimum Loss (deg) | Minimum Velocity Loss (m/sec) | Injection True Anomoly (deg) |
| 1 | July 3 | Jan. 16 | 114 | 2,798 | 190.1 | 66 | 1,835 | 215.4 |
| 2 | Aug. 1 | Jan. 22 | 114 | 2,659 | 171.1 | 66 | 1,461 | 222.5 |
| 3 | Aug. 20 | Jan. 26 | 114 | 2,782 | 167.7 | 66 | 1,082 | 241.0 |
| 4 | Aug. 22 | Mar. 5 | 114 | 2,860 | 170.5 | 66 | 1,294 | 232.8 |
| 5 | Aug. 2 | Mar. 5 | 114 | 2,758 | 185.0 | 66 | 2,113 | 204.6 |
| 6 | July 4 | Jan. 24 | 114 | 2,904 | 185.7 | 66 | 2,165 | 206.8 |
| 7 | July 23 | Feb. 16 | 114 | 2,763 | 184.0 | 66 | 2,167 | 203.1 |
| 8 | Aug. 1 | Feb. 16 | 114 | 2,611 | 189.8 | 66 | 1,750 | 213.4 |
| 9 | Aug. 11 | Feb. 16 | 114 | 2,710 | 171.4 | 66 | 1,466 | 223.3 |

- Tangential injection with impulsive burn
- Parking orbit period = 10.1 hours<br>(Spacecraft-assist $\Delta V \simeq 1.5$ km/sec)
- Launch azimuth range investigated is between 66 and 114 degrees

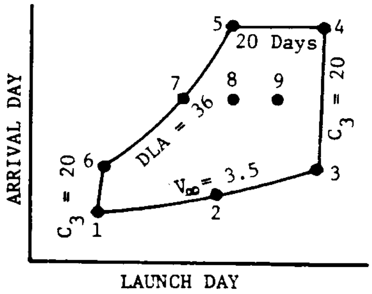

Figure 3.4-7: LAUNCH-ARRIVAL DATE EFFECTS ON INJECTION VELOCITY LOSS

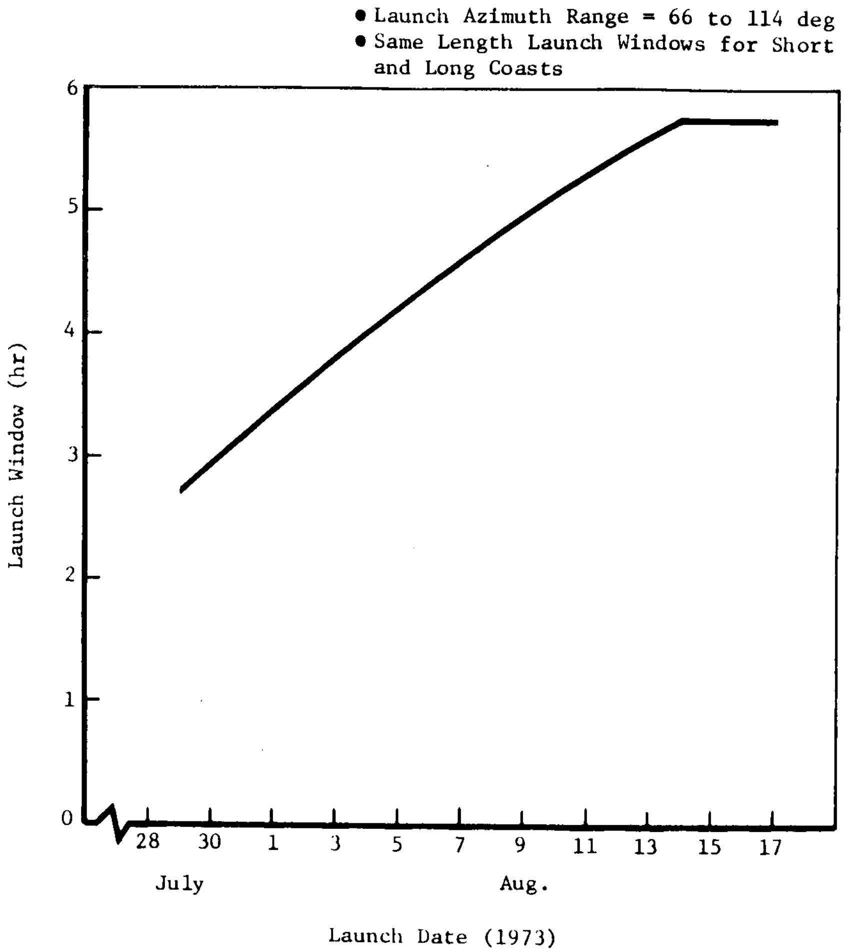

Figure 3.4-8: DAILY LAUNCH WINDOWS

### 3.4.2 Parametric Studies

The parametric studies were to result in a broad preliminary overview of the factors influencing performance and of performance capability. Initial analyses were concerned with reducing problem complexity by establishing reasonable design conditions on which to base further decisions. Because these decisions would be based primarily on useful in-orbit weight, it was necessary to parametrically establish nonuseful weight as a function of useful propellant, Figure 3.4-9 (nonuseful weight equals orbiter propulsion subsystem, propulsion residuals, and VCS and ACS propellants). It was recognized that since the nonuseful weight was based on an assumed configuration and structural concept, its reiteration for the refined analyses of the study (when a more accurate determination of flight capsule plus science payload was made) would be necessary.

Type I and Type II trajectories, launch period influences, and resulting arrival dates were examined using the data of Figure 3.4-9 and a minimum energy-fixed arrival date approach. From the results, shown in Figure 3.4-10, it was concluded that Type I trajectories were superior to Type II trajectories and that, for a 20-day launch period (chosen as being a reasonable compromise), February 16, 1974 was the best arrival date ($C_3$ = 16.139 km$^2$/sec$^2$ and $\Delta V$ post-injection = 1.404 km/sec).

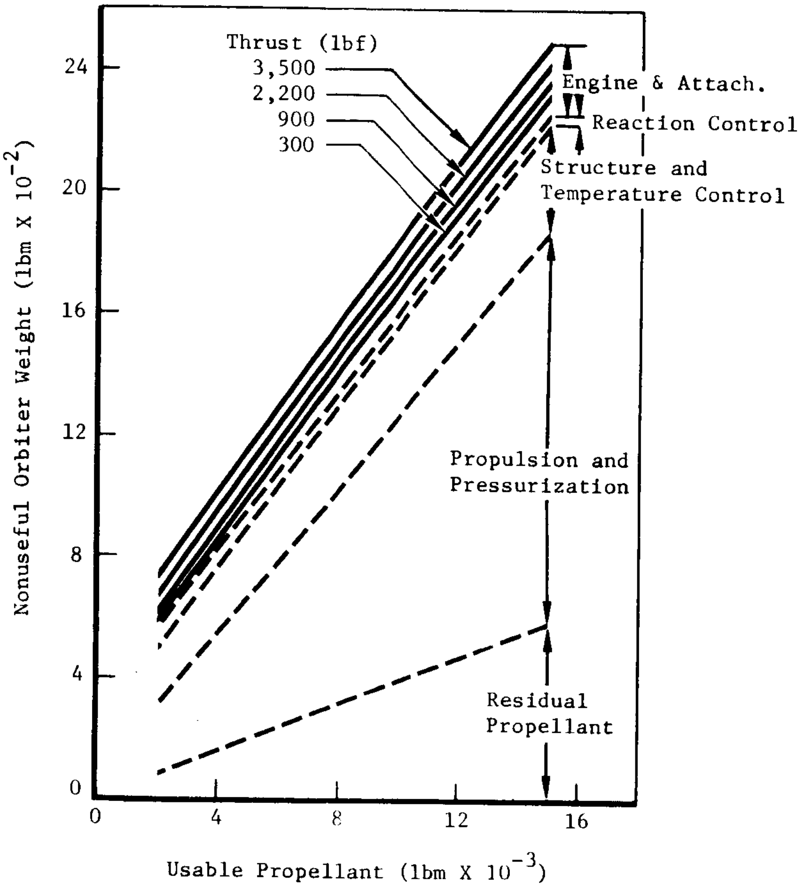

Figure 3.4-9: NONUSEFUL ORBITER WEIGHT

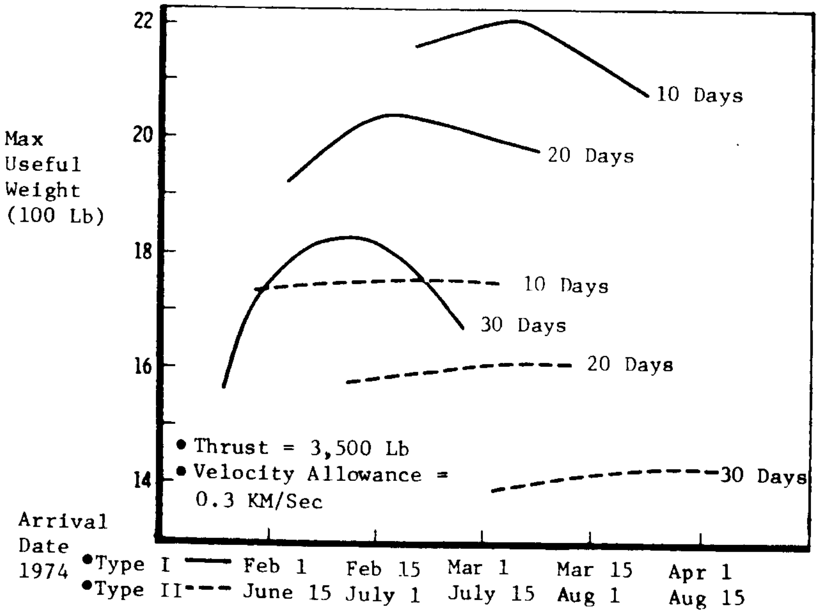

Figure 3.4-10: TITAN IIIC ARRIVAL DATE EFFECTS

The trajectory parameters associated with the best arrival date were then used in an engine selection study so that further analyses on holding orbit penalties and choice of separated spacecraft design point weight could be made at just one thrust level. Figure 3.4-11 presents the performance results of this study, while Table 3.4-1 presents a summary of the pertinent hardware results.

From a performance standpoint, the factors contributing to engine selection are engine inerts, thrust, and specific impulse. At low ΔV assist, the effects of inerts override the effects of thrust (finite burn losses) and specific impulse, while at moderate and large ΔV assists, the opposite is true. For the range of ΔV assists (1.2 to 1.8 km/sec) that provide reasonable separated spacecraft weights and near maximum useful in-orbit weights, the 2,200- and 3,500-pound-thrust engines are competitive, whereas the 300- and 900-pound (cluster of three 300-pound) thrust engines provide considerably less payload. An examination of the engine hardware summary (Table 3.4-1) that considered such important hardware factors as mission burn time versus engine design burn time, present

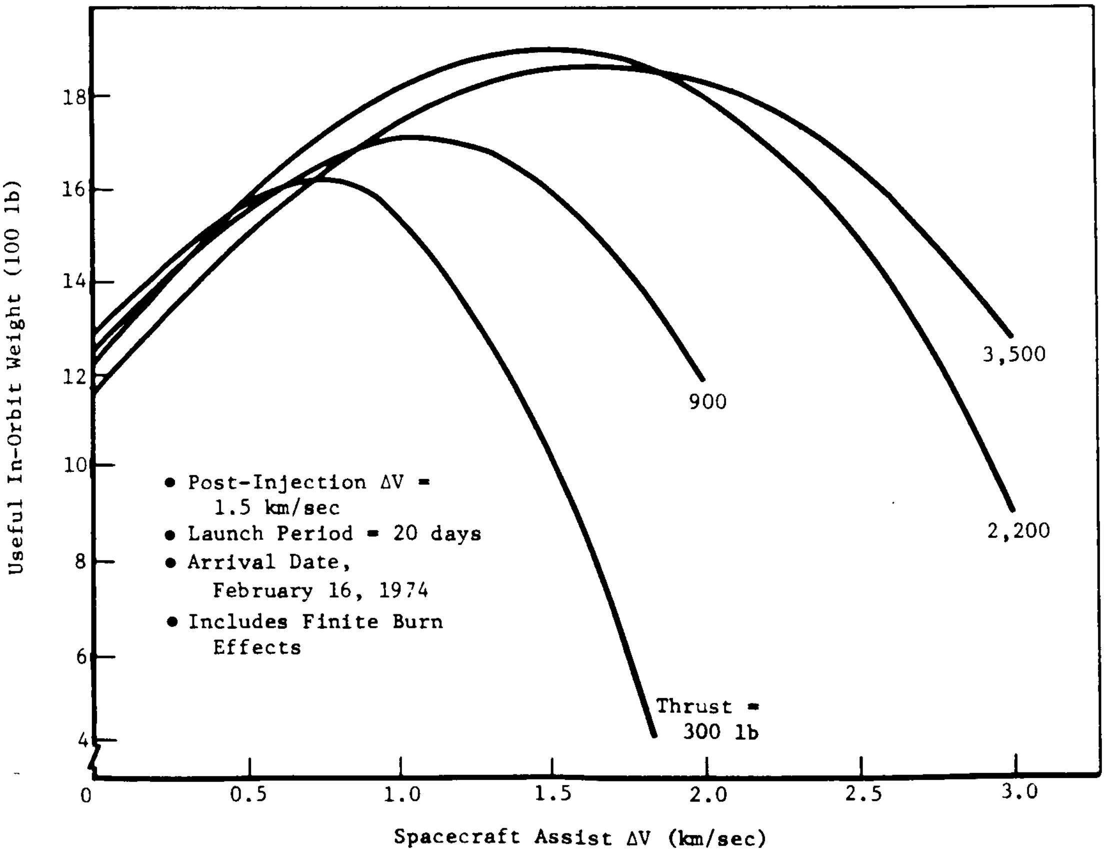

Figure 3.4-11: TITAN IIIC SPACECRAFT THRUST EFFECTS

Table 3.4-1: ENGINE SELECTION

| Engine<br>Thrust (lb) | Apollo Lunar Module Ascent Engine<br>3,500 | Apollo Subscale Engine<br>2,200 | PBPS Velocity Engine<br>3 x 300 |
|---|---|---|---|
| Useful Spacecraft Weight (lb) (Post-Injection ΔV = 1.5 km/sec) | 1,820 | 1,880 | 1,710 |
| Mars Mission Burn Time Requirements (sec) | ~360 | ≈575 | 1,400 |
| Engine Design Burn Time (sec) | >500 | 750 | 197 |
| Present Engine Status | In-Qualification for Apollo | Program Terminated (Subscale Test Engine) | In-Qualification for PBPS |
| Modifications Required | Gimbal Assembly | Gimbal Assembly<br>Bipropellant Valves | Radiation Nozzle Recontour<br>Throat Standoff<br>Valves |
| Qualification Required for Powered Spacecraft | Mission Simulation | Qualification | Qualification |

engine status, modifications required, and qualification required for powered spacecraft, in conjunction with the previously discussed performance capabilities, led to the selection of the 3,500-pound LEM Ascent engine for the powered spacecraft.

This choice of the 3,500-pound LEM Ascent engine required that propellant migration be eliminated and that unsymmetrical depletion of propellants be minimized if the required minimum velocity bits (approximately 1 m/sec) are to be achieved. Otherwise, weight penalties due to either increased attitude control authority or the ΔV penalties associated with "aim point biasing" or "ΔV dumping in a noncritical direction" would be incurred. The propulsion system has been designed to eliminate propellant migration (via check valves at tank outlets) and minimize unsymmetrical propellant depletion (by trimming orifices in tank outlet lines) so that the largest expected center-of-gravity shift (<0.5 inch) between engine burns is within the control authority of the guidance and control subsystem (Figure 3.4-12).

Having established launch vehicle capability, nonuseful parametric weight, trajectory type, best fixed arrival date with its associated performance parameters, and engine choice, the selection of a reasonable spacecraft weight was made. Figure 3.4-13 shows the relationship of separated spacecraft weight, ΔV assist, propellant weight, and useful in-orbit weight. From this data it was concluded, based on a desire to minimize spacecraft weight while not suffering too large a useful in-orbit weight penalty, that a separated spacecraft weight of 7,000 pounds represents a good design point, because further small increases in useful in-orbit weight are accompanied by large increases in separated spacecraft weight.

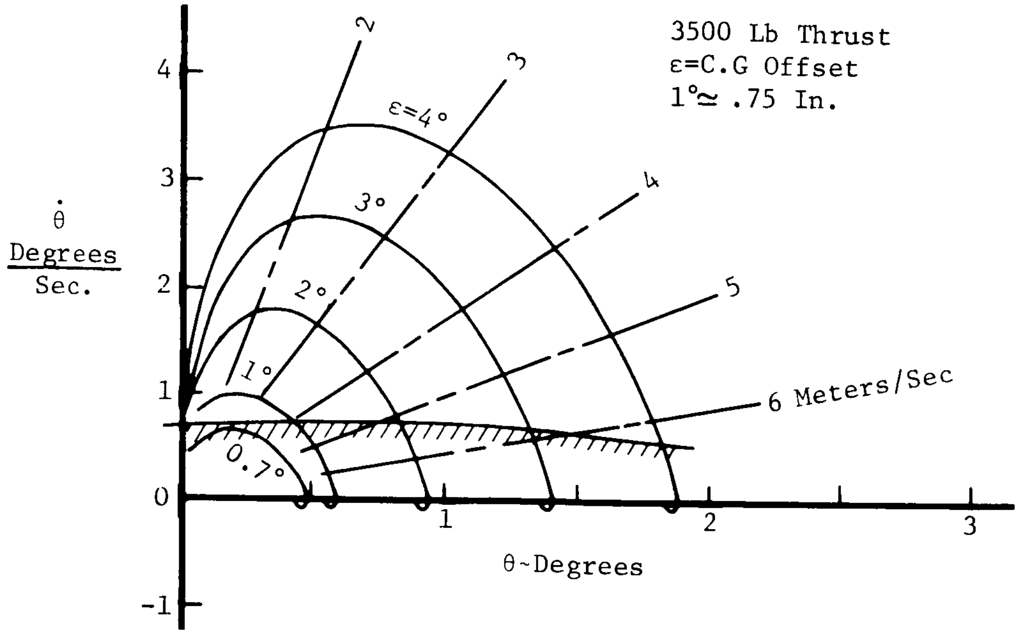

Figure 3.4-12: THRUST VECTORING SYSTEM CONTROL RESPONSE

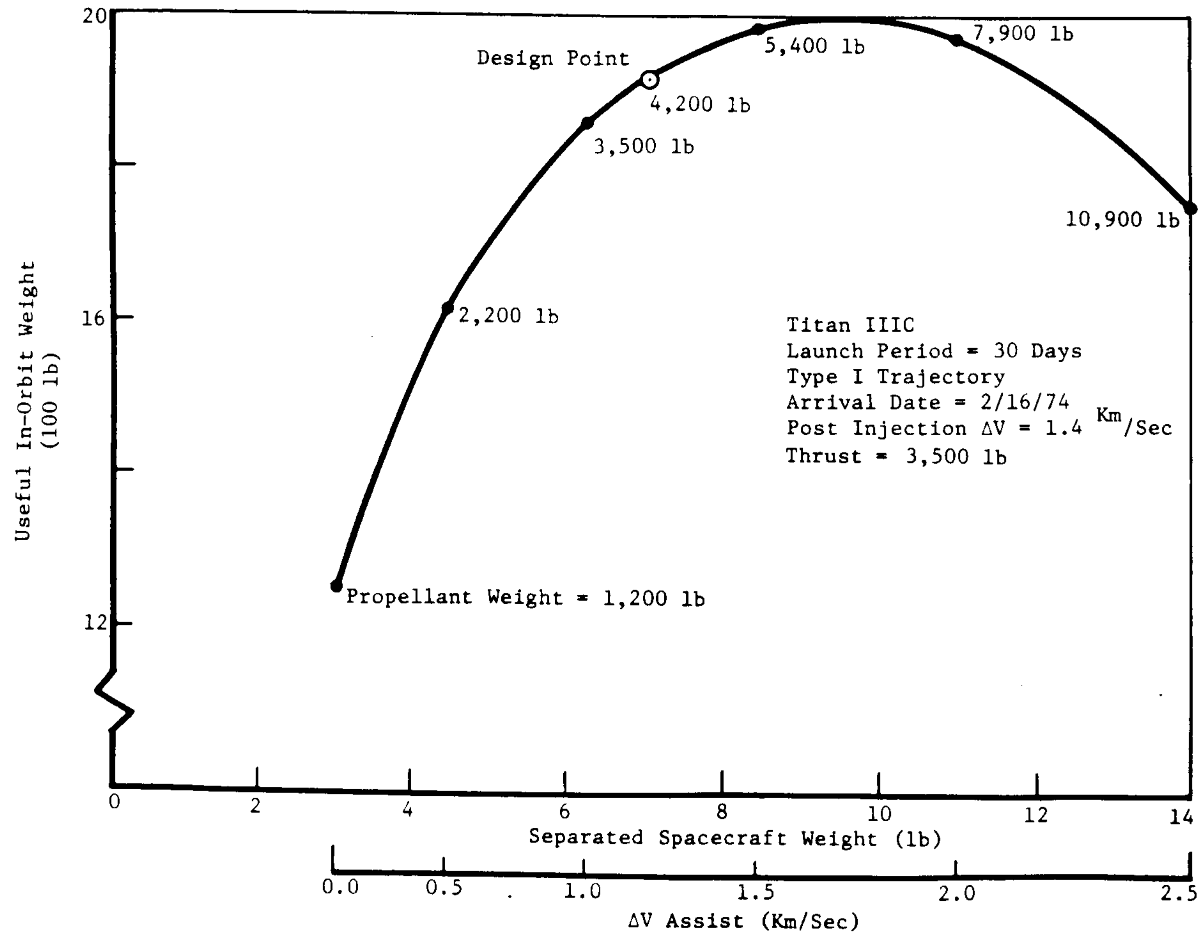

Titan IIIC
Launch Period = 30 Days
Type I Trajectory
Arrival Date = 2/16/74
Post Injection ΔV = 1.4 Km/Sec
Thrust = 3,500 lb

Figure 3.4-13: DESIGN POINT CHOICE

All parametric study results relating to useful in-orbit weight with the Titan IIIC have so far assumed an impulsive transtage second burn followed immediately by a spacecraft burn, with both occurring at perigee. Also, mission energy requirements were based on a best fixed arrival date for a 20-day launch period which, though representing the usual approach to planetary mission energy definition, normally results in greater energy requirements than those associated with a variable arrival date approach.

An examination of these two effects was conducted to assess their significance on powered spacecraft performance. This was done so that additional data would be available to establish the design conditions for the refined configuration and mission analysis and to more accurately define powered spacecraft performance.

The effect of nonimpulsive transtage second burn and spacecraft holding orbit (orbit after transtage second burn and before spacecraft ignition) is shown in Figure 3.4-14 as a function of ΔV assist and holding orbit coast time. The

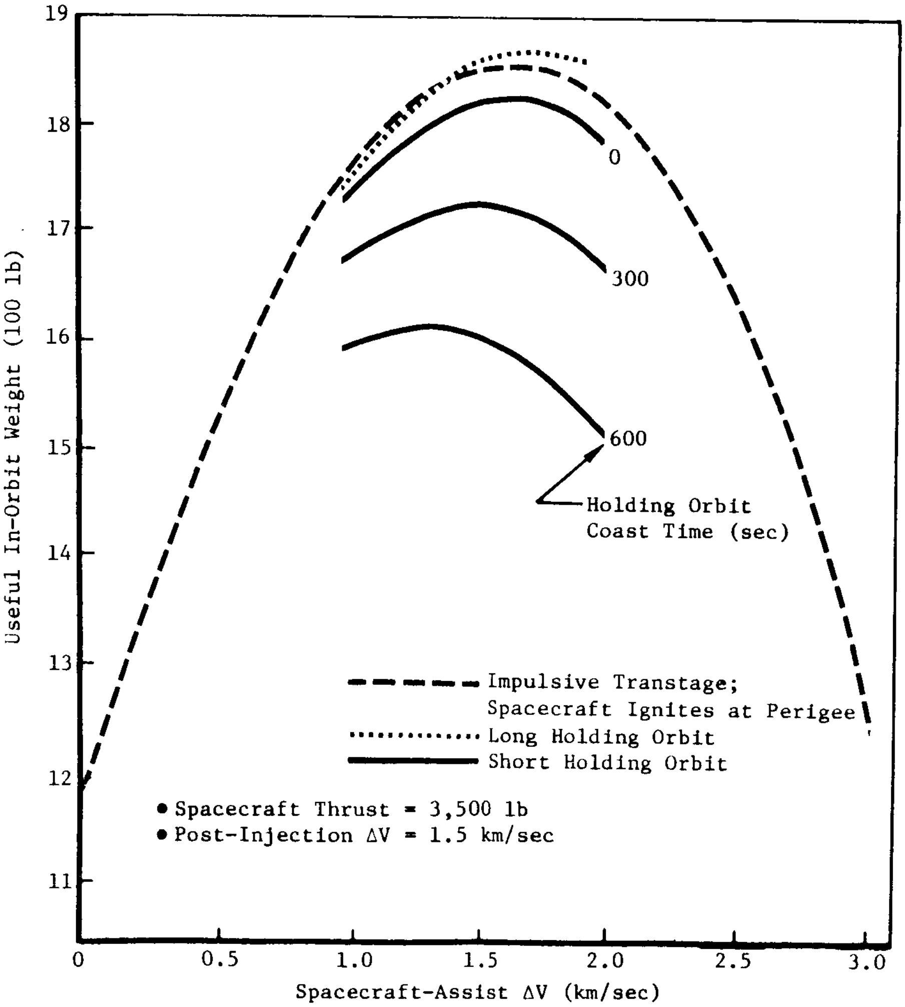

Figure 3.4-14: SHORT AND LONG HOLDING ORBIT COAST PENALTIES

performance penalties for both a once-around long holding orbit and a short holding orbit (Figure 3.4-15) are provided. For the short holding orbit condition, holding orbit times have been determined for both an engine-up and an engine-down (when seen in a launch-ready condition) configuration. These are shown pictorially in Figures 3.4-16 and -17.

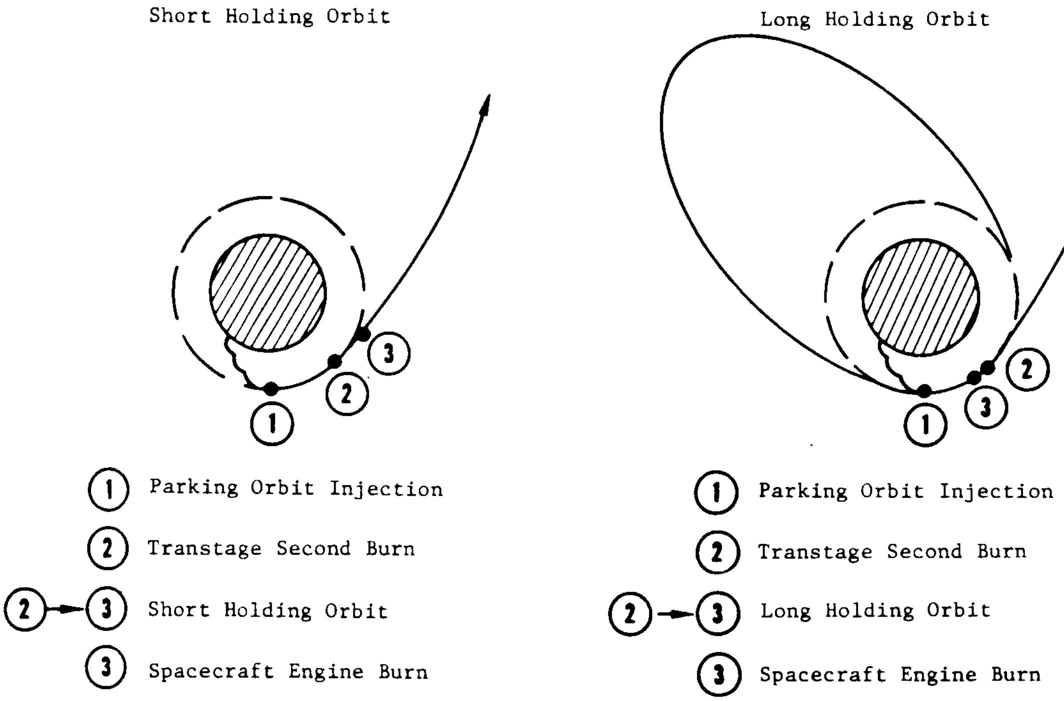
Short Holding Orbit
Long Holding Orbit
①
②
③
① Parking Orbit Injection
② Transtage Second Burn
② → ③ Short Holding Orbit
③ Spacecraft Engine Burn
① Parking Orbit Injection
② Transtage Second Burn
② → ③ Long Holding Orbit
③ Spacecraft Engine Burn

Figure 3.4-15: HOLDING ORBITS

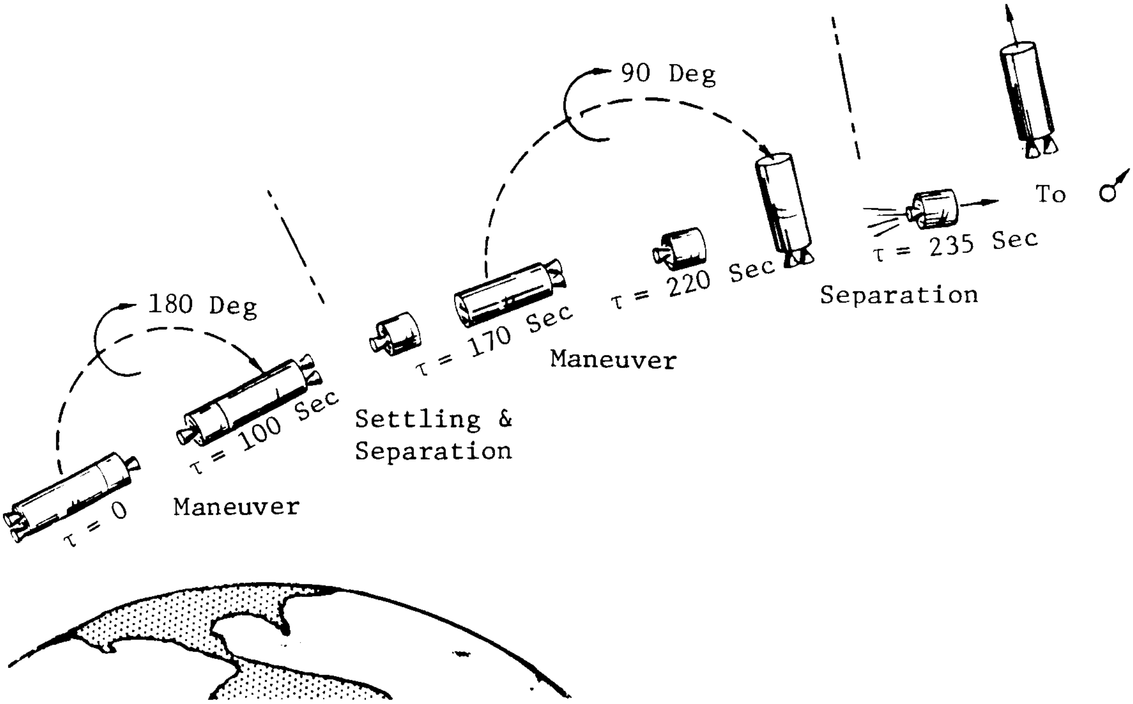
180 Deg
τ = 0
Maneuver
τ = 100 Sec
Settling &
Separation
τ = 170 Sec
90 Deg
Maneuver
τ = 220 Sec
Separation
τ = 235 Sec
To ♂

Figure 3.4-16: BOOST-ASSIST SEQUENCE---ENGINE UP

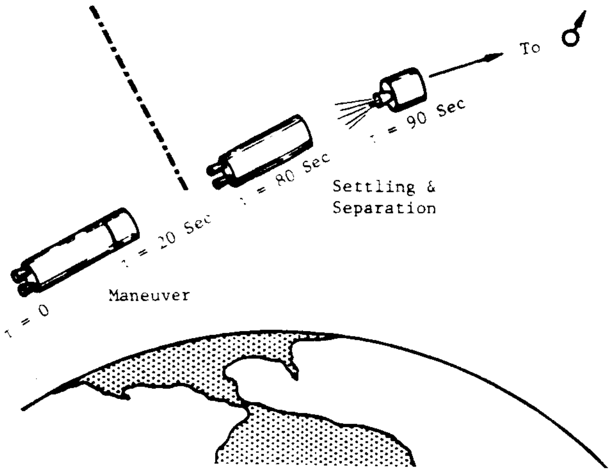

Figure 3.4-17: BOOST-ASSIST SEQUENCE---ENGINE DOWN

The short holding orbit is preferred because it does not require additional guidance and control hardware, orbit ephemeris updating, and establishing an Earth reference as does the long holding orbit option. However, meaningful useful in-orbit weight penalties result for this preferred mode because of off-perigee engine burn for boast assist; these were accounted for in the refined mission analyses.

Variable arrival date effects on useful in-orbit weight are shown in Figure 3.4-18 as a function of launch period. No ΔV losses are included in this data

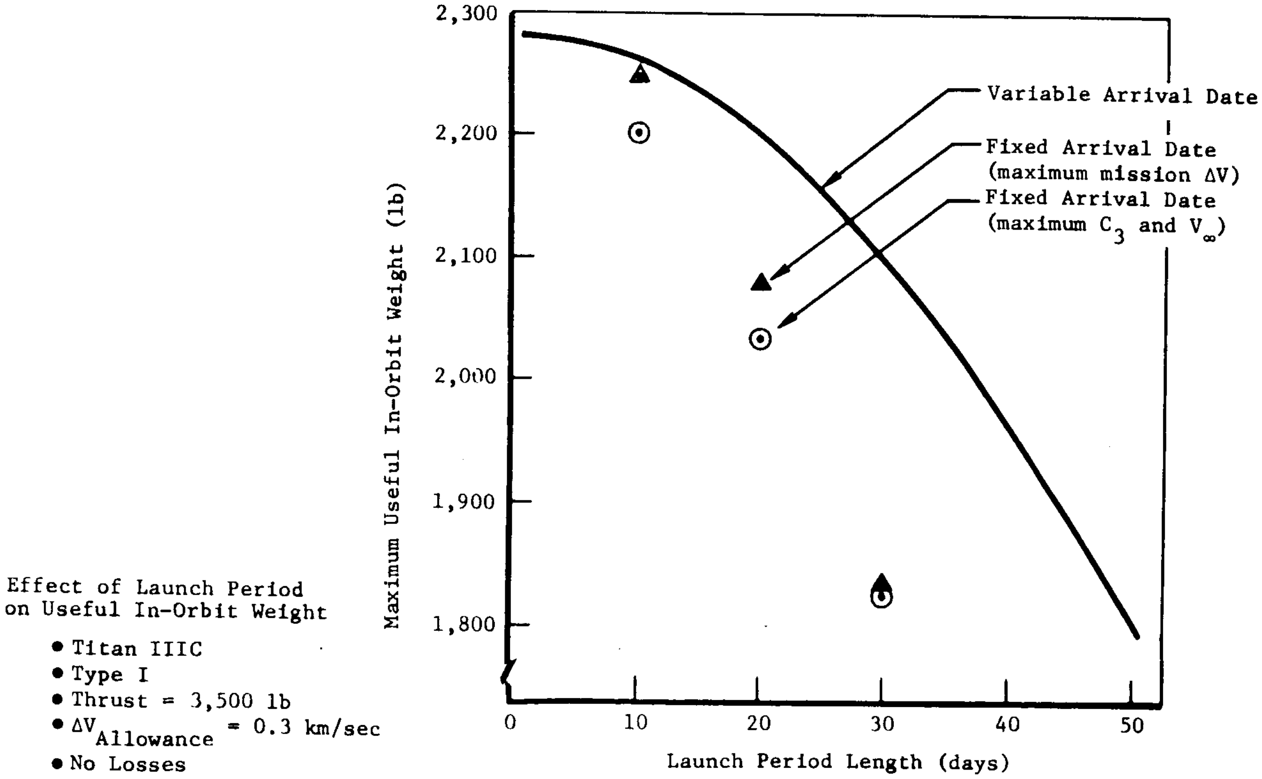

Figure 3.4-18: VARIABLE ARRIVAL DATE EFFECT ON USEFUL IN-ORBIT WEIGHT

because it is the performance differences that are significant. Three mission energy conditions are shown: (1) variable arrival date results; (2) maximum mission $\Delta V$ results; and (3) maximum $C_3$ and $V_\infty$ results. For a 20-day launch period, the performance gain resulting from a variable arrival date approach is considerable (approximately 150 pounds). Therefore, if a variable arrival date approach is compatible with the mission design, it should be used.

### 3.4.3 Subsystems

Three subsystems--propulsion, guidance and control, and electrical power--were examined in detail. They were chosen for detail evaluation because these subsystems were expected to be most influenced by a powered spacecraft concept. All other subsystems were evaluated only with regard to parametrically establishing their weights.

*Propulsion Subsystem*--- The propulsion subsystem is of conventional design. It uses existing technology, developed hardware, and selective redundancy. Functionally, it is a regulated gas (helium), pressure-fed, liquid bipropellant ($N_2O_4$-A50) system with a gimbaled 3,500-pound LEM Ascent engine. Propellants are contained in four spherical tanks having elastomeric bladders; valves are provided to regulate gas and liquid flows and to isolate the system as required; and liquid check valves and trimming orifices are incorporated in outlet lines to prevent propellant migration and minimize unsymmetrical propellant depletion. Table 3.4-2 is a weight breakdown for the subsystem.

Table 3.4-2: PROPULSION SUBSYSTEM WEIGHT

| | Indirect Lander Weight (lb) | Direct Lander Weight (lb) |
|---|---|---|
| Engine Assembly (including valves) | 135 | 135 |
| TVC Gimbal Assembly (excluding actuators) | 39 | 39 |
| Structural Support and Attachments, and Thermal Control | 122 | 96 |
| Propellant Tankage | 161 | 148 |
| Pressurization Tankage | 110 | 95 |
| Propellant and Pressurization Feed System | 62 | 62 |
| Inert Fluids and Helium Gas: | | |
| Trapped Propellant | 82 | 73 |
| Mixture Ratio Allowance | 72 | 64 |
| Helium Gas (Propellant Expulsion and Residual) | 10 | 9 |
| Total Inert Weight | 793 | 721 |
| Minimum Usable Propellant Weight | 3,965 | 3,482 |

*Guidance and Control Subsystem*---The guidance and control subsystem is of conventional design. It too uses existing technology, developed hardware, and selective redundancy. Functionally, it uses celestial references (Sun and Canopus) to establish attitude position and rate during coast periods and an interial reference unit to maintain position and rate during celestial occulations. The inertial reference unit is also used to provide rate outputs during angular maneuvers and to maintain attitude position once an angular maneuver is completed. A linear accelerometer whose output is integrated is used to establish velocity burn termination. These all operate in conjunction with a cold-gas nitrogen reaction control system and a computer sequencer that programs and computes mission events initiation time, attitude maneuvers, and velocity maneuvers. Table 3.4-3 provides physical data for the subsystem.

*Electrical Power Subsystem*---The electrical power subsystem is also of conventional design. It uses solar panels for electrical power generation when in the Sun and nickel cadmium batteries when in the shadow (and for peak loads). Power is supplied to the spacecraft over a voltage range of 22 to 31 volts. A dissipative shunt regulator augmented with solar panel shorting logic provides voltage control for solar illuminations ranging between 130 and 48 watts/ft$^2$.

Table 3.4-3: GUIDANCE AND CONTROL WEIGHT, POWER, AND VOLUME

| Component | Weight (Pounds) | Average Power (Watts) | Volume (Cubic Inches) | Comments |
|---|---|---|---|---|
| Inertial Reference Units | 15.0 | 30 | 600 | Includes accelerometer; gyro and accelerometer off shelf. Develop package. |
| Star Tracker ▷1 | 7.5 | 3.5 | 800 | Canopus---incrementing type. |
| Sun Sensor ▷1 | 2 | | 45 | Fine, coarse, and remote. |
| Reaction Control ▷1 | 52 | Neg | 1,950 | Complete system (includes 17 pounds $N_2$). |
| Gimbal Actuator | 18.5 | ▷3 | | New design. |
| Computer Sequencer ▷2 | 15 | 25 | 1,000 | Includes required guidance and control electronics. |
| Supports | 11 | | | |
| Total Preferred System | 121 | 58.5 | 4,395 | |

▷1 Off Shelf

▷2 Design Available

▷3 Occurs During Engine Burn Only 500 w Max.
250 w Rated

A charge controller, voltage booster, and discharge controller control battery charging and discharging over this same solar illumination range and during shadow operations. Table 3.4-4 gives a weight breakdown for the subsystem.

## Table 3.4-4: POWER SUBSYSTEM WEIGHT AND SIZE

| | Weight (pounds) | Size (square feet) |
|---|---|---|
| Solar Array | 82.0 | 94.3 (net area used for cells) |
| Battery (Ni-Cd) | 44.4 | 102.4 (gross area) |
| Power Control and Distribution | | |
| Charge Controller | 5 | |
| Voltage Booster | 4 | |
| Discharge Control | 4 | |
| Shunt Regulator (2 each) | 6 | |
| Dissipation Unit | 6 | |
| T/M Signal Conditioning | 5 | |
| Solar Array Shorting Logic | 6 | |
| Weight Total | 162.4 | |
| Plus Deployment Mechanisms and Supports | 14 | |
| Total | 176.4 | |

Weights for additional orbiter subsystems--telecommunications, computing and sequencing, pyrotechnics, temperature control, and electrical cabling--are given in Table 3.4-5. Each of these weights is for a subsystem using present-day technology and/or available hardware.

## Table 3.4-5: ADDITIONAL SUBSYSTEM WEIGHTS

| Subsystem | Weight (lb) | Remarks |
|---|---|---|
| Telecommunications | 192 | Includes Radio, Telemetry, Data Storage, & Antennas<br>Two 10W TWTA's; 6 ft. dia high gain & 3 ft. dia relay antennas<br>Provides $3.5 \times 10^9$ bits in 10 days over a $2.3 \times 10^8$ Km range<br>Empirical fit to available data. |
| Temperature Control | 94 | Includes radiator plates & passive control components (coatings, insulation, & louvers). Empirical fit to available data. |
| Cabling | 140 | Includes wire, coax, connectors, & supports. Empirical fit to available data. |
| Pyrotechnics | 13 | Includes 9 lb for pyrotechnic devices & 4 lb for switching circuits. |
| Computing & Sequencing | 15 | Includes 3 lb for attitude control electronics & 12 lb for a 120 input-output programmer. |
| Useful Orbiter Structure | 132 | Determined from preliminary analysis of Model 971-105 & 971-106 configurations. |

### 3.4.4 Refined Configurations and Mission Analysis

From the preceding data, a NASA-Boeing team established design conditions for conducting refined configuration and mission analyses. Of these, the most significant were:

- Launch Date = 1973
- Type I Trajectory
- Variable Arrival Date
- 24.6-hour, 1,000-kilometer Periapsis Altitude Mars Orbit
- 20-degree Apsidal Rotation
- 20-day Launch Period
- Short Holding Orbit
- Engine Thrust = 3,500 pounds
- ΔV Allowance = 125 m/sec
- Separated Spacecraft Weight = 7,000 pounds
- Orbiter Science = 200 pounds

They were used to establish both indirect (out of orbit lander) and direct (lander deployed before Mars arrival) lander performance, configurations, weights, and costs.

*Performance and Mission Analysis*---Table 3.4-6 summarizes mission velocity requirements for the best 20-day variable arrival date launch period in 1973. The ΔV's shown include trans-Mars injection maneuver losses that consist of finite burn effects for both the transtage and spacecraft, and the 4-minute coast time penalties associated with a preferred engine-up configuration. From these, the largest total mission ΔV (2.498 km/sec) established the mission energy design point for determining powered spacecraft performance. Additional ΔV capability is therefore available for other launch-arrival date combinations in the 20-day launch period.

Table 3.4-6: MISSION VELOCITY REQUIREMENTS

| Launch Date (1973) | Arrival Date (1974) | Trip Time (days) | Injection $C_3$ ($km^2/sec^2$) | Arrival $V_\infty$ (km/sec) | Impulsive Spacecraft-Assist ΔV (km/sec)[1] | Trans-Mars Injection ΔV Loss (km/sec)[2] | Orbit Insertion ΔV (km/sec)[3] | Total Mission ΔV (km/sec)[4] |
|---|---|---|---|---|---|---|---|---|
| July 29 | Feb. 23 | 209 | 14.925 | 2.754 | 1.145 | 0.081 | 1.143 | 2.494 |
| Aug. 2 | Feb. 28 | 210 | 15.072 | 2.671 | 1.151 | 0.081 | 1.099 | 2.456 |
| Aug. 7 | Mar. 6 | 211 | 15.660 | 2.580 | 1.176 | 0.084 | 1.053 | 2.438 |
| Aug. 12 | Mar. 12 | 212 | 16.758 | 2.504 | 1.223 | 0.088 | 1.015 | 2.451 |
| Aug. 17 | Mar. 17 | 212 | 18.386 | 2.450 | 1.292 | 0.093 | 0.988 | 2.498 |

[1] Spacecraft weight = 7,000 pounds

[2] Assumes 4-minute coast between transtage final cutoff and spacecraft ignition

[3] Mars orbit definition: Periapsis altitude = 1,000 kilometers
Period = 24.6 hours
Apsidal rotation = 20 degrees

[4] Includes midcourse and orbit trim allowance of 125 m/sec

In addition to mission energies, both nonuseful weight versus usable propellant, and useful in-orbit weight versus separated spacecraft weight, were required before capsule plus orbiter science capability could be established. Refined nonuseful weights are shown in Figure 3.4-19 for a 3,500-pound-thrust propulsion module. The reduction in nonuseful weights form those used in the preliminary sizing study (Figure 3.4-9) are a result of the final configurations, subsystems, and structural concepts selected. Useful in-orbit weight,

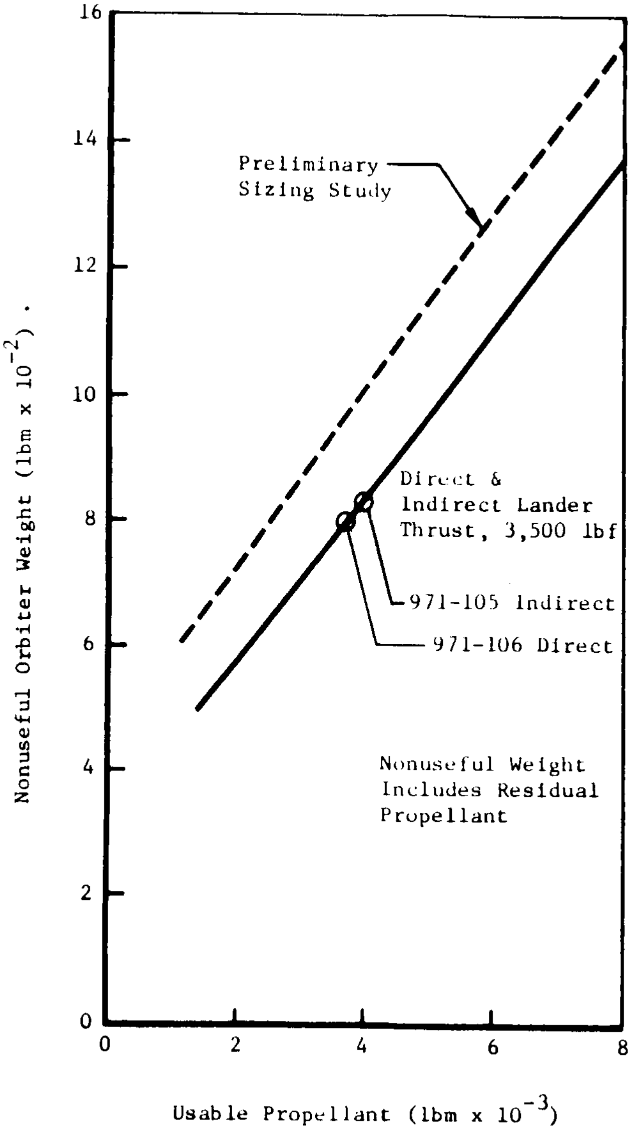

Figure 3.4-19: REFINED NONUSEFUL ORBITER WEIGHT

Figure 3.4-20, was determined through detail analyses of the propulsion, guidance and control, electrical power, and structural subsystems, and by using parametric weights data for telecommunications, computing and sequencing, pyrotechnics, temperature control, and electrical cabling.

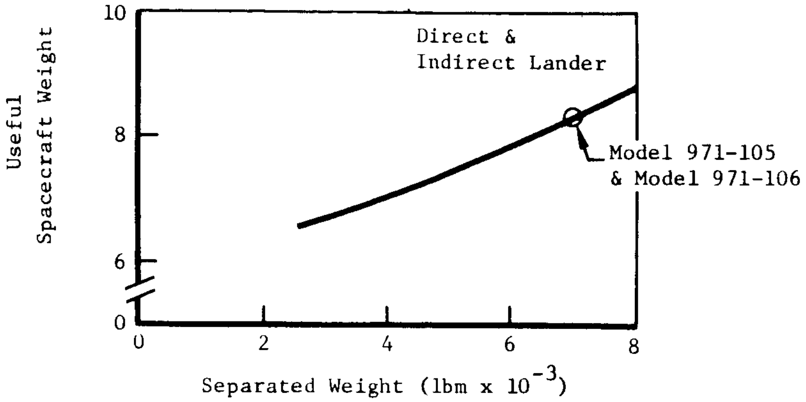

Figure 3.4-20: USEFUL SPACECRAFT WEIGHT

The combination of mission requirements, useful in-orbit weight, nonuseful weight, and the 3,500-pound LEM Ascent engine ($I_{sp}$ = 305), resulted in the capsule capability of Figure 3.4-21 for the indirect lander and of Figure

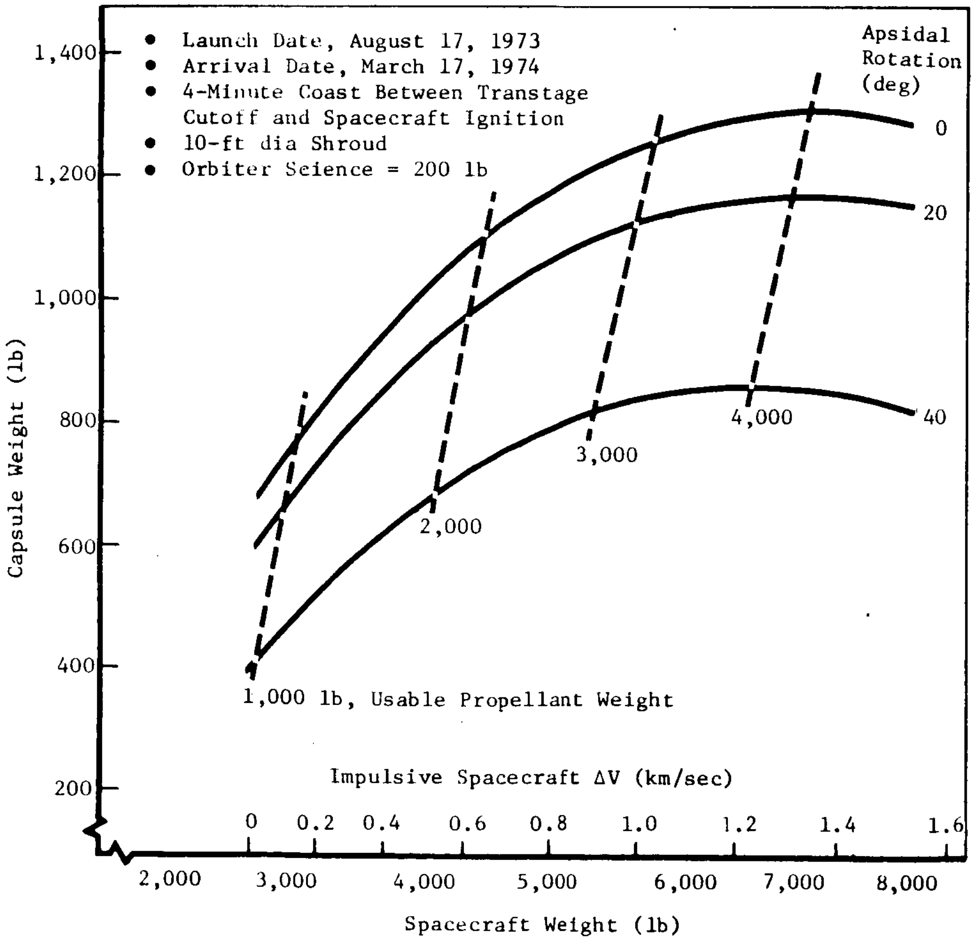

Figure 3.4-21: CAPSULE PLUS SCIENCE WEIGHTS---INDIRECT ENTRY

3.4-22 for the direct lander. The useful in-orbit weight for the indirect lander is shown in Figure 3.4-23. For the nominal mission (20-degree apsidal rotation) and a 7,000-pound separated spacecraft, an indirect lander capsule of about 1,146 pounds (usable propellant = 3,965 pounds) and a direct lander capsule of about 1,700 pounds (usable propellant = 3,482 pounds) results. For both cases, the orbiter science payload is 200 pounds.

Though the increased performance capability of the powered spacecraft over a nonpowered spacecraft is desirable, a performance judgment as to its suitability to Mars missions was deferred until an operational assessment was made. This is necessary because the powered spacecraft employs a critical operation, spacecraft engine burn, to achieve a trans-Mars trajectory.

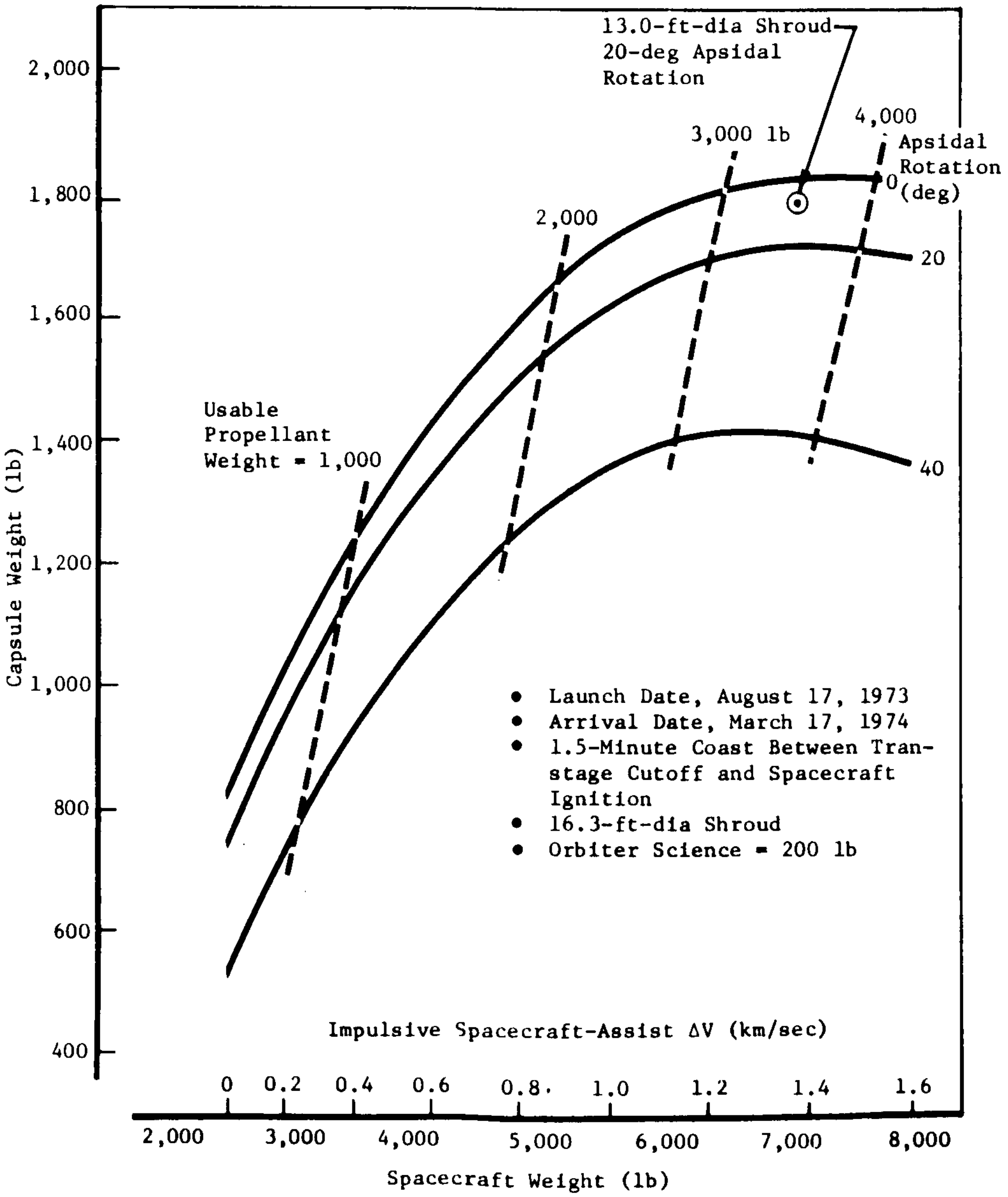

- Launch Date, August 17, 1973
- Arrival Date, March 17, 1974
- 1.5-Minute Coast Between Transtage Cutoff and Spacecraft Ignition
- 16.3-ft-dia Shroud
- Orbiter Science = 200 lb

Figure 3.4-22: CAPSULE PLUS SCIENCE WEIGHTS---DIRECT ENTRY

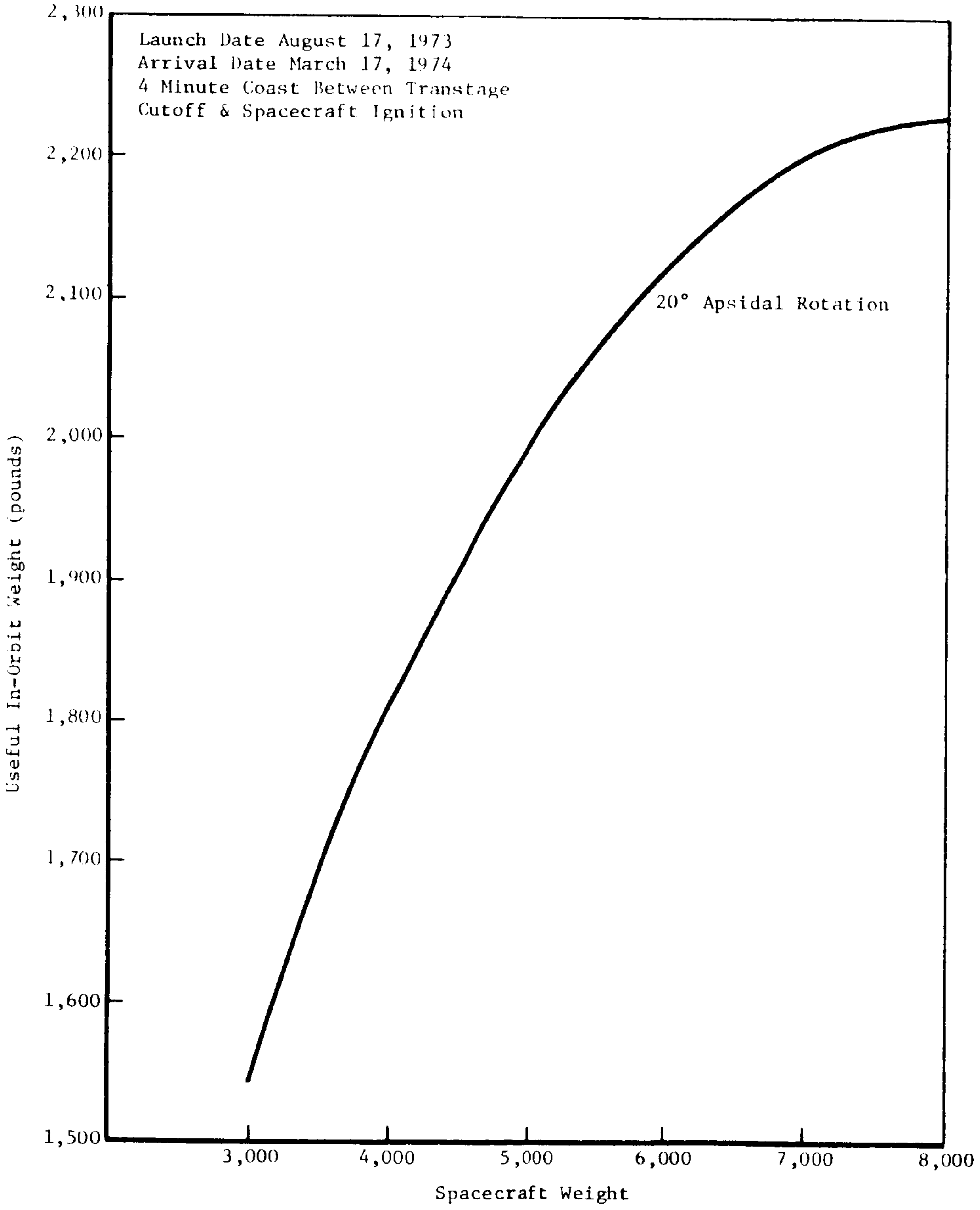

Figure 3.4-23: USEFUL IN-ORBIT WEIGHT---INDIRECT ENTRY

Figure 3.4-24 shows a typical event sequence from prelaunch to spacecraft Sun acquisition. Though no command capability is available during this sequence, a stored program within the computer and sequencer can readily handle the events shown. Engineering telemetry during the critical spacecraft burn will be available in real time if receiving stations are in view and the travelling wave tube amplifier (TWTA) can be turned on during velocity burn. If either of these conditions do not exist, then this telemetry will have to be tape stored and read out in nonreal time. An examination of tracking station view periods for an August 17, 1973 launch date, Figures 3.4-25 and -26, shows that tracking coverage for real-time telemetry during the entire trans-Mars injection maneuver can be readily obtained by using one or two tracking ships to fill in the regions where no DSIF coverage exists. Similar results would be true for other launch days. Therefore, real-time telemetry will be available unless a TWTA hardware problem exists.

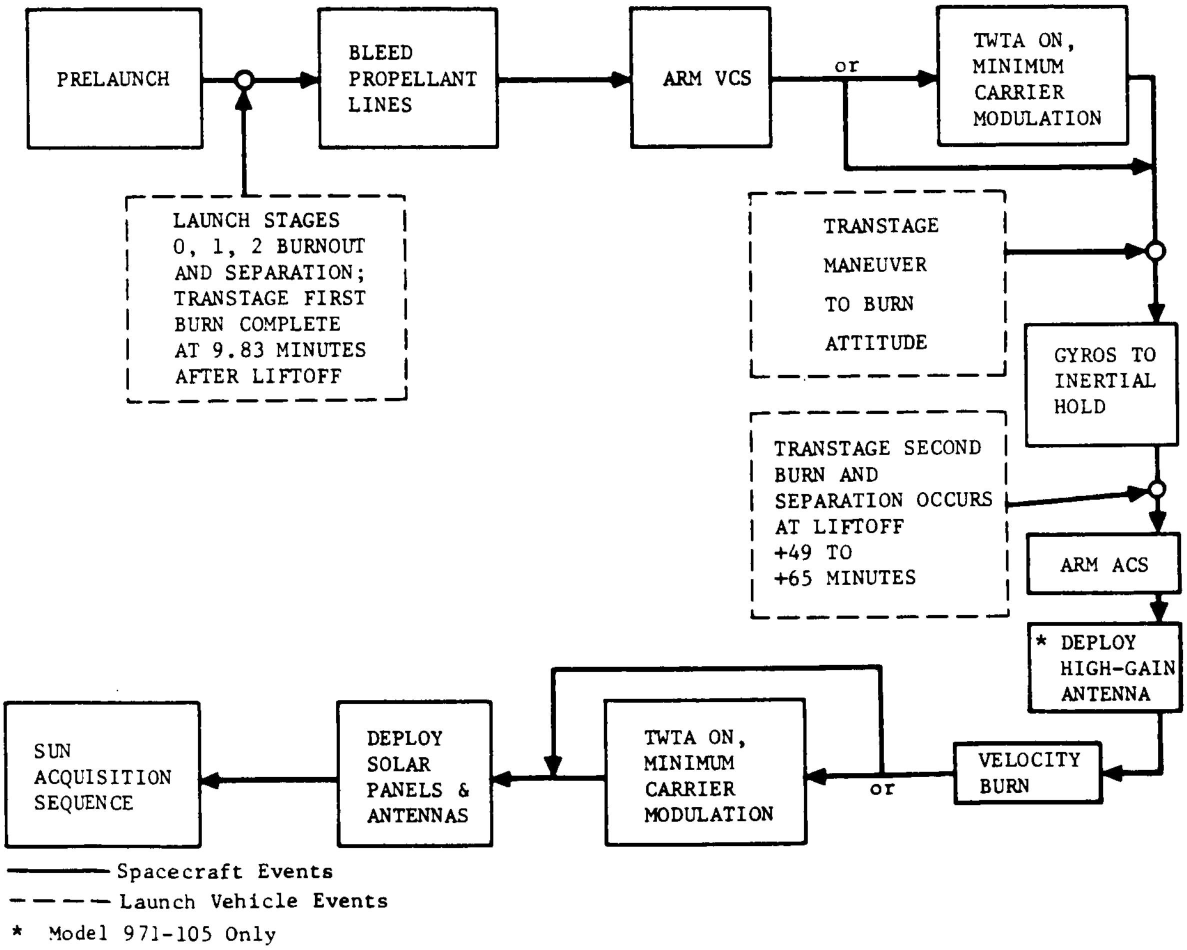
PRELAUNCH
BLEED PROPELLANT LINES
ARM VCS
or
TWTA ON, MINIMUM CARRIER MODULATION
LAUNCH STAGES 0, 1, 2 BURNOUT AND SEPARATION; TRANSTAGE FIRST BURN COMPLETE AT 9.83 MINUTES AFTER LIFTOFF
TRANSTAGE MANEUVER TO BURN ATTITUDE
GYROS TO INERTIAL HOLD
TRANSTAGE SECOND BURN AND SEPARATION OCCURS AT LIFTOFF +49 TO +65 MINUTES
ARM ACS
* DEPLOY HIGH-GAIN ANTENNA
VELOCITY BURN
or
TWTA ON, MINIMUM CARRIER MODULATION
DEPLOY SOLAR PANELS & ANTENNAS
SUN ACQUISITION SEQUENCE
Spacecraft Events
Launch Vehicle Events
* Model 971-105 Only

Figure 3.4-24: EVENT SEQUENCE --- SHORT HOLDING ORBIT

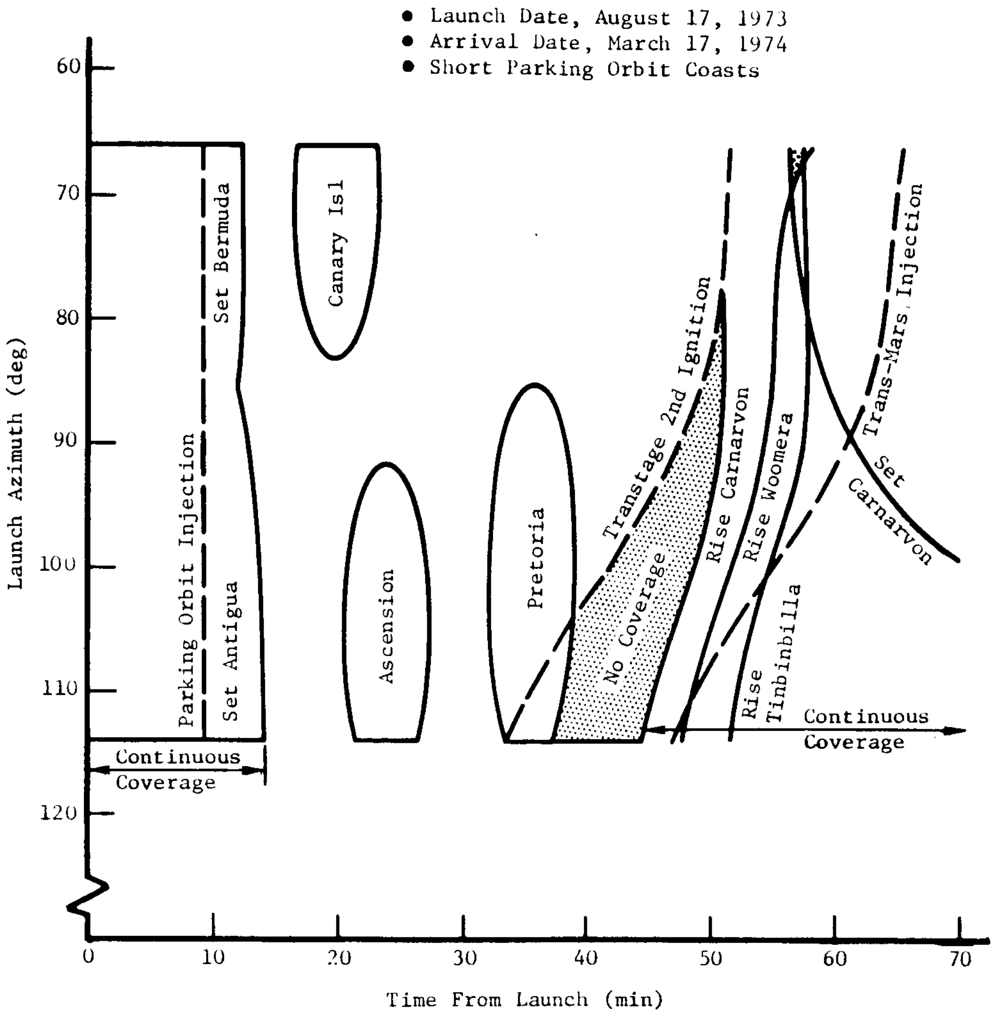
- Launch Date, August 17, 1973
- Arrival Date, March 17, 1974
- Short Parking Orbit Coasts

Figure 3.4-25: TRACKING STATION COVERAGE---
LAUNCH PHASE---SHORT PARKING ORBIT COAST

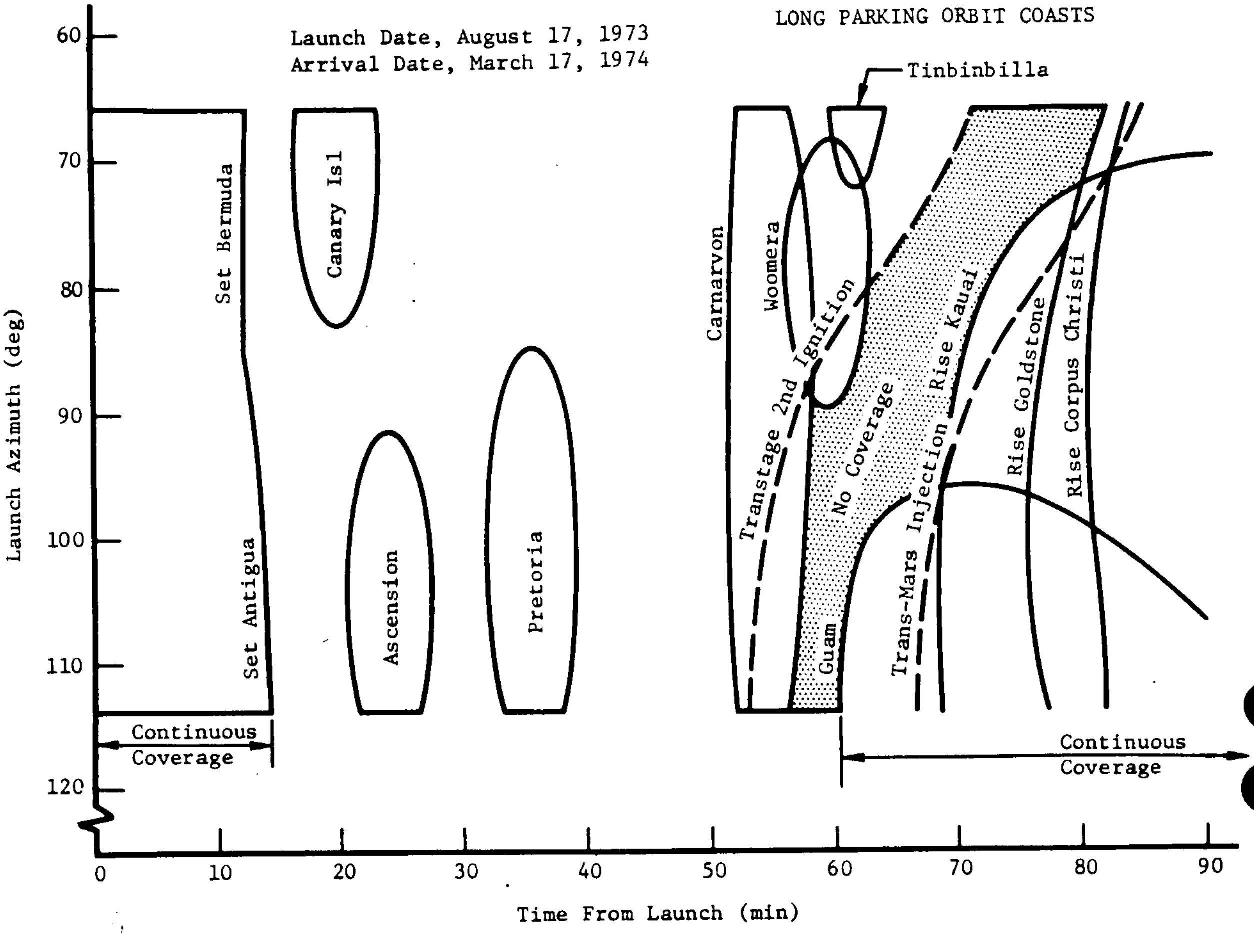

Figure 3.4-26:

TRACKING STATION COVERAGE---LAUNCH PHASE---LONG PARKING ORBIT COAST

The results of the performance payload and operational analysis leads to the conclusion that a powered spacecraft can provide considerably greater payloads to Mars orbit than a nonpowered spacecraft with no undue operational uncertainty or complexity.

*Configurations*---The design parameters used for spacecraft configuration development are shown in Table 3.4-7. These resulted from the various preceding parametric studies and data supplied by NASA-Langley before the refined configuration and mission analyses studies. Shown flight capsule weights are not indicative of actual performance. They were the values used for structural design only. With this data an indirect lander, Boeing Model 971-105, and a direct lander, Boeing Model 971-106, were configured.

Model 971-105 is shown in both its launch and space configuration in Figures 3.4-27 and -28. The vehicle is composed of an octagonal box body, an external engine support truss, and a capsule and propellant tank internal support truss. All orbiter equipment is plate-mounted on four of the eight faces of the body sides. The body top provides the mounting surface for the solar panels, main

Table 3.4-7: DESIGN PARAMETERS

| | Indirect Lander Entry | Direct Lander Entry |
|---|---|---|
| Launch Vehicle | Titan IIIC | Titan IIIC |
| Shroud Diameter (ft) | 10 | 16.33 |
| Shroud Weight (lb) | Variable | 4,525 |
| Capsule Diameter and Length (in.) | 102 x 60 | 178 x 104 |
| Capsule Weight (lb) | 1,500 | 2,000 |
| Separated Spacecraft Weight (lb) | 7,000 | 7,000 |
| Orbiter Engine Thrust (lb) | 3,500 | 3,500 |
| Propellant Weight (lb) | 4,119 | 3,619 |
| Propulsion System Type | Modular | Modular |
| Pressurant Weight and Type | 10 lb, Helium | 9 lb, Helium |
| ACS Propellant and Type | 18 lb, Nitrogen | 18 lb, Nitrogen |
| Solar Panel Area (sq ft) | 100 | 100 |
| High-Gain Antenna and Type | 72 in., Parabolic | 72 in., Parabolic |
| Capsule Antenna and Type | 36 in., Parabolic | 36 in., Parabolic |
| Omnidirectional Antenna and Type | 8 in., Biconical | 8 in., Biconical |
| Micrometeroid Protection | None | None |

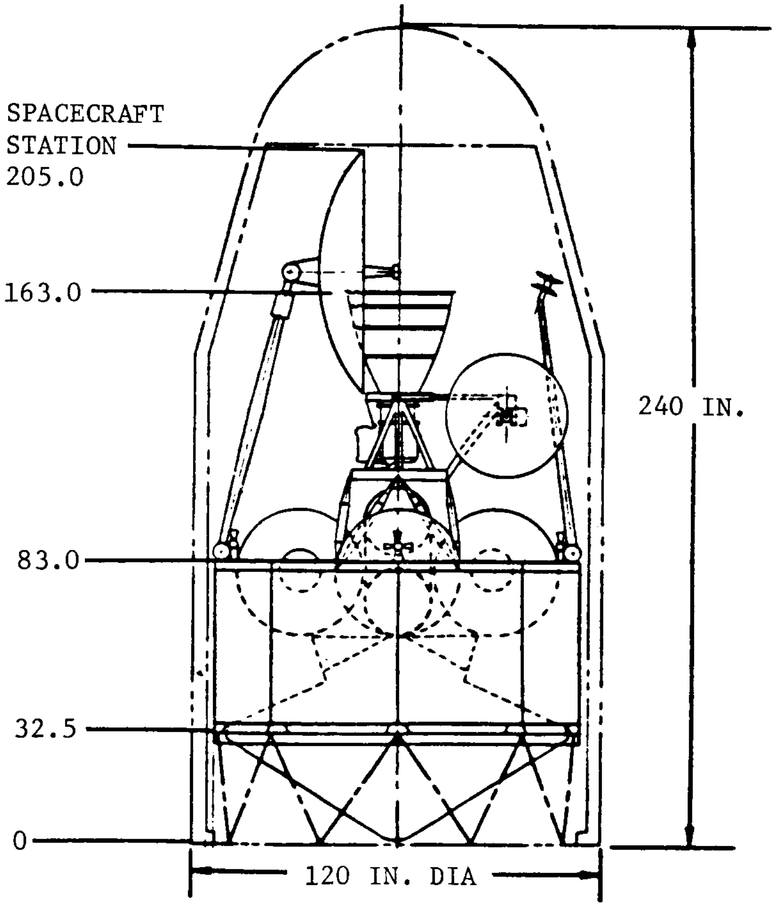

Figure 3.4-27: MODEL 971-105 LAUNCH CONFIGURATION

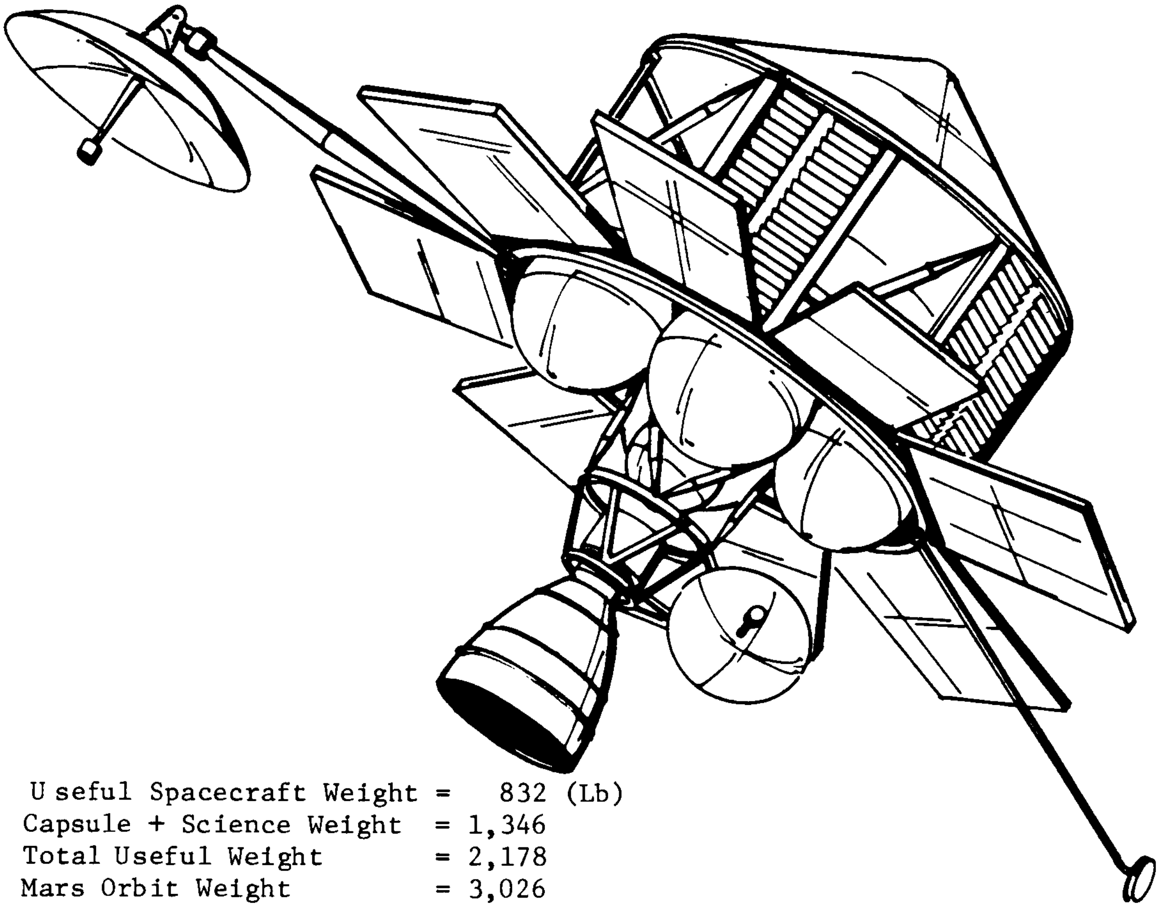

Useful Spacecraft Weight = 832 (Lb)
Capsule + Science Weight = 1,346
Total Useful Weight = 2,178
Mars Orbit Weight = 3,026

Figure 3.4-28: MODEL 971-105 SPACE CONFIGURATION

Table 3.4-8: MODEL 971-105 WEIGHTS

| | Useful | Non-Useful | Total |
|---|---|---|---|
| Orbiter Less Science (Dry) | 831 | 676 | 1,507 |
| Capsule<br>Science (Orbiter) | 1,146<br>200 | | 1,146<br>200 |
| In-Orbit Dry Weight | (2,177) | (676) | (2,853) |
| Residual Propellant | | 154 | 154 |
| ACS Gas-In Orbit | | 9 | 9 |
| Pressurization Gas | | 10 | 10 |
| In-Orbit Weight | (2,177) | (849) | (3,026) |
| Transplanet ACS Gas | | 9 | 9 |
| Usable Propellant | | 3,965 | 3,965 |
| Spacecraft Separated Weight | (2,177) | (4,823) | (7,000) |

propellant tanks, helium pressurant tanks, attitude control thrusters, nitrogen tank, omnidirectional antenna, and high-gain antenna. The lander relay antenna is located on a tripod mounted to the external engine support truss. An engine-up launch configuration is used because the diameter limitations of the Titan IIIC shroud and the propellant volume combine to force the deployable components toward one end of the vehicle. Because it is structurally desirable to mount the heavier elements of the spacecraft (orbiter structure, flight capsule, and propellant) closest to the spacecraft support plane, both the engine and the deployables must then be placed furthest from this plane. This structural advantage is the reason for an engine-up configuration which, though requiring the spacecraft to be inverted before engine ignition, showed an overall performance gain. A weight breakdown for Model 971-105 is given in Table 3.4-8.

Model 971-106 is shown in both its launch and space configuration in Figures 3.4-29 and -30. The vehicle octagonal body and engine support truss is similar to Model 971-105 with the main difference being the elimination of engine support dual tripods and capsule internal support. The capsule is now mounted directly on the top of the orbiter body. Propellant tank support is provided by four truss members that carry loads from the tanks to the orbiter/capsule interface. Fixed to the body at its base in a deployed condition are the solar array panels supported by diagonal struts. This fixed solar array provides the mounting surface for attitude control thrusters and all deployable components. An engine-down launch configuration is used because adequate space exists for side mounting deployable components and because a structurally efficient adapter to go around the flight capsule and mate with the smaller diameter orbiter was not realizable with the capsule mounted close to the spacecraft/transtage interface plane. A weight breakdown for Model 971-106 is given in Table 3.4-9.

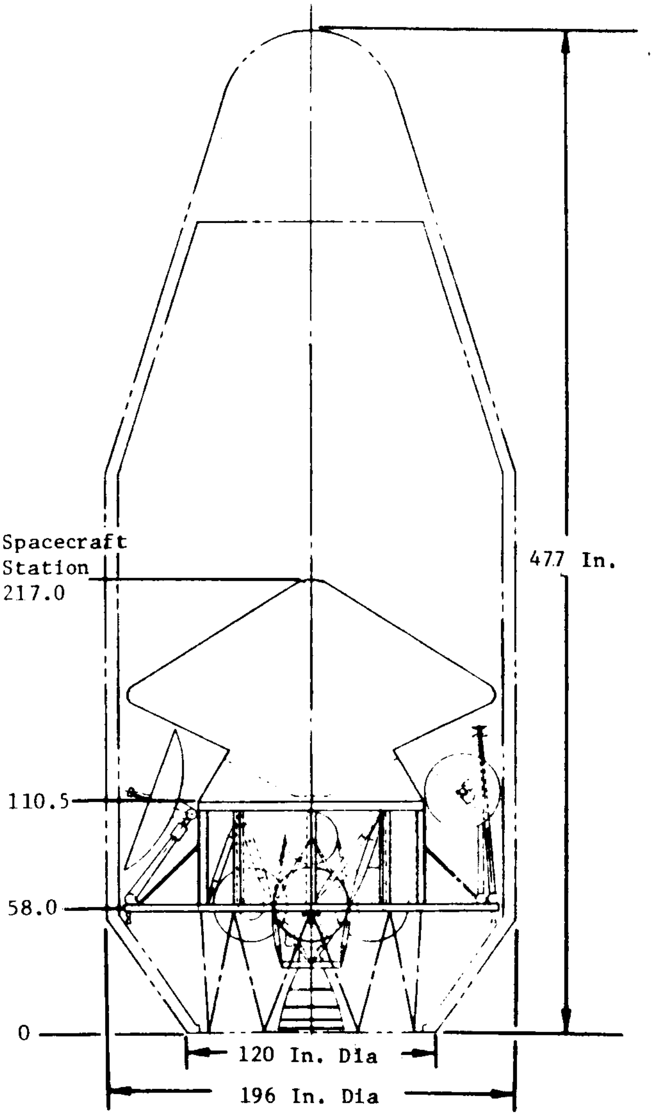

Figure 3.4-29:

MODEL 971-106 LAUNCH CONFIGURATION

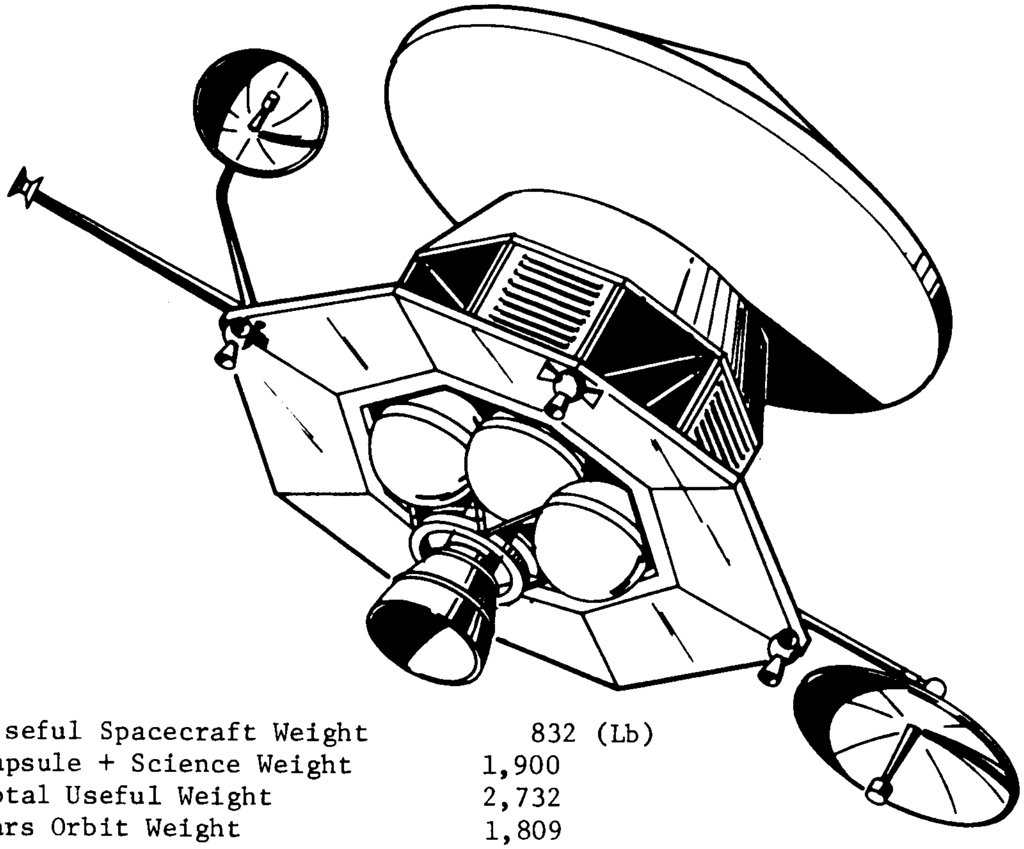

| | |
|---|---|
| Useful Spacecraft Weight | 832 (Lb) |
| Capsule + Science Weight | 1,900 |
| Total Useful Weight | 2,732 |
| Mars Orbit Weight | 1,809 |

Figure 3.4-30: MODEL 971-106 SPACE CONFIGURATION

Table 3.4-9: MODEL 971-106 WEIGHTS

| | Useful | Non-Useful | Total |
|---|---|---|---|
| Orbiter Less Science (Dry) | 832 | 622 | 1,454 |
| Science (Orbiter) | 200 | | 200 |
| In-Orbit Dry Weight | (1,032) | (622) | (1,654) |
| Residual Propellant | | 137 | 137 |
| ACS Gas-In Orbit | | 9 | 9 |
| Pressurization Gas | | 9 | 9 |
| In-Orbit Weight | (1,032) | (777) | (1,809) |
| Transplanet ACS Gas | | 9 | 9 |
| Usable Propellant | | 3,482 | 3,482 |
| Capsule | (1,700) | | (1,700) |
| Spacecraft Separated Weight | (2,732) | (4,268) | (7,000) |

# 4.0 TECHNICAL GUIDELINES

The technical guidelines for the study supplied by NASA in RFP L-8982, *Study of Powered Spacecraft for Mars Missions,* plus additions (*below and under Section 4.4) determined to be necessary for executing the intent of the study, are as follows.

## 4.1 MISSION PARAMETERS

- The analyses shall be directed toward solutions for the 1973 mission opportunity.
- Both Type I and II mission profiles shall be considered.
- The analyses shall be conducted parametrically for total after-injection ΔV requirements of 1.0, 1.5, and 2.0 km/sec that include allowances for midcourse corrections, Mars insertion, and Mars in-orbit maneuvers.
- The analyses shall be conducted to obtain 10-, 20-, and 30-day launch windows.
- "Useful spacecraft weights in Mars orbit" shall be calculated for the selected launch vehicles without spacecraft assist. These results will be used as baseline values in the parametric studies. In addition, the following values of "useful spacecraft weight in Mars orbit," assuming powered spacecraft assist, shall be considered in these studies:
  1) 1,600 pounds
  2) 1,800 pounds
  3) 2,000 pounds
  4) Maximum
- The declination of the departure launch asymptote shall have a value no greater than ±36 degrees.
- *Mars orbits shall be synchronous with a periapsis altitude of 1,000 kilometers, and an apoapsis altitude of ~33,000 kilometers.

## 4.2 SPACECRAFT PARAMETERS

### *Spacecraft Configurations*

- Original configuration concepts shall be generated. These designs shall be limited in detail to that necessary to establish overall spacecraft configuration concepts, pertinent subsystem realistic weights, and other properties necessary for refined evaluations of parameters selected by NASA during the course of the study.
- A goal of this study is that the powered spacecraft be compatible with existing or already under-development 10-foot-diameter Titan shrouds. Should the designs be severely compromised by this constraint, alternate approaches shall be recommended to NASA for concurrence.

- Antennas and solar panel requirements will not be defined by NASA during the course of this study. Size and weight estimates for these items and the appendages that support them shall be made. These estimates shall be used for configuration packaging and structural studies.
- The spacecraft shall be of a modular design so that propulsion and/or guidance systems developed for the 1973 Mars mission may be employed on other missions.

### *Spacecraft Propulsion*

- Only development or in-development engines shall be considered. Environmental conditions imposed on the spacecraft by the engines as well as the effects of mission environments on the engines shall be considered during engine selections. Multiple restart capability and thermal balance should be considered during engine selection. Realistic, attainable specific impulse values for propellants shall be used.

### *Guidance and Control*

- Spacecraft guidance and control concepts, applicable to the powered assist mode of flight, must be compatible with normal mission requirements.
- Spacecraft guidance and control concepts using the launch vehicle as a reference, or Canopus, Sun, or Earth references, or others may be considered.

## 4.3 LAUNCH VEHICLES

Analyses shall be based on use of the Titan IIIC and Titan IIID launch vehicles.

## 4.4 RANGE

- The vehicle shall be launched out of the Eastern Test Range (ETR).
- The Eastern Test Range, the NASA Deep Space Network, and other NASA tracking and data acquisition facilities may be used to support the Mars mission.
- *Range safety regulations shall be observed. A check on stage impact points is required to ensure that a major range safety problem does not exist.

# 5.0 PERFORMANCE AND MISSION ANALYSIS

The objective of the performance and mission analysis was to demonstrate the feasibility of the powered spacecraft concept and to parametrically establish the useful weight delivered to Mars orbit.

The study was scoped to encompass the following parametric analysis:

1) Determination of the nominal performance of both the Titan IIIC and Titan IIID launch vehicles;
2) Examination of the effects of applicable launch vehicle constraints on mission profiles;
3) Determination of the effects of interplanetary trajectory type, launch and arrival date, launch period length, and post-injection $\Delta V$ on separated spacecraft weight and useful weight in Mars orbit;
4) Comparison of attainable useful in-orbit weights as a function of launch vehicle, spacecraft thrust, mission mode, and other spacecraft sizing and mission-dependent parameters;
5) Evaluation of the impact on the powered spacecraft concept on operational parameters such as launch window, tracking and data acquisition, midcourse and orbit determination requirements, and event sequences.

The study involved a parametric analysis of many variables. Because the matrix of combinations was large, it was necessary to systematically select representative values of parameters for use in subsequent phases of the analysis. The flow of these intermediate selections closely followed the study tasks outlined above. After determining launch vehicle performance, a trajectory type was selected and a launch period defined. Selection of a preferred launch vehicle and spacecraft thrust level required consideration of mission-mode effects and subsystem requirements. Finally, the preferred spacecraft was used for the operational studies. In general, spacecraft-assist $\Delta V$ and post-injection $\Delta V$ were carried parametrically throughout the entire study.

A typical interplanetary mission involves the following events:

1) Injection into circular Earth parking orbit;
2) Injection into the desired transplanetary trajectory at the appropriate point in the parking orbit;
3) Heliocentric coast with as many as three midcourse corrections;
4) Injection into the desired Mars orbit;
5) Orbit trim maneuvers where required.

If a capsule is carried, it can be ejected from the spacecraft late in the heliocentric coast or it can be separated after the orbit injection and trim maneuvers are performed. Basically, a powered spacecraft mission is identical to the above. The only difference is that a two-stage maneuver is used for injection onto the interplanetary trajectory. The two stages include the last burn of the final launch vehicle stage and the initial burn of the spacecraft. These burns are separated by a coast phase that represents the period during which the spacecraft is in an elliptical Earth holding orbit. This aspect of the mission is discussed in detail in the section on mission mode selection.

## 5.1 LAUNCH VEHICLE ANALYSES

Launch vehicle performance, trajectory constraints, and empty-case splash points were examined for both the Titan IIIC and IIID to establish payload capability, that the induced dynamic and thermal environment met launch vehicle constraints, and that empty stages did not impact major land areas.

### 5.1.1 Performance

Launch vehicle payload capabilities for the 15-to-1 expansion ratio Titan IIIC and Titan IIID are shown in Figure 5.1-1 as a function of inertial velocity at a 100 n mi altitude. The launch vehicle characteristics used to simulate the trajectories are given in Reference 1. The launch vehicle payload is defined as the net payload plus the spacecraft adapter (see Appendix A3) and support equipment. The payload data shown in Figure 5.1-1 are based on the following assumptions:

1) Launch azimuth = 66 degrees; launch site is AFETR (Pad P-40).
2) Both the Titan IIIC and IIID trajectories attain circular satellite conditions at a 100 n mi altitude.
3) No velocity losses are included after circular satellite conditions have been attained.
4) Both launch vehicles retain reserve propellants in the last stage that correspond to an RSS of 2.5% of the ideal velocity increments of all stages.
5) The jettisoned payload fairing (shroud) weights vary with the launch vehicle payload in the following manner:

| Launch Vehicle Payload (pounds) | Payload Fairing Weight (pounds) |
|---|---|
| 0 to 2,500 | 1,213 |
| 2,501 to 7,500 | 1,440 |
| 7,501 to 15,000 | 1,668 |
| 15,001 to 25,000 | 1,896 |
| 25.001 to 31,000 | 2,143 |

6) U.S. Standard Atmosphere, 1962, is used.

Figure 5.1-2 shows the burnout altitude effect on Titan IIID burnout velocity capability for 10,000-pound payload. Assumptions similar to the preceding are used except the last stage burnout occurs at zero flight-path angle at the specified altitude. Figure 5.1-2 shows that increasing the Titan IIID burnout altitude from 100 to 200 n mi decreases the burnout velocity by 850 m/sec. This corresponds to an approximate payload capability reduction from 10,000 to 6,000 pounds at a burnout velocity of 9.75 km/sec. However, note that some

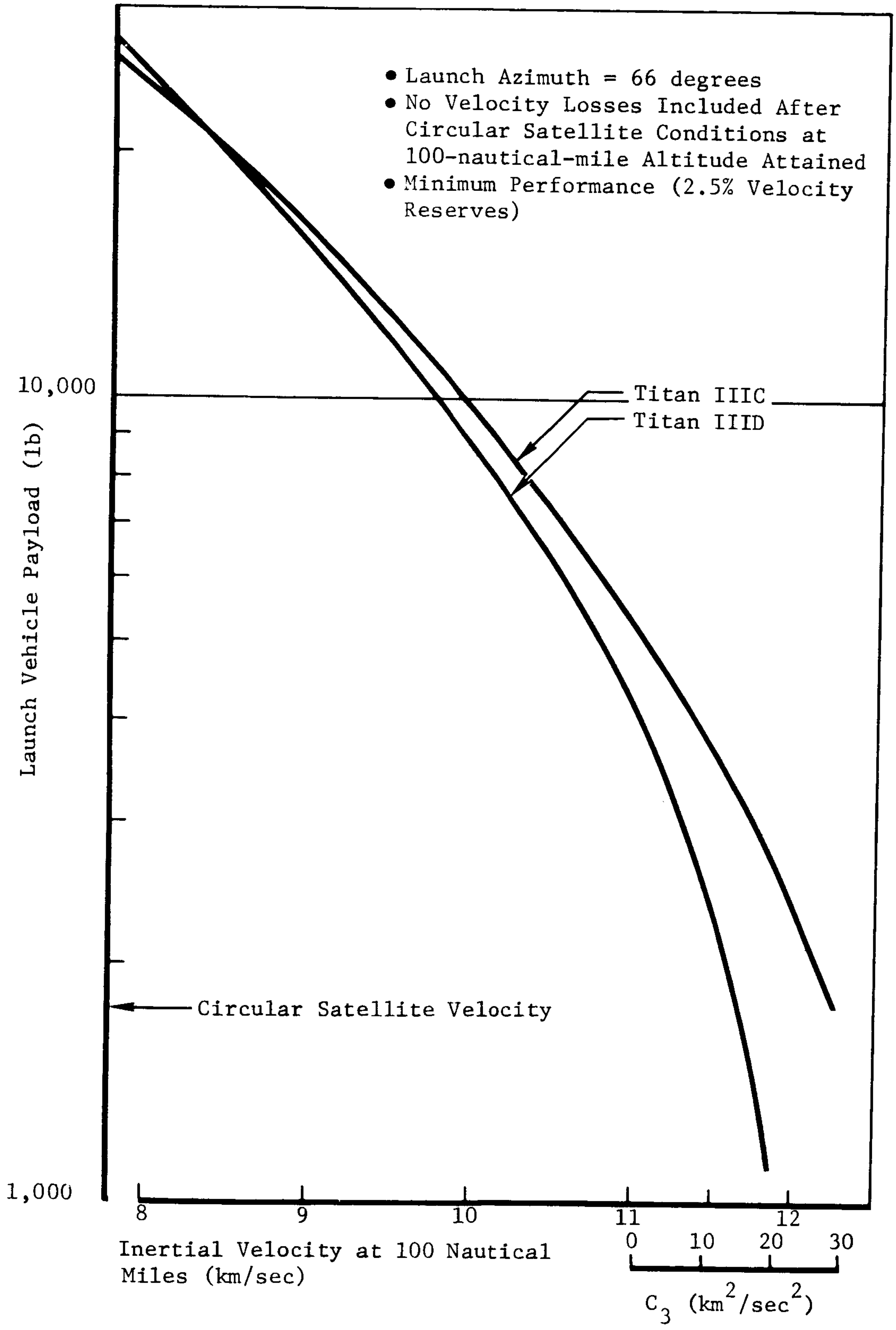

Figure 5.1-1: LAUNCH VEHICLE PAYLOAD CAPABILITIES

- Titan IIID
- Payload Weight = 10,000 lb
- Burnout Flight Path Angle = 0 degree
- Minimum Performance (2.5% Velocity Reserves)

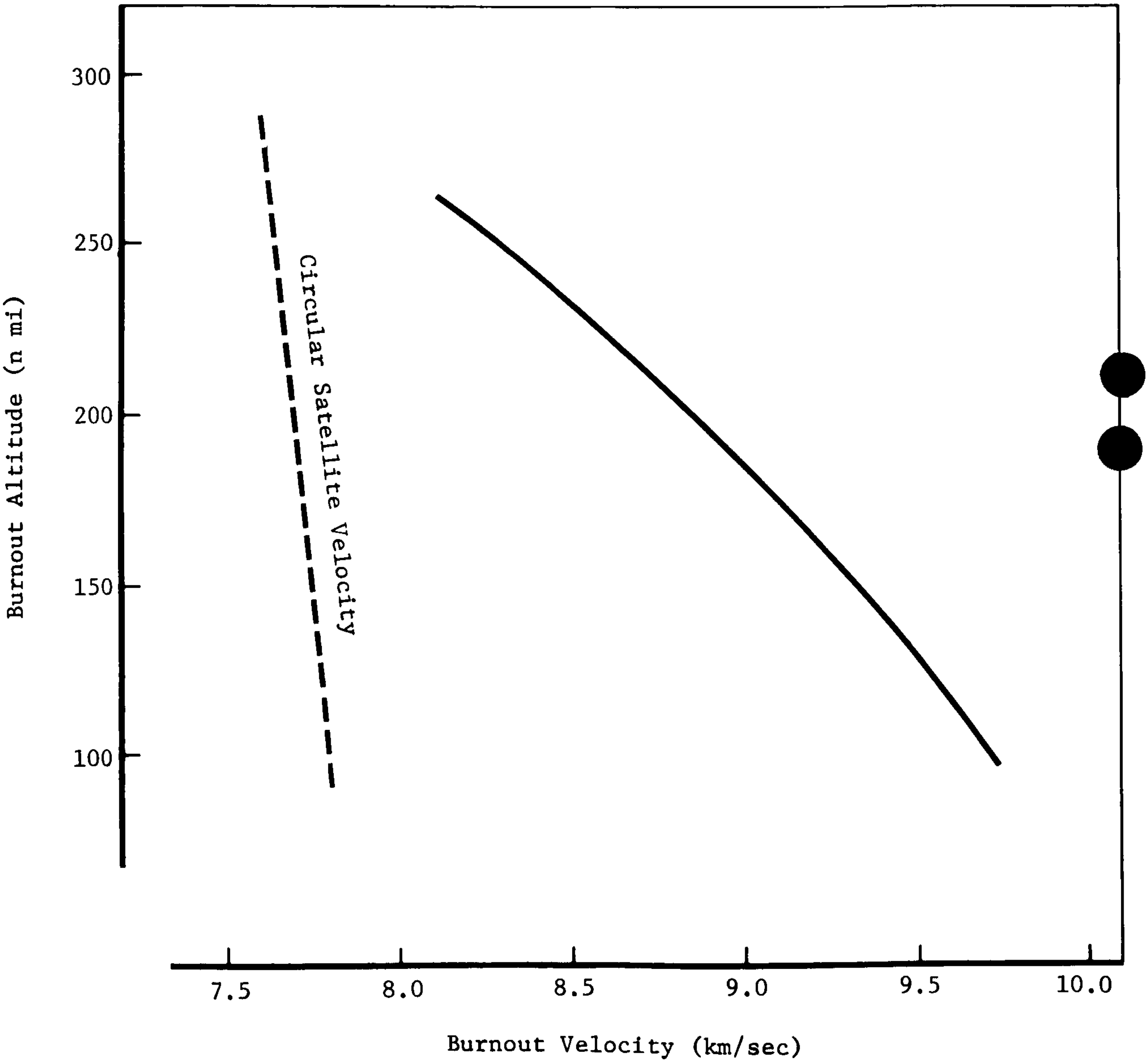

Figure 5.1-2: BURNOUT ALTITUDE EFFECT ON BURNOUT VELOCITY

reduction in the off-perigee injection ΔV losses incurred with Titan IIID will result from higher perigee altitudes. These effects are discussed in Section 5.5.2.

Figures 5.1-1 and 5.1-2 show burnout velocity capabilities for a 66-degree launch azimuth. Similar velocities are obtained at 114 degrees, but launching at azimuths between these limits yields higher burnout velocities. Launching at 90 degrees results in an increase of approximately 35 m/sec in both the Titan IIIC and IIID burnout velocities. This results in an approximate payload increase of 300 pounds at a burnout velocity of 10 km/sec.

The trajectory simulations employ a vertical rise for 20 seconds followed by an instantaneous tilt. Following the tilt maneuver, the vehicle flies a gravity turn trajectory (zero angle of attack) until the dynamic pressure has decreased to 10 psf. Then the vehicle maintains a constant angle of attack until burnout. The tilt angle and the constant angle of attack values are control parameters uniquely determined to satisfy specified end conditions. Two sets of end conditions are used. For injection into a circular orbit altitude, velocity and flight-path angle are specified. When a circular parking orbit is not assumed, burnout altitude, flight-path angle, and time are specified.

The instantaneous tilt maneuver is an approximation of an actual tilt maneuver performed at a finite rate. Such an instantaneous maneuver is a convenient tool for simulating the approximate trajectory of a point mass vehicle. Previous studies have shown that the use of an instantaneous tilt angle has a negligible effect on the subsequent trajectory characteristics and the launch vehicle payload.

### 5.1.2 Trajectory Constraints

Reference 1 lists various constraints that the trajectories must observe. Table 5.1-1 shows that the Titan IIIC and IIID nominal trajectories observe all these constraints for the range of payloads investigated.

### 5.1.3 Empty Stage Splash Points

Impact points have been computed for empty stages of the Titan IIIC and IIID launch vehicles flying nominal trajectories. The entire range of payload weights and launch azimuths under consideration were studied.

Figures 5.1-3 and 5.1-4 show the various empty stage impact points for Titan IIIC and IIID, respectively. Core Stage 2 of Titan IIIC impacts on or near the west coast of northern Africa when the launch azimuths are less than 93 degrees and payloads are less than 6,000 pounds. Because the powered spacecraft weights are generally greater than 6,000 pounds, mission design will not be constrained by consideration of impact on Africa.

For both launch vehicles a launch azimuth of 114 degrees causes the solid rocket motors to impact near the Bahamas. For Titan IIIC, a launch azimuth of 72 degrees causes the Core 1 stage and the standard payload fairing to impact near Bermuda. However, to realistically determine the probabilities

Table 5.1-1: LAUNCH VEHICLE TRAJECTORY CONSTRAINTS

| Launch Vehicle | Payload (lb) | Maximum Dynamic Pressure (psf) | Maximum Heat Integral (ft-lb/ft$^2$) | At Stage 0 Separation |  |  | At Core Stage 1 Separation |  |  | Minimum Transtage Burn Time (sec) |
|---|---|---|---|---|---|---|---|---|---|---|
|  |  |  |  | q (psf) | α (deg) | q α (lb-deg/ft$^2$) | q (psf) | α (deg) | q α (lb-deg/(ft$^2$) | |
| Constraints |  | 900 | $95 \times 10^6$ | 180 | 4 | 360 | 30 | 15 | 360 | 20 |
| Titan IIIC | 5,000 | 806 | $70.6 \times 10^6$ | 18 | 0.0 | 0.0 | 0.001 | 2.80 | 0.0 | 49 |
|  | 7,000 | 806 | $71.2 \times 10^6$ | 19 | 0.0 | 0.0 | 0.001 | 3.56 | 0.0 | 79 |
|  | 10,000 | 806 | $72.6 \times 10^6$ | 22 | 0.0 | 0.0 | 0.001 | 4.95 | 0.0 | 125 |
|  | 15,000 | 806 | $76.2 \times 10^6$ | 27 | 0.0 | 0.0 | 0.002 | 7.78 | 0.0 | 202 |
|  | 19,000 | 807 | $80.1 \times 10^6$ | 34 | 0.0 | 0.0 | 0.007 | 10.62 | 0.1 | 164 * |
|  | 24,000 | 809 | $86.3 \times 10^6$ | 44 | 0.0 | 0.0 | 0.034 | 14.98 | 0.5 | 69 * |
| Titan IIID | 5,000 | 838 | $69.6 \times 10^6$ | 12 | 0.0 | 0.0 | 0.0004 | -3.3 | 0.0 | -- |
|  | 7,000 | 836 | $69.7 \times 10^6$ | 12 | 0.0 | 0.0 | 0.0004 | -2.8 | 0.0 | -- |
|  | 10,000 | 832 | $69.8 \times 10^6$ | 13 | 0.0 | 0.0 | 0.0004 | -2.2 | 0.0 | -- |
|  | 15,000 | 827 | $69.9 \times 10^6$ | 14 | 0.0 | 0.0 | 0.0005 | -1.1 | 0.0 | -- |
|  | 19,000 | 821 | $70.0 \times 10^6$ | 15 | 0.0 | 0.0 | 0.0005 | -0.3 | 0.0 | -- |
|  | 24,000 | 815 | $70.0 \times 10^6$ | 16 | 0.0 | 0.0 | 0.0006 | 0.8 | 0.0 | -- |

* Second transtage burn

- Burnout at 100-n-mi circular satellite conditions
- Gravity turn until q decreases to 10 psf

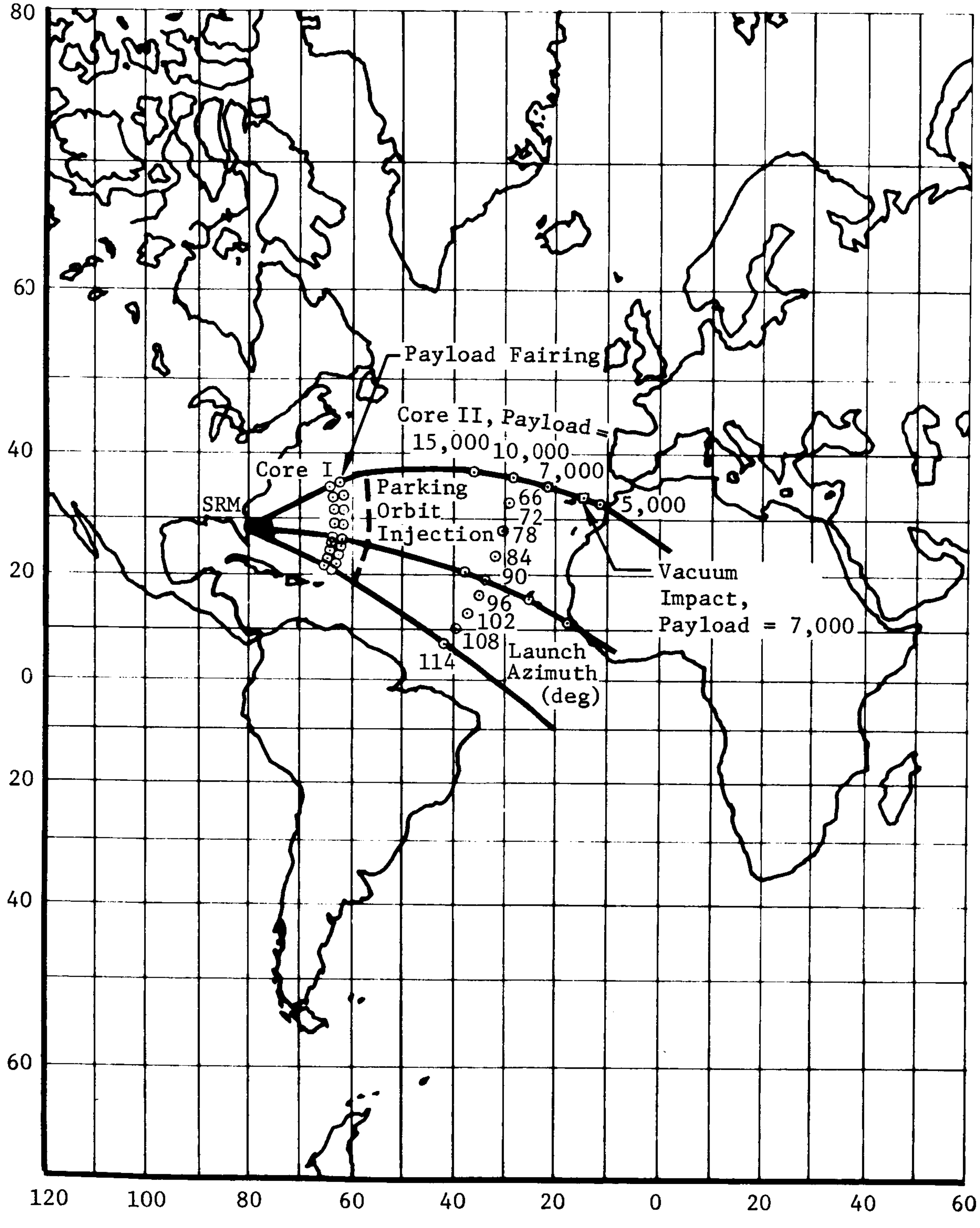
Payload Fairing
Core II, Payload =
15,000
10,000
7,000
5,000
Core I
SRM
Parking Orbit Injection
66
72
78
84
90
96
102
108
114
Vacuum Impact, Payload = 7,000
Launch Azimuth (deg)
80
60
40
20
0
20
40
60
120
100
80
60
40
20
0
20
40
60

Figure 5.1-3: EMPTY STAGE SPLASH POINTS---TITAN IIIC

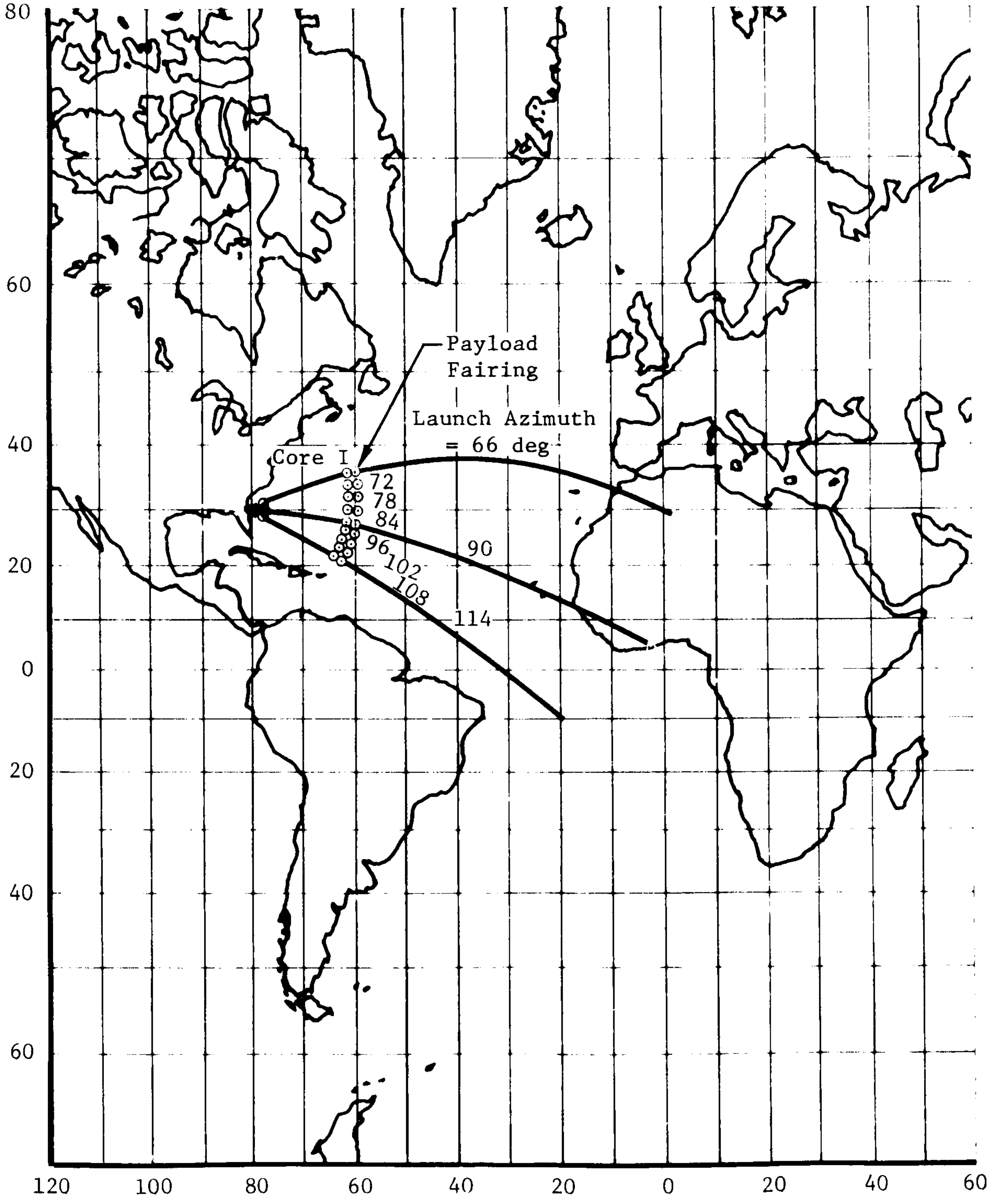
80
60
40
20
0
20
40
60
120
100
80
60
40
20
0
20
40
60
Payload Fairing
Launch Azimuth = 66 deg
Core I
72
78
84
90
96
102
108
114

Figure 5.1-4: EMPTY STAGE SPLASH POINTS---TITAN IIID

of hitting the various land masses, off-nominal ascent trajectories must be investigated and more precise trajectories must be generated for the various entering pieces. Note that the problem of stage impact on land masses within the ETR is common to any orbital mission and not peculiar to the powered spacecraft concept.

The aerodynamic data assumed for the various entering stages are shown in Appendix A1.

## 5.2 PRELIMINARY SPACECRAFT AND PROPULSION SIZING

Preliminary spacecraft and propulsion sizing in support of the parametric performance and mission analysis studies was performed to determine the "nonuseful" spacecraft weight as defined by the standard space vehicle terminology shown in Section 2.0. The difference between total spacecraft weight and nonuseful weight provided the resultant useful weight in Mars orbit.

### 5.2.1 Nonuseful Weight

Nonuseful weight is defined for this study as:

1) Orbiter propulsion system including its fuel pressurant gas and hardware;
2) The orbiter reaction control gas supply system;
3) That portion of the orbiter structure used to support and attach the propulsion and attitude control system.

A preliminary configuration concept, as shown below, was defined as representative of the powered spacecraft propulsion system design. Propellant loading was varied from 2,000 to 15,000 pounds with engine thrust varying from 300 to 3,500 pounds. Nonuseful inert weight was determined analytically and empirically for the following elements:

Propulsion Subsystem

- Propellant Tanks and Support (including expulsion)
- Pressurization Tanks and Support
- Pressurization and Propellant Feed System
- Pressurization Gas (Nitrogen)
- Engine and Attachments

Propulsion Support Structure and Tank Temperature Control

- Upper Deck
- Lower Deck
- Insulation, Paint, Engine Heat Shield

Attitude Control System

- Tankage and Support
- Plumbing
- Thrusters
- Gas ($N_2$)

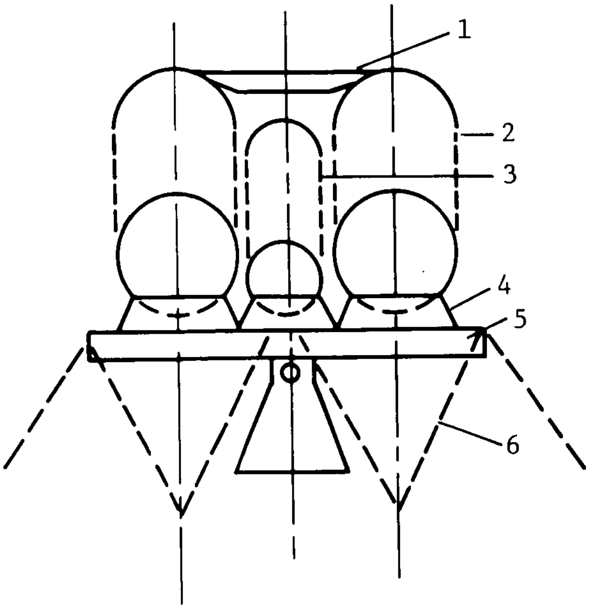

1 Upper Deck
2 Propellant Tanks
3 Pressurization Tank
4 Tank Support
5 Lower Deck
6 Separated Spacecraft - Launch Vehicle Adapter

Conditions

Maximum overall diameter: 96.5 in.

Maximum propellant tank diameter: 28.5 in.

Maximum pressure tank diameter: 25.5 in.

Upper tank deck: Lateral loads only

Lower tank deck: Axial loads and bending moments

Structural Materials

Basic load structure: Aluminum
Tanks: Titanium

Tank Burst Pressure

Propellant tank: 407 psia
Pressure tank: 7,700 psia

Figure 5.2-1 summarizes the results of this preliminary sizing study. Total nonuseful in-orbit weight is shown as a function of usable propellant and engine thrust. Subsystem and residual propellant weight variation is also shown. Residual propellant, which is a constant 3.75% of total propellant, allows 2% for nonusable and 1.75% for mixture ratio tolerance. Propellants used in the study were $N_2O_4$/Az-50 with a 1.6 O/F mixture ratio. The total nonuseful in-orbit weight reflected in Figure 5.2-1 as a function of usable propellant can be very closely approximated by the following equation:

$$\text{Weight}_{\text{nonuseful}} = 270 + 0.139 (W_p) + 0.05 T$$

where: $W_p$ = usable propellant weight (lbm)

$T$ = engine thrust (lbf)

Note that subsequent refined analyses of more efficient configurations reduced structural inerts for the entire range of usable propellants. This plus other changes ($N_2$ to $H_e$ for pressurant gas) are not reflected in the useful in orbit parametric weights shown in Sections 5.3 through 5.5 and in Appendix A3.

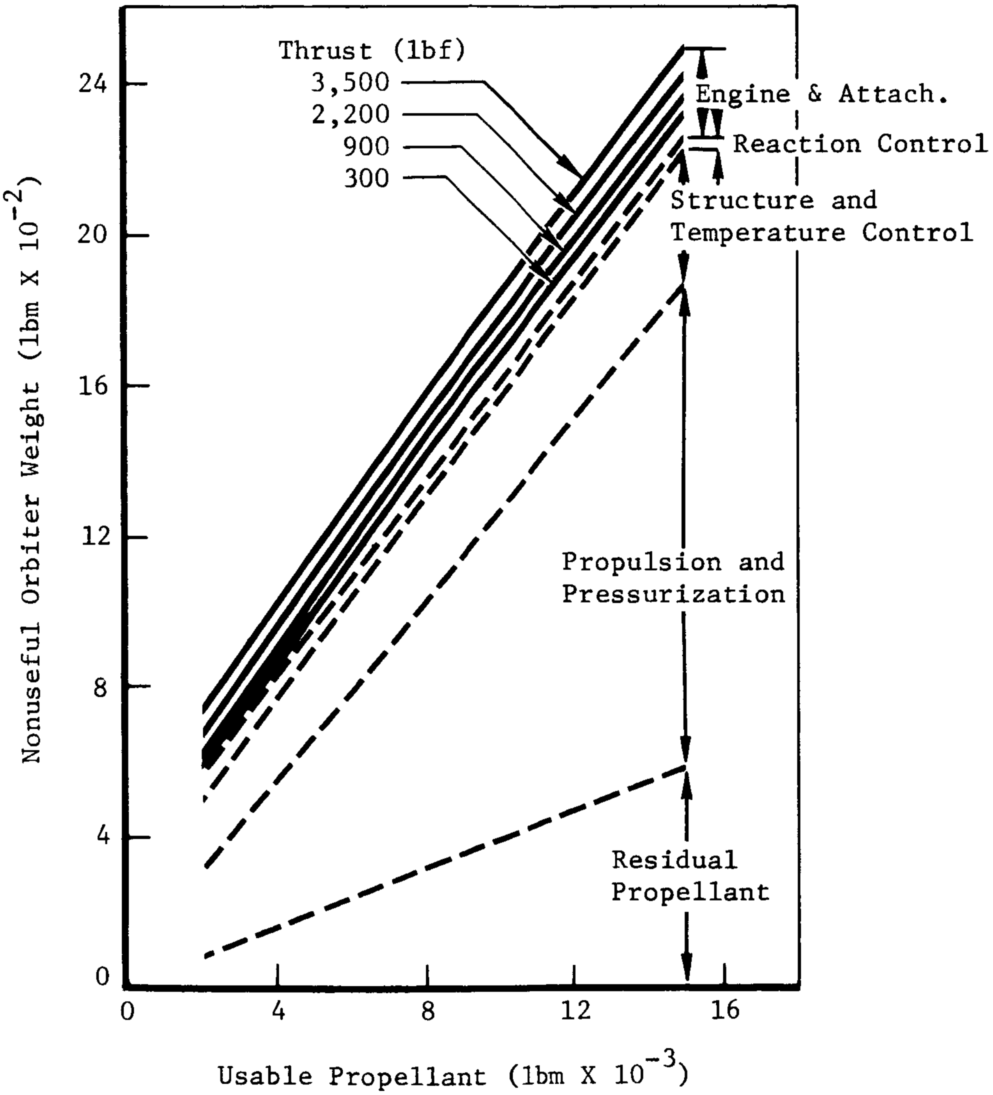

Figure 5.2-1: NONUSEFUL ORBITER WEIGHT

### 5.2.2 Data Correlation

During and after completion of the preliminary spacecraft and propulsion sizing task, actual data were collected and correlated for engine, pressurant, and propellant tanks, and pressurization and propellant feed systems. This data, presented in Figures 5.2-2 through 5.2-4 and in Table 5.2-1, has been compared as shown with the data developed during the initial sizing task. The dry inert weight items compared here represent from 60 to 72% of the total nonuseful in-orbit orbiter weight. The close comparison of component actual data with that used in the initial sizing task provides confidence in the initial performance and mission analysis work completed.

Table 5.2-1: ENGINE WEIGHT---INITIAL SIZING STUDY

| Thrust (lbf) | Weight | |
|---|---|---|
| | *Sizing Study (pounds) | Manufacturer's Data |
| 300 | 35 | 25 lb, Long Duration RS-14 (PBPS) Engine |
| 900 | 85 | 75 lb, (3) RS-14 Engines |
| 2,200 | 135 | 125 lb, Apollo Subscale Engine |
| 3,500 | 210 | 196 lb, Apollo Lunar Module Ascent Engine |

* Sizing study weight includes a 10-pound allowance for structural attachments. Engine weight includes thrust chamber, gimbal mount and engine attachment, and TVC actuators.

## 5.3 MISSION PARAMETER EFFECTS

The initial task in the study involved the selection of representative values of mission parameters for use throughout the analysis. These mission parameters include interplanetary trajectory type, arrival date, and launch period length. The basis for comparison is useful in-orbit weight.

### 5.3.1 Fixed Arrival Date

Analysis of the effect of variations in trajectory type and launch period length are based on a launch period with fixed arrival date at Mars. For a given arrival date, a range of consecutive launch dates that minimize the total impulsive velocity requirement can be identified. The effects of arrival date on total mission $\Delta V$ and the corresponding maximum values for $C_3$ and $V_\infty$ are defined in Appendix A2.

The maximum useful in-orbit weight, corresponding to the optimum spacecraft-assist $\nabla V$, was calculated for each arrival date-launch period combination, each launch vehicle, and each trajectory type. These data are shown in Figures 5.3-1 through 5.3-4 for both the Titan IIIC and IIID launch vehicles. The analysis assumed

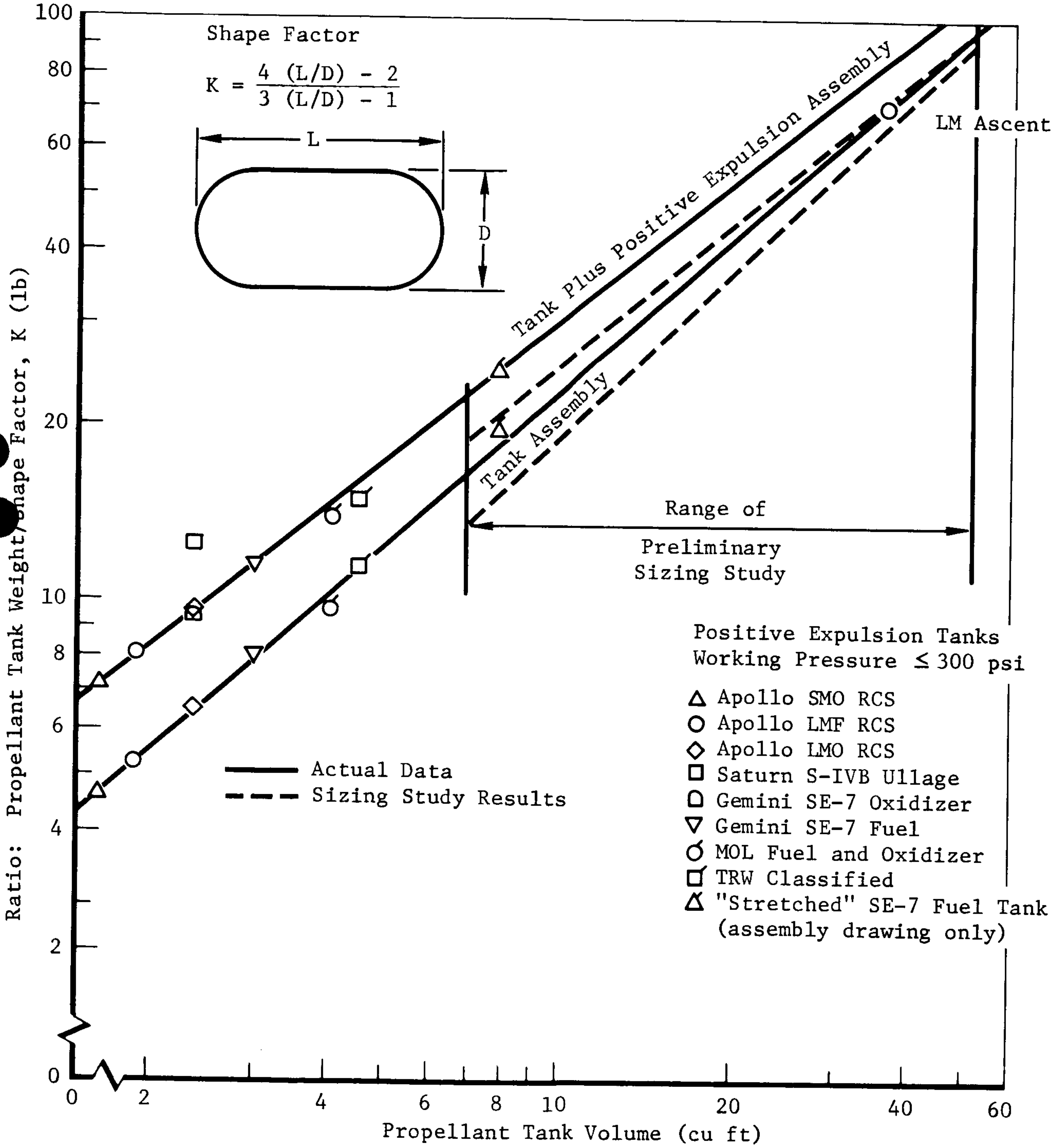

Figure 5.2-2: BLADDER EXPULSION PROPELLANT TANK WEIGHT CORRELATION

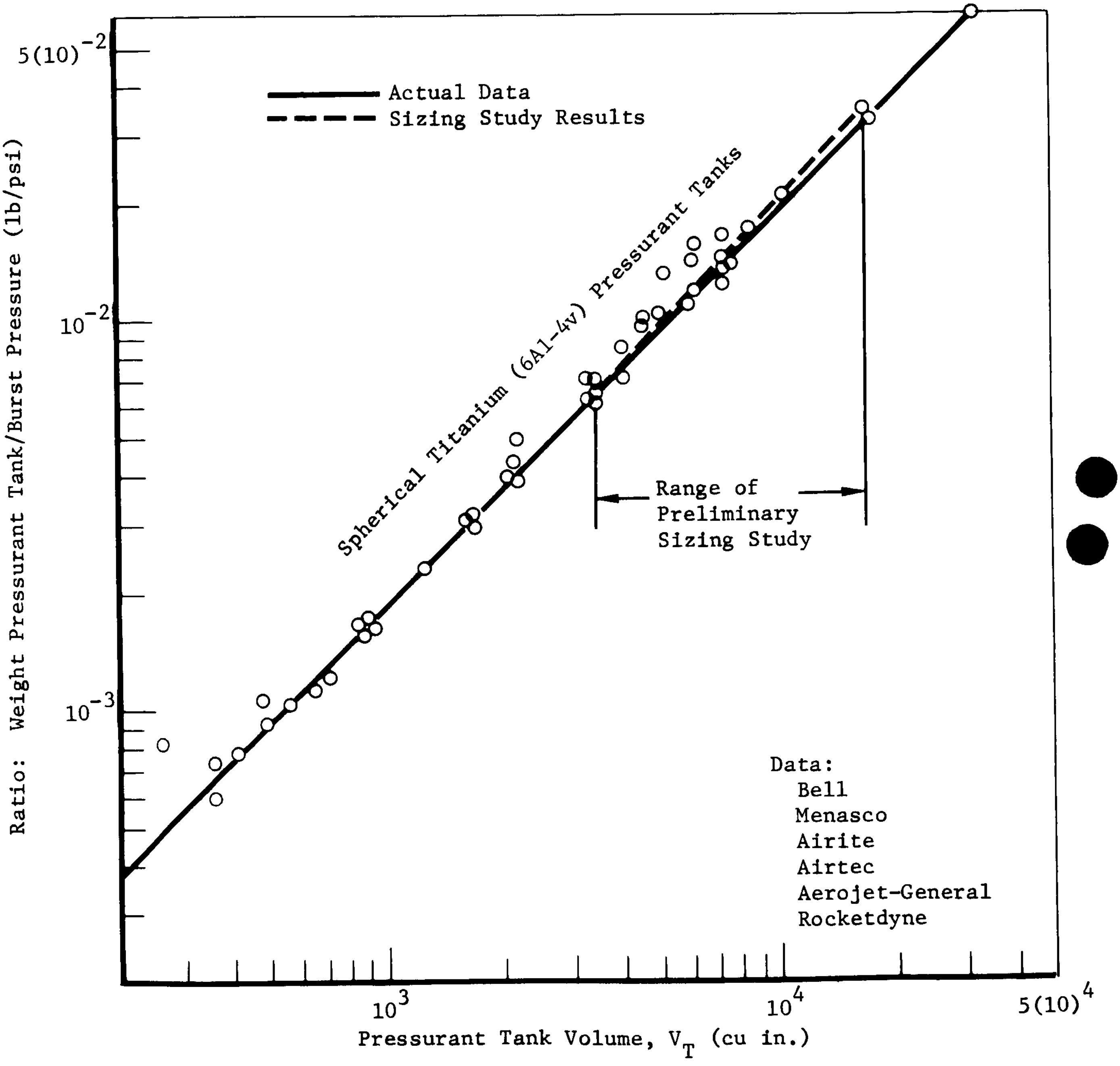

Figure 5.2-3: PRESSURANT TANK WEIGHT CORRELATION

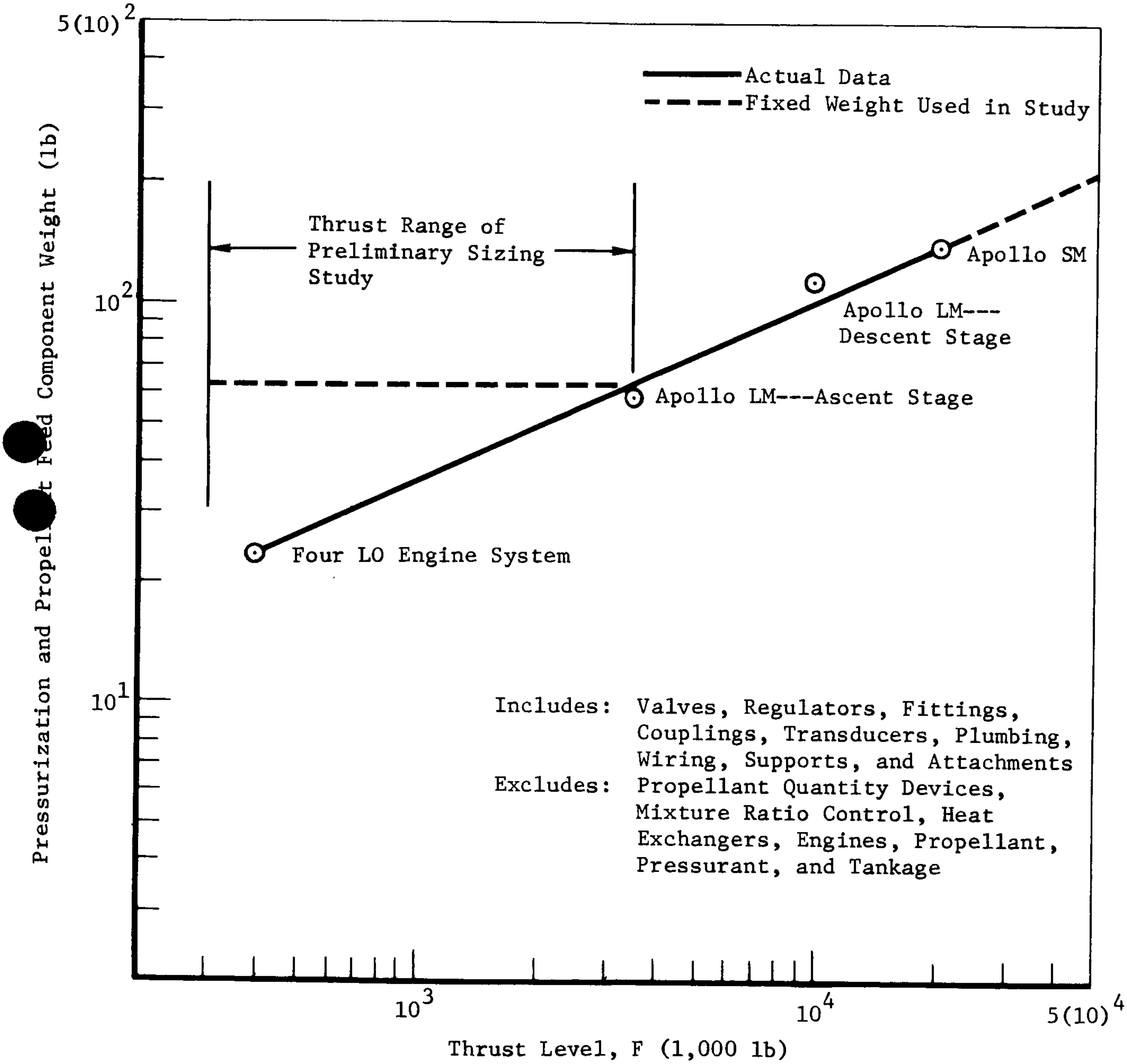

Figure 5.2-4: PRESSURIZATION AND PROPELLANT FEED SYSTEM WEIGHT CORRELATION

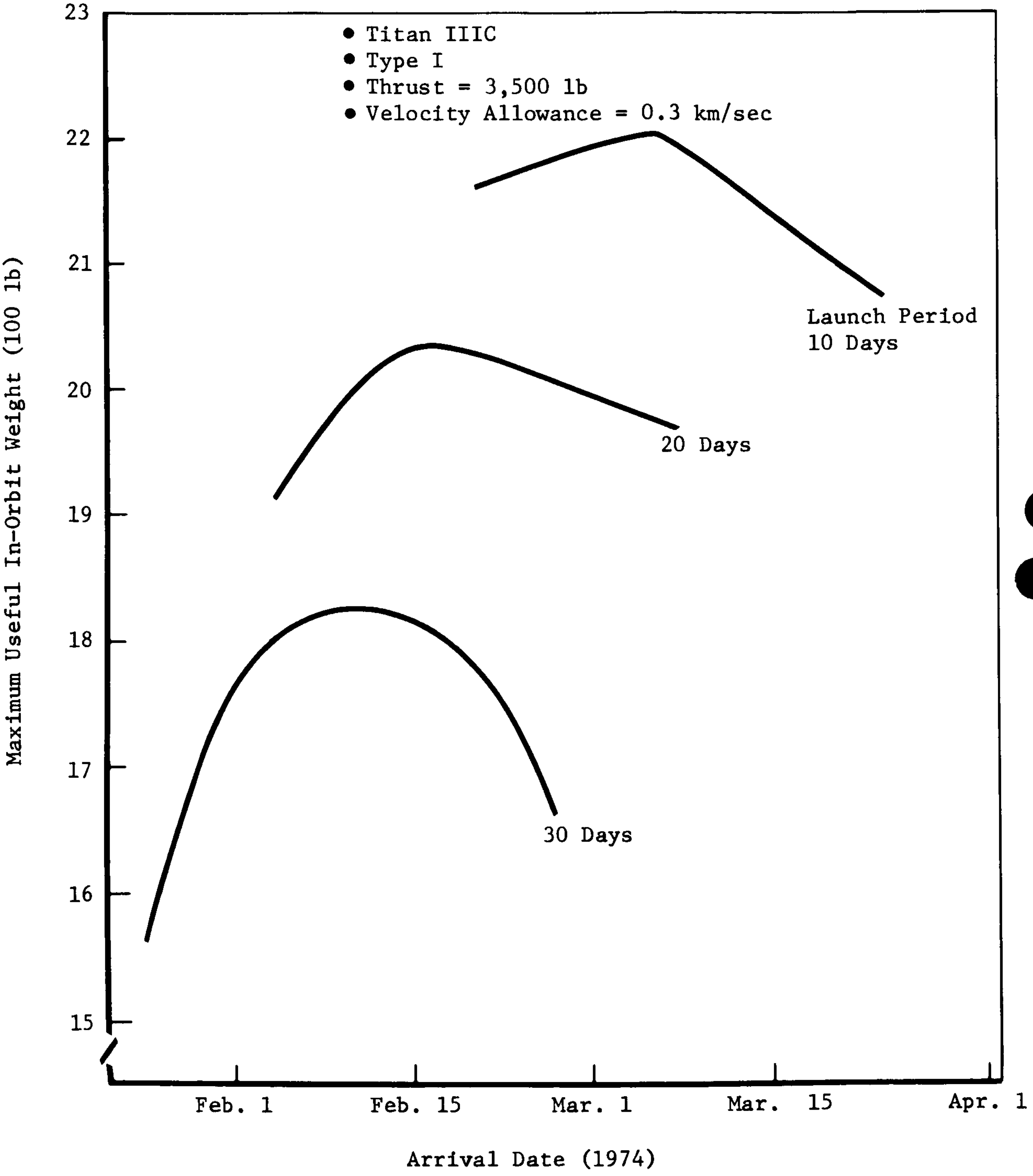

Figure 5.3-1: ARRIVAL DATE EFFECTS---TITAN IIIC TYPE I

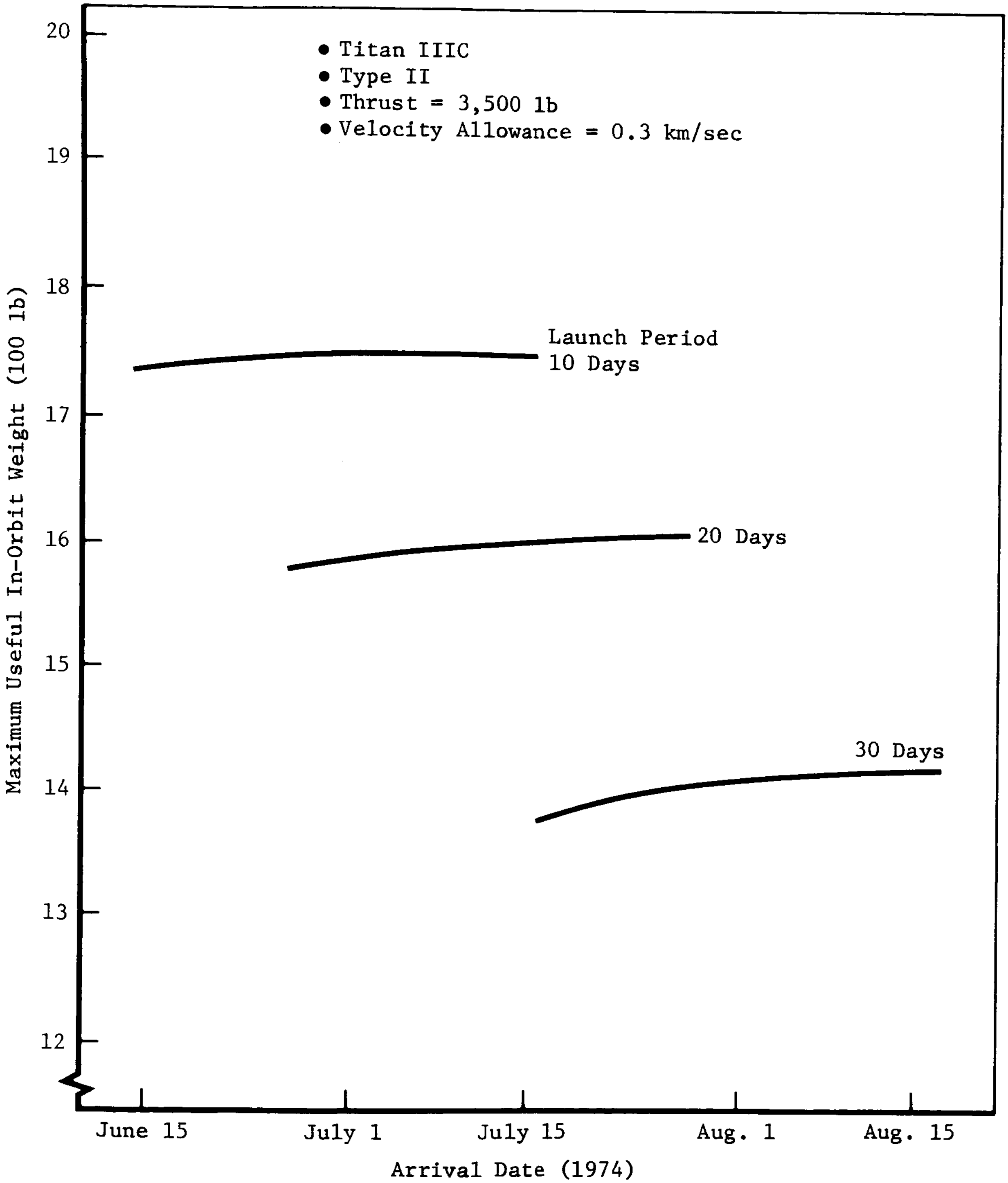

Figure 5.3-2: ARRIVAL DATE EFFECTS---TITAN IIIC TYPE II

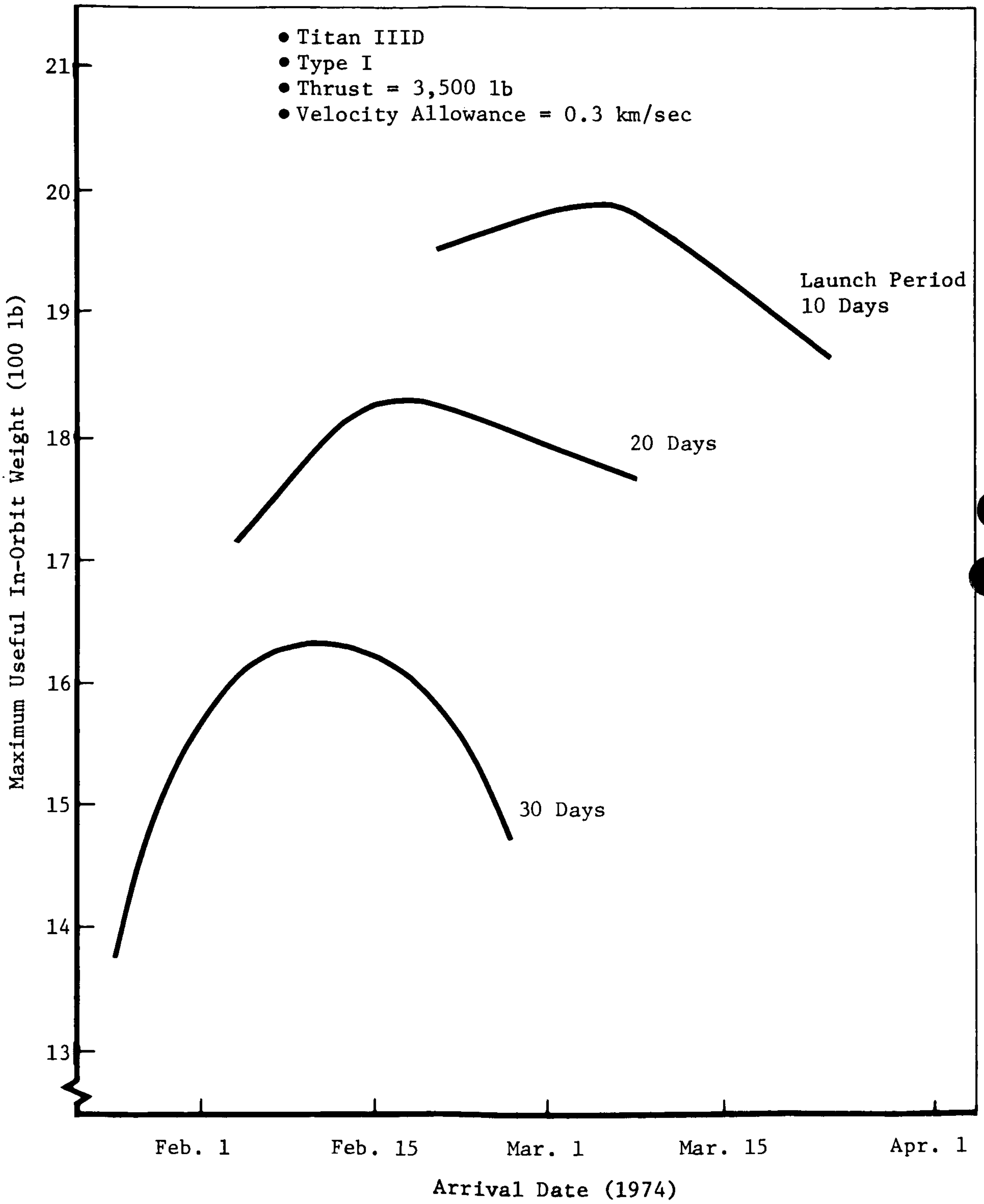

Figure 5.3-3: ARRIVAL DATE EFFECTS---TITAN IIID TYPE I

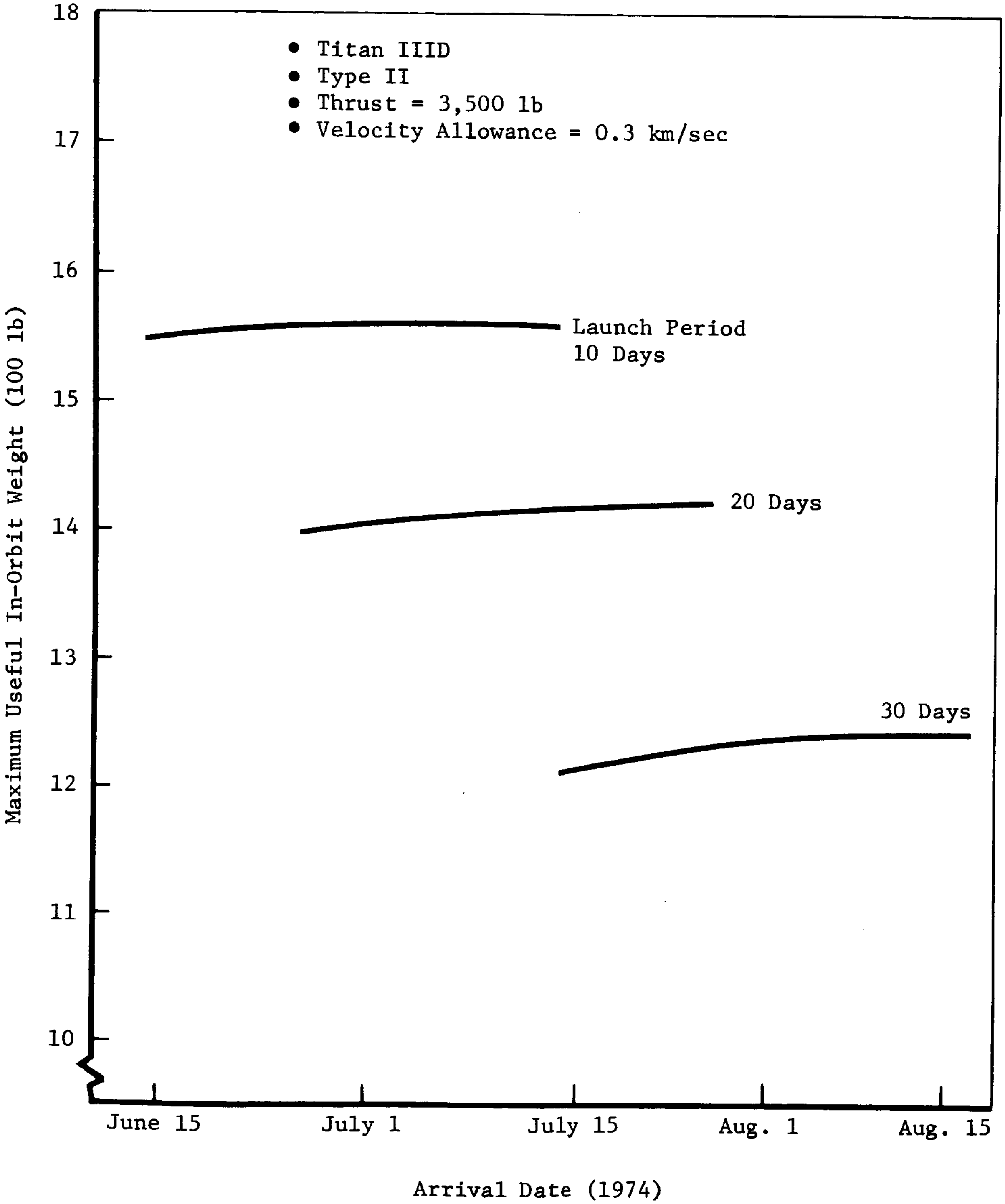

Figure 5.3-4: ARRIVAL DATE EFFECTS---TITAN IIID TYPE II

the nonuseful weights corresponding to the 3,500-pound-thrust engine identified in Section 5.2. In addition to the required spacecraft-assist and orbit-injection $\Delta V$, an allowance of 300 m/sec was assumed in the calculation. This allowance provides capability for midcourse and trim maneuvers and for changing the orientation of the Mars orbit at injection. The arrival date for minimum total mission $\Delta V$ is very near the optimum for Type I missions. The Type II results are quite flat and indicate that the selection of arrival date is not particularly critical.

Several major conclusions can be drawn from an overall view of the results of this portion of the study. For the best arrival date and a given launch vehicle-launch period length combination, Type I trajectories result in approximately 400 pounds more useful in-orbit weight than Type II for the 1973 Mars missions under consideration herein. At a given trajectory type and launch period length, Titan IIIC delivers approximately 200 pounds more useful in-orbit weight than Titan IIID. In addition, useful in-orbit weight is reduced considerably as launch period length is increased. Based on these results, the following assumptions can be specified and retained for the remainder of the parametric performance studies:

| | |
|---|---|
| • Trajectory Type | I |
| • Launch Period Length | 20 days (typical) |
| • Launch Dates | July 23 to August 11, 1973 |
| • Arrival Date | February 16, 1974 |
| • Injection $C_3$ | 16.139 $km^2/sec^2$ |

### 5.3.2 Variable Arrival Date

Consideration of a launch period with fixed arrival date results in some advantages to the mission designer. For example, the fixed Earth-Mars-Sun geometry at arrival is a favorable situation for orbit selection. In addition, if two spacecraft are to be launched in a given opportunity, it is desirable to have the spacecraft arrival separated by a minimum number of days to minimize the complexity of mission operations. Two fixed arrival date launch periods can be selected to ensure this result. However, from an energy standpoint, a performance gain can be realized if variable arrival dates are considered.

Figure 5.3-5 illustrates the maximum useful in-orbit weight (no losses) attainable for optimum launch-arrival day combinations in 1973 with a Titan IIIC launch vehicle. The energy relationships corresponding to these combinations are given in Appendix A2. These data are based on Type I trajectories. The useful in-orbit weights resulting from given launch period lengths are shown in Figure 5.3-6. In addition, the corresponding useful in-orbit weights attainable with fixed arrival dates are shown. These points are based on two options. In the one case, the spacecraft is sized to provide the maximum daily mission $\Delta V$ required in the launch period. In the second case, the spacecraft is sized to achieve the maximum $C_3$ and the maximum $V_\infty$ that occur during the launch period. If the maximum $C_3$ and $V_\infty$ occur on the same day, the options will be identical. This is nearly the case for a 30-day launch period. At a typical

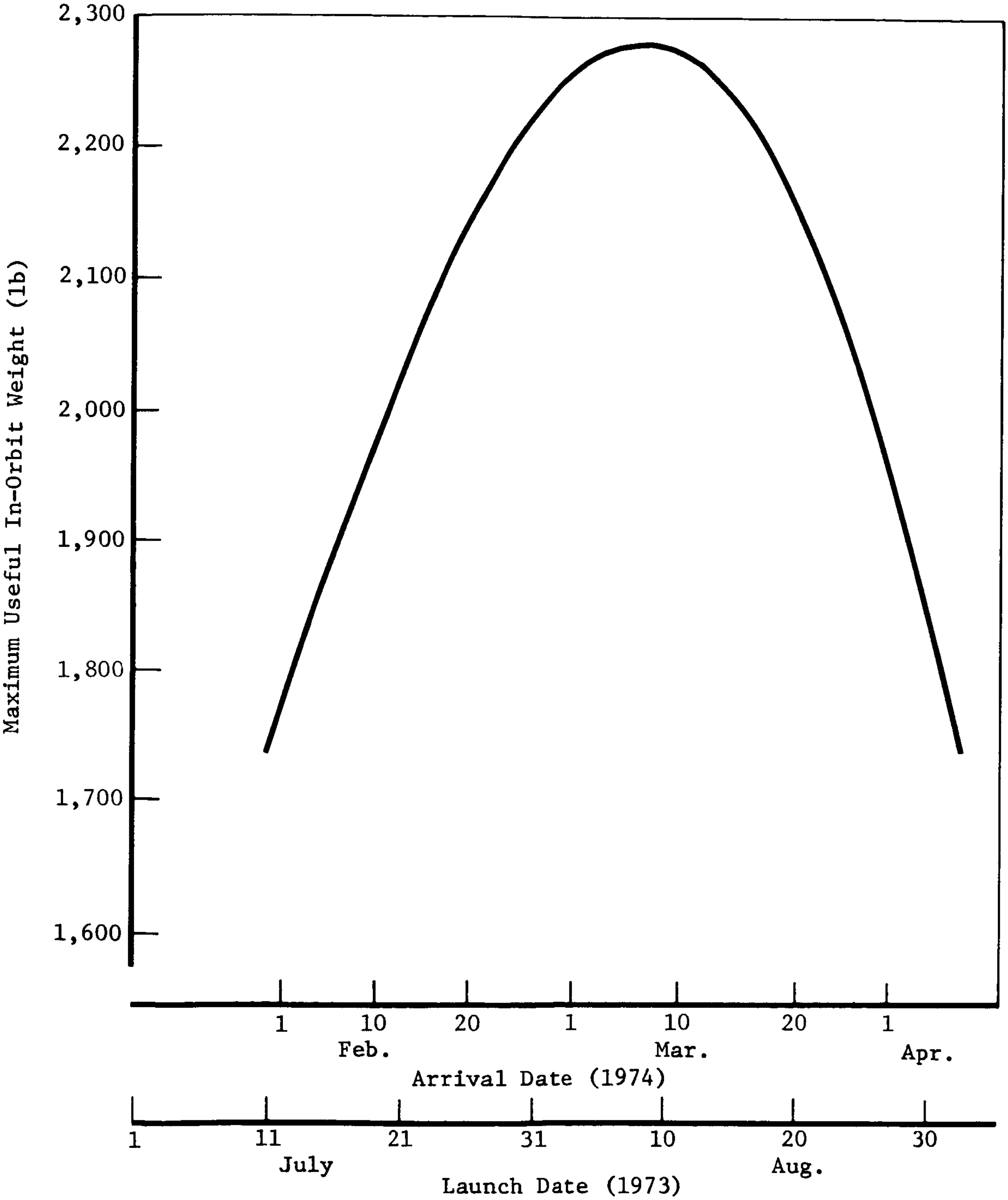

- Titan IIIC
- Type I
- Thrust = 3,500 lb
- $\Delta V_{Allowance}$ = 0.3 km/sec
- No Losses

Figure 5.3-5: MAXIMUM USEFUL IN-ORBIT WEIGHT WITH VARIABLE ARRIVAL DATE

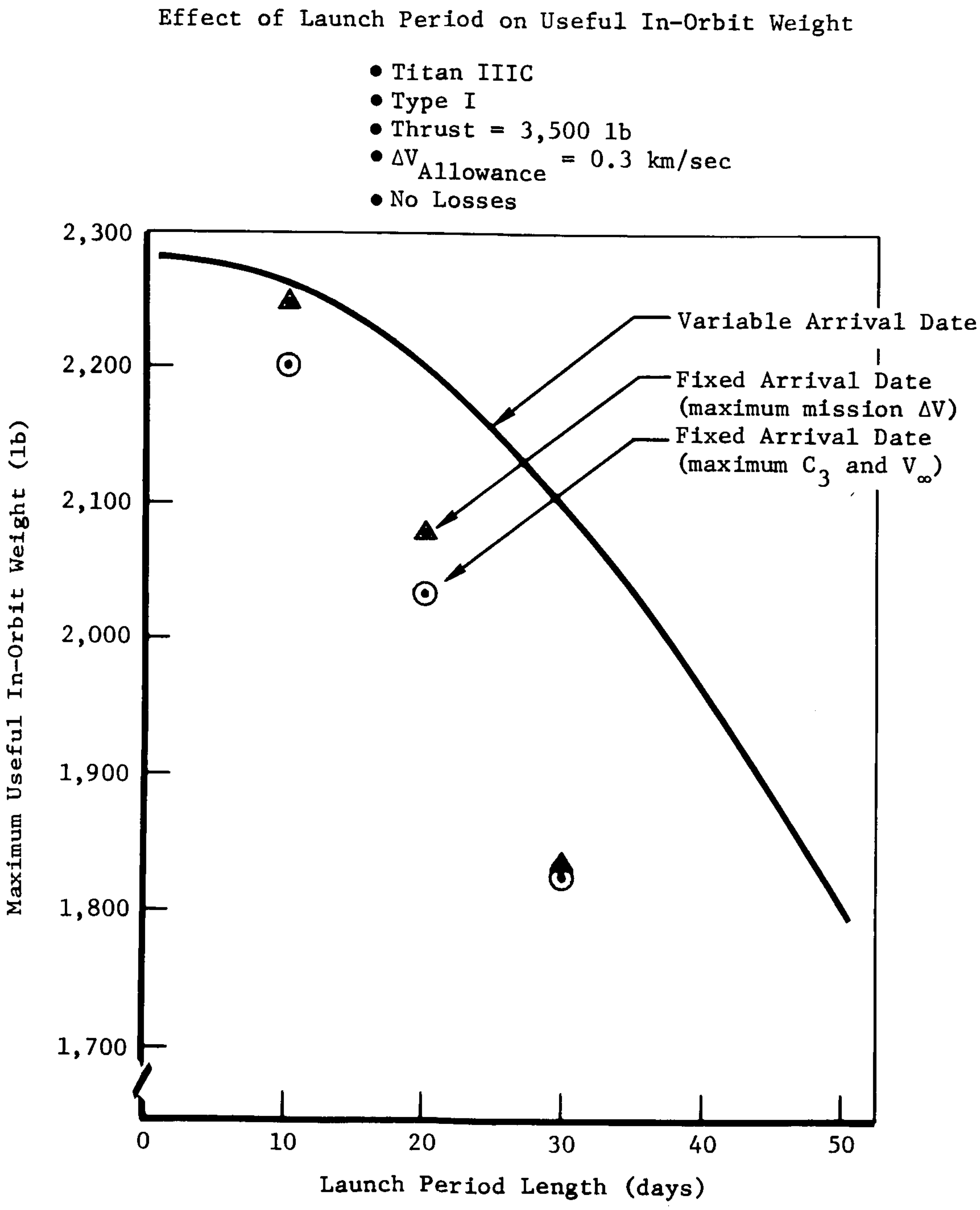

Figure 5.3-6: VARIABLE ARRIVAL DATE EFFECT ON USEFUL IN-ORBIT WEIGHT

launch period of 20 days, the useful weight gain associated with variable arrival date is 120 pounds for the maximum mission $\Delta V$ option and 165 pounds for the maximum $C_3$ and $V_\infty$ option. Figure 5.3-7 illustrates the effect of variations in the velocity allowance on useful in-orbit weight for a 20-day launch period. The curve illustrates the importance of minimizing the allowance because an increase of only 0.1 km/sec results in a useful in-orbit weight loss of 130 pounds.

## 5.4 SPACECRAFT SIZING PARAMETERS

The parameters critical to spacecraft sizing that were considered in the analysis include launch vehicle, spacecraft thrust level, nonuseful weight, post-injection $\Delta V$, and injection $C_3$. The effect of variations in these parameters on useful in-orbit weight has been identified for values of spacecraft-assist $\Delta V$ from 0 to 3 km/sec. The data are based on the 20-day fixed arrival date launch period defined in Section 5.3, and on an impulsive transtage burn, a finite spacecraft engine burn with ignition at perigee, and an optimum inertially fixed attitude during $\Delta V$ injection. The complete parametric results of this analysis and an example of their use in preliminary sizing of a spacecraft are given in Appendix A3.

### 5.4.1 Launch Vehicle Selection

The launch vehicles considered in the analysis are the Titan IIIC and IIID. The characteristics of these vehicles are defined in Reference 1; their performance is described in Section 5.1.1 of this volume. The relative capability of the launch vehicles is illustrated in Figure 5.4-1. These results, based on a spacecraft thrust of 3,500 pounds and a post-injection $\Delta V$ of 1.5 km/sec, show that the useful in-orbit weight attainable with Titan IIIC always exceeds the corresponding Titan IIID performance. Similar results occur at other thrust and post-injection $\Delta V$ levels. However, the Titan IIID results do not include the potential penalty associated with the fact that the final stage of this launch vehicle (Core 2) is not restartable. Consequently, spacecraft weighing less than 27,000 pounds will be placed in an elliptical parking orbit by the launch vehicle. The relative orientation between perigee of the parking orbit and the desired trans-Mars hyperbola requires that the spacecraft burn take place at a point off the perigee of the parking orbit (see Figure 5.5-8b). This results in an additional velocity loss of approximately 1 km/sec and a corresponding reduction in useful in-orbit weight of approximately 1,100 pounds. Because this penalty is completely unacceptable, the Titan IIID is removed from further consideration as a launch vehicle for powered spacecraft missions to Mars in 1973. Section 5.5.2 contains a detailed discussion of the penalties resulting from the use of elliptical parking orbits.

### 5.4.2 Spacecraft Thrust Selection

Three engines, at thrust levels of 3,500, 2,200, and 300 pounds, were considered in the parametric performance analysis. These engines were selected from a large group of candidates as a result of the propulsion subsystem parametric studies discussed in the propulsion section. In addition, a thrust level of 900 pounds was studied. This propulsion system was comprised of a cluster of three of the 300-pound-thrust engines.

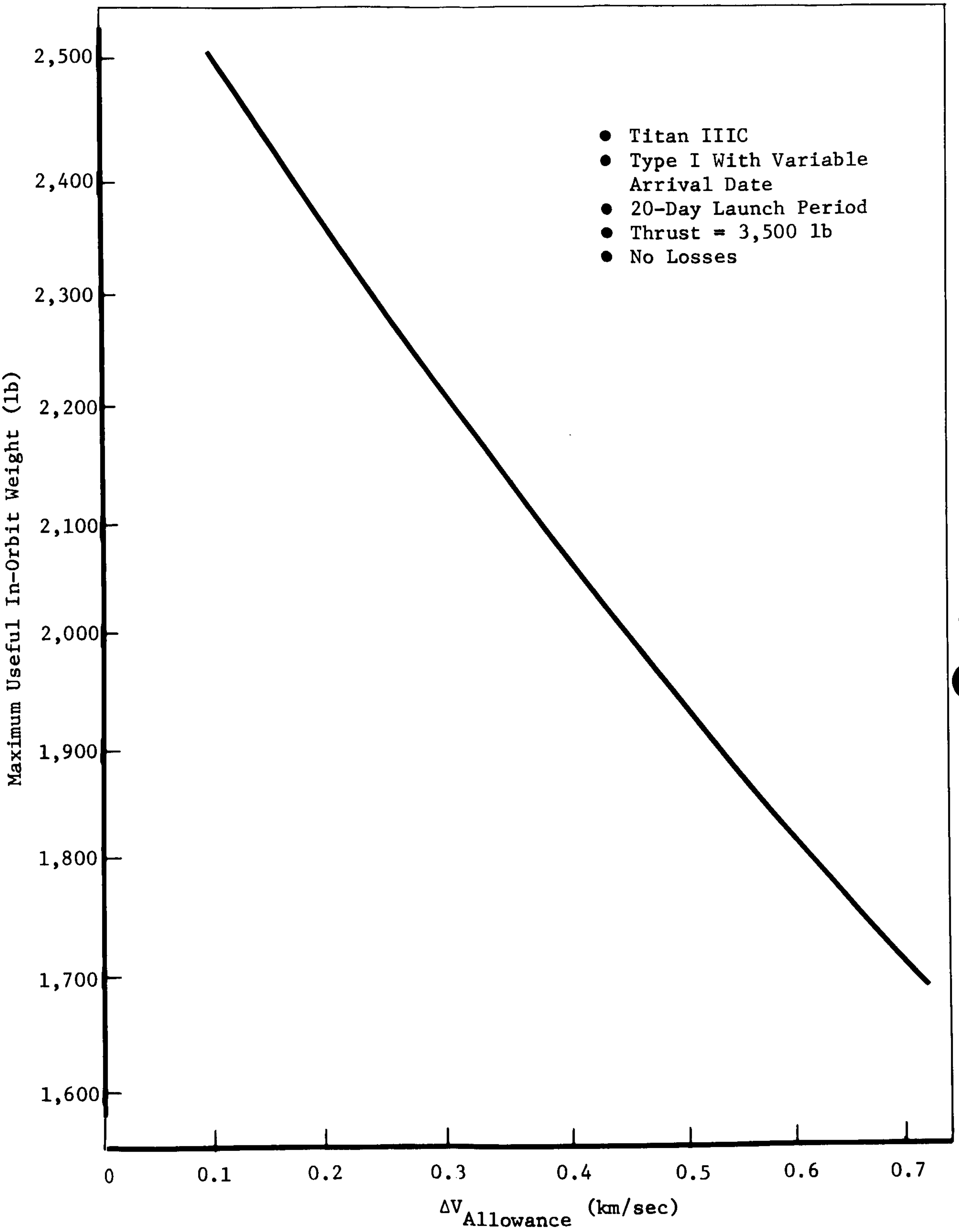

Figure 5.3-7: EFFECT OF VELOCITY ALLOWANCE ON USEFUL IN-ORBIT WEIGHT

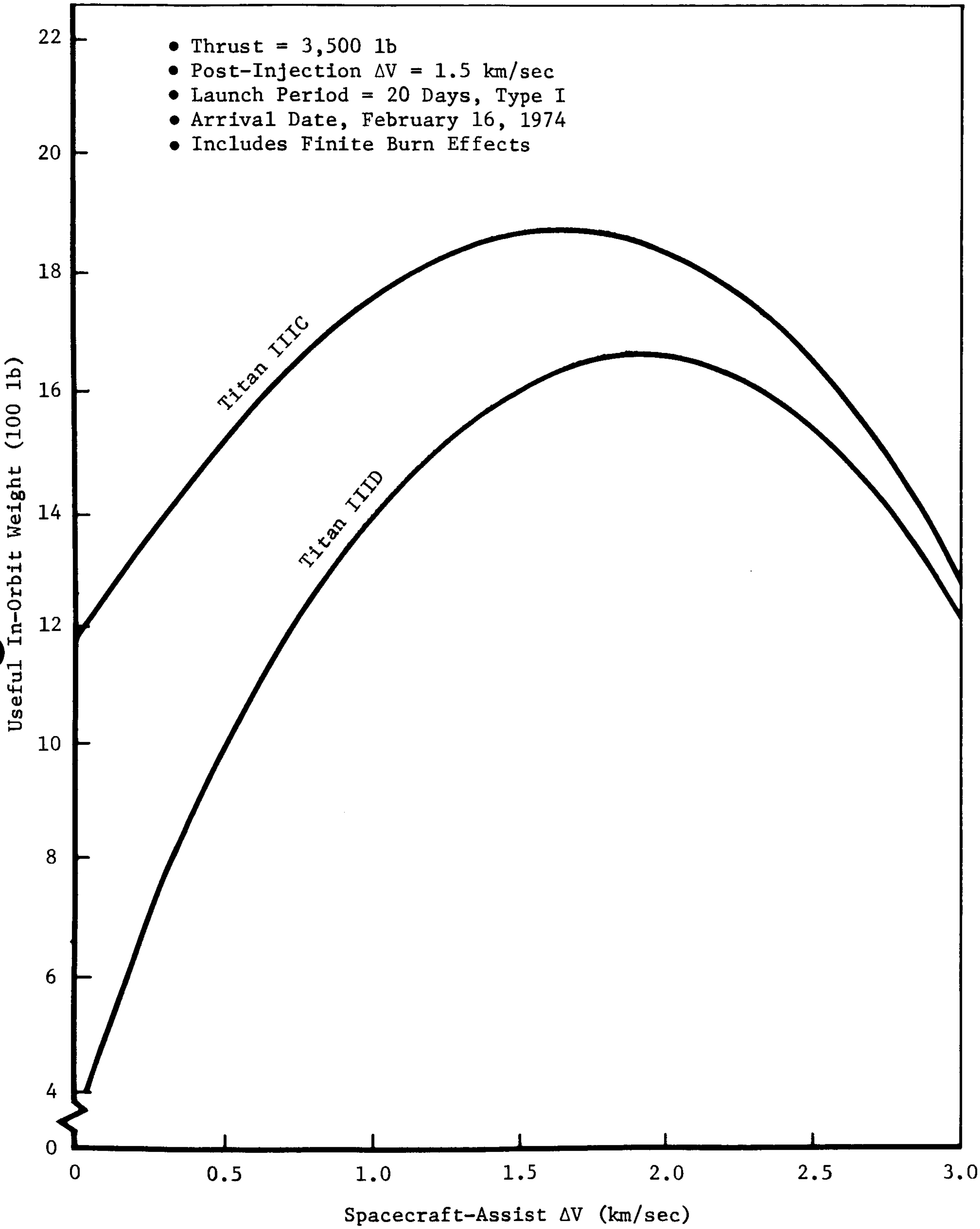

Figure 5.4-1: LAUNCH VEHICLE COMPARISON

Variations in the spacecraft thrust level affect useful in-orbit weight in several ways. First, the specific impulse of the 300-pound engine is 290 seconds, while the 2,200- and 3,500-pound engines have a value of 305 seconds. In addition, reduction in the thrust level reduces the nonuseful weight of the propulsion system. This, in turn, increases useful in-orbit weight. However, the corresponding reduction in spacecraft thrust-to-weight ratio increases the velocity losses due to finite burn effects and provides for a corresponding decrease in useful in-orbit weight. The combined effects of thrust variation are shown in Figure 5.4-2 for a typical post-injection $\Delta V$ of 1.5 km/sec. The finite burn losses and lower specific impulse degrade the performance of the 300- and 900-pound systems rather severely relative to the comparable results obtained for 2,200 and 3,500 pounds. Although the 2,200-pound system enjoys a slight performance advantage over the 3,500-pound-thrust system, the status of engine development, production, and funding, discussed in Appendix B, favors 3,500 pounds. Consequently, this thrust level was selected for the baseline system.

### 5.4.3 Post-Injection $\Delta V$ Effects

All spacecraft maneuvers subsequent to injection onto the transplanetary trajectory must be considered in the post-injection $\Delta V$ budget. This includes the Mars orbit injection maneuver as well as all required midcourse and orbit trim impulses. This total budget cannot be sized exactly without detailed knowledge of the mission design. In particular, it is necessary to know the size and orientation of the Mars orbit. Because these data cannot be defined with certainty at this time, post-injection $\Delta V$ was carried as a variable in the parametric analysis. Figure 5.4-3 illustrates the useful in-orbit weights attainable with post-injection $\Delta V$ varying between 1 and 2 km/sec. The data clearly indicate the importance of selecting a mission that minimizes post-injection $\Delta V$, because a useful in-orbit weight loss in excess of 1 pound results from every 1 m/sec increase in required velocity.

### 5.4.4 $C_3$ Effects

The results presented thus far are based on the launch period and arrival date defined in Section 5.3.1. The injection $C_3$ associated with this fixed arrival date mission (16.139 $km^2/sec^2$) is typical of a minimum energy mission to Mars in 1973. However, to provide the mission designer with sufficient information to determine useful in-orbit weights for other missions, a parametric analysis of the effect of variations in injection $C_3$ has been conducted. Figure 5.4-4 illustrates the useful in-orbit weights attainable with injection $C_3$ variations between 12 and 28 $km^2/sec^2$. This covers the range of $C_3$ that might be selected for Mars orbital missions in 1973. The data are based on a post-injection $\Delta V$ of 1.5 km/sec. The variation in maximum useful weight is almost linear with $C_3$. It amounts to approximately 50 pounds of useful in-orbit weight for each 1 $km^2/sec^2$. Additional parametric results are given in Appendix A3.

### 5.4.5 Spacecraft Weights

The separated spacecraft weights attainable with a Titan IIIC launch vehicle are shown in Figure 5.4-5 as a function of spacecraft-assist $\Delta V$. The data are based on a nominal $C_3$ of 16.139 $km^2/sec^2$. This weight is defined as the

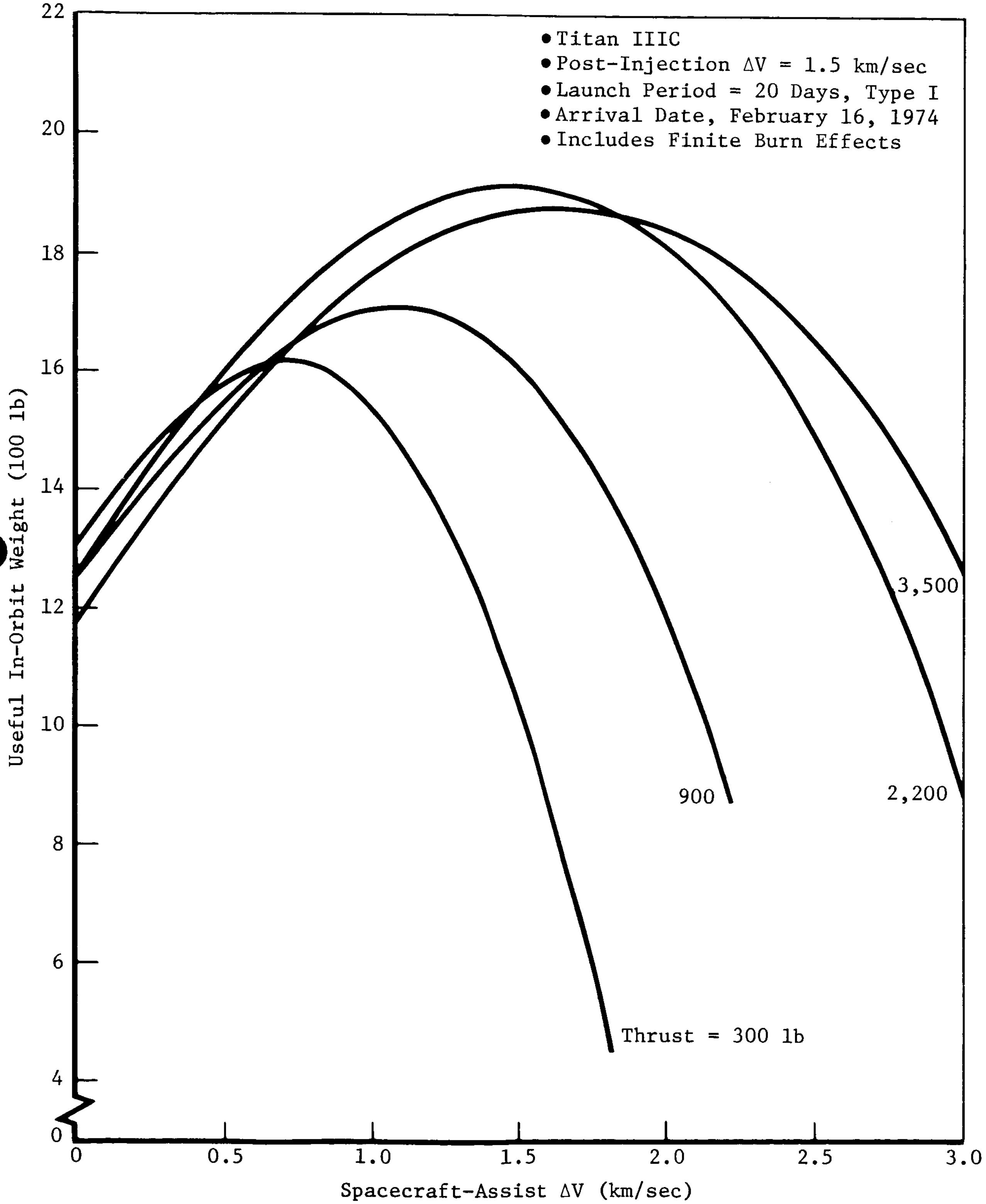

Figure 5.4-2: SPACECRAFT THRUST EFFECTS---TITAN IIIC

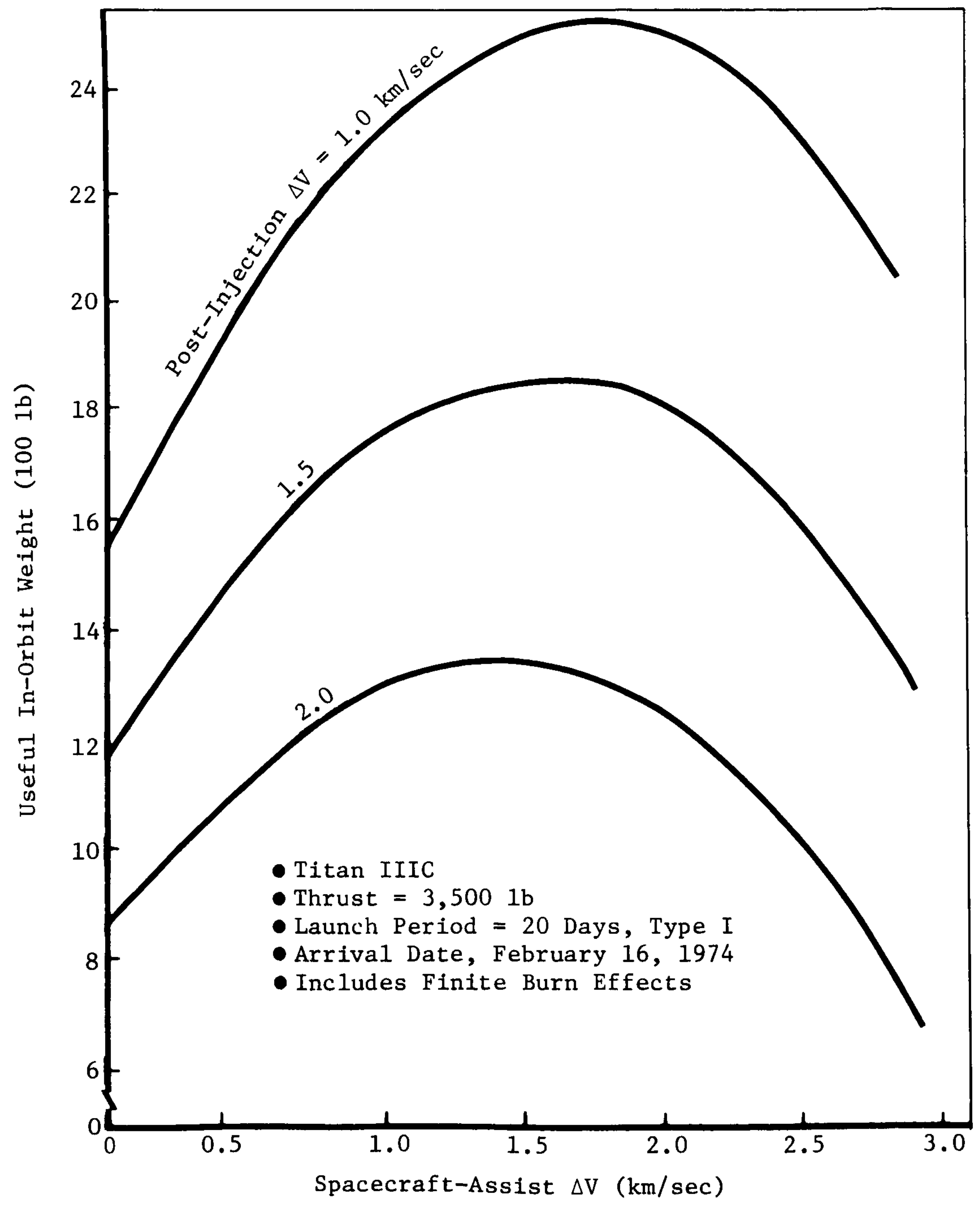

Figure 5.4-3: EFFECT OF POST-INJECTION ΔV ON USEFUL IN-ORBIT WEIGHT

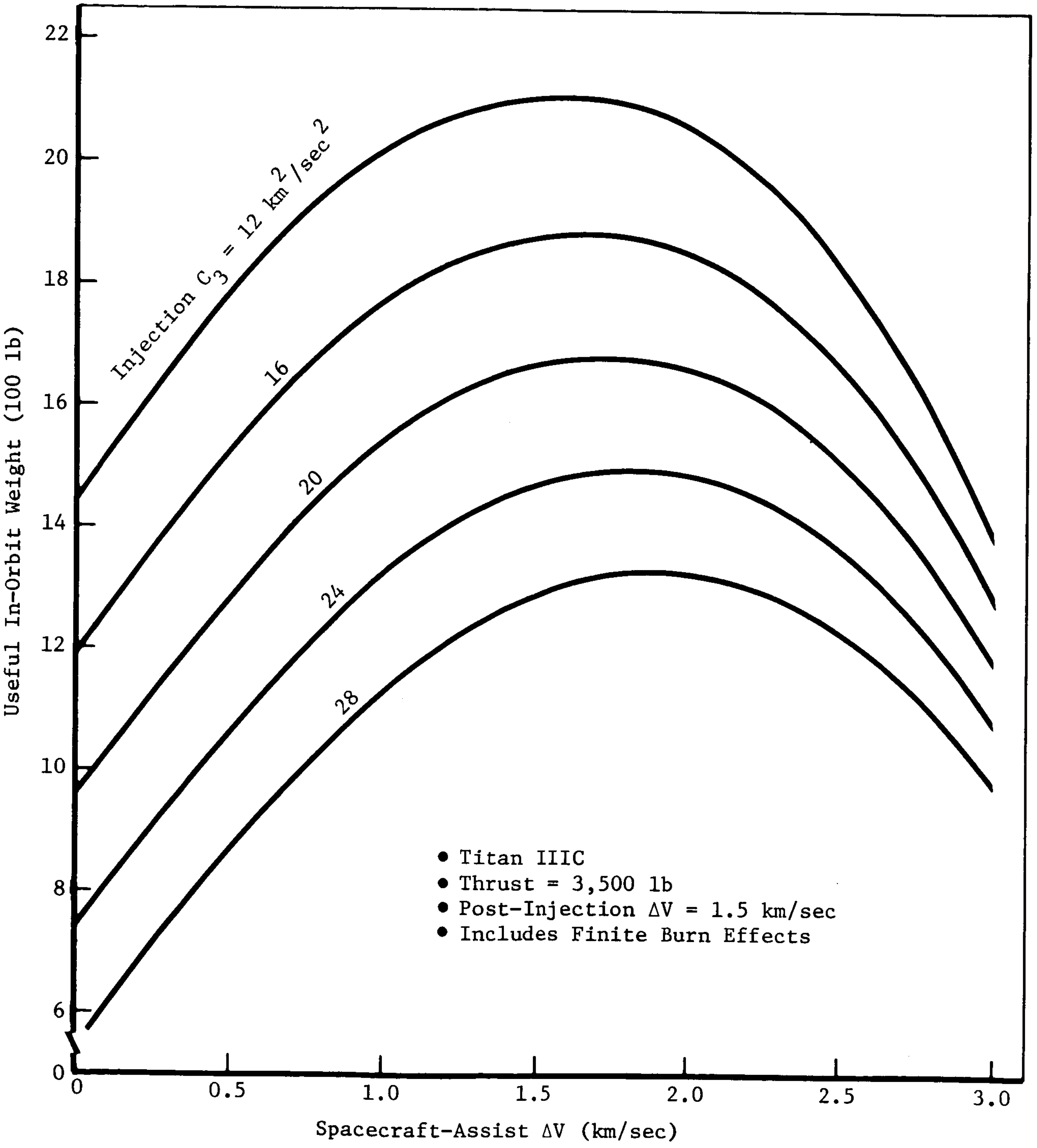

Figure 5.4-4: $C_3$ EFFECTS ON USEFUL IN-ORBIT WEIGHT

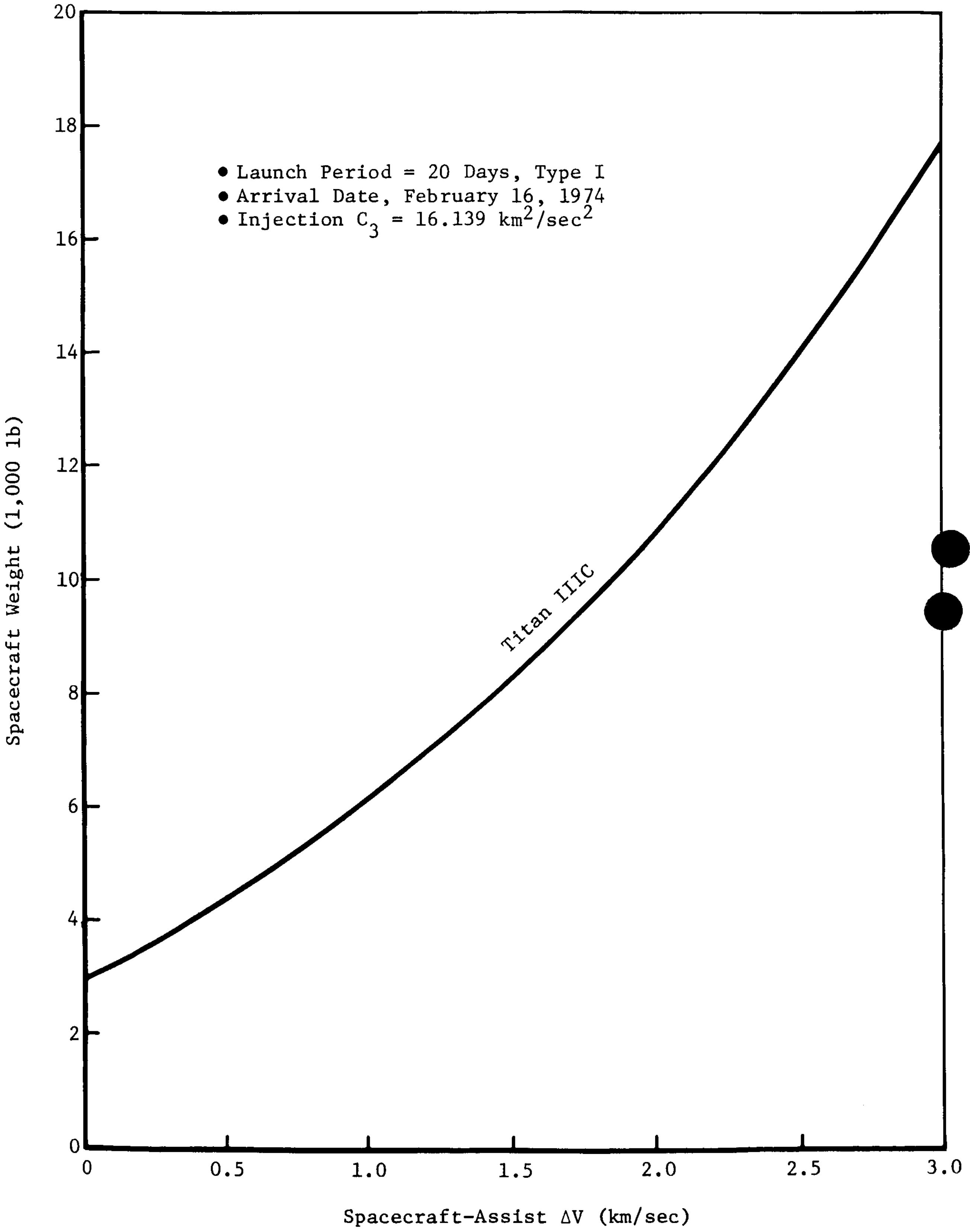

Figure 5.4-5: POWERED SPACECRAFT WEIGHT

fully loaded weight of the spacecraft after separation from the spacecraft-launch vehicle adapter. Comparable data for other values of $C_3$ and the corresponding propellant weights are given in Appendix A3.

Figure 5.4-6 relates spacecraft size directly to useful in-orbit weight. The data illustrate that a slight deviation from maximum useful in-orbit weight can result in substantial change in spacecraft size. For example, the maximum useful in-orbit weight for a spacecraft with 3,500-pound thrust is 1,870 pounds when $\Delta V_{PI}$ = 1.5 km/sec. This requires a spacecraft weighing 9,000 pounds and carrying 6,100 pounds of propellant. However, with only a 50-pound reduction in useful in-orbit weight, the spacecraft size shrinks to 7,000 pounds with only 4,200 pounds of propellant.

## 5.5 NEAR-EARTH MISSION DESIGN

Design of the near-Earth portion of an interplanetary mission involves a compromise between the performance and operational aspects of the trajectory. The mission must be designed to minimize the inefficiency of the energy transfer while retaining the capability of providing adequate daily launch window.

In the usual interplanetary mission, a circular parking orbit and a single-stage injection maneuver are used. The injection maneuver must be timed to provide the desired interplanetary trajectory orientation. This type of mission profile is shown in Figure 5.5-1. Powered spacecraft missions on the Titan IIIC launch vehicle are similar. However, the final stage of the Titan IIID is not restartable. Consequently, the spacecraft is placed into an elliptical parking orbit by the launch vehicle. Missions using both circular and elliptical parking orbits were studied.

### 5.5.1 Titan IIIC

The Titan IIIC launch vehicle is able to inject spacecraft weighing less than 26,000 pounds into a 100 n mi circular orbit without completely expending the propellants in the transtage. The remaining transtage capability is then used to provide the initial portion of the required transplanetary energy. Following transtage cutoff, the spacecraft propulsion system provides the remainder of the required energy. The coast period between final transtage cutoff and spacecraft ignition is called the holding orbit. If this coast time is a minimum value, based on the shortest time allowable from an operational standpoint, it is called a short holding orbit. This type of powered spacecraft mission closely resembles the standard interplanetary mission shown in Figure 5.5-1.

The holding orbit established by the transtage second burn is elliptical. During the coast, the spacecraft is moving away from perigee, which is the optimum point to perform an impulsive spacecraft injection maneuver. Significant $\Delta V$ penalties result when the ignition point moves from perigee (particularly if the orbit is highly eccentric). It is these penalties that suggest use of a long holding orbit. In this case, the spacecraft is maintained in holding orbit for approximately one revolution. The final injection burn is initiated at the optimum point before perigee passage to minimize the combined $\Delta V$ losses due to finite burn effects and the inefficient energy transfer. This mission profile, depicted in Figure 5.5-2, results in an energy transfer

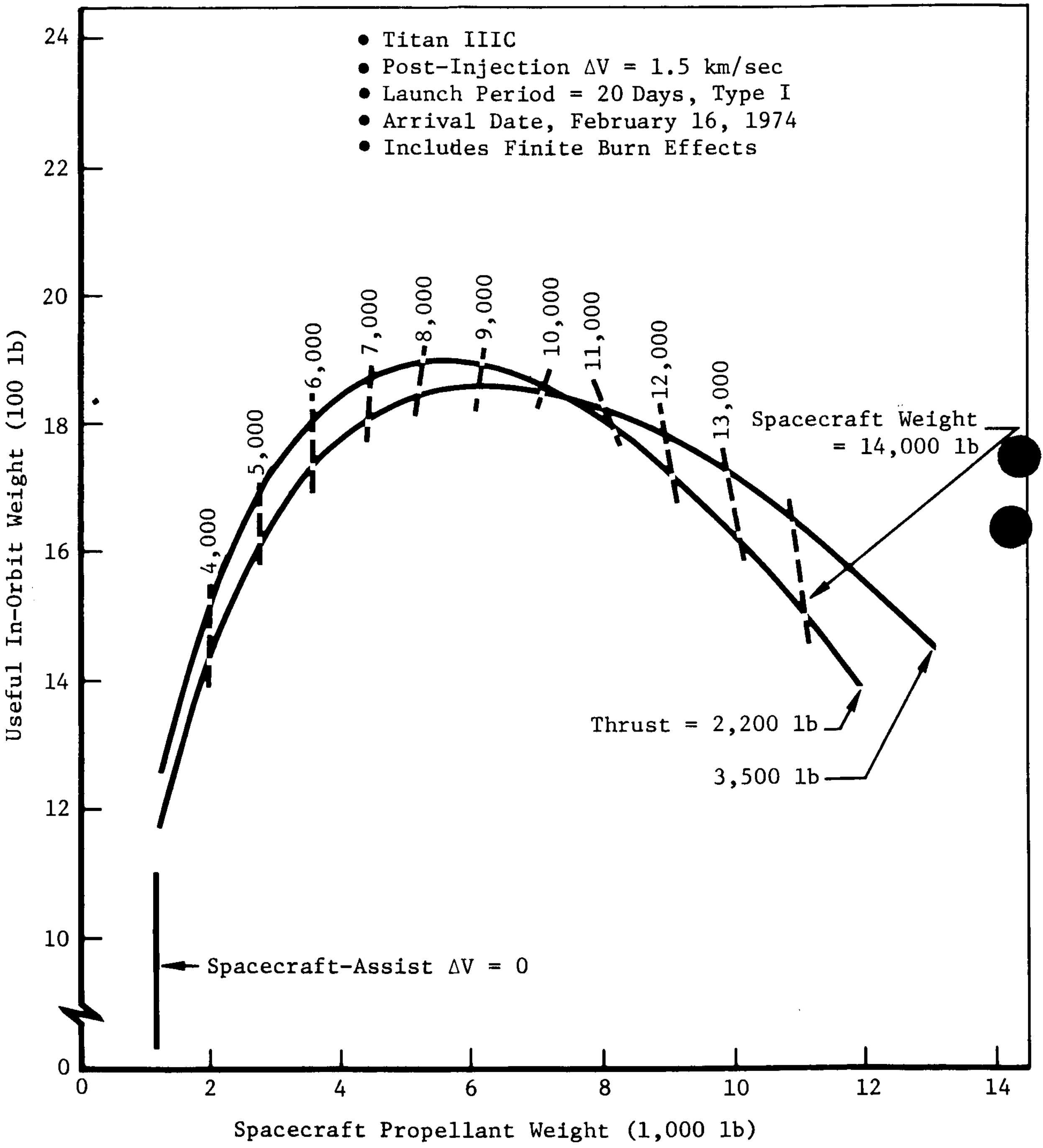

Figure 5.4-6: EFFECT OF SPACECRAFT SIZE ON USEFUL IN-ORBIT WEIGHT---TITAN IIIC

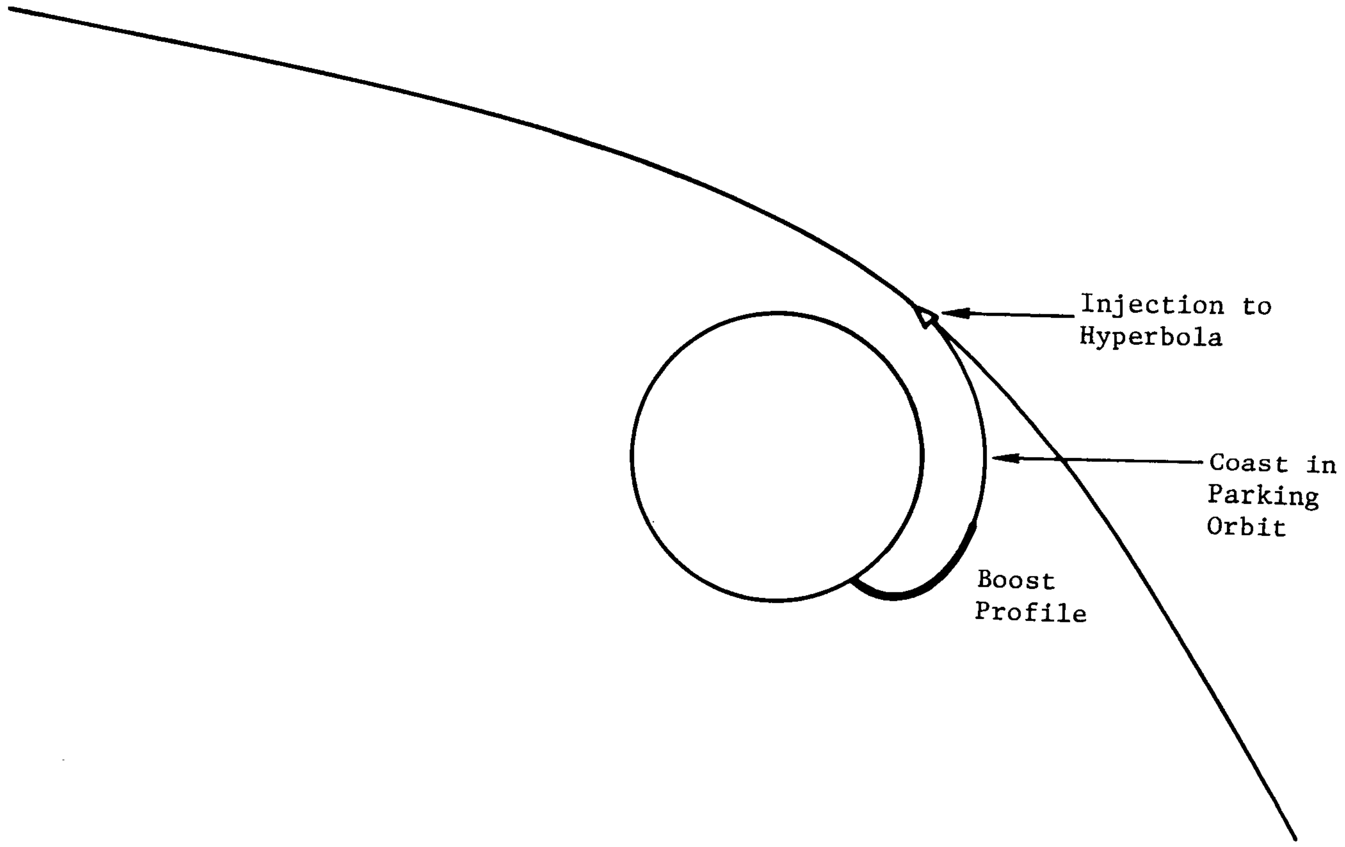
Injection to
Hyperbola
Coast in
Parking
Orbit
Boost
Profile

Figure 5.5-1: MISSION PROFILE---CIRCULAR PARKING ORBIT (SHORT HOLDING ORBIT)

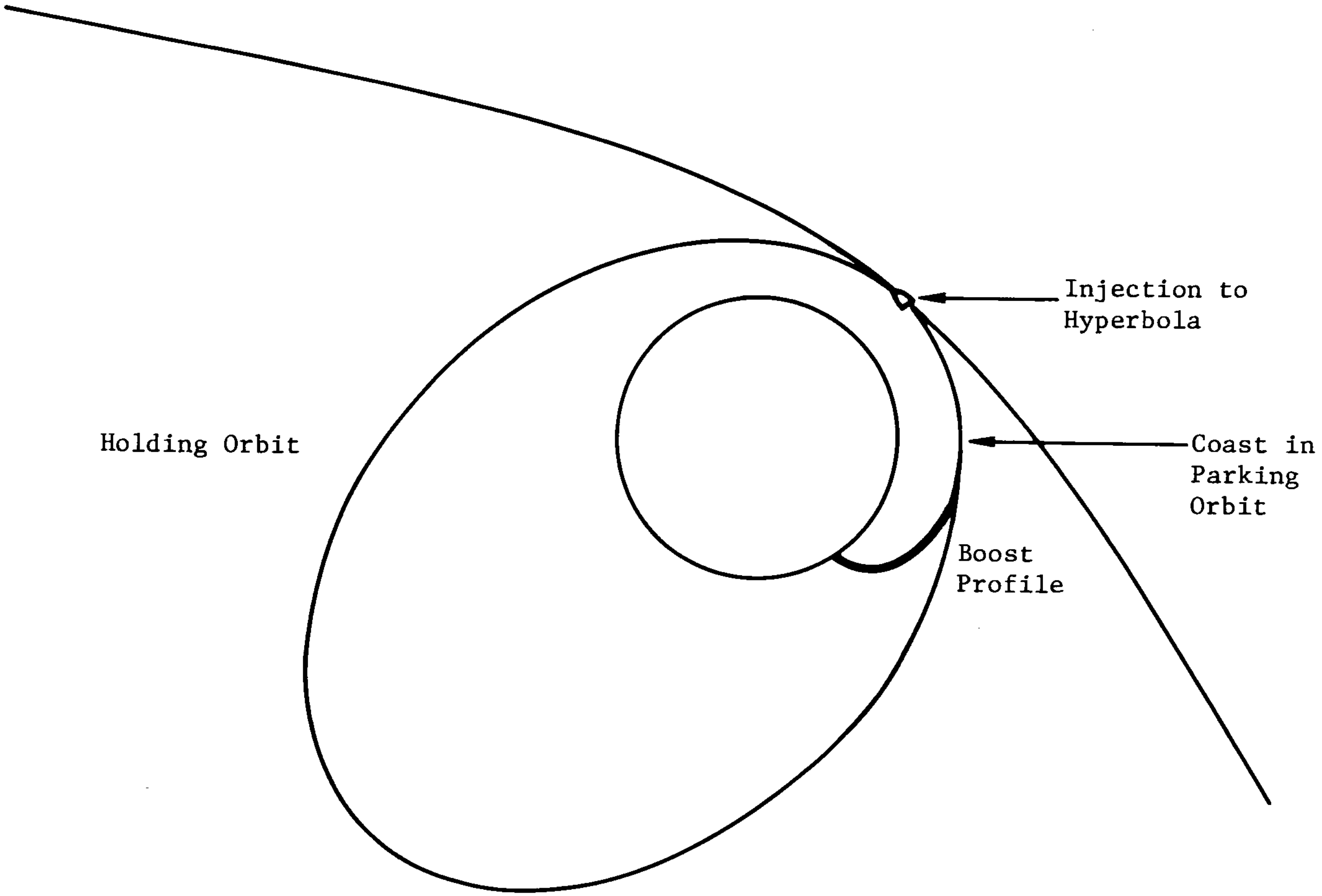
Injection to Hyperbola
Coast in Parking Orbit
Holding Orbit
Boost Profile

Figure 5.5-2: MISSION PROFILE---CIRCULAR PARKING ORBIT (LONG HOLDING ORBIT)

that is more efficient than the short holding orbit. However, it does place additional requirements on subsystem design. These specific requirements are discussed in the individual subsystem sections of the report.

To make a valid comparison between the short and long holding orbit options, trajectories leaving parking orbit were optimized. The assumed steering profile considered a fixed inertial attitude rate for transtage and a fixed inertial attitude for the spacecraft. The search technique determined the magnitude of these parameters necessary to maximize the useful weight in Mars orbit. Fixed coast times were used in the short holding orbit analysis. However, in the long holding orbit cases, the spacecraft ignition time before perigee was also optimized.

The useful weights attainable with both short and long holding orbits are compared in Figure 5.5-3. The parametric data given in Section 5.4 was based on impulsive transtage burn with spacecraft ignition occurring at perigee and spacecraft attitude held at the optimum inertial value. Results based on this assumption are also shown in Figure 5.5-3. For the short holding orbit solutions, there is approximately a 30-pound bias between zero coast and the parametric result. This is due to two factors. First, the zero coast cases reflect the finite thrust losses incurred during the transtage burn. In addition, spacecraft ignition now occurs past perigee because the transtage burnout flight-path angle is positive. The additional loss incurred with increasing coast time reflects the fact that the spacecraft position is rapidly moving away from perigee and picking up the associated velocity penalty. The long holding orbit results are very comparable to the parametric data. In fact, the performance for the cases involving longer spacecraft burn times (higher spacecraft-assist $\Delta V$) actually exceeds the parametric solution. In these cases, the loss incurred in the transtage burn is overcome by the gain associated with ignition of the spacecraft at the optimum point before perigee passage.

Analysis conducted during the attitude control parametric study indicated that holding orbit coast times of as little as 90 seconds are attainable. For moderately sized spacecraft weighing approximately 7,000 pounds, this represents a useful in-orbit weight reduction of approximately 45 pounds when compared with the long holding orbit solution. This penalty is quite moderate and does not provide sufficient motive for selecting the long holding orbit mission mode. In fact, the subsystem penalties and operational difficulties peculiar to the long holding orbit mode override the performance advantage. Consequently, the short holding orbit mode is considered as the primary mode for powered spacecraft missions launched on Titan IIIC.

The effect of post-injection $\Delta V$ on useful in-orbit weights attainable with both short and long holding orbits is given in Figures 5.5-4 and 5.5-5. The variation in useful in-orbit weight is quite similar to the results discussed in Section 5.4.3.

To determine the adequacy of the constant attitude rate-constant attitude steering profile, the results shown in Figure 5.5-4 were compared with optimum solutions generated with a calculus of variations optimization technique. The steering angle was continually allowed to vary optimally during both the

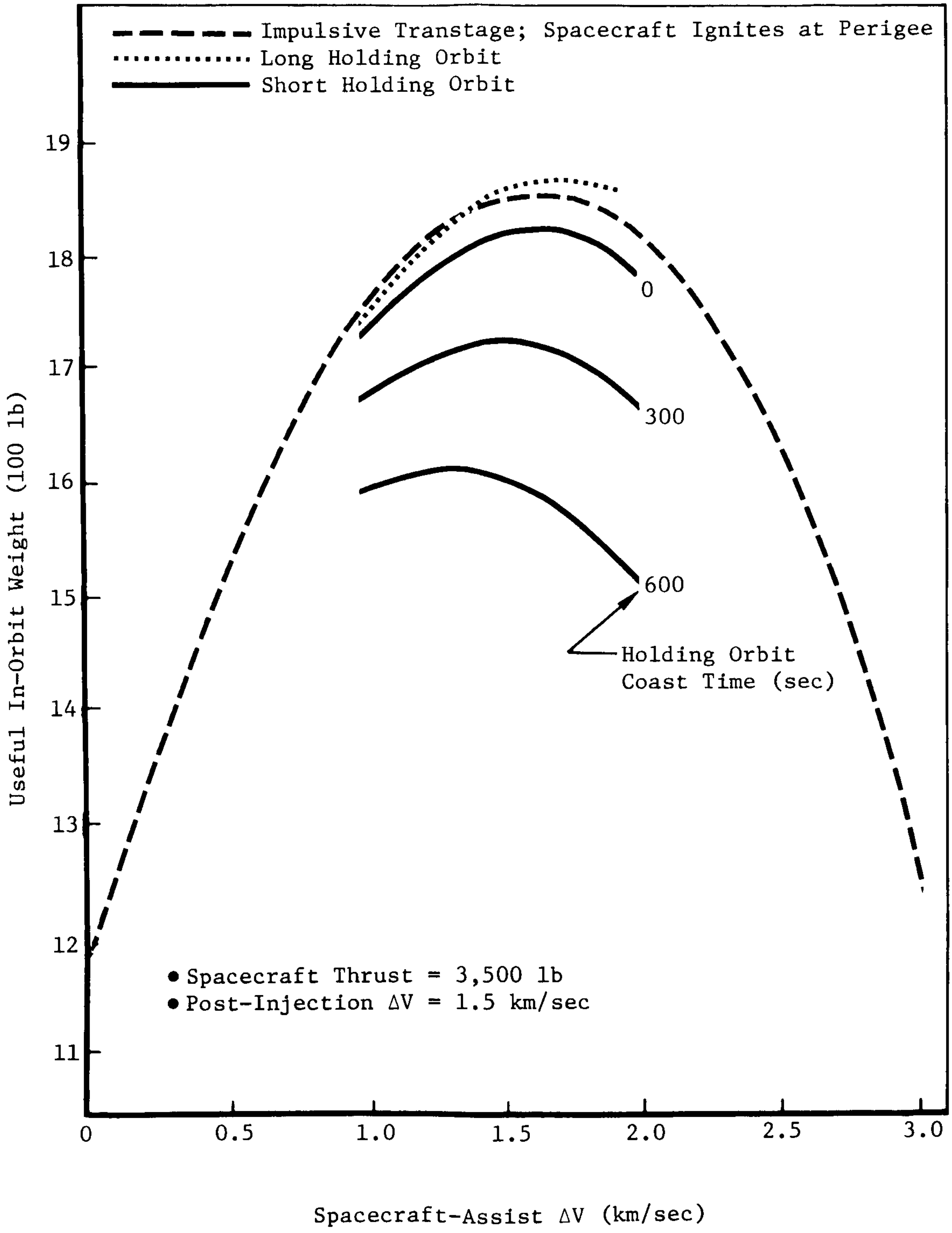

Figure 5.5-3: USEFUL IN-ORBIT WEIGHT COMPARISON---SHORT AND LONG HOLDING ORBITS

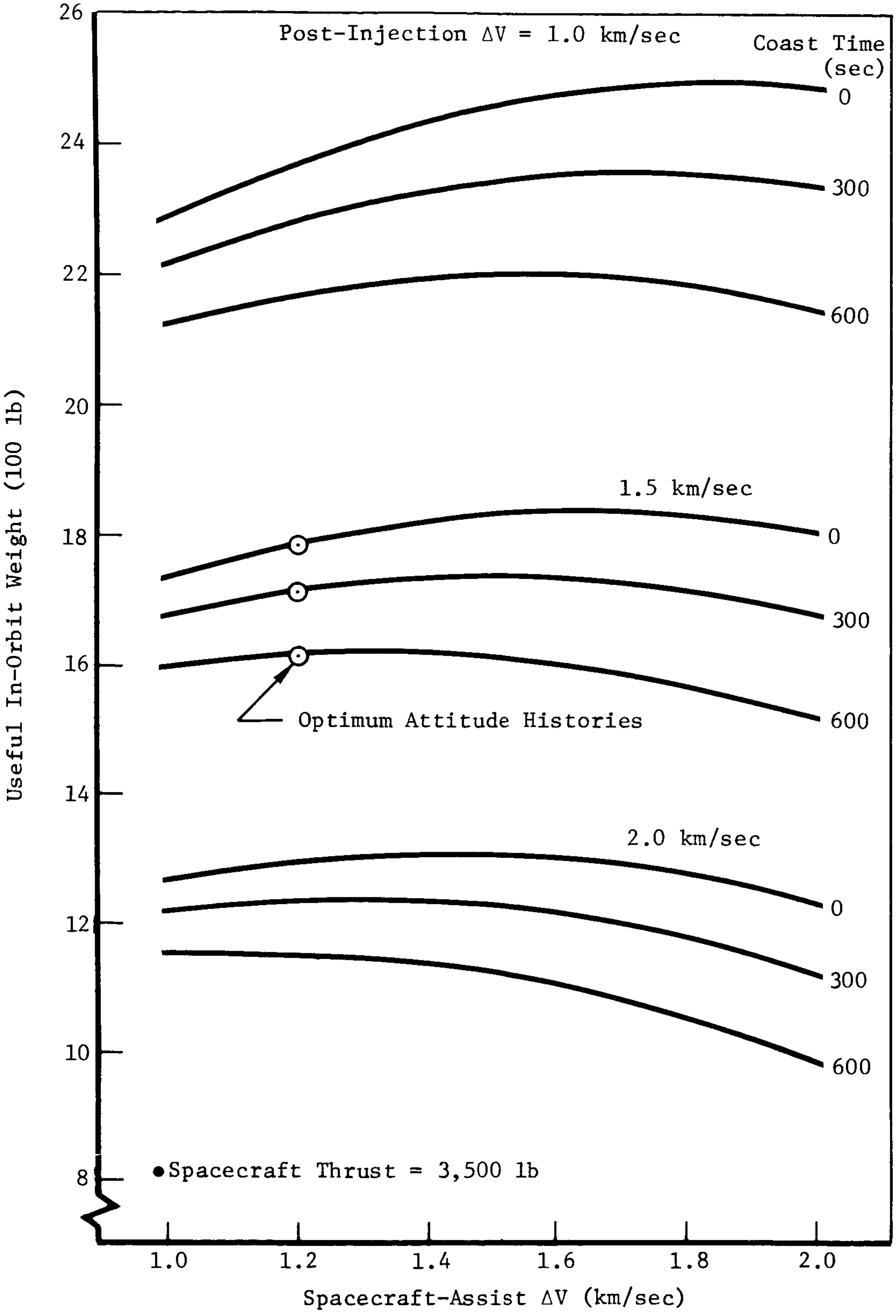

Figure 5.5-4: USEFUL IN-ORBIT WEIGHTS FOR SHORT HOLDING ORBITS

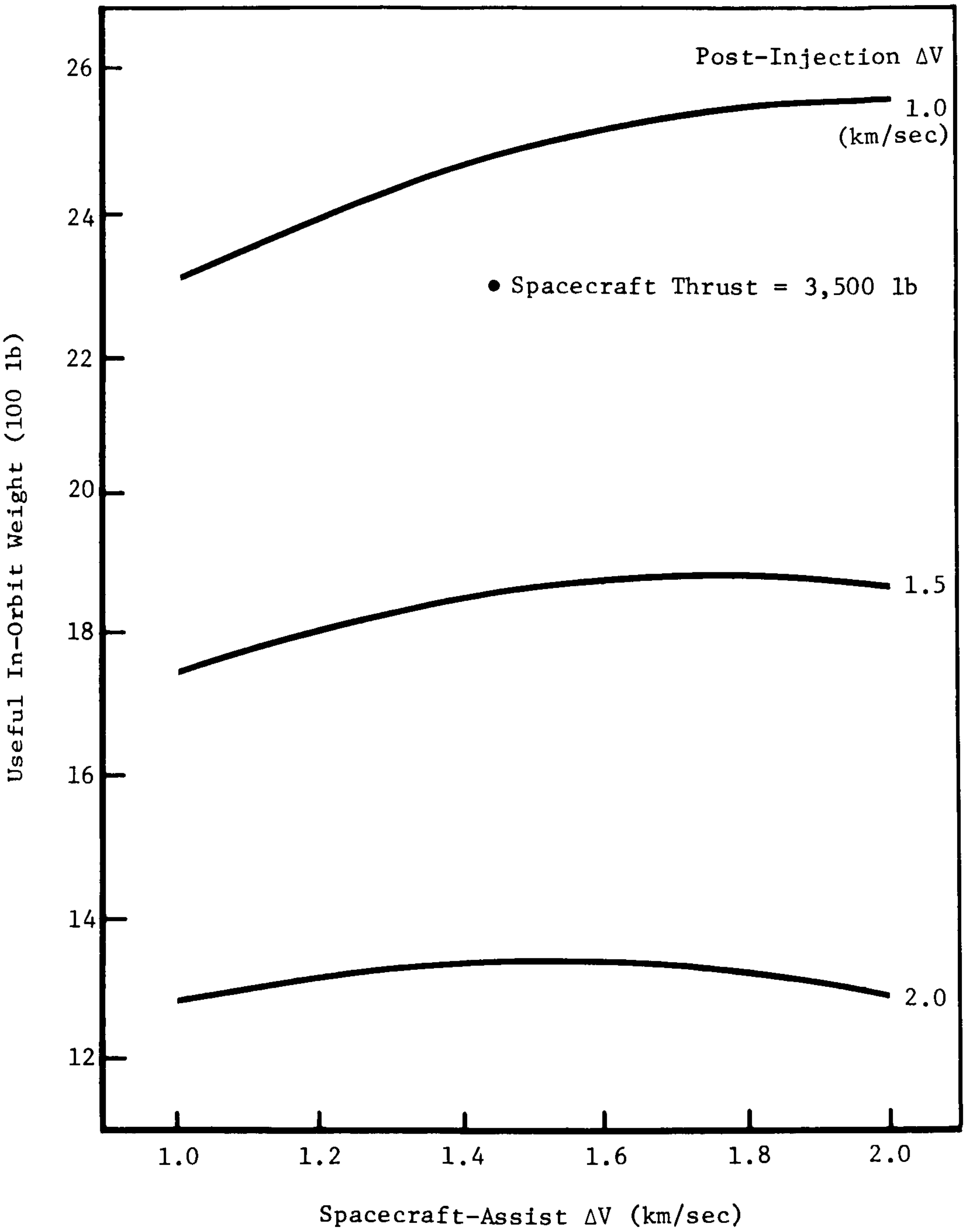

Figure 5.5-5: USEFUL IN-ORBIT WEIGHTS FOR LONG HOLDING ORBITS

transtage and spacecraft burns. The results, determined for a spacecraft-assist ΔV of 1.5 km/sec, are virtually identical with the study results. The variation in useful in-orbit weight amounted to less than 1 pound.

The optimum steering angles and rates calculated for both the short and long holding orbit modes are given in Figure 5.5-6. The negative sign represents pitchdown from the local horizontal at ignition. The only data not shown are the transtage initial attitude and attitude rate for the long holding orbit cases. These values are -2 and -0.055 deg/sec, respectively, and they are invariant with spacecraft-assist ΔV.

The characteristics of the holding orbits are given in Figure 5.5-7. Data are shown for both impulsive and optimum transtage maneuvers. The small decrease in orbit period with the optimum transtage burn is due to the energy lost to finite thrust effects.

### 5.5.2 Titan IIID

Because the final stage of the Titan IIID launch vehicle cannot restart, the spacecraft will be placed into an elliptical parking orbit about Earth. The main purpose of this investigation is to determine the velocity losses incurred during the trans-Mars injection maneuver from the elliptical parking orbit. These losses result from performing the injection maneuver at a high-altitude, low-velocity region on the elliptical orbit. In the analysis, the "injection velocity loss" is defined as the difference between the injection ΔV at the required true anomaly and the ΔV for tangential injection at perigee. This velocity loss represents a velocity increment that must be added to the basic mission ideal velocity requirement, as obtained from analysis based on either a circular parking orbit or an elliptical parking orbit with perigee injection. To obtain the total mission ideal velocity requirement, the velocity losses due to finite burn effects also must be included. These are not treated here.

The trans-Mars injection maneuver often must be performed at a true anomaly on the ellipse that results in high velocity losses. The outgoing trajectory asymptote (parallel to the S-vector) is essentially fixed on a given launch day for a specified arrival day. Launch is possible when the plane established by the center of Earth, launch site location, and a specified launch azimuth has rotated to such a position that it includes the S-vector. (Generally this occurs twice per day. The two launch-time,solutions are identified as the "short coast" and "long coast" solutions, because one has a longer parking orbit coast time than the other.) Thus, the location of the launch site in the trajectory plane is established relative to the S-vector. The launch vehicle characteristics and a specified payload weight establish the inertial geocentric burn arc between the launch site vector (vector from center of Earth through launch site) and the elliptical parking orbit injection vector, as well as the size of the elliptical orbit. This information is sufficient to define the near-Earth trajectory geometry illustrated in Figures 5.5-8a and 5.5-8b.

Figure 5.5-8a shows a case where the outgoing S-vector has such an orientation that trans-Mars injection is possible near the perigee of the elliptical parking orbit. This case requires an injection ΔV that is very close to the minimum ΔV requirement. (This minimum ΔV is required when the maneuver is performed near the closest point to Earth, which is at the perigee of the parking

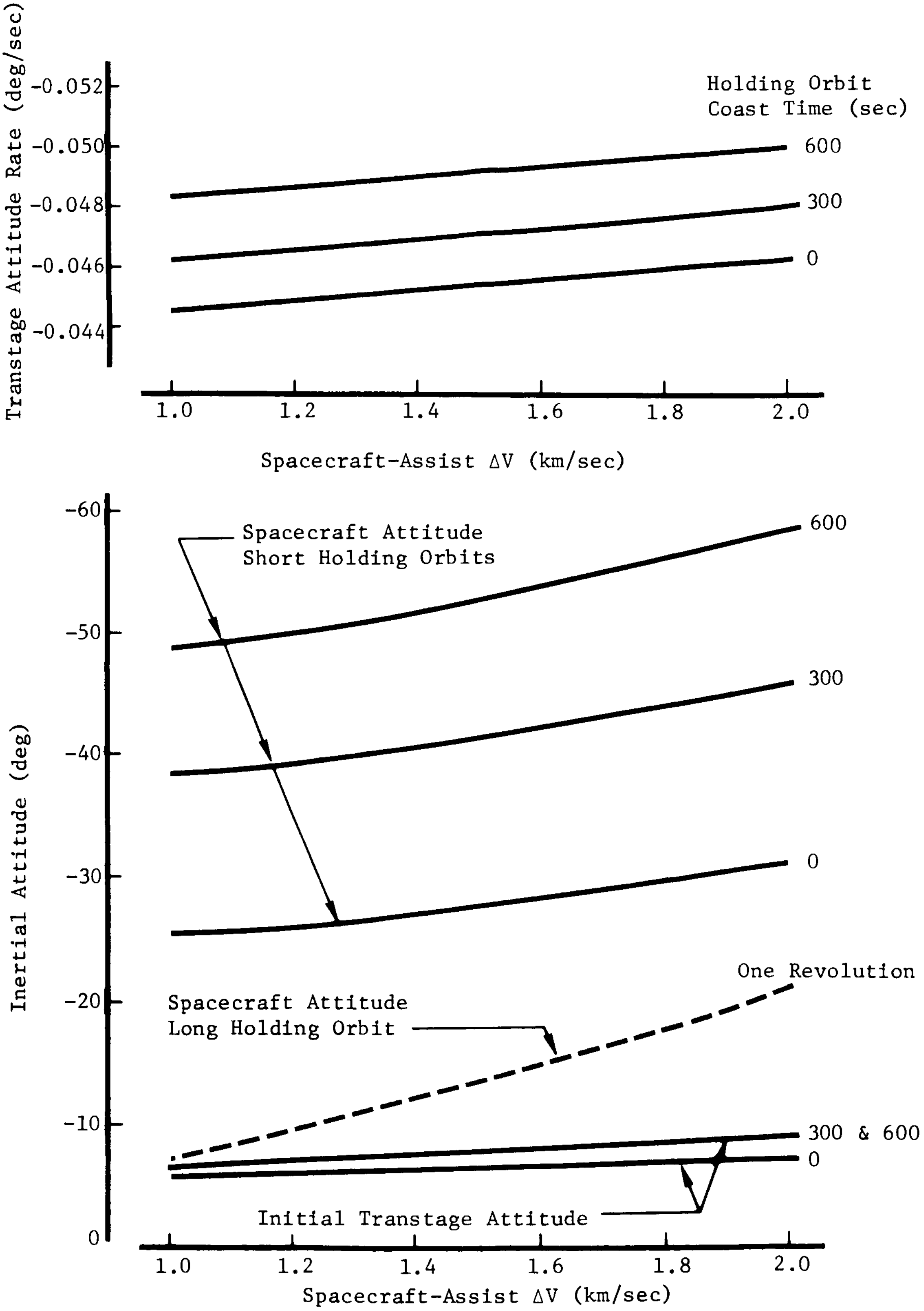

Figure 5.5-6: STEERING PROFILE DEFINITIONS

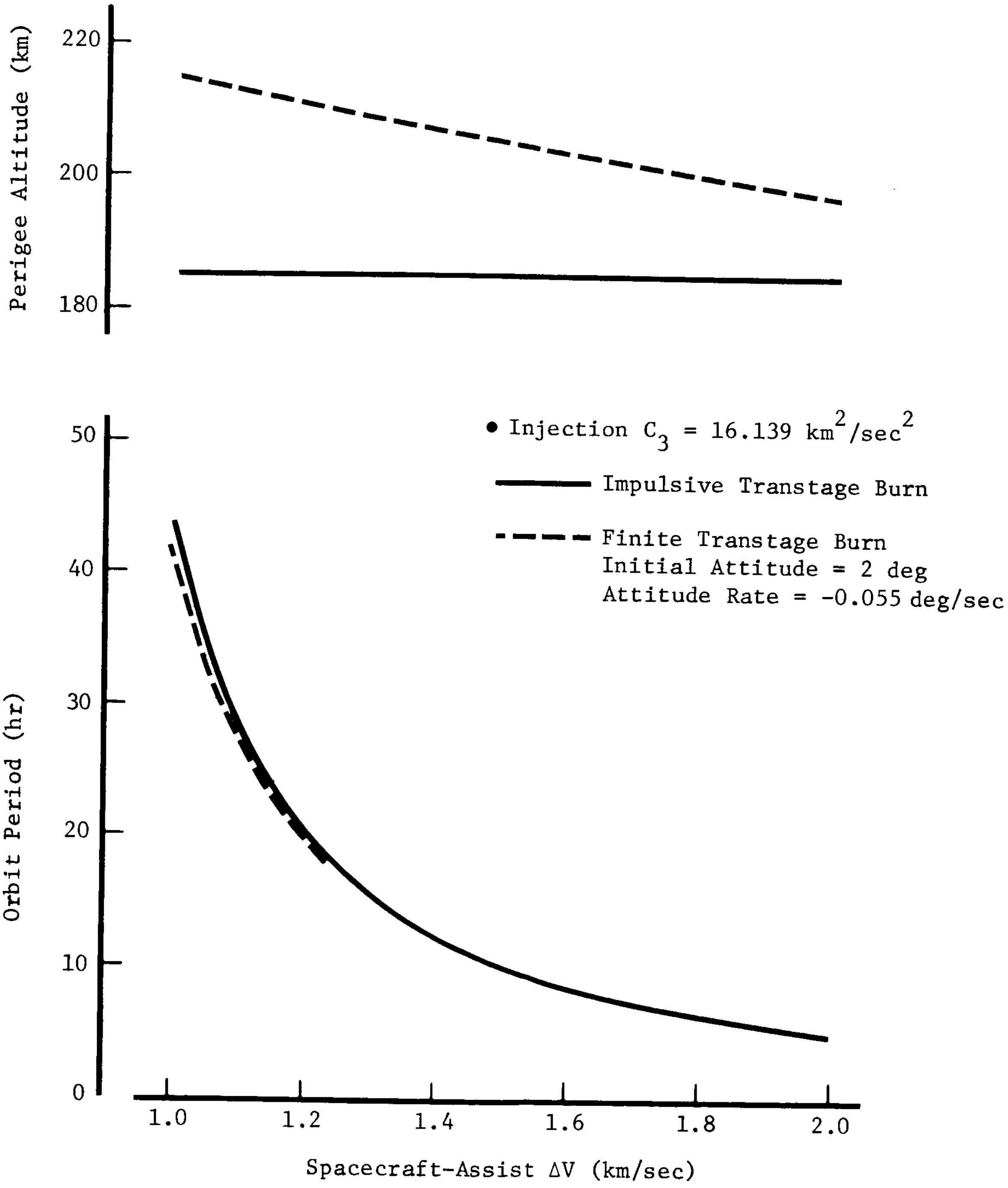

Figure 5.5-7: HOLDING ORBIT CHARACTERISTICS

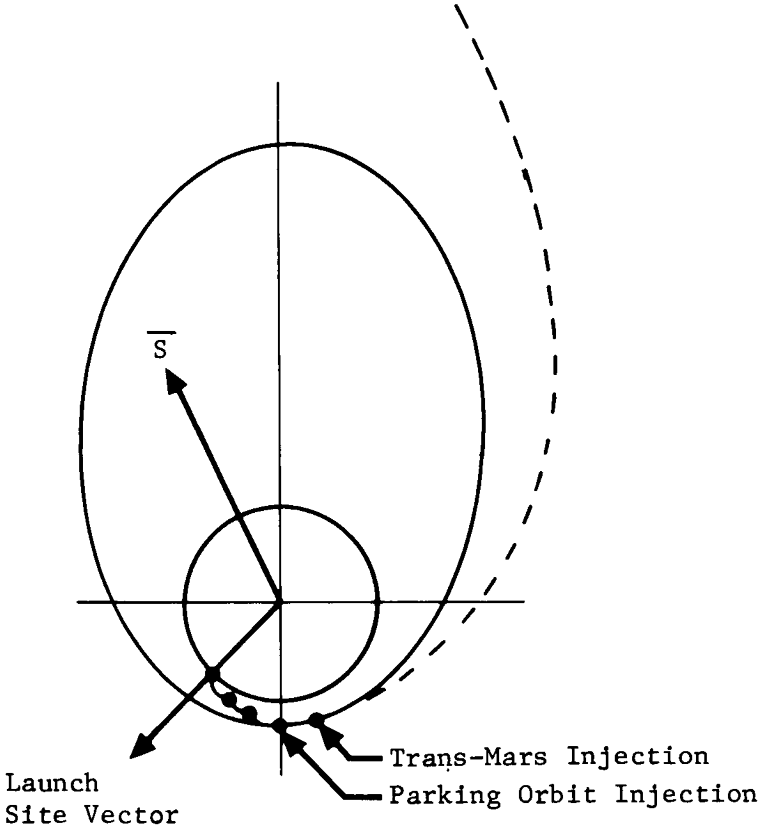
$\overline{S}$
Trans-Mars Injection
Parking Orbit Injection
Launch
Site Vector

Figure 5.5-8a: NEAR-EARTH TRAJECTORY GEOMETRY -- PERIGEE INJECTION

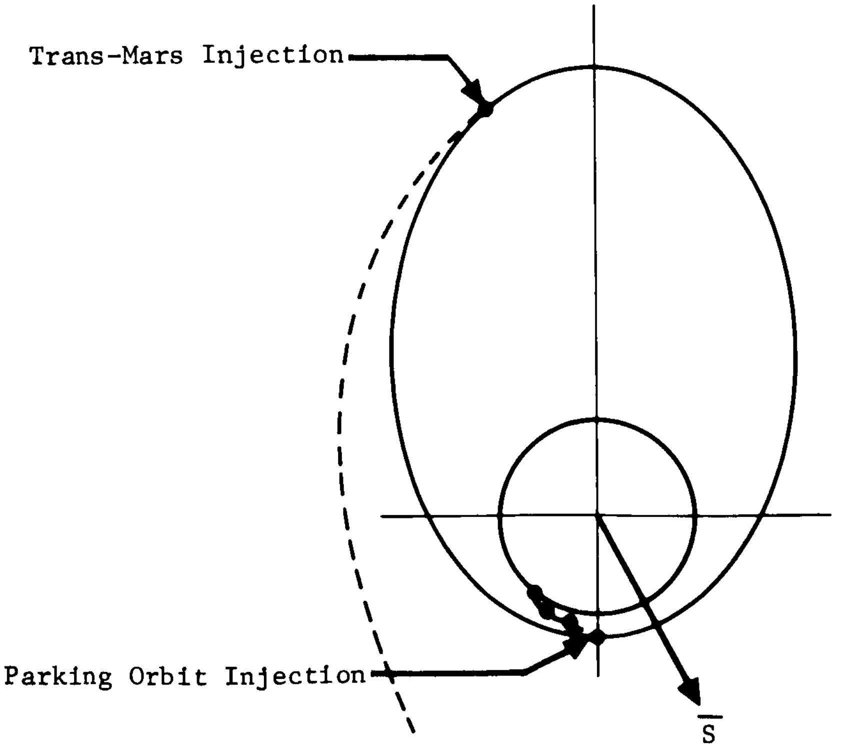
Trans-Mars Injection
Parking Orbit Injection
$\overline{S}$

Figure 5.5-8b: NEAR-EARTH TRAJECTORY GEOMETRY -- OFF-PERIGEE INJECTION

orbit.) The type of near-Earth trajectory geometry shown in the figure is desirable, but it cannot be attained for the Mars 1973 Type I mission.

Figure 5.5-8b illustrates the trajectory geometry typical for the Mars 1973 missions. For these trajectories, the S-vector is so located that trans-Mars injection must occur near apogee of the elliptical parking orbit, and hence high velocity losses are incurred.

Figure 5.5-9 shows the injection velocity loss dependence on launch azimuth and parking orbit size for a typical launch-arrival day combination with a short parking orbit coast. Two guidance laws are considered in the analysis. The first, or "tangential," requires that the velocity vector on the trans-Mars trajectory is parallel to that on the ellipse at injection. Tangential solutions are considered because they can be handled in closed form. The second guidance law, or "optimum," minimizes the injection $\Delta V$ by using a search routine to find the optimum vehicle attitude and injection true anomaly. Three spacecraft-assist $\Delta V$'s are used. These yield the elliptical parking orbit sizes indicated in Figure 5.5-9. These $\Delta V$'s represent the velocity increments the spacecraft would provide for trans-Mars injection if the velocity losses were zero. The actual velocity requirements are obtained by adding the velocity losses to the spacecraft-assist $\Delta V$.

The injection true anomalies are shown in Figure 5.5-10. Note that the injection occurs near apogee (true anomaly = 180 degrees). This explains the high velocity losses.

Figures 5.5-11 and 5.5-12 show the injection velocity losses and injection true anomalies for the same launch-arrival date combination employing a long parking orbit coast. Decreasing the launch azimuth moves the injection point away from apogee and the injection velocity loss decreases. Thus, for the specific launch-arrival day combination considered, the injection velocity loss can be reduced by using a long parking orbit coast, considering northerly launch azimuths, and increasing the spacecraft-assist $\Delta V$. The data also shows that the injection $\Delta V$'s for tangential injection maneuvers approach those for optimum maneuvers as the parking orbit eccentricity is reduced (spacecraft-assist $\Delta V$ is increased) and the injection true anomaly approaches 180 degrees.

Table 5.5-1 gives the minimum velocity losses for the launch-arrival day combinations that encompass the Mars 1973 Type I envelope. Tangential injection is employed and the parking orbit period is 10.1 hours (spacecraft-assist $\Delta V$ = 1.5 km/sec). The launch-arrival day envelope used is established by the $V_\infty$, $C_3$, DLA, and launch period length constraints indicated in the sketch on the table. The long coast solutions give the minimum velocity losses for the launch-arrival day combinations investigated. These minimum velocity losses are about, 1,000 m/sec and are obtained by launching at the lowest allowable launch azimuth of 66 degrees.

In summary, the velocity losses encountered due to the use of elliptical parking orbits vary from 1 to 3 km/sec for Type I missions to Mars in 1973. A loss of 1 km/sec reduces useful in-orbit weight by approximately 1,100 pounds. Consequently, the useful in-orbit weights that Titan IIID can deliver to Mars are very small and may even be negative. This result clearly eliminates Titan IIID from consideration as a launch vehicle for a Mars 1973 powered spacecraft mission.

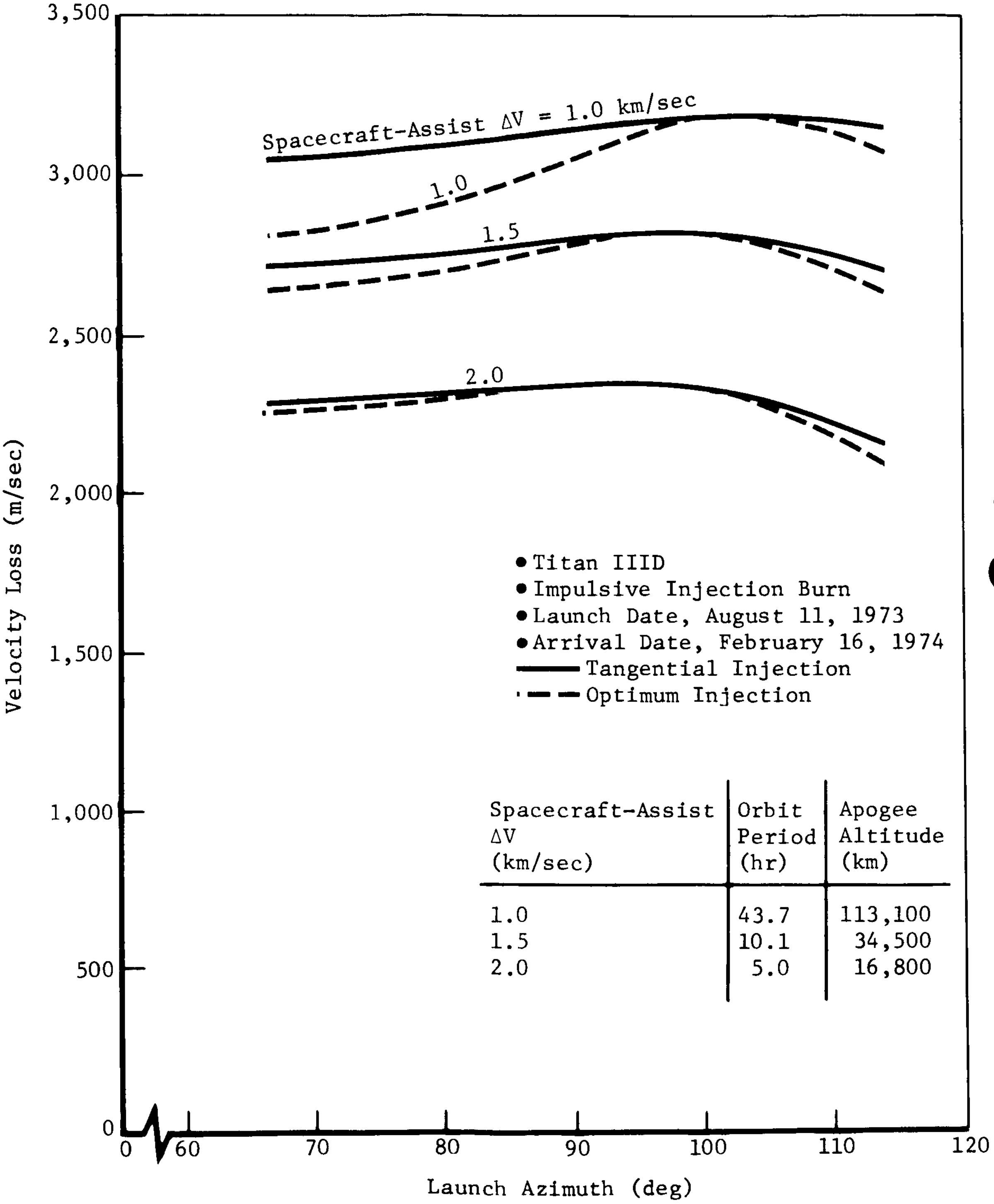

| Spacecraft-Assist ΔV (km/sec) | Orbit Period (hr) | Apogee Altitude (km) |
|---|---|---|
| 1.0 | 43.7 | 113,100 |
| 1.5 | 10.1 | 34,500 |
| 2.0 | 5.0 | 16,800 |

Figure 5.5-9: INJECTION VELOCITY LOSS WITH ELLIPTICAL PARKING ORBITS---SHORT COAST

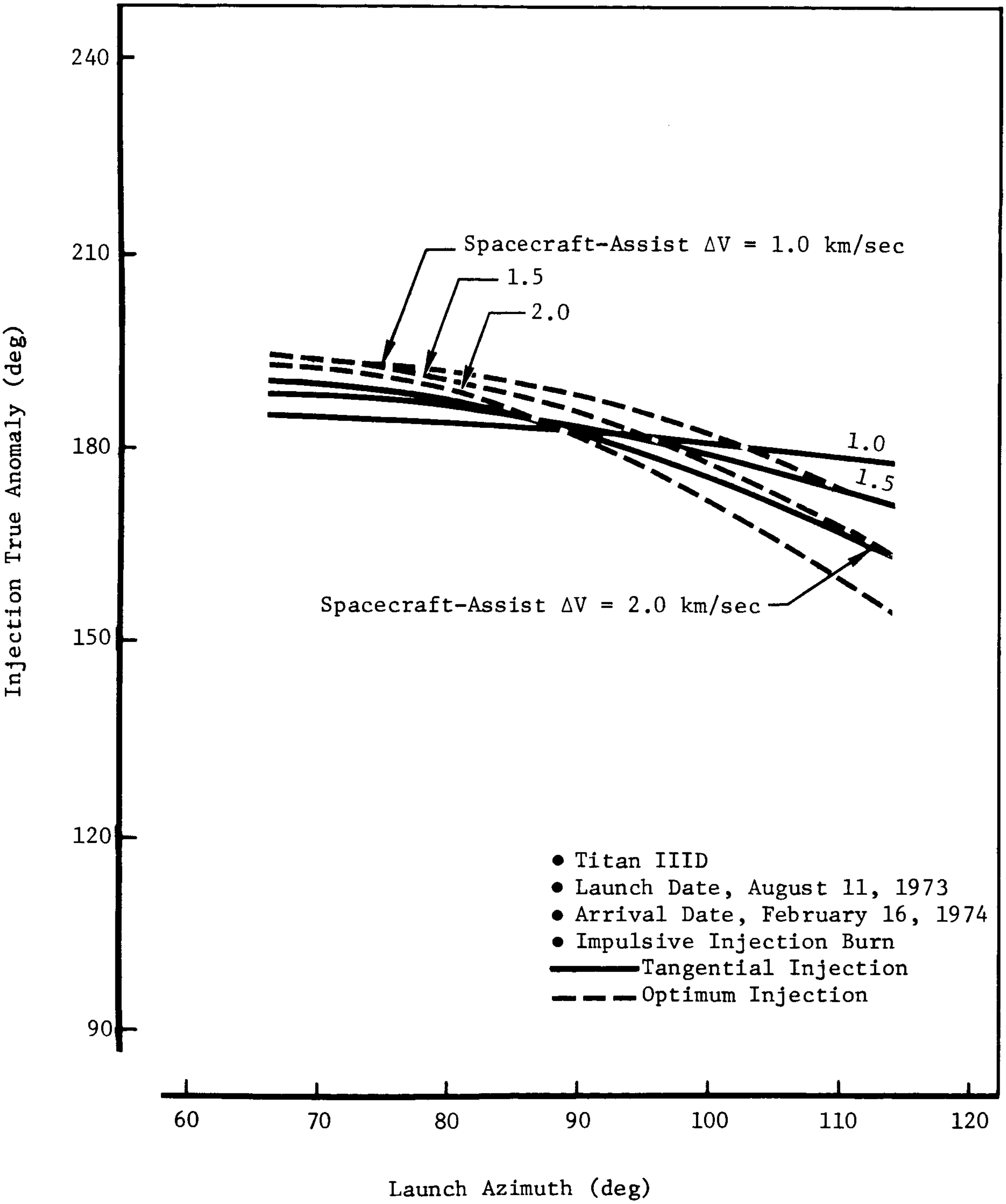

Figure 5.5-10: INJECTION TRUE ANOMALIES WITH ELLIPTICAL PARKING ORBITS---SHORT COAST

LONG COAST

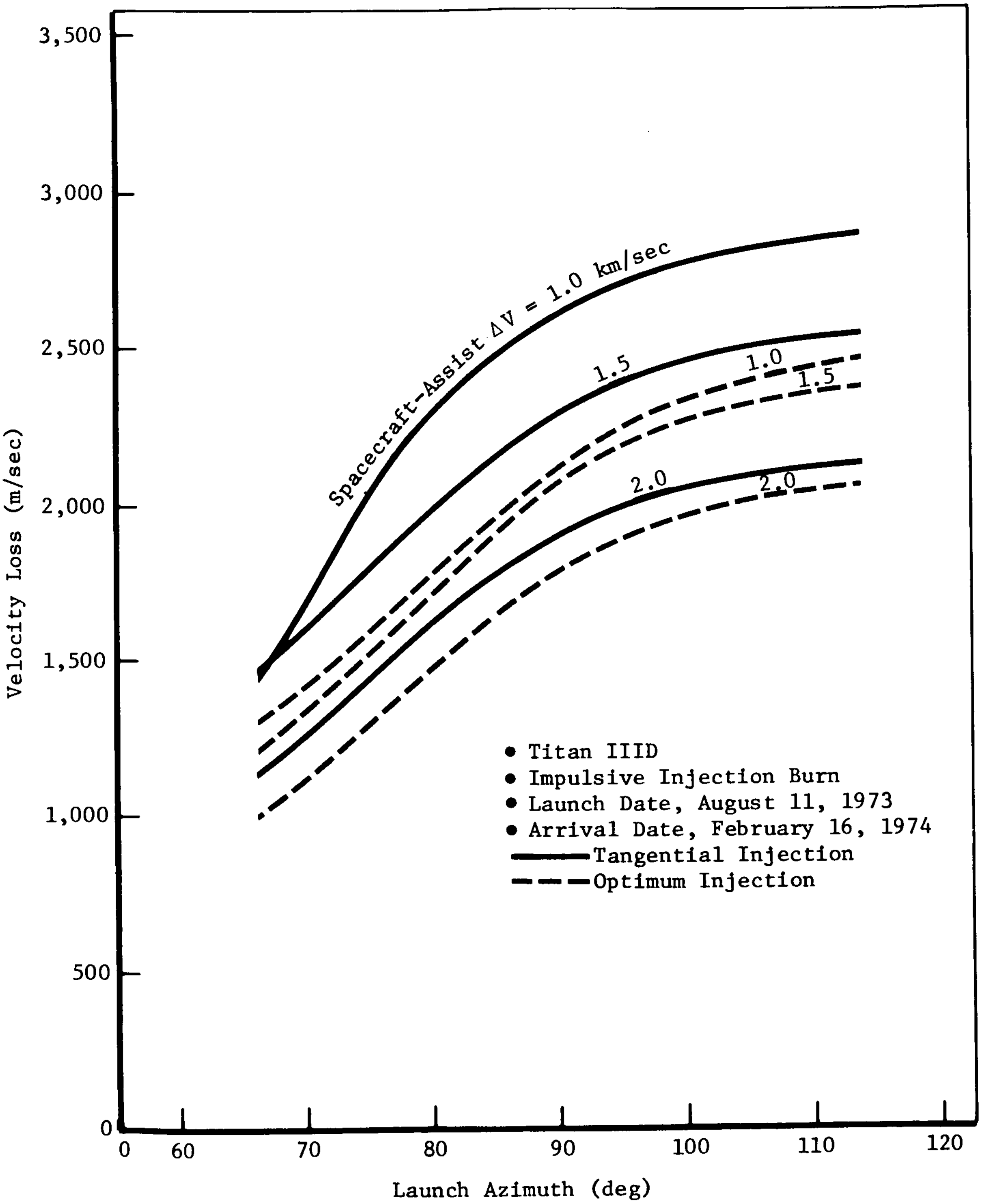

Figure 5.5-11: INJECTION VELOCITY LOSS WITH ELLIPTICAL PARKING ORBITS---LONG COAST

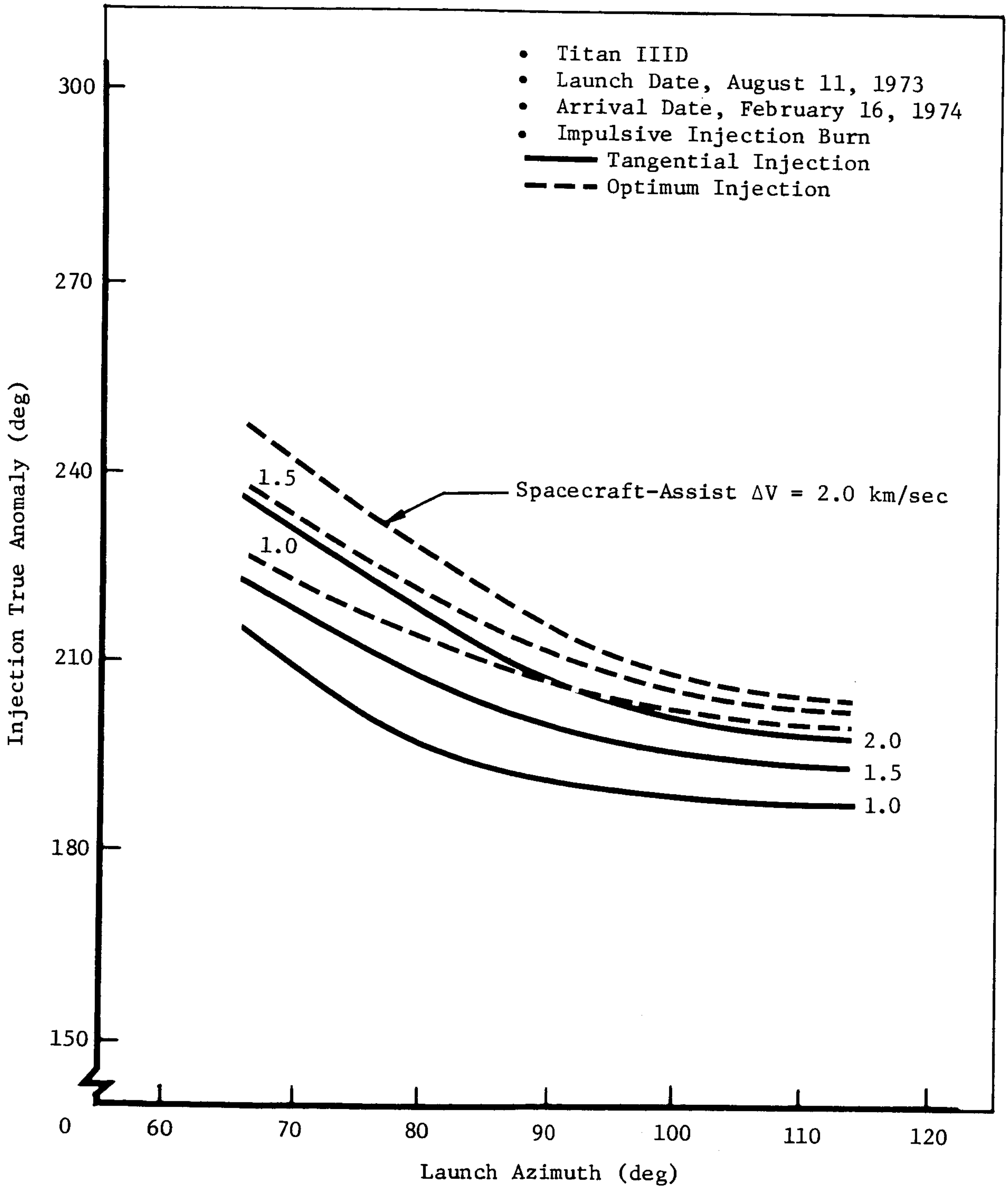

Figure 5.5-12: INJECTION TRUE ANOMALIES WITH ELLIPTICAL PARKING ORBITS---LONG COAST

## Table 5.5-1: LAUNCH-ARRIVAL DATE EFFECTS ON INJECTION VELOCITY LOSS

| Trajectory Number | Launch Day 1973 | Arrival Day 1974 | Short Coast | | | Long Coast | | |
|---|---|---|---|---|---|---|---|---|
| | | | Launch Azimuth For Minimum Loss (deg) | Minimum Velocity Loss (m/sec) | Injection True Anomaly (deg) | Launch Azimuth For Minimum Loss (deg) | Minimum Velocity Loss (m/sec) | Injection True Anomoly (deg) |
| 1 | July 3 | Jan. 16 | 114 | 2,798 | 190.1 | 66 | 1,835 | 215.4 |
| 2 | Aug. 1 | Jan. 22 | 114 | 2,659 | 171.1 | 66 | 1,461 | 222.5 |
| 3 | Aug. 20 | Jan. 26 | 114 | 2,782 | 167.7 | 66 | 1,082 | 241.0 |
| 4 | Aug. 22 | Mar. 5 | 114 | 2,860 | 170.5 | 66 | 1,294 | 232.8 |
| 5 | Aug. 2 | Mar. 5 | 114 | 2,758 | 185.0 | 66 | 2,113 | 204.6 |
| 6 | July 4 | Jan. 24 | 114 | 2,904 | 185.7 | 66 | 2,165 | 206.8 |
| 7 | July 23 | Feb. 16 | 114 | 2,763 | 184.0 | 66 | 2,167 | 203.1 |
| 8 | Aug. 1 | Feb. 16 | 114 | 2,611 | 189.8 | 66 | 1,750 | 213.4 |
| 9 | Aug. 11 | Feb. 16 | 114 | 2,710 | 171.4 | 66 | 1,466 | 223.3 |

- Tangential injection with impulsive burn
- Parking orbit period = 10.1 hours
  (Spacecraft-assist $\Delta V \cong 1.5$ km/sec)
- Launch azimuth range investigated is between
  66 and 114 degrees

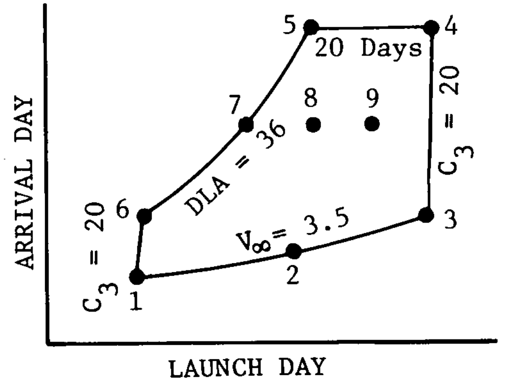

## 5.6 OPERATIONAL ANALYSES

These analyses were conducted to determine the operational feasibility of the powered spacecraft mission. Operational feasibility was to be established by conducting: (1) launch analyses, (2) tracking and data acquisition analyses, (3) event-sequence analyses, and (4) guidance analyses.

### 5.6.1 Launch Analysis

The task of designing an interplanetary trajectory includes finding an ascent trajectory that satisfies both geometric and launch constraints. The analysis required is briefly defined in Section 5.5.2. This section examines the near-Earth trajectory characteristics over the 20-day launch period with fixed arrival date defined in Section 5.3. Launch times, launch windows, parking orbit coast times, and near-Earth shadow times are shown. Only the Titan IIIC launch vehicle using a 100 n mi parking orbit is considered.

Figure 5.6-1 shows the launch time variation with launch azimuth for 3 launch days spanning the launch period. For each launch day two launch windows exist. These windows correspond to short and long parking orbit coast periods. For July 23 and August 1 launches, azimuths around 90 degrees cannot be used because the required declinations of the outgoing asymptote (DLA) exceed the latitude of the launch site.

The launch window durations are shown in Figure 5.6-2 for all days in the 20-day launch period. The window length varies from a minimum of 1.1 to a maximum of 5.74 hours. (Two such windows can be obtained per day---one for the short parking orbit coast and the other for the long coast solutions.) The maximum launch window is obtained for all days having a DLA less than the launch site geocentric latitude (28.56 degrees).

Figure 5.6-3 shows the parking orbit coast time variations with launch azimuth for 3 launch days. This data assumes impulsive trans-Mars injection at a zero flight-path angle. A typical finite burn trans-Mars injection maneuver employing a 120-second coast between transtage final cutoff and spacecraft ignition will reduce all parking orbit coast times shown by about 300 seconds.

Near-Earth shadow entry and exit times for each day are shown in Figures 5.6-4 and 5.6-5 for the short and long parking orbit coast solutions. Maximum launch-to-shadow exit times of about 90 minutes are encountered. For each day, event times are shown for the launch azimuth that has the longest launch-to-shadow exit time. Launches on or before August 2 have values of DLA greater than the launch latitude. Launches after August 2 have smaller DLA's. As a result, the longest launch-to-shadow exit times occur at different launch azimuths and discontinuities result.

The circled points show event times for a typical finite burn injection maneuver that employs a 120-second coast between transtage final cutoff and spacecraft ignition (short holding orbit). For this finite burn maneuver, the shadow exit time occurs about 3 minutes later.

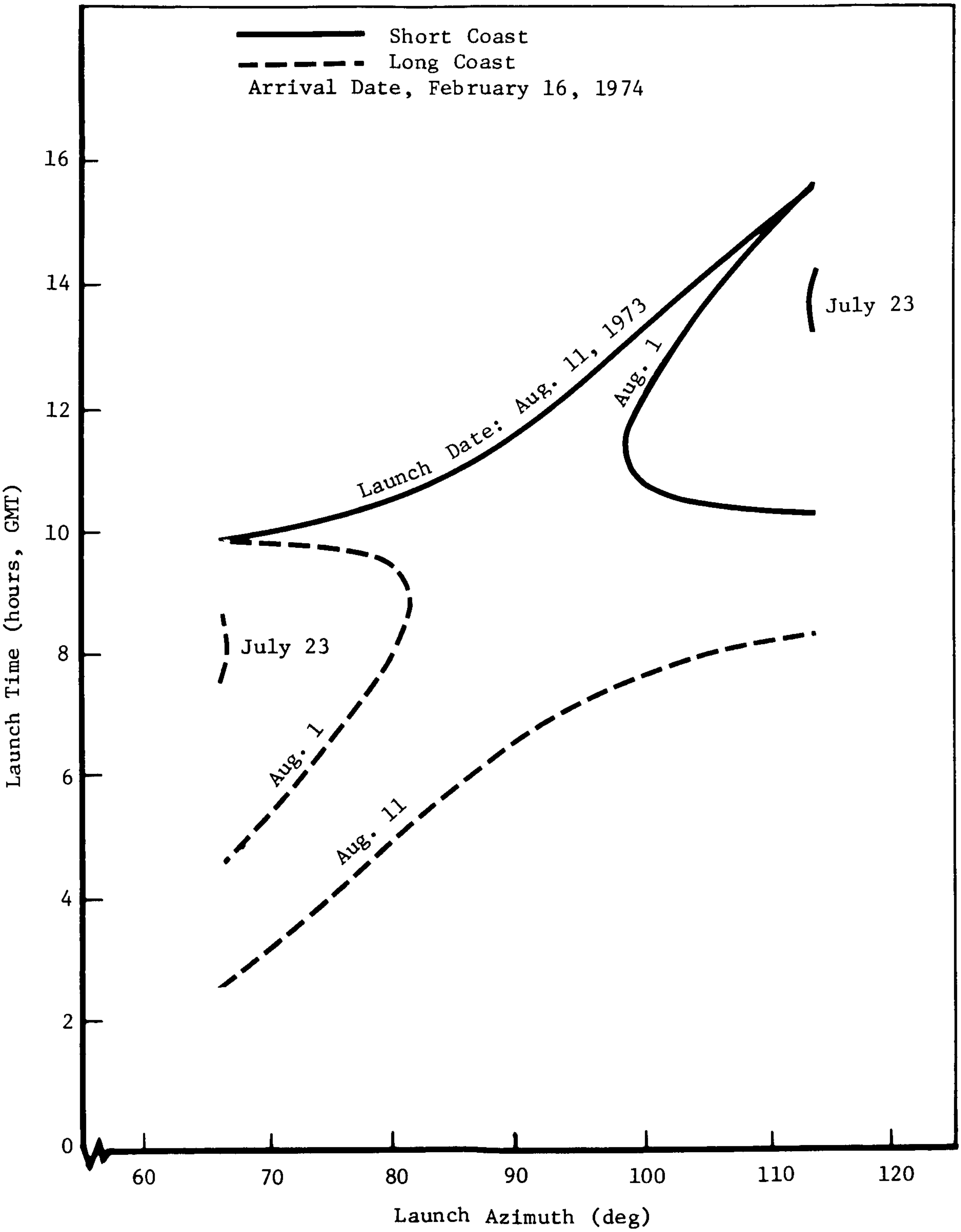

Figure 5.6-1: LAUNCH TIME VARIATION WITH LAUNCH AZIMUTH

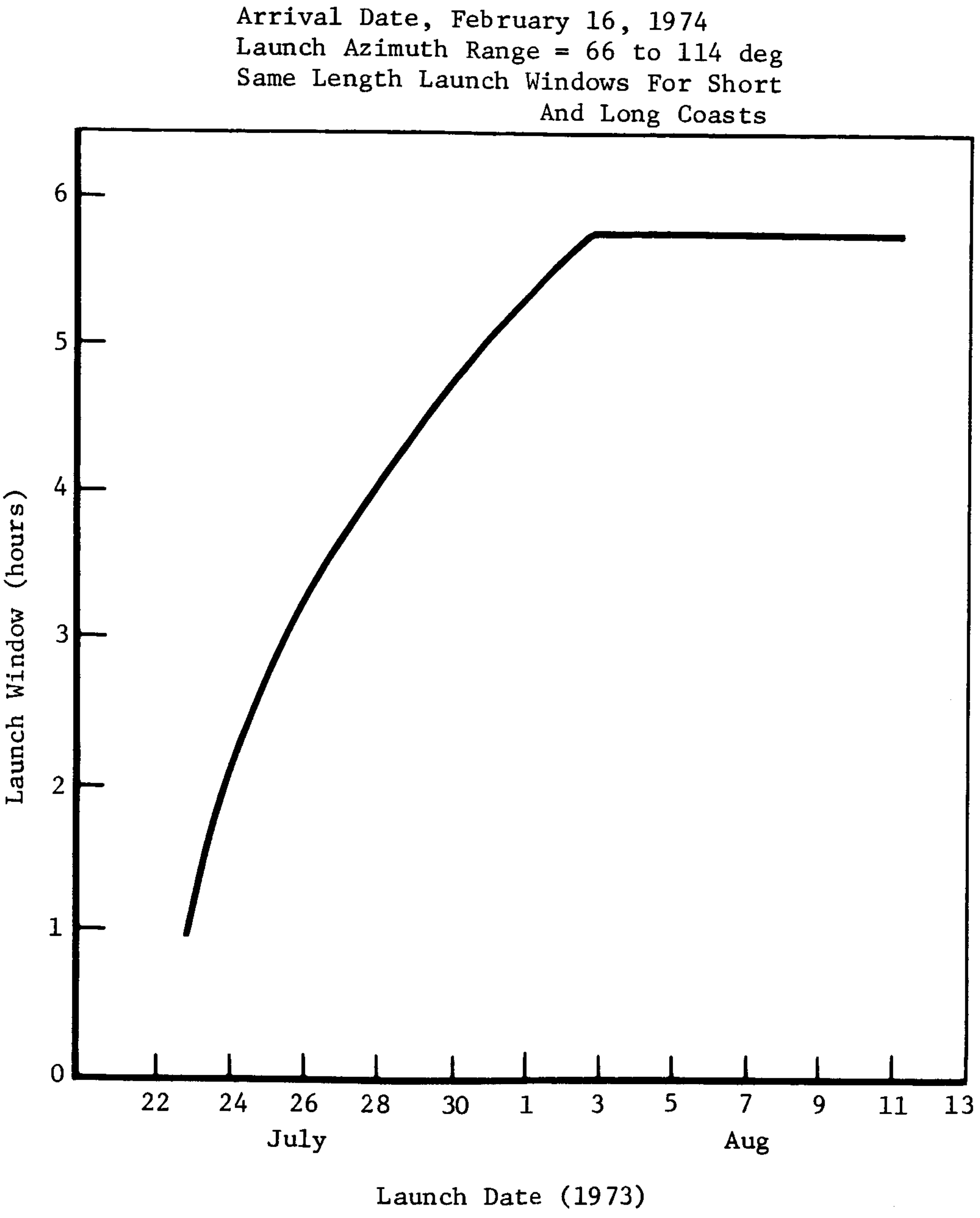

Figure 5.6-2: LAUNCH WINDOW DURATIONS

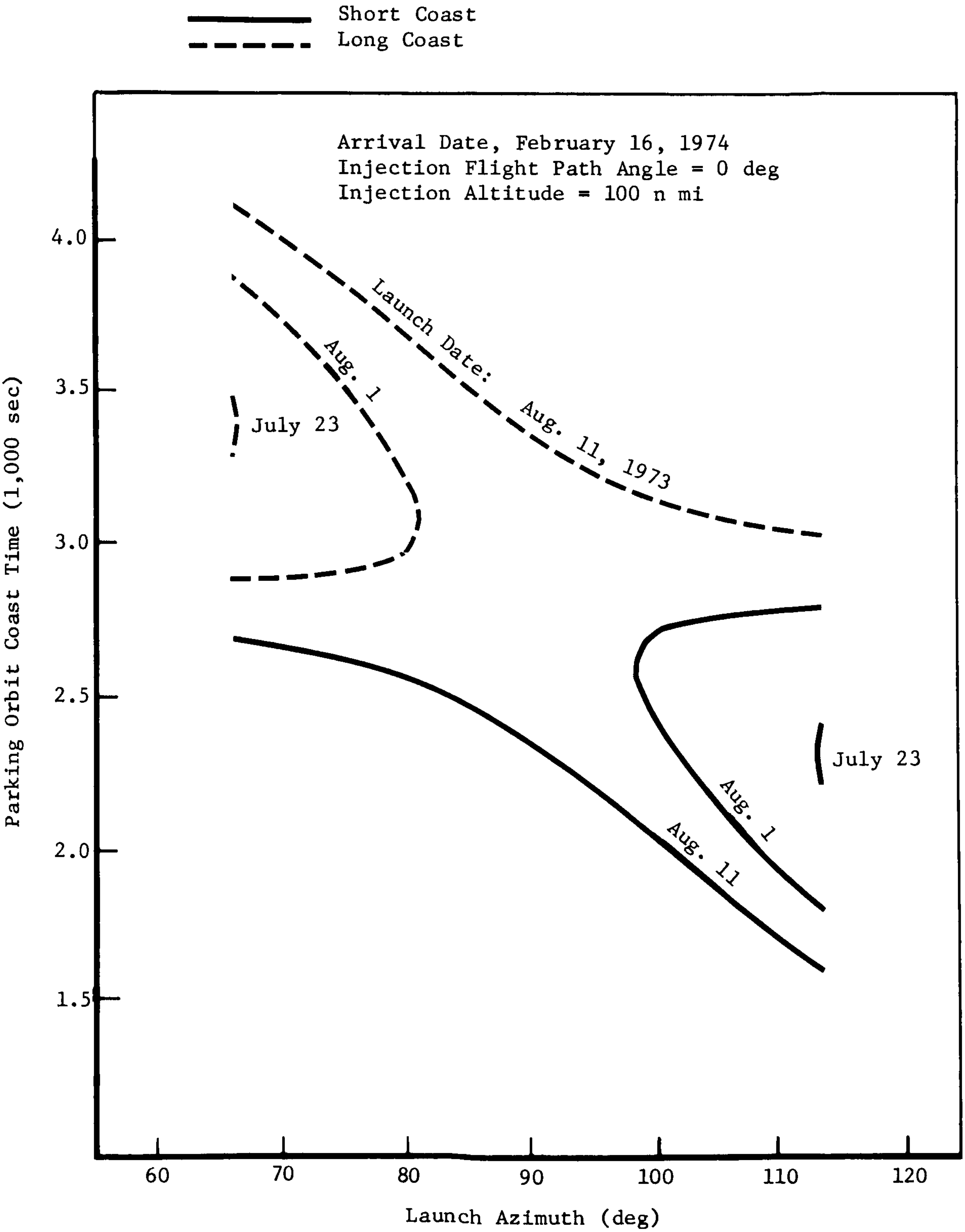

Figure 5.6-3: PARKING ORBIT COAST TIME

Arrival Date, February 16, 1974
Injection Flight Path Angle = 0 deg
Injection Altitude = 100 n mi

On Each Day Data Are Shown For That Launch Azimuth That Gives Longest Launch To Shadow-Exit Time

⊙ Finite Burn Injection With $\gamma_{Inj}$ = 15 deg

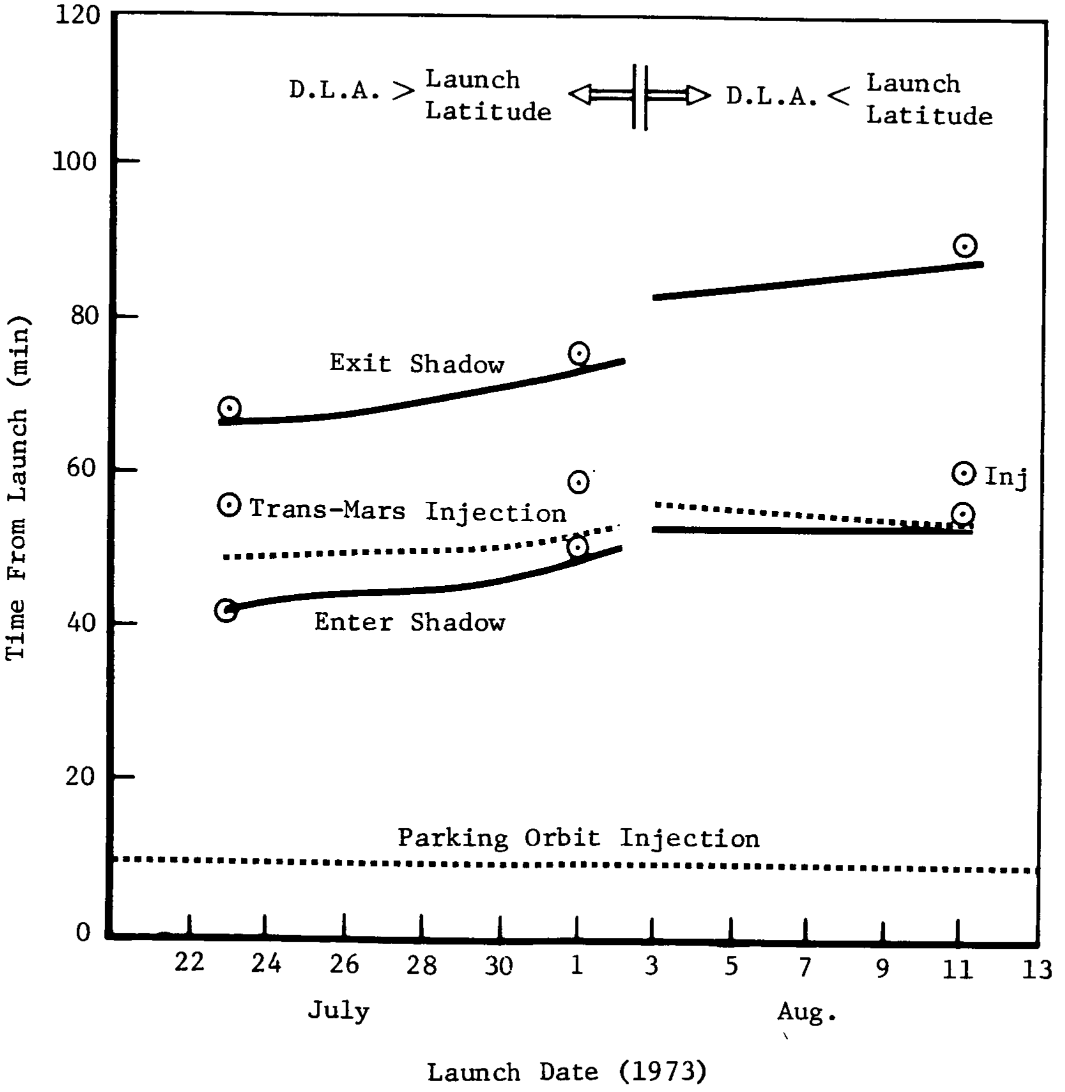

Figure 5.6-4: NEAR-EARTH SHADOW ENTRY AND EXIT TIME---SHORT COAST

Arrival Date, February 16, 1974
Injection Flight Path Angle = 0 deg
Injection Altitude = 100 n mi

On Each Day Data Are Shown For That Launch Azimuth That Gives Longest Launch To Shadow-Exit Time

⊙ Finite Burn Injection With $\gamma_{Inj}$ = 15 deg

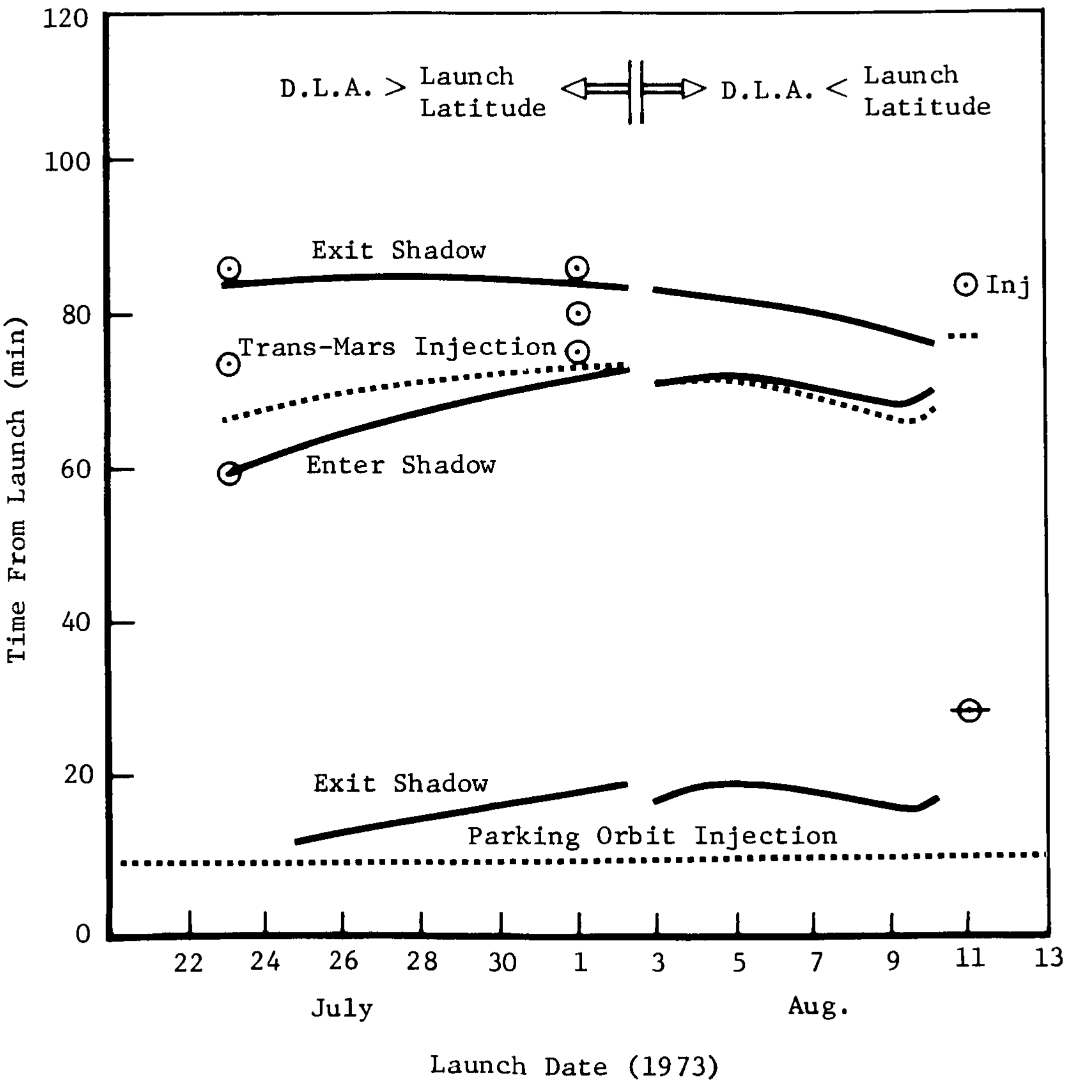

Figure 5.6-5: NEAR-EARTH SHADOW ENTRY AND EXIT TIME---LONG COAST

The data are based on the assumption that the holding orbit coast times are short. If the spacecraft spends a full revolution in the holding orbit (long holding orbit), then the trans-Mars injection times can be interpreted as the holding orbit injection times. Consequently, the data are applicable to the long holding orbit case. After one revolution in the holding orbit, the spacecraft will encounter another similar shadow period near the trans-Mars injection point.

Although a specific 20-day launch period with a constant arrival day has been considered here, other studies indicate that the event times shown are representative for launches occurring anywhere in the Mars 1973 Type I opportunity.

### 5.6.2 Tracking and Data Acquisition

Study of the ascent, parking orbit, long holding orbit, and trans-Mars mission phases shows that no unusual tracking problems result from the use of a powered spacecraft. Tracking ships may have to be employed if real-time telemetry is desired during the long holding orbit and trans-Mars injection maneuvers.

Tracking station visibility of the vehicle during the various trajectory phases has been determined for the tracking stations defined in Appendix A4. Figure 5.6-6 shows the tracking coverage obtained during the ascent and parking orbit phases. Continuous station coverage is obtained during the ascent phase (launch to parking orbit injection). However, coverage in the parking orbit is very spotty. The tracking data shown is applicable for any launch and arrival day.

Superimposed on Figure 5.6-6 are the injection loci for 3 days spanning the 20-day launch period defined in Section 5.3. Both short and long parking orbit coast loci are shown. The injection maneuver is not visible by any tracking station for some launch days and launch azimuths. Injection refers to trans-Mars injection when short holding orbit coasts are employed and holding orbit injection when long holding orbits are employed. It is assumed that the injection occurs impulsively at zero flight-path angle and an altitude of 100 n mi.

Tracking ships may be used to increase tracking coverage of the injection maneuver. Figure 5.6-7 illustrates how three stationary ships (shaded region) cover the entire injection loci for the short parking orbit coast solutions of the 20-day launch period. Figure 5.6-8 shows the trajectory ground tracks, the injection loci for the 3 launch days, and the position and approximate tracking coverage of each ship. Complete coverage from only two ships is possible if the ships are allowed to change their position from day to day during the launch period. This is the normal mode of operation.

Station coverage for the entire near-Earth portion of typical trajectories employing a long holding orbit is shown in Figures 5.6-9 and -10 for short and long parking orbit coasts, respectively. Redundant coverage is obtained everywhere except during injection into the long holding orbit and trans-Mars injection maneuvers. Tracking ships may have to be used to see these two maneuvers at certain launch days and launch azimuths. Almost continuous station viewing exists during the long holding orbit. Continuous DSIF station

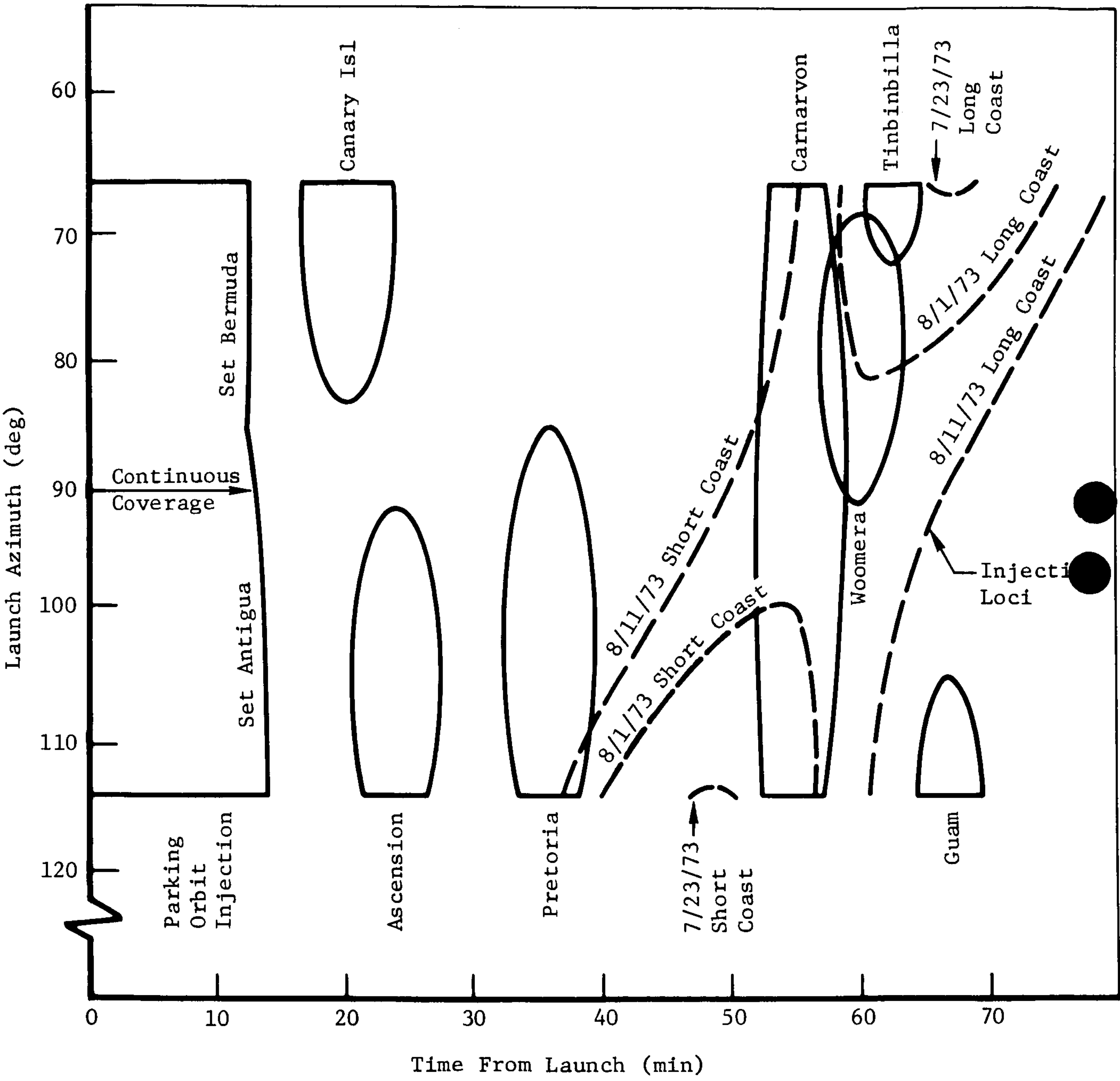

Figure 5.6-6: STATION TRACKING COVERAGE---LAUNCH PHASE---SHORT PARKING ORBIT COAST

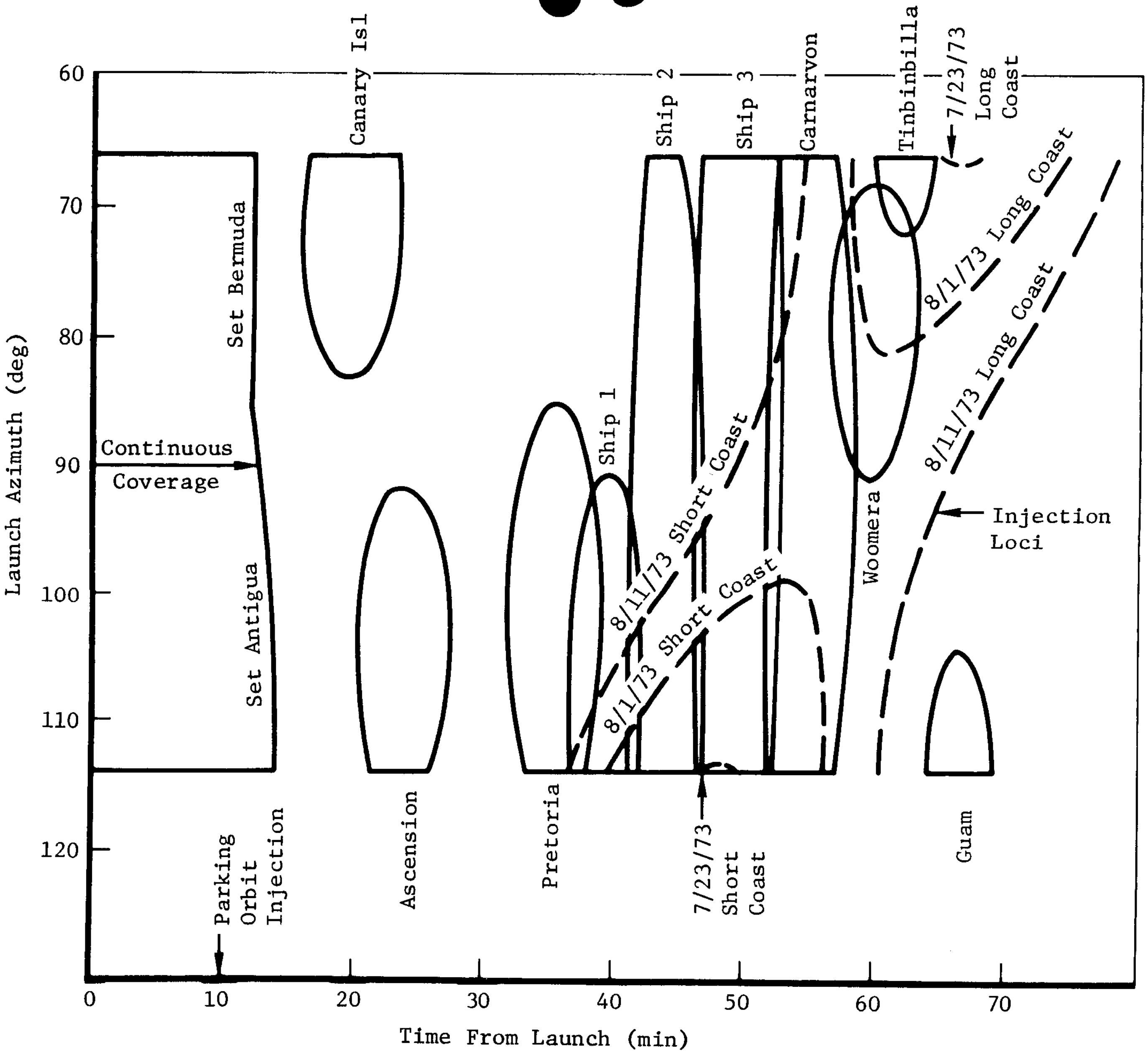

Figure 5.6-7: STATION TRACKING COVERAGE---LAUNCH PHASE---LONG PARKING ORBIT COAST

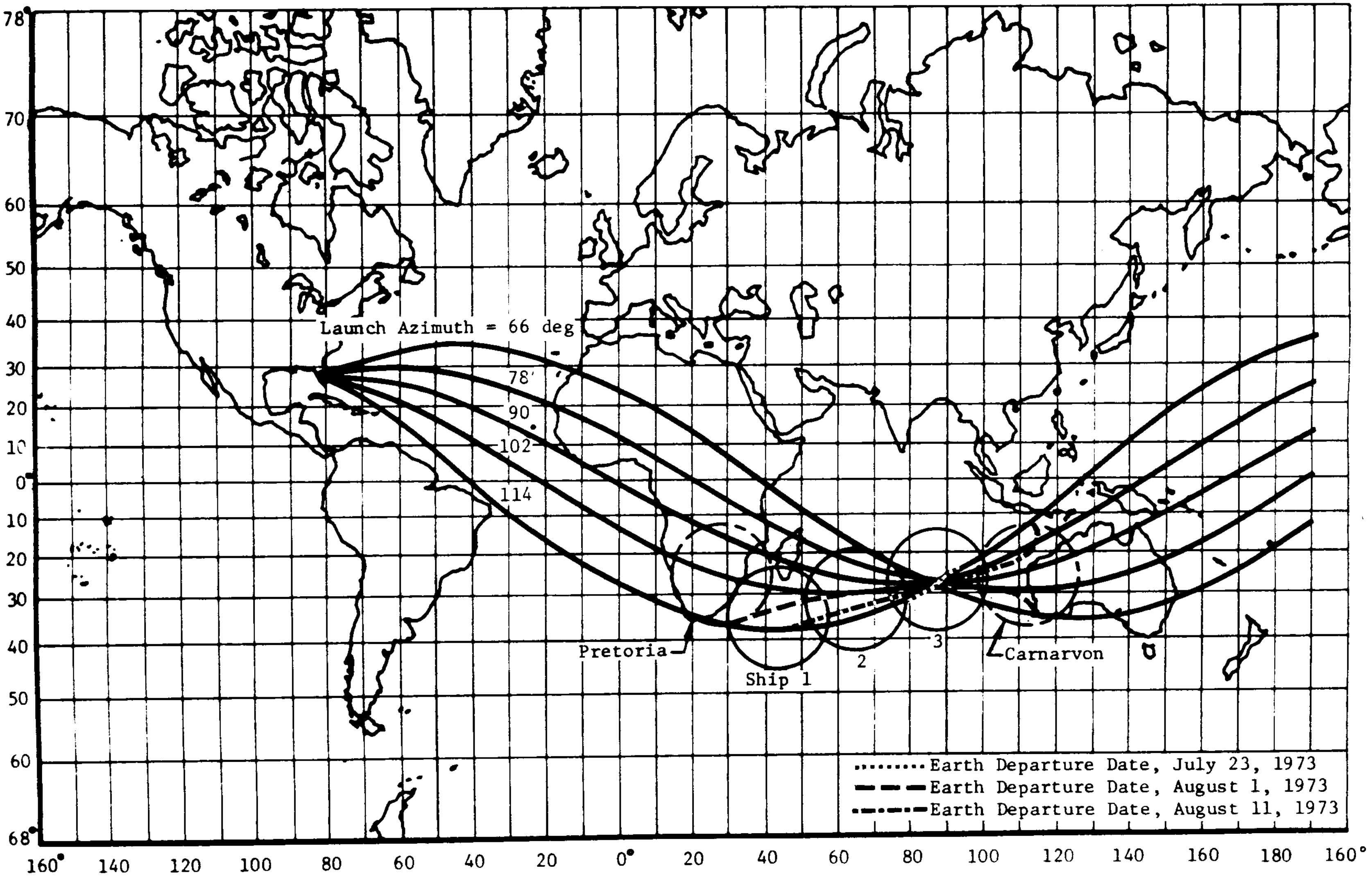
Launch Azimuth = 66 deg
78
90
102
114
Pretoria
Ship 1
2
3
Carnarvon
Earth Departure Date, July 23, 1973
Earth Departure Date, August 1, 1973
Earth Departure Date, August 11, 1973
78
70
60
50
40
30
20
10
0
10
20
30
40
50
60
68
160°
140
120
100
80
60
40
20
0°
20
40
60
80
100
120
140
160
180
160°

Figure 5.6-8: SHIP COVERAGE OF INJECTION MANEUVER

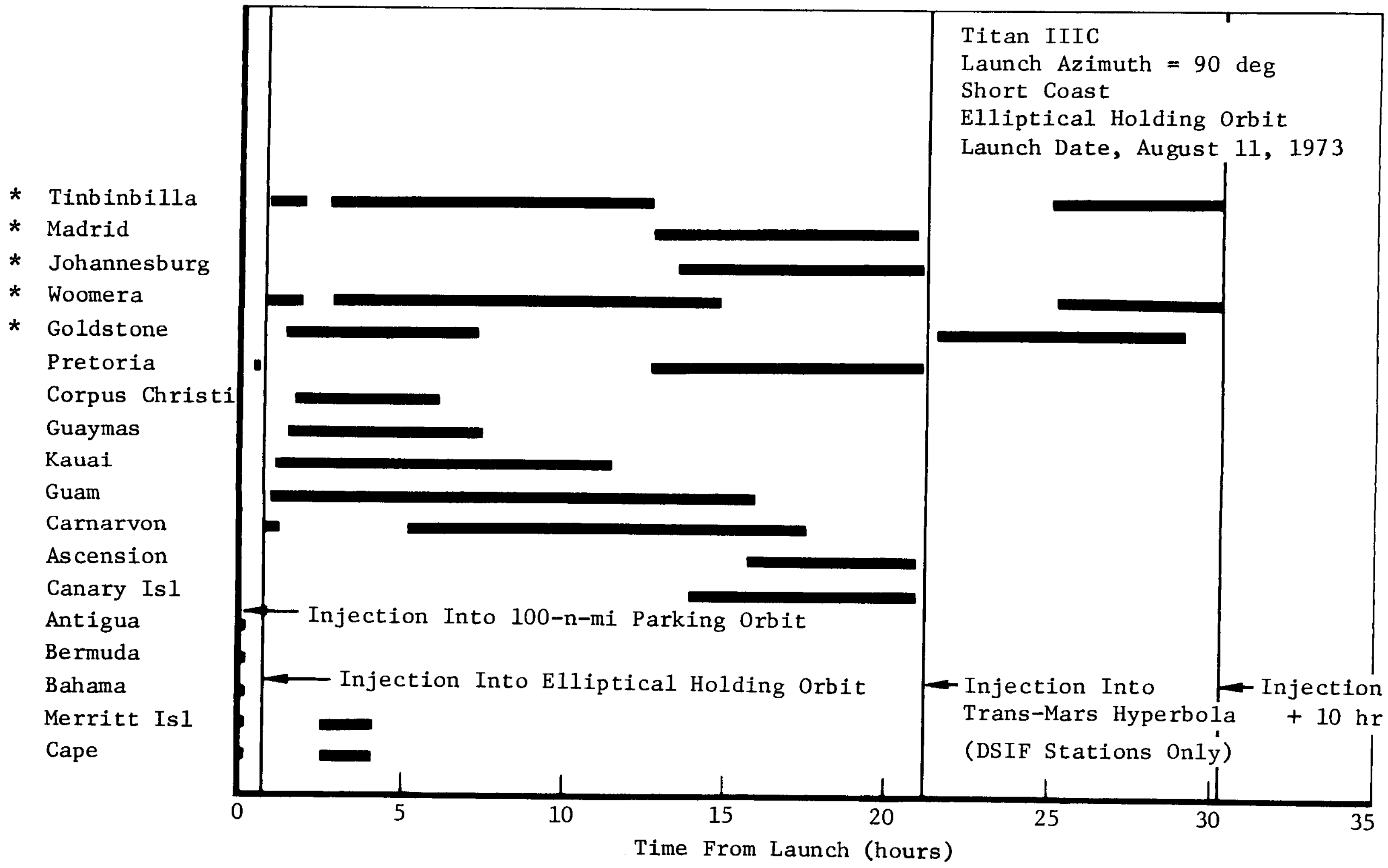

*DISF Stations

Figure 5.6-9: TRACKING STATION VIEW PERIODS (SHORT COAST)

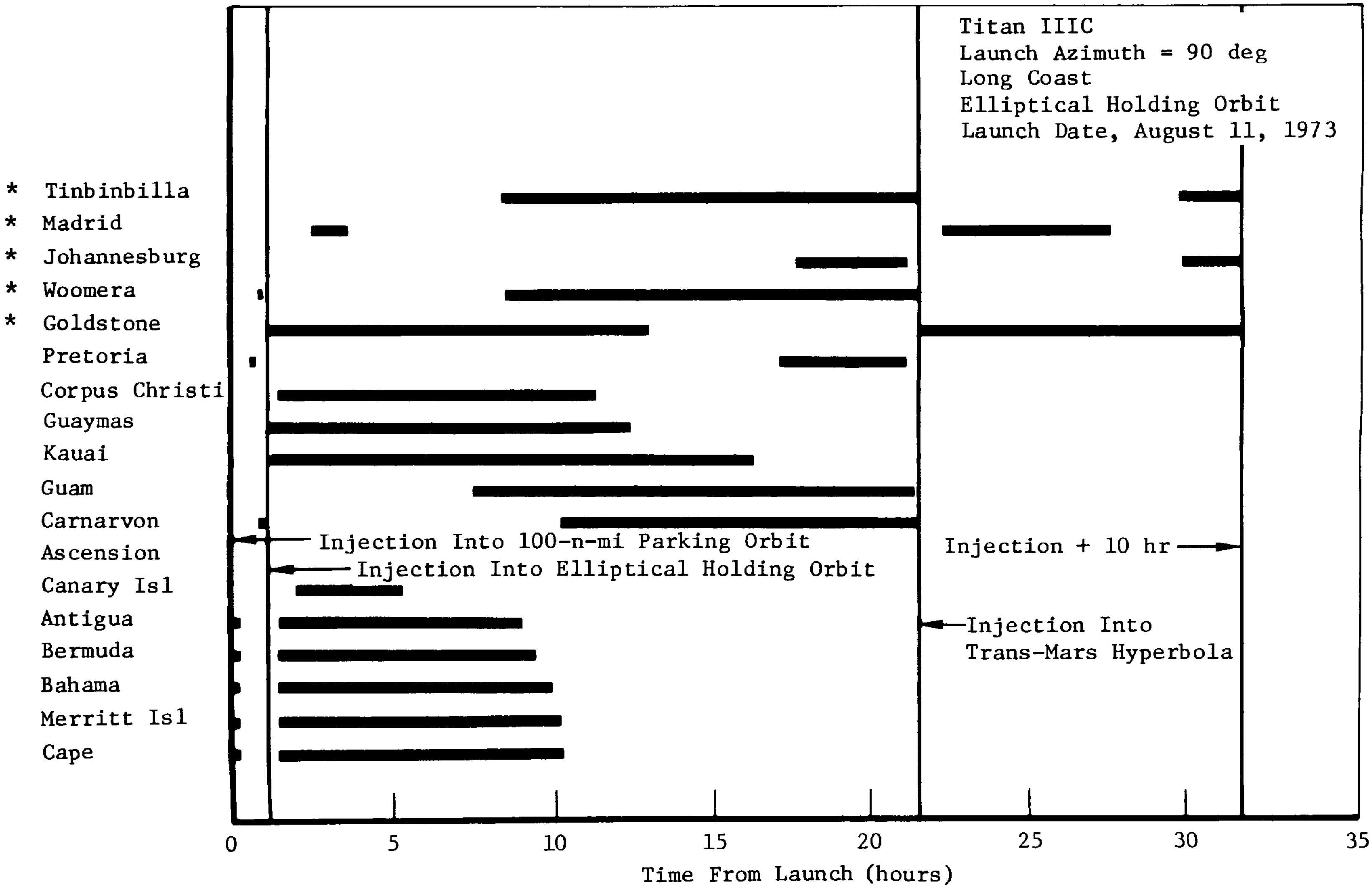

*DISF Stations

Figure 5.6-10: TRACKING STATION VIEW PERIODS (LONG COAST)

coverage during the trans-Mars phase is obtained within 0.5 hour of injection for the cases investigated. Tracking coverage in the first 0.5 hour of the trans-Mars trajectory will be the same as for the long holding orbit when the short holding orbit mode is used.

Appendix A4 defines the tracking station coordinates and constraints and presents parametric station viewing data.

### 5.6.3 Event-Sequence Analysis

In performing the event-sequence analysis, three prime tracking stations with 85-foot antennas are used: DSS-12 at Goldstone, California; DSS-42 at Tinbinbilla, Australia; and DSS-62 at Madrid, Spain. In addition, 11 MSFN stations (all those with 30-foot antennas and unified S-band capability), as well as three ETR launch stations, are included. The view period for the 85-foot antenna at Woomera is also included.

Two major categories (cases), missions with short and long holding orbits, are considered with the Titan IIIC launch vehicle. The Titan IIID was not evaluated because it lacks performance capability (see Section 5.5.2); however, the long holding orbit case with the Titan IIIC is representative of an operational analysis with the Titan IIID. For the case of the short holding orbit, the spacecraft transplanetary injection burn occurs as soon as practical after transtage second burn. For the long holding orbit case, the transtage second burn places the spacecraft in a highly elliptical Earth orbit, and the spacecraft transplanetary injection burn occurs at or near the following perigee.

For each case, event sequences are developed. However, only the preferred short holding orbit mode is discussed in this section. A long holding orbit operational analysis is given in Appendix A5.

The event sequences shown are general; as a rule event times are not specified. This approach was taken because an exact event sequence is always tied to a specific spacecraft design (i.e., the requirement to bleed propellant lines is tied to a specific propulsion technique). In like manner, an accurate description of event times (such as the time it takes a solar panel to deploy) is tied to a specific configuration.

*Short Holding Orbit Case*---Figure 5.6-11 shows a general event sequence for the short holding orbit case.

Prelaunch spacecraft activities include all the spacecraft tests and checkouts required during the countdown. These activities are a function of the spacecraft design, and work on accurately describing them cannot be undertaken until detail design of the spacecraft is underway. For the purposes of this analysis, it is sufficient to say that there are no operational aspects of the prelaunch phase of the mission that would make it unfeasible. Prelaunch activities for the powered spacecraft mission would be very similar and basically no more operationally complex than for a baseline Mars Mission.

Shortly before liftoff, the spacecraft programmer is enabled to control spacecraft activities during the launch and transplanetary injection phase. Titan IIIC launch and burnout of Stages 0, 1, and 2 occur as indicated in

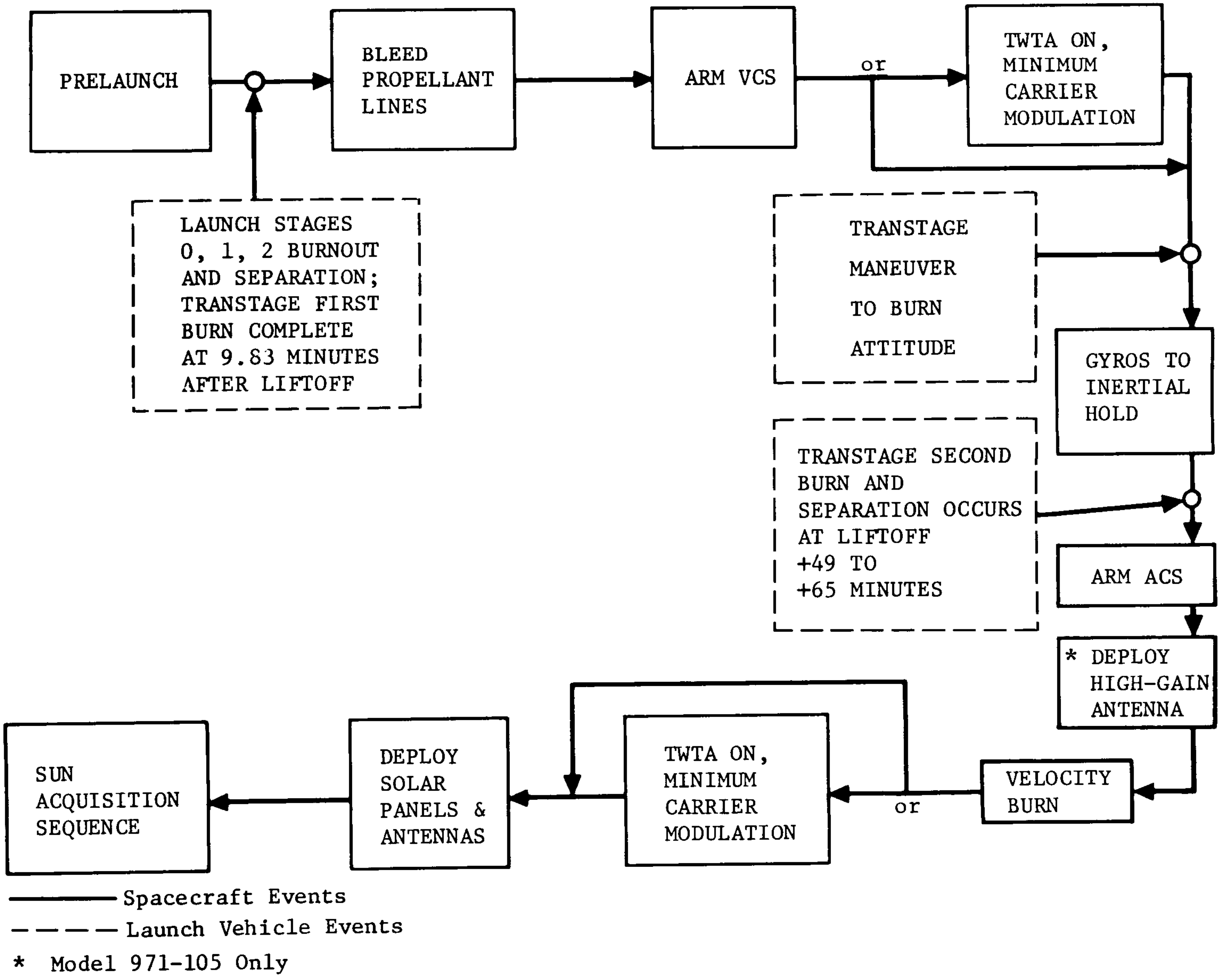
PRELAUNCH
BLEED PROPELLANT LINES
ARM VCS
or
TWTA ON, MINIMUM CARRIER MODULATION
LAUNCH STAGES 0, 1, 2 BURNOUT AND SEPARATION; TRANSTAGE FIRST BURN COMPLETE AT 9.83 MINUTES AFTER LIFTOFF
TRANSTAGE MANEUVER TO BURN ATTITUDE
GYROS TO INERTIAL HOLD
TRANSTAGE SECOND BURN AND SEPARATION OCCURS AT LIFTOFF +49 TO +65 MINUTES
ARM ACS
* DEPLOY HIGH-GAIN ANTENNA
VELOCITY BURN
or
TWTA ON, MINIMUM CARRIER MODULATION
DEPLOY SOLAR PANELS & ANTENNAS
SUN ACQUISITION SEQUENCE
Spacecraft Events
Launch Vehicle Events
* Model 971-105 Only

Figure 5.6-11: EVENT SEQUENCE---SHORT HOLDING ORBIT

Figure 5.6-11. The transtage is then ignited for the first time to place the transtage and attached spacecraft in a 100 n mi circular Earth orbit. No spacecraft activity is anticipated during this period from liftoff until the end of the transtage first burn.

The tracking station view periods shown in Appendix A4, of which Figure 5.6-12 is typical, are for the launch and 100 n mi parking orbit phases of flight. As can be seen from these figures, the view periods are all less than 10 minutes in duration and provide very spotty coverage except for the period from liftoff to parking orbit injection, which is entirely covered. Between the time of parking orbit injection and transtage second burn, certain spacecraft events will occur as required by the particular spacecraft design employed. If spacecraft activities such as bleeding the propellant lines and arming the velocity control subsystem (VCS) are necessary, these activities would be performed during this period. Tracking station coverage appears to be available for all launch azimuths until approximately 12 minutes after liftoff. Thus, it may be desirable to perform the propellant line bleed and VCS arming sequences at a typical time of liftoff plus 11 minutes to ensure tracking station coverage. Note that for all launch azimuths, injection will have occurred before 80 minutes after liftoff. Because the three 85-foot antennas are capable of tracking the spacecraft shortly after the transplanetary injection burn, the use of several of the MSFN 30-foot antennas would not be required for this case. The stations not required are Guaymas, Corpus Christi, Kauai, Merritt Island (ETR facilities are used for the launch phase), and possibly Guam.

For a Mars mission, the spacecraft will most likely not have a "low level" communication system; therefore, a traveling wave tube amplifier (TWTA) will be required for communications from the spacecraft. To receive real-time engineering data during the spacecraft velocity maneuver via a stub antenna (antennas do not have to be deployed except when they interfere with engine burn), some time must be allowed for tracking stations or ships to acquire the spacecraft signal and lockup. Therefore, it may be desirable to turn on the traveling wave tube amplifier and select the best modulation mode for acquisition at some convenient time before separation of the spacecraft from the transtage. A good time to do this is shortly before the transtage second burn, because a preferential transtage roll attitude should allow tracking station acquisition of the spacecraft downlink (via the stub omniantenna). This would provide several minutes for lockup before separation and the subsequent loss of the spacecraft engineering data via transtage telemetry. Because the TWTA causes a significant power drain, it should not be turned on too early. It may also prove to be unacceptable to turn it on before transtage second burn and/or the spacecraft velocity burn for other considerations, such as vibration.

From the tracking station view periods, it is evident that tracking station coverage after liftoff plus about 15 minutes through spacecraft injection is very spotty. Therefore, two or more tracking ships around the injection loci (see Section 5.6.2) would be required to provide coverage during the spacecraft injection velocity burn. However, it would still be desirable to have spacecraft capability to record engineering data during the velocity burn and transmit the data back to Earth at a later time in the mission. In this

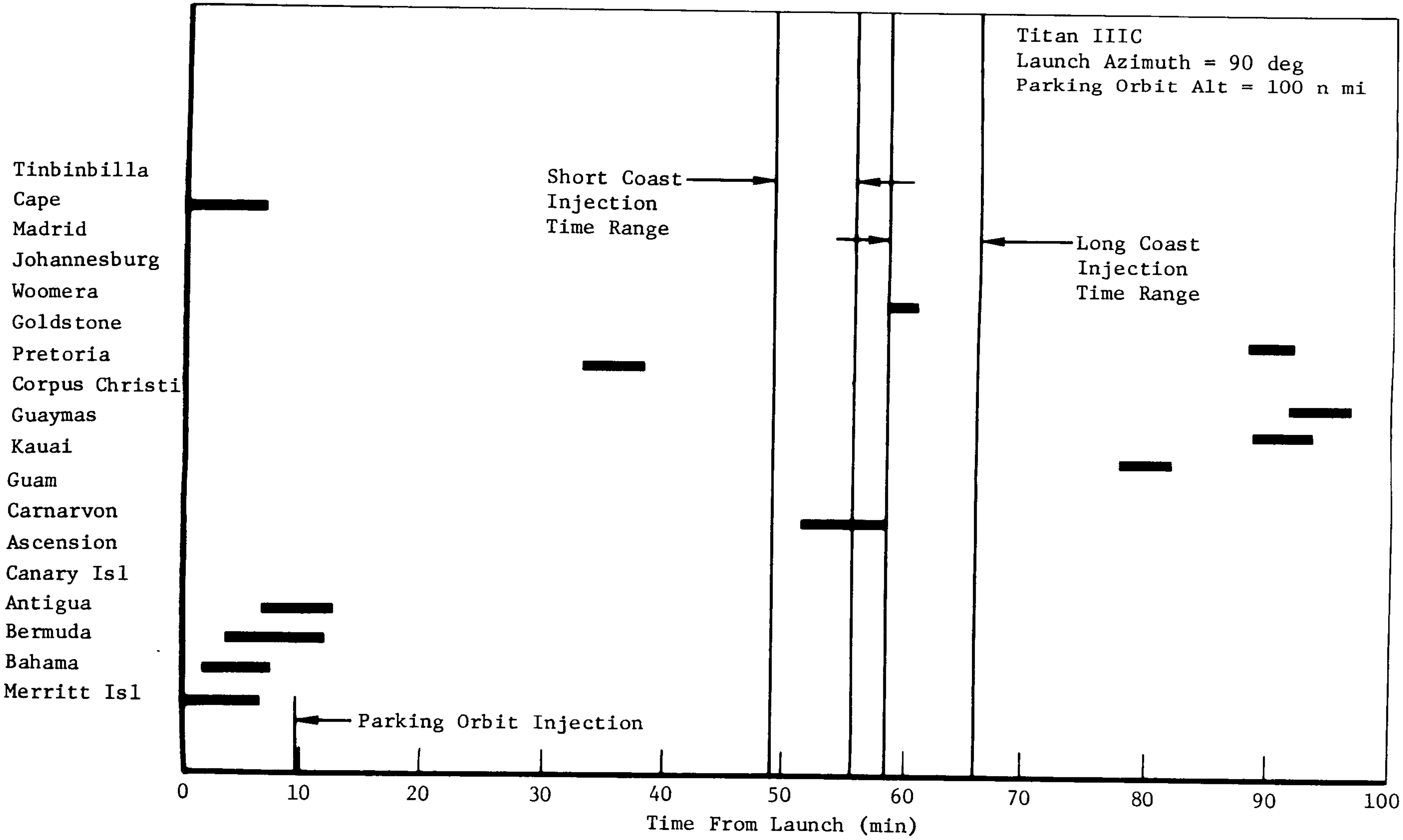

Figure 5.6-12: TRACKING STATION VIEW PERIODS (SHORT AND LONG COAST)

manner, engineering data on the spacecraft velocity burn would be obtained for all cases except a catastrophic condition causing destruction of the spacecraft or failure of the communications capability.

Following the transtage maneuver to the required attitude for the second burn, the spacecraft gyros are switches from the rate to the inertial hold mode. Transtage second burn then occurs, followed by spacecraft separation. As soon as practical following separation, the attitude control system is armed, the spacecraft is maneuvered to an optimum inertially fixed attitude, and spacecraft velocity burn occurs. For this sequence, it may prove desirable to initiate the spacecraft activities following separation by separation itself (as opposed to using the programmer clock).

If the TWTA was not turned on before the spacecraft velocity burn, it would be turned on immediately after it so that tracking station coverage could be obtained during the Sun-acquisition sequence. The deployment and Sun-acquisition sequences would follow. At some later time, the communication system could be switched to a more suitable modulation mode for the transplanetary cruise period. This would complete the major events and injection before transplanet coast.

The following conclusions can be drawn for the short holding orbit case:

1) There are no operational problems for this mission as compared to a baseline Mars mission, because all spacecraft functions, as for the baseline mission, have to be programmed until the Sun-acquisition sequence is completed. Thus, there is no operational risk over a baseline mission.
2) Because command capability is not feasible until after the spacecraft velocity burn, the spacecraft must have the capability to perform all required functions such as bleeding the propellant lines and conducting the velocity burn independent of real-time command activity.
3) It is desirable to place a reasonable number of tracking ships (probably two) in a pattern that allows tracking the spacecraft during velocity burn. It is also desirable for the spacecraft to record data during spacecraft velocity burn to further ensure engineering data acquisition.

### 5.6.4 Guidance Error Analysis

The primary purpose of the guidance error analysis was to define the first midcourse $\Delta V$ requirement resulting from launch vehicle dispersion and control systems errors. In addition, trade data was generated to evaluate the effect of variations in pointing error. The guidance implications of minimum $\Delta V$ bit size is reviewed.

#### 5.6.4.1 First Midcourse $\Delta V$ Requirements

The total first midcourse $\Delta V$ requirements for two representative spacecraft-assist trajectories are 26 m/sec, $3\sigma$, for the selected spacecraft control system errors. The trajectories are based on a short holding orbit option though both short and long parking orbit coast times are considered. Details of the trajectories are given below.

POWERED SPACECRAFT CONIC TRAJECTORIES FOR ERROR ANALYSES

| Parking Orbit Coast | Launch Time (hr) | Launch to Injection Time (hr) | Altitude (km) | Velocity (km/sec) | Flight-Path Angle (deg) | Incl (deg) | Mode (deg) | Arg. of Periapsis (deg) |
|---|---|---|---|---|---|---|---|---|
| Short | 11.69473 | 0.81756 | 185.2 | 11.73039 | 0 | 28.32 | 324.67 | -86.59 |
| Long | 6.65854 | 1.09825 | 185.2 | 11.73039 | 0 | 28.32 | 248.92 | 342.209 |

- Launch Date = August 11, 1973
- Arrival Date = February 16, 1974
- Launch Azimuth = 90 degrees
- Impulsive Second Burn
- Powered Spacecraft-Assist $\Delta V$ = 1.19039 km/sec

The following procedure was used in the calculation of midcourse $\Delta V$. The launch vehicle (Titan IIIC) dispersion as provided by NASA (Reference 2) was scaled to 0- and 68.7-degree parking orbit coasts. Velocity errors resulting from spacecraft attitude and velocity control subsystem errors acting through the spacecraft-assist $\Delta V$ were computed and added to the launch vehicle dispersion. The specific attitude error of 1.025 degrees, $3\sigma$, used for both the long and short parking orbit cases, is per the analysis of Appendix C. The combined launch vehicle dispersion and spacecraft-assist velocity errors were mapped to the first midcourse time (launch plus 5 days) for calculation of the corrective midcourse $\Delta V$.

The above analysis was based on conic trans-Mars trajectories. More precise integrated search solutions were used to generate the solid line given in Figure 5.6-13. This was done to check the use of conic solutions. The analysis was performed on an integrated trajectory defined for Voyager guidance studies. The launch vehicle dispersion for the long parking orbit case and a range of control errors were considered. The results using conic trajectories are in excellent agreement with the integrated trajectory solution when the midcourse $\Delta V$ is properly scaled with spacecraft-assist $\Delta V$, and allowances are made for nonvariation of the launch vehicle errors. The lower dashed curve of Figure 5.6-13 is an extrapolation from the upper curve through the point calculated for 1-degree pointing error. It permits estimating the midcourse $\Delta V$ for a range of powered spacecraft pointing errors and injection $\Delta V$'s.

The use of a long holding orbit results in a downrange uncertainty at powered spacecraft ignition of up to 46 degrees from perifocus (or 9.2 minutes), $3\sigma$. This results in unacceptable midcourse requirements. Consequently, a navigation update from ground tracking and orbit determination is required for this option.

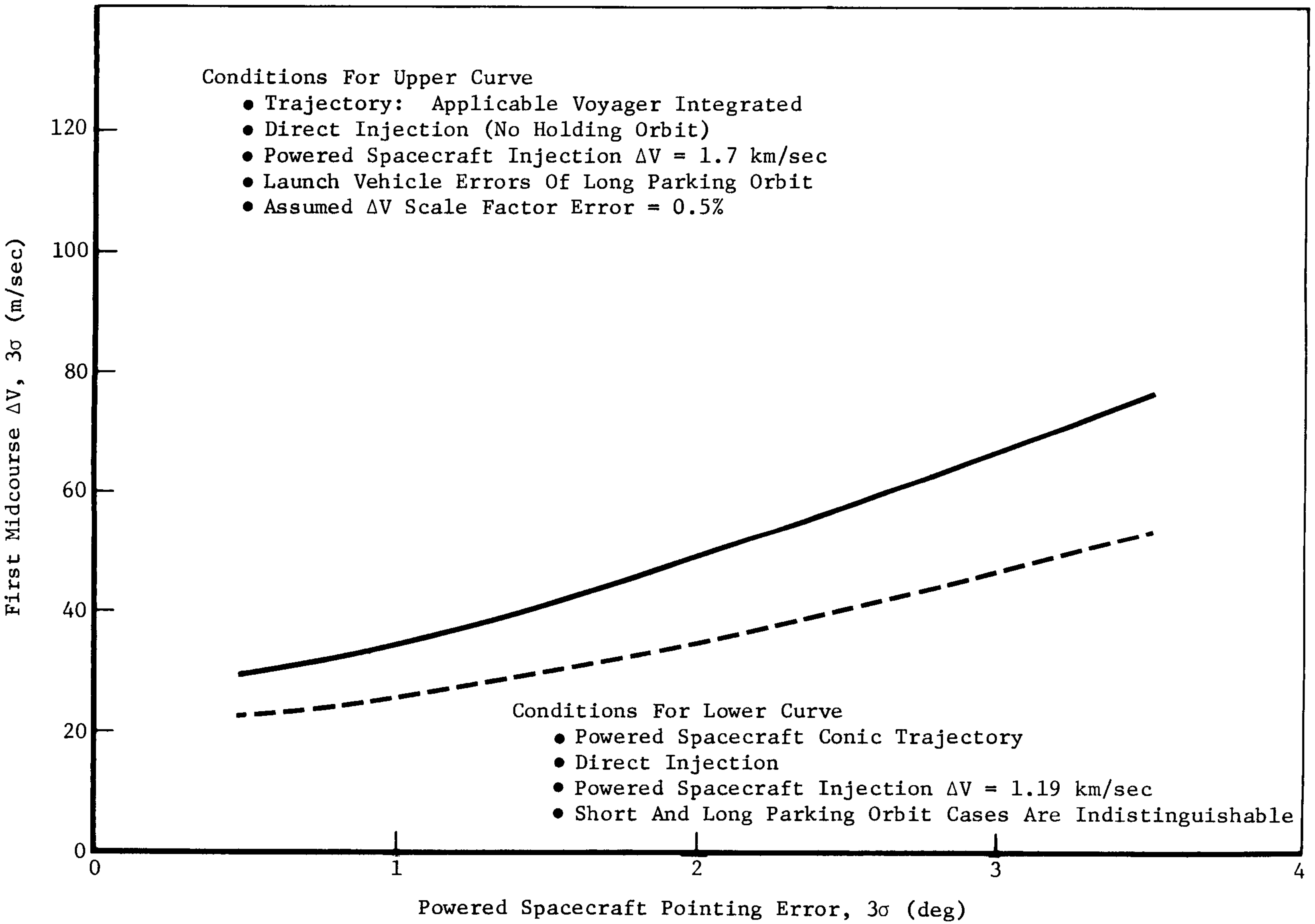

Figure 5.6-13: FIRST MIDCOURSE ΔV

### 5.6.4.2 Minimum $\Delta V$ Bit Size

The effects of minimum $\Delta V$ bit size (MVB) on mission control must be known to avoid unnecessary overspecification of MVB in designing for adequate mission control capability. The 3500-pound LEM Ascent engine can provide an MVB of 1.0 meter/second, which, though probably larger than required for second and third midcourse corrections, will result in insignificant performance penalties. Means are possible by which MVB's can be used that are larger than individual midcourse $\Delta V$ requirements. Three such approaches for tolerating significant MVB's for a 1973 Mars flight have been explored:

1) Adjust midcourse aim point biasing (to always require at least the MVB for each maneuver);
2) $\Delta V$ dumping in the noncritical direction (normal to the plane for correcting $\vec{B} \cdot \hat{T}$ and $\vec{B} \cdot \hat{R}$, hence degrading encounter time);
3) Shift midcourse correction times.

The first two approaches have been investigated for three sizes of MVB---1, 3, and 6 m/sec. Data to evaluate the potential of the third approach is also presented.

The study resulted in the following conclusions.

1) Aim point biasing and $\Delta V$ dumping in the noncritical direction are both feasible means for tolerating MVB's larger than required minimum $\Delta V$ maneuvers.
2) Shifting midcourse correction times is not a practical means for tolerating larger MVB's.
3) The aim point shifts required in aim point biasing are sufficiently large for MVB's over about 3 m/sec to cause some degradation in data from a flyby mission in case of engine failure. This may be an important factor in method selection.
4) The midcourse $\Delta V$ penalties of the $\Delta V$ dumping approach are lowest, but because of the direction of the $\Delta V$, the arrival altitude error is larger (essentially $\vec{B} \cdot \hat{R}$). Consequently, the Mars orbit insertion and trim $\Delta V$ penalties are larger. The total $\Delta V$ penalty for the $\Delta V$ dumping approach is lowest for MVB's under 2.5 m/sec.
5) The encounter time variations of the $\Delta V$ dumping approach are under 2 hours for MVB's under 4.4 m/sec, with a break point at about 4 m/sec, beyond which the variation in encounter time increases rapidly. Goldstone visibility of insertion could be maintained for MVB's of up to 6 m/sec.

A discussion of these results is given in Appendix A6, "Minimum Velocity Bit (MVB)."

## 6.0 PRELIMINARY CONFIGURATIONS

Preliminary configurations were developed to more definitively establish useful in-orbit weight, capsule and science weight, and spacecraft size, shape, and arrangement. Four concepts were evaluated. These include three liquid-rocket-powered vehicles and one solid/liquid-rocket-powered configuration. All spacecraft arrangements were based on the requirements and general parameters shown below.

| | |
|---|---|
| Launch Vehicle | Titan IIIC |
| Shroud Internal Diameter (Dynamic) | 112 in. |
| Separated Weight | 7,000 lb |
| Engine Thrust | 3,500 lb Liquid, 17,000 lb Solid |
| Propellant Weight (All Liquid System) | 4,200 lb |
| Propulsion System Design | Modular |
| Pressurant | Nitrogen |
| Attitude Control Gas | Nitrogen |
| Flight Capsule Diameter and Length | 102 in., 60 in. |
| Solar Panel Area | 100 sq ft |
| High-Gain Antenna and Type | 72 in., Parabolic |
| Capsule Antenna Diameter and Type | 36 in., Parabolic |
| Ominidirectional Antenna Diameter and Type | 8 in., Biconical |
| Micrometeroid Protection | None |

During the development of these configurations, various propellant tank arrangements were considered. These included a single spherical tank with a thrust-axis-oriented metallic membrane center bulkhead, two dual-tank on-axis designs, two-tank transverse asymmetrical arrangements, and transverse symmetrical four-tank layouts. The single spherical tank was not weight competitive because a small pressure differential across the flat center bulkhead could not be easily maintained. This results in a requirement for a thick center bulkhead with attendant weight penalties. The two dual-tank on-axis designs, one with a common bulkhead and one with two spherical tanks, proved to be the wrong shape for proper integration into the overall spacecraft design. These tank arrangements tend to be about 40 to 50 inches in diameter (depending on head configuration) and from 60 to 90 inches in overall length. Both designs complicate the spacecraft and propulsion module structure, extend the overall spacecraft length, and increase structural weight. The two-tank transverse asymmetrical design has much the same problem. The different densities of the propellants require that the tanks be offset with respect to the thrust axis or vice versa. The moment arm ratio is 1 to 1.6. With the required propellant volumes and the limited shroud diameter of the Titan, it becomes difficult to get the weight distributed so as to maintain spacecraft balance as propellant is used. Because the more common four-tank system provides weights comparable to the other examined approaches without their associated complexity or dynamic unbalance problems, it was used on all configurations (in both spherical and cylindrical shapes).

## 6.1 MODEL 971-101

Figures 6.1-1, -2, and -3 show Model 971-101 in the launch and space configurations. In this concept, the flight capsule and propulsion module are placed close to the launch vehicle interface to minimize bending moments on the spacecraft structure. This arrangement minimizes the shroud length because the largest spacecraft diameter is nearest the launch vehicle. Launch loads are carried from the transtage interface plane through a 21-inch-long truss adapter and an adapter ring to eight longerons arranged at the apexes of a 108-inch-diameter octagon that forms the orbiter body. These longerons are stabilized by eight shear panels that also provide interior equipment mounting surfaces and exterior space for temperature control louvers. The eight longerons are joined at the top (Station 71.5) by an octagonal ring and shear deck. Four 37.1-inch-diameter spherical tanks contain 62 cubic feet for the liquid propellant and its expulsion system. These are mounted in skirt rings and supported by four main longerons and four internal truss members. Eight truss members, joined to the shear deck at the internal truss member connection point, support a 28-inch-diameter nitrogen tank, a 28-inch-diameter semimonocoque engine thrust cylinder, and an engine support ring. The 3,500-pound-thrust Lunar Module ascent engine gimbal is joined to the engine support ring by two tripod trusses. Thrust vector actuators are connected between the engine aft face and the periphery of the engine support ring.

The octagonal ring and shear deck provide the mounting surface for the four attitude control thruster clusters and all deployable components. The high-gain and omnidirectional antennas are stowed alongside the engine during launch and are deployed by single-plane rotation. The eight 41- by 45-inch solar panels, hinged from the octagonal ring at the top of the orbiter body, are stowed over the equipment louvers during launch and are deployed by knee-action struts.

The flight capsule relay antenna is not deployed, but is mounted on a tripod-supported dual-axis drive. The tripod is mounted from the engine gimbal points and the engine support ring.

### 6.1.1 Configuration Assessment

A review of the configuration resulted in the following assessment.

- Positive Features

  *20-foot shroud requirement*---Placement of the capsule near the launch vehicle interface allows the use of a short shroud.

  *Symmetrical spacecraft arrangement*---The natural symmetry of the design minimizes center-of-gravity offset and movement.

  *Good control authority*---The relationship of the gimbal position to the spacecraft masses provides a good positive control margin.

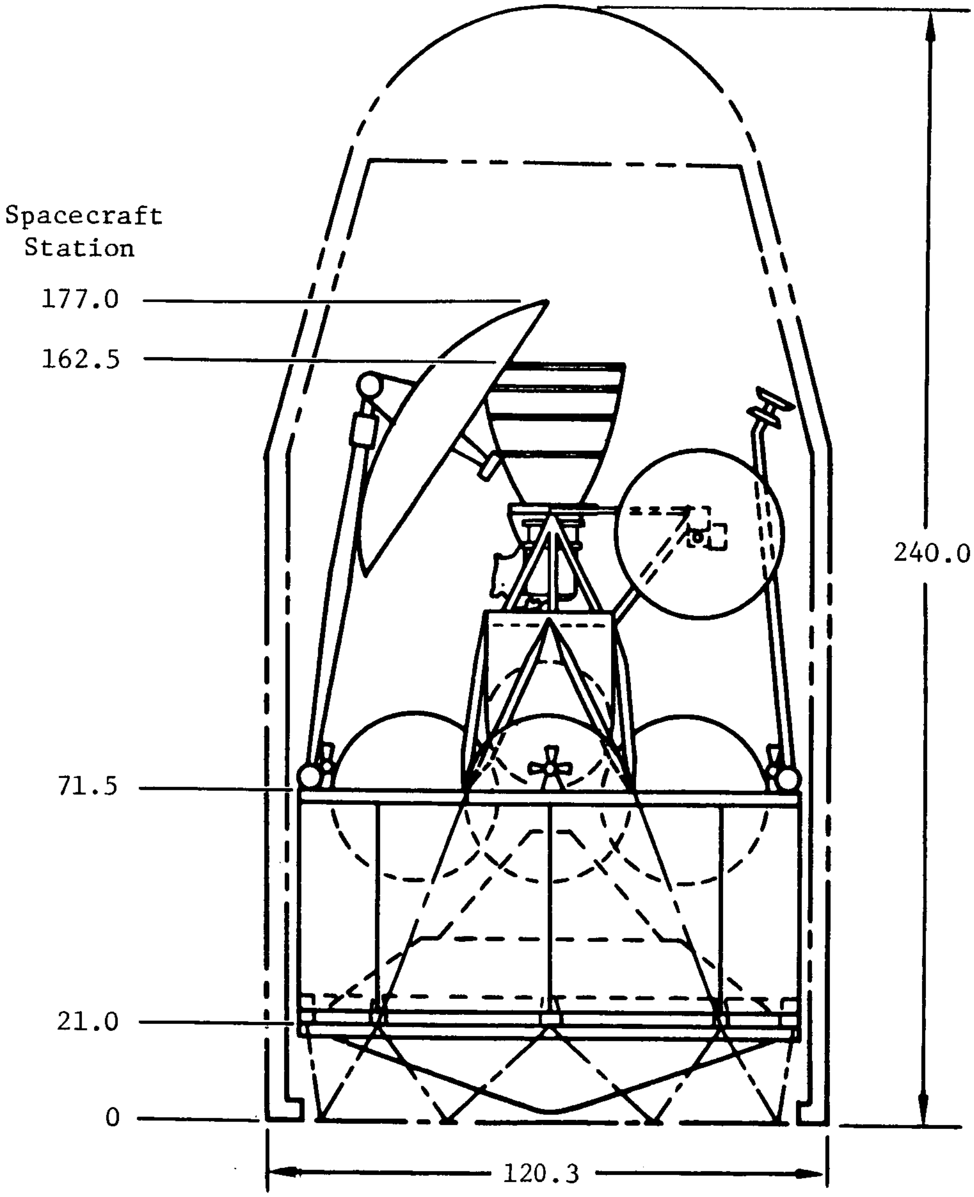
Spacecraft
Station
177.0
162.5
71.5
21.0
0
240.0
120.3

Figure 6.1-1: MODEL 971-101 LAUNCH CONFIGURATION

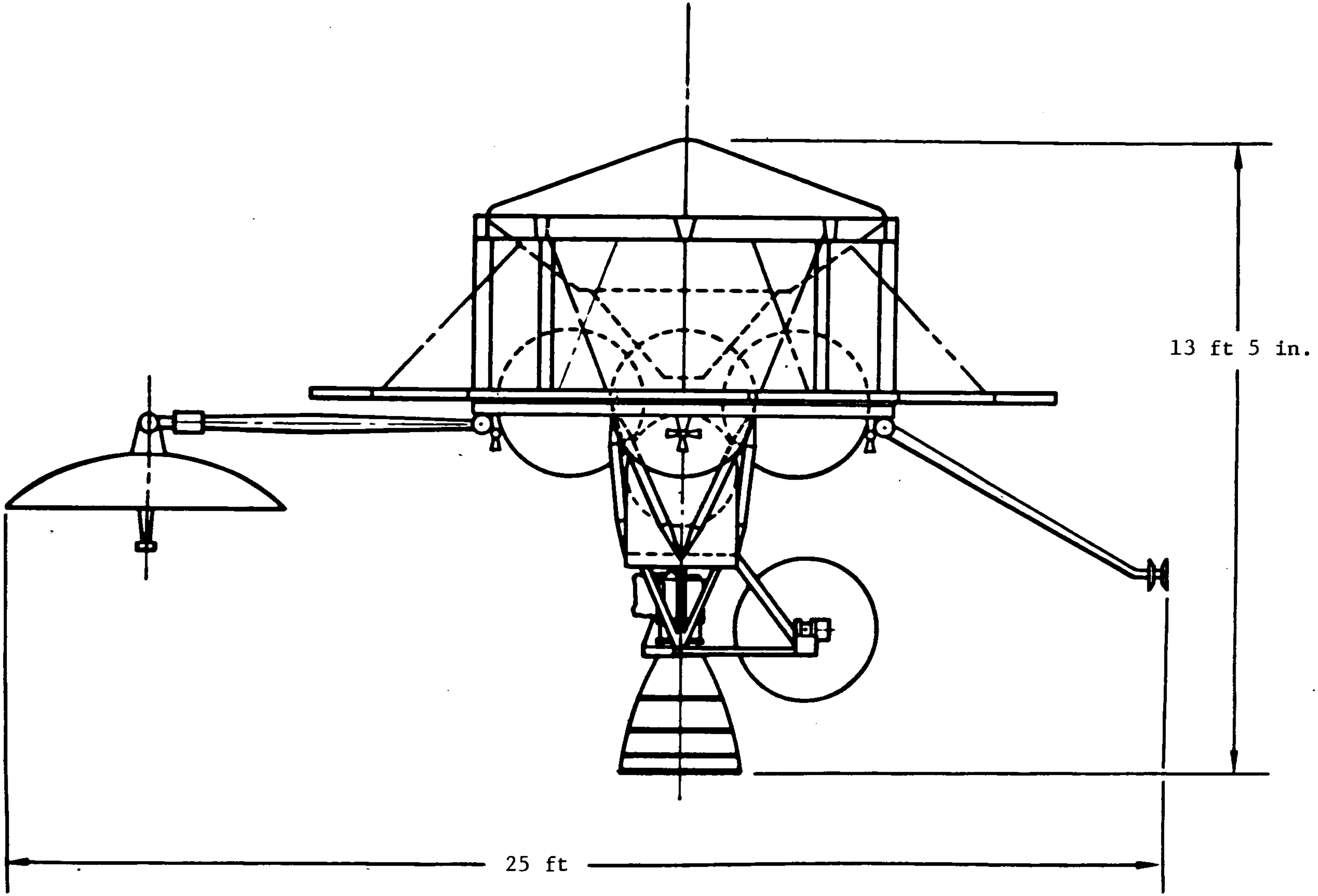
13 ft 5 in.
25 ft

Figure 6.1-2: MODEL 971-101 SPACE CONFIGURATION

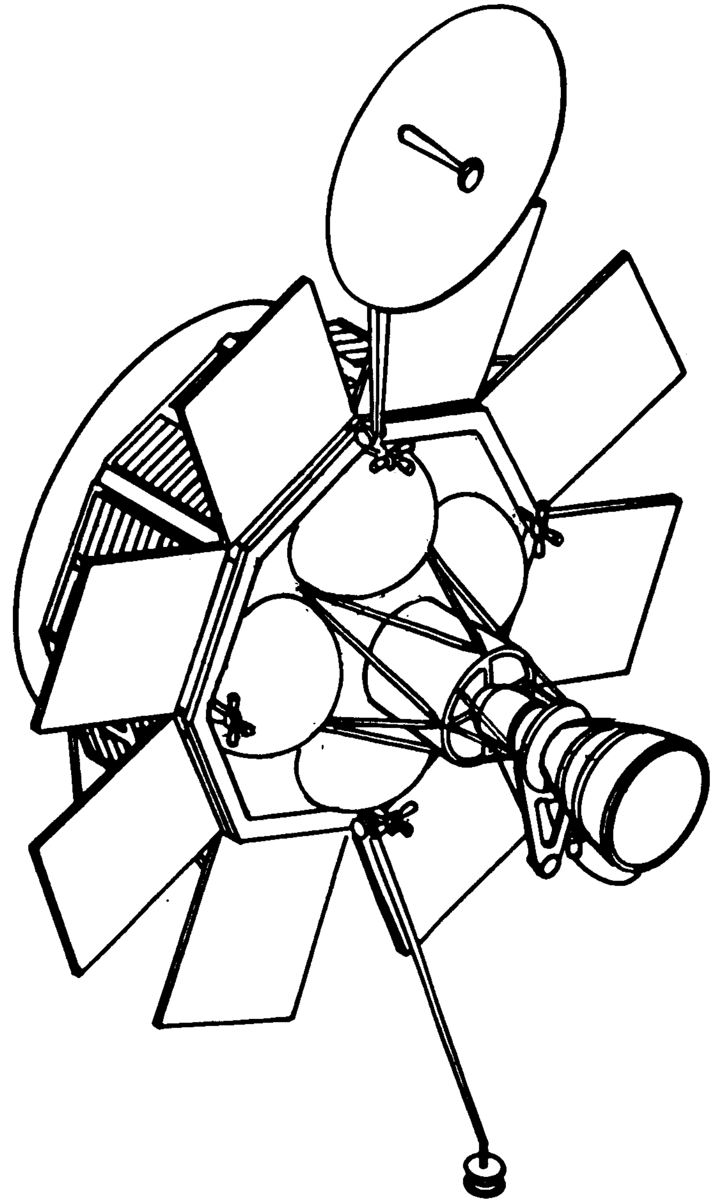

Figure 6.1-3: MODEL 971-101 SPACE CONFIGURATION (ISOMETRIC)

*Good thermal control capability*---The position of the louvers on the shadow side of the solar panels and the compactness of the vehicle contribute toward good thermal control.

*Good sensor views*---All sensors and antennas have unobstructed views.

*Simple antenna deployment motions*---Only two of the three major antennas are deployed, and these are single-plane motions.

- Negative Features

  *Spacecraft reversal required at separation from launch vehicle*---Like all engine-up arrangements, it has a turnaround performance penalty at transplanetary injection, but this is offset by the reduced structural weight of a low center-of-gravity boost configuration.

  *Limited equipment access with flight capsule in place*---Placement of the capsule at the end of the equipment bay, and mounting equipment inside the shear panels, make it necessary to remove the flight capsule or sections of the shear deck to service equipment.

  *Special flight capsule interface required to get lightest arrangement*---The best flight capsule interface for this design would be a joint at the outside diameter of the flight capsule. When this is not the case, special flight capsule adapter structure must be added.

### 6.1.2 Weight Analysis

Analysis of Model 971-101 showed that a flight capsule plus science weight of 1,249 pounds is available. Total useful weight is 2,041 pounds and total weight in Mars orbit is 2,951 pounds. These weights are based on the general design parameters shown in Table 6.4-1 and the weight statement of Table 6.4-2.

## 6.2 MODEL 971-102

Figures 6.2-1, -2, and -3 show Model 971-102 in the launch and space configurations. In this concept, the solar panels are mounted so that they are edge-loaded by the 17,000-pound thrust of the Thiokol TE-M-364-4-01 solid rocket spacecraft-assist engine. Launch loads are carried from the transtage interface plane through a 42-inch-long truss adapter to a deck that supports the solid rocket case, four Marquardt R4D 100-pound-thrust liquid rocket engines, four 22-inch-diameter by 38-inch-long cylindrical propellant tanks, four attitude control thruster clusters, and an equipment support collar. The equipment collar is the orbiter body. It is composed of eight longerons and shear panels. The shear panels provide interior equipment mounting panels and exterior space for temperature control louvers. The flight capsule is supported from the equipment collar by an eight-point star truss. The four propellant tanks are supported on thrust cones from the deck and are stabilized at the top by a horizontal bulkhead that contains a 24-inch-diameter nitrogen tank. This assembly is attached to the equipment collar by sway braces and to the lower deck by a semimonocoque cone, which also provides a temperature control barrier for the solid rocket engine.

The four 85- by 42-inch solar panels are double-folded so that they can be stowed against the body sides between the lower deck and the flight capsule.

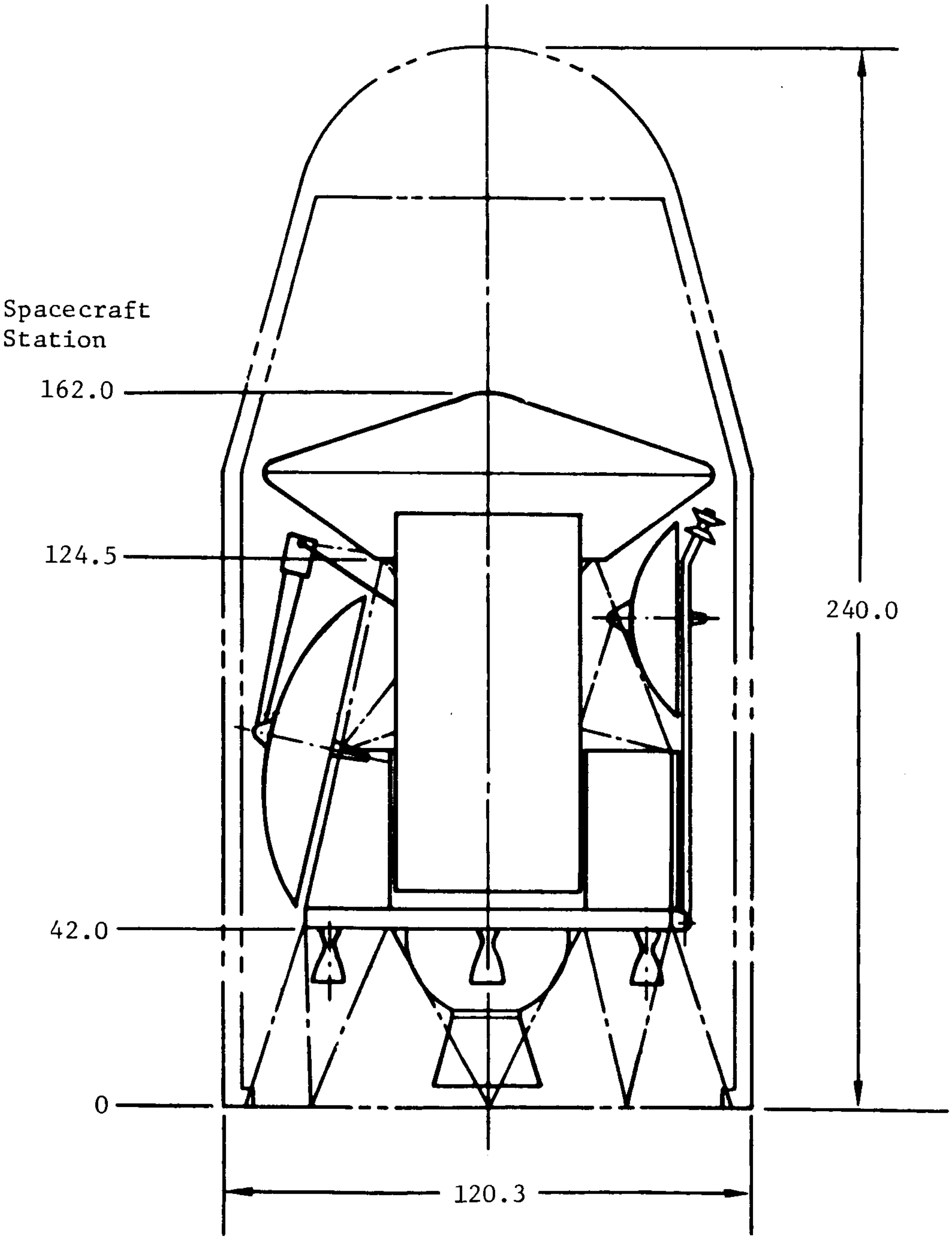
Spacecraft Station
162.0
124.5
42.0
0
240.0
120.3

Figure 6.2-1: MODEL 971-102 LAUNCH CONFIGURATION

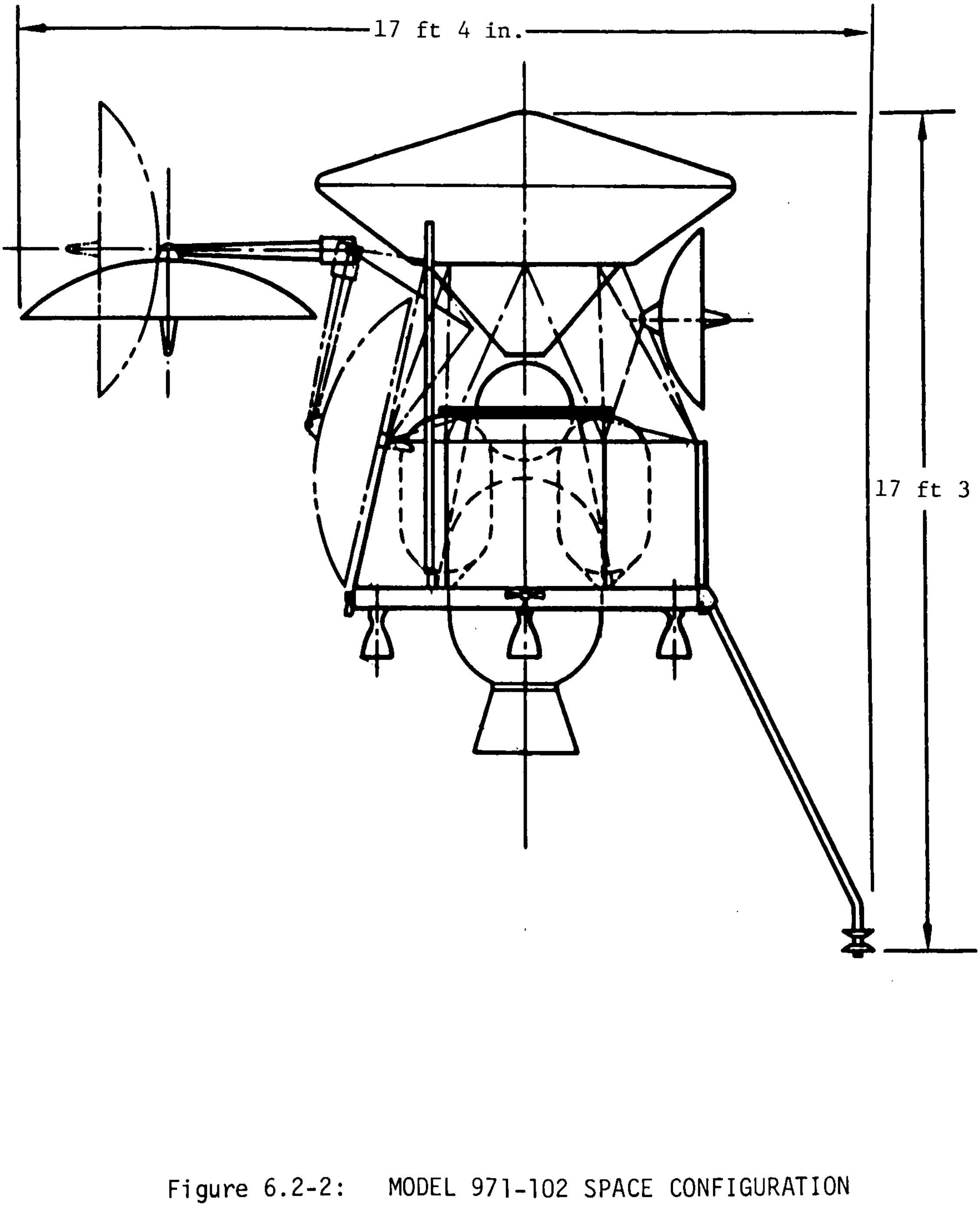
17 ft 4 in.
17 ft 3 in.

Figure 6.2-2: MODEL 971-102 SPACE CONFIGURATION

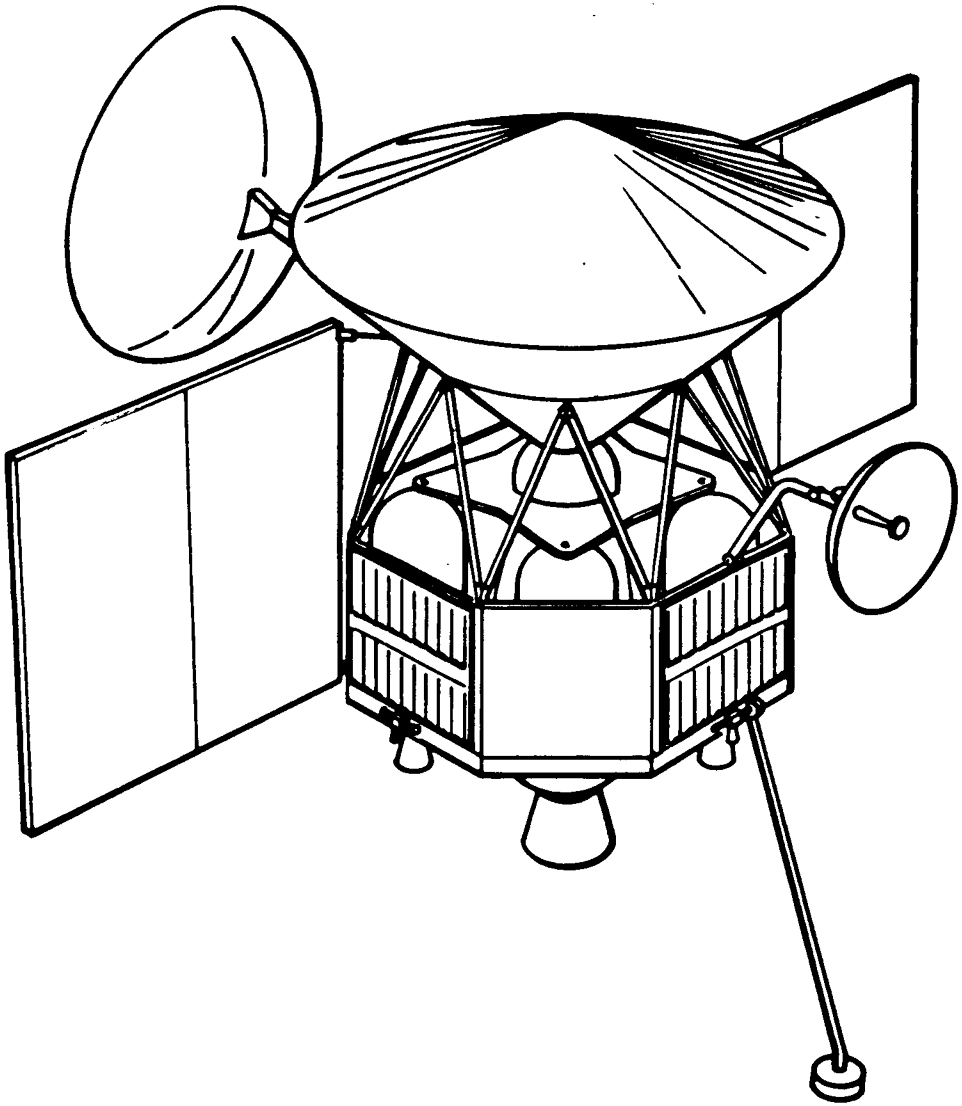

Figure 6.2-3: MODEL 971-102 SPACE CONFIGURATION (ISOMETRIC)

The omnidirectional antenna attaches to the lower deck and stows along the thrust axis on the vehicle periphery. The two parabolic antennas are mounted from the capsule support truss work and are deployed by single-plane rotation.

### 6.2.1 Configuration Assessment

A review of this configuration resulted in the following assessment.

- Positive Features

  *20-foot shroud requirement*---Use of the compact solid rocket engine allows the use of a short shroud.

  *Staged inerts*---The solid rocket can be released from the spacecraft after the spacecraft-assist mode. This decreases the orbiter inert weight by 156 pounds.

  *Good thermal control capability*---The position of the louvers on the shadow side of the solar panels and the compactness of the vehicle result in good thermal control authority.

  *Simple antenna deployment motions*---All antenna deployments are single-plane motions.

  *Simple flight capsule support*---Good flight capsule support is provided by the eight-point star truss at the natural flight capsule interface.

  *Good solar panel loading*---Edge-loading the solar panels minimizes the effects of the high acceleration forces of the solid rocket engine.

  *Good solar panel growth capability*---Side mounting allows solar panel growth without modifying the spacecraft structure.

- Negative Features

  *Assymetrical spacecraft*---Placement of the solar panels on the side of the spacecraft creates an unbalance that may be difficult to offset by equipment placement. It also allows Sun exposure of the flight capsule when on Sun-lock.

  *Limited control authority to overcome center-of-gravity offsets*---All steering is accomplished by pulsing the R4D engines. This results in limited control authority during the spacecraft-assist phase. Lateral center-of-gravity shifts or offsets are limited to about 0.25 inch.

  *High acceleration forces*---The solid rocket engine introduces acceleration loads of about 3.5 g. This requires that all deployed components remain stowed during the spacecraft-assist phase.

  *Limited star tracker view*---The Canopus tracker view is limited to ±37.5 degrees.

  *Extensive deployment*---All antennas require deployment. The solar panels require deployment from a double-fold position.

### 6.2.2 Weight Analysis

Analysis of Model 971-102 showed that a flight capsule plus science weight of 1,373 pounds is available. Total useful weight is 2,155 pounds and total weight in Mars orbit is 2,699 pounds. In this case the separated spacecraft weight is 7,100 pounds. This occurs because of the fixed weight of the solid rocket engine. However, increasing the separated weight of the other configurations by 100 pounds would have a negligible effect on their available flight capsule plus science weight; therefore, it can be concluded that this configuration has not been given undue benefit and that the differences shown in flight capsule plus science weight are realistic. These weights are based on the general design parameters shown in Table 6.4-1 and the weight statement of Table 6.4-2.

## 6.3 MODEL 971-103

Figures 6.3-1, -2, and -3 show Model 971-103 in the launch and space configurations. This design is the liquid-rocket-powered equivalent of Model 971-102. Basically, the same structure was used. The main deck now supports the 3,500-pound-thrust Lunar Module engine, four 26-inch-diameter by 59.3-inch-long cylindrical propellant tanks, four attitude control thruster clusters, and an equipment mounting collar. Two 22.2-inch-diameter spherical nitrogen tanks are dumbbell-mounted from a semimonocoque cylindrical intertank structure supported on a star truss from the main deck. The thrust-cone-mounted propellant tanks are stabilized by a flat cone structure at the top. This cone joins the upper nitrogen tank, the propellant tanks, and the flight capsule support truss that provides structural continuity between the flight capsule and the equipment mounting collar.

The four stowed 95- by 40-inch solar panels are wrapped around the body between the main deck and the flight capsule. They are deployed along the thrust axis at the side of the spacecraft. The omnidirectional antenna attaches to the lower deck and stows along the thrust axis on the vehicle periphery. Because of the larger propellant capacity, it was not possible to stow the high-gain antenna at the side of the vehicle as in Model 971-102. This antenna stows over the flight capsule on specialized truss work. The flight capsule antenna is mounted from the capsule support truss work and stows at the side of the spacecraft. Both parabolic antennas are deployed by single-plane rotation.

### 6.3.1 Configuration Assessment

A review of this configuration resulted in the following assessment.

- Positive Features

  *Good control authority*---The relationship of the gimbal position to the spacecraft masses provides a good positive control margin.

  *Good thermal control capability*---The position of the louvers on the shadow side of the solar panels and the compactness of the vehicle result in good thermal control authority.

  *Simple antenna deployment motions*---All antenna deployments are single-plane motions.

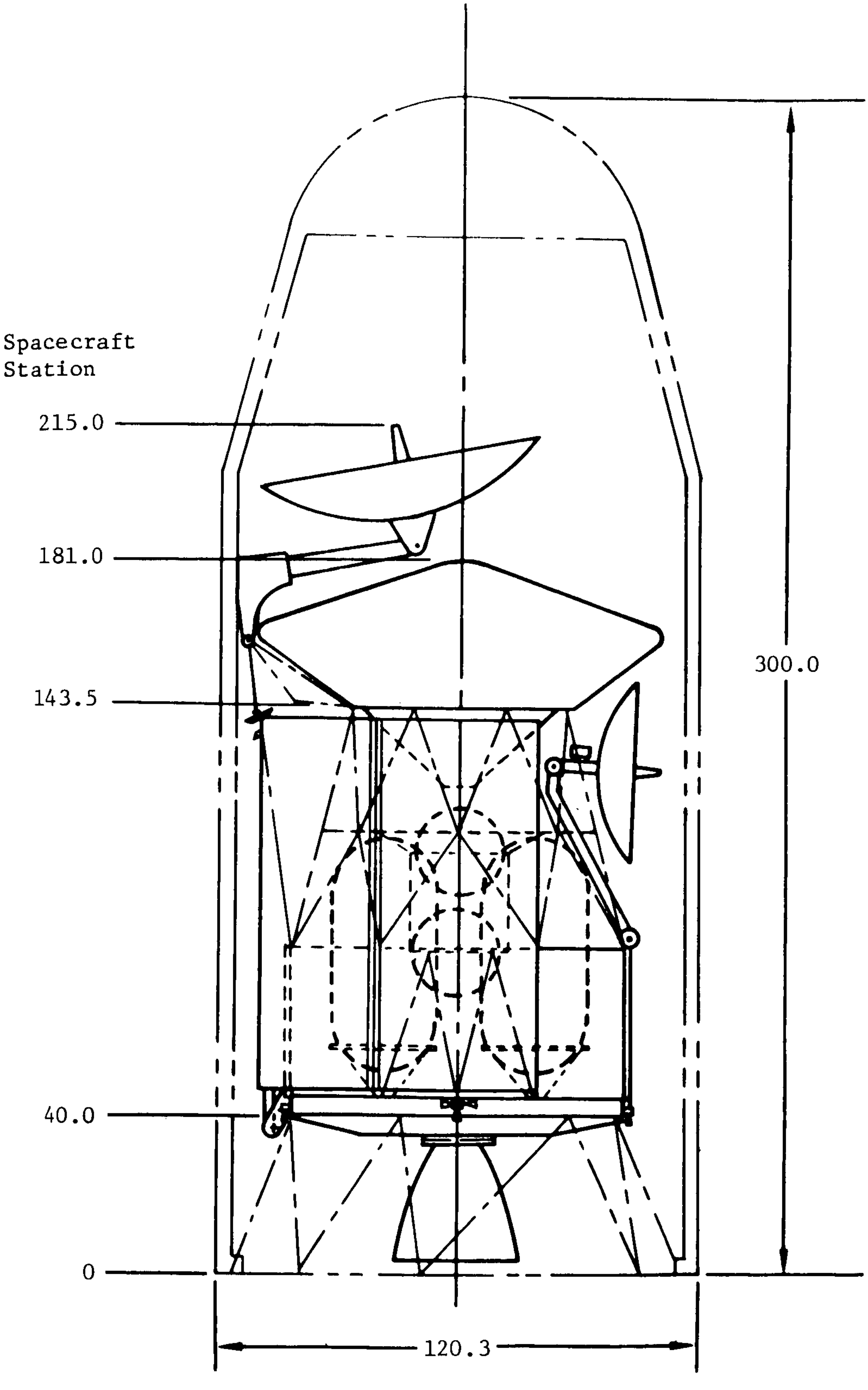
Spacecraft
Station
215.0
181.0
143.5
40.0
0
300.0
120.3

Figure 6.3-1: MODEL 971-103 LAUNCH CONFIGURATION

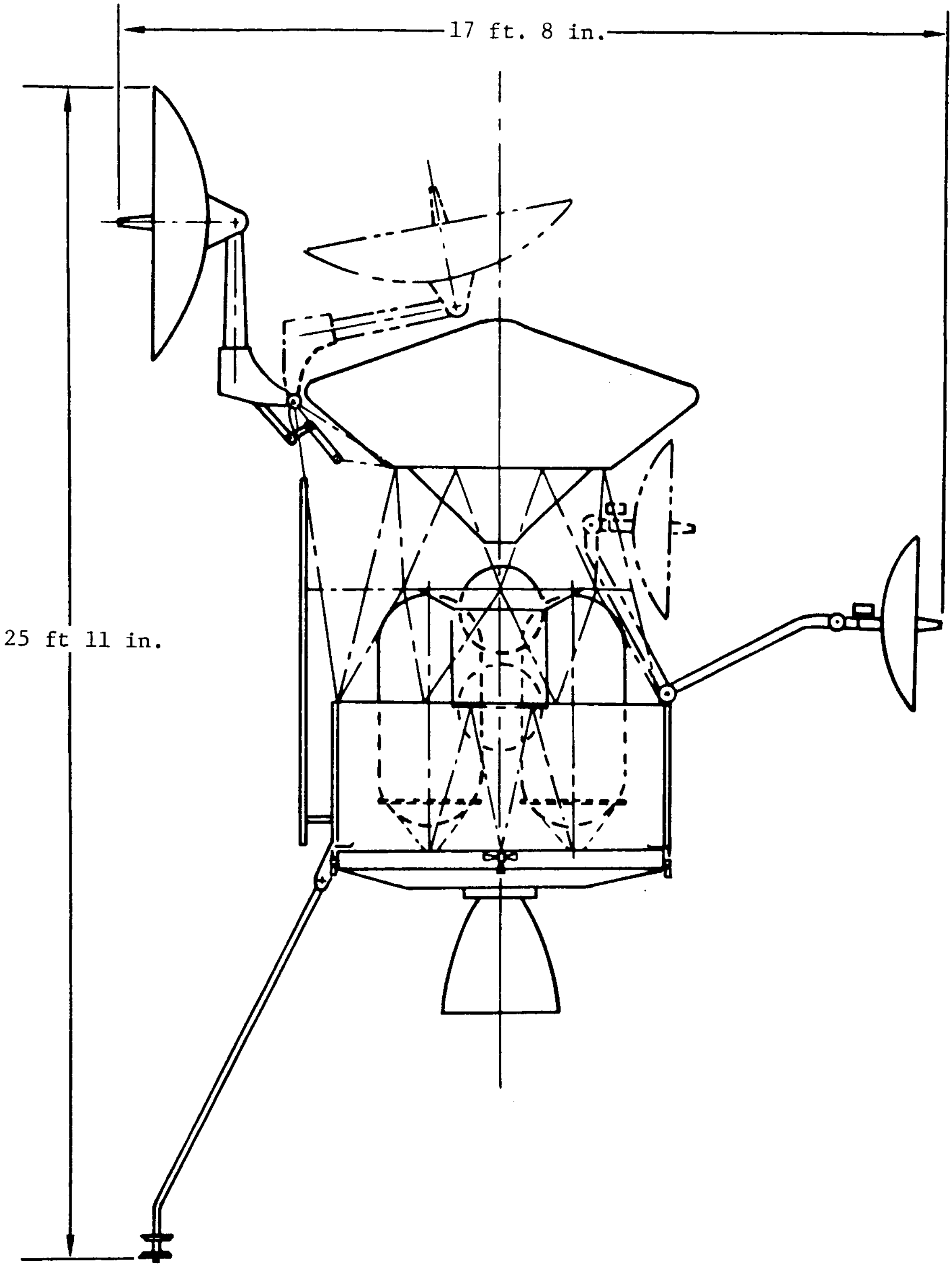
17 ft. 8 in.
25 ft 11 in.

Figure 6.3-2: MODEL 971-103 SPACE CONFIGURATION

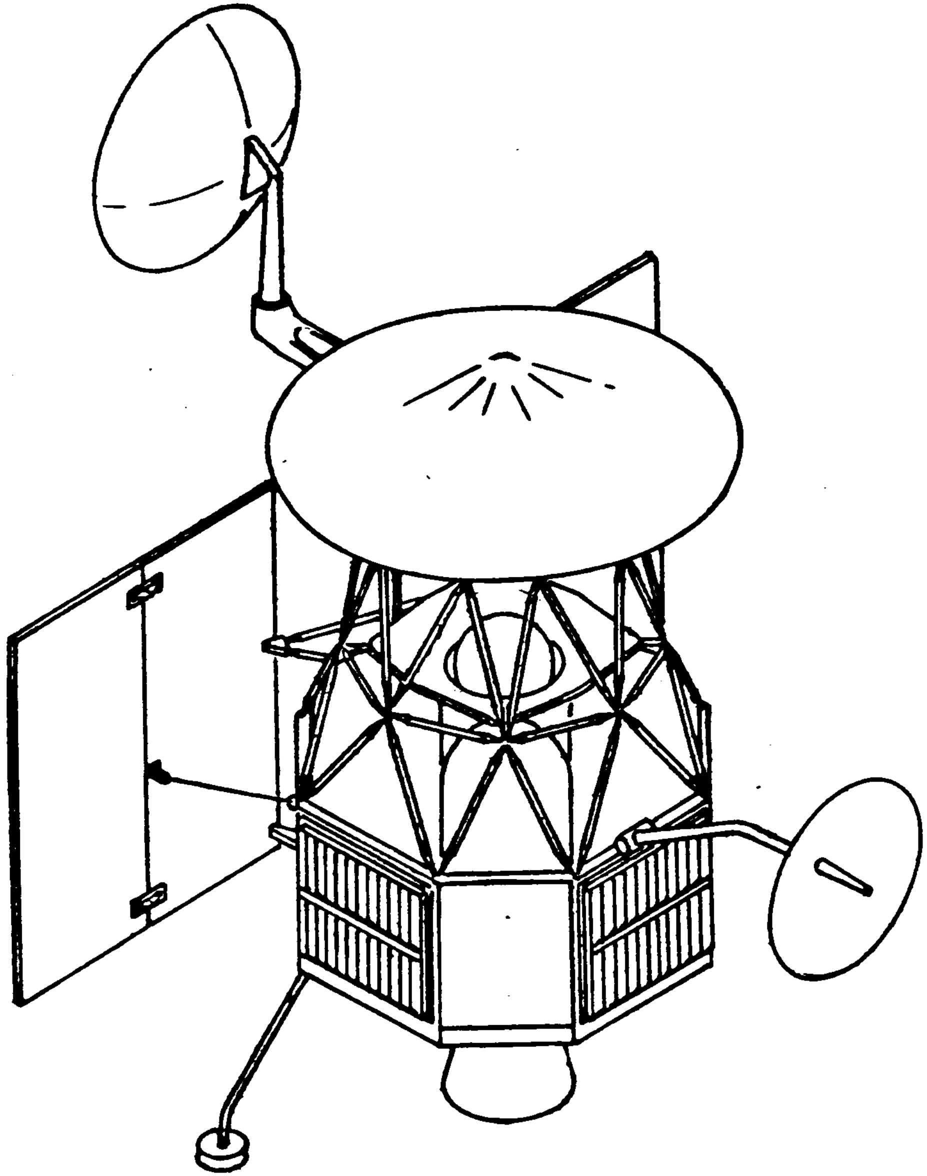

Figure 6.3-3: MODEL 971-103 SPACE CONFIGURATION (ISOMETRIC)

*Simple flight capsule support*---Good flight capsule support is provided by the eight-point star truss at the natural flight capsule interface.

*Good solar panel loading*---Edge-loading the solar panels minimizes the effects of the high acceleration forces of the solid rocket engine.

*Good solar panel growth capability*---Side mounting allows solar panel growth without modifying the spacecraft structure.

- Negative Features

  *Asymmetrical spacecraft*---Placement of the solar panels on the side of the spacecraft creates an unbalance that may be difficult to offset by equipment placement. It also allows Sun exposure of the flight capsule when on Sun-lock.

  *25-foot shroud requirement*---Placement of the flight capsule at the upper end of the spacecraft requires the shroud length to be increased to the next standard size.

  *Limited star tracker view*---The Canopus tracker view is limited to ±30 degrees.

  *Extensive deployment*---All antennas require deployment. The solar panels require deployment from a double-fold position.

### 6.3.2 Weight Analysis

Analysis of Model 971-103 showed that a flight capsule plus science weight of 1,120 pounds is available. Total useful weight is 1,929 pounds and total weight in Mars orbit is 2,951 pounds. These weights are based on the general design parameters shown in Table 6.4-1 and the weight statement of Table 6.4-2.

## 6.4 MODEL 971-104

This configuration (Figure 6.4-1) was developed to examine the effect of launching Model 971-101 with its engine facing aft. The spacecraft general arrangement is the same as that discussed in Section 6.1. The 971-101 design is not well-suited to an engine-facing-aft launch mode because it requires an adapter 115 inches long.

### 6.4.1 Configuration Assessment

A review of the configuration resulted in the following assessment.

- Positive Features

  *Symmetrical spacecraft arrangement*---The natural symmetry of the design minimizes center-of-gravity offset and movement.

  *Good control authority*---The relationship of the gimbal position to the spacecraft masses provides a good positive control margin.

  *Good thermal control capability*---The position of the louvers on the shadow side of the solar panels and the compactness of the vehicle result in good thermal control authority.

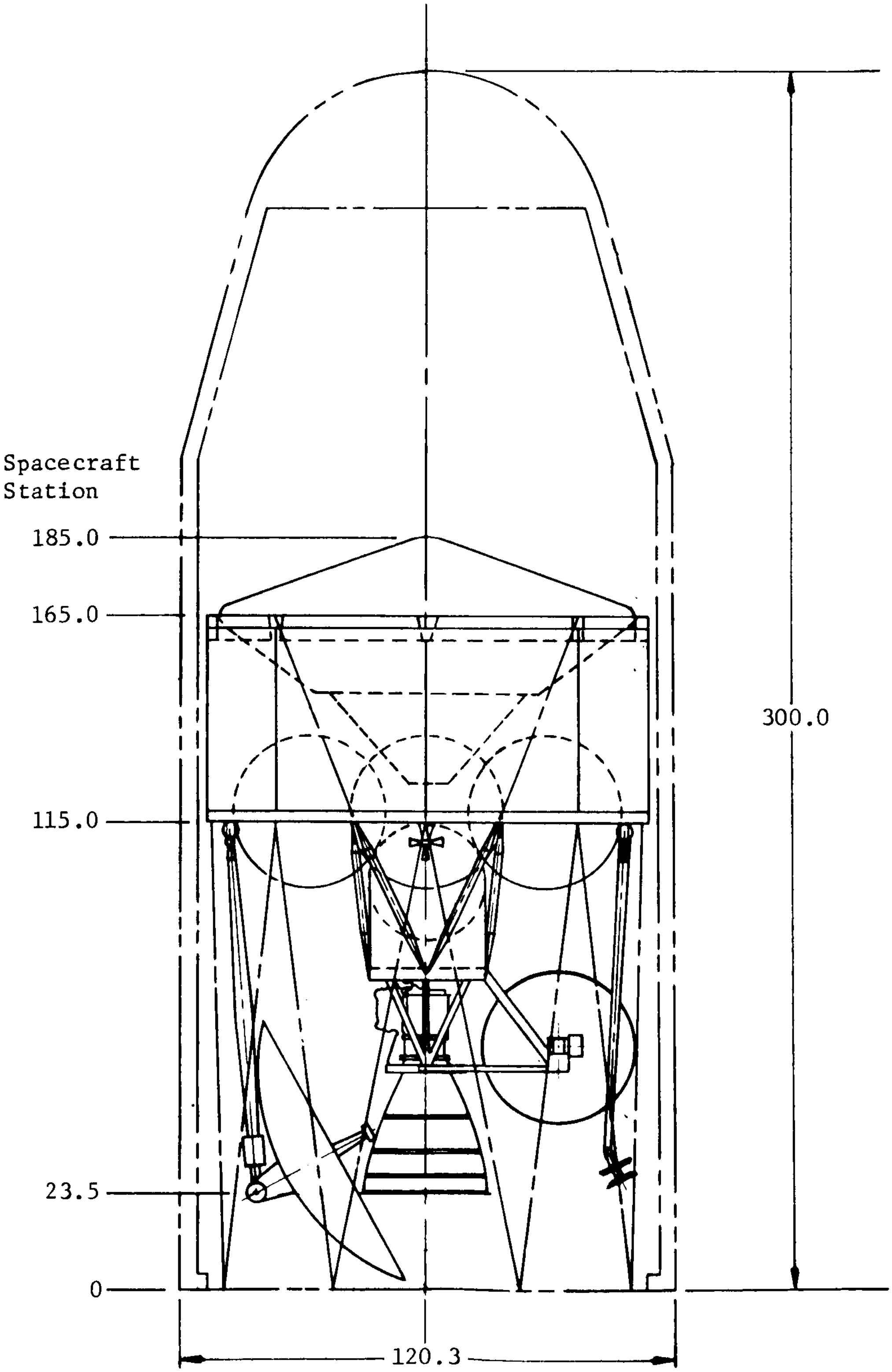
Spacecraft
Station
185.0
165.0
115.0
23.5
0
300.0
120.3

Figure 6.4-1: MODEL 971-104 LAUNCH CONFIGURATION

*Good sensor views*---All sensors and antennas have unobstructed views.

*Simple antenna deployment motions*---Only two of the three major antennas are deployed and these are single-plane motions.

- Negative Features

  *Long adapter required*---The weight of the adapter required for this vehicle more than offsets the gain that can be realized by engine-aft launching. The payload penalty for the adapter required with the engine-aft configuration is about 85 pounds, whereas the penalty for spacecraft reversal as required for the engine-up configuration is approximately 50 pounds.

  *Limited adapter clearance unless a deployable or petal adapter is used*---In addition to its weight and complexity, the long adapter makes it very doubtful that the spacecraft will clear the adapter during separation. This may require a special deployable adapter.

  *25-foot shroud requirement*---Placement of the flight capsule at the upper end of the spacecraft requires the shroud length to be increased to the next standard size.

  *Limited equipment access with flight capsule in place*---Placement of the capsule at the end of the equipment bay, and mounting equipment inside the shear panels, make it necessary to remove the flight capsule or sections of the shear deck to service equipment.

  *Special flight capsule interface required to get lightest arrangement*---The best flight capsule interface for this design would be a joint at the outside diameter of the flight capsule. When this is not the case, special flight capsule adapter structure must be added.

### 6.4.2 Weight Analysis

Analysis of Model 971-104 showed that a flight capsule plus science weight of 1,174 pounds is available. Total useful weight is 1,969 pounds and total weight in Mars orbit is 2,871 pounds. These weights are based on the general design parameters shown in Table 6.4-1 and the group weight statement of Table 6.4-2.

## Table 6.4-1: GENERAL DESIGN PARAMETERS

| Item | Model | | | |
|---|---|---|---|---|
| | 971-101 | 971-102 | 971-103 | 971-104 |
| Structural Arrangement | | | | |
| Capsule Support | Truss & Ring | Truss | Truss | Truss & Ring |
| Propellant Tank Support | Truss | Deck | Deck | Truss |
| Solid Motor Support | -- | Ring | -- | -- |
| Load Factors (Limit) | | | | |
| Lateral | | | | |
| At launch vehicle interface | 2.0 | 2.0 | 2.0 | 2.0 |
| At lander CG or equivalent distance from launch vehicle interface | 4.0 | 4.0 | 4.0 | 4.0 |
| Axial | 4.25 | 4.25 | 4.25 | 4.25 |
| Propulsion | | | | |
| Liquid Propellant Tank | | | | |
| Shape | Sphere | Cylinder | Cylinder | Sphere |
| *Pressure (psia) | 250 | 250 | 250 | 250 |
| Pressurization Tank | | | | |
| Shape | Sphere | Sphere | Sphere | Sphere |
| *Pressure (psia) | 3,500 | 3,500 | 3,500 | 3,500 |

*Nominal operating pressure: Limit Pressure = 1.1 (nominal)
Ultimate Pressure = 2.0 (limit)

Table 6.4-1: GENERAL DESIGN PARAMETERS (Cont)

| Other Subsystems (All Models) | |
|---|---|
| Reaction Control | Extended mission, 180 days Mars orbit<br>$N_2$ gas, 17 lb<br>Bottle pressure, 3,500 psia (contained in propellant pressurization bottles) |
| Guidance and Control | Weight includes: 18.5-lb gimbal actuator and 15-lb computer and sequencer; no horizon scanner included |
| Electrical Power | Weight includes: Solar array, 0.80 psf (excluding deployment and support)<br>Battery, Ni-Cd at 44 lb |
| Telecommunication | Telemetry, 18 lb<br>Data storage, 37 lb<br>Ratio, 55 lb with two 10-watt travelling wave tube amplifiers<br>Antenna, 82 lb (includes 6-foot-diameter high-gain antenna, 3-ft-diameter capsule antenna, omni-antenna, and probe antenna) |
| Pyrotechnics | Fixed weight, 13 lb includes pyrotechnics and switching circuits |
| Temperature Control | Function of spacecraft useful weight, prime power, RF power output, and spacecraft diameter |
| Cabling | Function of electrical-electronic weight |

## Table 6.4-2: GROUP WEIGHT STATEMENT

| | 971-101 | | | 971-102 | | | 971-103 | | | 971-104 | | |
|---|---|---|---|---|---|---|---|---|---|---|---|---|
| | Useful | Non-useful | Total | Useful | Non-useful | Total | Useful | Non-useful | Total | Useful | Non-useful | Total |
| Orbiter Less Science (Dry)* | 792 | 672 | 1,464 | 782 | 428 | 1,210 | 809 | 784 | 1,593 | 795 | 664 | 1,459 |
| Capsule & Science (Weight Available)** | 1,249 | | 1,249 | 1,373 | | 1,373 | 1,120 | | 1,120 | 1,174 | | 1,174 |
| In-Orbit Dry Weight | (2,041) | ( 672) | (2,713) | (2,155) | ( 428) | (2,583) | (1,929) | ( 784) | (2,713) | (1,969) | ( 664) | (2,633) |
| Residual Propellant | | 160 | 160 | | 70 | 70 | | 160 | 160 | | 160 | 160 |
| RCS Gas---In Orbit | | 8 | 8 | | 8 | 8 | | 8 | 8 | | 8 | 8 |
| Pressurization Gas | | 70 | 70 | | 38 | 38 | | 70 | 70 | | 70 | 70 |
| In-Orbit Weight | (2,041) | ( 910) | (2,951) | (2,155) | ( 544) | (2,699) | (1,929) | (1,022) | (2,951) | (1,969) | ( 902) | (2,871) |
| SRM Inerts | | | | | 156 | 156 | | | | | | |
| Transplanet RCS Gas | | 9 | 9 | | 9 | 9 | | 9 | 9 | | 9 | 9 |
| Usable Propellant | | 4,040 | 4,040 | | 4,236 | 4,236 | | 4,040 | 4,040 | | 4,120 | 4,120 |
| Spacecraft Separated Weight | (2,041) | (4,959) | (7,000) | (2,155) | (4,945) | (7,100) | (1,929) | (5,071) | (7,000) | (1,969) | (5,031) | (7,000) |

*Subsystem weights are shown in Section 6.3

**Impulsive transtage burn---spacecraft burn at perigee

# 7.0 REFINED CONFIGURATION AND MISSION ANALYSIS

After reviewing results of the Performance and Mission Analysis, Orbiter Subsystems, and Preliminary Configuration studies, a NASA-Boeing team chose the design conditions of Table 7.0-1 for conducting the Refined Configuration and Mission Analysis studies. From these studies, a final definition of expected performance, spacecraft configurations, and costs resulted.

Table 7.0-1: DESIGN CONDITIONS

| Case I---Out of Orbit Lander | Case II---Direct Entry Lander |
|---|---|
| 1973 launch date | 1973 launch date |
| Best attainable mission | Best attainable mission |
| Mars orbit period = 24.6 hr | Mars orbit period = 24.6 hr |
| Mars orbit periapsis alt = 1,000 km | Mars orbit periapsis alt = 1,000 km |
| 20-deg apsidal rotation + payload for 0 and 40 deg | 20-deg apsidal rotation + payload for 0 and 40 deg |
| Type I trajectories | Type I trajectories |
| 20-day launch period | 20-day launch period |
| ΔV allowance = 125 m/sec | ΔV allowance = 125 m/sec |
| Short holding orbits | Short holding orbits |
| Thrust = 3,500 lb | Thrust = 3,500 lb |
| Separated spacecraft weight = 7,000 lb + payload at 4,000, 6,000, and 8,000 lb | Separated spacecraft weight = 7,000 lb + payload at 4,000, 6,000, and 8,000 lb |
| 6-month Mars orbit | 6-month Mars orbit |
| First 30 days of Mars orbit active | First 30 days of Mars orbit active |
| 10-foot-diameter shroud | 16-foot-diameter shroud + payload Δ weight for 13-foot diameter |
| Capsule diameter, 102 to 111 in. | Capsule diameter, 170 to 180 in. |
| Capusle length, 60 in. | Capsule length in proportion to diameter |
| Orbiter science + scan platform = 200 lb | Orbiter science + scan platform = 200 lb |
| "Inhouse" redundancy philosophy | "Inhouse" redundance philosophy |

## 7.1 PERFORMANCE AND MISSION ANALYSIS

The performance and mission analysis conducted for the selected design configurations paralleled the corresponding parametric analysis. The objective was to provide detailed definition of mission parameters such as spacecraft velocity requirements, launch period and daily launch window, injection maneuvers, and tracking station view periods.

The analysis was based on the design conditions shown in Table 7.0-1. The basic difference between the two configurations is the time of capsule release. The capsule is released from Mars orbit for the "indirect" entry case. In the "direct" entry mission, the capsule is jettisoned before arrival at Mars.

Additional analysis was conducted to parametrically establish the effect, on payload, of variations in separated spacecraft weight and apsidal rotation during the Mars orbit insertion maneuver.

### 7.1.1 Mission Velocity Requirements

Proper orientation of periapsis of the Mars orbit is an important factor in mission design. It is desirable to have the capability of locating the periapsis within specific latitude and illumination bands. This will require rotation of the orbit line of apsides and/or plane change during the orbit insertion maneuver. Orbit insertion velocity requirements are given in Figure 7.1-1 for varying amounts of apsidal rotation. No plane change was considered. The ΔV shown is the requirement for establishing a Mars orbit with a periapsis altitude of 1,000 kilometers and a period of 24.6 hours. Note that the penalty for apsidal rotation is invariant with $V_\infty$. This allows selection of a fixed allowance, through the entire launch period, for a given desired apsidal rotation. The amount of this allowance is shown in Figure 7.1-2. In addition, the midcourse and orbit trim allowances are given as 50 and 75 m/sec, respectively. The buildup in total required ΔV is very rapid with increasing apsidal rotation. This factor is a major consideration in the selection of the desired orbit orientation. Note that the value of 300 m/sec used for ΔV allowance in the parametric analysis provides capability for 25 degrees apsidal rotation.

Table 7.1-1 summarizes the mission velocity requirements for the 20-day variable-arrival-date launch period discussed in Section 5.3. The ΔV buildup shown includes an allowance for losses in the trans-Mars injection maneuver. These losses combine the effect of finite burn in the transtage and spacecraft with the loss due to a 4-minute coast between transtage cutoff and spacecraft ignition. Detailed discussion of these losses is found in Section 5.5. Note that the total mission ΔV is approximately equal at the start and end of the launch period with a decrease of 60 m/sec in the center of the period. This reduction represents an additional ΔV available for contingencies.

### 7.1.2 Spacecraft Weights

Refined mission analysis calculations are based on modified parametric weight data developed from spacecraft configuration and structural studies. Nonuseful orbiter weight as a function of usable propellant, and useful in-orbit weight (less science and capsule) as a function of separated weight, are shown in Figures 7.1-3 and 7.1-4, respectively.

The nonuseful weight parametric data used for the refined studies is compared to the results from the preliminary propulsion sizing study (Figure 5.2-1) to show the reduction in nonuseful weight that resulted from the final configuration and structural concepts selected. This difference is due to two factors:

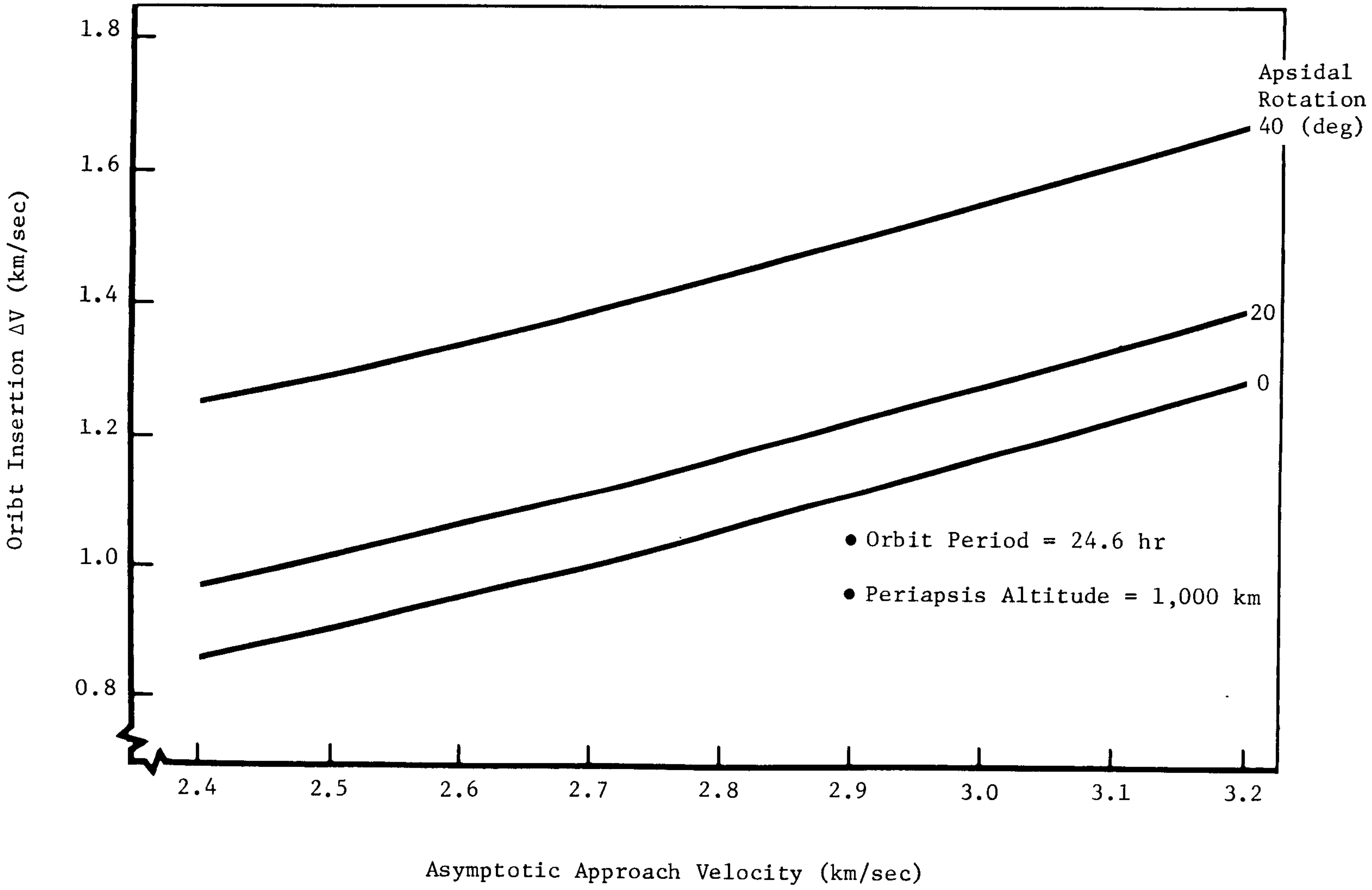

Figure 7.1-1: MARS ORBIT INSERTION VELOCITY REQUIREMENTS

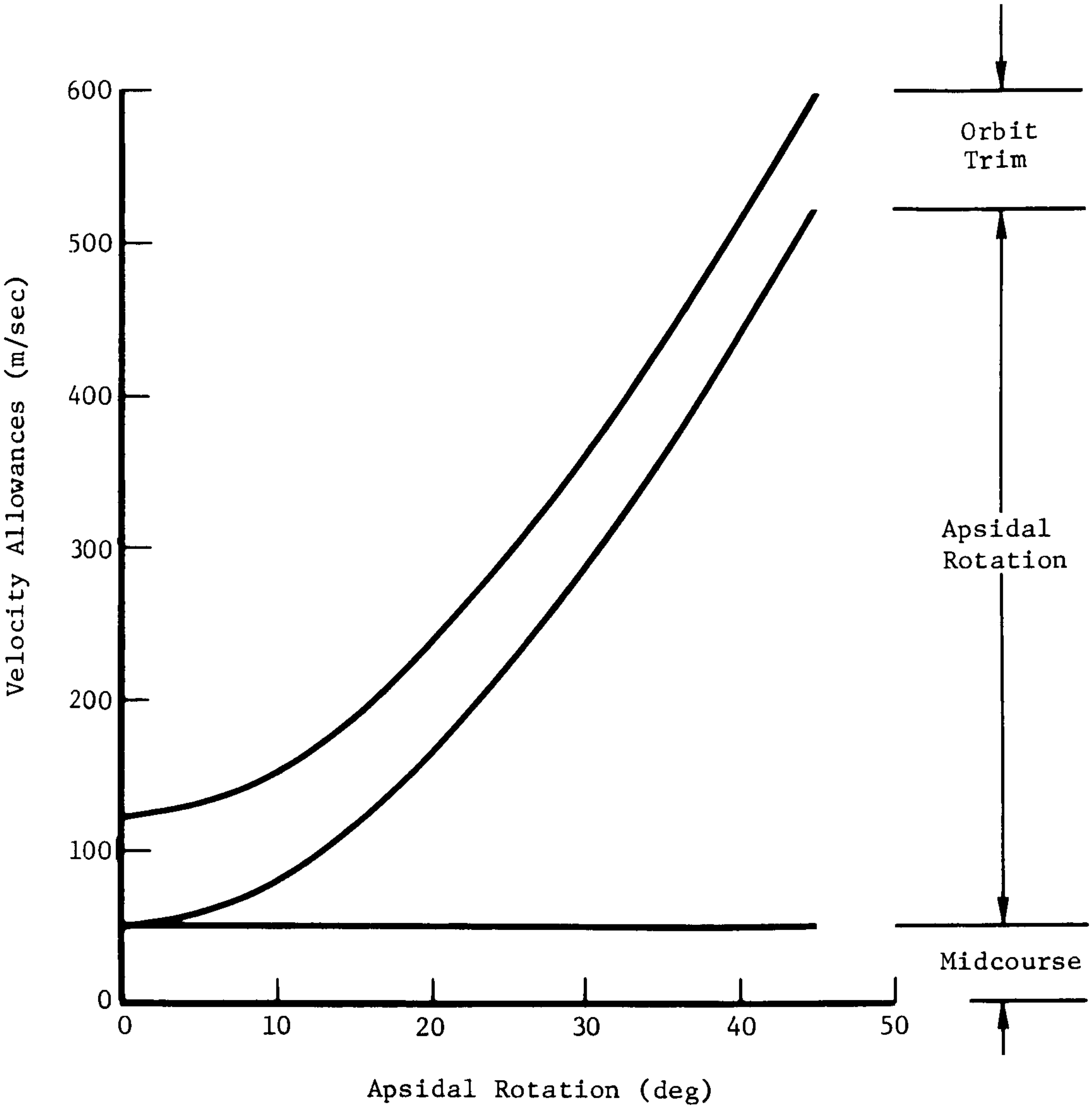

Figure 7.1-2: VELOCITY ALLOWANCE REQUIREMENTS

Table 7.1-1: MISSION VELOCITY REQUIREMENTS

| Launch Date (1973) | Arrival Date (1974) | Trip Time (days) | Injection $C_3$ ($km^2/sec^2$) | Arrival $V_\infty$ (km/sec) | Impulsive Spacecraft-Assist $\Delta V$ (km/sec)[1] | Trans-Mars Injection $\Delta V$ Loss (km/sec)[2] | Orbit Insertion $\Delta V$ (km/sec)[3] | Total Mission $\Delta V$ (km/sec)[4] |
|---|---|---|---|---|---|---|---|---|
| July 29 | Feb. 23 | 209 | 14.925 | 2.754 | 1.145 | 0.081 | 1.143 | 2.494 |
| Aug. 2 | Feb. 28 | 210 | 15.072 | 2.671 | 1.151 | 0.081 | 1.099 | 2.456 |
| Aug. 7 | Mar. 6 | 211 | 15.660 | 2.580 | 1.176 | 0.084 | 1.053 | 2.438 |
| Aug. 12 | Mar. 12 | 212 | 16.758 | 2.504 | 1.223 | 0.088 | 1.015 | 2.451 |
| Aug. 17 | Mar. 17 | 212 | 18.386 | 2.450 | 1.292 | 0.093 | 0.988 | 2.498 |

[1] Spacecraft weight = 7,000 pounds

[2] Assumes 4-minute coast between transtage final cutoff and spacecraft ignition

[3] Mars orbit definition: Periapsis altitude = 1,000 kilometers
Period = 24.6 hours
Apsidal rotation = 20 degrees

[4] Includes midcourse and orbit trim allowance of 125 m/sec

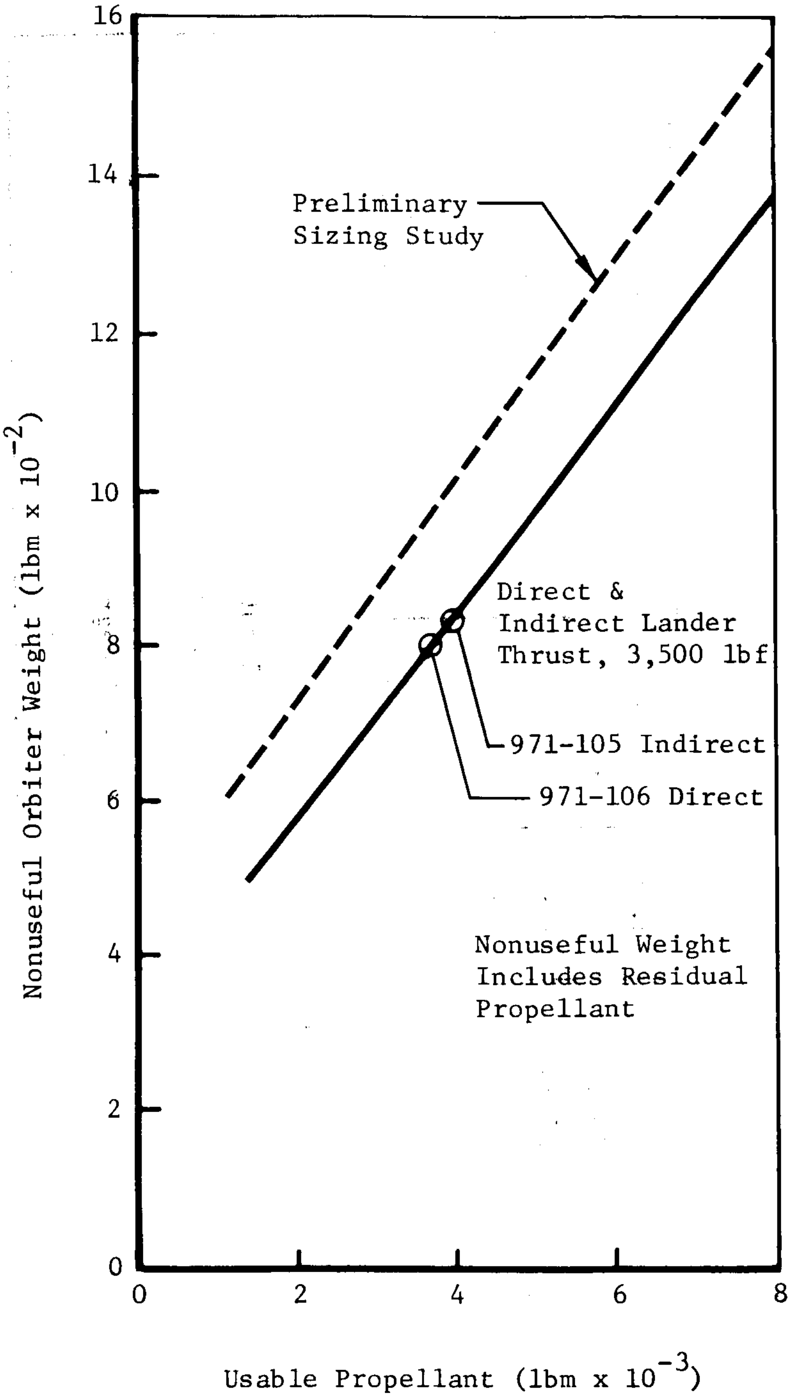

Figure 7.1-3: REFINED NONUSEFUL ORBITER WEIGHT

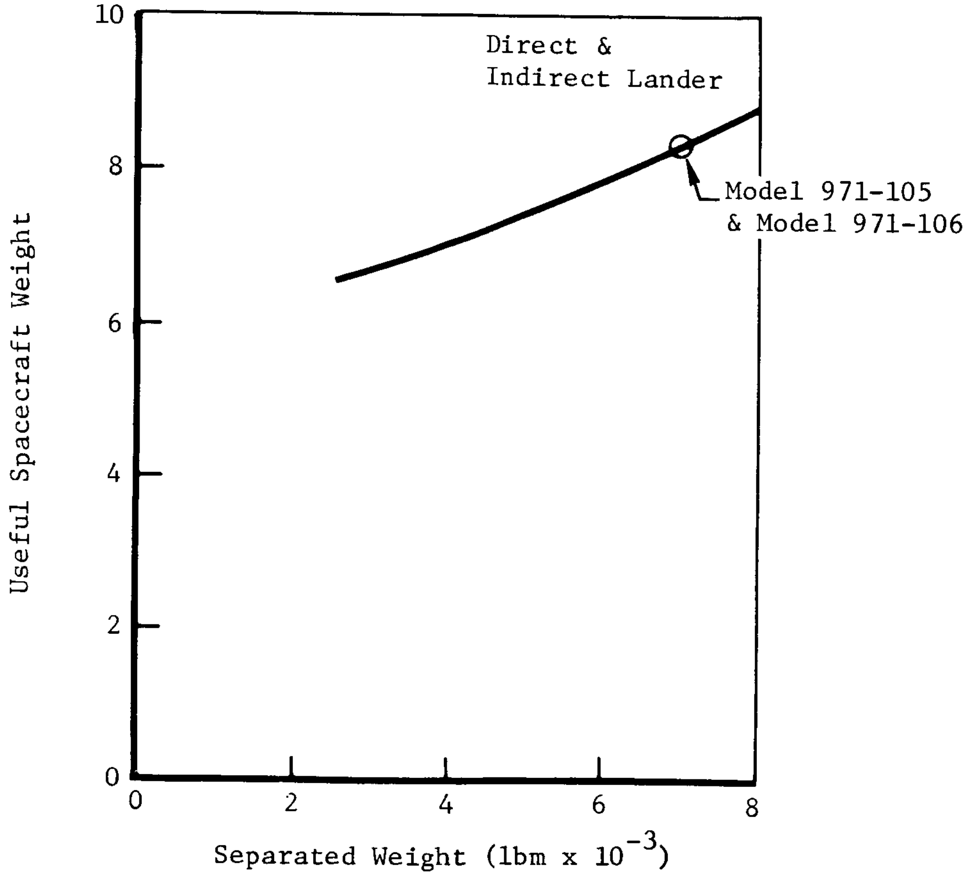

Figure 7.1-4: USEFUL WEIGHT MINUS SCIENCE AND CAPSULE

1) Structural Weight---These have been reduced by approximately 100 pounds because the final configurations (Models 971-105 and 971-106) provide propulsion system structural support more efficiently than the configuration (Section 5.2.1; similar to Model 971-103) used to initially evaluate nonuseful structure. This reduction in nonuseful structure is also manifested in the preliminary configurations, Models 971-101 and 971-104.

2) Propulsion System Pressurization Weight---Propellant pressurization nonuseful weights are reduced by approximately 50 pounds for a propellant load of 4,000 pounds because helium rather than nitrogen is being used for propellant expulsion. This change is a direct result of a new capsule shape (NASA supplied) that permits the increased volumes associated with helium for propellant expulsion and nitrogen for RCS (as opposed to an all nitrogen approach) without attendant weight penalties.

Figure 7.1-4 shows the variations in useful in-orbit weight as a function of separated weight. This data was obtained by considering all useful subsystem weights, except for temperature control, cabling, and orbiter structure, invariant with separated weight. For the variable weight subsystems, orbiter geometry and design loads determine estimated weight allocations.

### 7.1.3 Spacecraft Payload Capability

Spacecraft payload capability has been parametrically determined as a function of separated spacecraft weight, apsidal rotation, and capsule entry mode. The short holding orbit mission option defined in Section 5.5 was considered in the analysis. Figure 7.1-5 illustrates the capsule weight that can be placed in Mars orbit when an indirect capsule entry is assumed. The data considered the finite burn losses encountered in a trans-Mars injection maneuver with 4 minutes coast between transtage cutoff and spacecraft ignition. A $\Delta V$ allowance of 125 m/sec for midcourse and orbit trim is also included. The launch-arrival date assumed is the last day in the 20-day variable-arrival-date launch period. Because this is the most severe combination in the launch period, the capsule weights shown will be attainable anywhere in the period. A capsule weight of approximately 1,170 pounds is attainable at the design point of 7,000-pound spacecraft weight and 20-degree apsidal rotation. This requires a usable propellant load of approximately 4,000 pounds. Note that this payload represents a gain of 95% over the corresponding payload with no spacecraft assist. Figure 7.1-6 illustrates similar data for the direct capsule entry mode. The increased performance ($\sim$1,700 pounds for the design configuration) is primarily due to the propellant saved in eliminating the requirement to put the cpasule in orbit before its deployment. In addition, there is a decrease in losses due to the reduction in required coast between transtage cutoff and spacecraft ignition from 4 to 1.5 minutes. However, there are compensating losses due to the large payload fairing that must be used to enshroud the capsule during launch. This shroud, defined in the configurations section of the report, is 16.33 feet in diameter and weighs 3,085 pounds more than the standard 10-foot-diameter payload fairing used for the indirect entry case. The increase in weight results in a reduction in velocity at transtage cutoff of 69 m/sec for a mission with a 7,000-pound spacecraft. In this capsule entry mode, the payload gain over a mission without spacecraft assist is 127%. An additional gain in capsule weight of 72 pounds can be achieved if the shroud diameter is reduced to 13 feet.

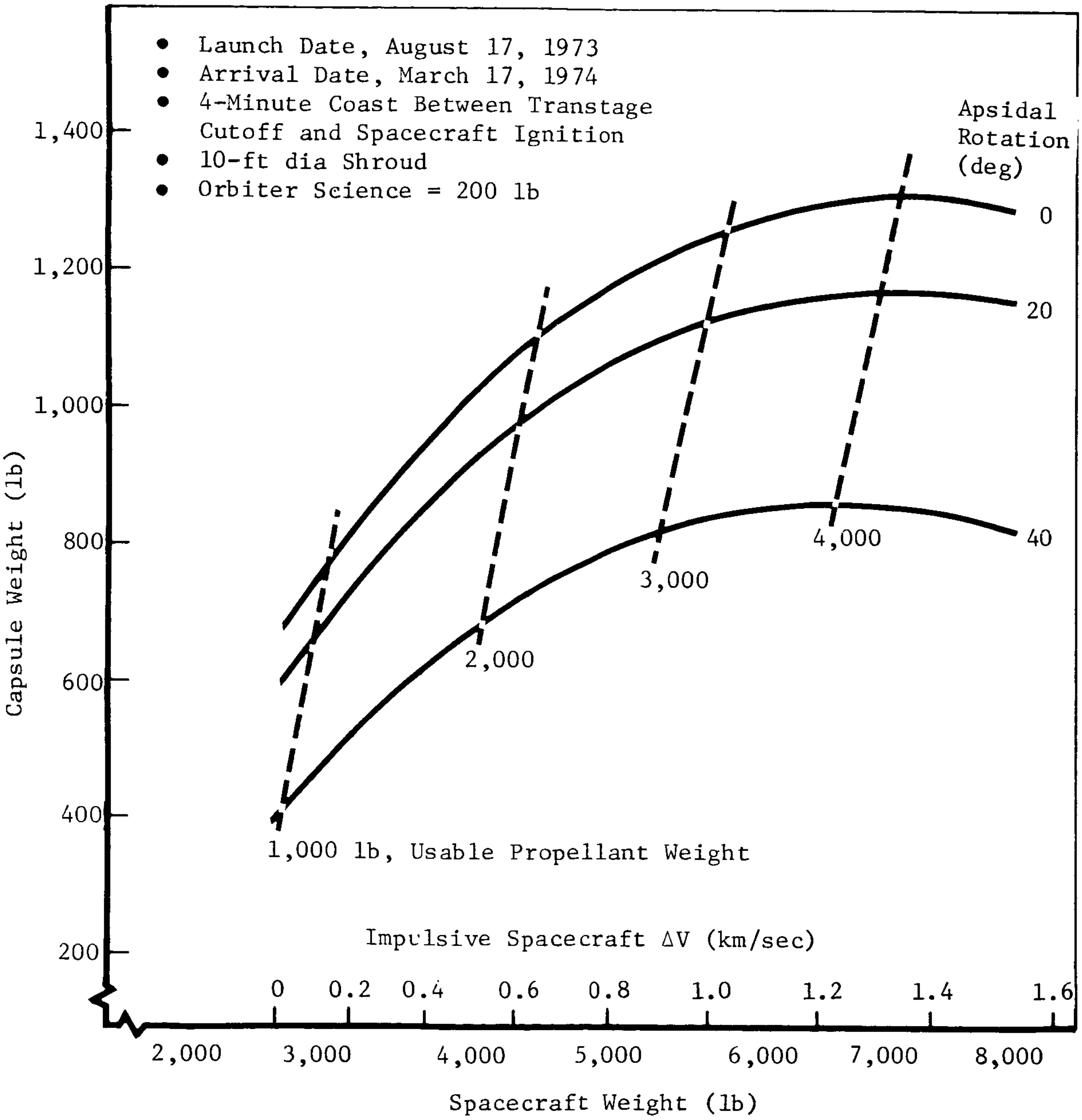

Figure 7.1-5: CAPSULE WEIGHTS---INDIRECT ENTRY

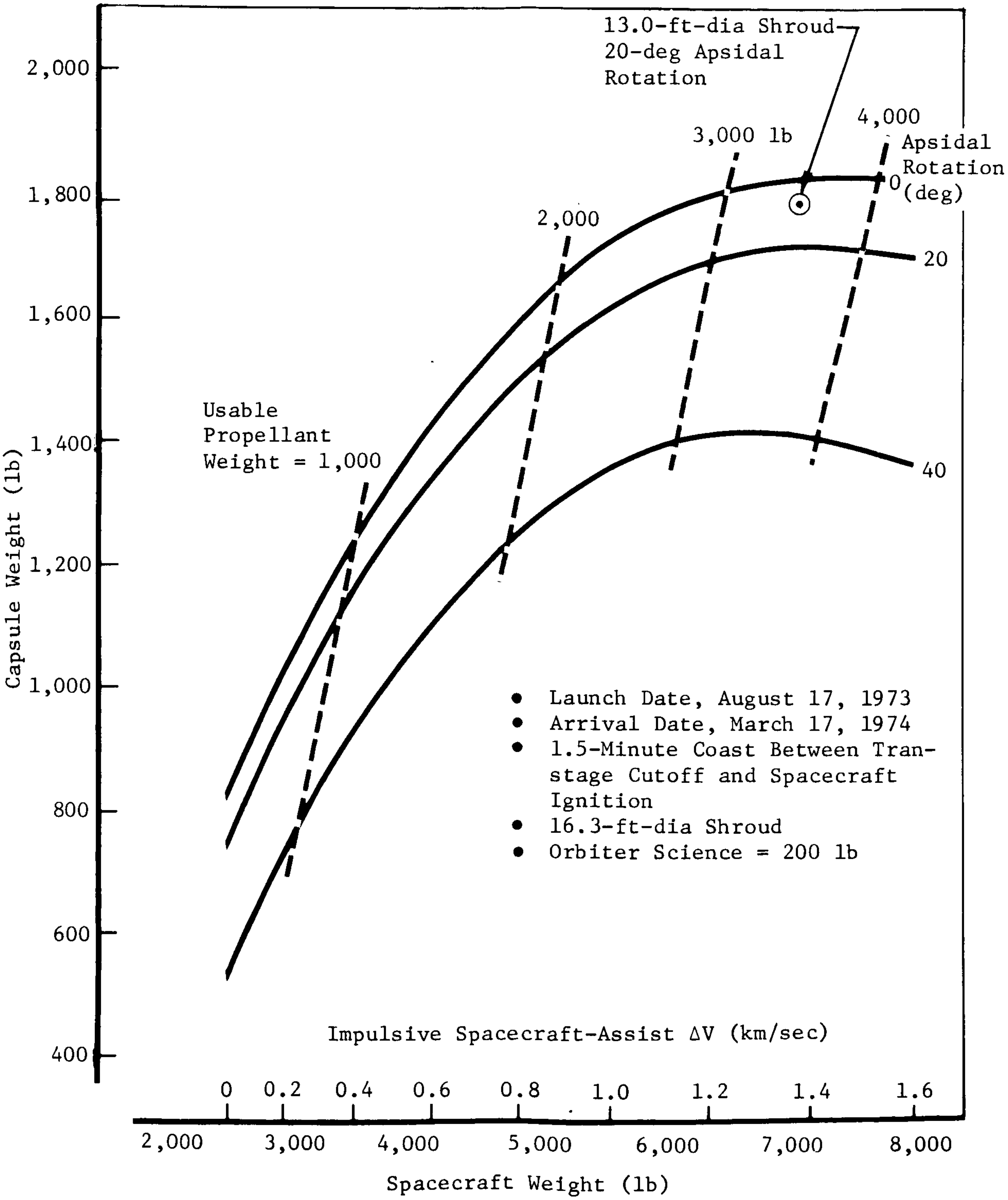

Figure 7.1-6: CAPSULE WEIGHTS---DIRECT ENTRY

The steering profile considered in the trans-Mars injection maneuver assumes a fixed attitude rate during transtage second burn and a constant inertial attitude angle for the spacecraft burn. These angles are optimized to achieve the desired $C_3$ with a minimum expenditure of spacecraft propellant. The resulting steering profiles are defined in Figure 7.1-7.

### 7.1.4 Launch Analysis

Near-Earth trajectory characteristics were examined for the 20-day variable-arrival-date launch period. Detailed discussion of a similar analysis appears in Section 5.6.1 for a different launch period employing a constant arrival day. The analysis assumes an injection burn arc corresponding to a mission with a 7,000-pound spacecraft and a 4-minute coast between transtage final cutoff and spacecraft ignition.

Two launch windows exist on each day of the 20-day launch period. These windows correspond to the short and long parking orbit coast time solutions. Figure 7.1-8 shows the usable launch azimuth range for both launch windows for each launch day. For the early days of the launch period, only the launch azimuths near 114 degrees (short parking orbit coasts) and 66 degrees (long parking orbit coasts) can be used. For August 14 through August 17 launches, the entire launch azimuth range from 66 to 114 degrees is available for each launch window. All launch azimuths can be used on these later days because the declination of the outgoing asymptote (DLA) is less than the launch site latitude.

Figure 7.1-9 shows the launch times during both launch windows for each day of the launch period. The required launch azimuths are also shown. The duration of each nominal launch window varies from a minimum of 2.7 hours for launch on the first day of the period to 5.7 hours for August 14 through August 17 launches. Figure 7.1-10 illustrates the variation in nominal launch window during the launch period.

Parking orbit coast times for both the short and long parking orbit coasts are shown in Figure 7.1-11. All coast times encountered are above 1,400 seconds. This data is based on a 4-minute coast between transtage second shutdown and spacecraft ignition. A reduction in this coast time will increase the parking orbit coast time.

Near-Earth shadow entry and exit times for both the short and long parking orbit coasts are shown in Figures 7.1-12 and 7.1-13. All event times for each day are shown for that launch azimuth with the longest launch-to-shadow exit time. Note that the vehicle usually enters Earth's shadow during the trans-Mars injection maneuver and exits after the maneuver has been completed. The maximum time from launch to shadow exit is 95 minutes. This is comparable to the parametric result discussed in Section 5.6.1.

### 7.1.5 Tracking and Data Acquisition

Section 5.6.2 discusses tracking station visibility of trajectories having impulsive trans-Mars injection maneuvers. This section investigates the effect of an actual finite burn injection maneuver. The data shown assumes a 7,000-pound spacecraft and a 4-minute coast between the transtage second shutoff and spacecraft ignition.

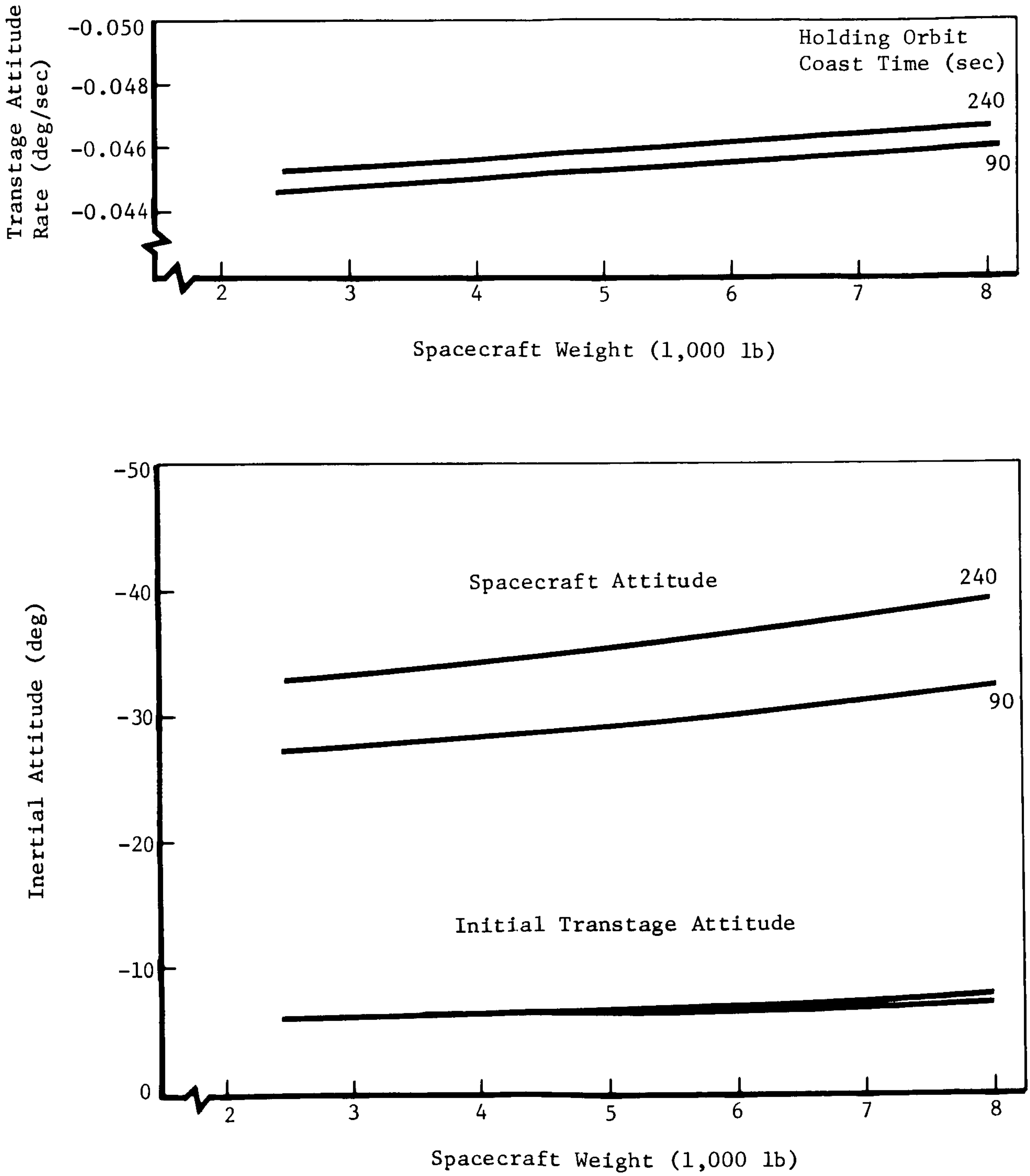

Figure 7.1-7: STEERING PROFILE DEFINITIONS

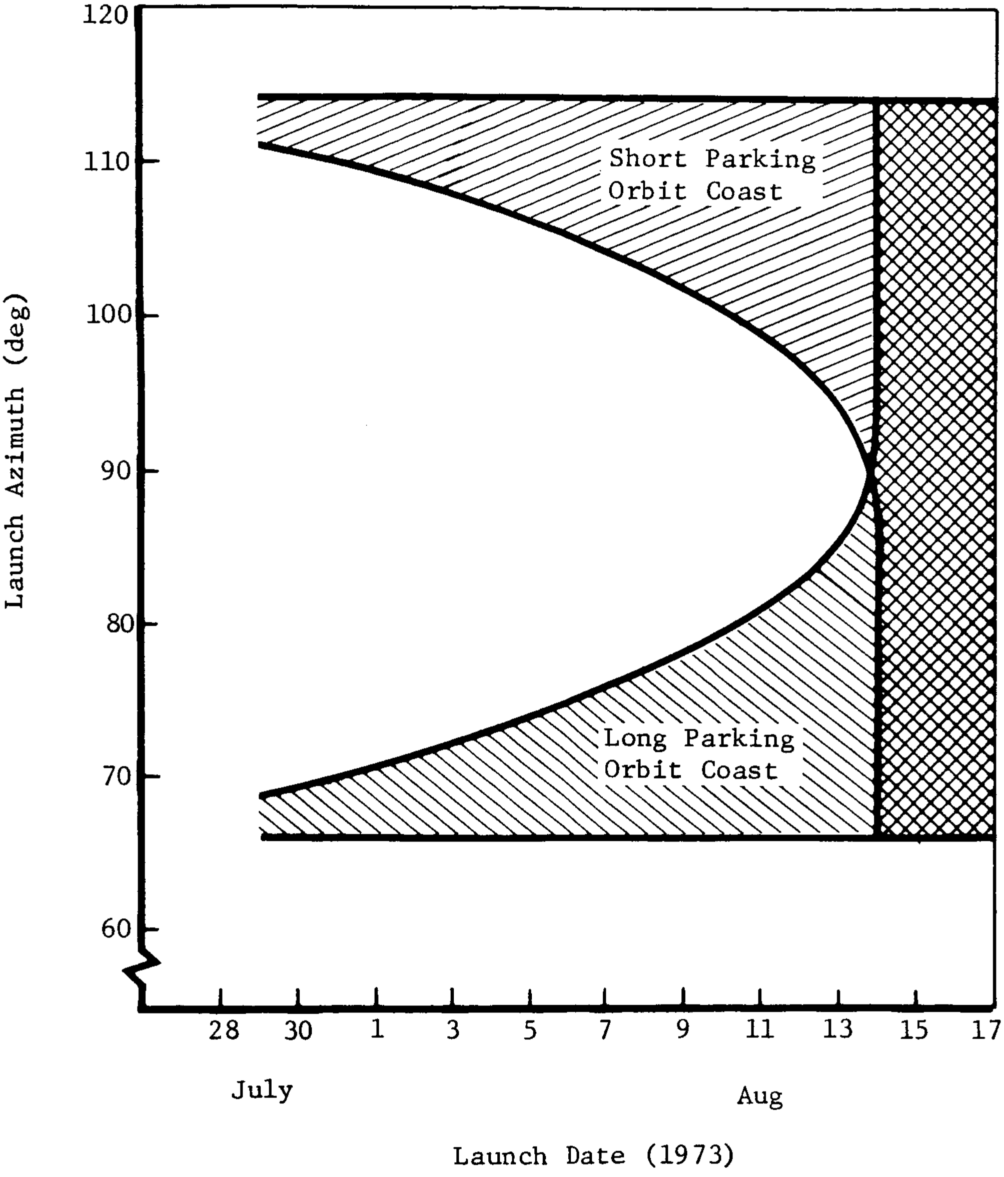

Figure 7.1-8: USABLE LAUNCH AZIMUTHS

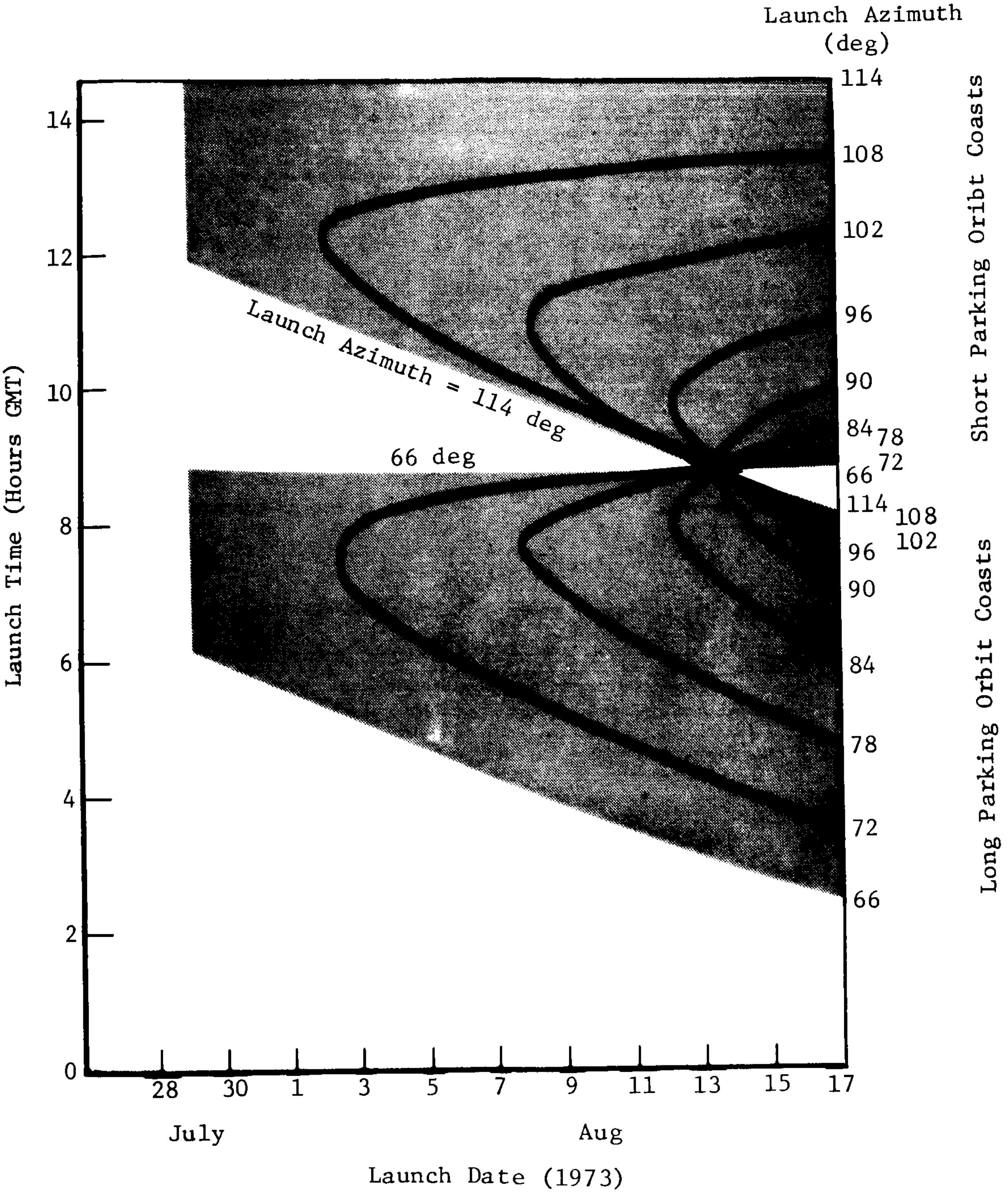

Figure 7.1-9: LAUNCH TIMES

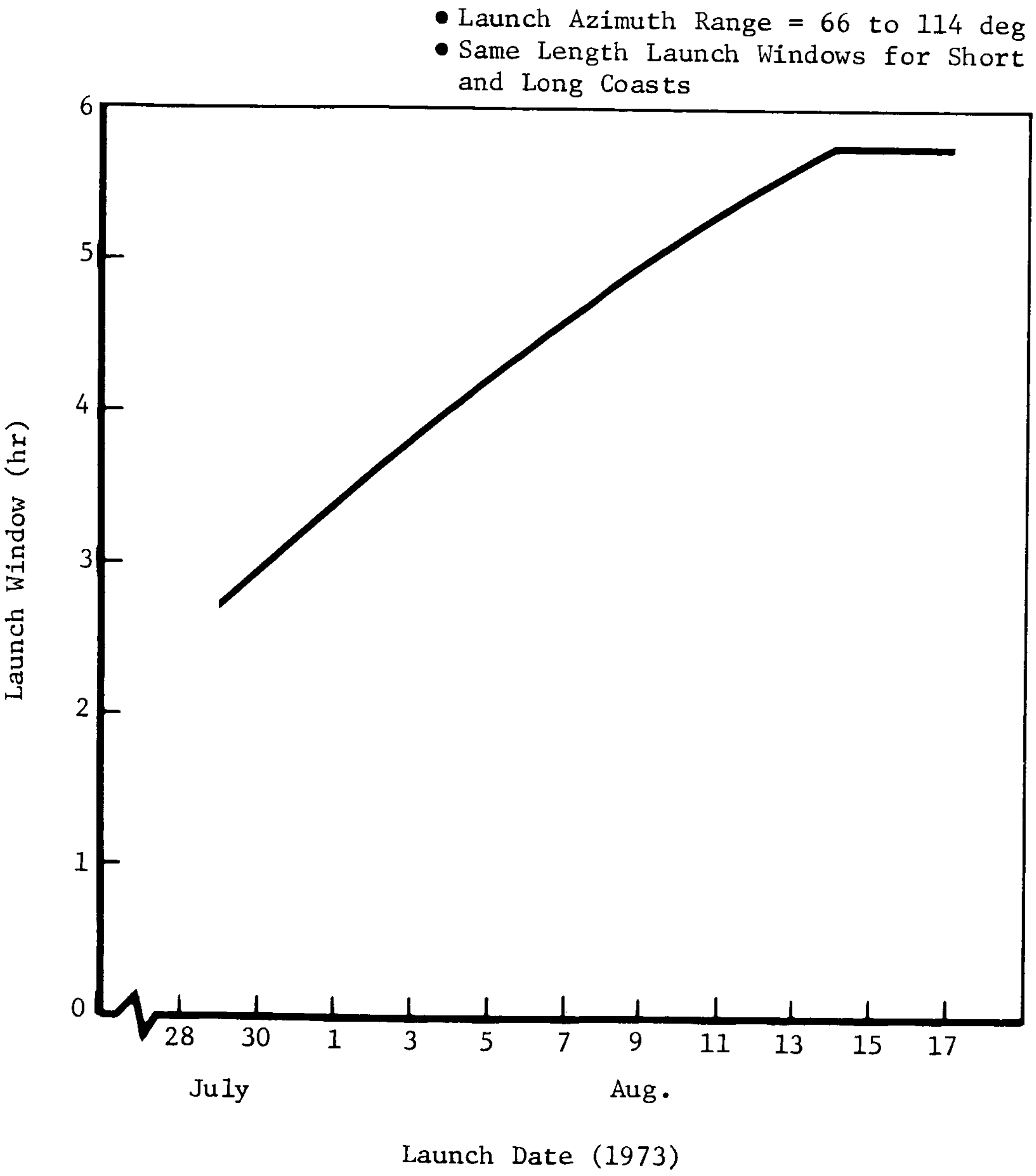

Figure 7.1-10: DAILY LAUNCH WINDOWS

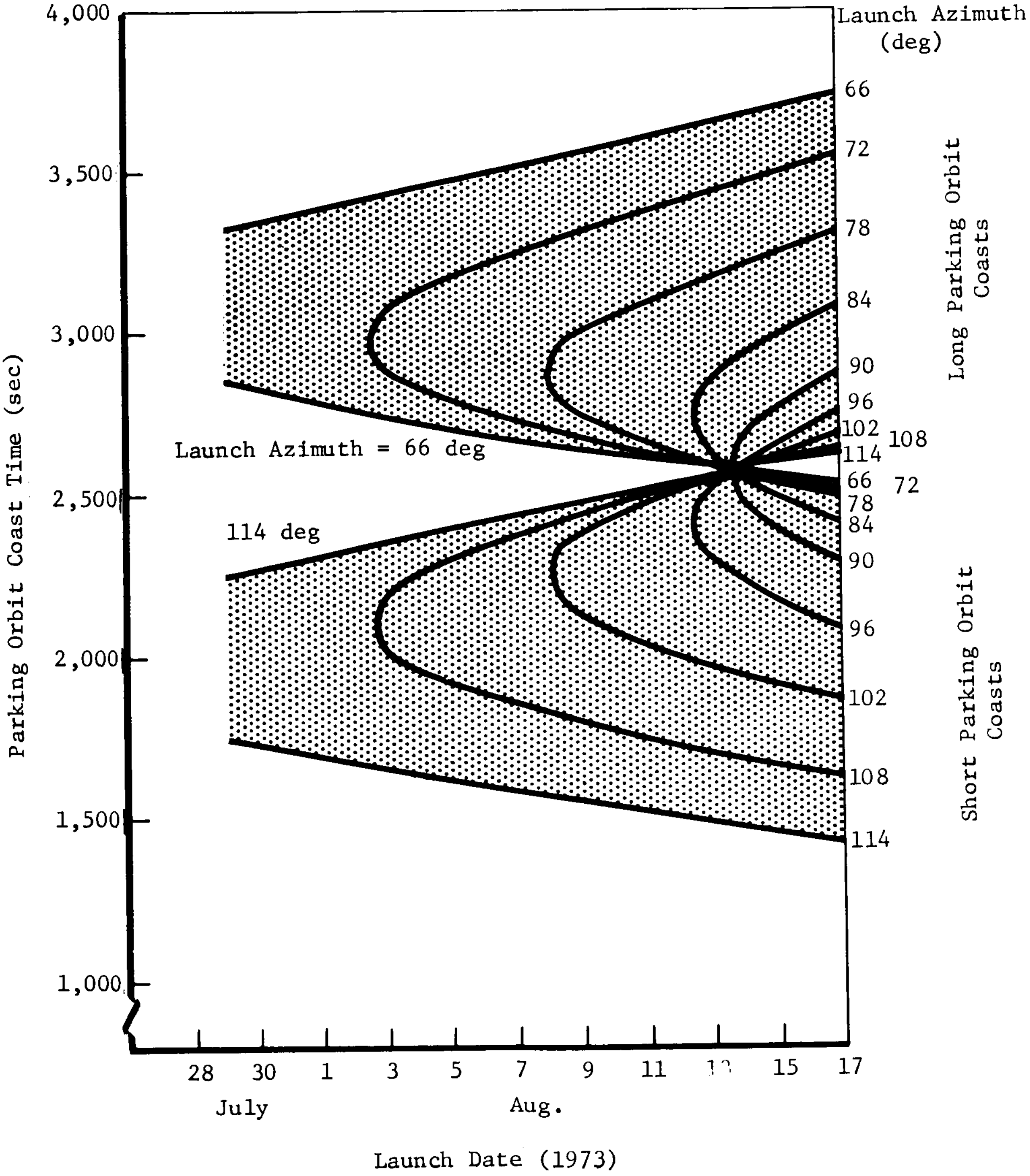

Figure 7.1-11: PARKING ORBIT COAST TIMES

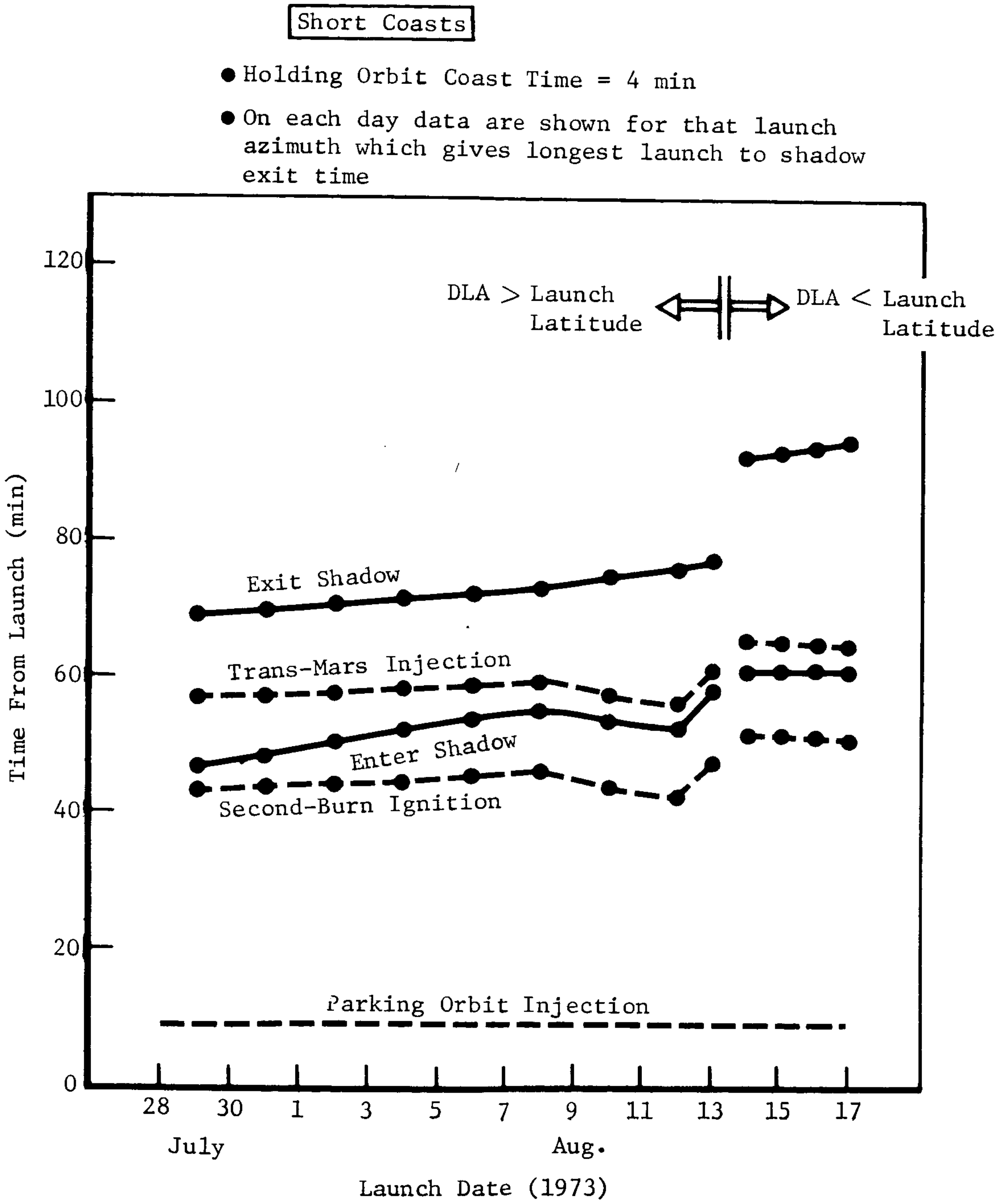

Short Coasts

- Holding Orbit Coast Time = 4 min
- On each day data are shown for that launch azimuth which gives longest launch to shadow exit time

Figure 7.1-12: NEAR-EARTH SHADOW ENTRY AND EXIT TIMES---SHORT COASTS

Long Coasts

- Holding Orbit Coast Time = 4 min
- On each day data are shown for that launch azimuth which gives longest launch to shadow exit time

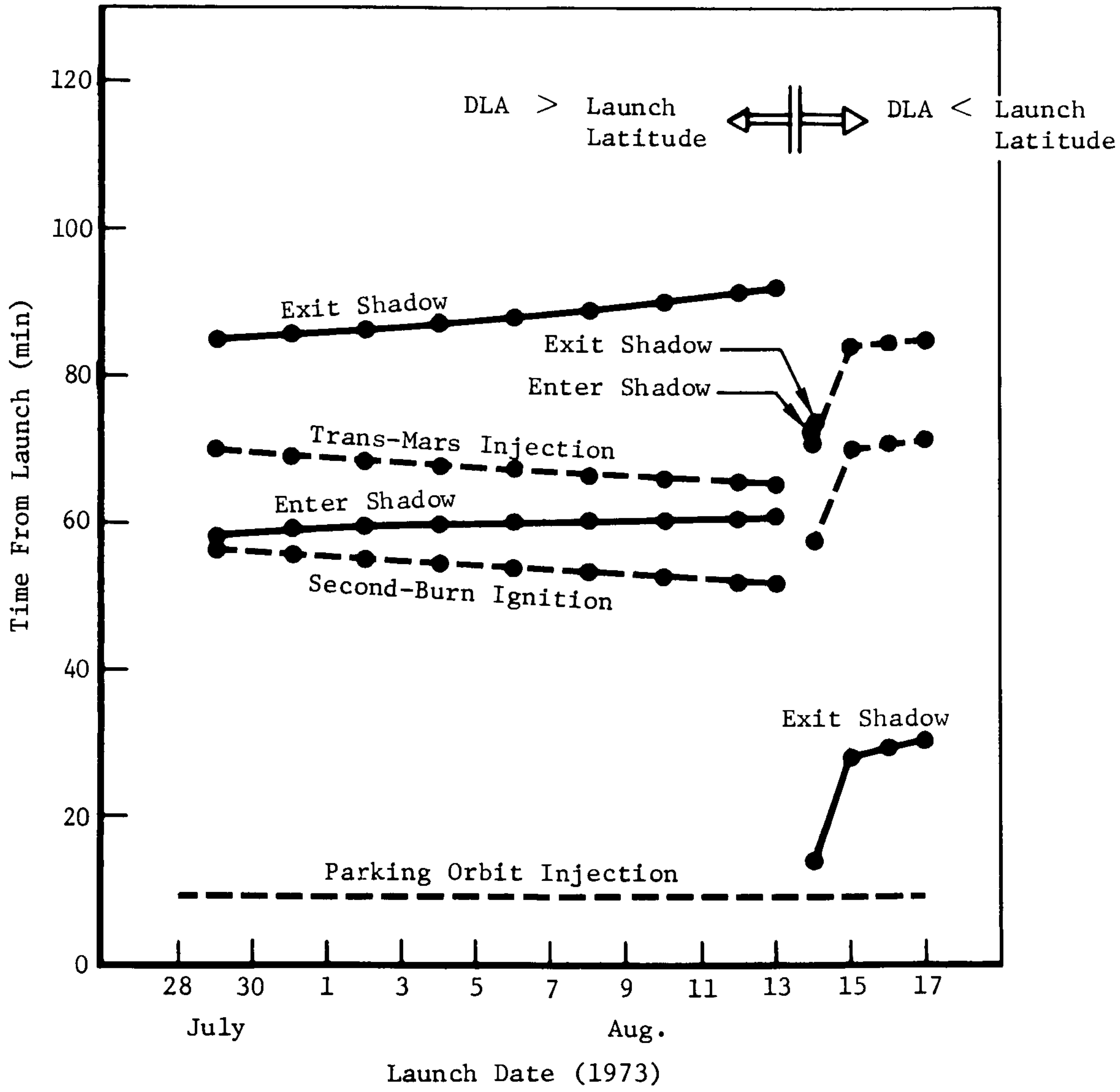

Figure 7.1-13: NEAR-EARTH SHADOW ENTRY AND EXIT TIMES---LONG COASTS

Figure 7.1-14 shows the station visibility regions during the launch phase as functions of time from launch and launch azimuth for launch on August 17. Short parking orbit coast is assumed. Similar results would occur on other launch days. For the launch day investigated, no coverage exists for parts of the early portion of the trans-Mars injection maneuver (shaded regions). However, after the vehicle starts gaining altitude, it comes into the view of one or more tracking stations so that the actual trans-Mars injection point has multi-station coverage. Figure 7.1-15 shows similar data for the August 17 launch employing long parking orbit coast times. No tracking coverage is obtained during most of the injection maneuver, but the burnout is generally visible by one or more stations. Tracking ships will have to be employed if real-time telemetry is required for the entire trans-Mars injection maneuver. The additional coverage obtained with ships is described in Section 5.6.2.

Figures 7.1-16 and 7.1-17 show the tracking coverage during the trans-Mars phase for August 17 launch employing short and long parking orbit coasts, respectively. Only the DSIF stations are shown. It is seen that for all launch azimuths, continuous coverage is obtained within 0.5 hour of the trans-Mars injection. The shaded areas show the brief time periods when the vehicle is not in view of a DSIF station.

The tracking station coordinates and constraints considered in the analyses are defined in Appendix A4.

### 7.1.6 Guidance Analysis

The mission considered in the detailed performance and mission analysis is virtually identical with the candidate short holding orbit mission selected during the parametric analyses. Consequently, the estimate of first midcourse $\Delta V \approx 27$ m/sec, discussed in Section 5.6.4, is directly applicable to the refined analyses.

### 7.1.7 Mission Summary

Table 7.1-2 summarizes a typical event sequence and the corresponding spacecraft velocity requirements for missions considering direct and indirect capsule entry. The table illustrates the slight differences between the missions. From a velocity standpoint, the only difference is in the trans-Mars injection $\Delta V$. The extra 37 m/sec required for the direct entry option is primarily due to the large payload fairing required to enshroud the capsule.

In the direct entry mode, the capsule is released approximately 2 days before encounter. Deployment of the capsule much earlier than this might result in large errors in the position of the landing. If the capsule is released closer to the planet, the capsule velocity requirements begin to increase rapidly. The 2-day periods between trim maneuvers are required for orbit determination.

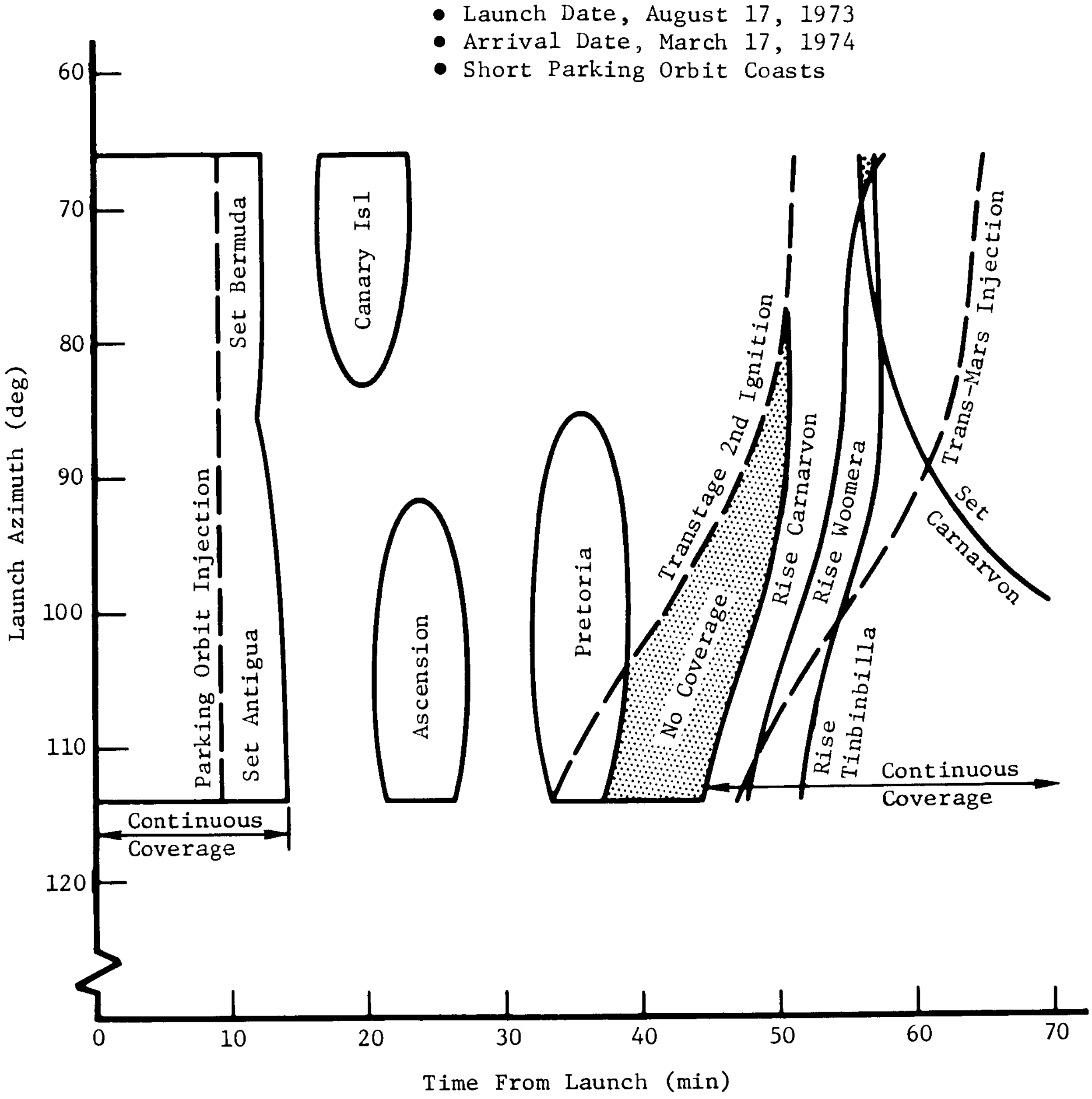

Figure 7.1-14: STATION TRACKING COVERAGE---LAUNCH PHASE---SHORT PARKING ORBIT COASTS

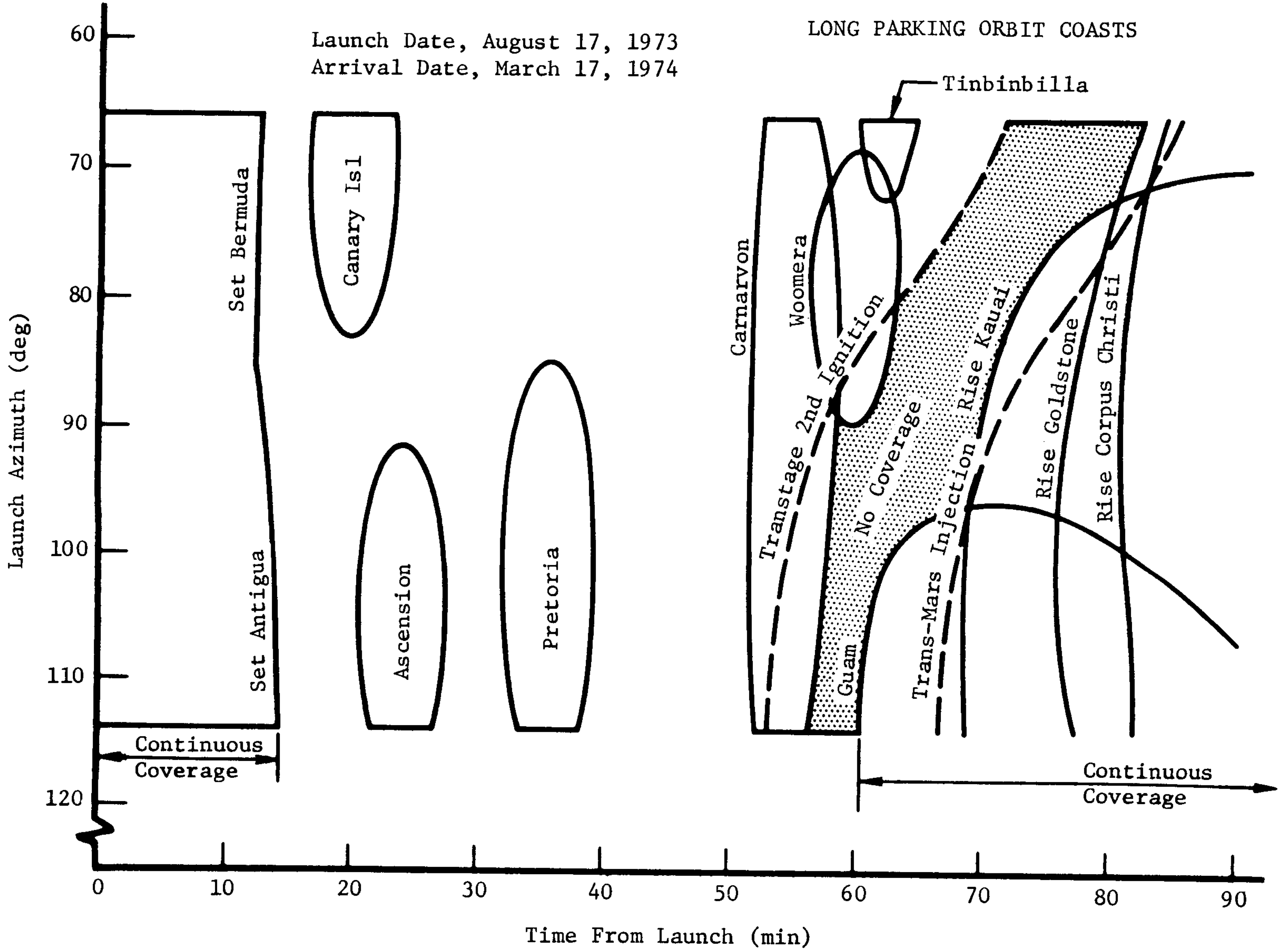

Figure 7.1-15: STATION TRACKING COVERAGE---LAUNCH PHASE---LONG PARKING ORBIT COASTS

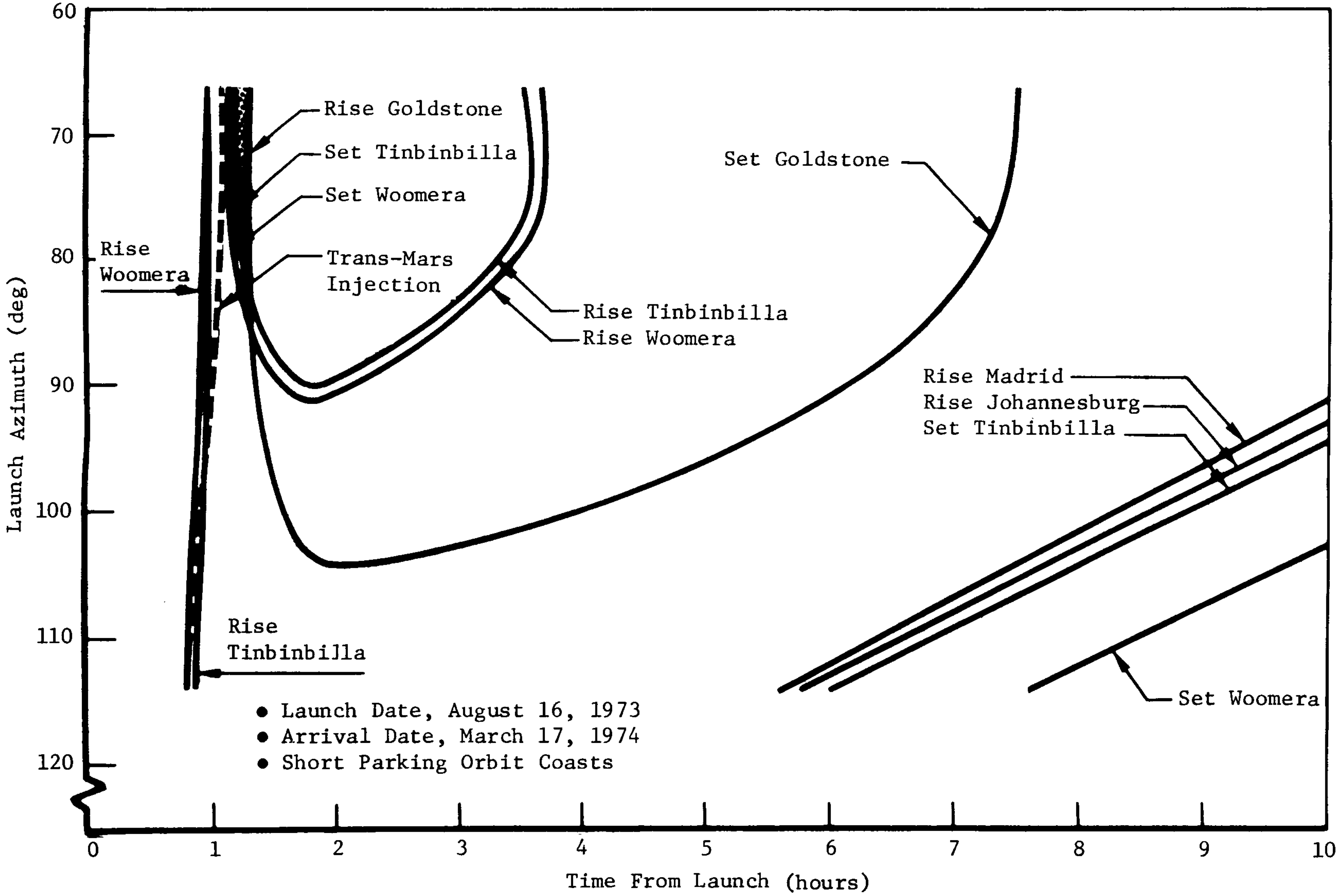

Figure 7.1-16: DSIF STATION COVERAGE---TRANS-MARS PHASE (SHORT COAST)

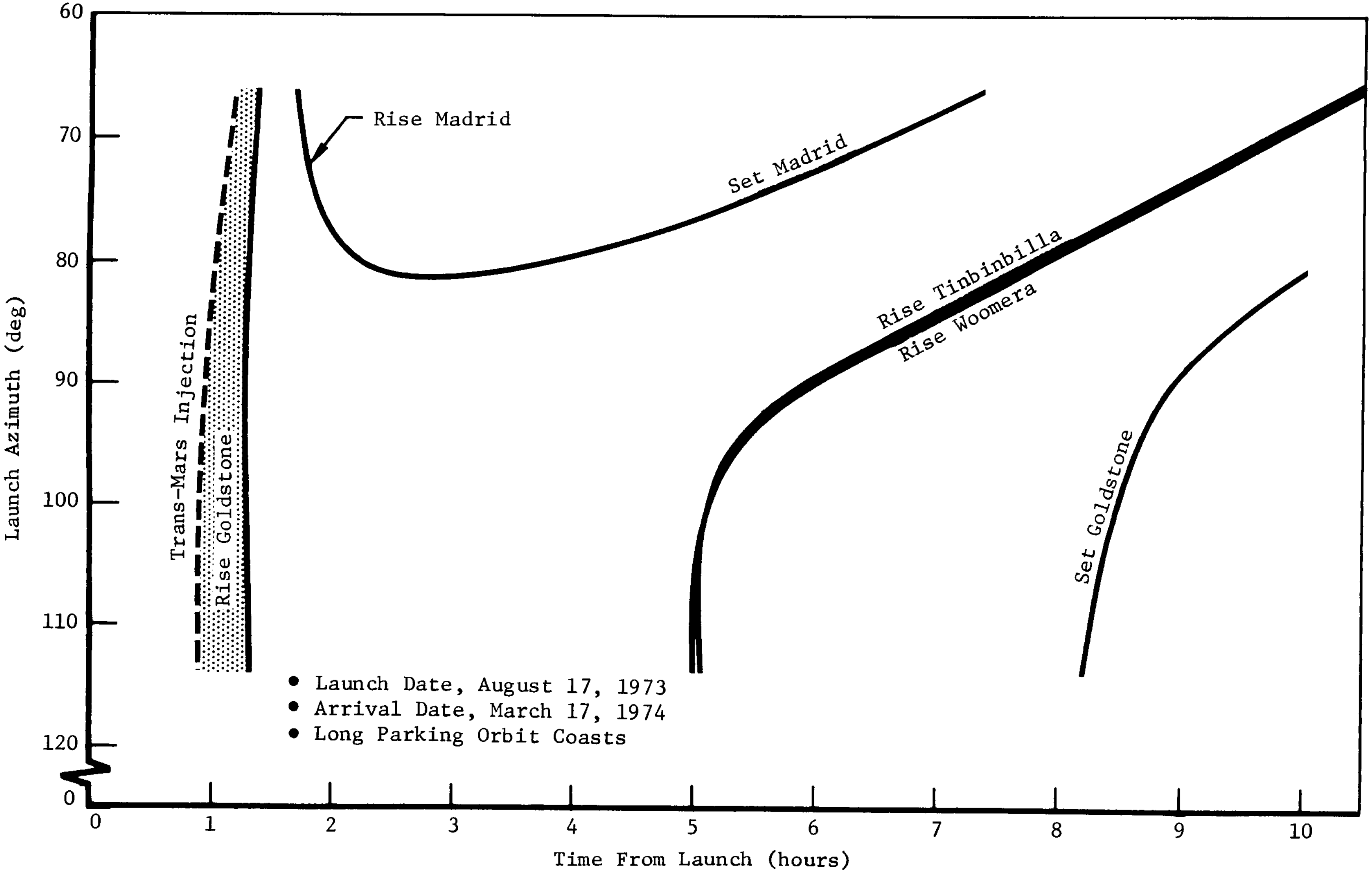

Figure 7.1-17: DSIF STATION COVERAGE---TRANS-MARS PHASE (LONG COAST)

## Table 7.1-2: TYPICAL MISSION EVENT SEQUENCE

| | Direct Entry | | Indirect Entry | |
|---|---|---|---|---|
| Event | Time from Liftoff | Spacecraft ΔV (m/sec) | Time from Liftoff | Spacecraft ΔV (m/sec) |
| | Minutes | | Minutes | |
| Liftoff, August 17, 1973 | 0 | | 0 | |
| Parking Orbit Injection | 9.4 | | 9.2 | |
| Transtage Second Ignition | 50.0 | | 47.4 | |
| Transtage Cutoff | 55.5 | | 53.2 | |
| Spacecraft Ignition | 57.0 | | 57.2 | |
| Trans-Mars Injection | 61.0 | 1,422 | 61.0 | 1,385 |
| | Days | | Days | |
| Midcourse Corrections (3 maneuvers) | 5, 25, & 172 | <50 | 5, 25, & 172 | <50 |
| Capsule Deployment | 170 | | | |
| Orbit Injection, March 17, 1974 | 172 | 988 | 172 | 988 |
| Orbit Trim (2 maneuvers) | 174 & 176 | 75 | 174 & 176 | 75 |
| Capsule Deployment | | | 178 | |

Short Parking Orbit Coast

Launch Azimuth = 90 degrees

Spacecraft Weight = 7,000 pounds

## 7.2 CONFIGURATIONS

This section contains configuration descriptions of the orbiters selected for both the indirect lander entry (orbit Mars before capsule release) and the direct lander entry (release capsule before orbiting Mars). Separate spacecraft descriptions are provided for each case.

The basic design parameters used for spacecraft development are shown in Table 7.2-1. Some of these, such as separated spacecraft weight, orbiter engine thrust, propellant, helium and nitrogen weight, solar panel size, and antenna size and type are the results of the various parametric studies that preceded the spacecraft configuration activity. Others, like launch vehicle type, shroud, and flight capsule size and weight, were specified by Langley Research Center before the refined configuration and mission analyses. Note that the shown flight capsule weights were used for structural design only. They do not indicate performance capability.

Table 7.2-1: DESIGN PARAMETERS

| | Indirect Lander Entry | Direct Lander Entry |
|---|---|---|
| Launch Vehicle | Titan IIIC | Titan IIIC |
| Shroud Diameter (ft) | 10 | 16.33 |
| Shroud Weight (lb) | Variable | 4,525 |
| Capsule Diameter and Length (in.) | 102 x 60 | 178 x 104 |
| Capsule Weight (lb) | 1,500 | 2,000 |
| Separated Spacecraft Weight (lb) | 7,000 | 7,000 |
| Orbiter Engine Thrust (lb) | 3,500 | 3,500 |
| Propellant Weight (lb) | 4,119 | 3,619 |
| Propulsion System Type | Modular | Modular |
| Pressurant Weight and Type | 10 lb, Helium | 9 lb, Helium |
| ACS Propellant and Type | 18 lb, Nitrogen | 18 lb, Nitrogen |
| Solar Panel Area (sq ft) | 100 | 100 |
| High-Gain Antenna and Type | 72 in., Parabolic | 72 in., Parabolic |
| Capsule Antenna and Type | 36 in., Parabolic | 36 in., Parabolic |
| Omnidirectional Antenna and Type | 8 in., Biconical | 8 in., Biconical |
| Micrometeroid Protection | None | None |

### 7.2.1 General Arrangement---Indirect Lander Entry

A discussion of the general arrangement of the indirect lander entry spacecraft follows. This configuration is designated Boeing Model 971-105.

The general arrangement drawing is shown in Figure 7.2-1. This design is a refinement of Model 971-101, which was shown and discussed in Section 6.0. The vehicle is composed of an octagonal box body, an external engine support truss, and an internal capsule and propellant tank support truss. All orbiter equipment is plate-mounted on four of the eight faces of the body. The top of the body provides the mounting surface for the solar panels, main propellant tanks, helium pressurant tanks, attitude control thruster clusters, attitude control nitrogen tanks, omnidirectional antenna, and high-gain antenna. The lander relay antenna is located on a tripod mounted on the external engine support truss.

#### 7.2.1.1 Launch Configuration

The engine-up launch position used for the Model 971-101 was retained because the diameter limitations of the Titan IIIC shroud and the propellant volume of the powered spacecraft combine to force the deployable components toward one end of the vehicle. From a structural weight standpoint it is best to mount the deployable components, and not the heavier basic orbiter structure, flight capsule, and propellant, furthest from the spacecraft support plane. This is the advantage of an engine-up configuration which, though requiring the spacecraft to be inverted (thus causing coast time penalties) before ignition, showed an overall performance gain (see Section 6.0). When the shroud diameter is large with respect to the basic spacecraft body (which allows side storage volume for deployable components) or when the shroud has the structural capability to support the spacecraft (which minimizes the distance between the spacecraft center of gravity and the launch vehicle interface), it is advantageous to use the more common aft-facing engine arrangement.

#### 7.2.1.2 Sensors and Deployable Components

Detailed view-angle/shadowgraph calculations were not conducted on this configuration because of the limited study time. Sensor placement was based on general view requirements and experience.

*Canopus Tracker*---The Canopus tracker is located in the orbiter body next to the capsule separation plane. Its view is centered on the +Z axis. A ±45-degree clear view cone is provided.

*Omnidirectional Antenna*---The biconical low-gain antenna is positioned on the +Z axis, stowed alongside the engine during boost, and deployed approximately 75 degrees in single-plane rotation to a point on the Sun side of the solar panel. This permits the antenna to have a 360-degree field of view centered about (±30 degrees cone ∢) the ecliptic plane.

*High-Gain Antenna*---The 72-inch-diameter high-gain antenna is located on the -Z axis, stowed alongside the engine during boost, and deployed about 150 degrees in single-plane rotation to a point outside the solar panel shadow. Two-axis drives provide rotation about both the swivel and hinge axes.

FOLDOUT FRAME 1 FOLDOUT FRAME 2 FOLDOUT FRAME 3

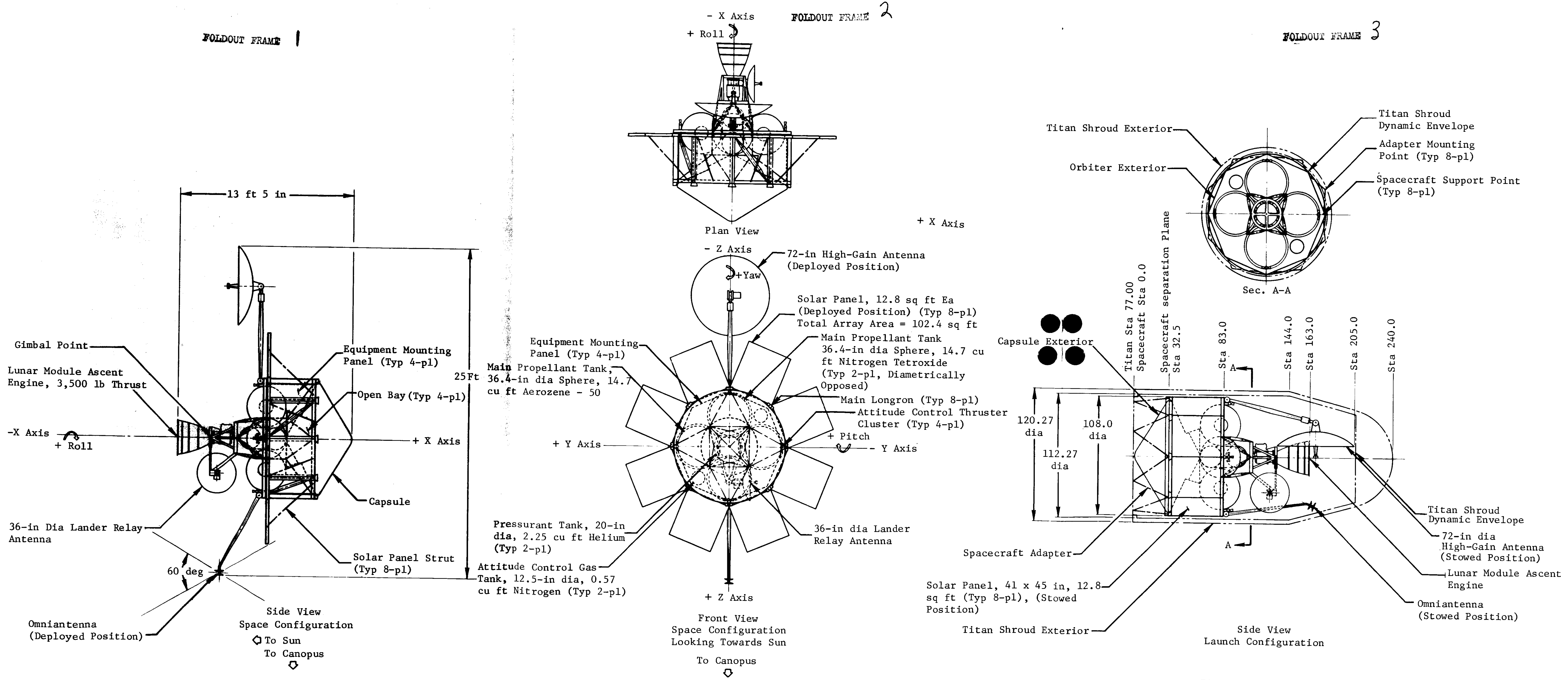

13 ft 5 in
25 Ft
Gimbal Point
Lunar Module Ascent Engine, 3,500 lb Thrust
-X Axis
+ Roll
36-in Dia Lander Relay Antenna
60 deg
Omniantenna (Deployed Position)
Equipment Mounting Panel (Typ 4-pl)
Open Bay (Typ 4-pl)
+ X Axis
Capsule
Solar Panel Strut (Typ 8-pl)
Side View
Space Configuration
To Sun
To Canopus
- X Axis
+ Roll
Plan View
+ X Axis
- Z Axis
+Yaw
72-in High-Gain Antenna (Deployed Position)
Solar Panel, 12.8 sq ft Ea (Deployed Position) (Typ 8-pl) Total Array Area = 102.4 sq ft
Main Propellant Tank 36.4-in dia Sphere, 14.7 cu ft Nitrogen Tetroxide (Typ 2-pl, Diametrically Opposed)
Main Longron (Typ 8-pl)
Attitude Control Thruster Cluster (Typ 4-pl)
+ Pitch
- Y Axis
+ Y Axis
Equipment Mounting Panel (Typ 4-pl)
Main Propellant Tank, 36.4-in dia Sphere, 14.7 cu ft Aerozene - 50
Pressurant Tank, 20-in dia, 2.25 cu ft Helium (Typ 2-pl)
Attitude Control Gas Tank, 12.5-in dia, 0.57 cu ft Nitrogen (Typ 2-pl)
36-in dia Lander Relay Antenna
+ Z Axis
Front View
Space Configuration
Looking Towards Sun
To Canopus
Titan Shroud Exterior
Orbiter Exterior
Titan Shroud Dynamic Envelope
Adapter Mounting Point (Typ 8-pl)
Spacecraft Support Point (Typ 8-pl)
Sec. A-A
Capsule Exterior
Titan Sta 77.00
Spacecraft Sta 0.0
Spacecraft separation Plane
Sta 32.5
Sta 83.0
Sta 144.0
Sta 163.0
Sta 205.0
Sta 240.0
A
120.27 dia
108.0 dia
112.27 dia
Spacecraft Adapter
Solar Panel, 41 x 45 in, 12.8 sq ft (Typ 8-pl), (Stowed Position)
Titan Shroud Exterior
Titan Shroud Dynamic Envelope
72-in dia High-Gain Antenna (Stowed Position)
Lunar Module Ascent Engine
Omniantenna (Stowed Position)
Side View
Launch Configuration

Figure 7.2-1: GENERAL ARRANGEMENT DRAWING---MODEL 971-105

PRECEDING PAGE BLANK NOT FILMED.

*Solar Panels*---The eight 12.8-square-foot trapezoidal solar panels, which are hinged from the octagonal ring at the top surface of the orbiter body, are stowed over the eight flat surfaces of the body during launch and deployed by 90-degree rotation. They are locked in position by knee-action deployment struts.

*Capsule Relay Antenna*---The 36-inch-diameter relay antenna is not deployed, but is driven in two axes from a tripod mounted on the engine truss. It is positioned so that its beam can be directed, without interference, toward the lander during lander-orbiter communication periods.

### 7.2.1.3 Thermal Considerations

Although no specific thermal analysis was conducted on this vehicle, good thermal design considerations have been observed. These include:

- Placing the capsule in the shade of the solar panels and orbiter body;
- Placing the temperature control louvers in the shade of the solar panel;
- Keeping a conservative engine exit plane to solar panel distance to prevent overheating the panel during engine firing;
- Placing the engine on the Sun side to keep the propellant valves and fittings from freezing;
- Making the orbiter body as compact as possible to provide a concentrated thermal mass while still maintaining adequate louver-controlled heat rejection surface areas.

The orbiter body is completely covered with either multilayer superinsulation or thermal control louvers. Eight louver assemblies are located on the sides of the orbiter body. Four of these control equipment mounting plate temperatures, the remainder control propulsion bay temperatures. The Sun-facing side of the body is covered with a conical-shaped insulation blanket with a high-temperature-resistant surface to prevent heat feedback from the engine during firing.

The position of the capsule antenna will require that the back surface of the parabolic dish be protected with a heat shield to prevent overheating during engine firing. Preliminary calculations show that, with proper insulation, the location is feasible. If an antenna temperature problem still exists after applying thermal control techniques, the antenna can be relocated and/or provided with a deployment mechanism.

### 7.2.2 General Arrangement---Direct Lander Entry

This section contains a discussion of the general arrangement of the spacecraft defined for the direct lander case. This configuration is designated Boeing Model 971-106.

The general arrangement drawing is shown in Figure 7.2-2. The vehicle is composed of an octagonal box body and an external engine support truss that is similar to Model 971-105. The main difference is the elimination of the dual

FOLDOUT FRAME 1

FOLDOUT FRAME 2

FOLDOUT FRAME 3

PRECEDING PAGE BLANK NOT FILMED.

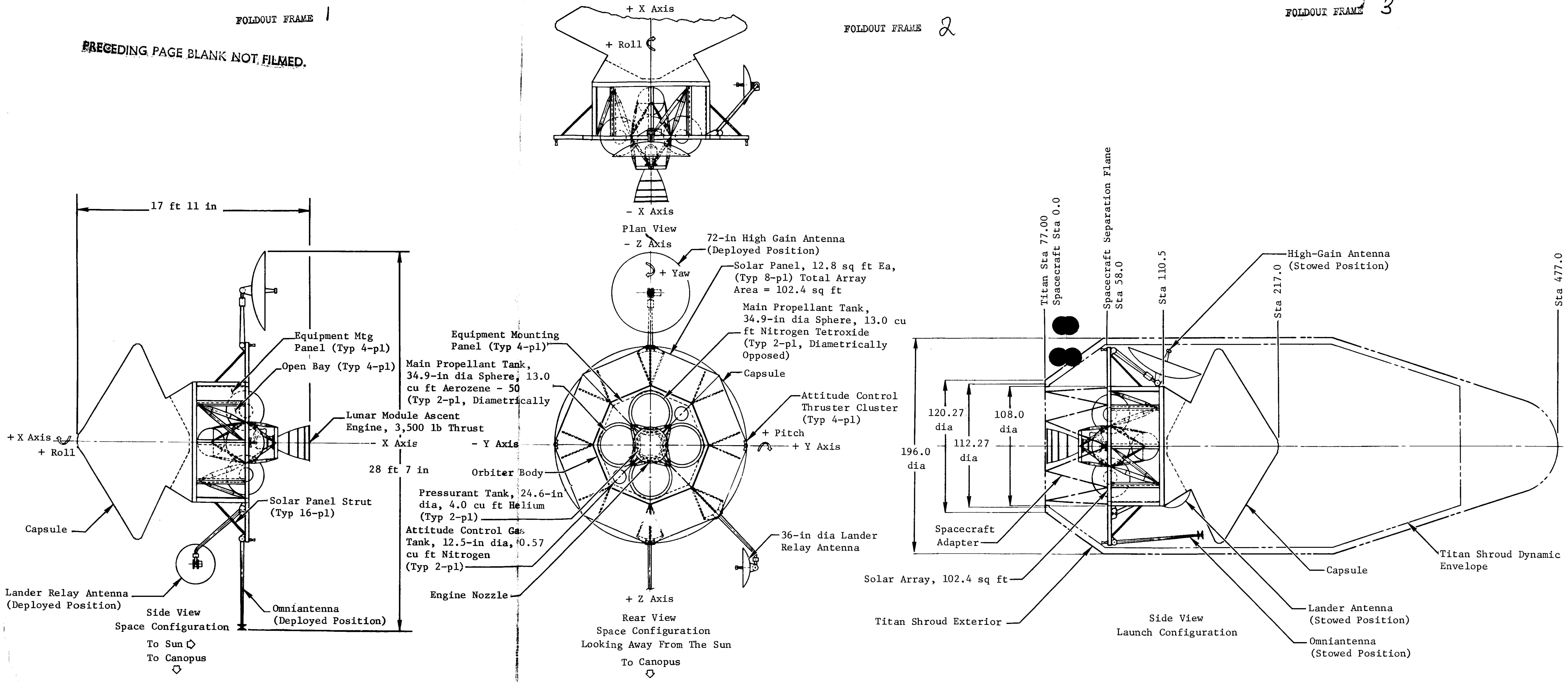
+ X Axis
+ Roll
- X Axis
Plan View
- Z Axis
+ Yaw
17 ft 11 in
Equipment Mtg Panel (Typ 4-pl)
Open Bay (Typ 4-pl)
Lunar Module Ascent Engine, 3,500 lb Thrust
+ X Axis
+ Roll
- X Axis
28 ft 7 in
Capsule
Solar Panel Strut (Typ 16-pl)
Lander Relay Antenna (Deployed Position)
Omniantenna (Deployed Position)
Side View
Space Configuration
To Sun
To Canopus
72-in High Gain Antenna (Deployed Position)
Solar Panel, 12.8 sq ft Ea, (Typ 8-pl) Total Array Area = 102.4 sq ft
Main Propellant Tank, 34.9-in dia Sphere, 13.0 cu ft Nitrogen Tetroxide (Typ 2-pl, Diametrically Opposed)
Capsule
Equipment Mounting Panel (Typ 4-pl)
Main Propellant Tank, 34.9-in dia Sphere, 13.0 cu ft Aerozene - 50 (Typ 2-pl, Diametrically
Attitude Control Thruster Cluster (Typ 4-pl)
+ Pitch
- Y Axis
+ Y Axis
Orbiter Body
Pressurant Tank, 24.6-in dia, 4.0 cu ft Helium (Typ 2-pl)
Attitude Control Gas Tank, 12.5-in dia, 0.57 cu ft Nitrogen (Typ 2-pl)
36-in dia Lander Relay Antenna
Engine Nozzle
+ Z Axis
Rear View
Space Configuration
Looking Away From The Sun
To Canopus
Titan Sta 77.00
Spacecraft Sta 0.0
Spacecraft Separation Plane
Sta 58.0
Sta 110.5
Sta 217.0
Sta 477.0
High-Gain Antenna (Stowed Position)
120.27 dia
108.0 dia
112.27 dia
196.0 dia
Spacecraft Adapter
Solar Array, 102.4 sq ft
Titan Shroud Exterior
Capsule
Titan Shroud Dynamic Envelope
Lander Antenna (Stowed Position)
Omniantenna (Stowed Position)
Side View
Launch Configuration

Figure 7.2-2: GENERAL ARRANGEMENT DRAWING---MODEL 971-106

PRECEDING PAGE BLANK NOT FILMED.

tripods that were used for engine support. This is possible because the flight capsule penetration into the orbiter body, which occurs in the Model 971-105, does not exist in this configuration. Thus, the helium can be contained in one tank that can be moved forward in the orbiter body. Consequently, the engine can be moved forward and be directly attached to the engine support ring without the dual tripods. The internal capsule support truss has also been eliminated because the capsule is now mounted directly on the orbiter body. Propellant tank support is provided by four truss members with direct load paths from the tank skirt rings to the orbiter/capsule interface. All orbiter equipment is plate-mounted on four faces of the body. The top of the body forms the mounting surface for the flight capsule. The solar array, which is composed of eight 12.8-square-foot trapezoidal panels, is fixed to the body at its base and is supported by diagonal struts at the solar panel beam points. The solar array provides the mounting surface for the attitude control thruster clusters and all deployable components.

### 7.2.2.1 Launch Configuration

An engine-down launch position was selected for this vehicle because of the following factors.

- The 196-inch-diameter bulbous shroud provides adequate space for side-mounting deployable components. This eliminates the requirement for end mounting this equipment.
- It is difficult to design a structurally efficient adapter around the capsule, which is larger in diameter than the basic launch vehicle, when it is located close to the transtage interface plane.
- Performance trade studies showed a loss for engine-up configurations in the 196-inch-diameter shroud. This occurs because structural gains in the orbiter structure were more than offset by the adapter weight gains and the performance penalties introduced by spacecraft turnaround requirements.

### 7.2.2.2 Sensors and Deployable Components

Detailed view-angle/shadowgraph calculations were not conducted on this configuration because of the limited study time. Sensor placement was based on general view requirements and experience.

*Canopus Tracker*---The Canopus tracker is located in the orbiter body next to the capsule interface plane. Its view is centered on the +Z axis. A ±45-degree clear view cone is available.

*Omnidirectional Antenna*---The biconical low-gain antenna is mounted on the edge of the solar array on the +Z axis. The antenna is stowed on the shade side of the solar array and when deployed lies in the solar panel plane. Its deployed position is such that the antenna has a 360-degree field of view centered about (±30 degrees cone ∢) the ecliptic plane.

*High-Gain Antenna*---The 72-inch-diameter high-gain antenna is located on the -Z axis at the edge of the solar array. It is stowed at the side of the spacecraft during launch and is deployed about 130 degrees in single-plane rotation to a point outside the solar array shadow. Two-axis drives provide rotation about both the swivel and hinge axes.

*Capsule Relay Antenna*---The 36-inch-diameter relay antenna is located 45 degrees from the +Z axis and on the edge of the solar array. It is stowed alongside the spacecraft body and is deployed by single rotation. It is driven on two axes and is positioned so that its beam can be directed without interference toward the lander during lander-orbiter communication periods.

### 7.2.2.3 Thermal Considerations

Although no specific thermal analysis was conducted on this vehicle, the thermal design considerations defined for Model 971-105 also apply to Model 971-106.

### 7.2.3 Structural Criteria and Design

The following structural design criteria were used for this study. These criteria are necessarily limited in scope because of the preliminary design nature of the study, but are adequate for realistic sizing of structure and calculation of the structural system weight.

*Design Load Factors*---The design load factors shown in Table 7.2-2 were used for sizing all primary and secondary structural members. These load factors were applied as static design loads multiplied by the appropriate factor of safety. The load factors apply at the interface between the spacecraft adapter and the launch vehicle. To account for dynamic amplifications due to the transitory nature of the actual load environment, the lateral load factors were varied as a function of distance from the spacecraft adapter/launch vehicle interface. This variation is shown in Figure 7.2-3.

Table 7.2-2: LIMIT DESIGN LOAD FACTORS

| Condition | Thrust (g) | Yaw (g) | Pitch (g) | Roll (rad/sec$^2$) |
|---|---|---|---|---|
| Combined | +4.25 | ±1.0 | 0 | 0 |
| Combined | -2.13 | ±1.0 | 0 | 0 |
| Combined | +4.25 | 0 | ±2.0 | 0 |
| Combined | -2.13 | 0 | ±2.0 | 0 |
| Singular | +4.25 | 0 | 0 | 0 |
| Singular | -2.13 | 0 | 0 | 0 |
| Singular | 0 | 0 | 0 | 10 |

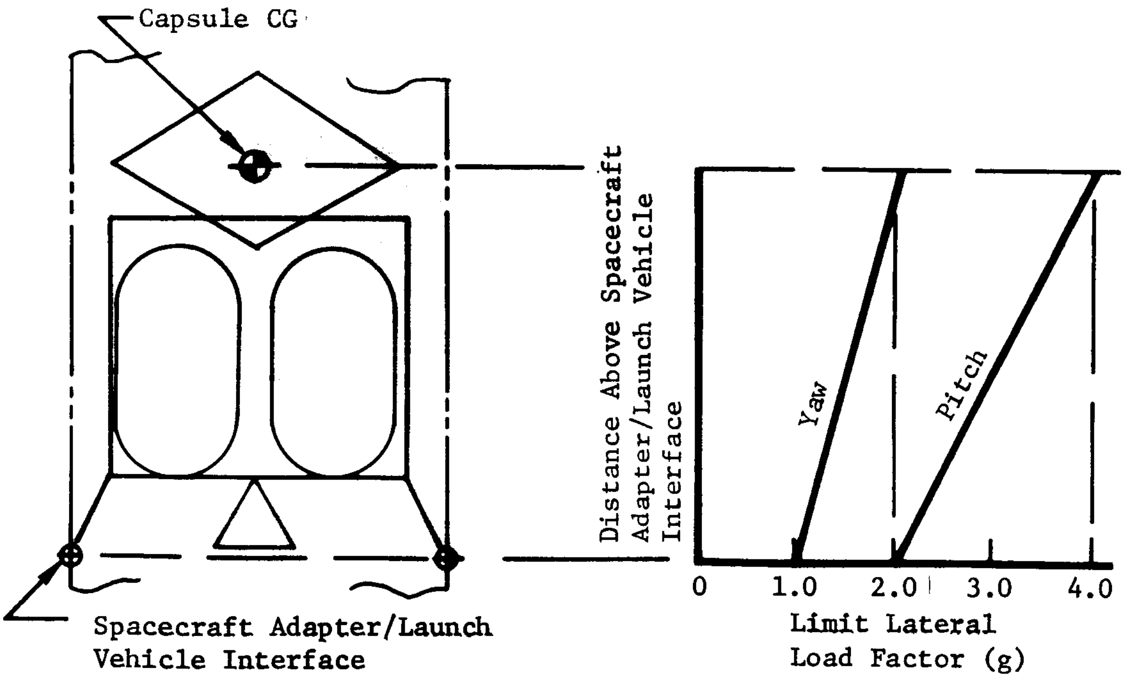

Figure 7.2-3: LATERAL LOAD FACTOR AMPLIFICATION

*Factors of Safety*---The factors of safety shown in Table 7.2-3 were applied to all design loads.

Table 7.2-3: FACTORS OF SAFETY

| Item | Limit | Proof | Yield | Ultimate |
|---|---|---|---|---|
| Primary Structure | 1.00 | 1.00 | 1.00 | 1.25 |
| Secondary Structure | 1.00 | 1.00 | 1.00 | 1.25 |
| Pressure Vessels | 1.00 | 1.50 | 1.65 | 2.00 |

*Limit Design Load*---The limit design load is the maximum anticipated load the structure is expected to encounter during specified conditions of operation and environment.

*Proof Load*---The proof load is only applicable to pressurized components as a singular loading condition before flight.

*Yield Design Load*---The yield design load is that load at which the structure will undergo a permanent deformation equivalent to not more than 0.2% permanent strain.

*Ultimate Design Load*---The ultimate design load is the maximum design load the structure will sustain without failure. It is the limit design load multiplied by the appropriate factor of safety.

*Margin of Safety*---The margin of safety shall be zero on all structure for the critical design load condition except where stiffness requirements preclude attainment of this objective.

*Structural Frequencies*---The structural frequency of the spacecraft as cantilevered from the launch vehicle was required to be a minimum of 10 cps for all axes. Appendages in the deployed configuration were required to have a minimum natural frequency of 2 cps to preclude adverse coupling with the attitude control system.

*Columns*---Compression truss members were designed with a 1% eccentricity to account for manufacturing misalignment and straightness tolerance.

*Shell and Plate Structure*---Shell and plate structures were designed so that they remain in an unbuckled state at ultimate design load.

### 7.2.3.1 Structural Arrangement---Model 971-105

In this design, the launch loads are carried from the transtage interface plans at Titan Station 77.0 through a 32.5-inch-long V-frame adapter to eight spacecraft support fittings and longerons located at the apexes of a 108-inch-diameter octagonal orbiter body. These longerons are stabilized by four shear panels and four diagonal struts joined to the inside flanges of the T-shaped longerons. The four shear panels provide 50 square feet of interior equipment mounting surfaces and exterior space for temperature control louvers. The alternating diagonal struts provide shear continuity in the open bays, which allows local access for equipment servicing. The eight longerons are joined at the top (Station 83.0) by an octagonal ring and shear deck. Four 36.4-inch-diameter spherical propellant tanks provide storage for 4,119 pounds of propellant (1,584 pounds of fuel, 2,535 pounds of oxidizer). The tanks are centered on a 58-inch-diameter circle and are located so that opposed pairs balance. The web of the shear deck employs ring-reinforced cutouts to accept propellant tank mounting. The tanks are attached so that radial expansion due to pressure is free to occur without restraint. Only vertical and tangential loading is permitted. Each tank is supported at three points equally spaced around the periphery of the tank skirt ring. A longeron in the orbiter body provides the outside support while the two inner supports are provided by vertical thrust tubes. All lateral loads originating from the tank inertias are reacted by the orbiter body shell and truss diagonals. Vertical inertia loads from the tanks are reacted by the longerons and thrust tubes. The lower ends of these thrust tubes are connected to a four-point star truss that supports all flight capsule loads and engine and propellant tank vertical loads. Thus, all transverse loads, except capsule loads, are carried in the orbiter body wall and are reacted at the spacecraft-adapter launch vehicle interface. Torque loads are carried in the upper shear deck, distributed in shear in the orbiter body wall, and reacted through the adapter to the spacecraft adapter/launch vehicle interface. Vertical loads from the orbiter engine, engine support structure, helium tanks, flight capsule, and two thirds of the propellant and tanks are carried in the internal star truss and are reacted at the spacecraft adapter/launch vehicle interface. All other vertical loads are carried down the longerons to the spacecraft adapter.

The two 20-inch-diameter spherical helium tanks are dumbbell-mounted on semi-monocoque skirts attached to the shear deck and are stabilized at the capsule support truss. Eight truss members, joined to the shear deck at the thrust tube attachment points, support a 28-inch-diameter engine support ring. The 3,500-pound-thrust Lunar Module Ascent engine gimbal is joined to the engine support ring by two tripod trusses. Thrust vector actuators are connected between the engine aft face and the periphery of the engine support ring.

The structural system was sized to the axial and lateral load factors shown in Figure 7.2-4. Figure 7.2-5 shows the results of the preliminary structural sizing. All truss members are fabricated from 2219-T851 aluminum tubes with machined end fittings welded to the tube ends. All remaining structural elements are fabricated from 7075-T6 aluminum sheet, extrusions, and machined fittings. These data were used to establish the structural weights shown in Section 7.2.4. No attempt to verify the stiffness requirements was made.

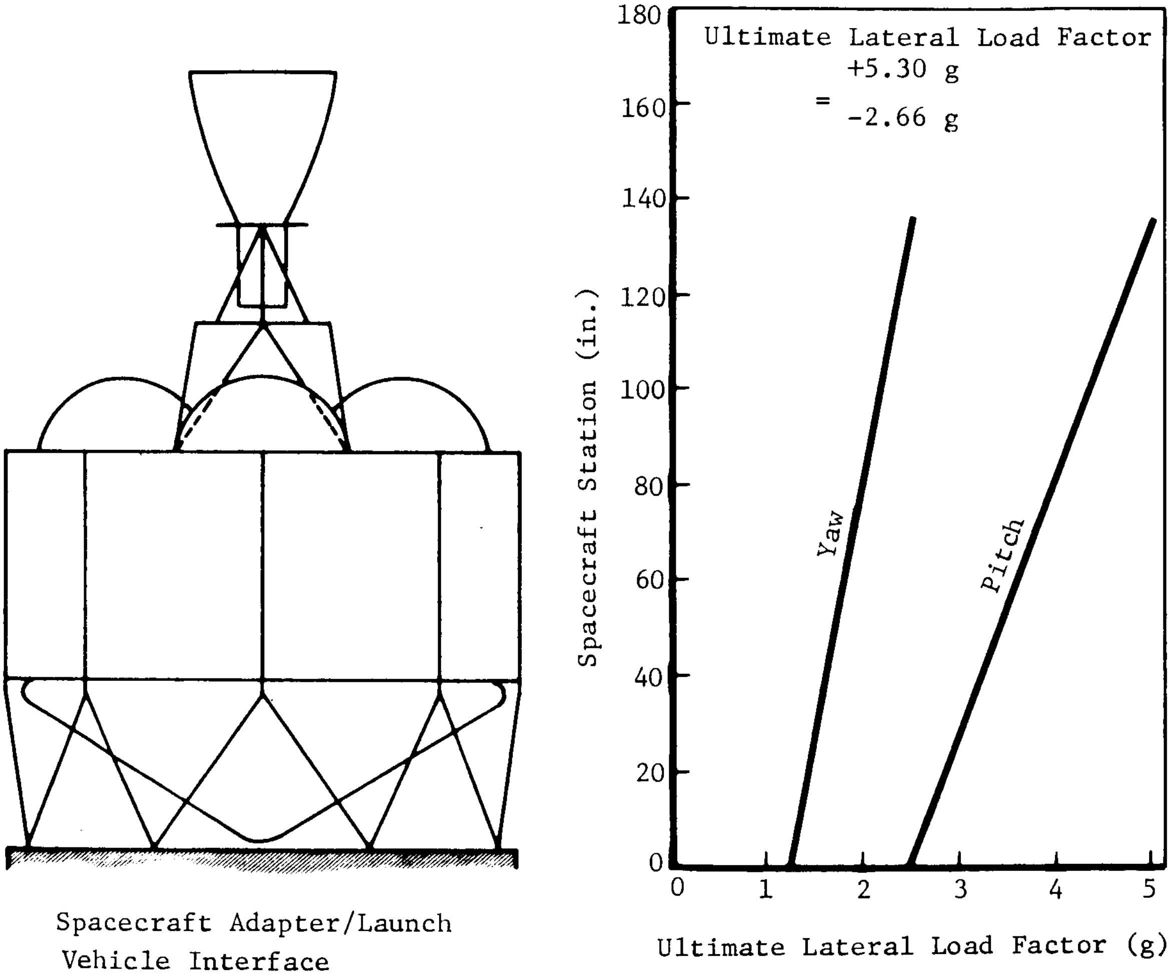
Spacecraft Adapter/Launch Vehicle Interface

Figure 7.2-4: LOAD FACTORS---MODEL 971-105

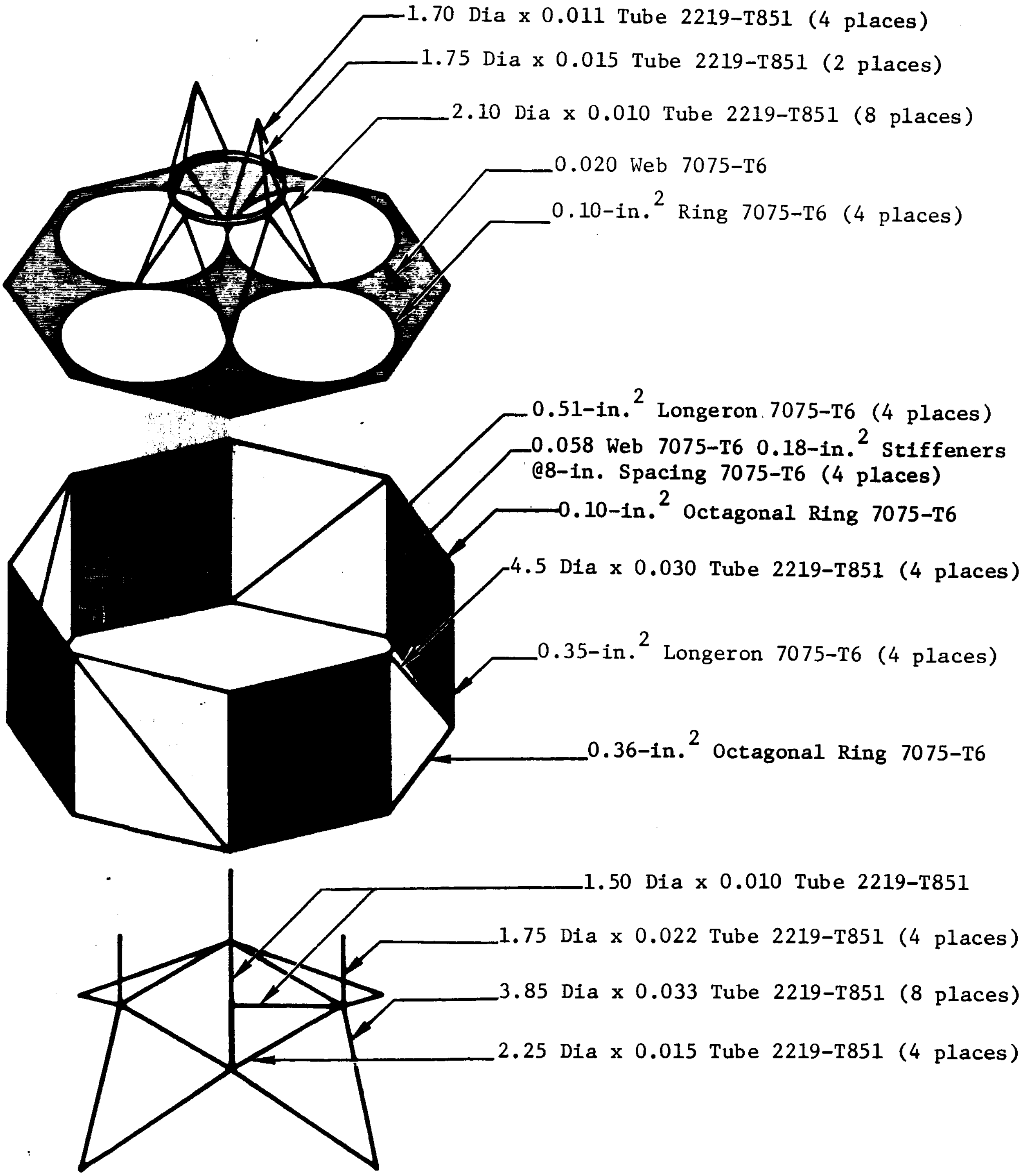
1.70 Dia x 0.011 Tube 2219-T851 (4 places)
1.75 Dia x 0.015 Tube 2219-T851 (2 places)
2.10 Dia x 0.010 Tube 2219-T851 (8 places)
0.020 Web 7075-T6
0.10-in.$^2$ Ring 7075-T6 (4 places)
0.51-in.$^2$ Longeron 7075-T6 (4 places)
0.058 Web 7075-T6 0.18-in.$^2$ Stiffeners @8-in. Spacing 7075-T6 (4 places)
0.10-in.$^2$ Octagonal Ring 7075-T6
4.5 Dia x 0.030 Tube 2219-T851 (4 places)
0.35-in.$^2$ Longeron 7075-T6 (4 places)
0.36-in.$^2$ Octagonal Ring 7075-T6
1.50 Dia x 0.010 Tube 2219-T851
1.75 Dia x 0.022 Tube 2219-T851 (4 places)
3.85 Dia x 0.033 Tube 2219-T851 (8 places)
2.25 Dia x 0.015 Tube 2219-T851 (4 places)

Figure 7.2-5: STRUCTURAL SIZING---MODEL 971-105

### 7.2.3.2 Structural Arrangement---Model 971-106

In this design the launch loads are carried from the transtage interface plane at Titan Station 77.0 through a 58-inch-long V-frame adapter to eight spacecraft support fittings and longerons located at the apexes of a 108-inch-diameter octagonal orbiter body similar to that described in Section 7.2.3.1, the main difference being the elimination of the capsule support truss. The capsule, because of its increased size, can now be mounted directly to the orbiter body. Four 34.9-inch-diameter spherical propellant tanks provide storage for 3,619 pounds of propellant (1,392 pounds of fuel, 2,227 pounds of oxidizer). Propellant tank location and mounting are similar to Model 971-105. Each tank is supported at three points equally spaced around the periphery of the tank skirt ring. A longeron in the orbiter body provides the outside support while the two inner supports are provided by a single truss member that attaches to the capsule interface ring. The lateral component from this member is reacted by a four-member spider frame at the capsule interface plane. All lateral loads originating from the tank inertias are reacted by the orbiter body shell and truss diagonals. Vertical inertia loads from the tanks are reacted by the longerons and truss members. Thus, all transverse loads are carried in the orbiter body wall and are reacted at the spacecraft/adapter launch vehicle interface. Torque loads are carried in the upper shear deck and are distributed in shear in the orbiter body wall and reacted through the adapter to the spacecraft adapter/launch vehicle interface. Vertical loads from the orbiter engine, engine support structure, helium tank, and flight capsule and two thirds of the propellant and tanks are carried in the internal truss members and are reacted at the spacecraft adapter/launch vehicle interface. These are then combined with all other vertical loads and are carried down the main longerons to the spacecraft adapter.

The 24-inch-diameter spherical helium tank is truss-mounted from the shear deck and stabilized at the capsule interface spider frame. Eight truss members, joined to the shear deck at the internal truss member attachment points, support a 28-inch-diameter engine support ring, which supports the 3,500-pound-thrust Lunar Module Ascent engine gimbal. Thrust vector actuators are connected between the engine aft face and the shear deck.

The structural system was sized to the axial and lateral load factors shown in Figure 7.2-6. Figure 7.2-7 shows the results of the preliminary structural sizing. All truss members are fabricated from 2219-T851 aluminum tubes with machined end fittings welded to the tube ends. All remaining structural elements are fabricated from 7075-T6 aluminum sheet, extrusions, and machined fittings. These data were used to establish the structural weights shown in Section 7.3.4. No attempt to verify the stiffness requirements was made.

### 7.2.4 Spacecraft Weights

This section contains the results of a weight analysis of the final configuration Models 971-105 and 971-106.

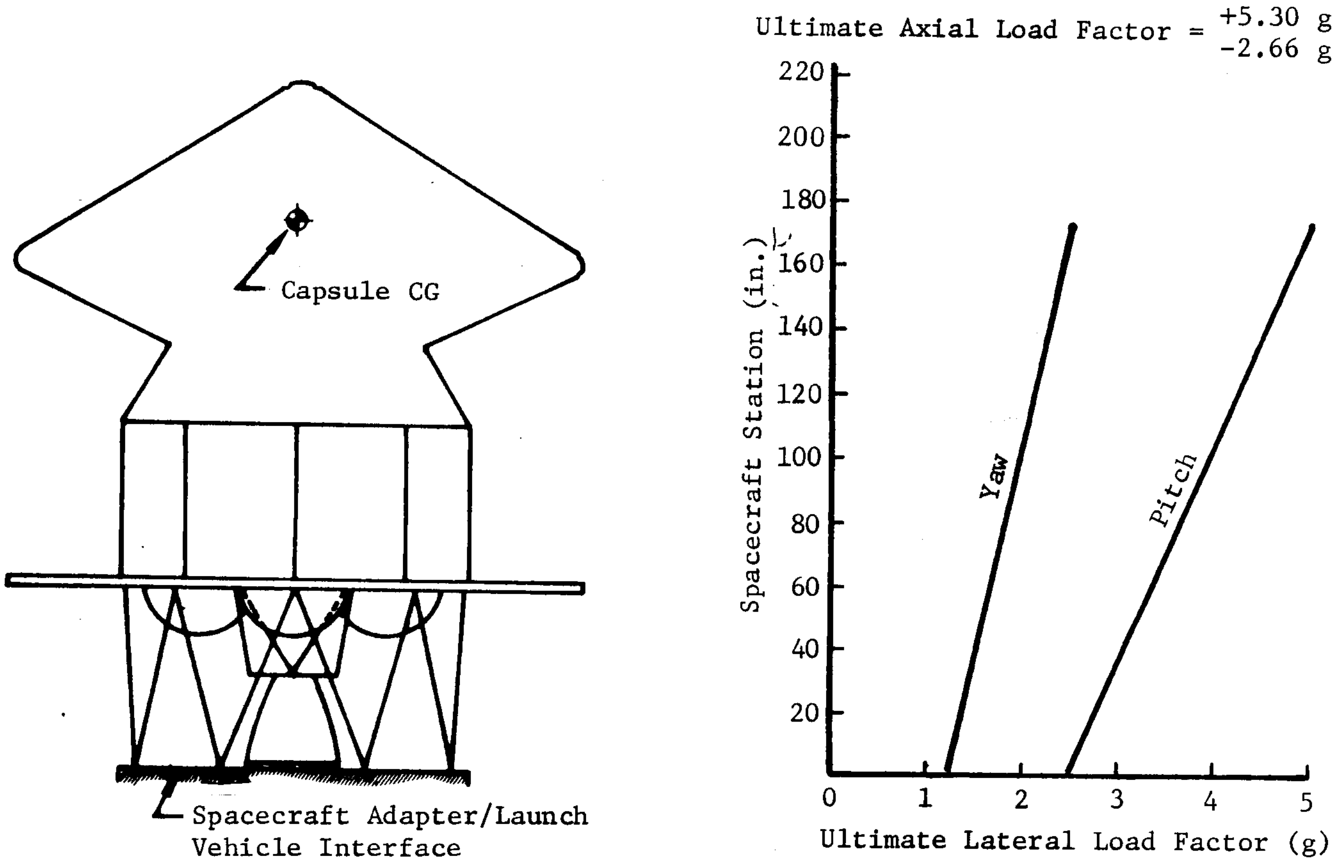

Figure 7.2-6: LOAD FACTORS---MODEL 971-106

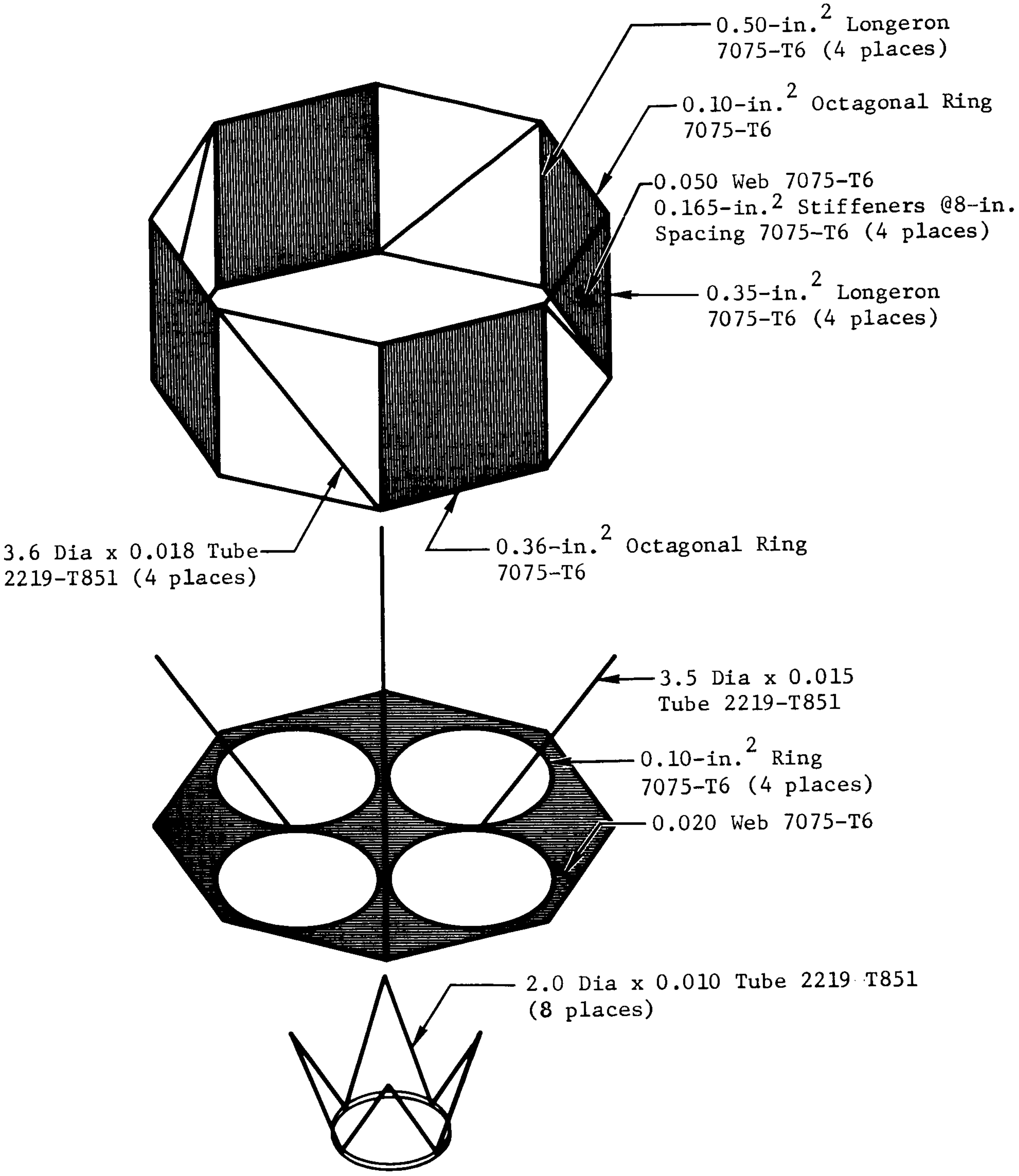
0.50-in.$^2$ Longeron
7075-T6 (4 places)
0.10-in.$^2$ Octagonal Ring
7075-T6
0.050 Web 7075-T6
0.165-in.$^2$ Stiffeners @8-in.
Spacing 7075-T6 (4 places)
0.35-in.$^2$ Longeron
7075-T6 (4 places)
3.6 Dia x 0.018 Tube
2219-T851 (4 places)
0.36-in.$^2$ Octagonal Ring
7075-T6
3.5 Dia x 0.015
Tube 2219-T851
0.10-in.$^2$ Ring
7075-T6 (4 places)
0.020 Web 7075-T6
2.0 Dia x 0.010 Tube 2219 T851
(8 places)

Figure 7.2-7: STRUCTURAL SIZING---MODEL 971-106

### 7.2.4.1 Weight Statement---Model 971-105

Table 7.2-4 is a summary weight statement for Model 971-105. Spacecraft preliminary weights were calculated by a combination of analytical and empirical methods. An allocation of 200 pounds was made for the science system (see Table 7.0-1). The flight capsule is defined as the weight available after all other weight has been calculated and subtracted from the spacecraft separated weight. Useful and nonuseful weights are distributed in accordance with the standard space vehicle terminology shown in Section 2.0.

Propulsion, guidance and control, and electrical power subsystem descriptions and physical data are discussed in detail in Sections 7.3, 7.4, and 7.5. Subsystem weight reflected in the weight statement is consistent with these data except as noted.

*Propulsion Subsystem*---The total propulsion system inert weight shown in Table 7.2-4 includes 97 pounds of orbiter propulsion load-carrying structure and 25 pounds of attachments and thermal control. Also included is the 164 pounds of residual propellant and pressurization gas. Propellant tank weight includes the expulsion system. Engine gimbal actuator weight is carried in the guidance and control subsystem.

*Guidance and Control*---The subsystem weight shown in Table 7.2-4 includes attitude control system components and nitrogen, the engine gimbal actuator, and the computer sequencer. Weight statement totals include an additional inertial reference unit (15 pounds) based on a selective Boeing redundancy approach.

*Electrical Power*---The electrical subsystem weight shown in Table 7.2-4 is the basic system weight. The additional 12 pounds carried in the summary weight statement provides an additional 5 pounds for a redundant charge controller and 7 pounds for other power distribution and control miscellaneous attachments and brackets.

The remaining subsystems and the methods used to calculate their weight are discussed in Section 7.2.4. No provisions have been made for possible meteoroid protection weight penalties or weight contingency allowances.

Launch vehicle to spacecraft adapter weight for the refined configurations is shown in Figure 7.2-8 as a function of spacecraft separated plus adapter weight. Shroud weight is as provided by NASA-Lewis for a 20-foot-long universal payload fairing.

### 7.2.4.2 Weight Statement---Model 971-106

Table 7.2-5 is a summary weight statement for Model 971-106. The method of calculating spacecraft weight is identical to that used for Model 971-105 except that an estimated capsule weight of 2,000 pounds was used for structural analysis. All subsystem weight is the same as for 971-105 except in the case of structure and propulsion. These weight differences are due to the difference in design loads, propellant quantity, and spacecraft geometry. The structural arrangement of this configuration is such that an adapter height of 60 inches is required. Figure 7.2-8 shows the adapter weight as a function of spacecraft separated plus adapter weight. Shroud weight was established at 4,525 pounds by NASA-Lewis during the midterm review of this study.

## Table 7.2-4: SUMMARY WEIGHT STATEMENT---MODEL 971-105 ( Indirect Lander Entry )

| | Useful | Nonuseful | Total |
|---|---|---|---|
| Flight Capsule (Weight Available) | (1,146) | | (1,146) |
| In-Orbit Orbiter | (1,031) | (849) | (1,880) |
| Science | 200 | | 200 |
| Subsystems | | | 747 |
| Attitude Control | 8 | 28 | |
| Guidance and Control | 65 | 19 | |
| Electrical Power | 188 | | |
| Telecommunications | 192 | | |
| Pyrotechnics | 13 | | |
| Temperature Control | 94 | | |
| Cabling | 140 | | |
| Structure | | | 228 |
| Orbiter Structure | 131 | | |
| Orbiter Propulsion Structure | | 97 | |
| Propulsion Subsystems | | 532 | 532 |
| Residuals and Reserves | | | 173 |
| ACS Gas, $N_2$ | | 9 | |
| Pressurization Gas, He | | 10 | |
| Propellant | | 154 | |
| In-Orbit Weight | (2,177) | ( 849) | (3,026) |
| Expendables | | | 3,974 |
| Velocity Control Propellant | | 3,965 | |
| Attitude Control Gas, $N_2$ | | 9 | |
| Spacecraft Weight (Separated Weight) | (2,177) | (4,823) | (7,000) |
| Adapter: Launch Vehicle to Spacecraft | | | 72 |
| Shroud: Jettisonable | | | 1,440 |
| Nonjettisonable | | | 70 |
| All-Up Weight | | | (8,582) |

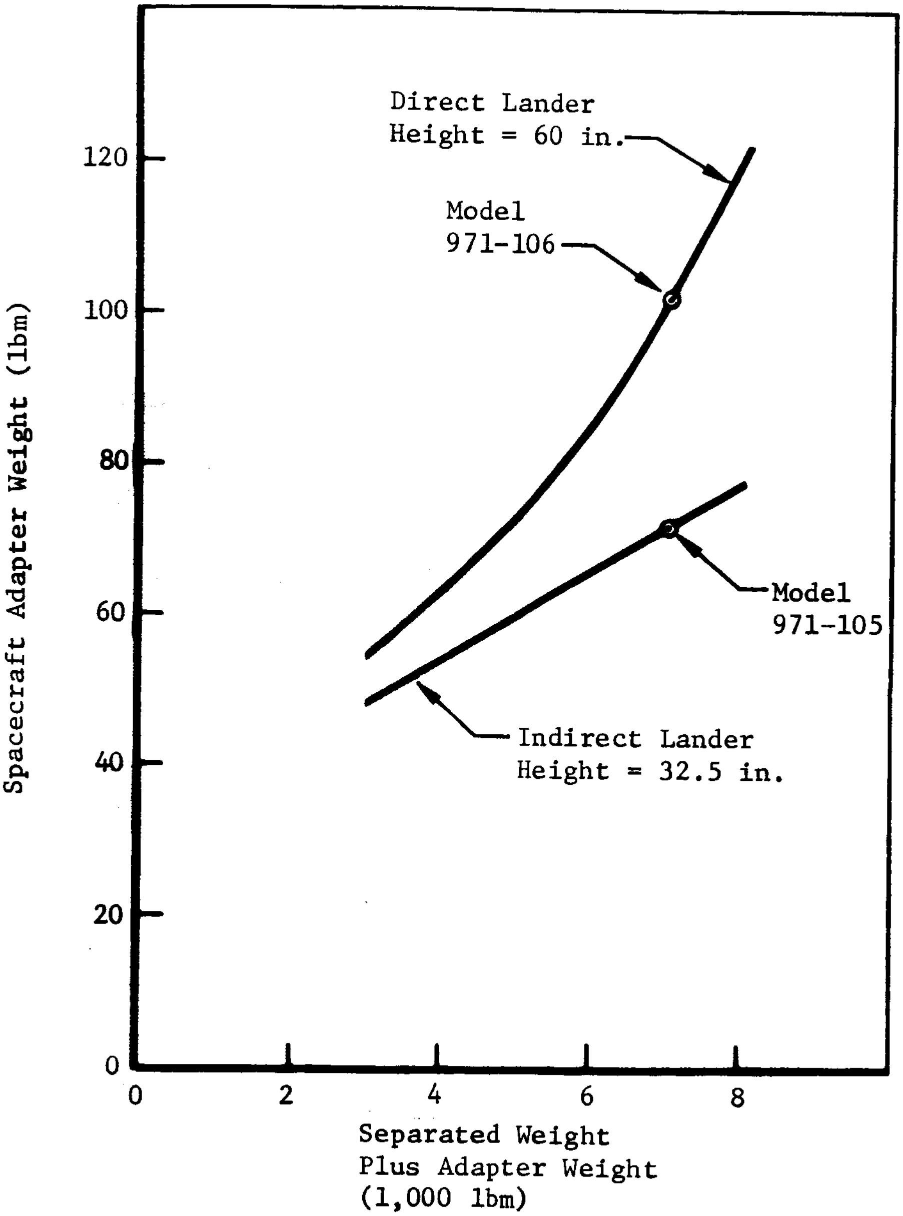

Figure 7.2-8: ADAPTER WEIGHT

Table 7.2-5: SUMMARY WEIGHT STATEMENT---MODEL 971-106 (Direct Lander Entry)

| | Useful | Nonuseful | Total |
|---|---|---|---|
| In-Orbit Orbiter | (1,032) | (777) | (1,809) |
| Science | 200 | | 200 |
| Subsystems | | | 747 |
| Attitude Control | 8 | 28 | |
| Guidance and Control | 65 | 19 | |
| Electrical Power | 188 | | |
| Telecommunications | 192 | | |
| Pyrotechnics | 13 | | |
| Temperature Control | 94 | | |
| Cabling | 140 | | |
| Structure | | | 204 |
| Orbiter Structure | 132 | | |
| Orbiter Propulsion Structure | | 72 | |
| Propulsion Subsystem | | 503 | 503 |
| Residuals and Reserves | | | 155 |
| ACS Gas, $N_2$ | | 9 | |
| Pressurization Gas, He | | 9 | |
| Propellant | | 137 | |
| Flight Capsule (Weight Available) | (1,700) | | (1,700) |
| Expendables | | | 3,482 |
| Velocity Control Propellant | | 3,482 | |
| Attitude Control Gas, $N_2$ | | 9 | |
| Spacecraft Weight (Separated Weight) | (2,732) | (4,268) | (7,000) |
| Adapter: Launch Vehicle to Spacecraft | | | 102 |
| Shroud: Jettisonable | | | 4,525 |
| Nonjettisonable | | | 70 |
| All-Up Weight | | | (11,697) |

## 7.3 ORBITER SUBSYSTEMS

Of the utility subsystems aboard the orbiter, the propulsion, guidance and control, and electrical power subsystems were examined in detail; all others were cataloged under "Additional Subsystems." For these, only subsystem weight was estimated.

### 7.3.1 Propulsion System

The powered spacecraft primary propulsion assists in transplanet injection "boost assist," performs midcourse corrections, establishes an orbit at Mars in retro maneuver, and performs selected orbit trim maneuvers.

#### 7.3.1.1 Design Conditions and Constraints

The system described in this section has resulted, in part, from the following system trades discussed in Appendix B:

- Engine Selection Study
- Pressurization Study
- Propellant Control Study
- Solid-Liquid Staging Study*

1) The spacecraft propulsion system must provide a total velocity increment of 2,498 m/sec to a 7,000-pound spacecraft. Of this total ΔV, the boost-assist velocity is nominally 1.385 km/sec and the post-injection velocity requirement for midcourse correction, orbit insertion, and orbit trim maneuvers is 1.113 km/sec. This represents a total impulse requirement of approximately 1.21 ($10^6$) lb-sec. The propulsion system must also provide maneuver capability consistent with the minimum maneuver ΔV defined by guidance requirements.

2) The propulsion system must operate in the space environment for a period of 1 year within a temperature range of 70 ±30°F. It should provide no hazard to the spacecraft from launch through flight termination.

3) The propulsion system should use engine(s) developed or in development. This engine must be capable of at least seven start sequences in the space environment.

#### 7.3.1.2 Preliminary Design

The specified powered spacecraft propulsion system is of conventional design. It uses existing technology, developed hardware, and selected redundancy. It has been designed for considerable operational flexibility to prevent single-thread failures. A system schematic is shown in Figure 7.3-1. General propulsion system features are summarized in Table 7.3-1.

---

*Not discussed in this section because it is not the system selected by NASA-Boeing for further study.

PRECEDING PAGE BLANK NOT FILMED.

FOLDOUT FRAME 1

FOLDOUT FRAME 2

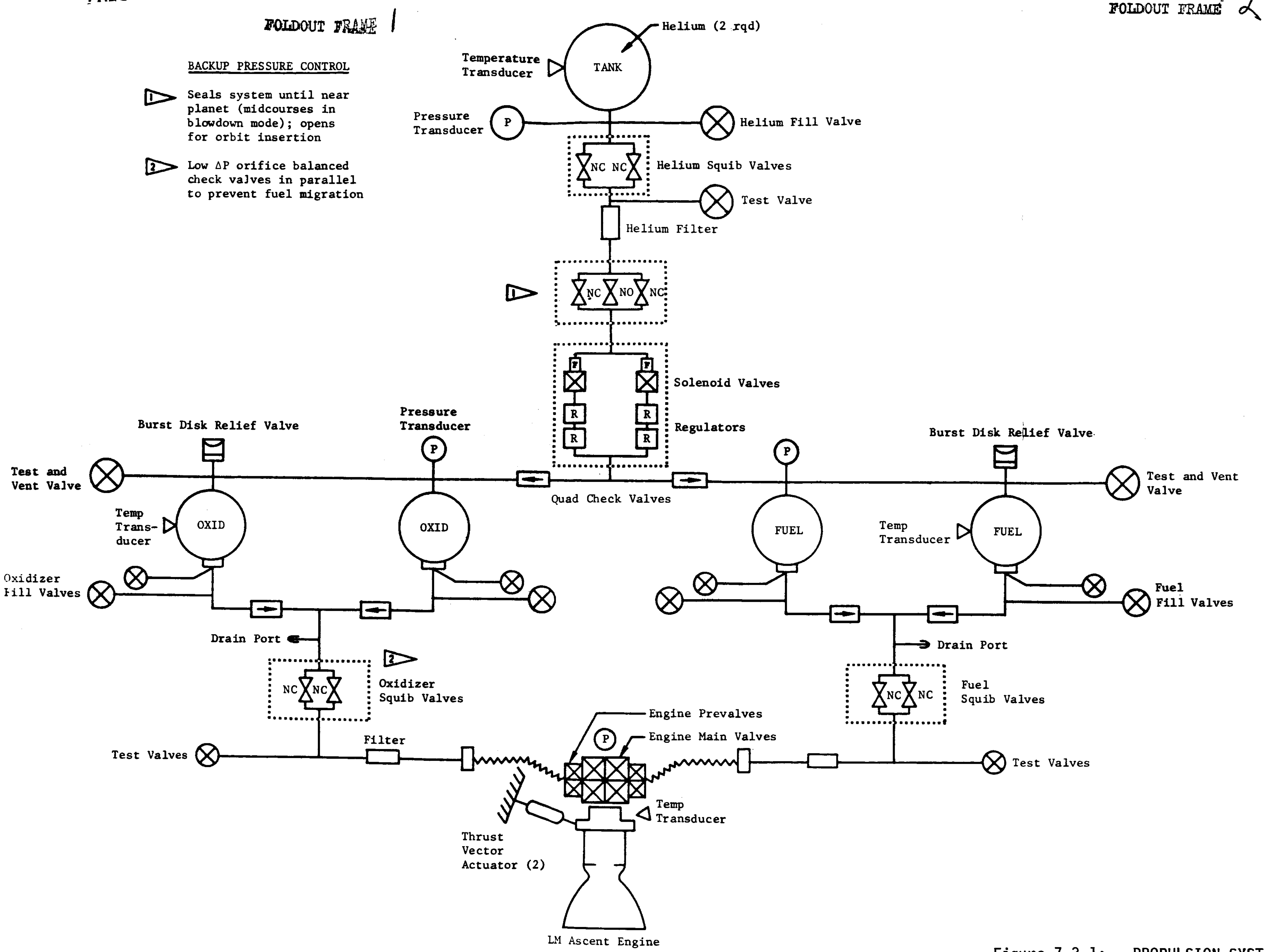
Helium (2 rqd)
Temperature Transducer
TANK
Pressure Transducer
P
Helium Fill Valve
NC NC
Helium Squib Valves
Test Valve
Helium Filter
1
NC NO NC
F
Solenoid Valves
R
Regulators
Burst Disk Relief Valve
Pressure Transducer
Test and Vent Valve
Quad Check Valves
Burst Disk Relief Valve
Test and Vent Valve
Temp Trans- ducer
OXID
OXID
FUEL
Temp Transducer
FUEL
Oxidizer Fill Valves
Fuel Fill Valves
Drain Port
2
Drain Port
NC NC
Oxidizer Squib Valves
NC NC
Fuel Squib Valves
Engine Prevalves
Engine Main Valves
Test Valves
Filter
Test Valves
Temp Transducer
Thrust Vector Actuator (2)
LM Ascent Engine

BACKUP PRESSURE CONTROL

1 Seals system until near planet (midcourses in blowdown mode); opens for orbit insertion

2 Low ΔP orifice balanced check valves in parallel to prevent fuel migration

Figure 7.3-1: PROPULSION SYSTEM SCHEMATIC

PRECEDING PAGE BLANK NOT FILMED.

Table 7.3-1: POWERED SPACECRAFT PROPULSION SYSTEM DESCRIPTION

| Type | Regulated Gas-Pressure-Fed |
|---|---|
| Propellants | $N_2O_4$/(50% $N_2H_4$ + 50% UDMH) |
| Mixture Ratio (Oxid/Fuel) | 1.6 |
| Total Impulse Available (lb-sec) | 1,210,000 |
| Design Temperature Range (°F) | 70 ± 30 |
| Engine Assembly: | |
| Model | Apollo LM Ascent Engine |
| Thrust (lb) | 3,500 |
| Specific Impulse (nom) (sec) | 310.4 |
| (min) (sec) | 306.3 |
| **Chamber Pressure (psia)** | 120 |
| **Engine Inlet Pressure (psia)** | 165 |
| **Nozzle Area Ratio ($A_E/A_T$)** | 45.6 |
| **Burn Time Capability (sec)** | 500 |
| **Minimum Impulse Bit (lb-sec)** | 462 * |
| **Restart Capability** | ≥ 35 |
| TVC Gimbal Angle (deg) | ± 6 * |
| Envelope (in.) | 34.0 x 51.5 |
| Chamber Cooling | Ablative |
| Nozzle Extension Cooling | Ablative (Radiation**) |
| Weight (Incl valves, gimbal) (lb) | 227 (174) |
| **Propellant Subsystem** | |
| **Propellant Tanks** | 4 - Spherical (6 AL-4V) |
| **Volume Per Tank ($ft^3$)** | 14.7 |
| **Ullage Volume (percent)** | 0% at 110°F ($N_2O_4$) |
| **Tank Diameter (in.)** | 36.4 |
| Storage Temperature Range (°F) | 70 ± 30 |
| Tank Pressure, Operating (psia) | 195 |
| Lockup (psia) | 200 |
| Propellant Control, Oxid Tanks | Teflon Bladders |
| Fuel Tanks | Teflon Bladders |
| Pressurization Subsystem | |
| Pressurant | Helium |
| Pressurant Tanks (2) | Spherical (6 Al-4V) |
| Tank Volume ($in.^3$) | 3,900 |
| Tank Diameter (in.) | 520 |
| Storage Temperature Range (°F) | 70 ± 30 |
| Storage Pressure (psia)(at 70°F) | 3,500 |

* To 90% steady-state thrust

** Modification

The powered spacecraft propulsion system is functionally a regulated gas-pressure-fed, liquid bipropellant propulsion system using Earth-storable propellants. It employs a 3,500-pound-thrust engine gimbaled for thrust vector control. Propellants are nitrogen tetroxide ($N_2O_4$) and Aerozine-50 (50% $N_2H_4$/ 50% UDMH) used at a nominal mixture ratio (oxidizer/fuel) of 1.6. Propellants are contained in four spherical tanks having elastomeric bladders. Helium pressurization gas is stored in two spherical pressurant tanks. Valves are provided to regulate gas and propellant flow and to isolate the system as required. Liquid check valves are incorporated to prevent propellant migration between tanks.

### 7.3.1.3 Major Subsystems

*Rocket Engine Assembly*---The 3,500-pound-thrust bipropellant engine assembly is a modification of the Apollo Lunar Module Ascent engine. It was selected from among 19 engine candidates encompassing a thrust range of 100 to 10,500 pounds. Eight of these engines were assigned a good or fair adaptability rating for the powered spacecraft mission. These were subsequently reduced to three major contenders after considering thruster weight, finite burn losses, and control requirements for small midcourse maneuvers. These were the 300-pound-thrust Post-Boost Propulsion System (PBPS) engine, the 2,200-pound-thrust Apollo Subscale engine, and the 3,500-pound-thrust Apollo Lunar Module Ascent engine (for characteristics see Appendix B). Subsequent evaluations of these three engines plus a three-engine cluster of the PBPS engine led to the final selection of the Apollo Lunar Module Ascent engine for the powered spacecraft mission. This selection was based primarily on considerations of useful payload attained in Mars orbit, and on the status of engine development, production, and funding.

The Lunar Module Ascent engine will be qualified in the Apollo program in a fixed (i.e., nongimbaled) installation. It is desirable that this engine be modified for the powered spacecraft mission to include gimbaling capability. This is considered to be a minor modification though additional qualification testing will be required. An optional modification involves replacing the existing, fully ablative nozzle skirt extension with a lighter weight, radiation-cooled extension. This modification has been assumed in the propulsion system weight statement, but further studies are required to determine whether this weight advantage is worth the development expense.

*Propellant Subsystem*---The propellant subsystem consists of propellant storage tanks, positive expulsion bladders, and the valves, filters, and orifices necessary for propellant servicing and control. Propellants are stored in four identical, spherical titanium (6AL-4V) tanks. New tanks were selected because the propellant tank survey (Reference 1) showed that existing tanks of the appropriate size were not available from other programs. Like propellant tanks are manifolded at both the pressurization gas supply and propellant feed lines.

Propellant control is accomplished with collapsing-type elastomeric bladders. Fuel and oxidizer tank bladders are identical and are constructed of teflon (TFE-FEP). These bladders were selected from among several methods evaluated in the propellant control study contained in Appendix A. Alternate methods included metal diaphragms, metal bellows, expulsion screens, separate start tanks, and separate ullage propulsion systems for propellant settling. Metal diaphragms and bellows were found to be heavier than the other approaches that were of essentially equal weight. The complexity of start tank and separate ullage propulsion systems, and concern over the operational status of start tanks and expulsion screens led to the selection of elastomeric bladders for the powered spacecraft mission.

Orificed, liquid check valves are included in the propellant feed system to prevent propellant migration between tanks due to propellant dynamics or pressure imbalances. Propellant migration is undesirable because it can produce large, unscheduled shifts in vehicle center of gravity (see thrust vector studies) and it increases residual propellant weight. It is particularly significant in the powered spacecraft because the boost-assist maneuver makes available large ullage volumes to which propellants can migrate. Methods considered to control propellant migration included not manifolding the propellant tanks, using check valves in the pressurization gas lines, and using check valves in propellant feed lines. Unmanifolded tankage was rejected because of increased residuals and the complexity of dual pressurization systems. Check valves were not used in the pressurization gas supply line to each tank because separate relief and service valves were then also required. This meant added complexity and extremely difficult pressure balancing of relief circuits. Liquid check valves were thus selected as the least complex, lightest-weight solution. However, separate propellant service valves were then required for each tank. Orifices were also required for balancing feed line pressure drop to prevent flow inequalities between tanks.

Dual, normally closed, squib valves are included in the propellant feed system to permit prelaunch engine purge and checkout.

*Pressurization Subsystem*---The pressurization subsystem consists of helium gas, a helium gas reservoir, and valves, regulators, and filters necessary for pressurant servicing and control. Approximately 10 pounds of helium gas are stored at high pressure in two spherical titanium (6AL-4V) reservoirs. No manifolding provisions are provided to the reaction control system because it uses a separate nitrogen gas supply as a propellant.

Helium was selected on a weight basis as the pressurizing gas in the final powered spacecraft configuration. Helium and nitrogen gas were both considered in the pressurization trade study discussed in Appendix A. Separate and common gas storage options were also evaluated when nitrogen, used as the reaction control propellant, was also used for pressurizing the main propellant tanks. Early powered spacecraft configurations, being quite compact, could not accommodate two gas reservoirs without incurring significant structural penalties for lengthening the spacecraft. This offset the 45- to 60-pound weight advantage obtained by using helium for pressurization because nitrogen was used as the reaction control propellant. (The dual-tank nitrogen system was correspondingly heavier than the dual-tank helium-nitrogen system.) However, subsequent spacecraft configurations readily accommodated two gas reservoirs without structural weight penalties; therefore, helium gas was selected as the pressurant in the final powered spacecraft configuration.

In this system, service and isolation valves are provided for prelaunch servicing. Squib valves, solenoid valves, check valves, and pressure regulators are provided in the gas supply circuit to control pressurant flow. Normally closed squib valves are provided immediately downstream of the gas reservoir to isolate the helium supply until the system is activated in Earth orbit. A latching solenoid valve-pressure regulator package used for primary pressurant control is located downstream of these valves. This package, used in the Apollo Lunar Module Ascent Stage, consists of dual valve-regulator assemblies arranged in parallel. Each valve-regulator assembly consists of a latching solenoid valve plus two regulators, packaged in series. These solenoid valves provide repeated isolation sequences as necessary. They are scheduled to be open during the major boost-assist and orbit-insertion maneuvers. When closed, they are used to minimize gas leakage through the regulators and into the propellant tanks. A backup squib valve package is provided between the helium tank and primary pressurant control packages to effectively isolate the pressurant between the boost-assist and orbit-insertion velocity maneuvers, if necessary.

The single pressurization gas outlet from the regulator package is manifolded to all propellant tanks. Check valves are included in these lines to prevent propellant vapor mixing. Reseating relief valves are included to prevent tank overpressure. Burst disks are incorporated in the relief valve to minimize gas leakage before valve actuation.

### 7.3.1.4 Physical Data

Propulsion system physical data are described in Tables 7.3-2 and 7.3-3. Much Apollo program hardware was used, particularly hardware developed for the Lunar Module Ascent Stage (LMAS).

### 7.3.1.5 Operations and Performance

The propulsion system may be fueled and serviced before installation at the launch pad. Checkout operations, however, will be performed on system instrumentation and engine valves while on the launch pad. When the spacecraft is in Earth orbit, the engine prevalves and main valves are cycling the normally closed lines. The pressurant circuit is then activated by cycling the normally closed squib valves. This is followed by an opening of the normally closed propellant squib valves which activates the propellant feed system.

After the spacecraft is separated from the Titan transtage and positioned for the final injection maneuver, an engine burn is initiated that continues until the desired velocity increment (1 to 1.3 km/sec) is attained. Engine shutdown is signaled by an integrating accelerometer output. After shutdown, the pressurization system latching solenoid valves are commanded closed.

The first midcourse correction is conducted within 5 days from injection. A second is scheduled for approximately 25 days from injection. A possible third correction may be required within 20 to 40 days of Mars encounter. These maneuvers can be accomplished in a blowdown mode without opening the pressurization system solenoid valves. Subsequent to the first or second midcourse correction, the backup isolation squib valve package may be actuated at the option of flight operations personnel.

Table 7.3-2: PROPULSION SYSTEM WEIGHT BREAKDOWN

| | Indirect Lander Weight (lb) | Direct Lander Weight (lb) |
|---|---|---|
| Engine Assembly (including valves) | 135 | 135 |
| TVC Gimbal Assembly (excluding actuators) | 39 | 39 |
| Structural Support and Attachments, and Thermal Control | 122 | 96 |
| Propellant Tankage | 161 | 148 |
| Pressurization Tankage | 110 | 95 |
| Propellant and Pressurization Feed System | 62 | 62 |
| Inert Fluids and Helium Gas: | | |
| Trapped Propellant | 82 | 73 |
| Mixture Ratio Allowance | 72 | 64 |
| Helium Gas (Propellant Expulsion and Residual) | 10 | 9 |
| Total Inert Weight | 793 | 721 |
| Minimum Usable Propellant Weight | 3,965 | 3,482 |

Before planet encounter, the propulsion system is reactivated for either the final midcourse correction or the orbit injection maneuver. The pressurization system latching solenoid valves are opened, and if the backup isolation squib package has not been used, the maneuver is initiated. If the backup squib package has been previously used, it must be reactivated to an open position before final maneuvers are conducted.

Orbit trim maneuvers may be conducted with pressurant being supplied to propellant tanks or in a blowdown mode (solenoid valve or the isolation package in a closed position). Performance of the propulsion system throughout the powered spacecraft mission is summarized in Table 7.3-4.

### 7.3.2 Guidance and Control System

As with a nonpowered spacecraft, the powered spacecraft requires full attitude stabilization and control during all mission phases to complete the mission successfully. It must have the capability to use fixed celestial references for establishing attitude position and rate and must be able to maintain its inertially fixed position during celestial occultations. It further requires a computer sequencer to program and compute mission events time to go, attitude maneuvers, and velocity maneuvers, because real-time command for these functions cannot be considered. And finally, it must contain an angular torquing system to offset disturbances causing attitude variations.

## Table 7.3-3: PROPULSION SYSTEM COMPONENTS

| Component | Description | Quantity | Weight (Each) | Avail-ability |
|---|---|---|---|---|
| Pressurant Tank | 0 to 3,500 psig, 70°F, 20 in. | 2 | 55.0 | Dev |
| Propellant Tank, Oxidizer | 36.4 in. dia, 250 psia | 2 | 40.0 | Dev |
| Propellant Tank, Fuel | 36.4 in. dia, 250 psia | 2 | 40.0 | Dev |
| Valve, Solenoid, Latching | 0 to 4,000 psig, 70°F | 2 | 2.3 | LMAS |
| Valve, Squib, $N_2$ | Normally open (1)<br>Normally closed (4) | 5 | 1.0 | LMAS |
| Valve, Relief (with burst disk) | 226 to 25 psig | 2 | 0.9 | LMAS |
| Valve, Service, Gas | 0 to 4,000 psig, 70°F | 5 | 0.3 | LMAS |
| Valve, Service, Propellant | 0 to 250 psig, 70°F | 10 | 0.4 | LMAS |
| Valve, Quad Check, Gas | 0 to 270 psig, 70°F | 2 | 1.0 | LMAS |
| Valve, Quad Check, Prop. | $N_2O_4$ Compatible, 250 psig | 4 | 2.0 | Dev |
| Pressure Regulator, Gas | Dual, Series | 2 | 2.7 | LMAS |
| Filter, Gas | 0 to 4,000 psig, 70°F | 3 | 0.4 | LMAS |
| Filter, Propellant | 0 to 250 psig, 70°F | 2 | 0.4 | LMAS |
| Orifice, Calibration | 0 to 250 psig, 70°F | 2 | 0.2 | Dev |
| Engine Assembly (with valve and gimbal assy) | Thrust = 3,500 lb | 1 | 173.7 | LMAS |
| Transducer | Temperature | 4 | 0.1 | LMAS |
| Transducer | Pressure | 4 | 0.1 | LMAS |
| Valve, Squib, Prop. | 0 to 250 psig, 70°F | 4 | 1.0 | Dev |

LMAS - Lunar Module Ascent Stage

Dev - Development Item

Table 7.3-4: PROPULSION SYSTEM PERFORMANCE SUMMARY

| Mission Phase | Duration (days) | Maneuver | ΔV (m/sec) | Operating Duration (sec) | Impulse (lb-sec) | Acceleration (Maximum) (g's) |
|---|---|---|---|---|---|---|
| Launch, In-Orbit | <1 | Boost Assist | 1,385 | 226 | 793,000 | 0.795 |
| Transfer to Planet | 200 | Miscourse No. 1 | ≤40 | ≤5 | ≤18,000 | 0.805 |
| | | Midcourse No. 2 | ≤6 | Minimum | ≤3,000 | |
| | | Midcourse No. 3 | ≤4 | Minimum | ≤2,000 | |
| Planet-Prime Mission | 30 | Orbit Insertion | 988 | 106 | 372,100 | 1.13 |
| | | Orbit Trim No. 1 | ≤45 | ≤4 | ≤14,000 | 1.14 |
| | | Orbit Trim No. 2 | ≤30 | ≤3 | ≤9,000 | 1.15 |
| Planet-Extended Mission | 180 | None | 0 | | | |
| Total<br>Prime<br>Extended | <br>231<br>381 | 7 starts | 2,498 | ≤346 | ≤1,211,000 | 1.15 |

The system described in this section meets these conditions. It has resulted from careful consideration of the trade studies reported in Appendix C, which are:

Initial Attitude Errors
Staging Rate
Reaction Control
Thrust Vector Control

### 7.3.2.1 Design Conditions and Constraints

The design conditions and constraints for the guidance and control system are set by the method chosen for Earth departure, the midcourse delta velocity accuracy, the communication requirements, and the mission requirements. They are given in Table 7.3-5 and briefly discussed below.

## Table 7.3-5: GUIDANCE AND CONTROL DESIGN CONDITIONS AND CONSTRAINTS

| Design Conditions | Origin |
|---|---|
| **Separation Transtage---Spacecraft** | |
| Rates to 0.62 deg/sec | Staging Rate Analysis |
| ±4 degree Gyro Gimbal Limit | Assumed |
| **Celestial Acquisition** | |
| Acquire Sun < 1.7 Hours After Launch | Battery Constraint |
| Programmed Sun and Canopus Requisition | Communication Range |
| **Pointing** | |
| High Gain Antenna ±0.6 degree | Communication Constraint at Mars |
| **Limit Cycle** | |
| Deadband ±0.3 degree | Communication Constraint, Minimize RCS Propellant |
| Rate 0.0003---0.002 deg/sec | Control Acceleration and Minimum Impulse |
| **Attitude Maneuver** | |
| Slew Rate 0.2 ±10% deg/sec | Battery Considerations, Minimize RCS Propellant |
| Accuracy $\le$ 0.5%/axis | 50 m/sec Midcourse $\Delta V$; from RFP |
| **Velocity Maneuver** | |
| Attitude Pointing Accuracy $\le$ 1.3 degrees | 50 m/sec Midcourse $\Delta V$; from RFP |
| Accelerometer Range 3.0 g's | Orbit Trim Maneuver |
| Accelerometer Accuracy 0.03 m/sec | Final Midcourse |
| Accelerometer Resolution 0.04 m/sec | Final Midcourse |
| Maximum Gimbal Rate Expected 4.5 deg/sec | TVC Analysis |
| Maximum Gimbal Deflection Expected 1.3 degrees | TVC Analysis |
| **Mission** | |
| 200 Days Transplanet---180 Days Mars Orbit | Assumed Mission |
| 4 Maneuvers Transplanet---30 Maneuvers in Mars Orbit | Assumed Mission |
| Stored Program Through Mars Orbit Insertion | |

*Pointing Accuracy*---The preferred method of boost assist is one in which the spacecraft engine burn takes place shortly after transtage-spacecraft separation. For this mode, the spacecraft initial inertial reference is taken from the transtage. A pointing accuracy < 1.3 degrees is required to meet a total midcourse allocation of ≤ 50 m/sec (see Figure 5.6-13).

*Sun-Acquisition Time*---Following injection, Sun acquisition is required to take place in ≤ 30 minutes so that battery discharge (approximately 60%) will not exceed the 280 watt-hours allowed (see Figure 7.3-1).

*Narrow Deadband Limit*---A ±0.3-degree deadband limit is required to meet the G&CS apportionment of 10.6 degree for high-gain antenna pointing (gives approximately 1-db loss at Mars).

*Maneuver Rate*---A maneuver rate of 0.2 deg/sec was chosen after considering such factors as off-Sun time, reaction control propellant expenditure, and end of maneuver settling time (see Appendix C).

*Maneuver Accuracy*---The accuracy requirement of 0.5% is conservative and was chosen after considering such errors as gyro drift, deadband, cross-axis coupling, and measurement inaccuracies.

*Thrust Vector Control (TVC)*---The thrust vector control design parameters of 10 deg/sec with a gimbal limit of 3 degrees resulted from the study reported in Appendix C. These design parameters will handle expected TVC deflection rates of 4.5 deg/sec and deflection angles of 1.3 degrees.

*Nitrogen Budget*---The nitrogen required to torque the spacecraft both for limit cycling, midcourse and scientific maneuvers, and rate damping is estimated to be 17.3 pounds (see Appendix C).

### 7.3.2.2 Preliminary Design

Listed below is the preferred design concept for guidance and control of the powered spacecraft:

1) The prime reference for attitude control is a Sun-Canopus system.
2) Backup reference for attitude control and guidance is a three-axis, orthogonal, rate-integrating gyro inertial reference unit, which maintains a stable base for attitude and velocity maneuvers.
3) Velocity control is provided by integrating the output of a linear accelerometer.
4) Maneuvers are measured by integrating gyro rate output in a digital computer.
5) Angular torque control about the roll, pitch, and yaw axes during limit cycle and attitude maneuvers is provided by a nitrogen cold-gas reaction control system.

6) Angular torque control during velocity maneuvers about the pitch and yaw axes is provided by an electromechanical gimbal actuator. Angular torque control about the roll axis during velocity maneuvers is provided by a nitrogen cold-gas reaction control system.

7) On-board guidance command and control is provided by a special-purpose digital computer; in addition, the computer provides event time to go, switching, gain changes, and control of all the spacecraft subsystems.

8) Boost-assist guidance reference is derived by the IRU from the transtage attitude immediately before separation.

The general block diagram of the guidance and control system is shown in Figure 7.3-2 for the pitch and yaw axes and 7.3-3 for the roll axis. In the preferred design, no major difference exists between the attitude control axes other than the different gains associated with the use of Sun sensors in pitch and yaw and Canopus tracker in roll. The system is a conventional rate-limited "On-Off" cold-gas attitude stabilization and control system.

The following equipment is used to perform these functions:

*Inertial Reference Unit*---The inertial reference unit (IRU) consists of three orthogonally mounted gyros and a linear accelerometer mounted to sense velocity changes along the thrust axis. Its gyros, mounted on ball bearings, are the single-degree-of-freedom, floated, rate-integrating type. This choice is based on availability, experience, and maturity of development in applications to space vehicles. The heater power for the gyros and accelerometer is switchable to permit control with IRU "off." The gyros are capable of operation in the rate or rate-integrating (inertial hold) mode. The rate mode is used for rate damping and maneuvers, and the inertial hold mode is used for limit cycle operation (attitude control) and thrust vector control. The IRU accelerometer provides an output proportional to the velocity increment gained during engine burn. This output is measured and integrated in the computer sequencer. Thrust is terminated on reaching a preset value of velocity change. A timed backup approach, based on $3\sigma$ burn tolerance, will be designed into the computer sequencer. The IRU gyros and accelerometer are available off the shelf; the electronics and packaging are readily designable with many designs being available. Table 7.3-6 lists their significant performance parameters.

*Canopus Tracker*---The selected Canopus tracker for roll reference is similar to Mariner '69 and the Lunar Orbiter. These sensors use an image dissector tube, allowing a wide field of view by electronic gimbaling. Further study is required to resolve the Canopus tracker problems experienced in previous space missions such as: (1) stray light or glint pulling the tracker off the star; (2) track loss due to illuminated stray particles; and (3) degradation of detector gain with time. The basic tracker is available off the shelf. Table 7.3-7 lists its major performance parameters.

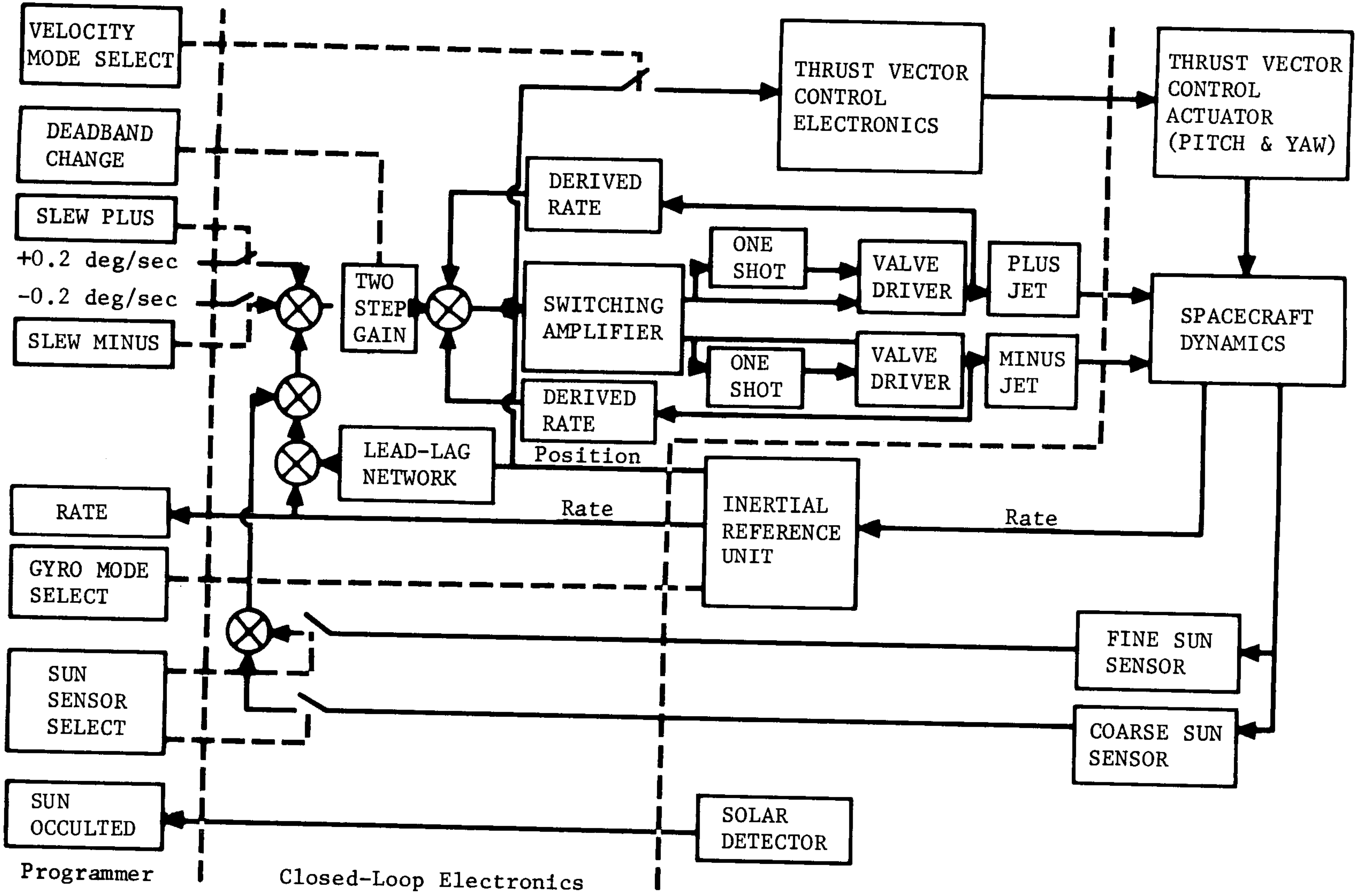
VELOCITY MODE SELECT
DEADBAND CHANGE
SLEW PLUS
+0.2 deg/sec
-0.2 deg/sec
SLEW MINUS
RATE
GYRO MODE SELECT
SUN SENSOR SELECT
SUN OCCULTED
Programmer
TWO STEP GAIN
LEAD-LAG NETWORK
DERIVED RATE
SWITCHING AMPLIFIER
DERIVED RATE
Position
Rate
ONE SHOT
ONE SHOT
VALVE DRIVER
VALVE DRIVER
PLUS JET
MINUS JET
THRUST VECTOR CONTROL ELECTRONICS
INERTIAL REFERENCE UNIT
SOLAR DETECTOR
Closed-Loop Electronics
THRUST VECTOR CONTROL ACTUATOR (PITCH & YAW)
SPACECRAFT DYNAMICS
Rate
FINE SUN SENSOR
COARSE SUN SENSOR

Figure 7.3-2: GUIDANCE AND CONTROL BLOCK DIAGRAM---PITCH AND YAW AXES

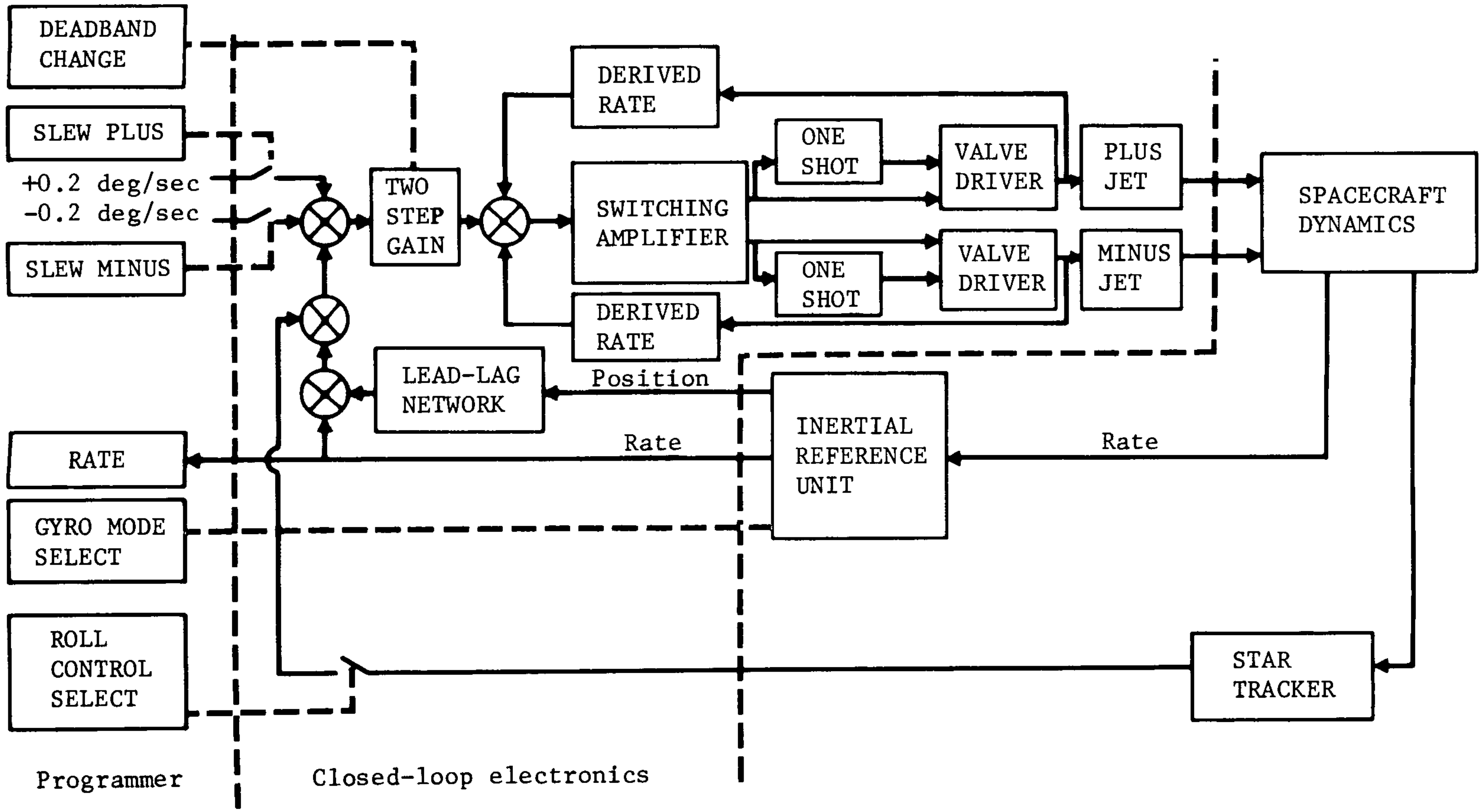
DEADBAND CHANGE
SLEW PLUS
+0.2 deg/sec
-0.2 deg/sec
SLEW MINUS
RATE
GYRO MODE SELECT
ROLL CONTROL SELECT
Programmer
TWO STEP GAIN
LEAD-LAG NETWORK
DERIVED RATE
SWITCHING AMPLIFIER
DERIVED RATE
ONE SHOT
ONE SHOT
VALVE DRIVER
VALVE DRIVER
PLUS JET
MINUS JET
Position
Rate
INERTIAL REFERENCE UNIT
Rate
SPACECRAFT DYNAMICS
STAR TRACKER
Closed-loop electronics

Figure 7.3-3: GUIDANCE AND CONTROL BLOCK DIAGRAM---ROLL AXIS

## Table 7.3-6: GUIDANCE AND CONTROL COMPONENT CHARACTERISTICS---INERTIAL REFERENCE UNIT

| | |
|---|---|
| Rate Mode | |
| Scale Factor | 4 volts/deg/sec over ±3 deg/sec |
| Error | 0.04% at ±0.2 deg/sec |
| Threshold | 0.2 deg/hr |
| Resolution | 1.0 deg/hr at 0.5 deg/sec |
| Rate Integrate Mode | |
| Scale Factor | 4 volts/1 deg ±0.5% over ±3 deg Input Angle |
| Input Angle | ±4 deg |
| G-Insensitive Drift | 0.3 deg/hr for IA's of ±0.3 deg |
| Attitude Error | ±0.01 deg for IA's ±0.2 deg |
| Threshold | 0.01 deg IA |
| Resolution | 0.01 deg for IA of ±0.5 deg |
| Accelerometer | |
| Range | ±5 g's |
| Stability | ±0.1% |
| Resolution | 0.04 m/sec/pulse |
| Bias | $10^{-4}$ g's |
| Accuracy | ±0.0006 g's at 5 g's |
| Alignment | |
| To Spacecraft Axes | ±0.18 degree ($3\sigma$) |

## Table 7.3-7: GUIDANCE AND CONTROL COMPONENT CHARACTERISTICS---CANOPUS TRACKER

Tracking Accuracy

- Short Term 0.802 degree
- Long Term 0.05 degree

Map Voltage

- Range---0.04 to 3 x Canopus

Recognition Gates

- Upper---4 Levels Programmable
- Lower---4 Levels Programmable

Field of View

- Instantaneous---1.05 x 11 degrees
- Scanned---3 x 11 degrees
- Acquisition---4 x 34 degrees
- Steps In Field of View---5 steps at 4.6 degrees each

Accuracy

- Null Accuracy---0.02 degree
- Roll Error---±6% over ±2 degrees from null linearity

Modes of Operation

- Acquisition---Automatic
- Tracking
- Reacquisition---Single Scan if star lost
- Recognition Override---Track any star above 0.04 x Canopus
- Override Star---Release acquired star on command

Sun Shutter

Activated 35 degrees from Sun

Activated 15 degrees from Mars

Mounting

No spacecraft structure within 40 degrees of boresight

*Sun Sensors*---The preferred Sun sensors for pitch and yaw reference are N/P silicon cells such as used on Lunar Orbiter. Three Sun sensor outputs will be provided: a fine Sun sensor with a 3-degree field of view in the linear range, a coarse Sun sensor having a 4π steradian field of view (used for backup Sun acquisition), and a Sun-acquisition sensor generating a presence signal when the Sun is within ±3 degrees of the fine Sun sensor null. The fine Sun sensor gain, sized for a ±0.3-degree limit cycle at Mars, controls the pitch and yaw axes during limit cycle operation. No compensation is provided for this Sun sensor, though its scale factor is changing because of the increasing Sun distance as the spacecraft approaches Mars. The two-step gain change shown in the functional diagram (Figure 7.3-2) could be sized to lessen this perturbation. The Sun sensors are available off the shelf. Table 7.3-8 lists major performance parameters.

*TVC Actuators*---Electromechanical actuators position the engine through the vehicle center of gravity during velocity maneuvers. The actuators are powered by a variable-speed d.c. motor driving a recirculating ball screw through reduction gearing. The actuator is irreversible; thus, it remains centered on the center of gravity after an engine firing. Rate and position sensors provide feedback signals for closed-loop operation. Actuator on and off time will be delayed some 200 milliseconds and 150 milliseconds, respectively, so as to avoid operation at low thrust levels.

## Table 7.3-8: GUIDANCE AND CONTROL COMPONENT CHARACTERISTICS---SUN SENSOR

Type Sun Sensor Photoelectric N/P Silicon

- Fine Sensor---Ball Brothers FE-5A
- Coarse Sensor---Ball Brothers CE-3
- Acquisition---Ball Brothers TE-4E

Quantity

- Fine Sensor---4
- Coarse Sensor---8
- Acquisition---1

| Fine | Coarse |
|---|---|
| • Field of View ±5 degrees | 180 degrees |
| • Null Error ±0.020 at 1 AU | ±0.2 degrees |
| • Scale Factor | |
| 1 AU 12 mv/deg ±10% | 1 AU 2 mv/deg ±10% |
| 1.67 AU 4.3 mv/deg ±10% | 1.67 AU 0.76 mv/deg ±10% |
| • Null Instability---±10% | ±0.5 degree |

Acquisition

- 100 mv over ±3 degrees

A block diagram of the system is shown in Figure 7.3-4. The gain change shown may be required for velocity maneuvers with capsule off. The actuator requires design and development because no comparable size is in production or has been built. Table 7.3-9 lists significant performance parameters.

## Table 7.3-9: GUIDANCE AND CONTROL COMPONENT CHARACTERISTICS---GIMBAL ACTUATOR

Type

- Electromechanical Reversible DC Motors. Irreversible Drive
- Recirculating Ball Jackscrew

| | |
|---|---|
| Gimbal Position Limit | ±3 degrees |
| Gimbal Angular Rate | 10 deg/sec |
| Maximum Actuator Limit Cycle | ±0.25 degree |
| Feedback Gain | 50 volts/rad |
| Position Gain | 109 volts/rad |
| Rate Gain | 47 volts/rad/sec |
| Forward loop gain | 0.3 rad/sec/volt |
| TVC Corner Frequency | 15 rad/sec |

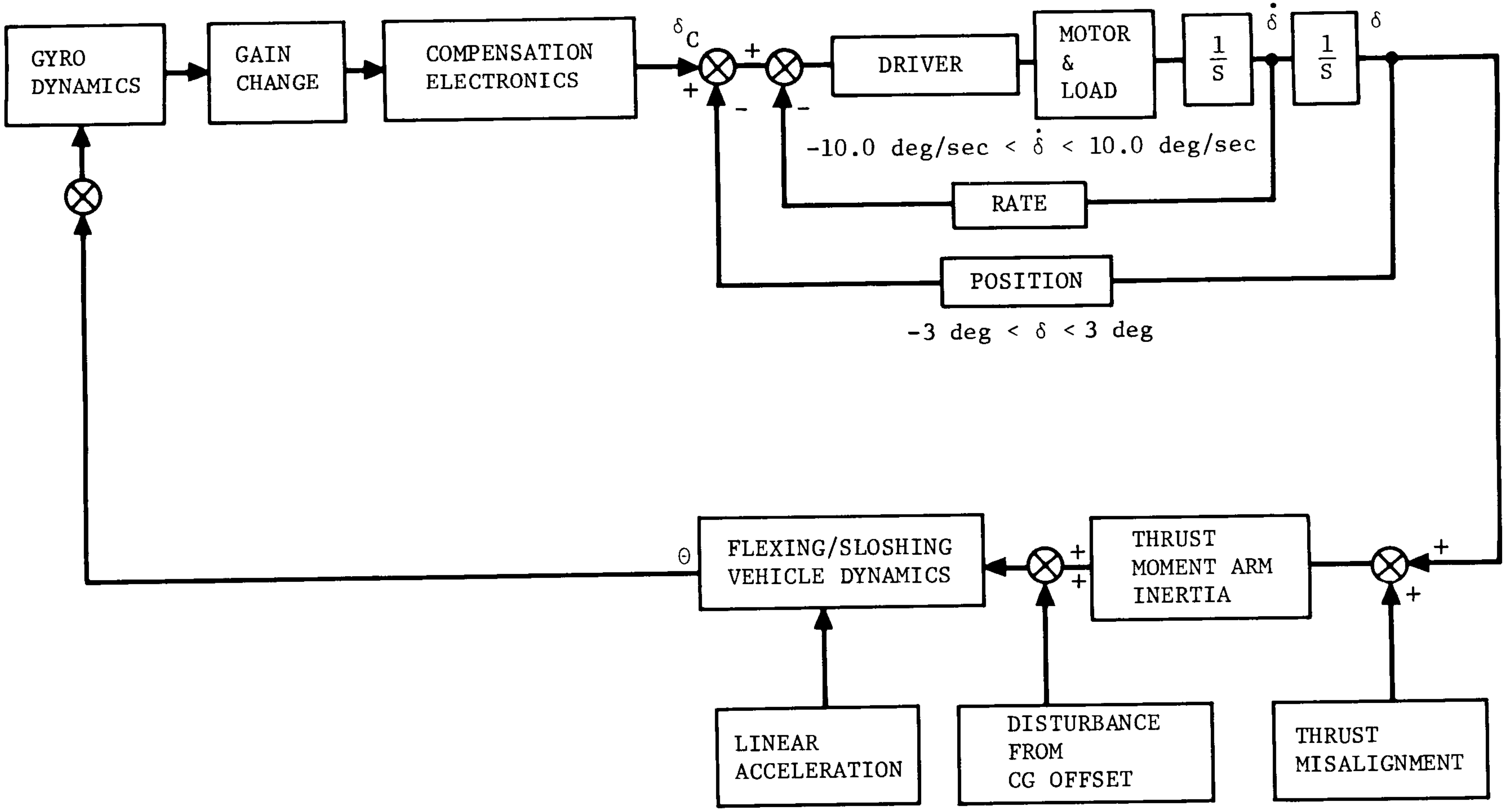
GYRO DYNAMICS
GAIN CHANGE
COMPENSATION ELECTRONICS
$\delta_C$
+
+
-
-
DRIVER
MOTOR & LOAD
$\frac{1}{S}$
$\dot{\delta}$
$\frac{1}{S}$
$\delta$
$-10.0$ deg/sec $< \dot{\delta} <$ $10.0$ deg/sec
RATE
POSITION
$-3$ deg $< \delta <$ $3$ deg
$\Theta$
FLEXING/SLOSHING VEHICLE DYNAMICS
+
+
THRUST MOMENT ARM INERTIA
+
+
LINEAR ACCELERATION
DISTURBANCE FROM CG OFFSET
THRUST MISALIGNMENT

Figure 7.3-4: THRUST VECTOR ACTUATOR BLOCK DIAGRAM

*Reaction Control*---The selected concept for reaction control is a pulsed, cold-gas, nitrogen system similar to Lunar Orbiter's. The system has eight thrusters: four in roll (0.07 pound each) and two each in pitch and yaw (0.29 pound each). A maneuver rate of 0.2 deg/sec has been selected as a compromise between expended propellant for maneuvers and the off-Sun constraint imposed by battery power considerations. The control acceleration of 0.05 deg/sec$^2$ in pitch and yaw was chosen after considering minimum propellant consumption, the retention of an inertial reference during transtage spacecraft separation, and a nominal settling time at the end of a maneuver. The roll control acceleration of 0.03 deg/sec$^2$ was sized to accommodate roll transients that may occur due to center-of-gravity misalignments at engine startup. Thruster performance degradation, due to short pulse operation, is minimized by the minimum on-time circuitry (one shot). Thrusters, test and fill valving, and regulators in the range desired are obtainable off the shelf. A block diagram of the system is shown in Figure 7.3-5. Table 7.3-10 lists significant performance characteristics.

*Computer Sequencer*---The computer sequencer performs the tasks of spacecraft timing, commanding, program storage, flight control logic, and attitude control switching, shaping, and gain changing. The selected programmer concept is a serial-data-cycled, special-purpose, 20-bit-word programmable digital computer. The conceptual design incorporates a 512-word random access, sequential, magnetic core memory. Computation is performed by a bit adder. Attitude position, velocity, and time to go are computed by this unit. Time

Table 7.3-10: GUIDANCE AND CONTROL COMPONENT CHARACTERISTICS---REACTION CONTROL

| | | | |
|---|---|---|---|
| Propellant | Cold $N_2$<br>Isp 68<br>Amount 17.3 pounds | | |
| Thrust Level | | | |
| Pitch | 0.29 pound | | |
| Yaw | 0.29 pound | | |
| Roll | 0.07 pound; 2 in couple | | |
| Control Acceleration - degrees/sec$^2$ | | | |
| | Startburn | Transit | Orbit |
| Pitch | 0.05 | 0.053 | 0.185 |
| Yaw | 0.05 | 0.053 | 0.185 |
| Roll | 0.03 | 0.04 | 0.065 |
| Limit Cycle Rate Minimum Impulse - degrees/sec | | | |
| Pitch | 0.0005 | 0.00053 | 0.00185 |
| Yaw | 0.0005 | 0.00053 | 0.00185 |
| Roll | 0.0003 | 0.0004 | 0.00065 |

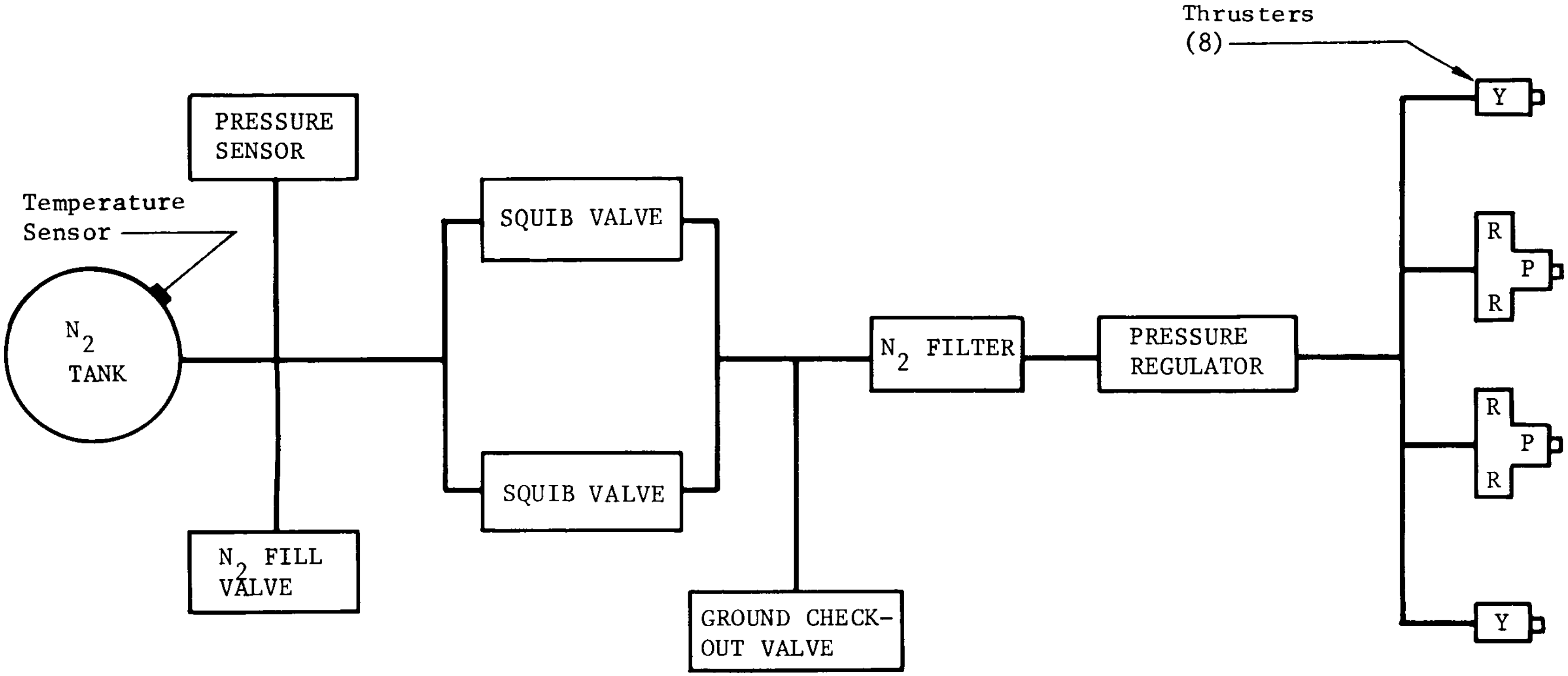
Thrusters
(8)
Y
R
P
R
R
P
R
Y
PRESSURE SENSOR
Temperature Sensor
$N_2$ TANK
SQUIB VALVE
SQUIB VALVE
$N_2$ FILL VALVE
GROUND CHECK-OUT VALVE
$N_2$ FILTER
PRESSURE REGULATOR

Figure 7.3-5: REACTION CONTROL BLOCK DIAGRAM

is resolved to 1 second, attitude position to 0.01 degree, and velocity to ±0.04 m/sec. Typical designs such as Lunar Orbiter or Mariner '69 are available. Table 7.3-11 lists the significant performance characteristics.

Alignment of all guidance sensors (except coarse Sun sensors) will be within 0.18 degree ($3\sigma$) of the respective spacecraft axes. Reference mirrors on the IRU, fine Sun sensors, and Canopus trackers are used for alignment.

### 7.3.2.3 Physical Data

The weight, volume, and average power consumption are shown in Table 7.3-12.

### 7.3.2.4 Operations and Performance

Significant guidance and control events for the powered spacecraft mission are shown in Figure 7.3-6. A discussion of the operations and performance associated with these events by mission phases follows.

*Launch*---The spacecraft is launched from Cape Kennedy by a Titan IIIC launch vehicle and placed in a 100 n mi parking orbit about Earth. During this portion of the mission, the G&C subsystem is essentially inactive with the exception of the computer sequencer.

- Nitrogen to the thrusters is cut off by normally closed squib valves.
- The Sun sensors are disconnected from the electronics to minimize thruster commands and consequent solenoid actuations.
- The Canopus tracker is off to prevent radiation and high voltage arcing damage during the launch phase and during passage through Van Allen belts.
- The gyros are in a rate mode as a protective measure to prevent their hitting the gimbal stops.

Before transtage second burn for the transplanet injection maneuver, the computer sequencer initiates spacecraft propellant line bleed and the arming of the velocity control subsystem.

*Transplanet Injection*---For departure from the 100 n mi parking orbit, a second burn of the transtage is applied at a constant attitude rate. Upon burn completion, the transtage maneuvers the transtage and spacecraft to the best inertially fixed position for spacecraft engine burn. The IRU is then placed in inertial hold, and separation occurs followed by spacecraft engine ignition. Since coast time before boost assist involved payload penalties (see Figure 5.5-3), the time is minimized by having separation transients in pitch and yaw removed during spacecraft engine burn by the TVC system. Spacecraft $3\sigma$ pointing errors at initiation of boost assist are estimated to be $< \pm 1$ degree (Appendix C).

After spacecraft velocity is terminated at a preprogrammed value by the computer sequencer, the appendages are deployed, the spacecraft is maneuvered to the Sun-acquisition attitude, and the Sun is acquired. A backup mode for Sun acquisition that provides for an autonomous acquisition will be initiated at a preprogrammed time. The time for launch to Sun lock will be approximately

## Table 7.3-11: GUIDANCE AND CONTROL COMPONENT CHARACTERISTICS---COMPUTER SEQUENCER

**General**

- Organized as a Cycled Special-Purpose Computer
- Automatic Selection of Guidance Modes
- Real-Time and Stored Program

Program Routines

- Stored Programs
- Interrupt Modes
- Immediate Execute
- A-D Conversion
- Adder

Memory

- 512 - 21-Bit Word Magnetic Core DRO
- Random access by Word Serial by Bit

Commands

- 90 Estimated, Expandable to 250

**Time**

- 12-Day Clock
- 1-Second Resolution

Maneuver Calculation

- 360 - 0.011 degree Resolution
- 2620 m/sec 0.08 m/sec Resolution (Long Burn)
- 1310 m/sec 0.04 m/sec Resolution (Short Burn)

Attitude Control

- Close Rate & Attitude Loops with Sensor Inputs
- Provide Lead/Lag on IRU Inertial Hold
- Amplify Limit Provide Derived Rate Sun Sensor
- Switch
  - Axis Gain
  - Slew Signals
  - Sensors

Provide Control Thrusters

Provide Control TVC

## Table 7.3-12: GUIDANCE AND CONTROL---WEIGHT POWER VOLUME

| Component | Weight (Pounds) | Average Power (Watts) | Volume (Cubic Inches) | Comments |
|---|---|---|---|---|
| Inertial Reference Units | 15.0 | 30 | 600 | Includes accelerometer; gyro and accelerometer off shelf. Develop package. |
| Star Tracker ▷1 | 7.5 | 3.5 | 800 | Canopus---incrementing type. |
| Sun Sensor ▷1 | 2 | | 45 | Fine, coarse, and remote. |
| Reaction Control ▷1 | 52 | Neg | 1,950 | Complete system (includes 17 pounds $N_2$). |
| Gimbal Actuator | 18.5 | ▷3 | | New design. |
| Computer Sequencer ▷2 | 15 | 25 | 1,000 | Includes required guidance and control electronics. |
| Supports | 11 | | | |
| Total Preferred System | 121 | 58.5 | 4,395 | |

▷1 Off Shelf

▷2 Design Available

▷3 Occurs During Engine Burn Only 500 w Max.
250 w Rated

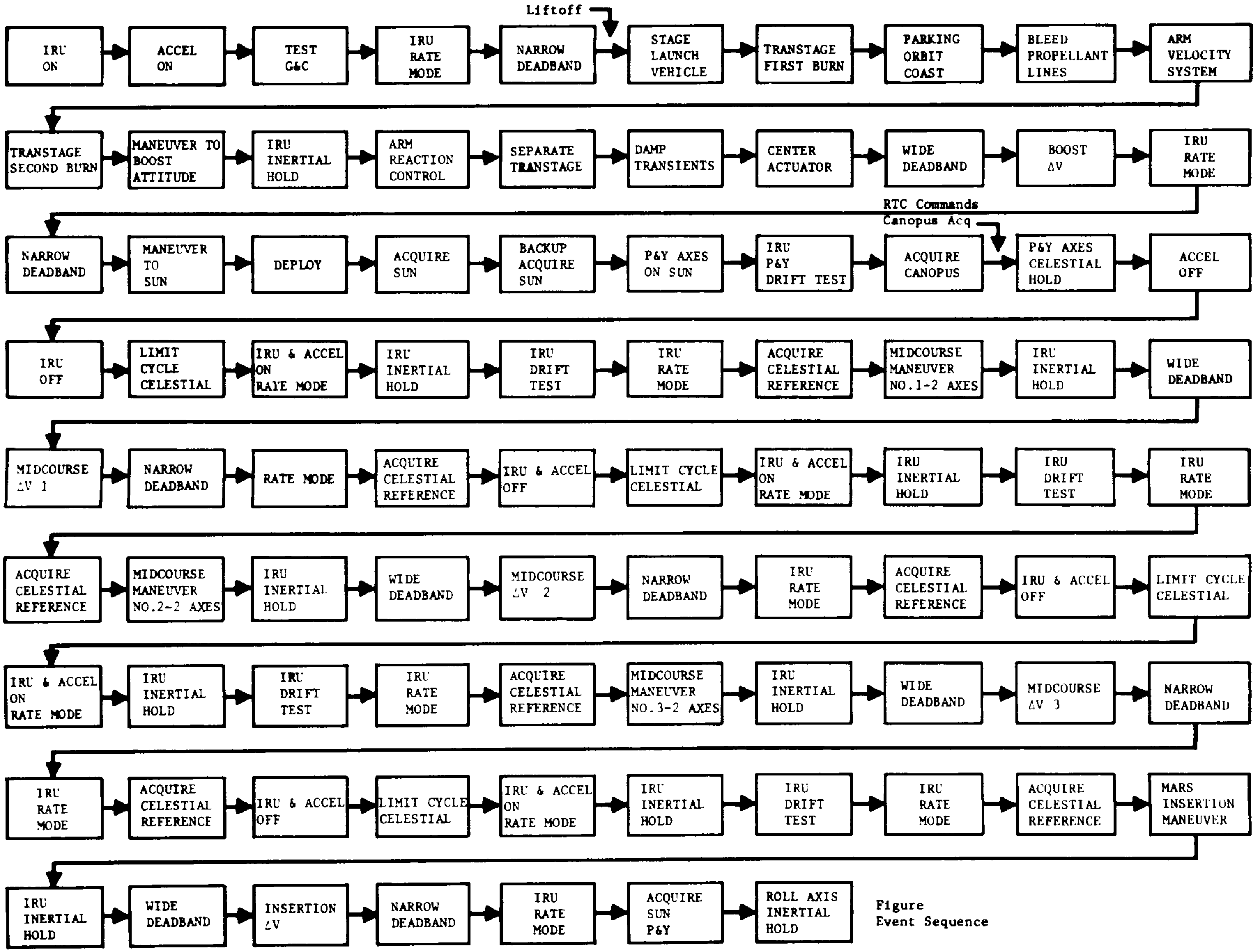
Liftoff
IRU ON
ACCEL ON
TEST G&C
IRU RATE MODE
NARROW DEADBAND
STAGE LAUNCH VEHICLE
TRANSTAGE FIRST BURN
PARKING ORBIT COAST
BLEED PROPELLANT LINES
ARM VELOCITY SYSTEM
TRANSTAGE SECOND BURN
MANEUVER TO BOOST ATTITUDE
IRU INERTIAL HOLD
ARM REACTION CONTROL
SEPARATE TRANSTAGE
DAMP TRANSIENTS
CENTER ACTUATOR
WIDE DEADBAND
BOOST ΔV
IRU RATE MODE
RTC Commands Canopus Acq
NARROW DEADBAND
MANEUVER TO SUN
DEPLOY
ACQUIRE SUN
BACKUP ACQUIRE SUN
P&Y AXES ON SUN
IRU P&Y DRIFT TEST
ACQUIRE CANOPUS
P&Y AXES CELESTIAL HOLD
ACCEL OFF
IRU OFF
LIMIT CYCLE CELESTIAL
IRU & ACCEL ON RATE MODE
IRU INERTIAL HOLD
IRU DRIFT TEST
IRU RATE MODE
ACQUIRE CELESTIAL REFERENCE
MIDCOURSE MANEUVER NO.1-2 AXES
IRU INERTIAL HOLD
WIDE DEADBAND
MIDCOURSE ΔV 1
NARROW DEADBAND
RATE MODE
ACQUIRE CELESTIAL REFERENCE
IRU & ACCEL OFF
LIMIT CYCLE CELESTIAL
IRU & ACCEL ON RATE MODE
IRU INERTIAL HOLD
IRU DRIFT TEST
IRU RATE MODE
ACQUIRE CELESTIAL REFERENCE
MIDCOURSE MANEUVER NO.2-2 AXES
IRU INERTIAL HOLD
WIDE DEADBAND
MIDCOURSE ΔV 2
NARROW DEADBAND
IRU RATE MODE
ACQUIRE CELESTIAL REFERENCE
IRU & ACCEL OFF
LIMIT CYCLE CELESTIAL
IRU & ACCEL ON RATE MODE
IRU INERTIAL HOLD
IRU DRIFT TEST
IRU RATE MODE
ACQUIRE CELESTIAL REFERENCE
MIDCOURSE MANEUVER NO.3-2 AXES
IRU INERTIAL HOLD
WIDE DEADBAND
MIDCOURSE ΔV 3
NARROW DEADBAND
IRU RATE MODE
ACQUIRE CELESTIAL REFERENCE
IRU & ACCEL OFF
LIMIT CYCLE CELESTIAL
IRU & ACCEL ON RATE MODE
IRU INERTIAL HOLD
IRU DRIFT TEST
IRU RATE MODE
ACQUIRE CELESTIAL REFERENCE
MARS INSERTION MANEUVER
IRU INERTIAL HOLD
WIDE DEADBAND
INSERTION ΔV
NARROW DEADBAND
IRU RATE MODE
ACQUIRE SUN P&Y
ROLL AXIS INERTIAL HOLD
Figure
Event Sequence

Figure 7.3-6: GUIDANCE AND CONTROL EVENT SEQUENCE

100 minutes (3σ). A few hours after injection, Canopus is acquired, the IRU turned off, and the transplanet cruise phase using celestial sensors for attitude reference begun. No problem is anticipated in rapidly acquiring Canopus, because even after about 10 hours, the undertainty in roll axis orientation will be only 3.5 degrees (3σ), which is within the tracker field of view. A backup mode for Canopus acquisition is programmed and will be initiated by ground command in the event Canopus is not acquired.

*Transplanet Cruise*---During the transplanetary cruise phase, the celestial sensors (Sun and Canopus) will serve as the primary attitude reference. Because of the fairly large variation in Sun-Canopus cone angle (20 to 27 degrees), the Canopus tracker will be electronically gimbaled to keep Canopus in the field of view. Because the IRU is off, a derived rate will also be used except for those periods when gyro drift rates are being established and when the spacecraft is being maneuvered. A maximum of three midcourse maneuvers is required during this phase: one at 5 days after injection, another at 25 days, and a final one at 40 days before Mars encounter. For each of these, the spacecraft will be maneuvered to a desired position, the gyros will be placed in inertial hold, the deadband will be set at its wide limits, and the engine will then be burned. After completing the engine burn, the spacecraft will be maneuvered back to its celestial references, the deadband will be set to its narrow limits, the IRU turned off, and the transplanet cruise mode will be reestablished.

*Mars Orbit Injection*---Upon arrival at Mars, an orbit insertion maneuver is performed to place the spacecraft in an orbit whose apoapsis and periapsis attitudes are respectively, about 33,000 and 1,000 kilometers, whose period is about 24.6 hours, and whose emphemeris matches the mission design. For this mode, the G&C subsystem operation is identical to that given for midcourse corrections except for increased engine burn time.

*Mars Orbit*---Once in Mars orbit, the IRU is assumed to be on continuously because Canopus and the Sun will be occulted or unavailable as a reference for certain portions of the orbit. Orbital trim maneuvers to shape the Mars orbit ephemeris will require G&C subsystem operations no different than for other maneuvers requiring engine burn. Maneuvers for scientific observations are scheduled at one per day for the first 30 days. G&C subsystem operations for these are identical to those for midcourse correction except that the spacecraft remains in narrow deadband and no velocity burn occurs.

### 7.3.3 Electrical Power Subsystem Studies

The electrical power subsystem serves as the sole source of all electrical power used by the planetary vehicle. The power subsystem collects radiant solar energy and converts it into electrical energy. This electrical energy is supplied in adequate quantity and quality to the spacecraft loads and is in part stored for use during planetary vehicle maneuvers when solar energy is not available. In addition, limited electrical power is supplied to the capsule for housekeeping. This study is carried to the depth necessary to determine the power subsystem's impact on a powered spacecraft's useful weight in Mars orbit. It can be concluded from the results that the power subsystem is not functionally or physically affected by whether a powered or nonpowered spacecraft is used.

### 7.3.3.1 Design Conditions and Constraints

The design requirements of the power subsystem are developed around the mission definition for 1973 launch opportunity into a Mars orbit. The applicable flight mechanics are listed in Table 7.3-13. In brief, the table reflects a direct launch into a Mars planet trajectory followed by a 6-month orbital period around Mars. The direct launch time, shown under "Boost Assist," must be sustained by battery energy. The parameters shown under "Transplanet" are estimates and do not affect the size of any power subsystem component and are shown here for comparison only. The "In Orbit" and "Loads for Design" parameters size the power subsystem. These orbital parameters define a representative and probable Mars orbit. The energy available from the Sun is a function of the spacecraft-to-Sun distance. For the 1973 launch opportunity, this distance is shown in Figure 7.3-7 for the 6-month orbital period.

Table 7.3-13: MISSION PARAMETERS APPLICABLE TO POWER SUBSYSTEM DESIGN

| | Hours |
|---|---|
| Boost Assist | |
| Boost assist duration (engine burn) | 0.06 |
| Adapter separation to Sun acquisition | ≃0.6 |
| T = 0 to adapter separation | ≃0.9 |
| Transplanet | |
| Midcourse maneuvers - Number | 0.3 |
| Maximum off-Sun time per maneuver | 0.33 |
| -Includes engine burn | 0.0017 |
| Orbit insertion - Off-Sun duration | 0.417 |
| -Includes engine burn | ≃0.042 |
| In Orbit | |
| Orbital period | 24.6 |
| Sun occult time per orbit - 1st 30 days | 0 |
| - Next 5 month | (Maximum) 1.64 |
| Orbit trim - Number | 2 |
| - Duration | 0.33 |
| - Includes engine burn | ≃0.0017 |
| Off-Sun maneuvers (exclusive of velocity maneuvers) | 0 |
| | Watts |
| Loads for Design | |
| On-Sun (loads on spacecraft bus) | 224 |
| Sun occult - Mars | 117 |
| - Earth (engine off/engine on) | 193/458 |
| - Mars encounter (engine off/engine on) | 152/417 |

Note:
Approximate
Arrival
Date = February 28, 1974

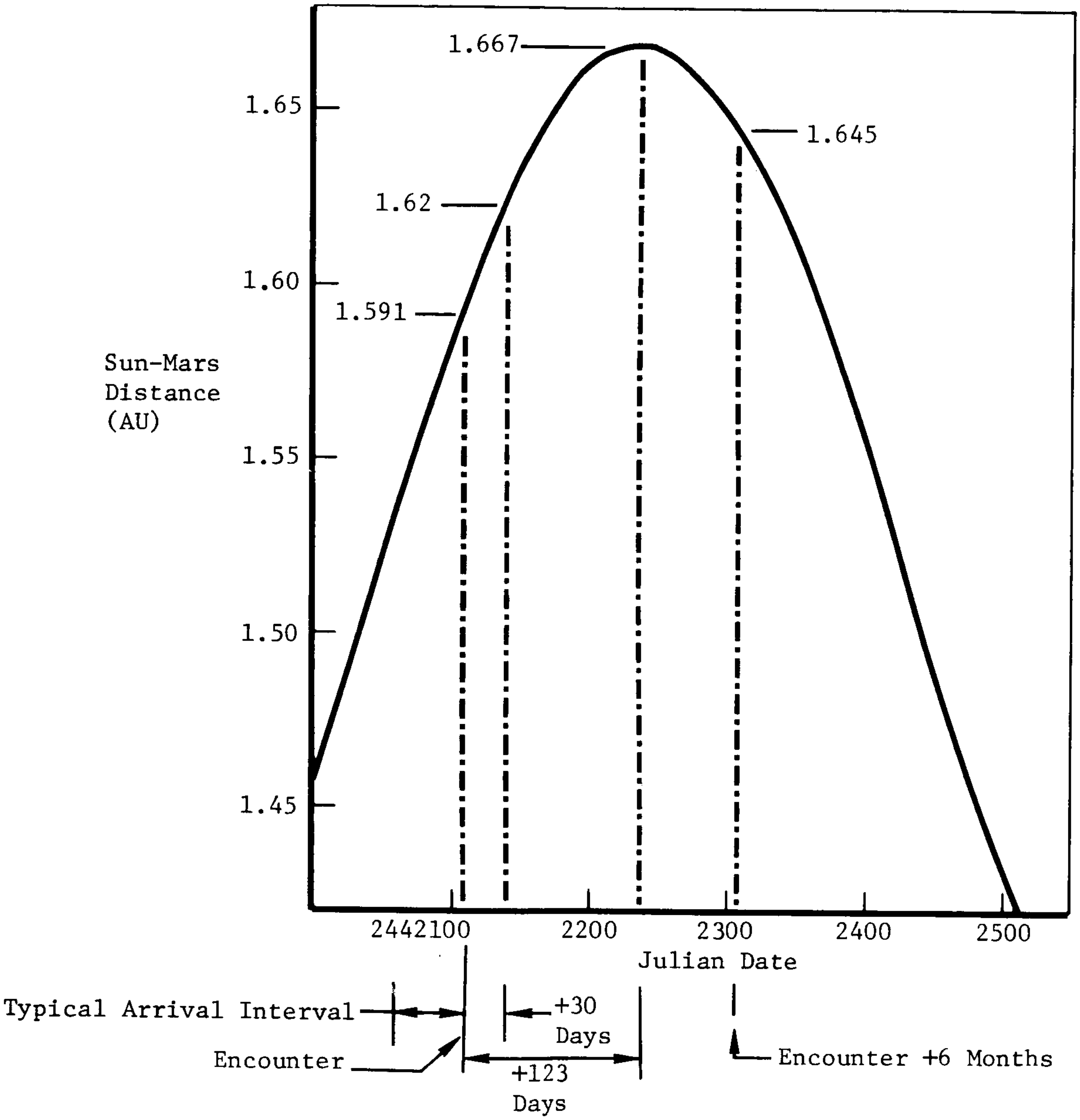

Figure 7.3-7: SUN-SPACECRAFT DISTANCE---MARS ORBIT

The electrical load breakdown to subsystems and flight modes is shown in Table 7.3-14. The loads are adequate to maintain a spacecraft in Mars orbit. The load totals are all under 300 watts except for engine burns. In Mars orbit, 41 watts is allocated to spacecraft science with an additional 10 watts for lander housekeeping. The latter is available from launch on. The communications loads include a 10-watt TWTA and two tape recorders. The transplanet loads and the orbital loads represent requirements to be satisfied by the solar array. The two delta velocity maneuvers and the orbit occult loads will be supplied by the battery.

### 7.3.3.2 Preliminary Design

The power subsystem consists of a solar array-battery system along with voltage control and charge control provisions. Power is supplied to the spacecraft over a total d.c. voltage range of 22 to 31 volts. During periods of on-Sun operation, a dissipative shunt regulator augmented with solar panel shorting logic maintains a nearly constant bus voltage of about 30.5 volts. During off-Sun operation, the battery supplies the necessary power over a slowly falling voltage (battery discharge characteristic) that will average approximately 24 volts. The power system block diagram is shown in Figure 7.3-8.

*Energy Source Control*---Photovoltaic energy sources have been the most commonly used type of spacecraft electrical power generation. The solar array (photovoltaic) size, weight, and minimum operating efficiency are determined for end-of-life degradation, maximum temperature, lowest solar energy, and largest load---all occurring simultaneously. During all other operating periods, excess power will be available from the solar array. This excess power is accommodated through a dissipative shunt regulator. This shunt regulator regulates the voltage available from the array and prevents high voltages from being applied to load equipment when the array is cold or the load is small. The solar array does not need protection because it can sustain open or short circuits. For this study an upper bus voltage regulation point of 30.5 ±0.5 volts was selected based on battery charge requirements at Mars.

The quantity of power available from the solar array between Earth and Mars rises to a peak of over twice that at Mars (Figure 7.3-9). To dissipate this excess energy would require a prohibitively large shunt regulator. Therefore, the shunt regulator is augmented by solar panel shorting logic. This logic shorts out solar panel circuits not required to maintain proper voltage regulation. Thus, a minimum capacity shunt regulator is adequate and has two advantages.

First, the shunt regulator can be designed to regulate within its tolerance band of 1 volt for a shunted power range of approximately 50 watts instead of 500 or 600 watts or more. Thus, the shunt regulator weight can be minimized. Second, if the excess electrical energy is never generated, it does not have to be disposed of thermally. Therefore, the spacecraft thermal problem is simplified.

## Table 7.3-14: ELECTRICAL LOAD ON POWER SUBSYSTEM COMPONENTS (Watts)

| | | Boost-Assist ΔV Maneuver | | Injection ΔV Maneuver | | Orbit | | Orbit |
|---|---|---|---|---|---|---|---|---|
| Subsystem | Transplanet | Engine Off | Engine Burn | Engine Off | Engine Burn | Lander Attached | Lander Released | Occult Period |
| Communications | | | | | | | | |
| TWTA | 54 | 54 | 54 | - | - | 54 | 54 | - |
| Tape Recorders | 25 | 12.5 | 12.5 | 25 | 25 | 12.5 | 25 | - |
| Comm w Lander | 8.5 | - | - | - | - | 8.5 | 8.5 | - |
| Comm w Earth | 33 | 33 | 33 | 33 | 33 | 33 | 33 | 33 |
| Attitude Control | | | | | | | | |
| Electronics & Heaters | 33.5 | 33.5 | 33.5 | 33.5 | 33.5 | 33.5 | 33.5 | 33.5 |
| Thrusters ◇ | | | 15 | | 15 | | | |
| Programmer | 25 | 25 | 25 | 25 | 25 | 25 | 25 | 25 |
| Propulsion | | | | | | | | |
| Actuators (2) | - | - | 150** | - | 150 | - | - | - |
| Engine Valves | - | - | 100** | - | 100 | - | - | - |
| Science | | | | | | | | |
| On Spacecraft | - | - | - | - | - | 41*** | 41 | - |
| On Lander | 10 | 10 | 10 | 10 | 10 | 10 | - | - |
| Power | | | | | | | | |
| Electronics | 25 | 25 | 25 | 25 | 25 | 25 | 25 | 25 |
| Battery Charge | 50 | - | - | - | - | 50 | 50 | - |
| Totals: Solar Array | 264 | - | - | - | - | 292 | 295 | - |
| Battery | - | 193 | 458 | 152 | 417 | - | - | 116.5 |

* 150 sec Max.

** 400 sec Max.

*** 3-w IR Spectrometer, G-w IR Radiometer, 32-w Vidicon

◇ 15 w for 50 m/sec, at Rate of 2.5 Times/Hour for Limit Cycle

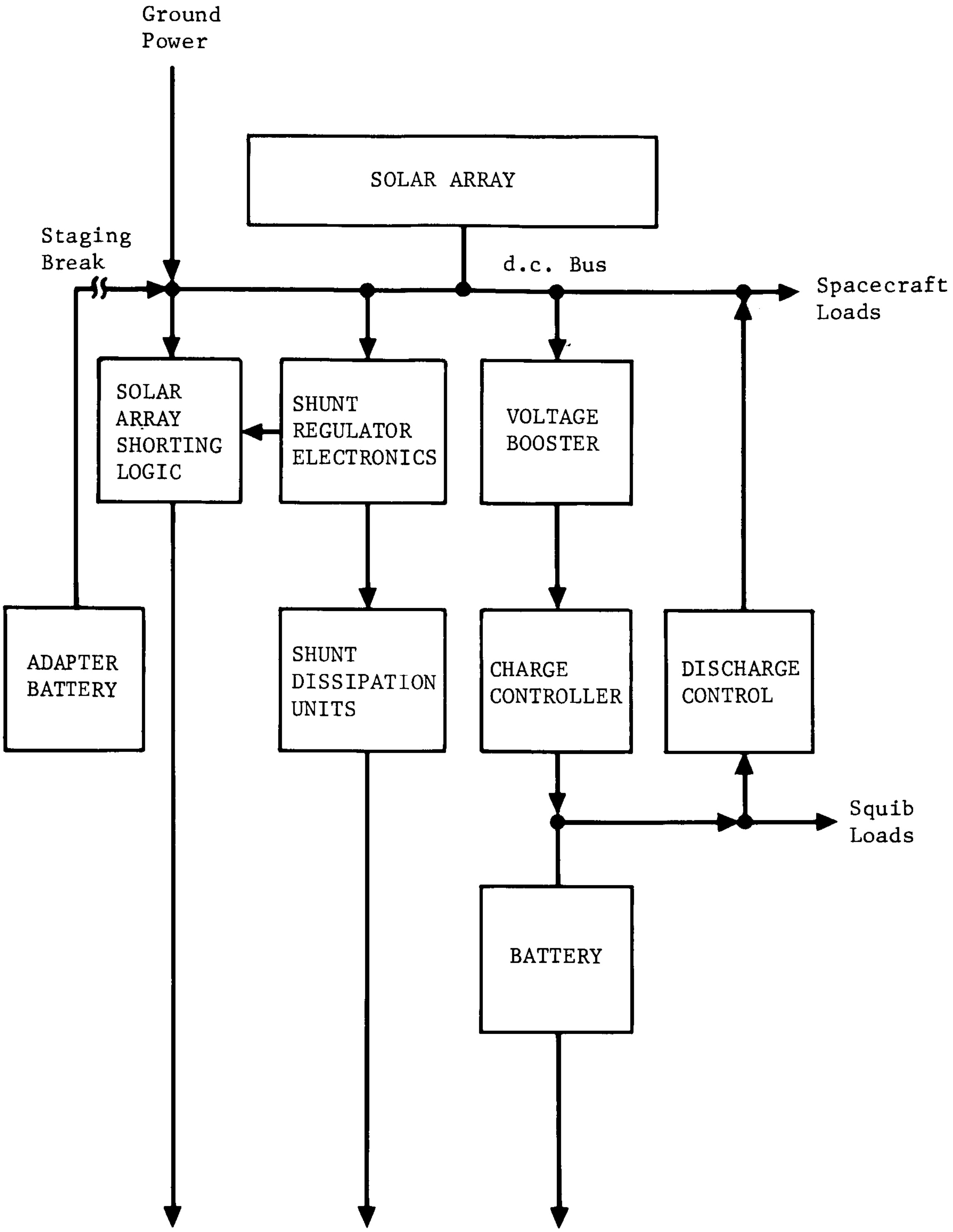
Ground Power
SOLAR ARRAY
Staging Break
d.c. Bus
Spacecraft Loads
SOLAR ARRAY SHORTING LOGIC
SHUNT REGULATOR ELECTRONICS
VOLTAGE BOOSTER
ADAPTER BATTERY
SHUNT DISSIPATION UNITS
CHARGE CONTROLLER
DISCHARGE CONTROL
Squib Loads
BATTERY

Figure 7.3-8: ELECTRICAL POWER BLOCK DIAGRAM

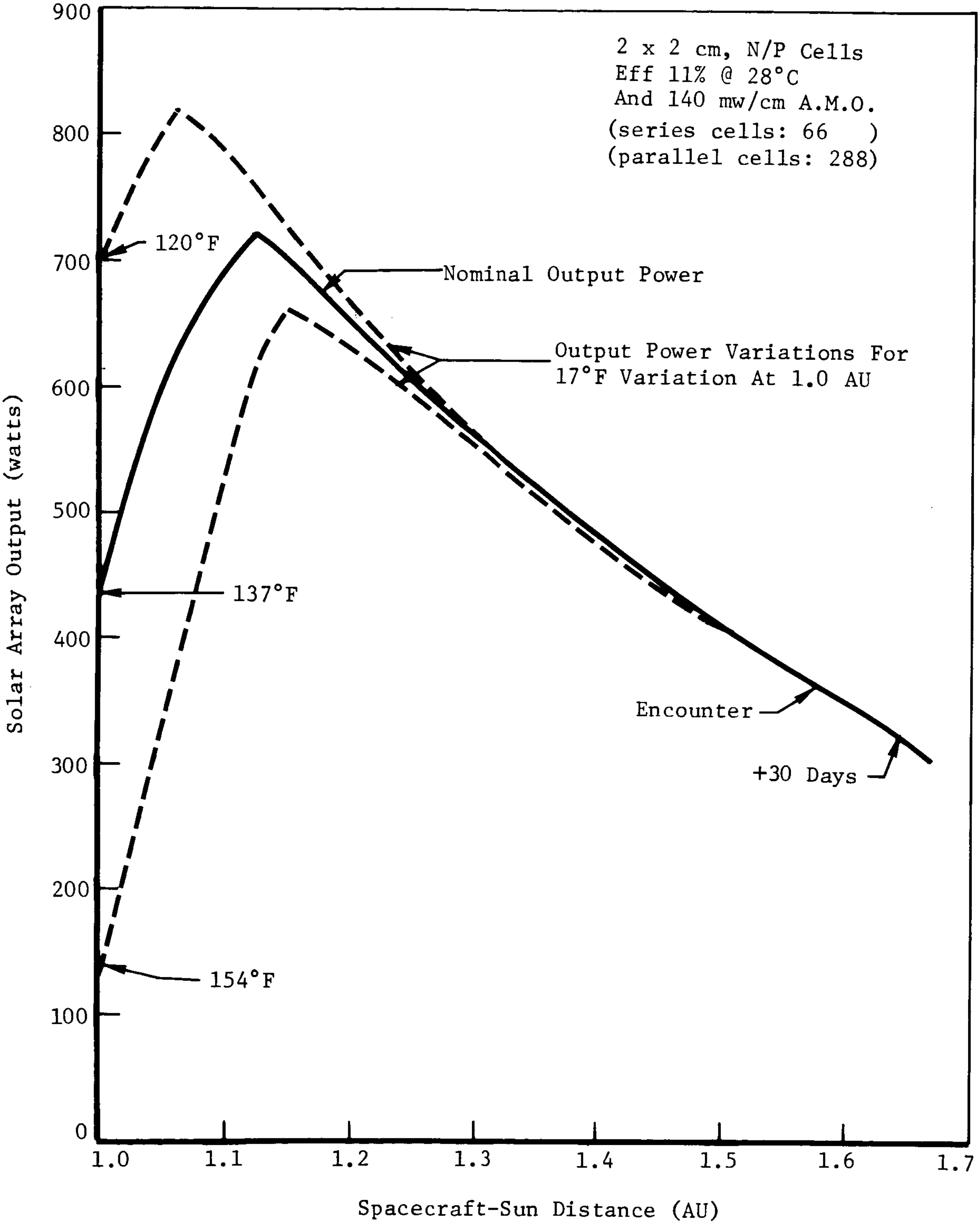

Figure 7.3-9: SOLAR ARRAY POWER OUTPUT TEMPERATURE EFFECTS AT EARTH AT 30.5 VOLTS ON BUS

*Energy Storage Control*---The energy storage medium used in this study is the nickel-cadmium battery. The trades shown in Table 7.3-15 justify the battery-type choice. The controls for energy storage regulate the energy input to the battery and indirectly control the energy out of the battery. Control of battery charge and discharge characteristics is a complex function. The battery charge and discharge rates directly affect battery efficiency, operating performance, and life. The addition of energy storage regulation and control equipment into the power subsystem contributes to equipment inefficiencies and reliability considerations. Therefore, this equipment is kept to a minimum. Battery charge and discharge characteristics and techniques are discussed fully in Reference 3.

The control parameters chosen for this study are current regulation with voltage and temperature limiting for charging. Discharge control is limited to an interruption of the discharge path when near Earth and charging. The latter is necessary because of a low bus voltage level when at and near Earth and is associated with the solar array design.

The solar array design, when optimized for Mars environment (AU distance and resultant temperature), will operate less efficiently at a low AU near Earth. This is illustrated in Figure 7.3-10. The 1 AU curve shows that a load of 100 watts or more could cause the solar array voltage to drop below the nominal 30.5 volts. The exact voltage point determination requires final electrical and thermal design of the solar array. This is beyond the scope of this study because it will not significantly impact weight. At the lesser voltage, the battery cannot be fully recharged without an intermediate voltage booster. During this same mode of operation when the battery charging voltage exceeds the bus voltage, the discharge control will open the battery discharge path.

During transplant flight to Mars when the solar array temperature drops sufficiently to permit all loads to be supplied at 30.5 volts, the voltage booster and discharge control will be bypassed and removed from the circuit. Thus, when power available at Mars is minimum, the inefficiencies of the two circuits do not exist.

*Weight Summation*---The total power subsystem weight summation is given in Table 7.3-16. The power control and conditioning weights are broken down into the performance functions. In addition, a separate weight called deployment mechanisms and supports is shown. This covers mounting bolts, nuts, and solar array deployment hardware.

## Table 7.3-15: CHOICE OF BATTERY TYPE (Ni-Cd VERSUS AG-Zn)

| Requirements on Battery | Ni-Cd | Ag-Zn |
|---|---|---|
| High Discharge Rate<br>Transplanet<br>6 to 8 amp<br>Orbit<br>4 to 5 amp | Well within performance range at C/2 | Acceptable for short life battery. Inconsistent with long life requirement. |
| Wet Life<br>Transplanet<br>7 Months<br>+<br>Orbit<br>6 Months | Well within performance range<br>1 year with no conditioning<br>3 years with conditioning | Reaching the state of the art. A long life battery plate separator design is in direct conflict with a plate separator designed for high current densities. May require temperature control to be kept cool during long term stands and then heated prior to each use. |
| Cycle Life<br>Estimate<br>100 cycles | Well within performance range<br>@ 40% DOD and 75°F cycle life is 1,000 to 3,000 cycles | Approaching state of the art<br>@ 40% DOD and 75°F cycle life estimate is 10 to 50 cycles<br>@ 20% DOD and 75°F cycle life may approach or exceed 100 cycles |
| Reliability | Actual numbers not available but will be similar to the cycle life margins | |
| Accessory Equipment | 1. Charge Controller<br>2. *Booster Regulator<br>3. *Discharge Control<br>Note: *Not required near and at Mars. Also upon final determination of bus voltage variation versus AU near Earth, Items 2 and 3 may not be required. Voltage variation with AU near Earth is a function of number of solar cells in series and their temperature excursions. That design detail is beyond the scope of this contract. | 1. Charge Controller<br>2. Booster Regulator<br>3. Discharge Control<br>Items 2 and 3 are necessary at Earth and at Mars because of the higher per cell charging voltage required by Ag-Zn batteries. |

## Table 7.3-15: CHOICE OF BATTERY TYPE (Ni-Cd VERSUS Ag-Zn) (Cont)

| Requirements on Battery | Ni-Cd | Ag-Zn | |
|---|---|---|---|
| Weight Comparison | | Orbital Mission | |
| | | 30 Day | 6 Month |
| Battery | 44.4 pounds | 17 pounds | 40 pounds |
| Booster Regulator | 4.0* pounds | 4 pounds | 4 pounds |
| Discharge Control | 4.0* pounds | 4 pounds | 4 pounds |
| Total | 44.4 pounds<br>or<br>52.4 pounds | 25 pounds | 48 pounds |
| *See note above | | | |
| Overcharge Capability | Good: Will accept continuous overcharge at C/10 or more depending on battery temperature. | Poor: Continuous overcharge requires special care. | |
| Battery Selection (For 6-month mission) | The Ni-Cd battery is selected with or without the booster regulator and discharge control being required. | The Ag-Zn battery inherent energy density advantage under short term use becomes insignificant and less reliable for a wet life of over one year, with the specified cycle life and discharge rates required. | |

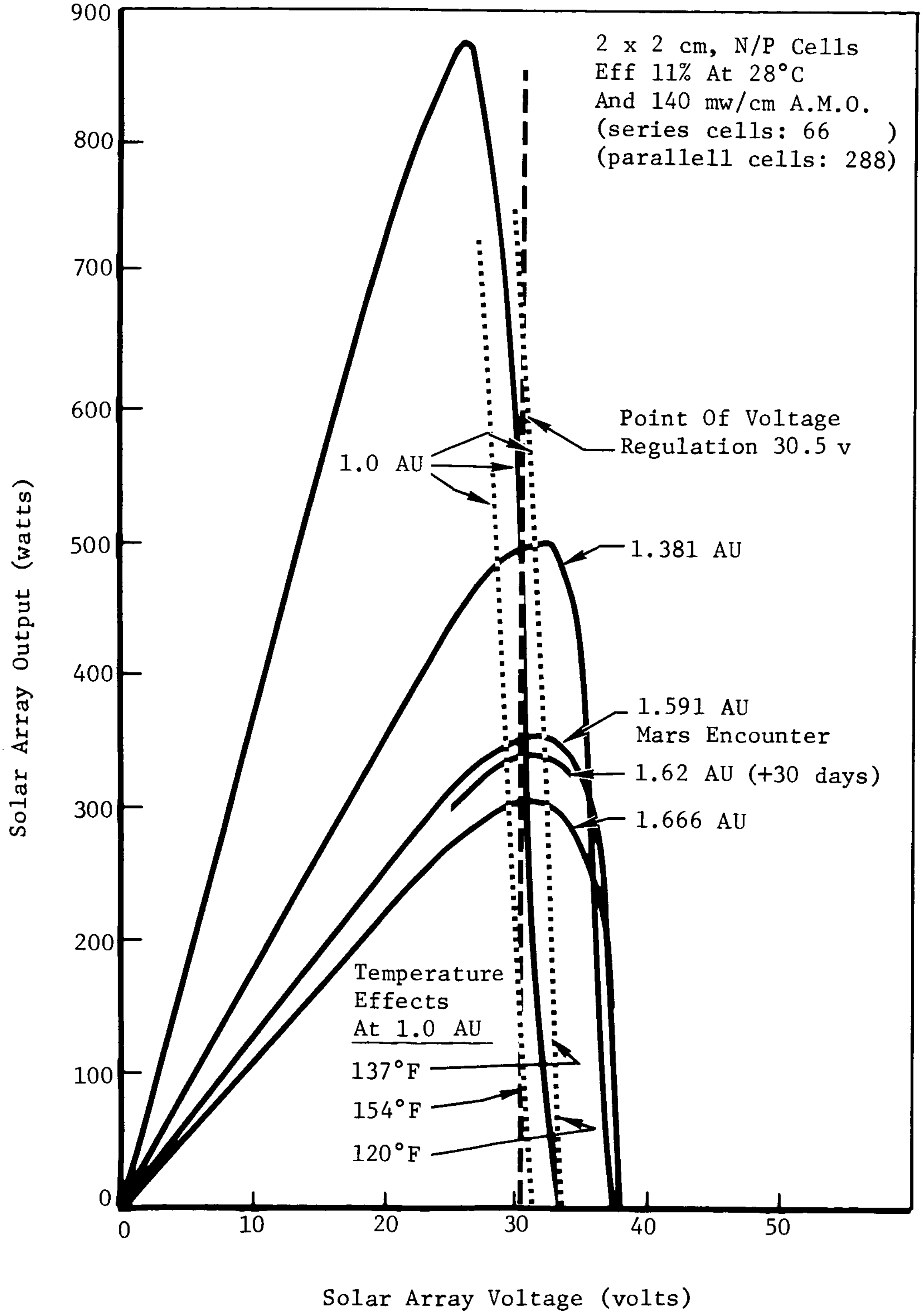

Figure 7.3-10: SOLAR ARRAY POWER OUTPUT

Table 7.3-16: POINT DESIGN---POWER SUBSYSTEM WEIGHT AND SIZE ESTIMATES

| | Weight (pounds) | Size (square feet) |
|---|---|---|
| Solar Array | 82.0 | 94.3 (net area used for cells) |
| Battery (Ni-Cd) | 44.4 | 102.4 (gross area) |
| Power Control and Distribution | | |
| Charge Controller | 5 | |
| Voltage Booster | 4 | |
| Discharge Control | 4 | |
| Shunt Regulator (2 each) | 6 | |
| Dissipation Unit | 6 | |
| T/M Signal Conditioning | 5 | |
| Solar Array Shorting Logic | 6 | |
| Weight Total | 162.4 | |
| Plus Deployment Mechanisms and Supports | 14 | |
| Total | 176.4 | |

### 7.3.3.3 Operation and Performance

The basic characteristics of the power subsystem major components are shown in Table 7.3-17. A general discussion of the subsystem performance must be done on a per-mission-phase basis. Therefore, the spacecraft mission is divided into five separate phases as follows:

1) Launch countdown to a few minutes prior to liftoff (about T-5 minutes);
2) T-5 minutes to Sun acquisition;
3) Sun acquisition to encounter (transplanet);
4) Encounter;
5) In orbit.

Table 7.3-17: POWER SUBSYSTEM COMPONENT CHARACTERISTICS

| Spacecraft Batteries | Solar Array | Power Control |
|---|---|---|
| Type: Nickel-Cadmium<br>Hermetically Sealed | Power Density:<br>3.26 w/ft$^2$ @ 1.66 AU | Voltage regulation by shunt dissipation augmented by solar panel shorting logic |
| Size: 20 a.h. | Weight:<br>0.80 lb/ft$^2$ | d.c. Power Bus:<br>22 to 31 volts |
| Discharge Voltage:<br>Nominal = 25 v (20 cells in series) | Solar Cells:<br>11% AMO<br>12 mil thick<br>N on P | |
| | Total power output:<br>308 watts | |

*Phase 1*---During Phase 1, all spacecraft electrical power will be supplied from a ground power source, except during internal power checks. These power checks will be scheduled to permit full battery recharge before launch. The external power supply will be capable of maintaining the spacecraft bus at 30.5 volts.

No details of the ground power supply are included herein because it is not relevant to the powered spacecraft weight.

*Phase 2*---At T-5 minutes, the external power source will be removed and the on-board spacecraft battery will take over. The spacecraft battery will continue to supply power to all spacecraft loads through boost, a short parking orbit, transtage (adapter) separation, powered spacecraft assist, and initial transplanet flight until Sun acquisition. This total time will be a maximum of about 1.5 hours (Table 7.3-13). During this interval, the bus voltage will slowly decay as it follows the battery discharge voltage characteristic. The minimum voltage should be above 24 volts. About 60% of the battery capacity will be used during this phase. This is a deviation from the 40% depth of discharge orbital design limit. At launch the nickel-cadmium battery is fresh (not degraded) and can easily sustain a 60% depth of discharge.

*Phase 3*---At Sun-acquisition, the solar array will supply power to the bus at a voltage that may be slightly less than 30.5 volts. The exact voltage will be a function of final series, i.e., parallel solar cell arrangement and cell temperatures. The voltage booster will raise the bus voltage to permit the battery to be charged fully. As transplanet flight continues and the spacecraft-Sun distance increases, the solar cell temperature will decrease. This will increase the solar array output voltage. When the bus voltage reaches 30.5 volts, two events may occur. First, the shunt regulator will commence to shunt excess solar array available energy and cause the bus voltage to remain below the prescribed maximum. Second, the booster regulator and the discharge control may be commanded off and shorted. From this point on the regulator and control are inert, having served their role. Also, their unreliability will be removed from the circuit.

During the transplanet trajectory, the solar array available energy will continue to increase to approach the combined capacity of the loads and shunt regulator. This available energy potential will peak at over 800 watts at about 1.1 AU. The solar panel shorting logic prevents the array power available from becoming too abundant by sequentially shorting the necessary solar array segments. Thus, actual power generated never exceeds the capacity of the loads plus the shunt regulator. Beyond 1.1 AU, the available array power will slowly decrease and the shorted array segments will be returned to useful service. During the initial Mars orbit, the solar array logic will continue to control the quantity of power produced to within the capacity of the shunt regulator. The array is sized to carry full load at the end of the 6-month orbital mission with all solar array segments on the line (none shorted).

*Phase 4*---During the encounter maneuver, the power subsystem can sustain the loads either with the solar array augmented by the battery during engine burn while on Sun, or off Sun with the battery supplying all loads. In the latter case, the energy removed from the battery will be about 17% of its capacity.

*Phase 5*---In orbit, the solar array will supply power continuously for the first 33 days. At this time a Sun occultation will be encountered each subsequent orbit. The Sun occultation duration will reach a maximum 82 days after encounter. From 110 days until the end of the 6-month orbital mission, the spacecraft will once again be in sunlight through its entire orbit. This maximum Sun occultation period was used to size the battery at a 40% depth of discharge. Figure 7.3-11 illustrates that a battery sized to carry the maximum orbital load at a 40% depth of discharge will also carry the launch load at a 60% depth of discharge. A 60% depth of discharge is permitted at launch and only a 40% maximum depth of discharge is permitted in Mars orbit for two reasons:

Prior To Initial Sun Acquisition

watt-hours = 280

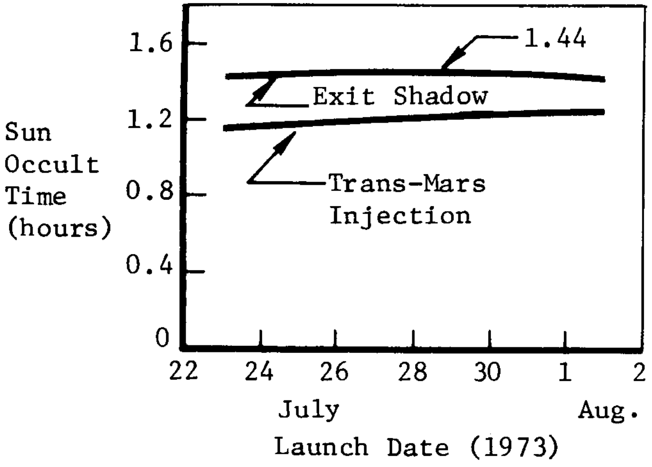

Mars Orbit

watt-hours = 191

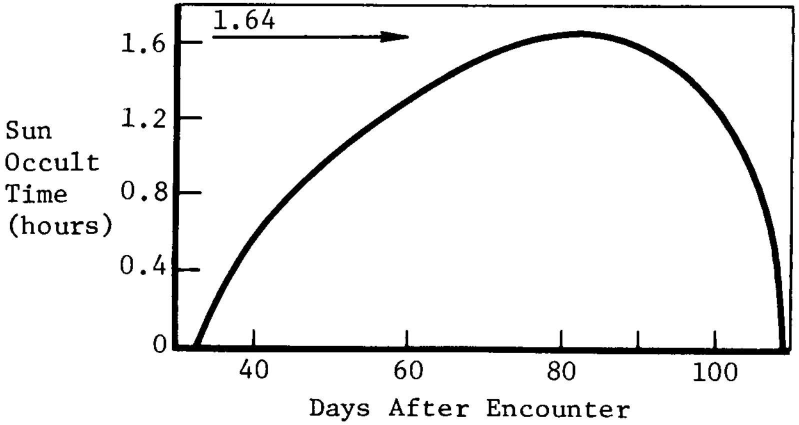

Once-Around Holding Orbit

watt-hours = 39

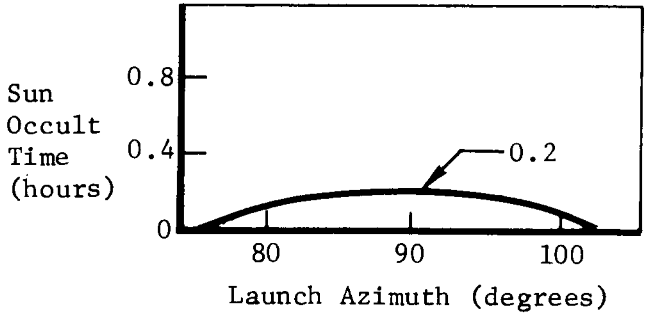

Using a 40% DOD For Mars Orbit And Allowing A 60% DOD For Single Discharge At Earth Makes Earth And Mars Battery Requirement Approximately The Same.

$$\text{Battery Capacity} = \frac{191\text{ w-hr}}{40\%} \simeq \frac{280\text{ w-hr}}{60\%}$$

$$477\text{ w-hr} \simeq 467\text{ w-hr}$$

Figure 7.3-11: BATTERY LOADS---ORBIT VERSUS LAUNCH

1) At launch the battery is new and has full or better rated capacity;

2) The launch load is a one-time discharge, where the orbital Sun occult loads are cyclic and follow 7 to 8 months of wet stand.

In addition, Figure 7-3.11 shows that the Earth-Sun occult encountered in a "once-around" holding orbit is minor and will not cause an impact on the power subsystem size.

### 7.3.4 Additional Subsystems

Propulsion, guidance and control, and electrical power subsystem descriptions and physical data have been discussed in detail in previous subsections. These subsystems represent approximately 55% of the orbiter less science dry inert weight. The remaining 45% of orbiter dry weight is associated with miscellaneous subsystems and orbiter structure.

Structural requirements are defined by specific load environment and geometry restraints and will be discussed only for a particular design configuration. The miscellaneous subsystems required are telecommunications, computing and sequencing, pyrotechnics, temperature control, electrical-electronic cabling, and science.

The intent of the Powered Spacecraft Study did not necessitate a detailed investigation of the miscellaneous subsystem requirements. Therefore, for the purposes of refined configuration analyses, the miscellaneous subsystem weight was defined through the use of weight prediction curves (Figures 7.3-12 and Figure 7.3-13) developed during the data collection study task. Individual subsystem weight was defined empirically as a function of pertinent design parameters or was fixed as a constant weight.

The components incorporated in these subsystems have been selected as a result of extensive system studies conducted by The Boeing Company during the Voyager NASA-funded studies and continuing independent studies on planetary systems.

*Telecommunication*---The telecommunication subsystem consists of radio, telemetry, data storage, and antenna components. Figures 7.3-12 and 7.3-13 provide a weight summary of these components. The radio subsystem selected includes a transponder, two 10-watt output TWT's, preamp, command detector, probe receiver, and supports. The telemetry system includes a multiplexer encoder, signal conditioner, and upper and lower subcarrier modulator. The data storage system weight of 37 pounds includes two recorders and data rate control, which provides for a total data transmittal of 3.5 x $10^9$ bits (equivalent) to Earth over a pericd of 10 days. This is based on a 24-hour Mars orbit with 20 hours of Earth viewing period.

Antenna weight is shown in Figure 7.3-13 as a function of diameter. Weight includes associated mechanism, stowage, and deployment. An additional weight of 12 pounds is provided for the omni and probe antennas. The refined configurations include a 6-foot-diameter high-gain antenna and a 3-foot-diameter capsule relay antenna.

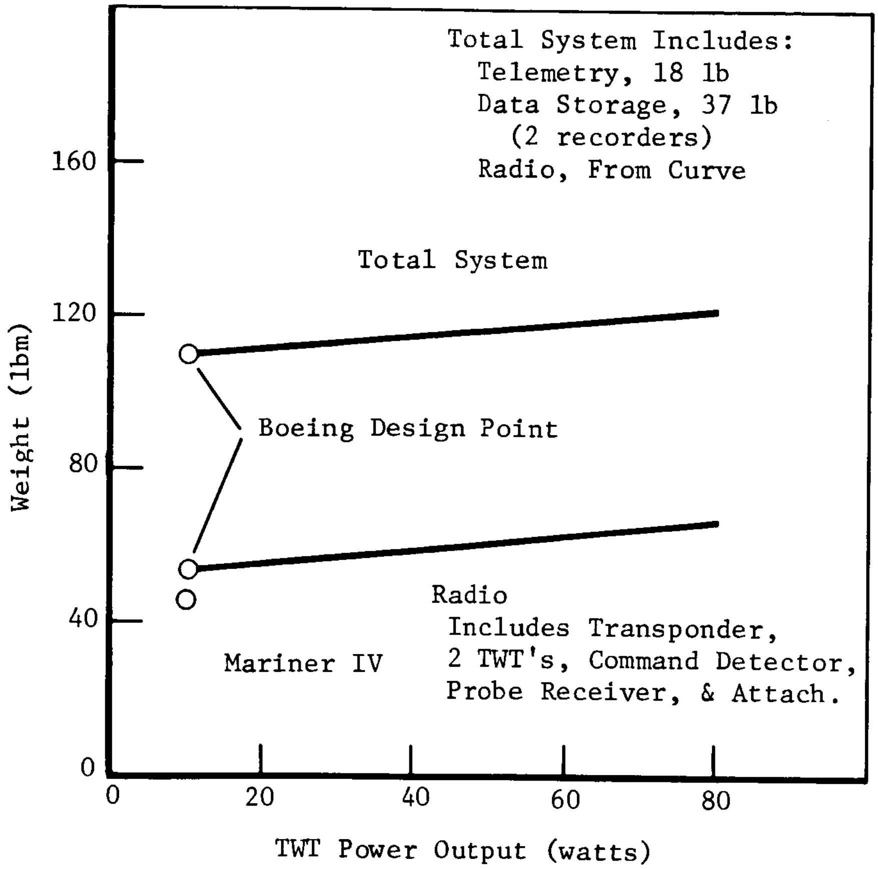

Figure 7.3-12: TELECOMMUNICATION SUBSYSTEM

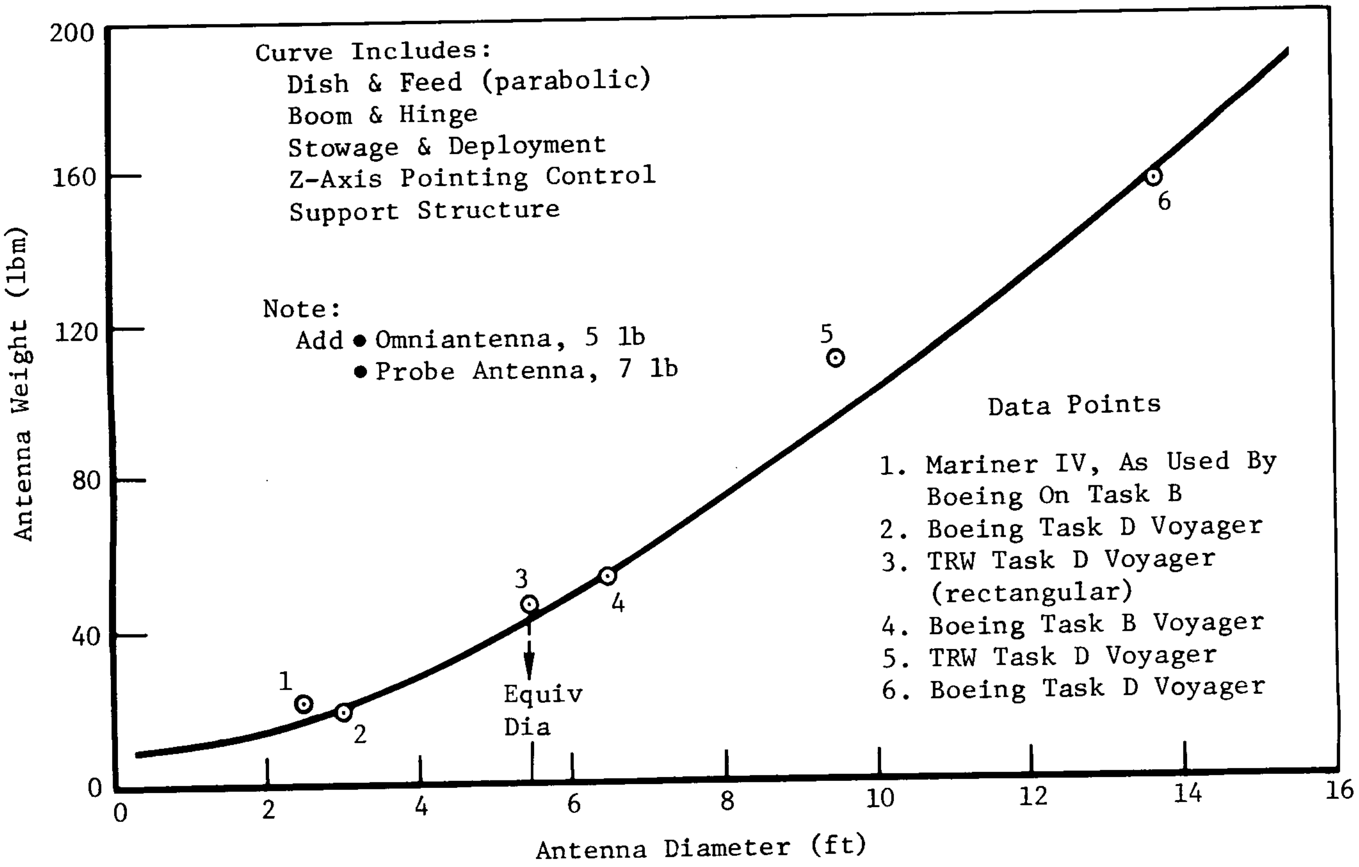

Figure 7.3-13: ANTENNA WEIGHT

*Computing and Sequencing and Pyrotechnic Subsystems*---Computing and sequencing weight of 15 pounds is provided for a single-thread system. This provides approximately 3 pounds for attitude control electronics and 12 pounds for a 120 input-output control function computer and sequencer. Computing and sequencing weight is carried with the guidance and control system in final configuration summary weight statements. Pyrotechnic subsystem weight of 13 pounds includes 9 pounds for pyrotechnic devices and 4 pounds for switching circuits. This provides for high current switching circuits for propulsion solenoid valves and antenna positioning drive.

*Temperature Control Subsystem*---Figure 7.3-14 provides the weight of the radiator plates as a function of the RF power output and the weight of passive control components as a function of spacecraft mass, prime power, environment, and size. The empirical data points are shown from which this curve was developed. Total system weight from these curves includes total equipment heat dissipation radiator plates, coatings, insulation, and louvers.

*Electrical-Electronic Cabling*---Figure 7.3-15 defines cabling weight as a function of total electrical-electronic component weight including science but excluding batteries and solar array.

*Science*---Final configuration analysis was based on a science weight of 200 pounds. This weight was estimated to be entirely electrical-electronic components when determining cable weight.

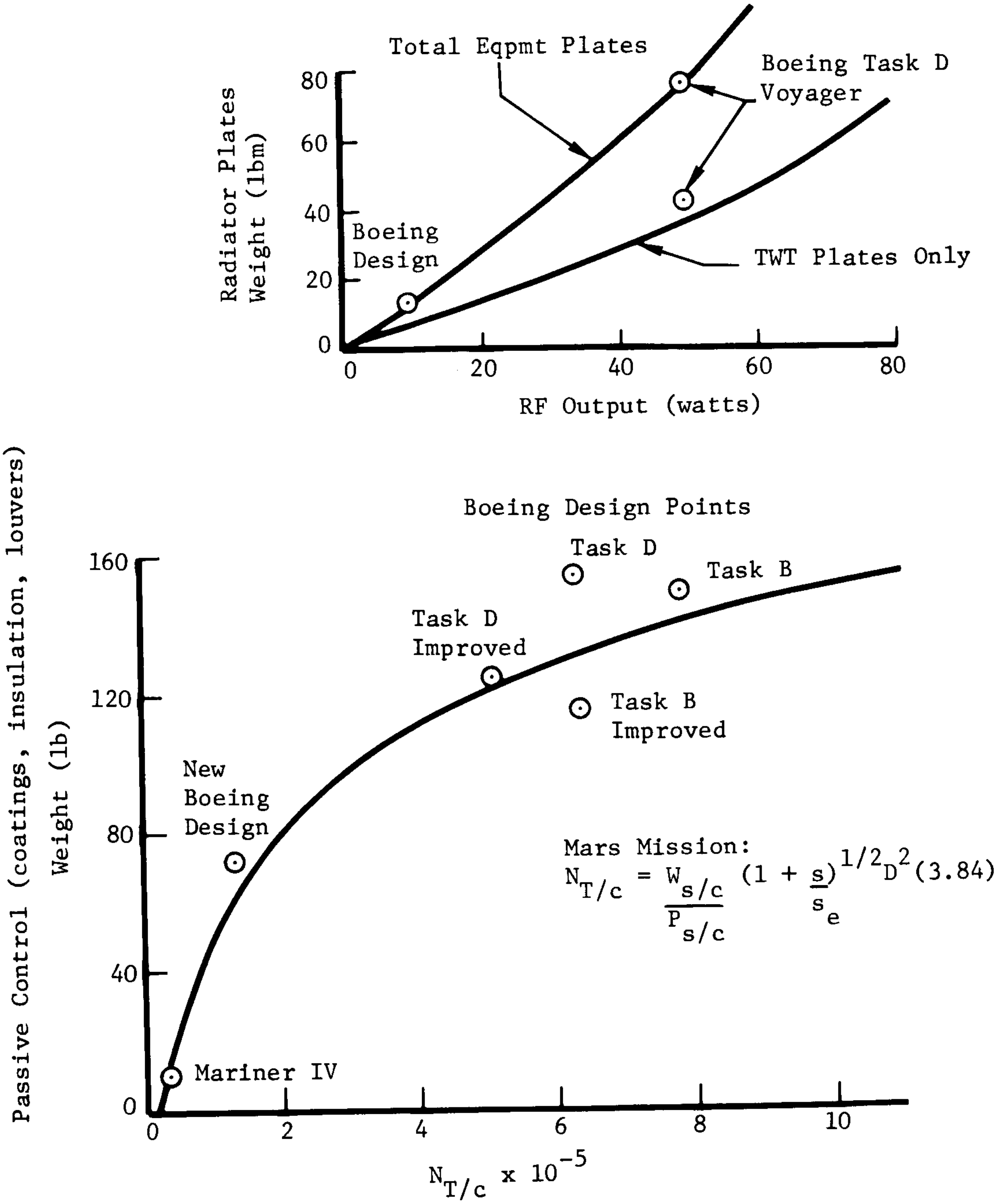

Mars Mission:

$$N_{T/c} = \frac{W_{s/c}}{P_{s/c}} \left(1 + \frac{s}{s_e}\right)^{1/2} D^2 (3.84)$$

$W_{s/c}$ = Useful In-Orbit Weight (pounds)
$P_{s/c}$ = Orbiter Prime Power (watts)
$S$ = Solar Constant At Mars (89 w/sq ft)
$S_e$ = Solar Constant At Earth
$D$ = Spacecraft Diameter (inches)

Figure 7.3-14: TEMPERATURE CONTROL

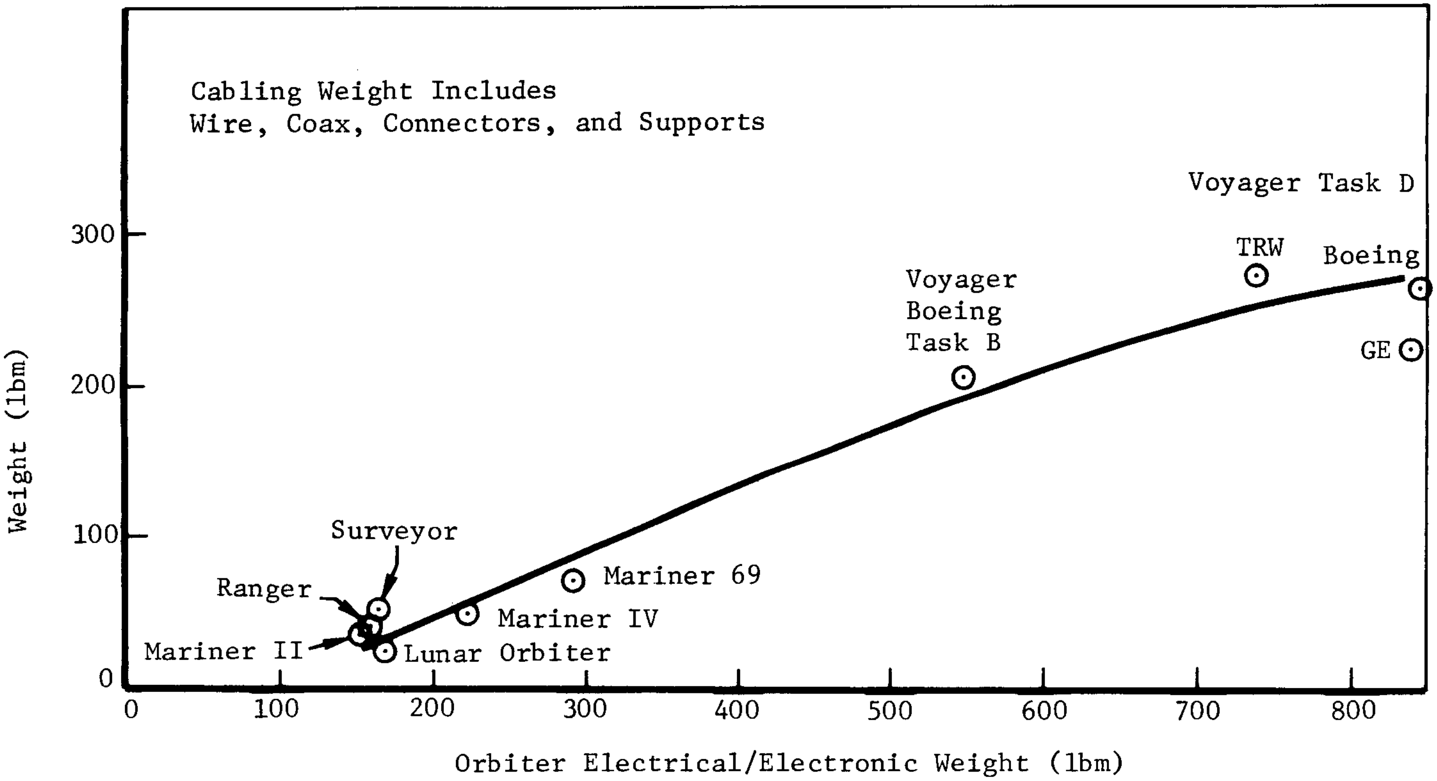

Electrical/Electronic Weight
Does Not Include Batteries
And Solar Array; Does Include
Science Equipment

Figure 7.3-15: CABLING WEIGHT

# APPENDIX A
# PERFORMANCE AND MISSION ANALYSIS

# APPENDIX A1
# AERODYNAMIC CHARACTERISTICS OF STAGES

The entry trajectory of each empty stage was integrated using the tumbling drag coefficients supplied by Aerospace Corporation (Reference 4). These drag coefficients are shown in Figures A1-1 through A1-3 for Core I, standardized payload fairing, and Core II, respectively. For the solid rocket motors (SRM), no such data were available. However, axial and normal force coefficients were available for various angles of attack at a Mach number of 3.71 (Figures A1-4 and A1-5). These data were converted to the drag coefficients shown in Figure A1-6, and an integrated average value of 5.76 was calculated. For other Mach numbers, the $C_D$ curve was assumed to be parallel to the Core I $C_D$ Mach number curve.

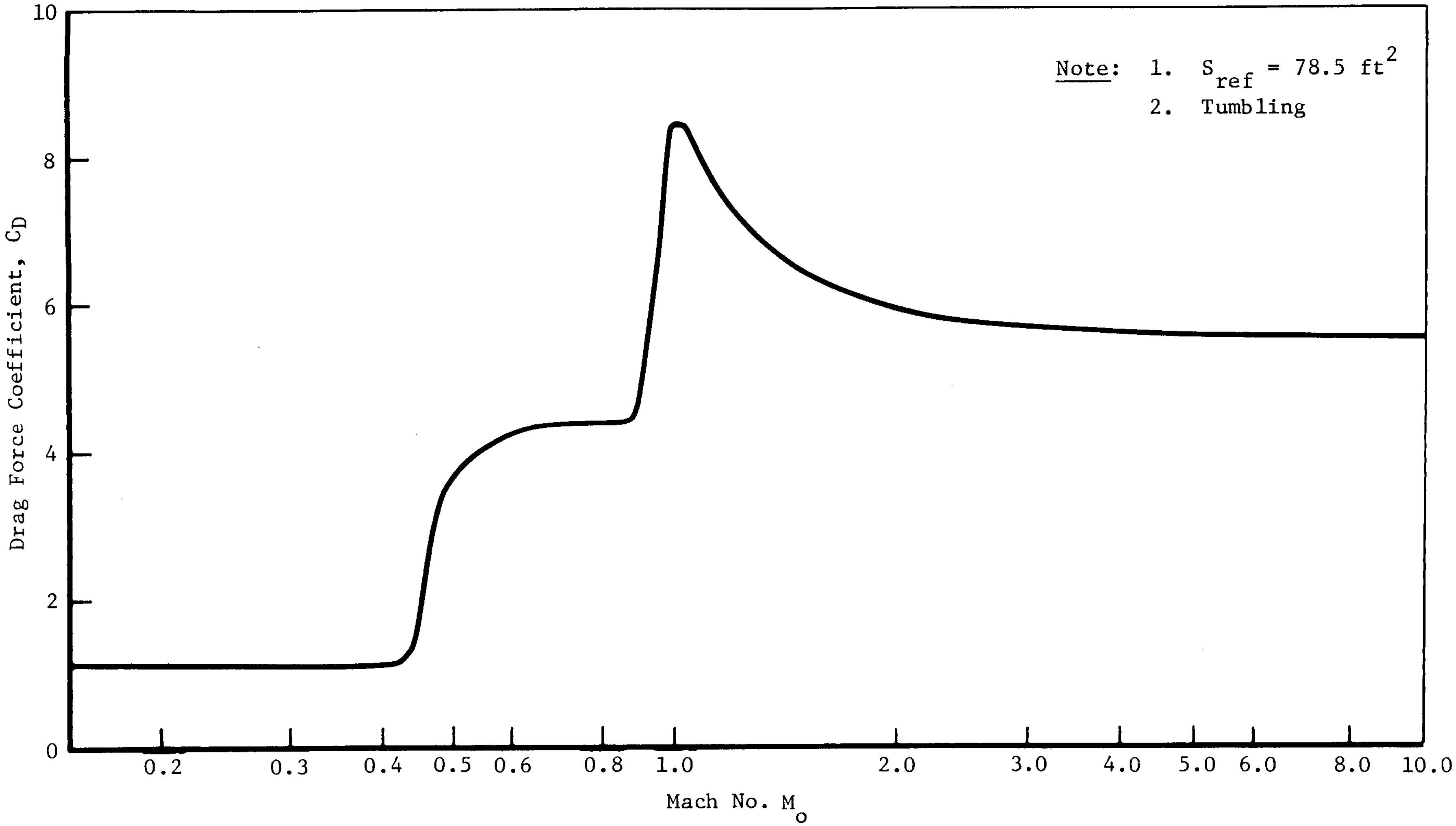

Note: 1. $S_{ref} = 78.5\ ft^2$
2. Tumbling

Figure A1-1: DRAG FORCE COEFFICIENT FOR STEP I (CORE I)

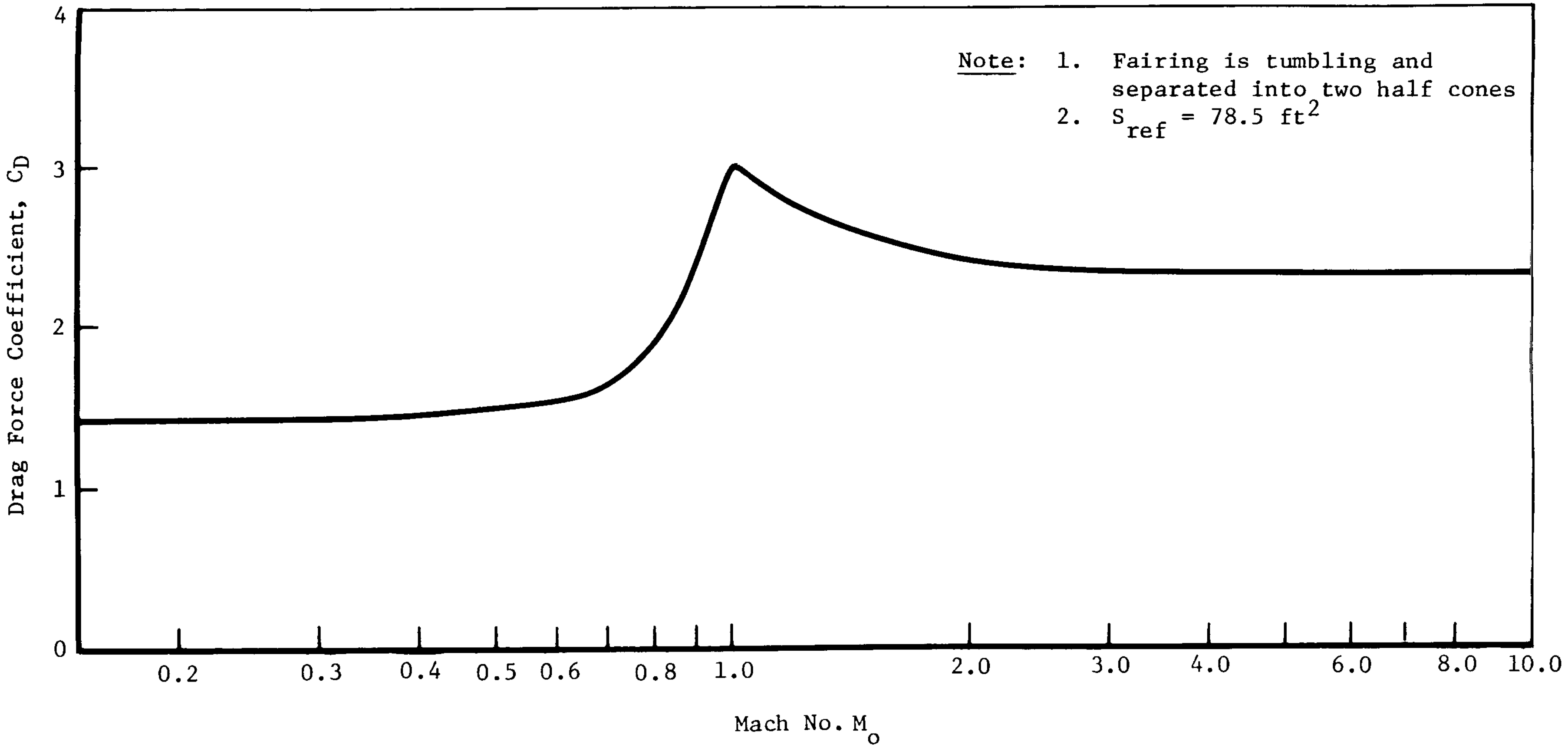

Figure A1-2: DRAG FORCE COEFFICIENT FOR STANDARDIZED PAYLOAD FAIRING

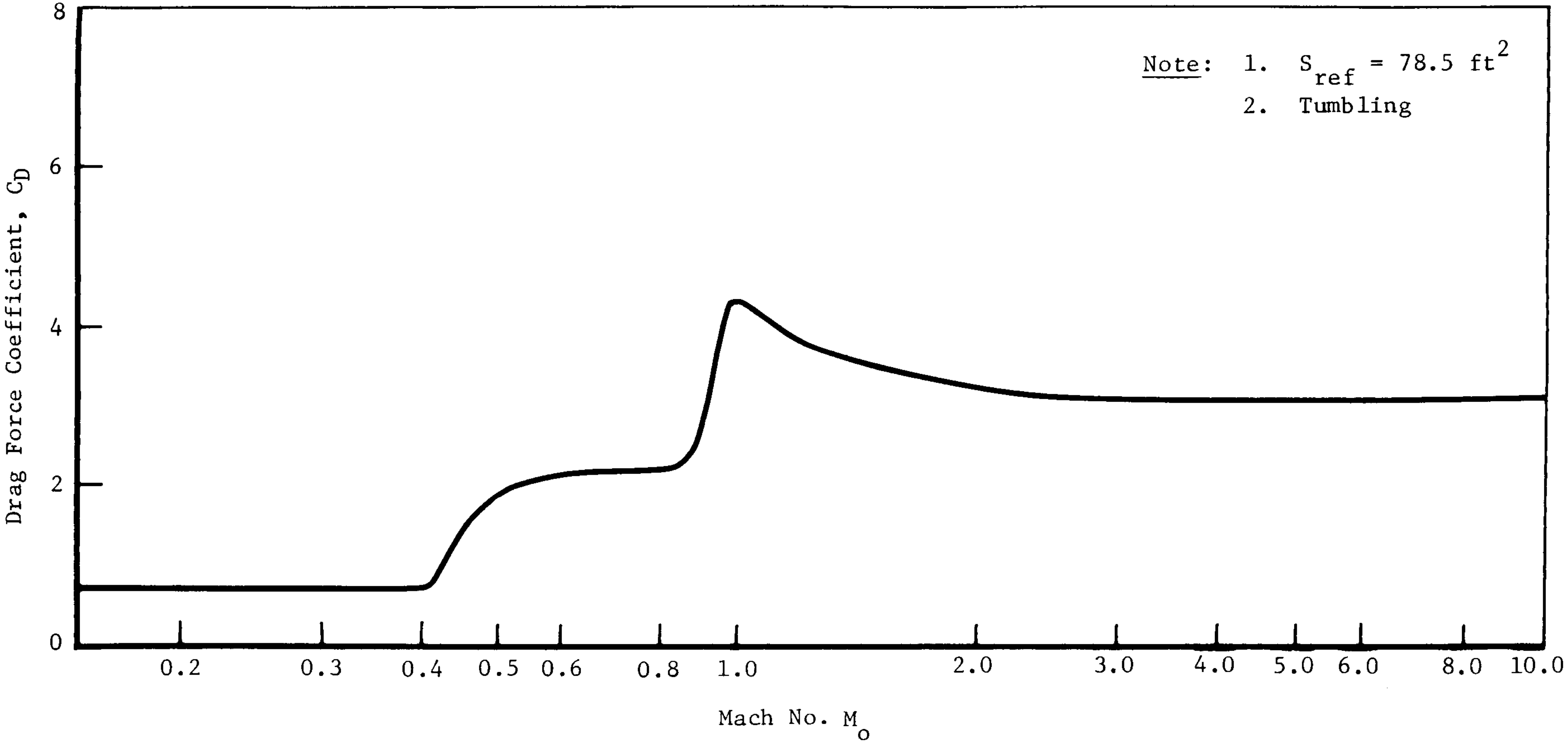

Figure A1-3: DRAG FORCE COEFFICIENT FOR STEP II (CORE II)

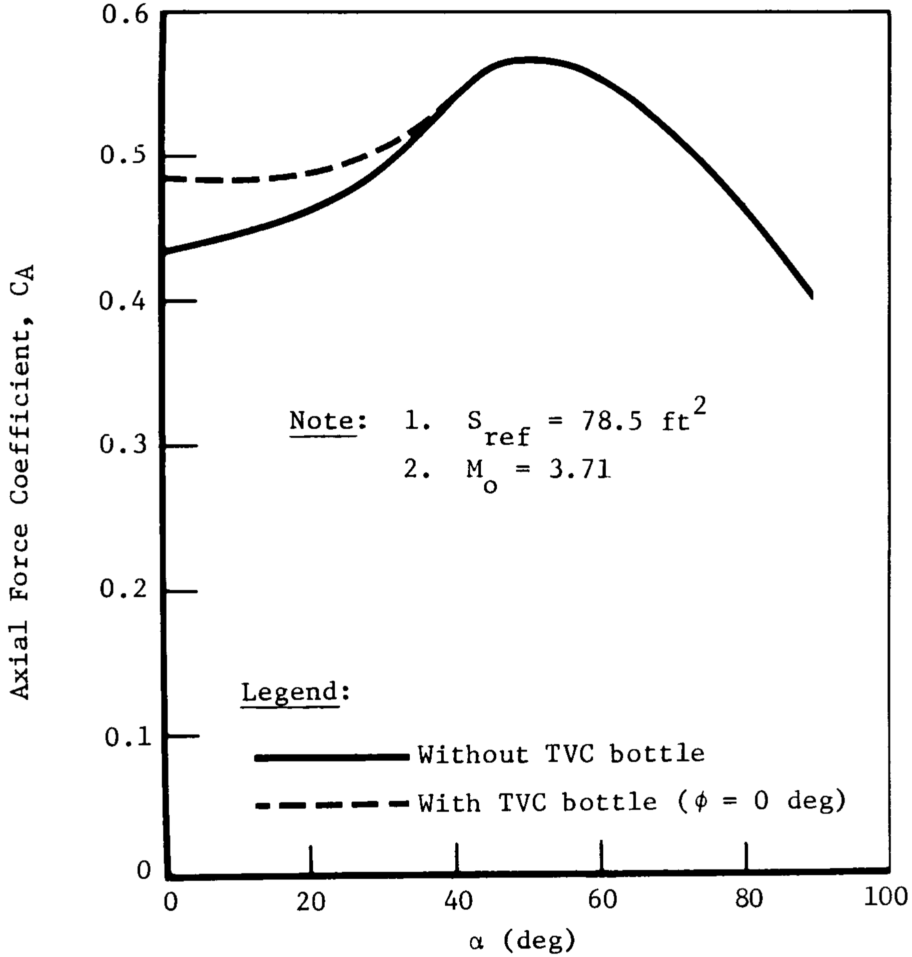

Figure A1-4: AXIAL FORCE COEFFICIENT FOR STEP 0 (SRM)

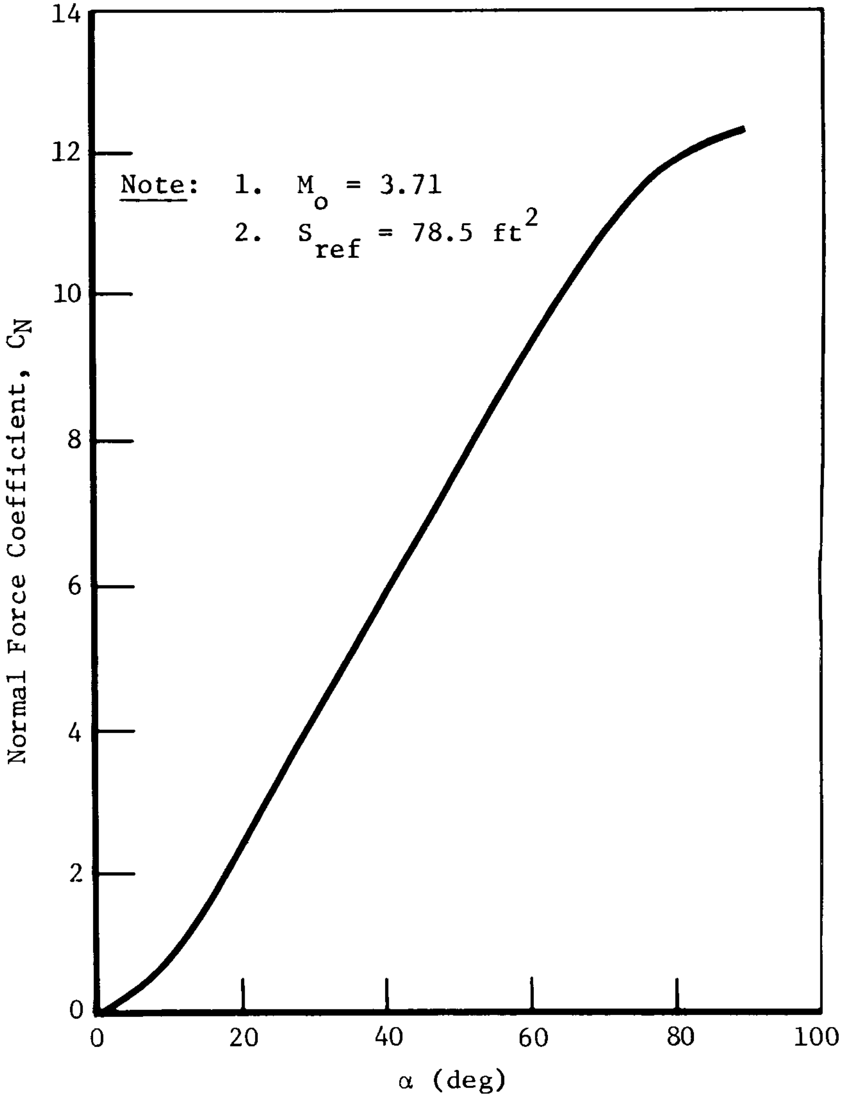

Figure A1-5: NORMAL FORCE COEFFICIENT FOR STEP 0 (SRM)

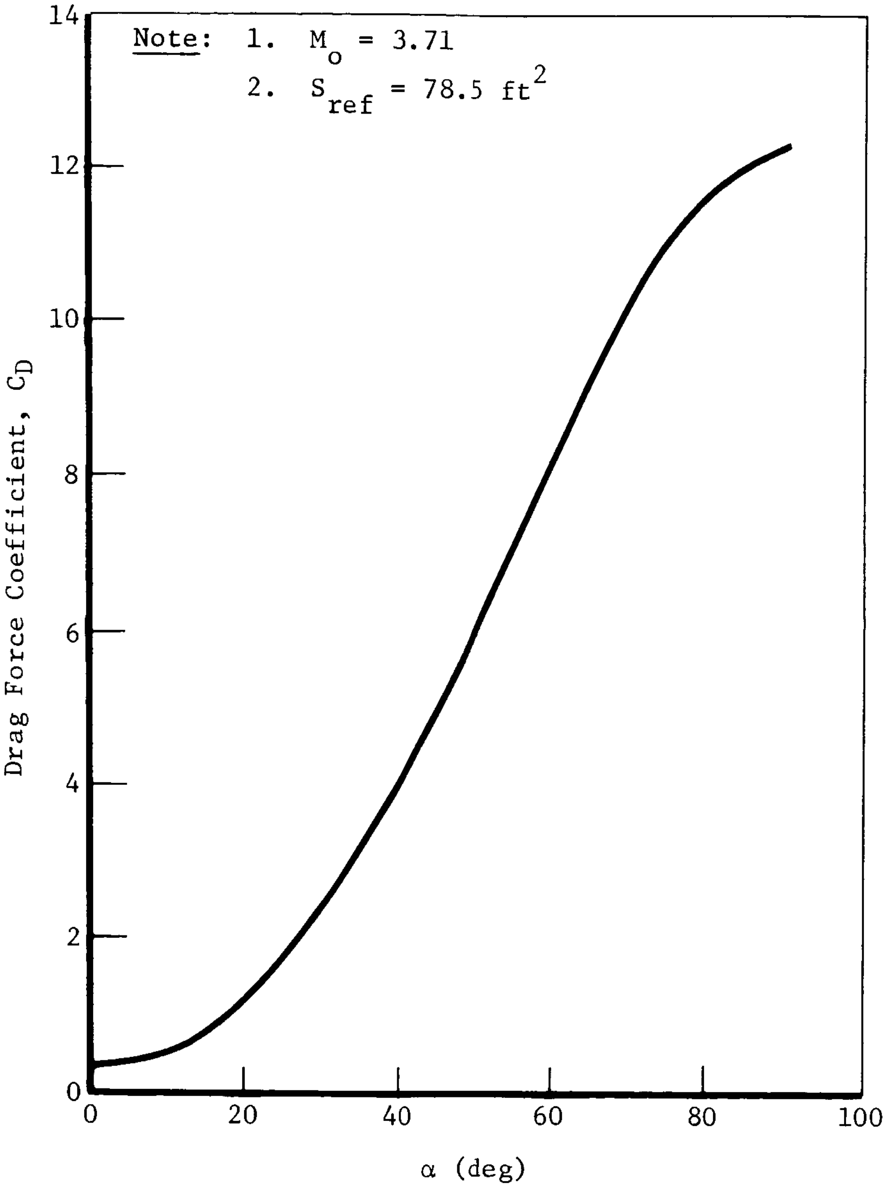

Figure A1-6: DRAG COEFFICIENT FOR STEP 0 (SRM)

# APPENDIX A2
# MISSION PARAMETER EFFECTS

*Fixed Arrival Day*---Selection of a fixed arrival date for a given interplanetary trajectory type and launch period length can involve a number of mission considerations. However, the primary one is the energy requirements for injecting onto the interplanetary trajectory and into Mars orbit. For a given arrival date, a range of consecutive launch dates that minimize the total mission velocity requirement can be identified. By definition, selection of the minimum velocity must be tempered by the requirement not to violate a maximum DLA of ± 36 degrees. Figure A2-1 illustrates the effect of arrival date on total $\Delta V$ for launch periods of 10, 20, and 30 days. These data represent 1973 Earth-Mars Type I interplanetary trajectories. Similar data for Type II trajectories are given in Figure A2-2. Mission $\Delta V$ is defined as the sum of the following velocity increments:

1) The difference between the velocity required at the desired $C_3$ level and satellite velocity at an altitude above Earth of 100 n mi;
2) The velocity required to inject into an orbit about Mars.

The data shown assumes a representative orbit with a periapsis altitude of 1,000 kilometers and an orbit period of 24.6 hours. The injection maneuver assumes a periapsis-to-periapsis transfer. Consideration of a different orbit size would change the magnitude of $\Delta V$, but it would not change the arrival date for minimum total $\Delta V$. The maximum values of $C_3$ and $V_\infty$ corresponding to the arrival date-launch period combinations of Figures A2-1 and A2-2 are given in Figures A2-3 and A2-4. Note that the minimum total velocity requirement does not correspond to minimum values of either $C_3$ and $V_\infty$.

*Variable Arrival Date*---The energy relationships, $C_3$ and $V_\infty$, corresponding to optimum launch-arrival day combinations for Type I Earth-Mars trajectories in 1973, are given in Figure A2-5. These optimum points were identified by selecting the arrival date that minimizes total mission $\Delta V$ for a given launch date.

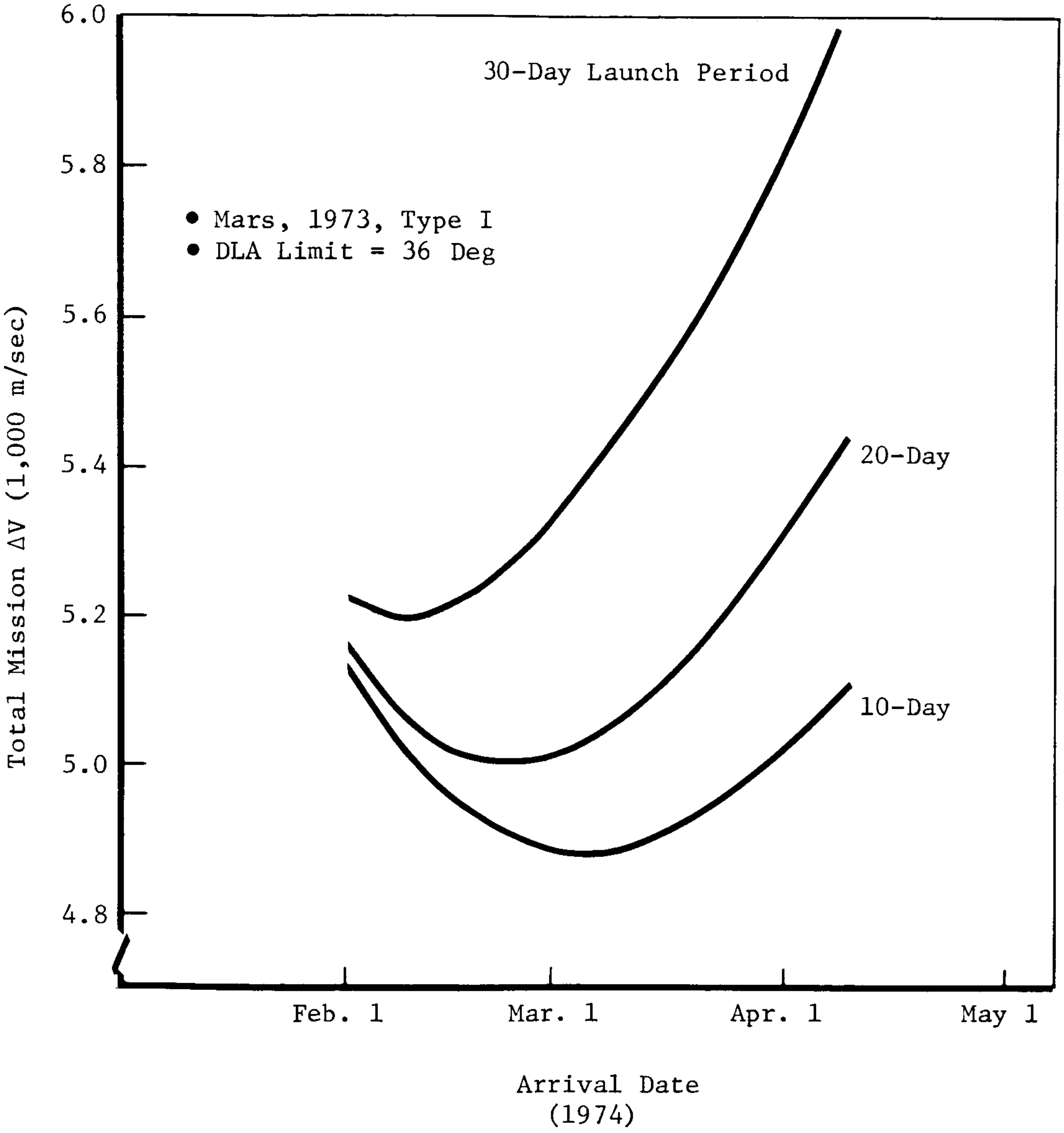

Figure A2-1: TOTAL MISSION ΔV REQUIREMENTS---TYPE I

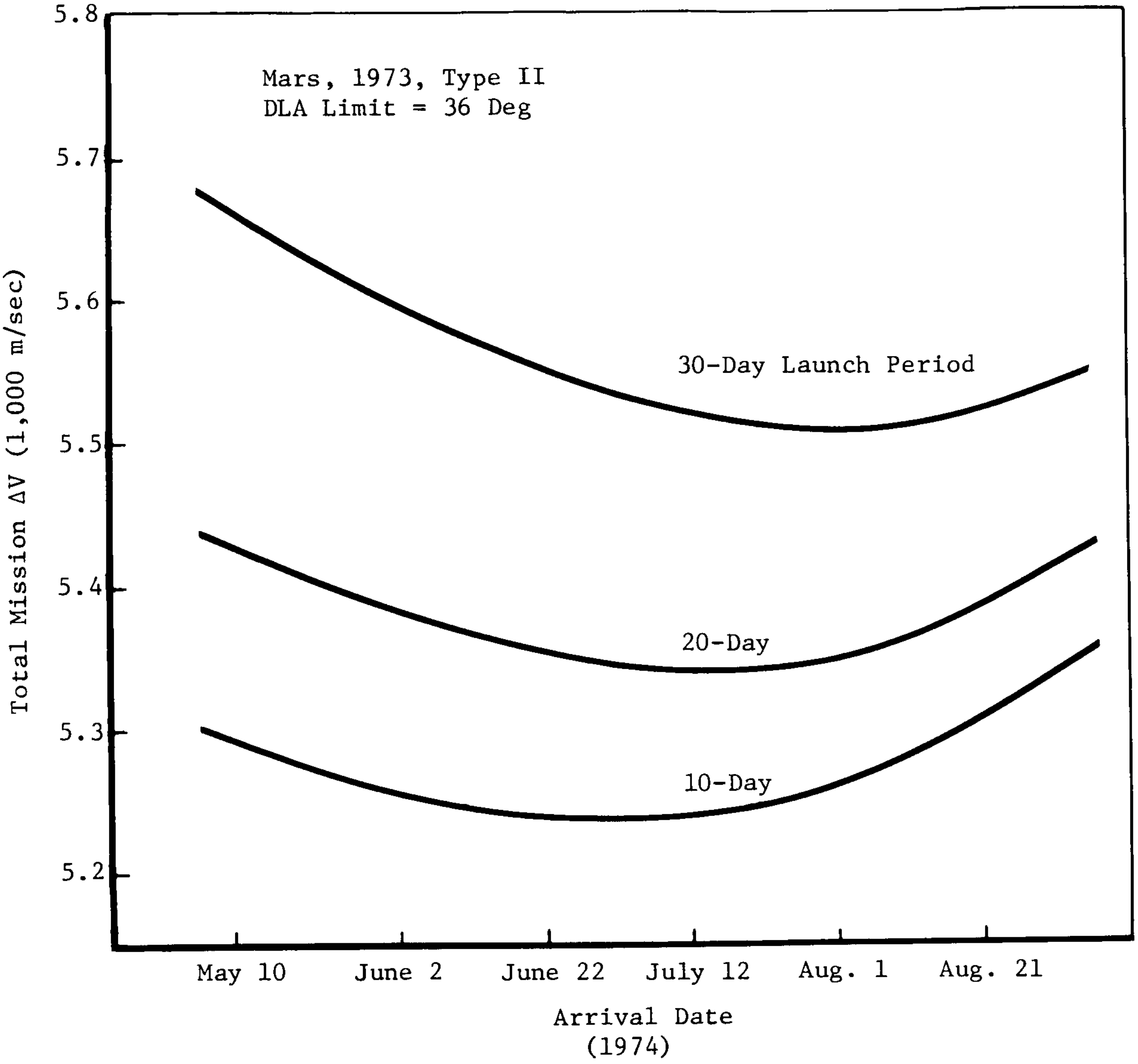

Figure A2-2: TOTAL MISSION ΔV REQUIREMENTS---TYPE II

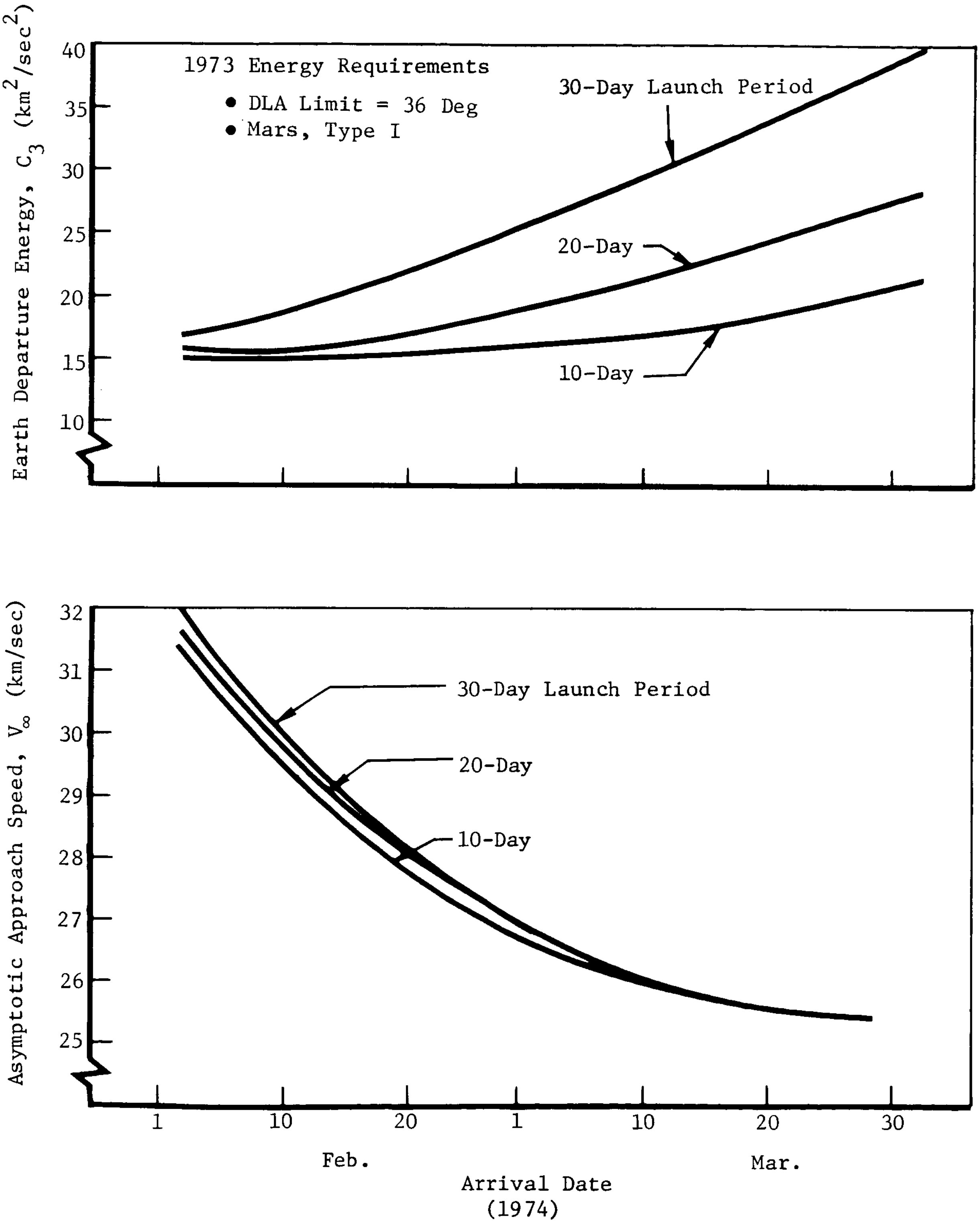

Figure A2-3: ENERGY RELATIONSHIPS---TYPE I

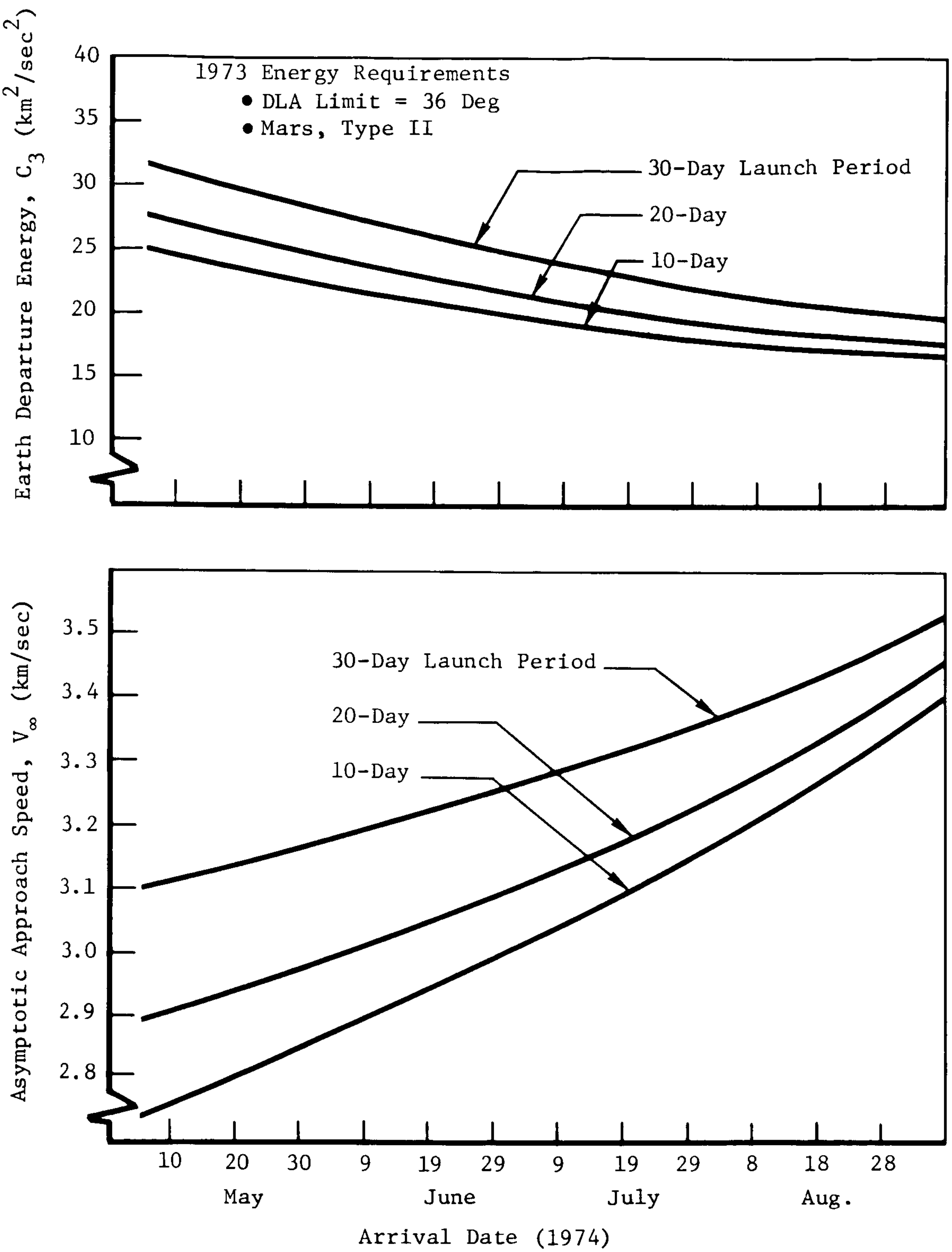

Figure A2-4: ENERGY RELATIONSHIPS---TYPE II

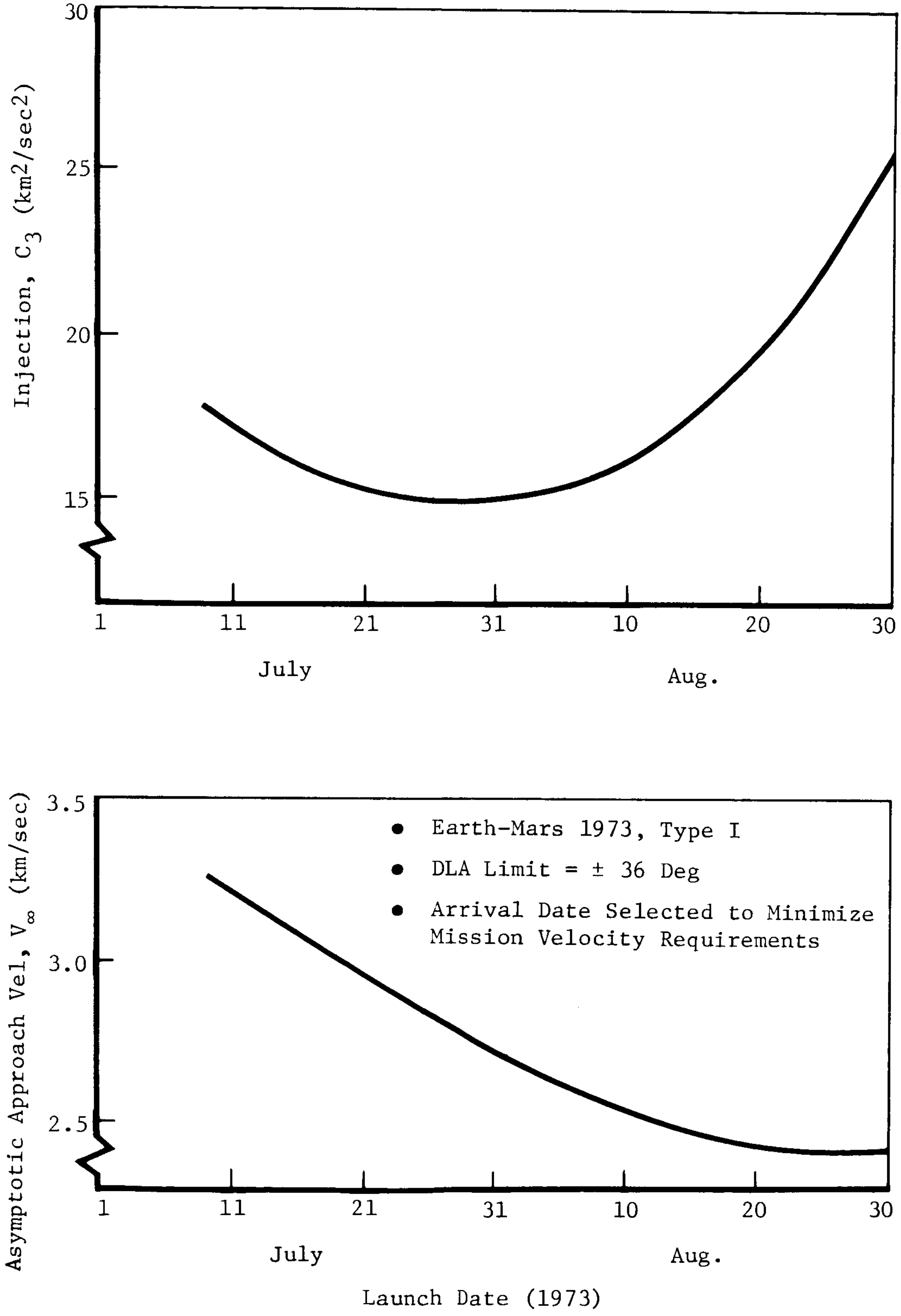

Figure A2-5: ENERGY RELATIONSHIPS---EARTH-MARS, 1973

# APPENDIX A-3
# SPACECRAFT SIZING PARAMETERS

The effect on useful in-orbit weight of a number of spacecraft sizing parameters is defined in this section. In addition, the corresponding spacecraft weights and propellant loads are given. The following parameters were considered.

1) Launch Vehicle---Titan IIIC and Titan IIID
2) Spacecraft Thrust---300, 900, 2,200, and 3,500 pounds
3) Post-Injection $\Delta V$---1, 1.5, and 2 km/sec
4) Injection $C_3$---12 through 28 $km^2/sec^2$
5) Specific Impulse (Thrust = 300 and 900 pounds)---290 seconds
6) Specific Impulse (Thrust = 2,200 and 3,500 pounds)---305 seconds

The basis for comparison between the study parameters is useful in-orbit weight. Calculation of this variable requires knowledge of launch vehicle performance and parametric weight information. These data must be combined with the mission velocity requirements to establish the useful in-orbit weight attainable with a given spacecraft size. The method of analysis is as follows.

1) Select a value for spacecraft-assist $\Delta V$. This is the amount of trans-Mars injection velocity contributed by the spacecraft.
2) Based on the desired $C_3$, calculate the inertial velocity required from the launch vehicle. The corresponding launch vehicle payload is obtained from the launch vehicle performance data in Section 5.1.1.
3) The spacecraft weight is obtained by deducting the weight of the adapter.

| Separated Spacecraft + Adapter Weight (lb) | Adapter Weight (lb) |
|---|---|
| 2,000 | 40 |
| 5,000 | 60 |
| 10,000 | 110 |
| 15,000 | 170 |
| 20,000 | 250 |
| 25,000 | 330 |

4) The amount of propellant required to provide the desired spacecraft-assist $\Delta V$ and post-injection $\Delta V$ is calculated.
5) The nonuseful weight corresponding to the required propellant is obtained from Section 5.2. (Important: See Section 5.2.1.)
6) Useful in-orbit weight is the amount remaining after the propellant and nonuseful weight are subtracted from the total spacecraft weight.

This procedure is followed for a number of values of spacecraft-assist $\Delta V$ to identify the maximum useful in-orbit weight attainable under a given set of weight and energy assumptions.

Two approaches to the determination of actual mission velocity requirements were considered in the parametric analysis. The first involved the assumption that all maneuvers performed after Earth parking orbit injection are impulsive. This results in solutions that become optimistic with decreasing thrust-to-weight ratio of the propulsion system. The second approach considered the effect of finite burn losses by actually integrating the trajectory for the spacecraft-assist maneuver. The velocity loss attributable to finite burning is defined as the difference between the actual $\Delta V$ required to increase the energy level of the spacecraft to the desired value and the corresponding impulsive velocity increment. Spacecraft ignition is assumed to take place at perigee of the elliptical orbit established by the launch vehicle. The spacecraft is held at a constant inertial attitude angle. This angle resulted from optimization techniques that minimized the $\Delta V$ required to achieve the desired energy. This method produces very realistic parametric results.

Figures A3-1 through A3-4 illustrate the useful in-orbit weights attainable with the Titan IIIC launch vehicle for various values of spacecraft thrust and post-injection $\Delta V$. The corresponding data for Titan IIID is given in Figures A3-5 through A3-8.

The relative spacecraft sizes required for Titan IIIC and Titan IIID are illustrated in Figure A3-9. This weight is the fully loaded weight of the spacecraft after the adapter has been jettisoned. Figures A3-10 through A3-15 present the total spacecraft propellant load required to perform the complete mission. This weight includes the 3.75% reserve propellant allowance.

The propellant requirements for the spacecraft-assist maneuver only are given in Figures A3-16 and A3-17. The propellant weight shown does not have any provision for reserves. It is simply the amount of propellant that must be expended to provide the energy change required to achieve the desired $C_3$ level. These data are all based on an injection of $C_3$ of 16.139 $km^2/sec^2$ as defined in Section 5.3.1. The effect of variations in $C_3$ is illustrated in Figures A3-18 through A3-25 for Titan IIIC only and a spacecraft thrust level of 3,500 pounds.

Parametric useful in-orbit weight envelopes for Titan IIIC and IIID are given in Figures A3-26 and A3-27. The constant post-injection $\Delta V$ loci represent the envelope of a family of spacecraft-assist $\Delta V$---useful in-orbit weight curves at various thrust levels. The constant thrust lines are the loci of the tangent points between the envelope and the family of constant thrust curves. These curves illustrate the maximum useful in-orbit weight attainable at a given spacecraft-assist $\Delta V$. Note that these curves are based on a constant specific impulse of 305 seconds. This deviates from the value of 290 seconds used previously for the 300- and 900-pound-thrust propulsion systems.

To aid in the interpretation of the parametric performance charts, the following example problems were considered.

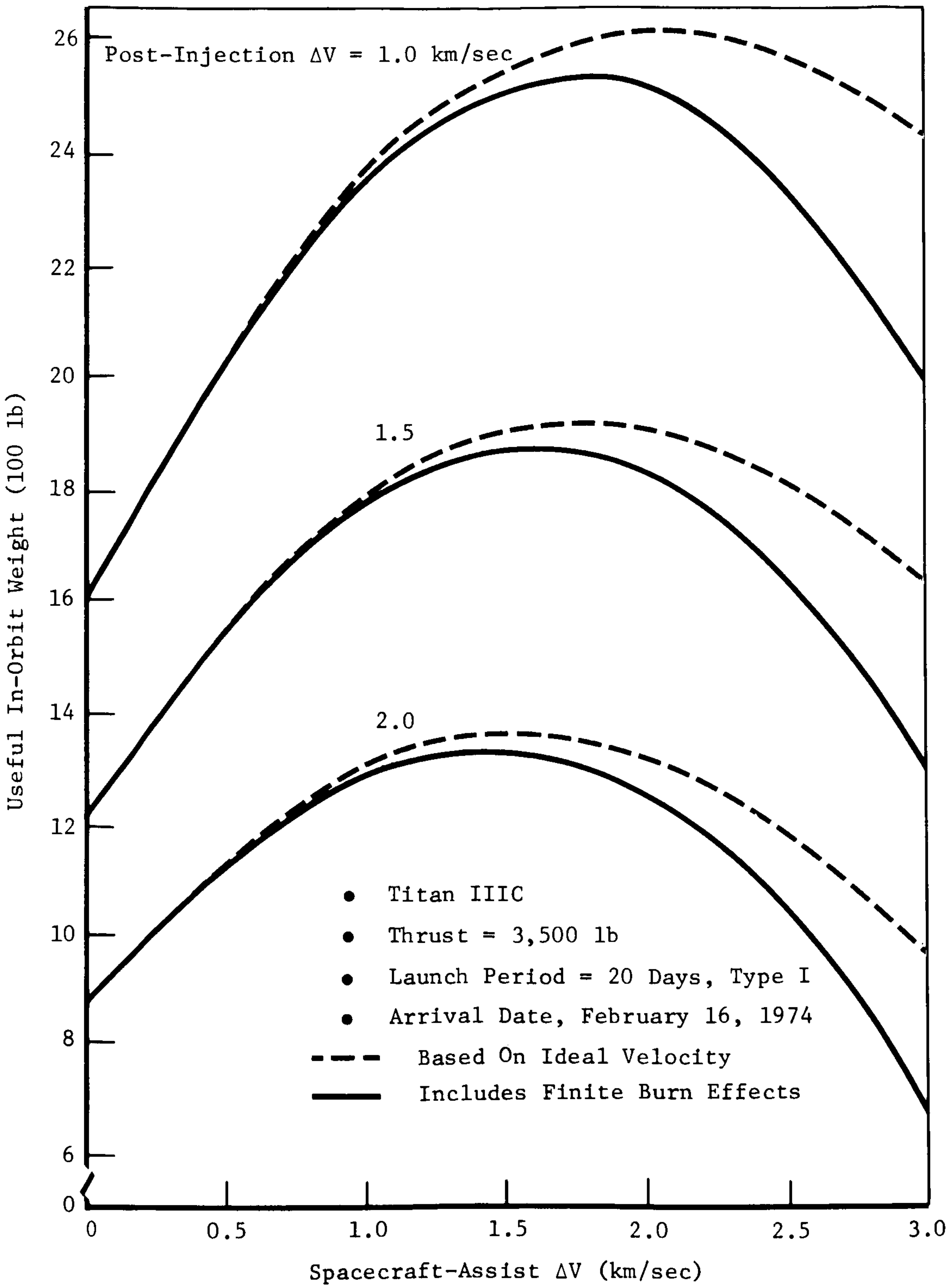

Figure A3-1: EFFECT OF POST-INJECTION ΔV ON USEFUL IN-ORBIT WEIGHT---SPACECRAFT THRUST---3,500-LB TITAN IIIC

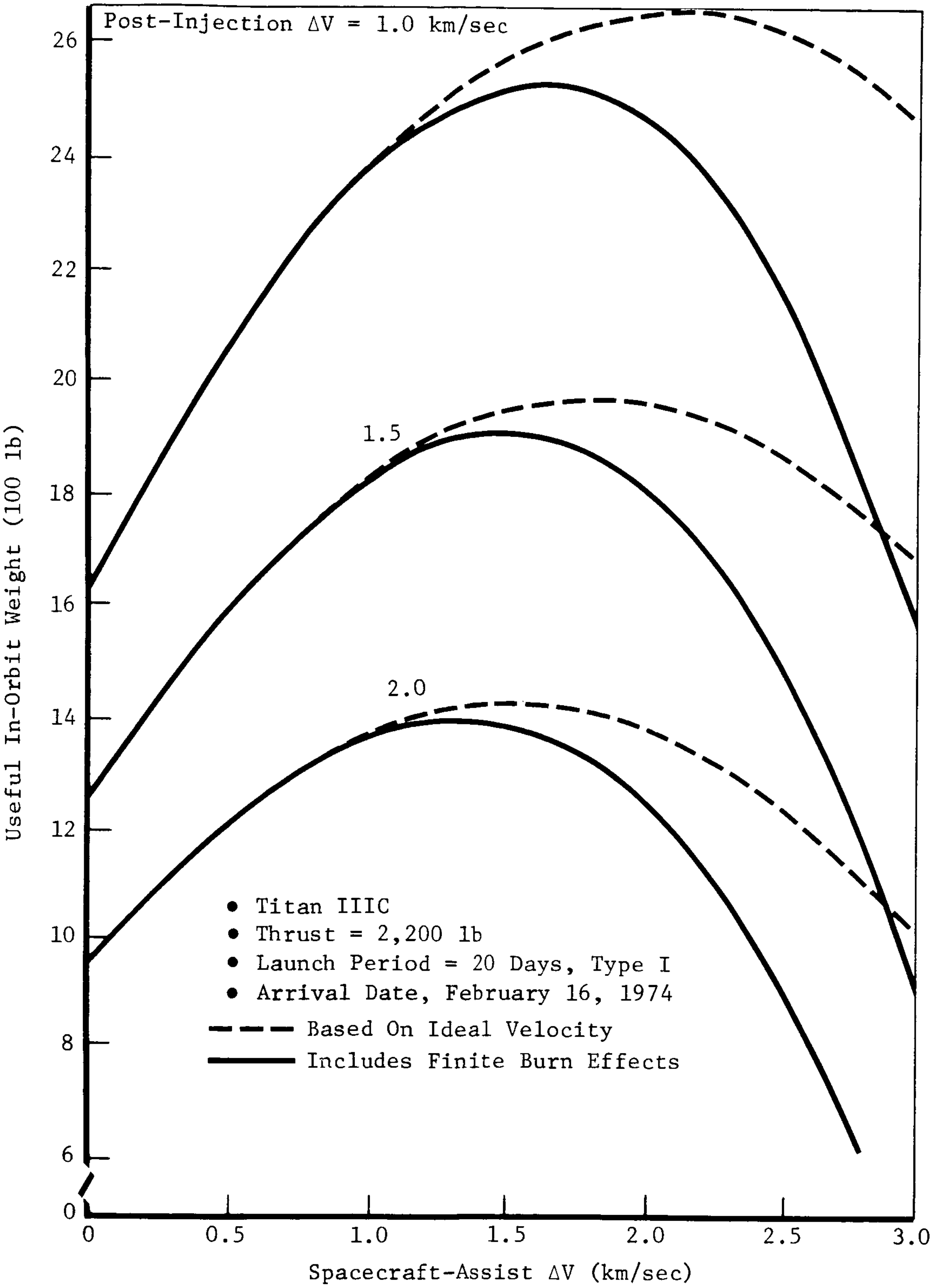

Figure A3-2: EFFECT OF POST-INJECTION ΔV ON USEFUL IN-ORBIT WEIGHT---SPACECRAFT THRUST---2,200-LB TITAN IIIC

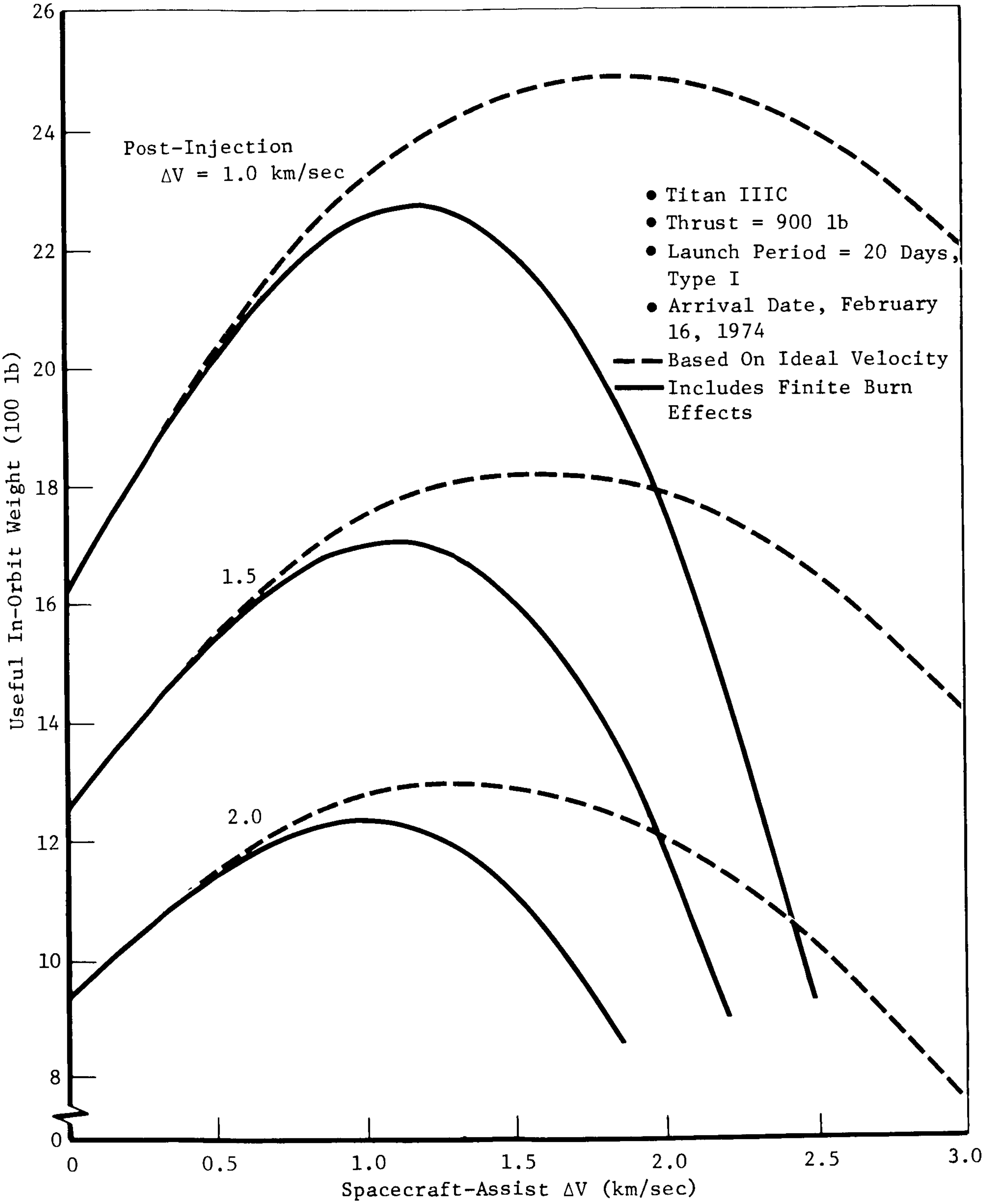

Figure A3-3: EFFECT OF POST-INJECTION ΔV ON USEFUL IN-ORBIT WEIGHT---SPACECRAFT THRUST---900-LB TITAN IIIC

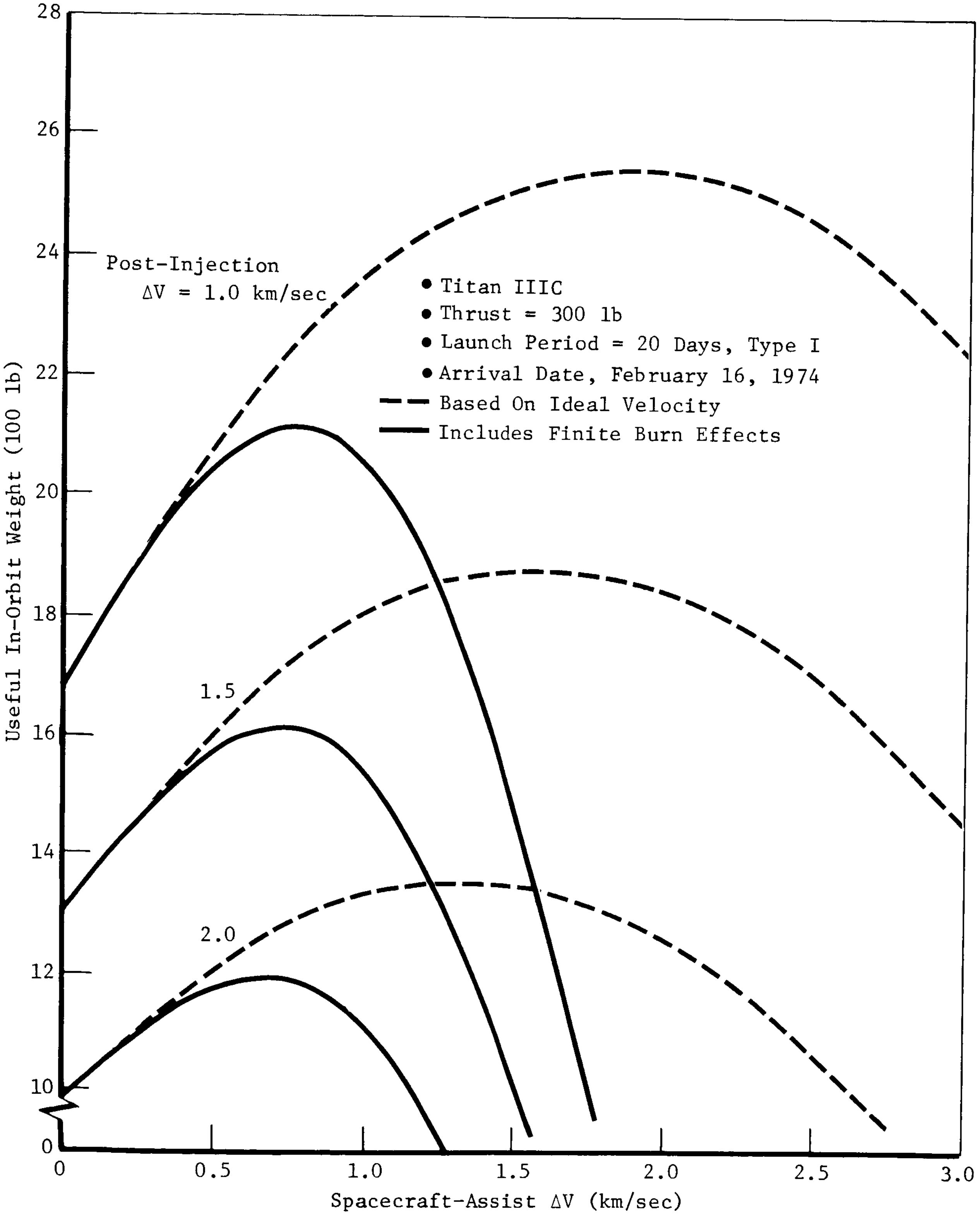

Figure A3-4: EFFECT OF POST-INJECTION ΔV ON USEFUL IN-ORBIT WEIGHT---SPACECRAFT THRUST---300-LB TITAN IIIC

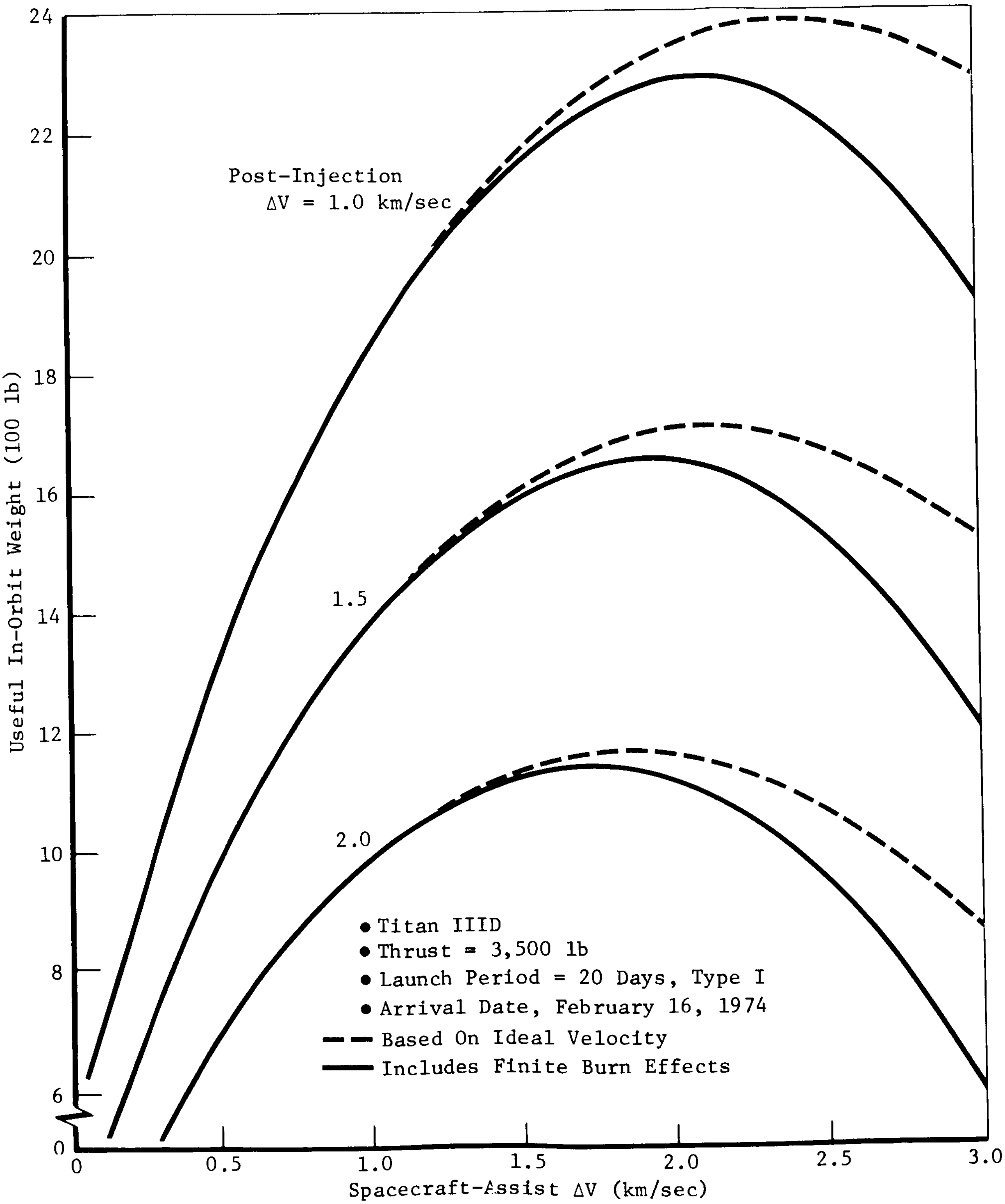

Figure A3-5: EFFECT OF POST-INJECTION ΔV ON USEFUL IN-ORBIT WEIGHT---SPACECRAFT THRUST---3,500-LB TITAN IIID

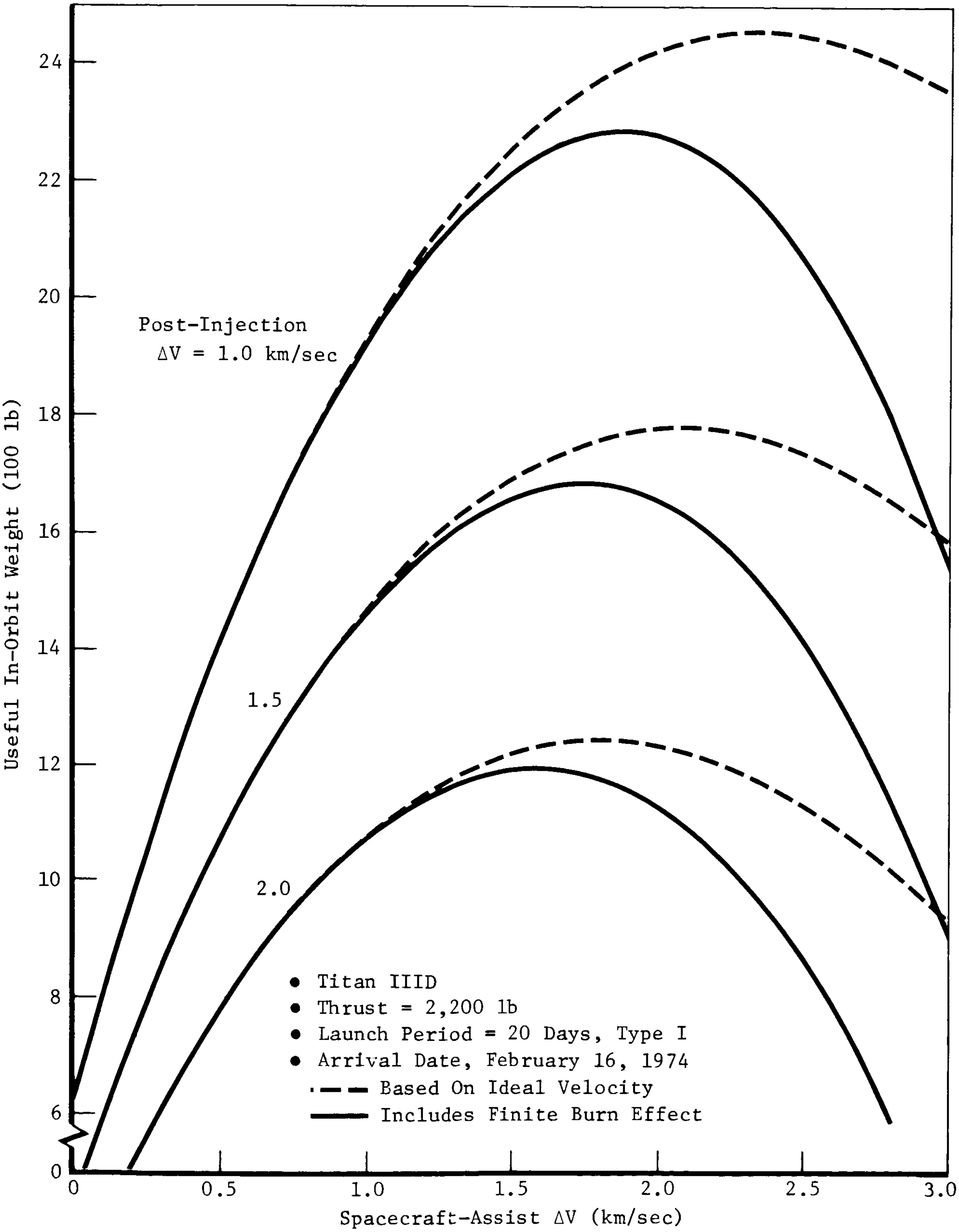

Figure A3-6: EFFECT OF POST-INJECTION ΔV ON USEFUL IN-ORBIT WEIGHT---SPACECRAFT THRUST---2,200-LB TITAN IIID

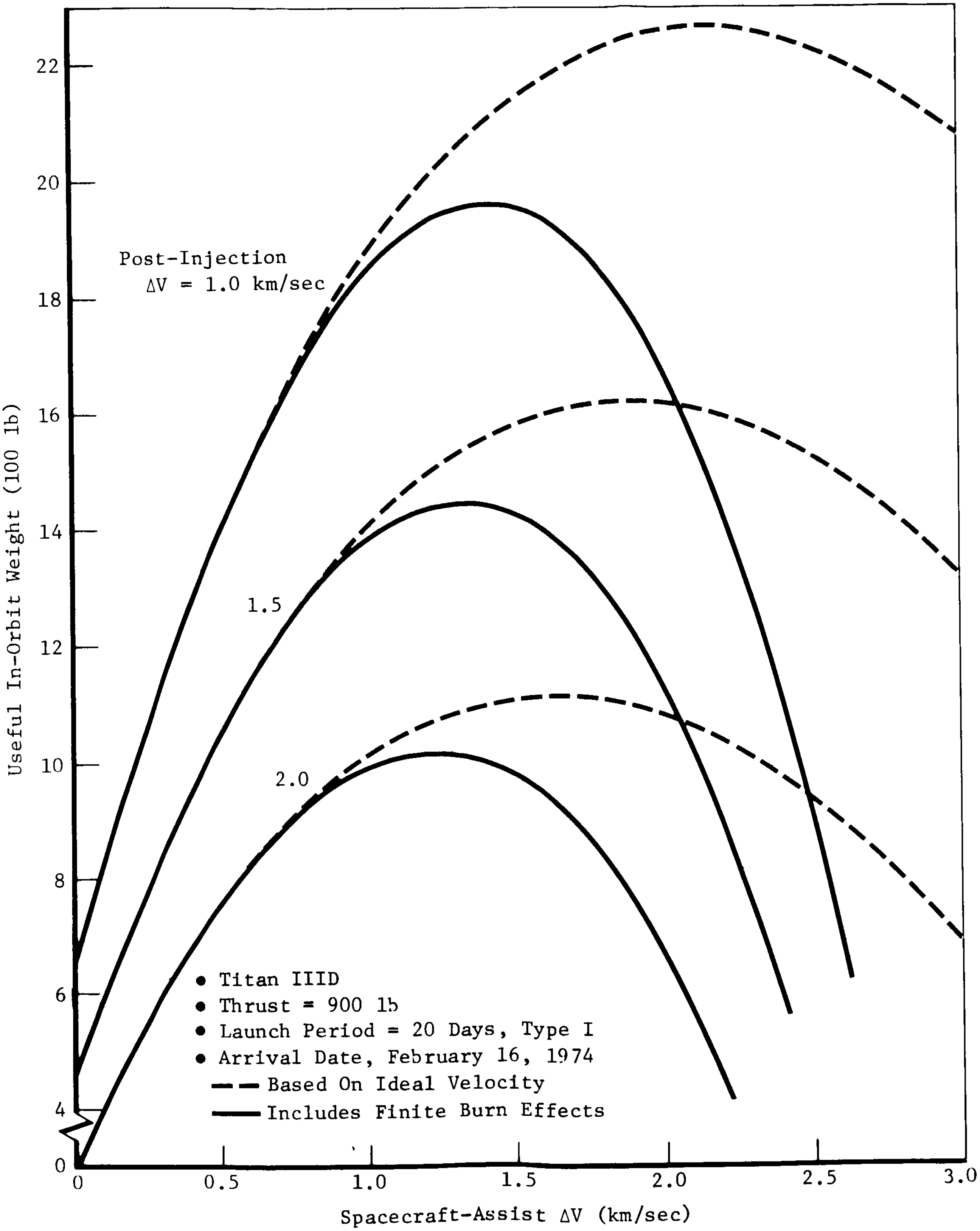

Figure A3-7: EFFECT OF POST-INJECTION ΔV ON USEFUL IN-ORBIT WEIGHT---SPACECRAFT THRUST---900-LB TITAN IIID

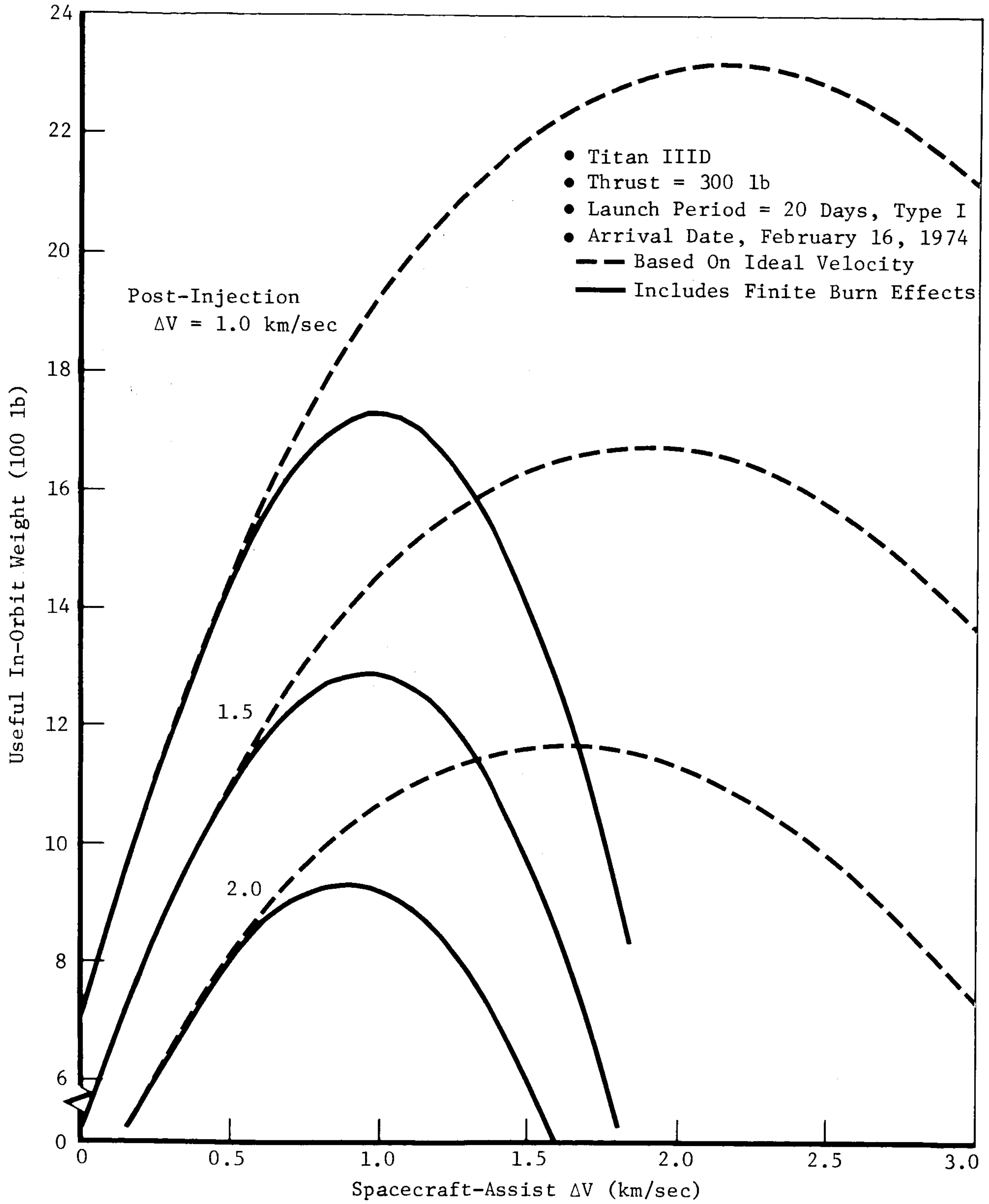

Figure A3-8: EFFECT OF POST-INJECTION ΔV ON USEFUL IN-ORBIT WEIGHT---SPACECRAFT THRUST---300-LB TITAN IIID

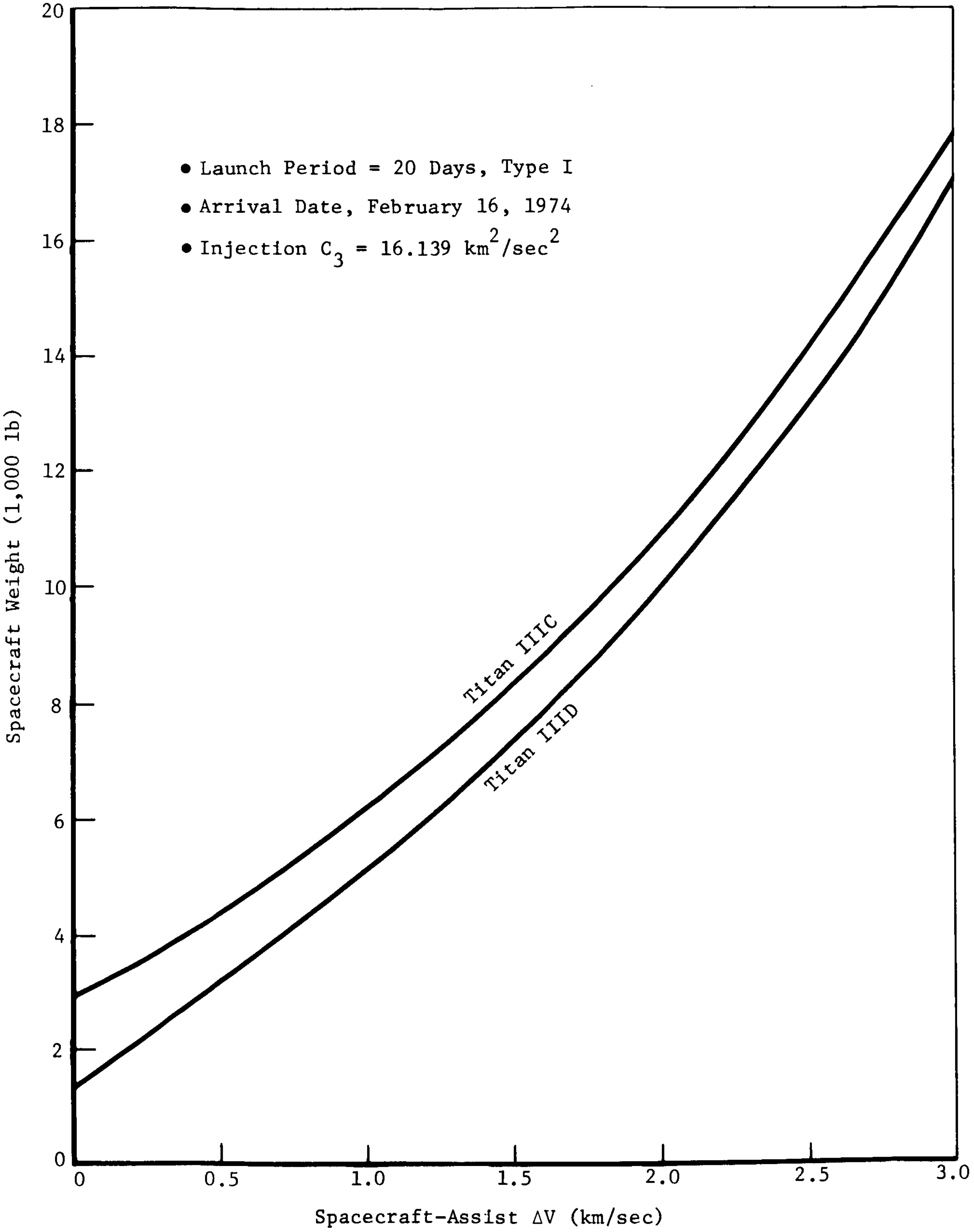

Figure A3-9: POWERED SPACECRAFT WEIGHT

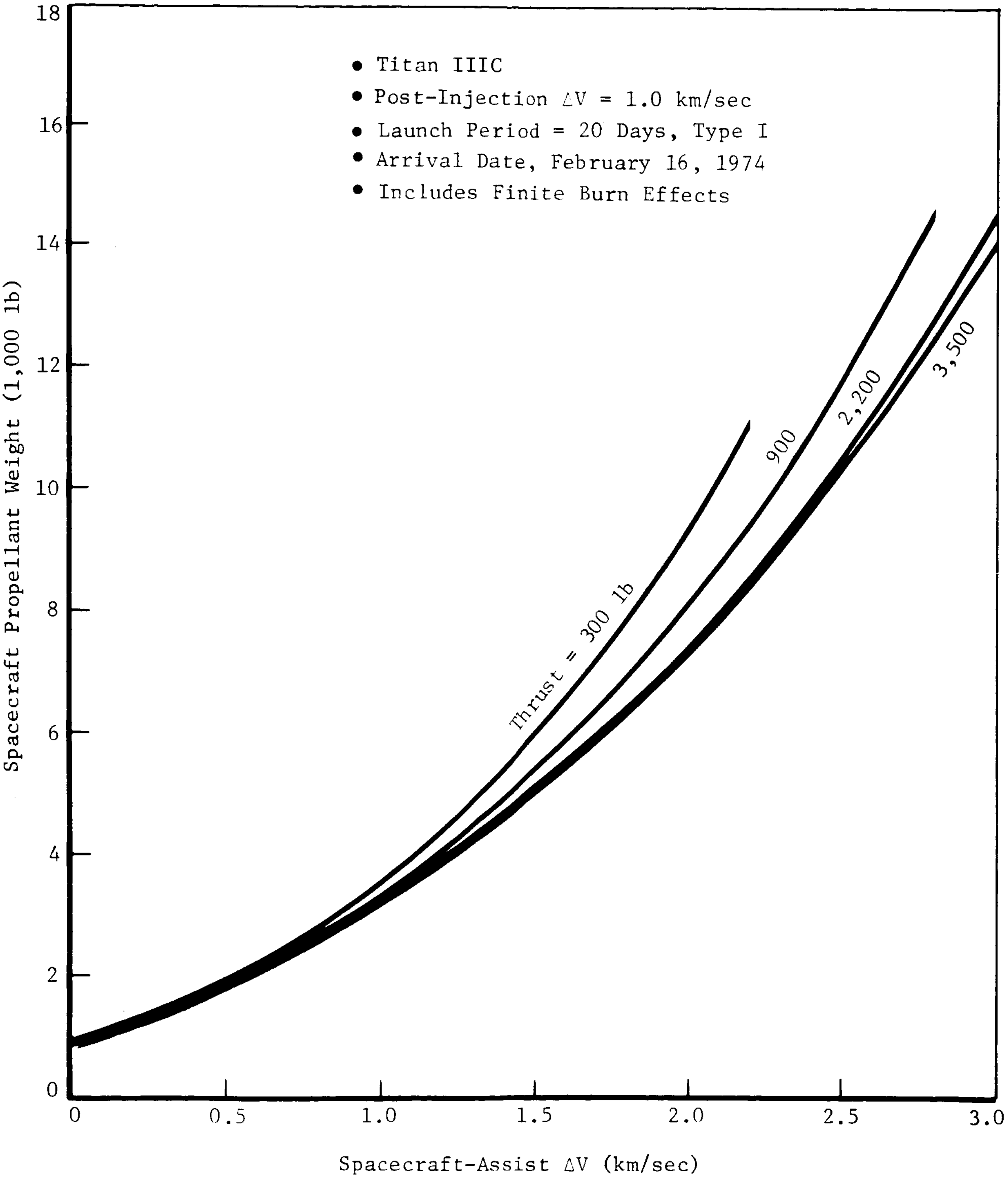

Figure A3-10: TOTAL SPACECRAFT PROPELLANT REQUIREMENTS---POST-INJECTION ΔV = 1.0 KM/SEC---TITAN IIIC

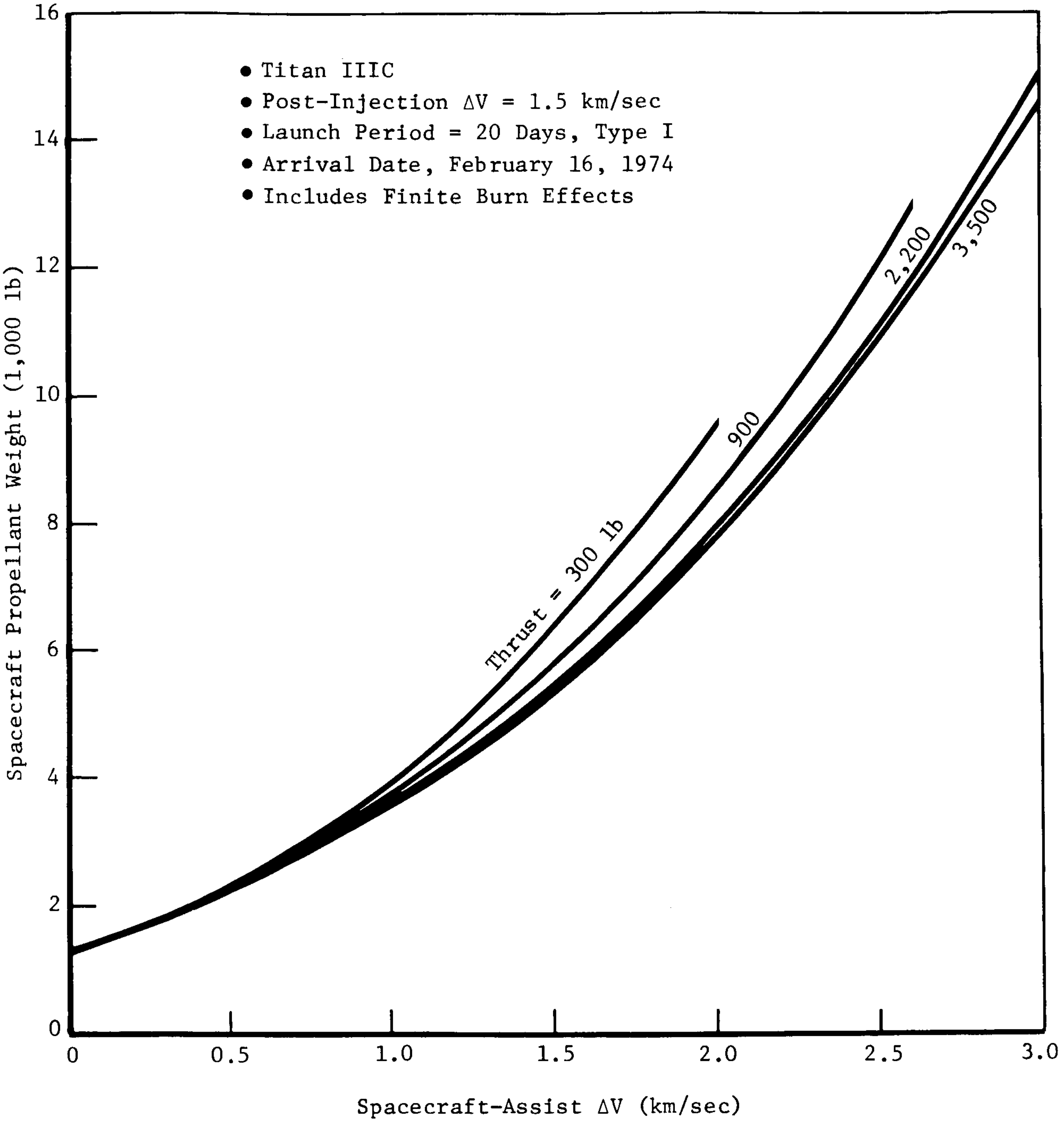

Figure A3-11: TOTAL SPACECRAFT PROPELLANT REQUIREMENTS---POST-INJECTION ΔV = 1.5 KM/SEC---TITAN IIIC

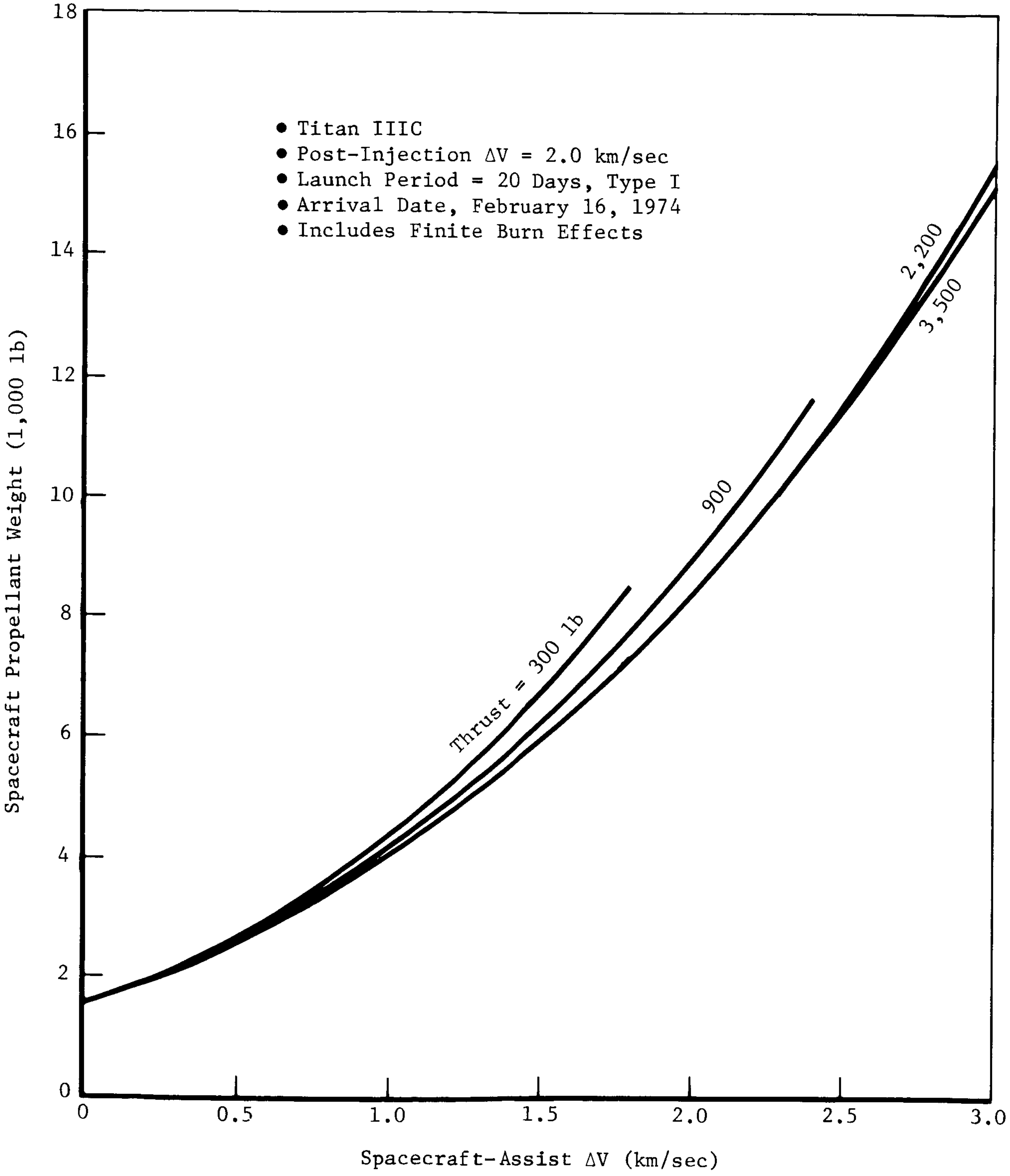

Figure A3-12: TOTAL SPACECRAFT PROPELLANT REQUIREMENTS---POST-INJECTION ΔV = 2.0 KM/SEC---TITAN IIIC

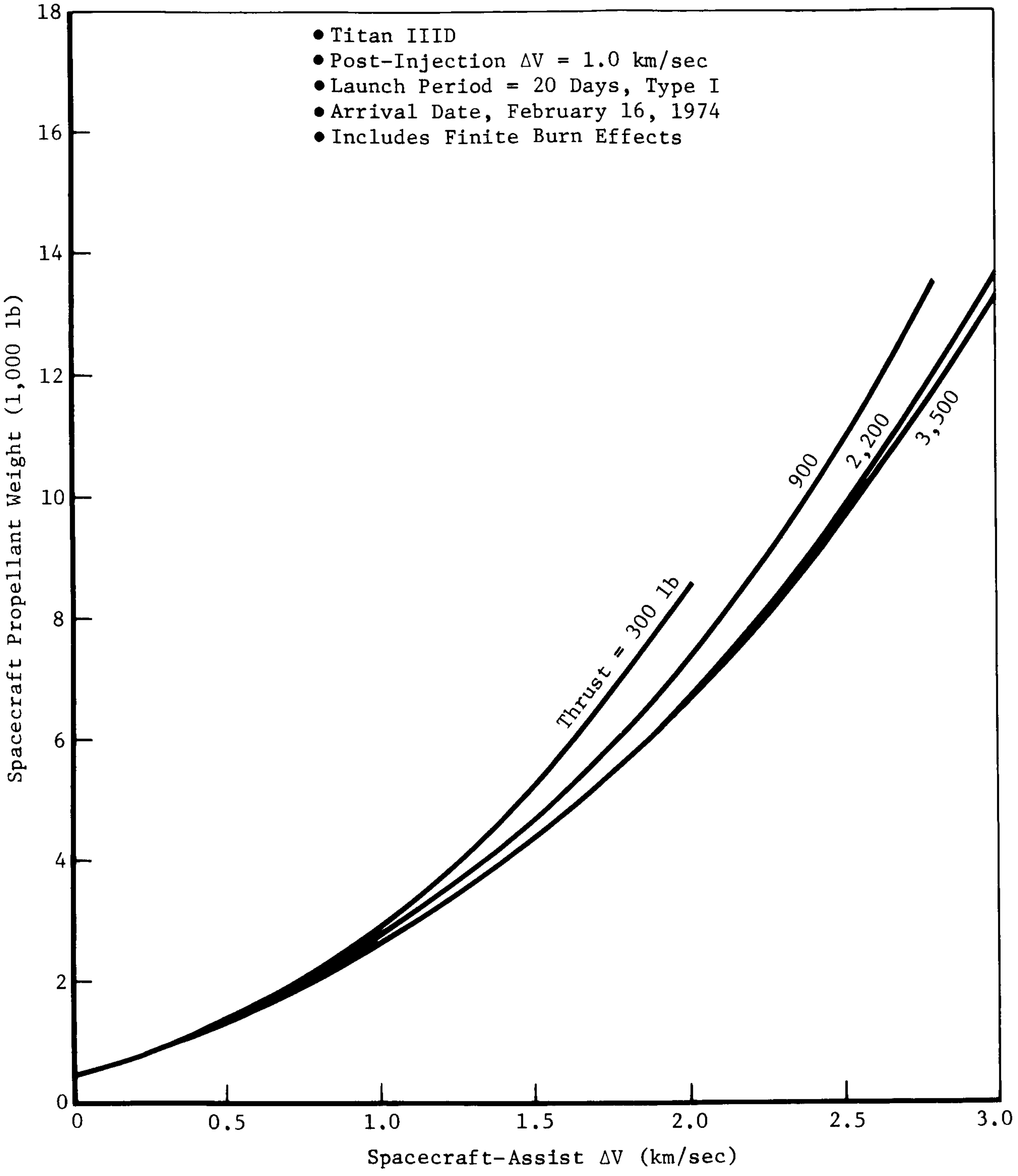

Figure A3-13: TOTAL SPACECRAFT PROPELLANT REQUIREMENTS---POST-INJECTION ΔV = 1.0 KM/SEC---TITAN IIID

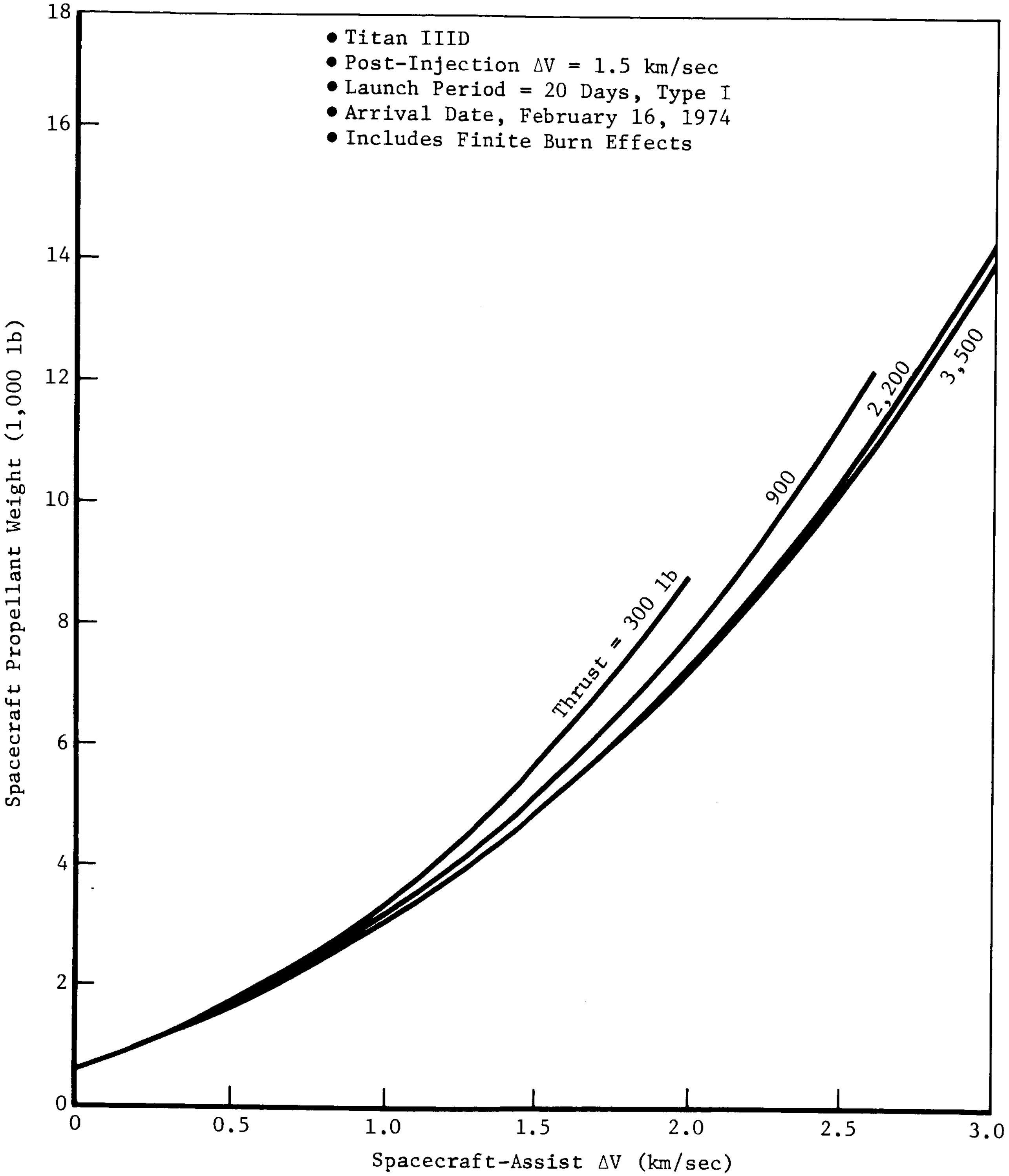

Figure A3-14: TOTAL SPACECRAFT PROPELLANT REQUIREMENTS---POST-INJECTION ΔV = 1.5 KM/SEC---TITAN IIID

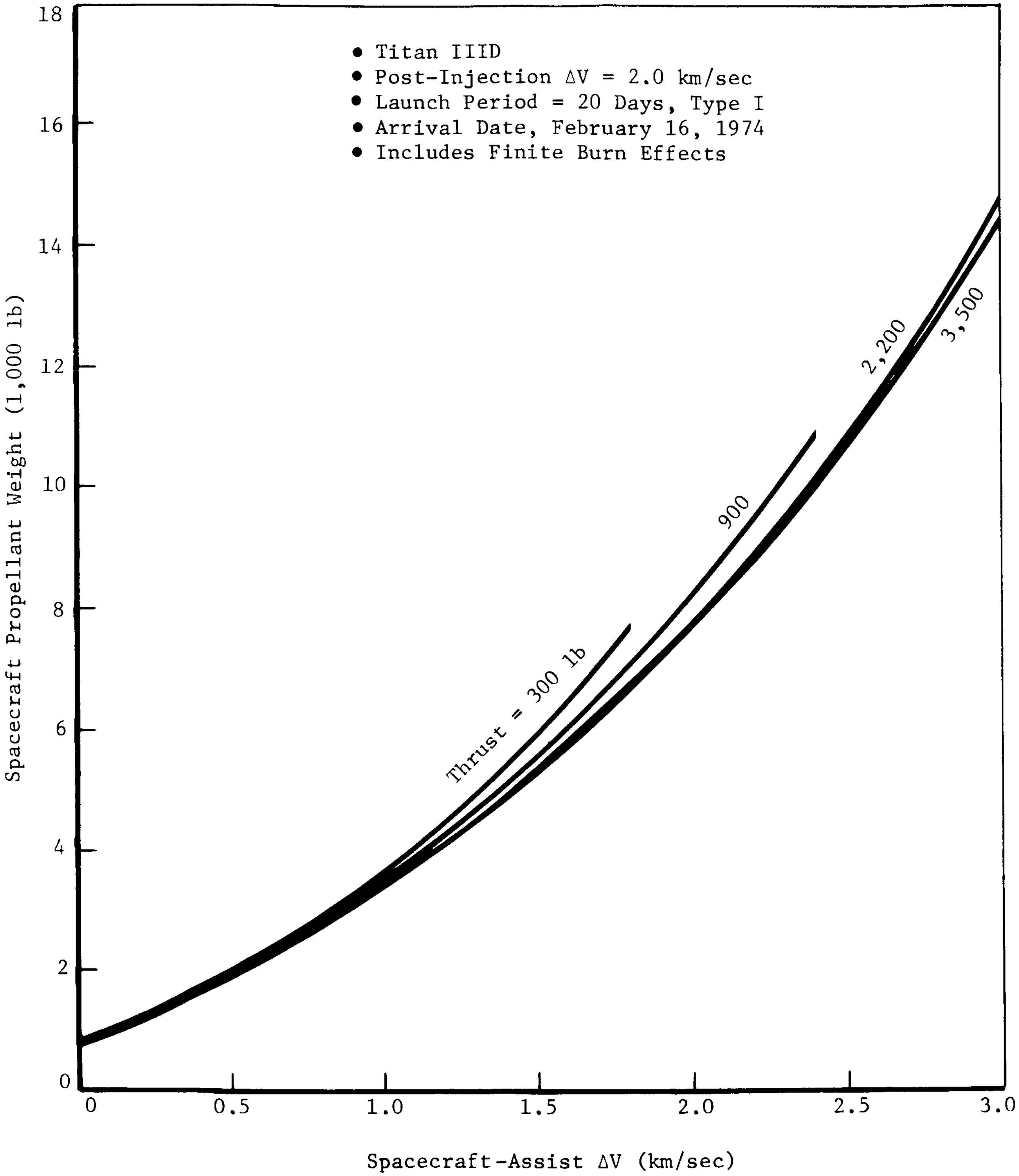

Figure A3-15: TOTAL SPACECRAFT PROPELLANT REQUIREMENTS---POST-INJECTION ΔV = 2.0 KM/SEC---TITAN IIID

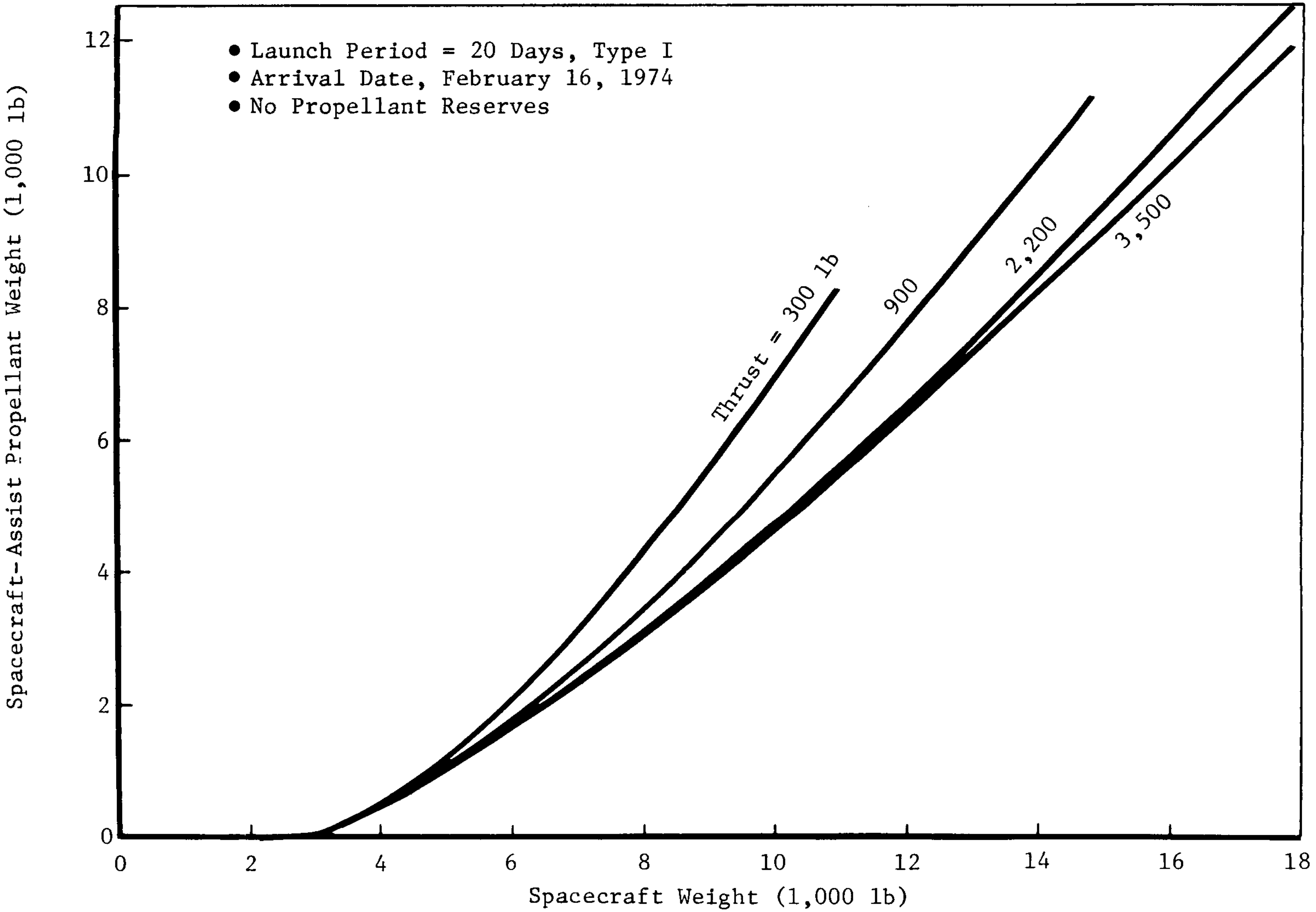

Figure A3-16: PROPELLANT REQUIREMENTS FOR SPACECRAFT-ASSIST MANEUVER---TITAN IIIC

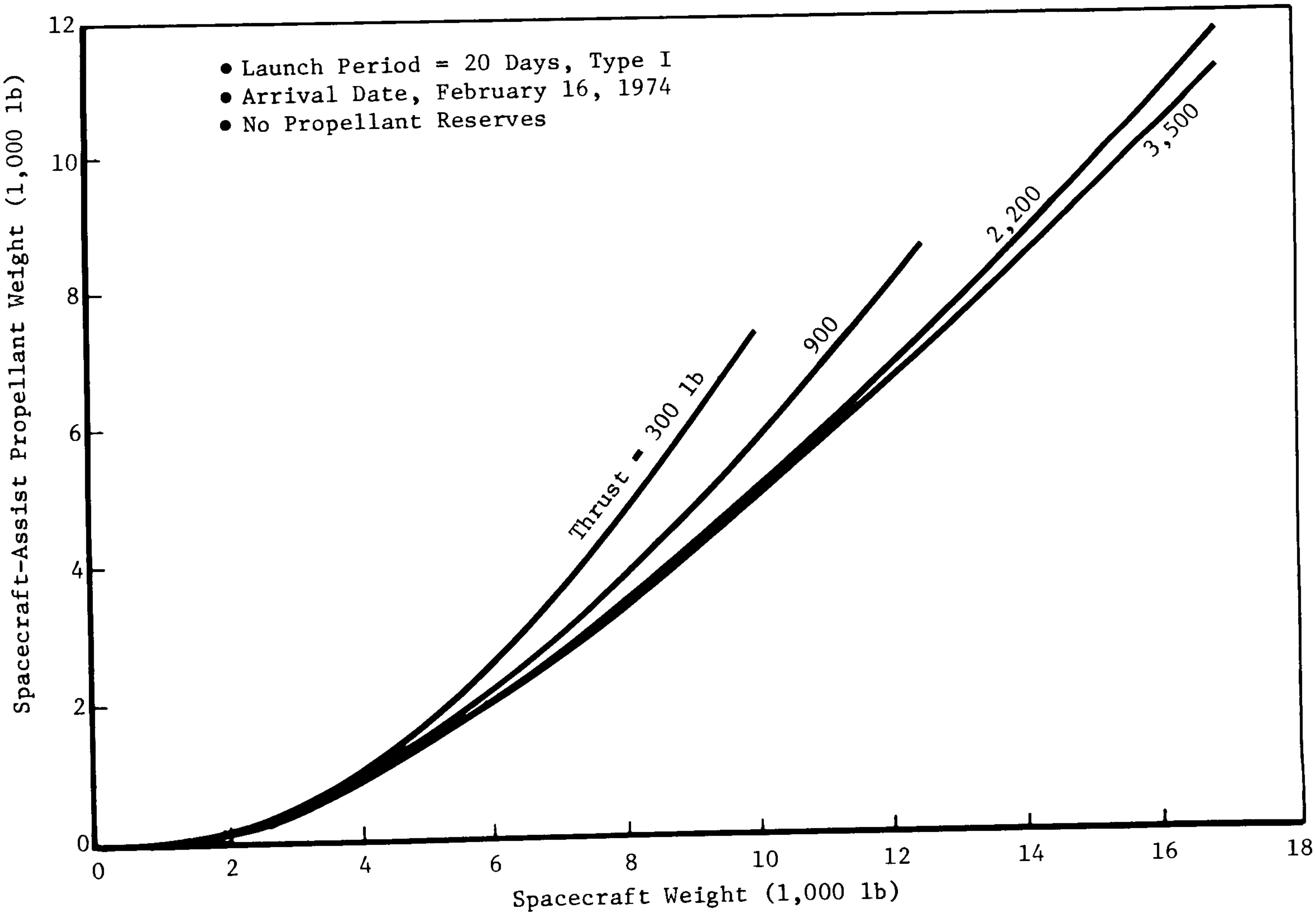

Figure A3-17: PROPELLANT REQUIREMENTS FOR SPACECRAFT-ASSIST MANEUVER---TITAN IIID

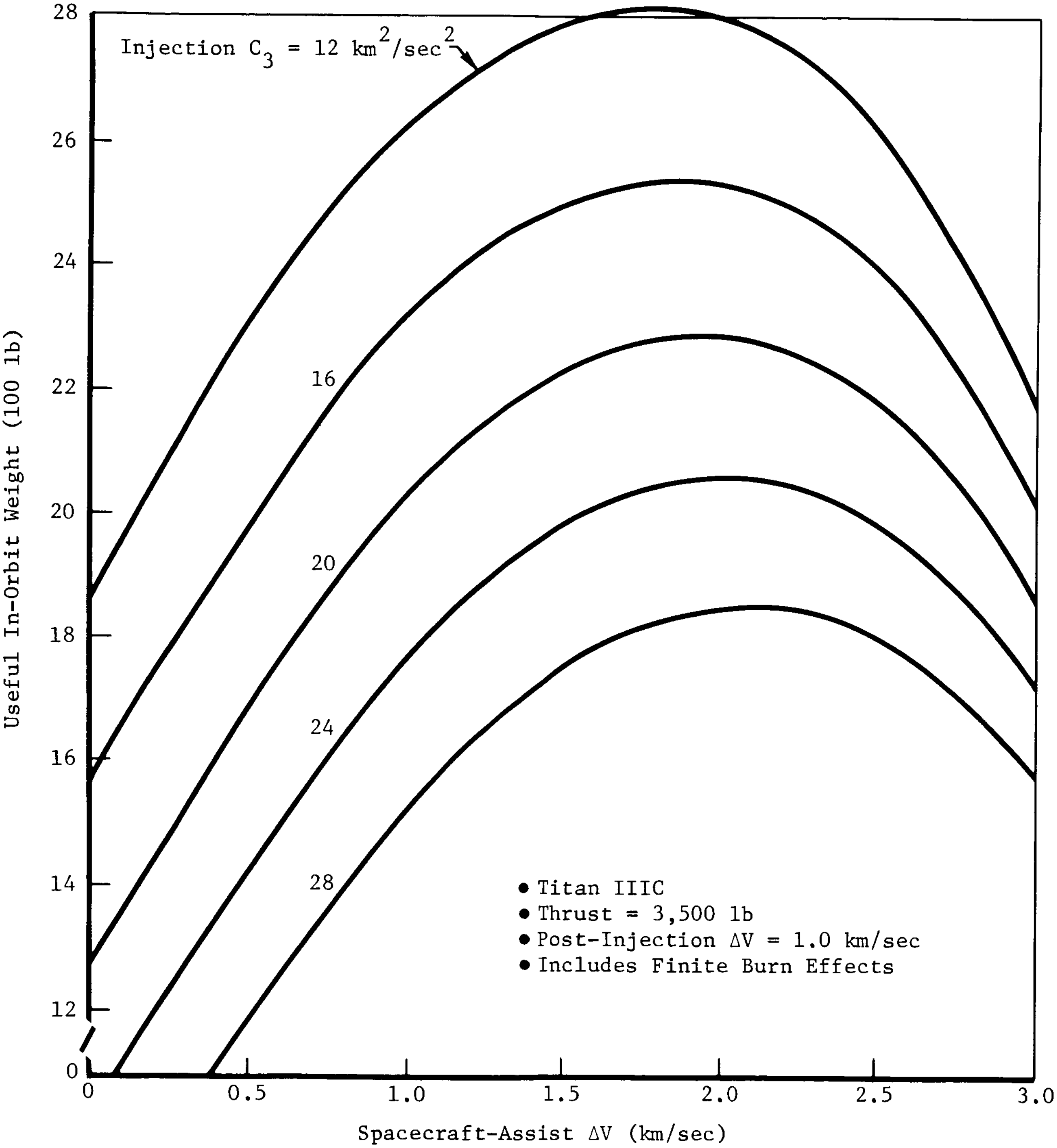

Figure A3-18: $C_3$ EFFECTS ON USEFUL IN-ORBIT WEIGHT---POST-INJECTION ΔV = 1 KM/SEC

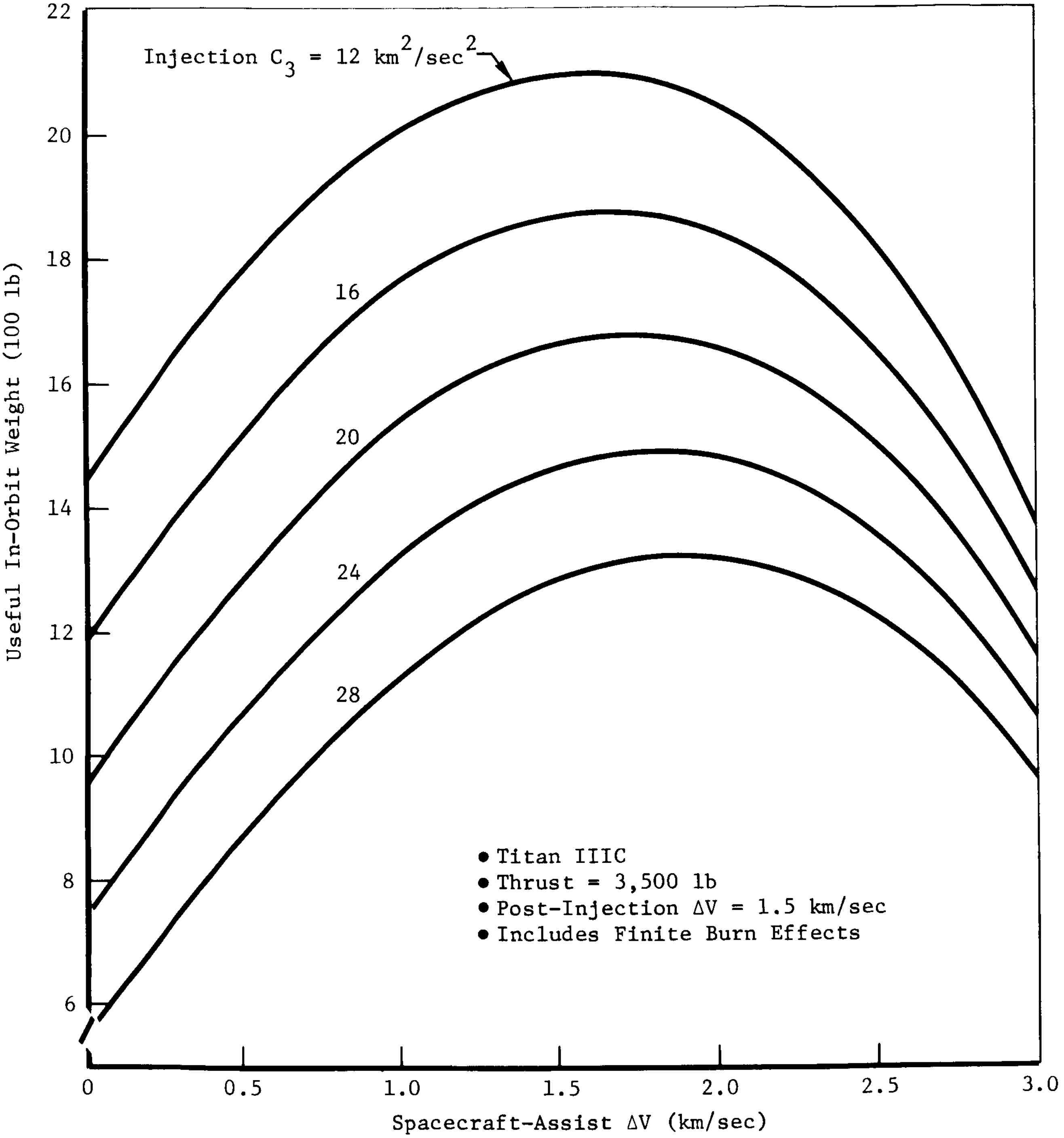

Figure A3-19: $C_3$ EFFECTS ON USEFUL IN-ORBIT WEIGHT---POST-INJECTION ΔV = 1.5 KM/SEC

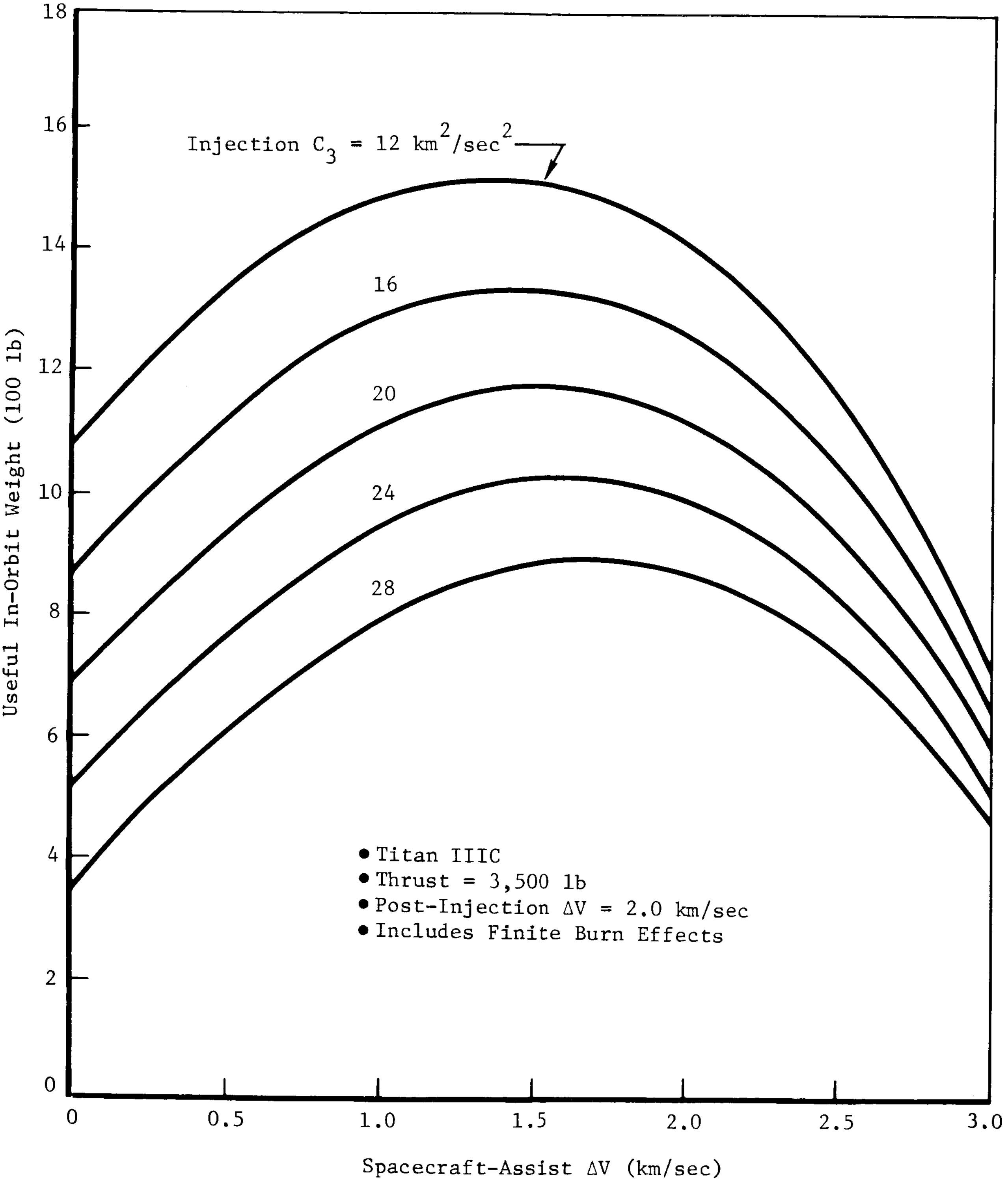

Figure A3-20: $C_3$ EFFECTS ON USEFUL IN-ORBIT WEIGHT---POST-INJECTION ΔV = 2 KM/SEC

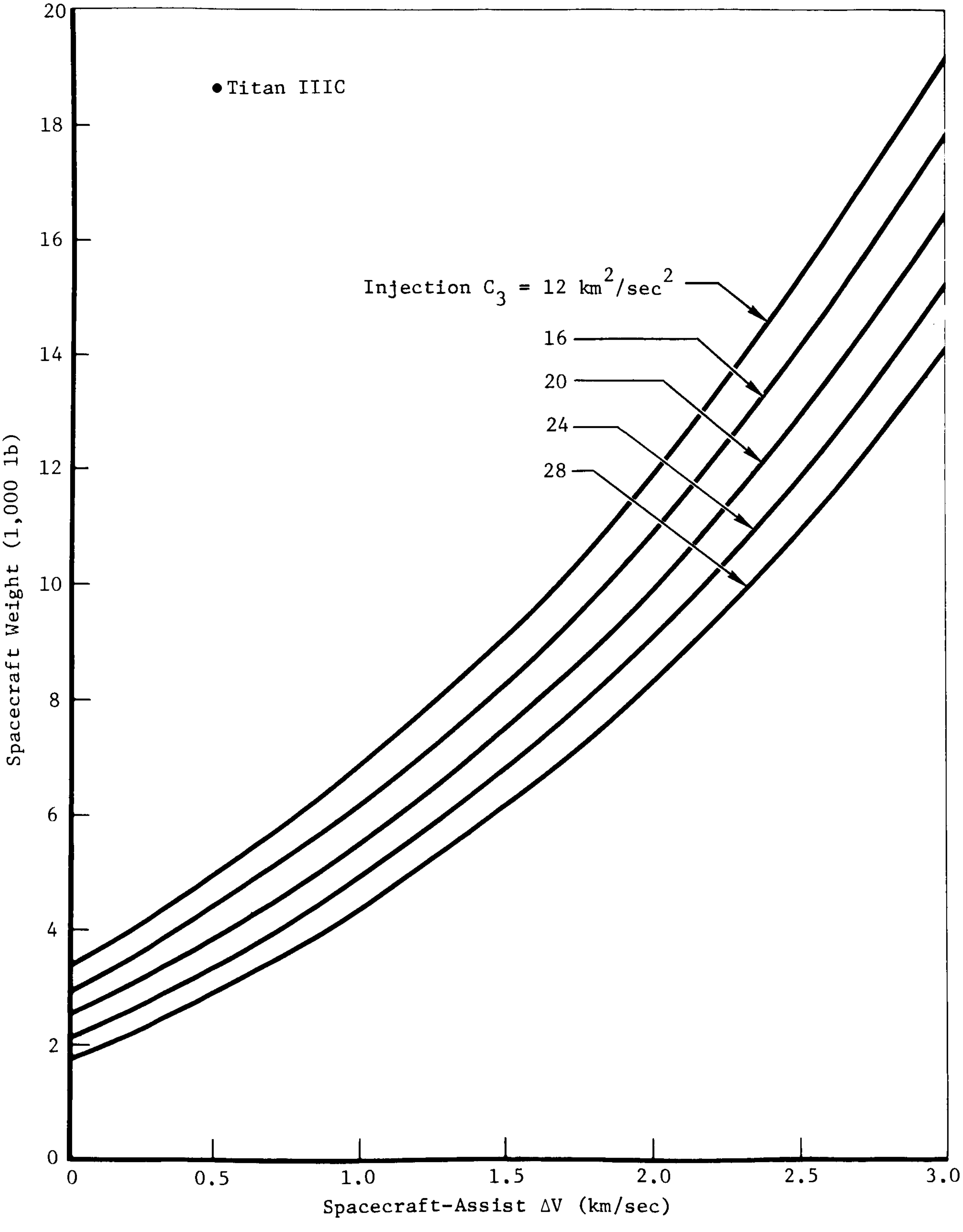

Figure A3-21: $C_3$ EFFECTS ON SPACECRAFT WEIGHT

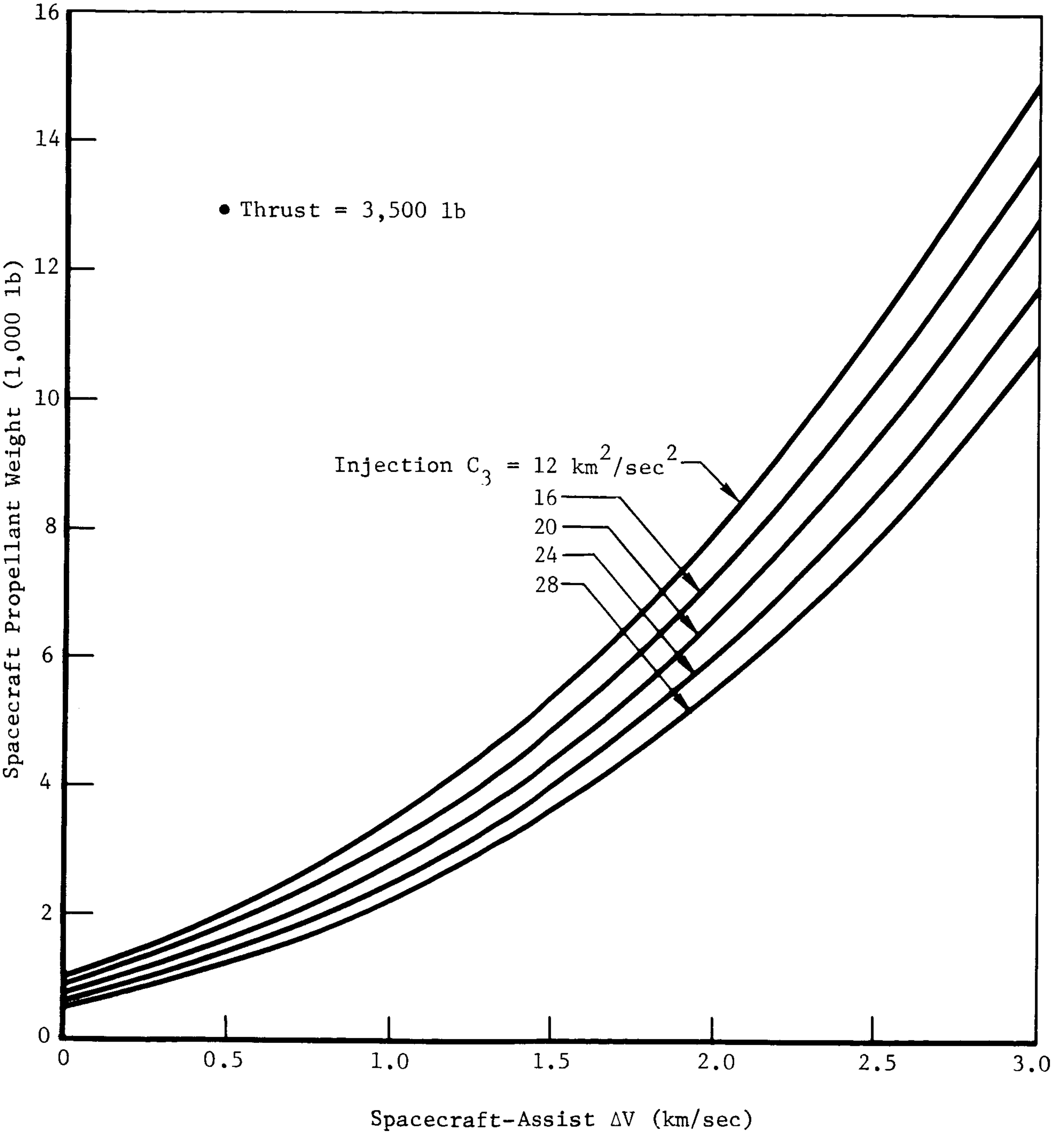

Figure A3-22: TOTAL SPACECRAFT PROPELLANT REQUIREMENTS---POST-INJECTION ΔV = 1.0 KM/SEC---TITAN IIIC

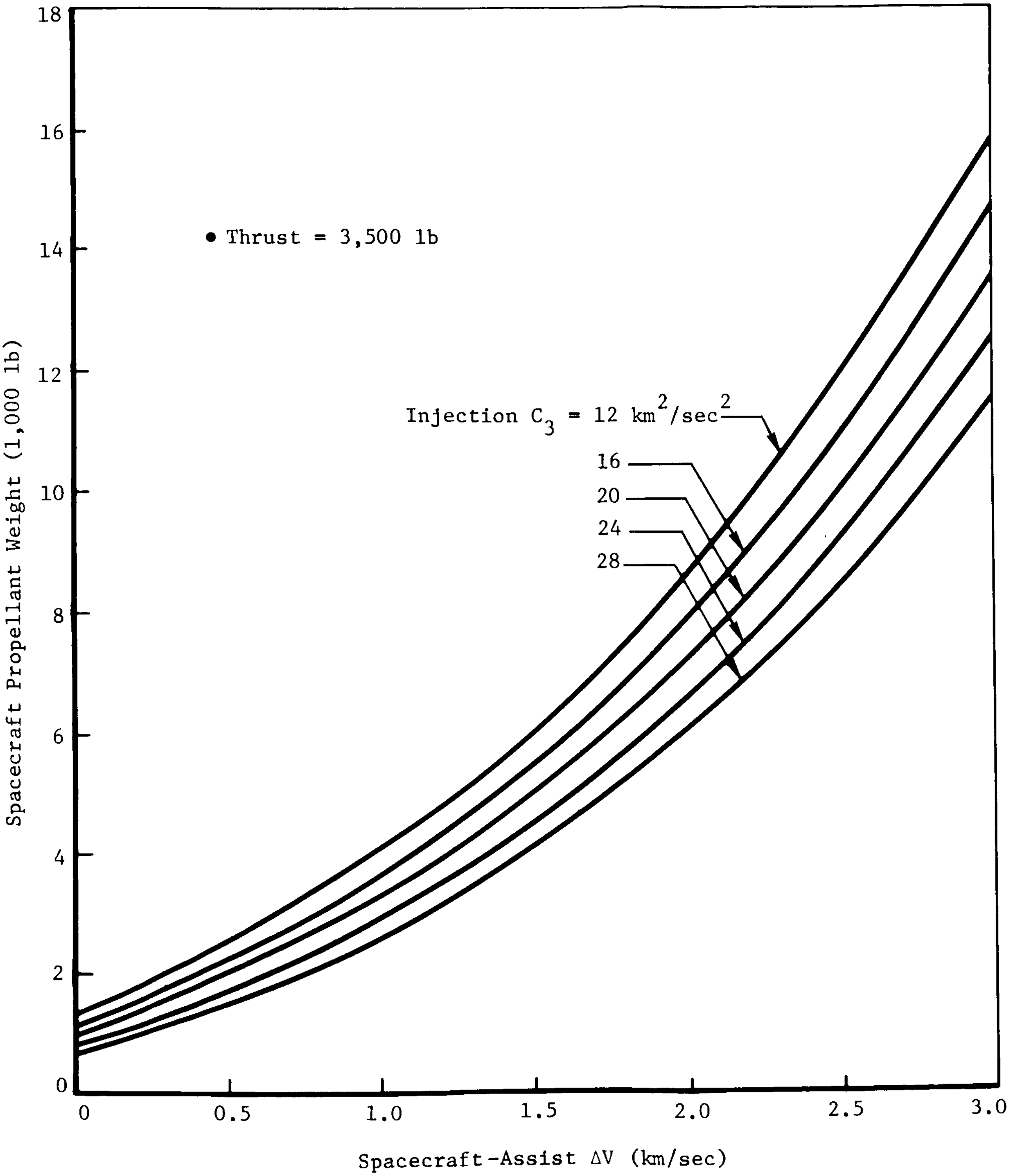

Figure A3-23: TOTAL SPACECRAFT PROPELLANT REQUIREMENTS---POST-INJECTION ΔV = 1.5 KM/SEC---TITAN IIIC

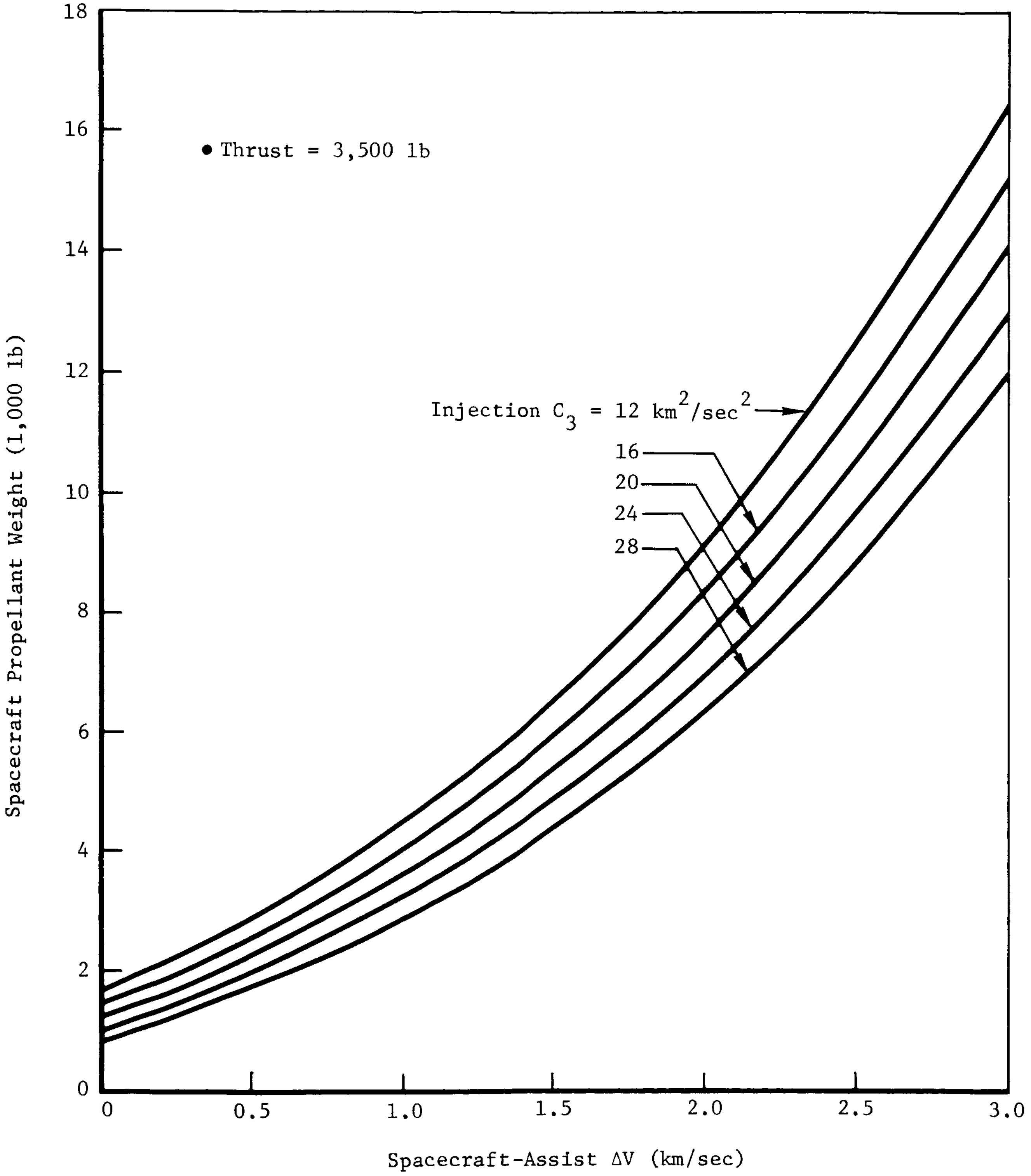

Figure A3-24: TOTAL SPACECRAFT PROPELLANT REQUIREMENTS---POST-INJECTION ΔV = 2 KM/SEC---TITAN IIIC

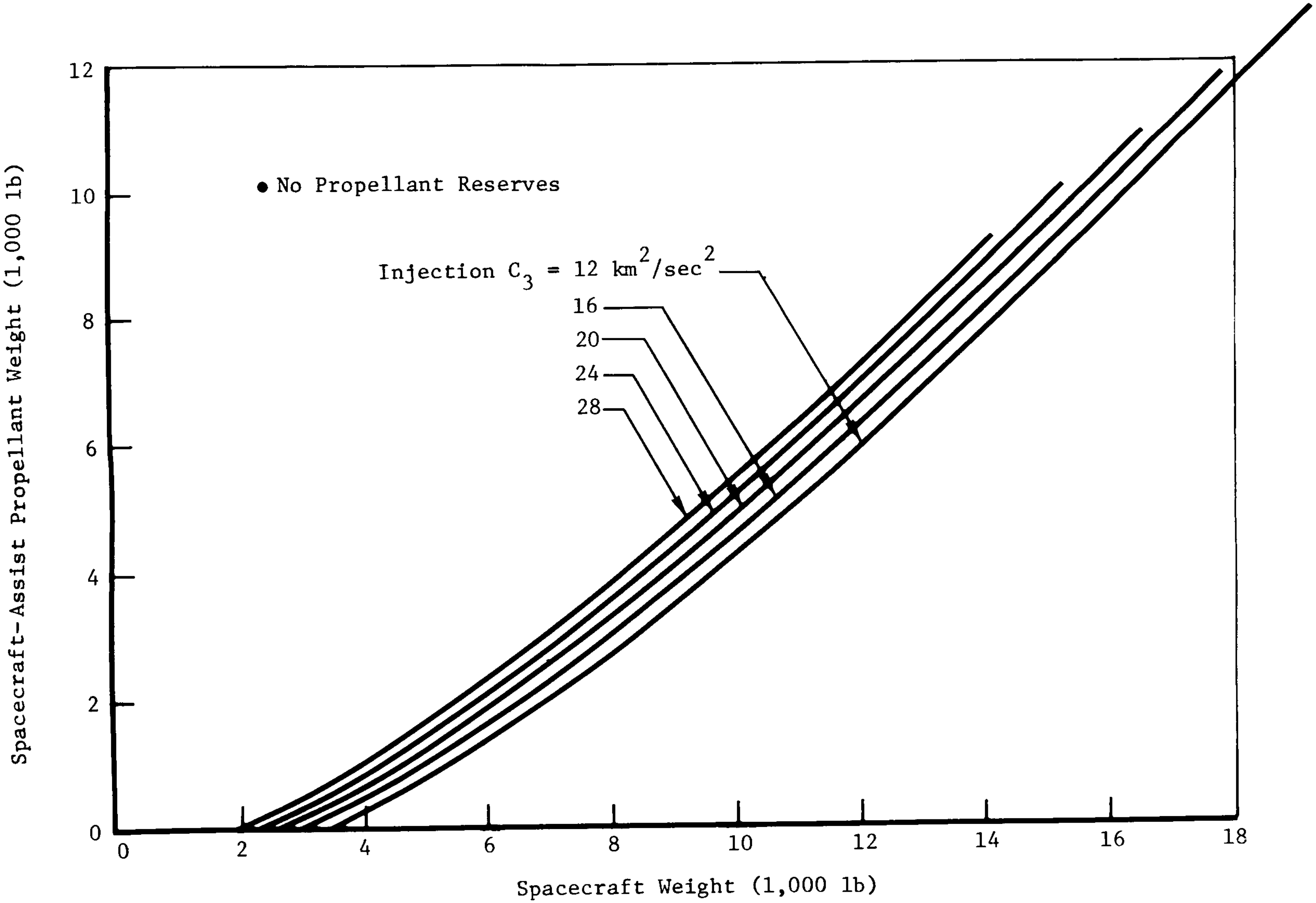

Figure A3-25: PROPELLANT REQUIREMENTS FOR SPACECRAFT-ASSIST MANEUVER---TITAN IIIC

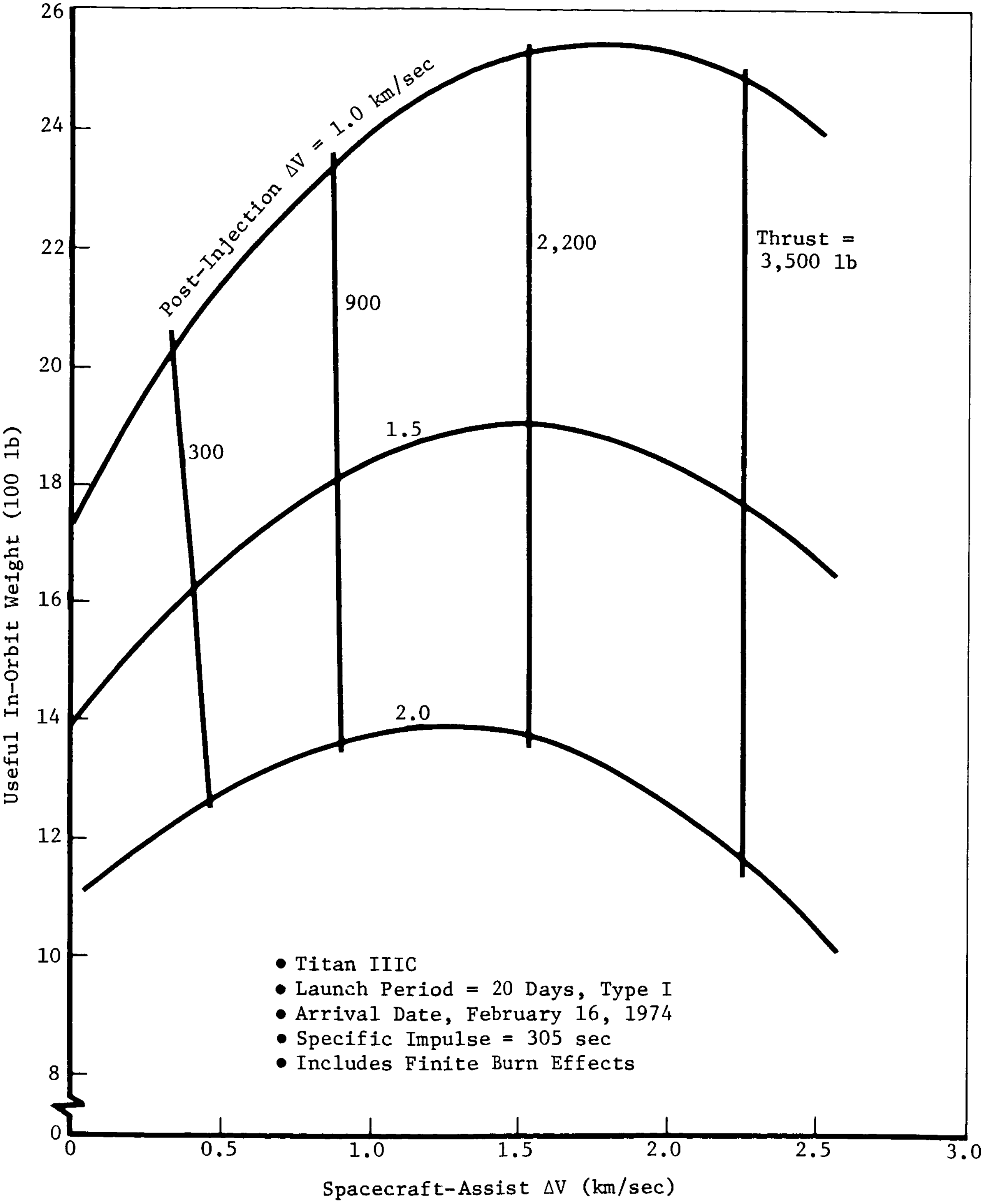

- Titan IIIC
- Launch Period = 20 Days, Type I
- Arrival Date, February 16, 1974
- Specific Impulse = 305 sec
- Includes Finite Burn Effects

Figure A3-26: USEFUL IN-ORBIT WEIGHT ENVELOPES---TITAN IIIC

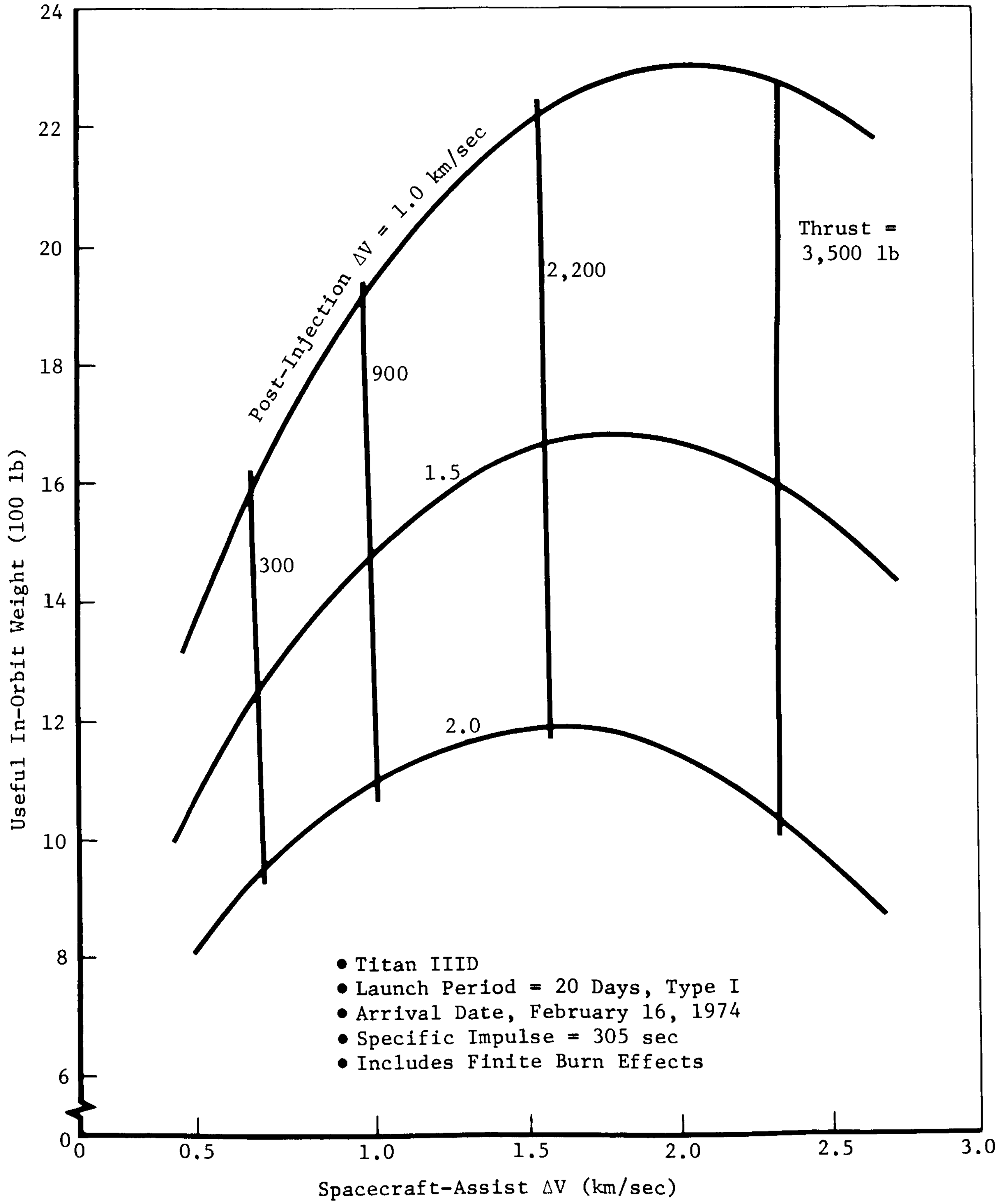

Figure A3-27: USEFUL IN-ORBIT WEIGHT ENVELOPES---TITAN IIID

*Example 1*

Given: Spacecraft Thrust = 3,500 pounds

Spacecraft-Assist ΔV = 1.5 km/sec

Post-Injection ΔV = 1.5 km/sec

$C_3 = 18 \text{ km}^2/\text{sec}^2$

Find: Spacecraft Weight

Total Propellant Weight

Useful In-Orbit Weight

Procedure:

1) From Figure A3-21, Spacecraft Weight = 7,950 pounds
2) From Figure A3-23, Total Propellant Weight = 5,200 pounds
3) From Figure A3-19, Useful In-Orbit Weight = 1,770 pounds

*Example 2*

Given: Spacecraft Thrust = 900 pounds

Spacecraft-Assist ΔV = 1.2 km/sec

Post-injection ΔV = 1.5 km/sec

$C_3 = 24 \text{ km}^2/\text{sec}^2$

Find: Spacecraft Weight

Total Propellant Weight

Useful In-Orbit Weight

Procedure:

1) From Figure A3-21, Spacecraft Separated Weight = 5,700 pounds
2) Since no data is provided that directly show the effect of $C_3$ on propellant and useful in-orbit weights, it is necessary to carefully manipulate the available data. The approach to be presented is approximate and should only be used for ΔV assists $\leq$ the ΔV assist that provides maximum useful in-orbit weight. (See Figures A3-1 through A3-4.)

   The first step is to obtain the propellant weight from the data for a 3,500-pound-thrust engine shown in Figure A3-23, i.e., total propellant weight = 3,495 pounds.
3) Next compare the propellant difference between the 900- and 3,500-pound-thrust engines as shown in Figure A3-11. This difference of 250 pounds (due to finite burn losses and $I_{SP}$ differences) when added to the 3,495 pounds of propellant gives a propellant total of 3,745 pounds. Herein lies the approximation since propellant differences are being established at a $C_3 = 16.139 \text{ km}^2/\text{sec}^2$ and not $24 \text{ km}^2/\text{sec}^2$.

4) Determine the usable propellant by dividing the total propellant by 1.0375 to account for unavailable fluid and mixture ratio losses. This results in a usable propellant of ≃3,605 pounds. The corresponding nonuseful weight, 815 pounds, can then be obtained from Figure 5.2-1.

5) Useful In-Orbit Weight = Separated Spacecraft Weight - Propellant Weight - Nonuseful Weight

Useful In-Orbit Weight = 5,700 - 3,605 - 815 = 1,280 pounds

Check: A comparison of these values versus analytically calculated values follows.

| | Approx | Actual | % Error |
|---|---|---|---|
| Spacecraft Separated Weight | 5,700 | 5,707 | -0.1 |
| Total Propellant Weight | 3,745 | 3,680 | +1.8 |
| Useful In-Orbit Weight | 1,280 | 1,351 | -5.3 |

# APPENDIX A4
# TRACKING AND DATA ACQUISITION

This appendix defines the tracking station coordinates and constraints and presents additional tracking station viewing data. The coordinates and constraints of the tracking stations considered in this study are given in Table A4-1. The constraints for some of the stations are obtained from Boeing Document D2-100767-1 (Reference 5). For those stations for which constraints are not available, 5-degree elevation angle and ±180-degree hour angle are assumed. For tracking ships, the elevation angle constraint is assumed to be 2.5 degrees.

Table A4-1: TRACKING STATIONS

| Station | Net-Work | Geocentric Latitude (deg) | Longitude (West of Greenwich) (deg) | Radius (km) | Contraints Elevation Angle (deg) | Used[1] Hour Angle (deg) |
|---|---|---|---|---|---|---|
| Merritt Island | MSFN | 28.345 | 279.306 | 6,373.337 | 5 | 180 |
| Grand Bahama | MSFN | 26.499 | 281.847 | 6,373.906 | 5 | 180 |
| Bermuda | MSFN | 32.176 | 295.342 | 6,373.102 | 0 | 180 |
| Antigua | MSFN | 16.908 | 298.247 | 6,376.392 | 0 | 180 |
| Canary Island | MSFN | 27.580 | 344.397 | 6,373.604 | 0 | 180 |
| Ascension | MSFN | - 7.902 | 345.672 | 6,378.322 | 0 | 180 |
| Carnarvon | MSFN | -24.759 | 113.724 | 6,374.458 | 0 | 180 |
| Guam | MSFN | 13.222 | 144.734 | 6,377.169 | 5 | 180 |
| Kauai | MSFN | 21.989 | 200.335 | 6,376.305 | 5 | 180 |
| Guymas | MSFN | 27.802 | 249.279 | 6,373.515 | 5 | 180 |
| Corpus Christi | MSFN | 27.494 | 262.621 | 6,373.601 | 5 | 180 |
| Pretoria | AFETR | -25.792 | 28.361 | 6,375.941 | 0 | 180 |
| Cape (Station 71) | AFETR | 28.317 | 279.434 | 6,373.350 | 5 | 180 |
| Goldstone | DSIF | 35.119 | 243.194 | 6,372.018 | 5 | 90 |
| Woomera | DSIF | -31.212 | 136.886 | 6,372.532 | 0 | 90 |
| Johannesburg | DSIF | -25.739 | 27.686 | 6,375.542 | 5 | 90 |
| Madrid | DSIF | 40.259 | 355.635 | 6,370.087 | 5 | 105 |
| Tinbinbilla | DSIF | -35.219 | 148.980 | 6,371.704 | 5 | 180 |
| Ships | MSFN | -- | -- | -- | 2.5 | 180 |

[1] No other constraints are considered.

Figures A4-1 through A4-5 show the station viewing periods for various launch azimuths during the ascent and parking orbit phases. These data are applicable for any launch and arrival day. Superimposed on the figures are the range of injection times for both short and long parking orbit coasts of the 20-day launch period discussed in Section 5.3. Injection refers to trans-Mars

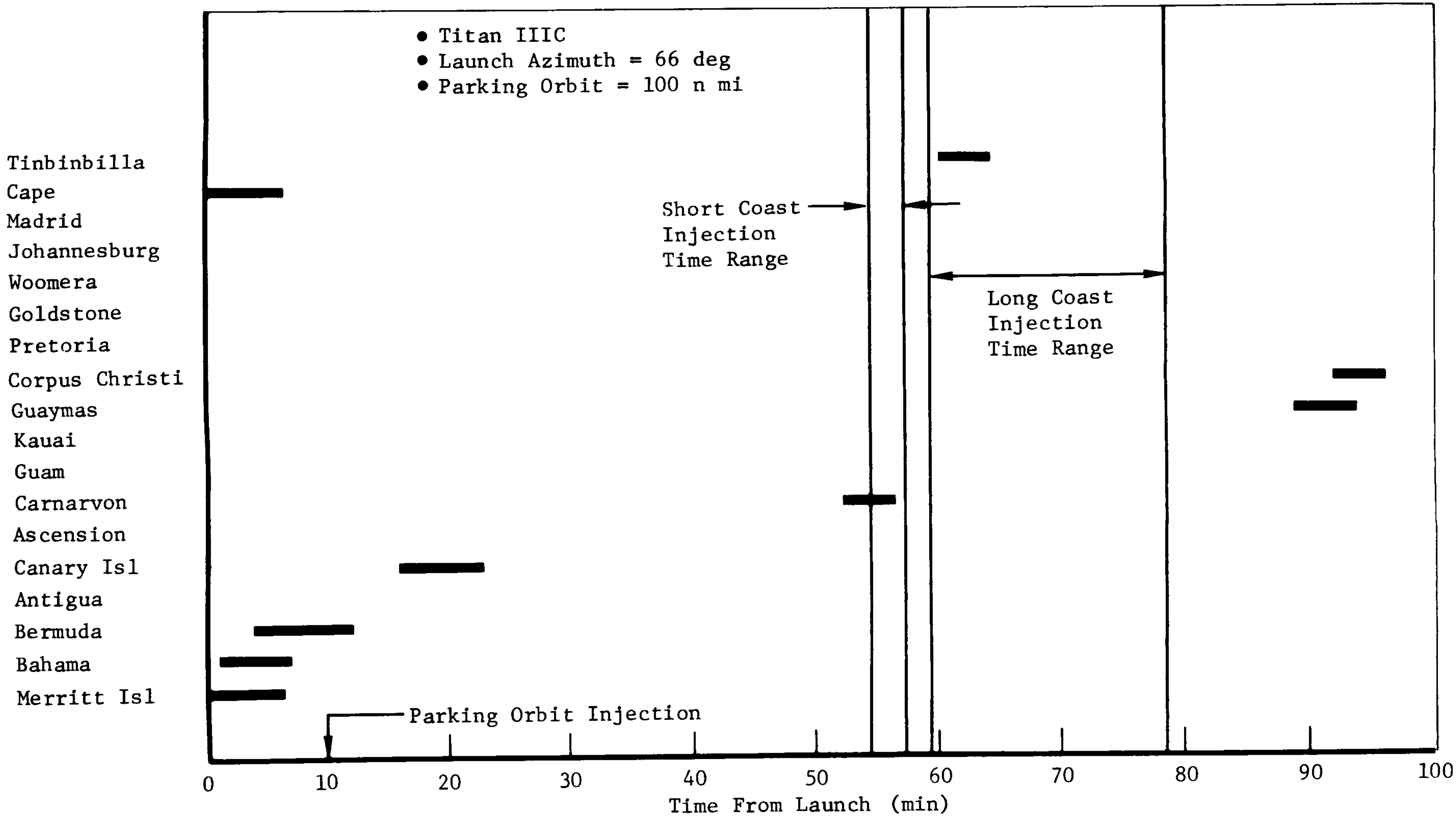

Figure A4-1: TRACKING STATION VIEW PERIODS---PARKING ORBIT COAST PHASE

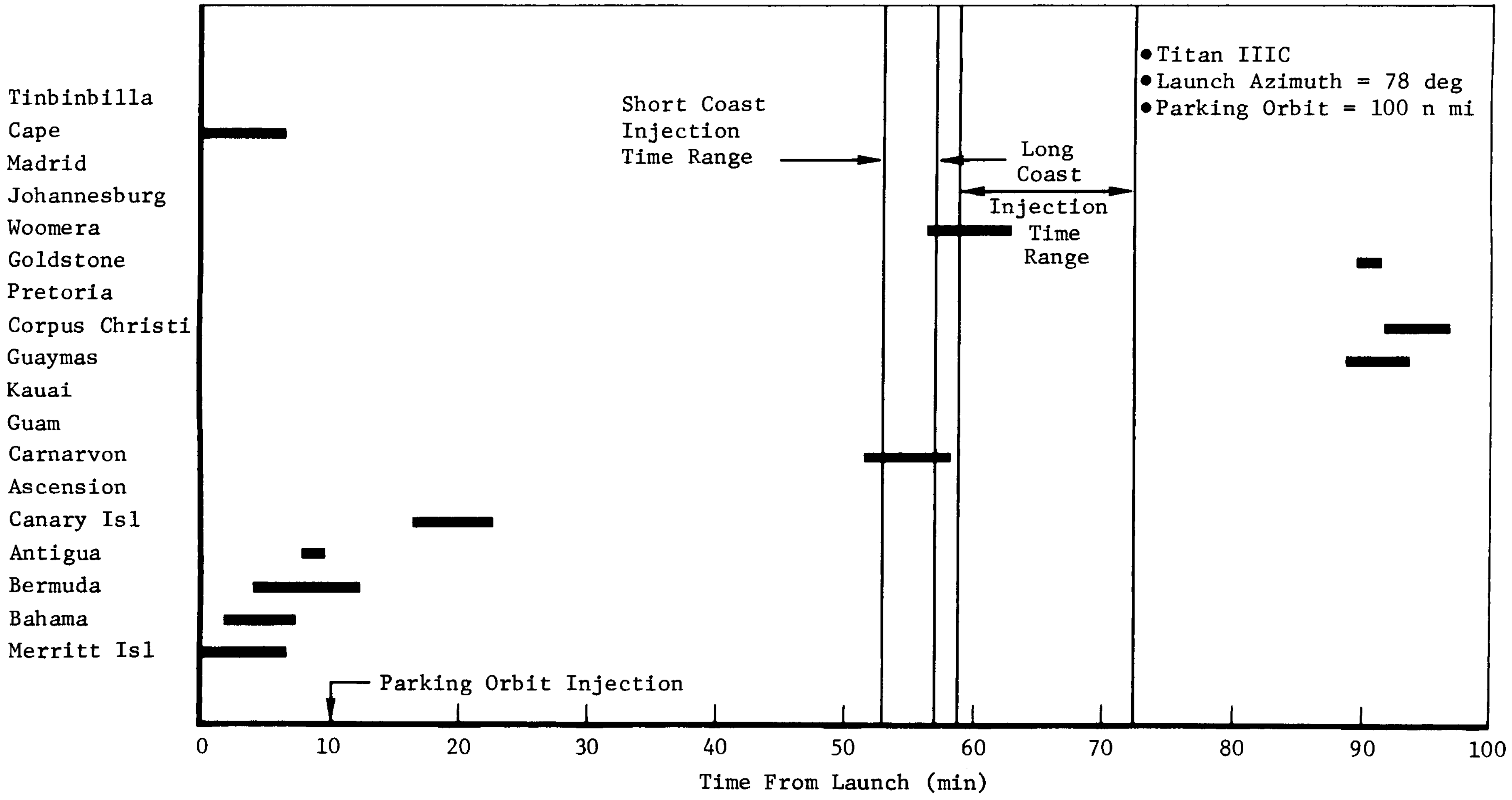

Figure A4-2: TRACKING STATION VIEW PERIODS---PARKING ORBIT COAST PHASE

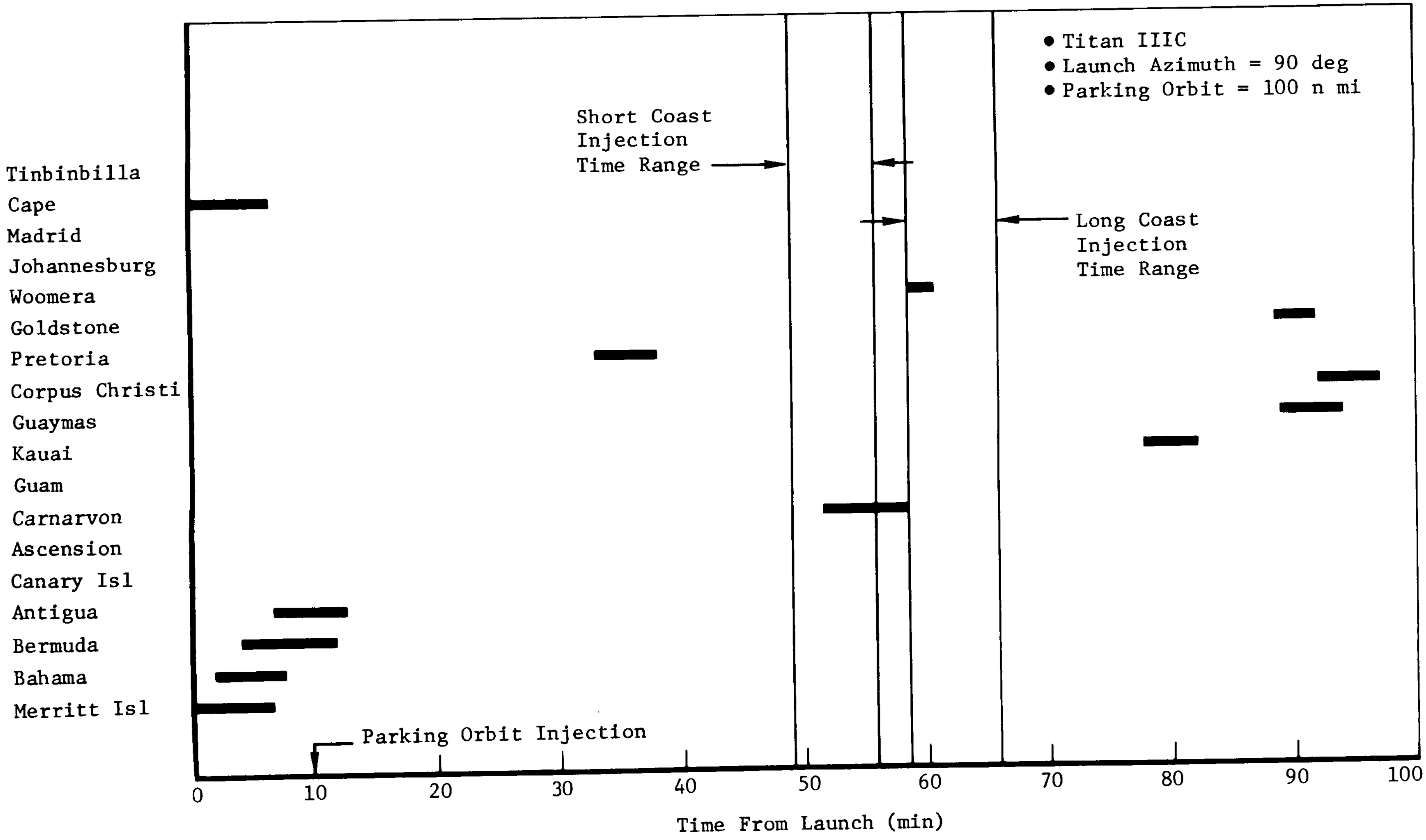

Figure A4-3: TRACKING STATION VIEW PERIODS---PARKING ORBIT COAST PHASE

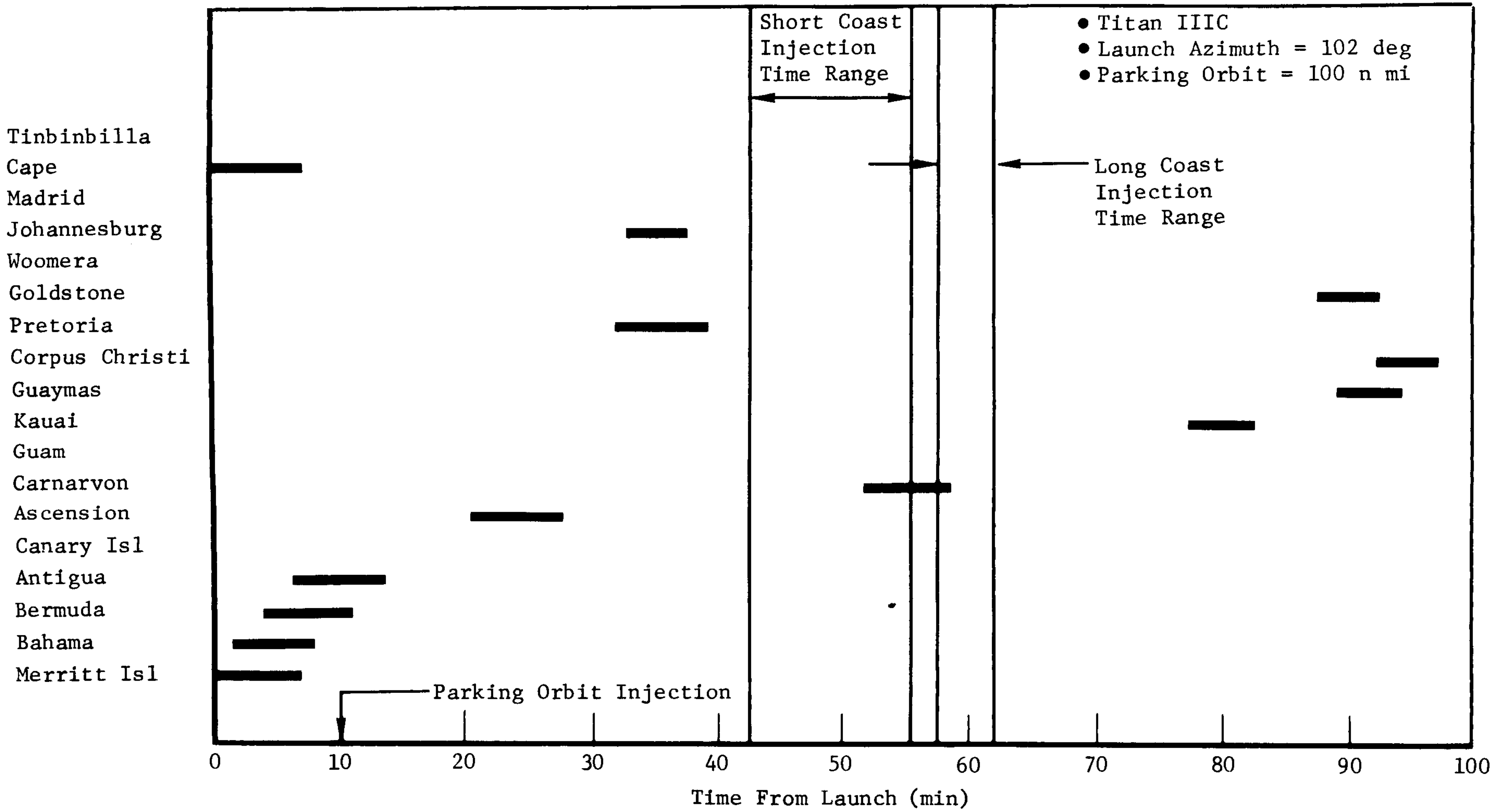

Figure A4-4: TRACKING STATION VIEW PERIODS---PARKING ORBIT COAST PHASE

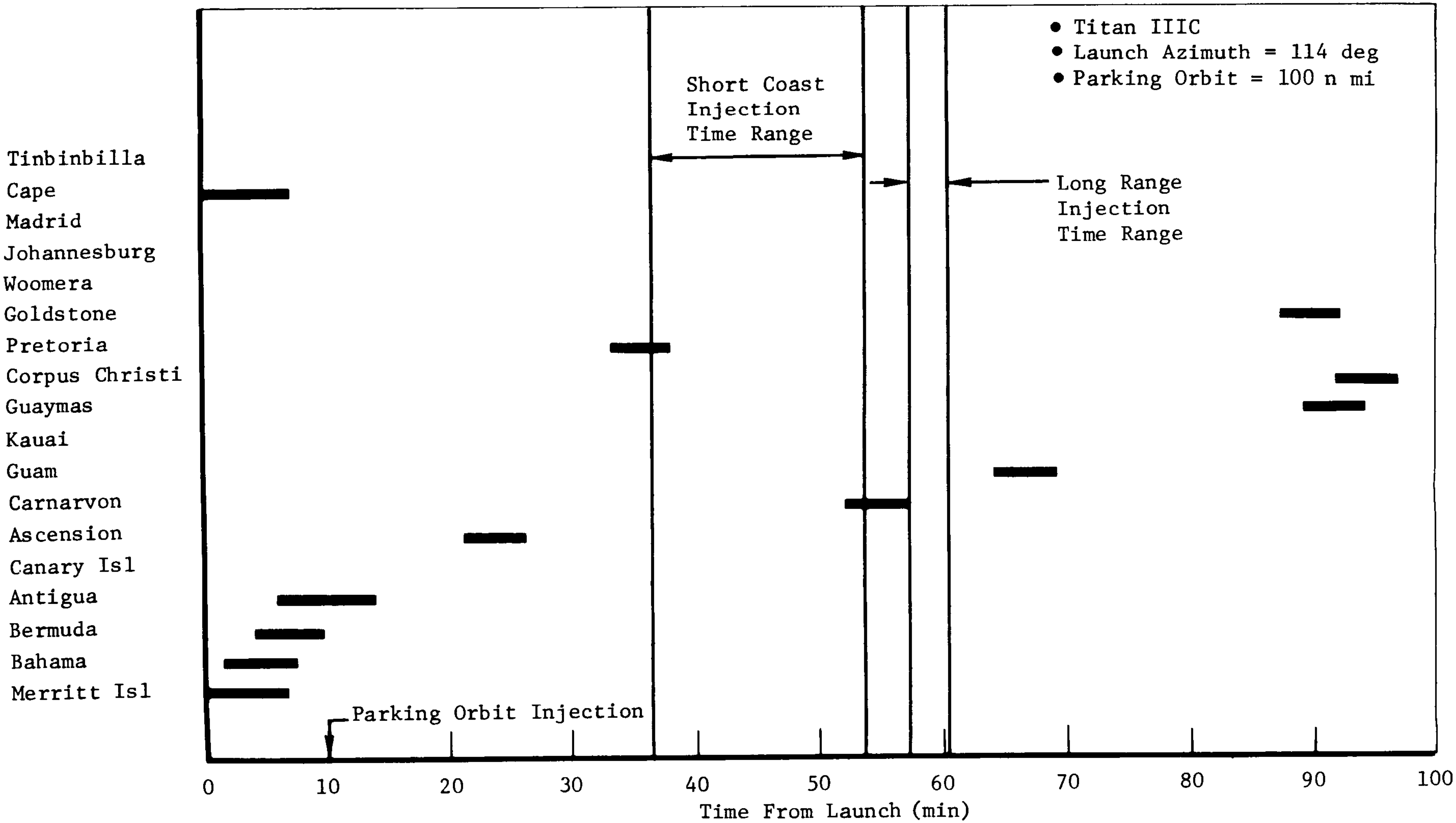

Figure A4-5: TRACKING STATION VIEW PERIODS---PARKING ORBIT COAST PHASE

injection when short holding orbit coasts are employed and long holding orbit injection when a full revolution is planned in the elliptical holding orbit. The injection is assumed to occur impulsively at zero flight-path angle at a 100 n mi altitude.

Figures A4-6 through A4-11 show the station coverage during the long holding orbit for launch on August 11, 1973. Three launch azimuths and both the short and long parking orbit coast solutions are investigated. Excellent station coverage is obtained everywhere except at perigee. Similar station coverage is obtained during the holding orbit for all launch days.

The tracking coverage obtained from the DSIF stations during the first 10 hours of the trans-Mars phase is shown in Figures A4-12 through A4-14. Figures A4-12 and A4-13 show tracking coverage for the short and long parking orbit coast solutions for missions where the spacecraft spends a full revolution in a long holding orbit with a period of 20.4 hours. Figure A4-14 illustrates the case where no holding orbit is employed. The data shown is typical and illustrates that continuous tracking during the trans-Mars phase is obtained soon after injection.

Ground tracks for the near-Earth phase are shown in Figures A4-15 through A4-17 for three launch azimuths for missions employing short parking orbit coasts and long holding orbits. If a short holding orbit is used, the spacecraft trans-Mars trajectory ground track will be coincident with the long holding orbit track for approximately 30 minutes. This track is shown in Figure A4-16.

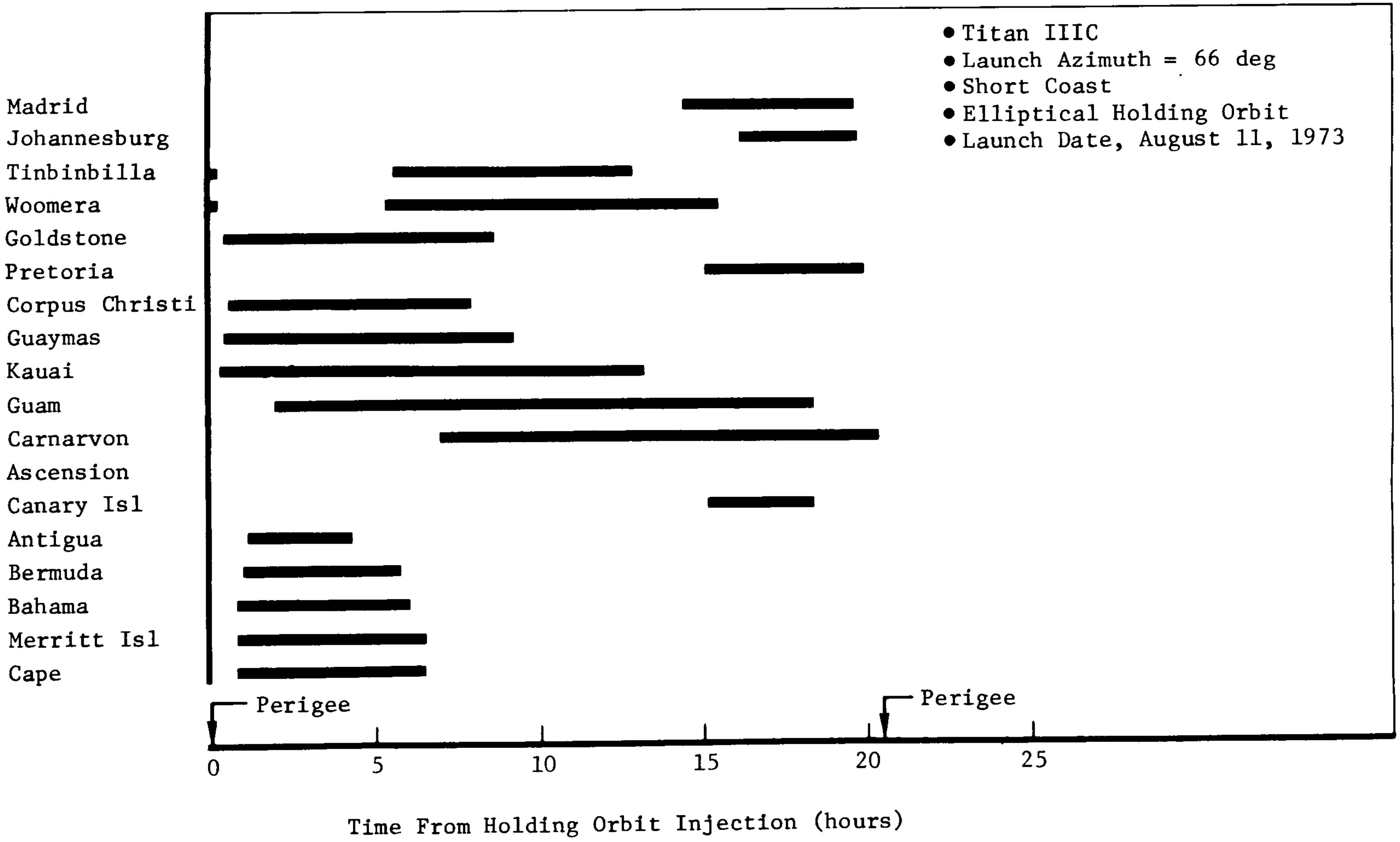

Figure A4-6: TRACKING STATION VIEW PERIODS---HOLDING ORBIT PHASE

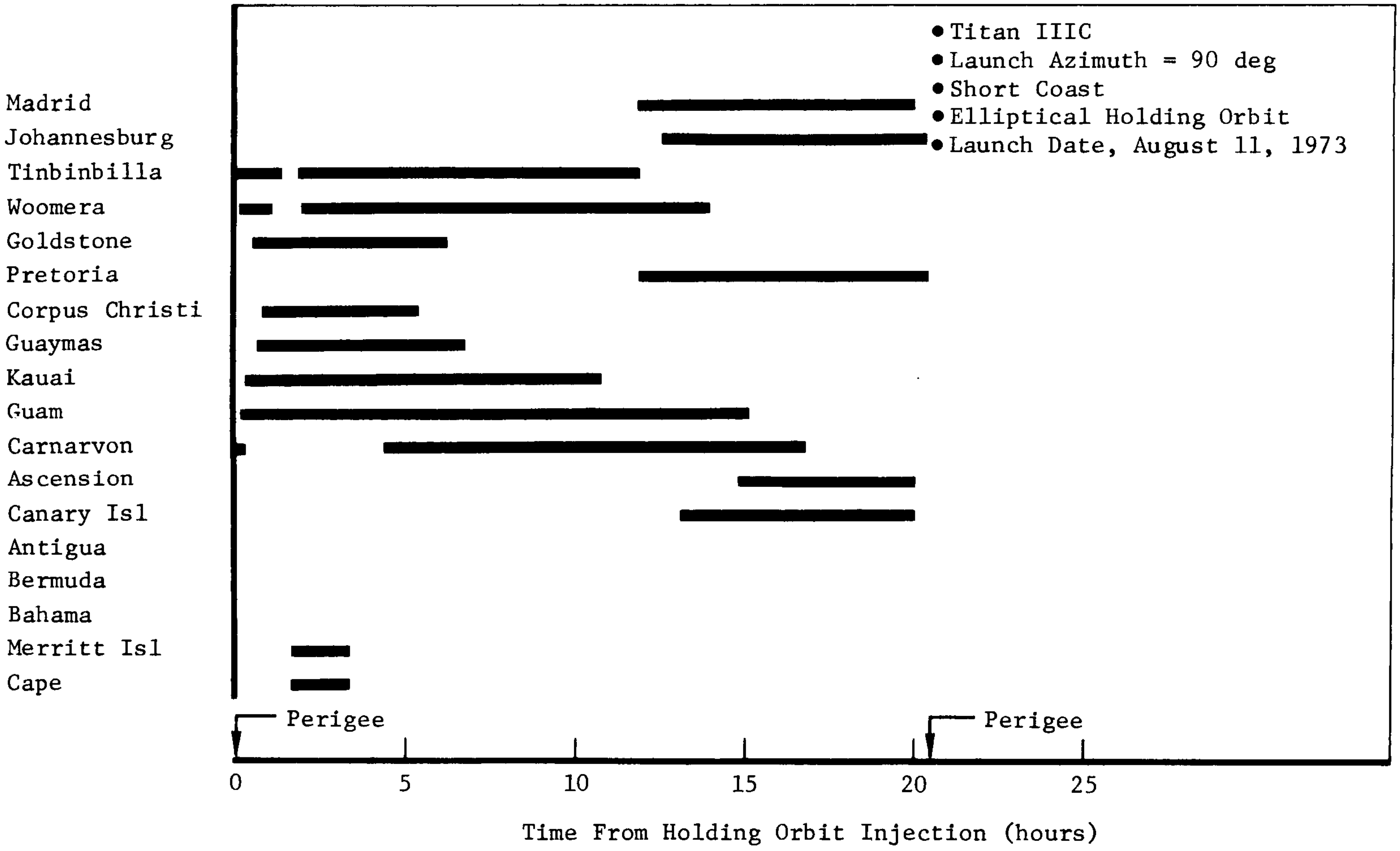

Figure A4-7: TRACKING STATION VIEW PERIODS---HOLDING ORBIT PHASE

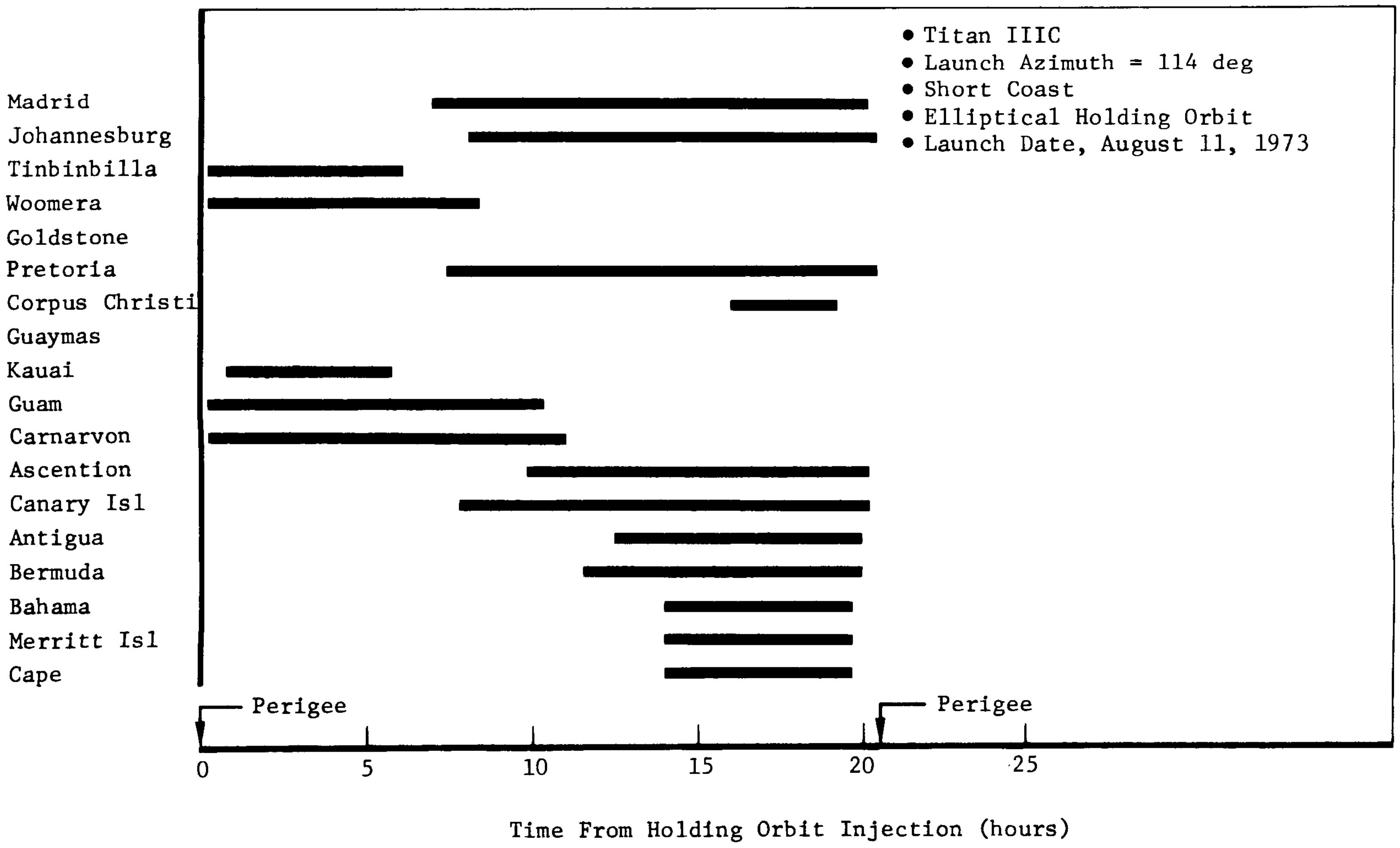

Figure A4-8: TRACKING STATION VIEW PERIODS---HOLDING ORBIT PHASE

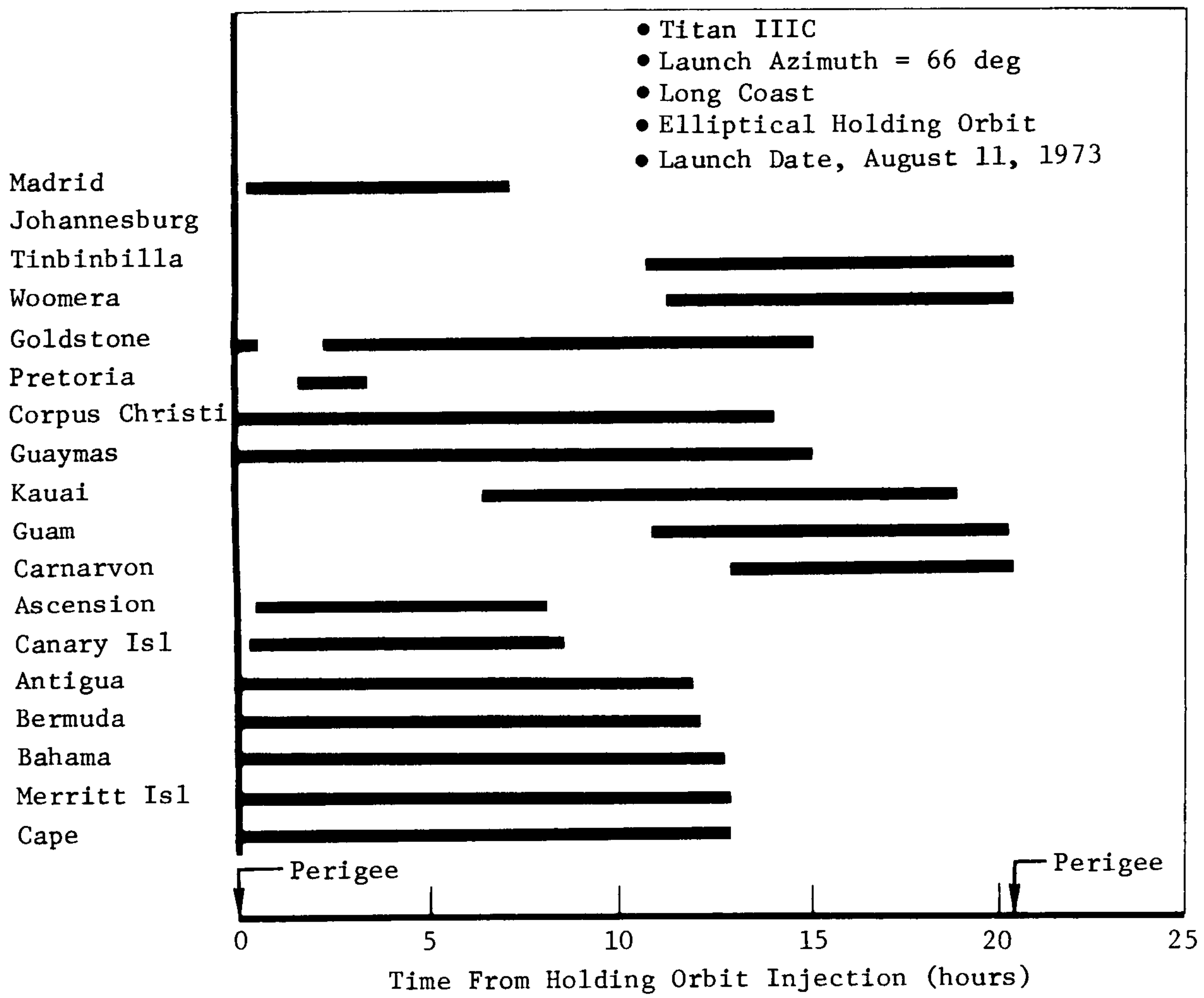

Figure A4-9: TRACKING STATION VIEW PERIODS---HOLDING ORBIT PHASE

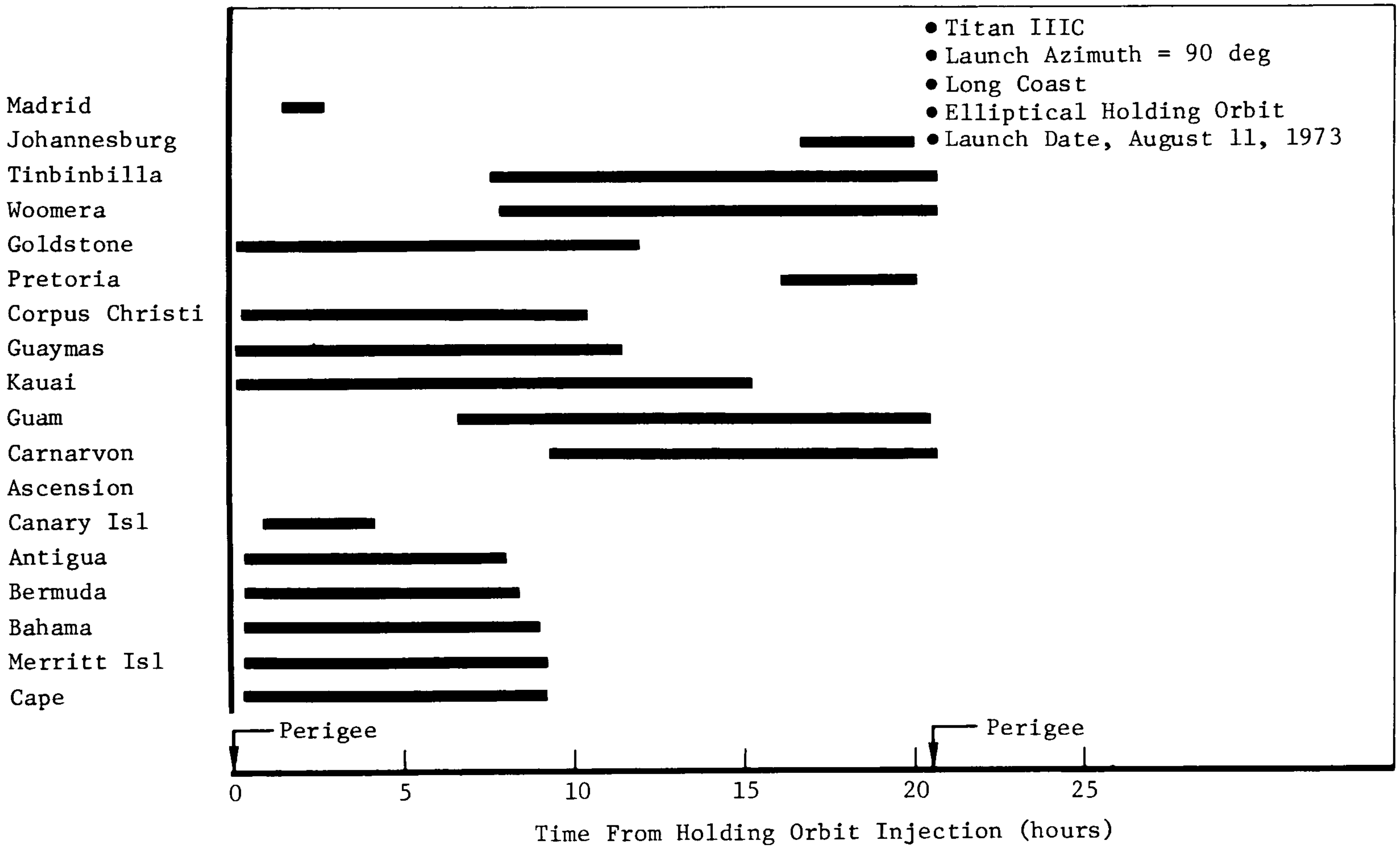

Figure A4-10: TRACKING STATION VIEW PERIODS---HOLDING ORBIT PHASE

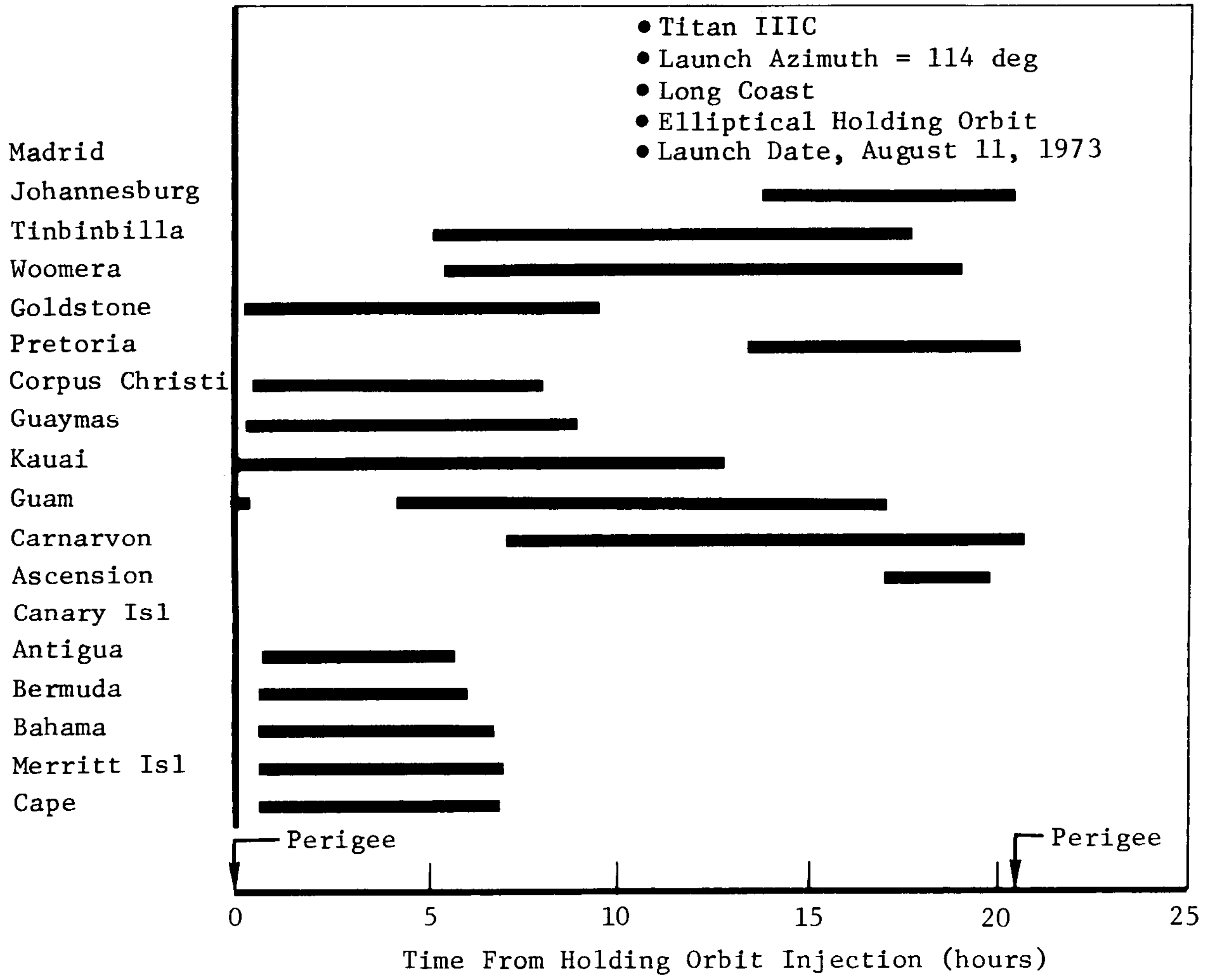

Figure A4-11: TRACKING STATION VIEW PERIODS---HOLDING ORBIT PHASE

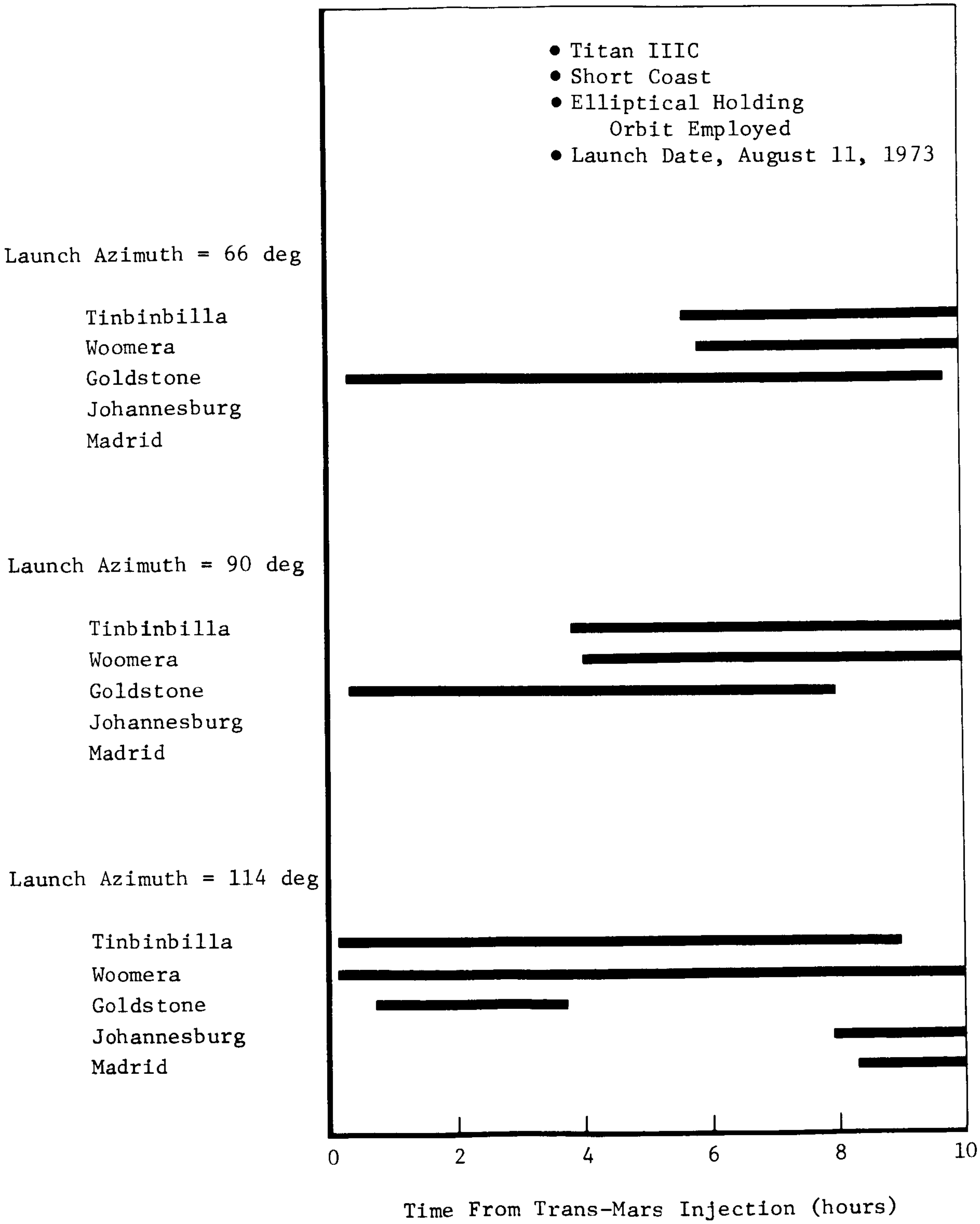

Figure A4-12: DSIF STATION COVERAGE---TRANS-MARS PHASE

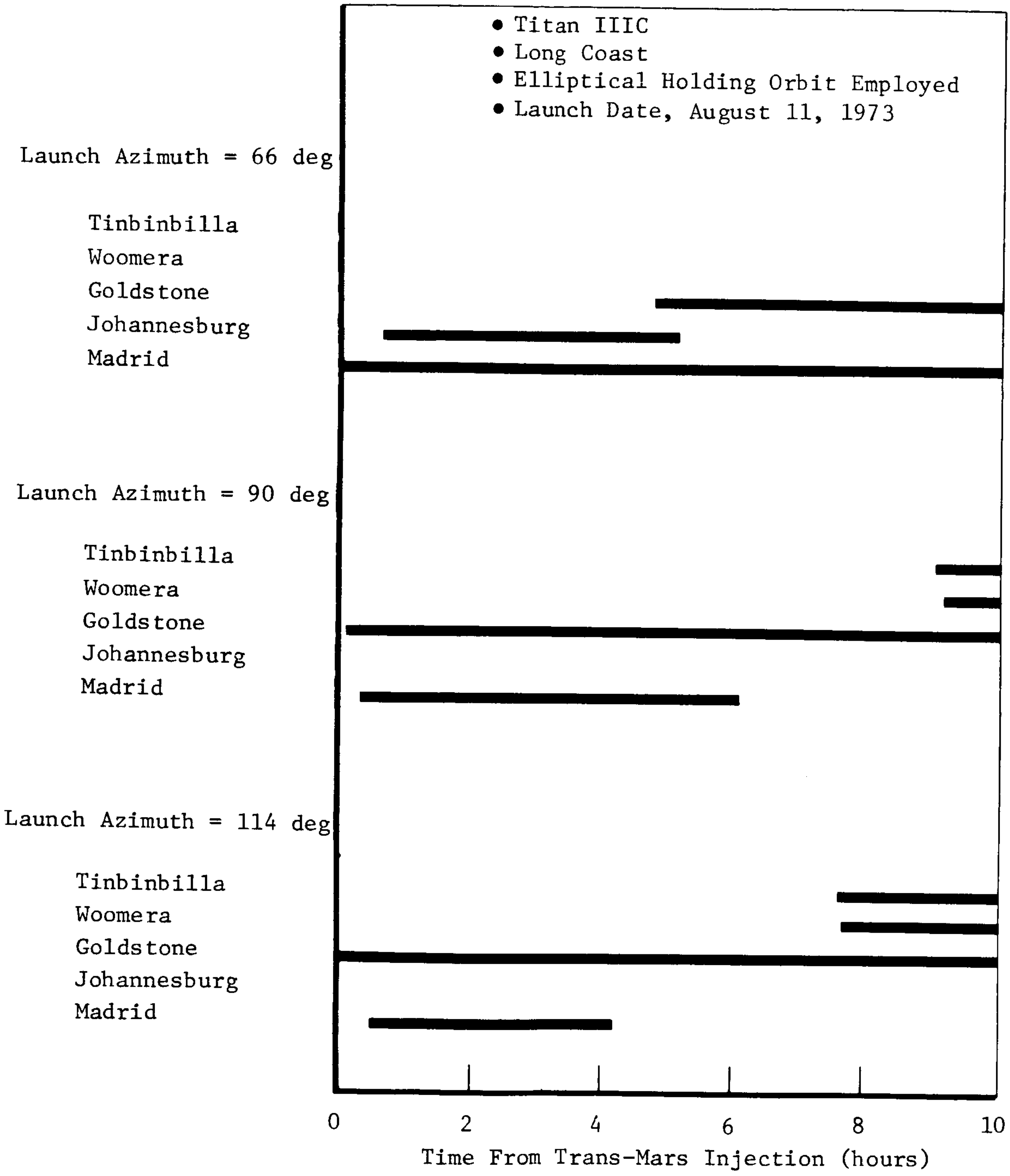

Figure A4-13: DSIF STATION COVERAGE---TRANS-MARS PHASE

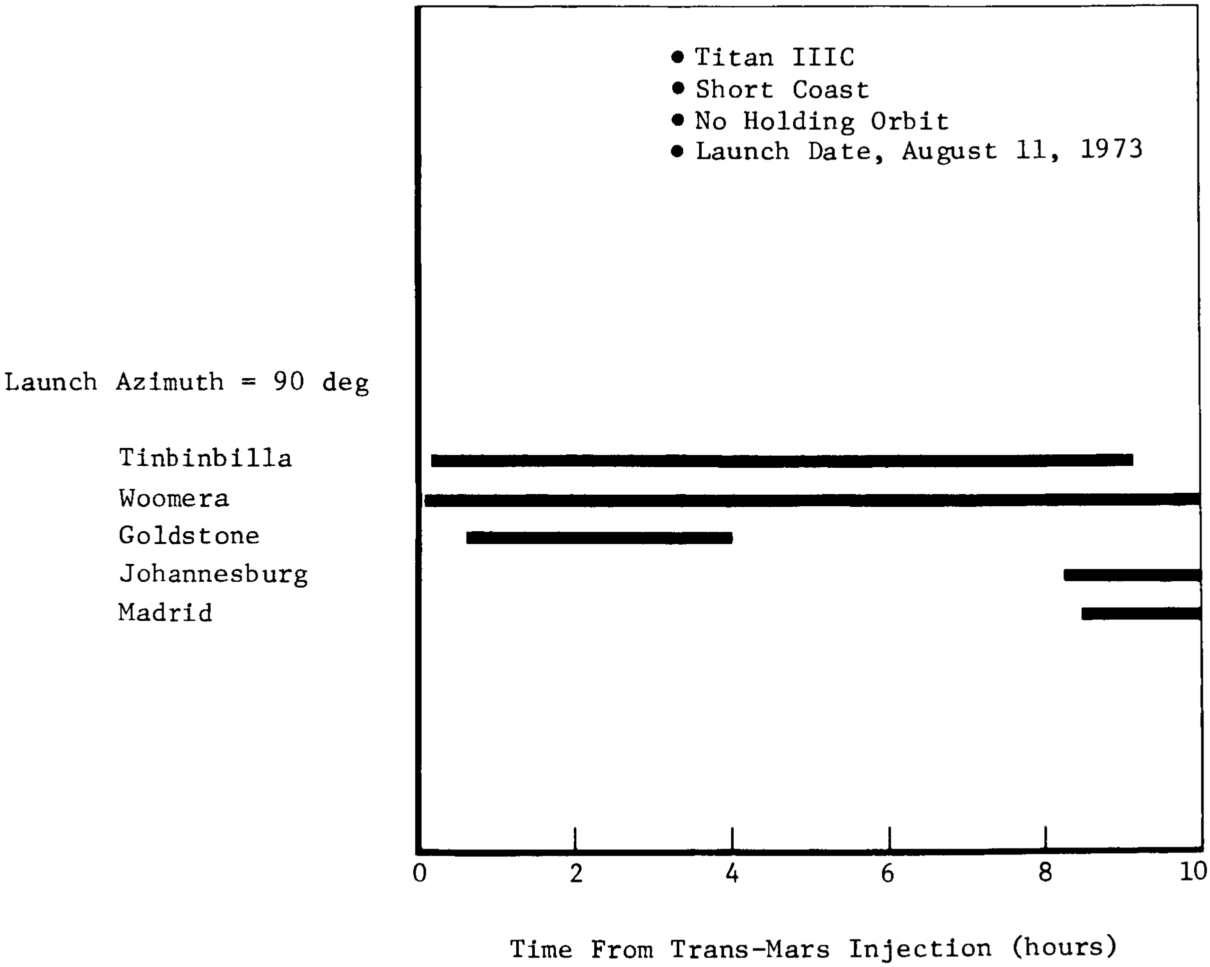

Figure A4-14: DSIF STATION COVERAGE---TRANS-MARS PHASE

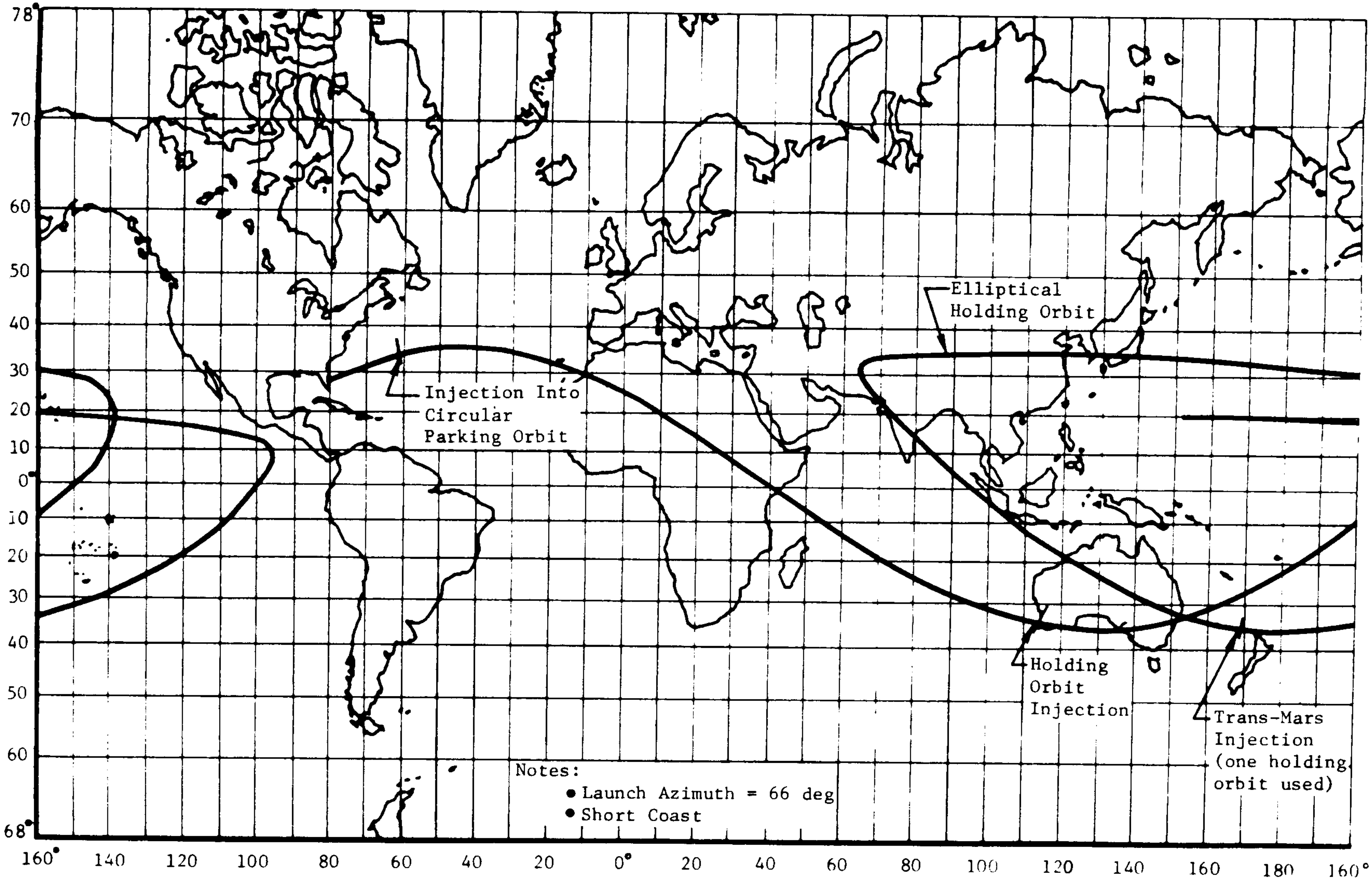
78
70
60
50
40
30
20
10
0
10
20
30
40
50
60
68
160
140
120
100
80
60
40
20
0°
20
40
60
80
100
120
140
160
180
160°
Elliptical Holding Orbit
Injection Into Circular Parking Orbit
Holding Orbit Injection
Trans-Mars Injection (one holding orbit used)

Notes:
- ● Launch Azimuth = 66 deg
- ● Short Coast

Figure A4-15: GROUND TRACK, LAUNCH TO TRANS-MARS INJECTION PLUS 10 HOURS

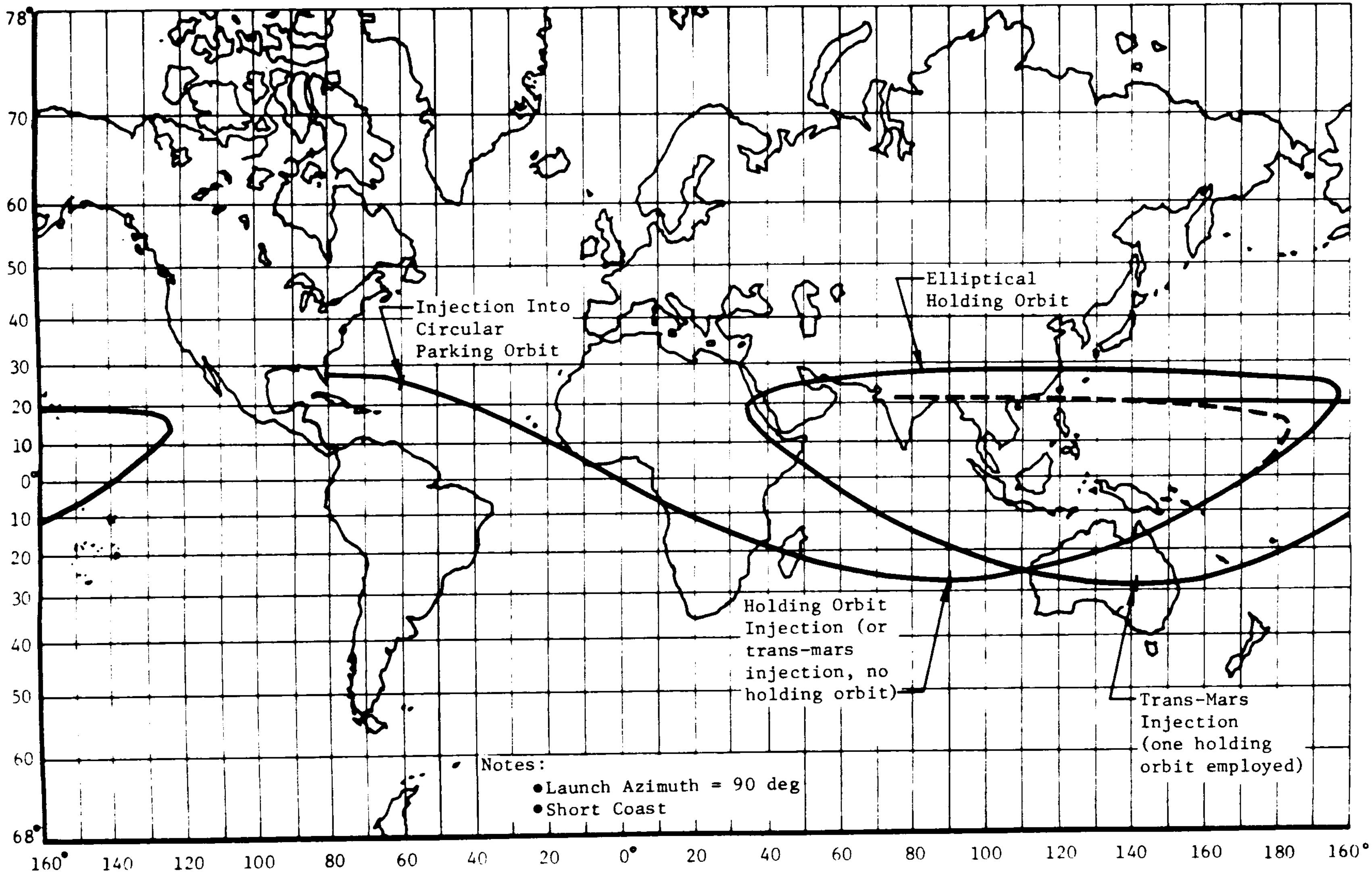
78
70
60
50
40
30
20
10
0
10
20
30
40
50
60
68
160
140
120
100
80
60
40
20
0
20
40
60
80
100
120
140
160
180
160
Injection Into Circular Parking Orbit
Elliptical Holding Orbit
Holding Orbit Injection (or trans-mars injection, no holding orbit)
Trans-Mars Injection (one holding orbit employed)
Notes:
● Launch Azimuth = 90 deg
● Short Coast

Figure A4-16: GROUND TRACK, LAUNCH TO TRANS-MARS INJECTION PLUS 10 HOURS

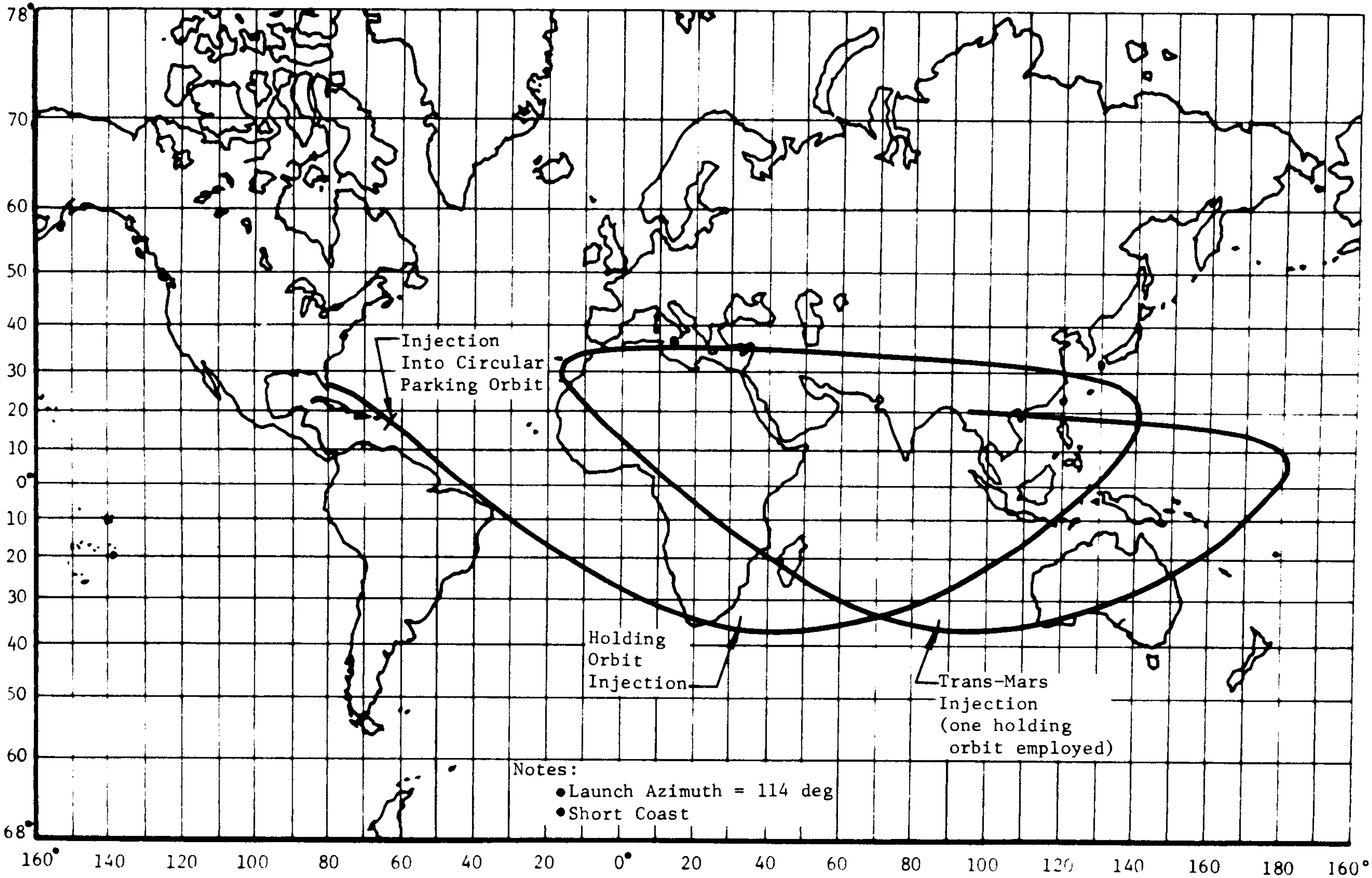

78
70
60
50
40
30
20
10
0
10
20
30
40
50
60
68
160
140
120
100
80
60
40
20
0
20
40
60
80
100
120
140
160
180
160°
Injection Into Circular Parking Orbit
Holding Orbit Injection
Trans-Mars Injection (one holding orbit employed)
Notes:
●Launch Azimuth = 114 deg
●Short Coast

Figure A4-17: GROUND TRACK, LAUNCH TO TRANS-MARS INJECTION PLUS 10 HOURS

# APPENDIX A5
# EVENT SEQUENCE ANALYSIS

*Long Holding Orbit Case*---The main problems affecting operational activities for this case are obtaining attitude references and sufficient tracking data to allow performance of orbit determination calculations. Obtaining celestial references is a problem because Van Allen belt radiation may preclude the use of a star tracker. Use of either a one- or two-axis horizon sensor is planned and described in detail in Appendix C. Two schemes of using horizon sensors were considered in the following operational analyses: use of a single-axis horizon sensor to determine the roll reference with the pitch and yaw axis in Sun lock, and use of a two-axis horizon scanner with a gyro-compassing technique to obtain a three-axis reference. Tracking data acquisition, orbit determination, and programmer updating are discussed as to how they affect operational aspects of the mission, and a schedule of the time period available for these activities is presented.

Tracking station view periods during the long holding orbit are shown in Appendix A4 for five launch azimuths. At time zero on these figures, the transtage is ignited the second time, placing it and the spacecraft in a highly elliptical Earth orbit. The burn is initiated while in the 100 n mi circular parking orbit, and it can be seen that the spotty coverage obtained at 100 n mi is quickly transformed into complete and redundant coverage for the 21-hour holding orbit, except for a few minutes near perigee. By 10 minutes after the transtage burn, the spacecraft is far enough from the Earth so as not to exceed the tracking rate capability of the prime 85-foot antennas. This is at a sufficiently early time in the holding orbit to allow tracking station coverage during the deployment and Sun-acquisition sequences (the 85-foot antennas can track when the spacecraft-to-Earth distance is approximately 600 n mi, which occurs early in the holding orbit). Therefore, command equipment is only required at the three prime 85-foot antenna sites, and there will be command capability during or very shortly after (a few minutes) the deployment sequence.

Figure A5-1 is an event sequence for the long holding orbit case. Prelaunch activities include countdown tests and checks, and impose no significant problems over a baseline Mars mission.

Launch of the Titan IIIC occurs followed by burnout of Stages 0, 1, 2, and transtage first burn, placing the transtage and attached spacecraft in a 100 n mi circular Earth orbit. After a coast period, the transtage is ignited a second time, placing the transtage and attached spacecraft in a highly elliptical Earth orbit (100 by 35,000 n mi). The transtage is then maneuvered so that the spacecraft solar panels will be oriented toward the Sun when deployment occurs. The transtage will also be maneuvered so that the spacecraft is in the best attitude for the Earth acquisition, which will occur later.

After completion of transtage maneuvering, the spacecraft gyros are switched from the rate mode to inertial hold, and separation of the spacecraft occurs followed by arming the attitude control subsystem. The TWTA is turned on,

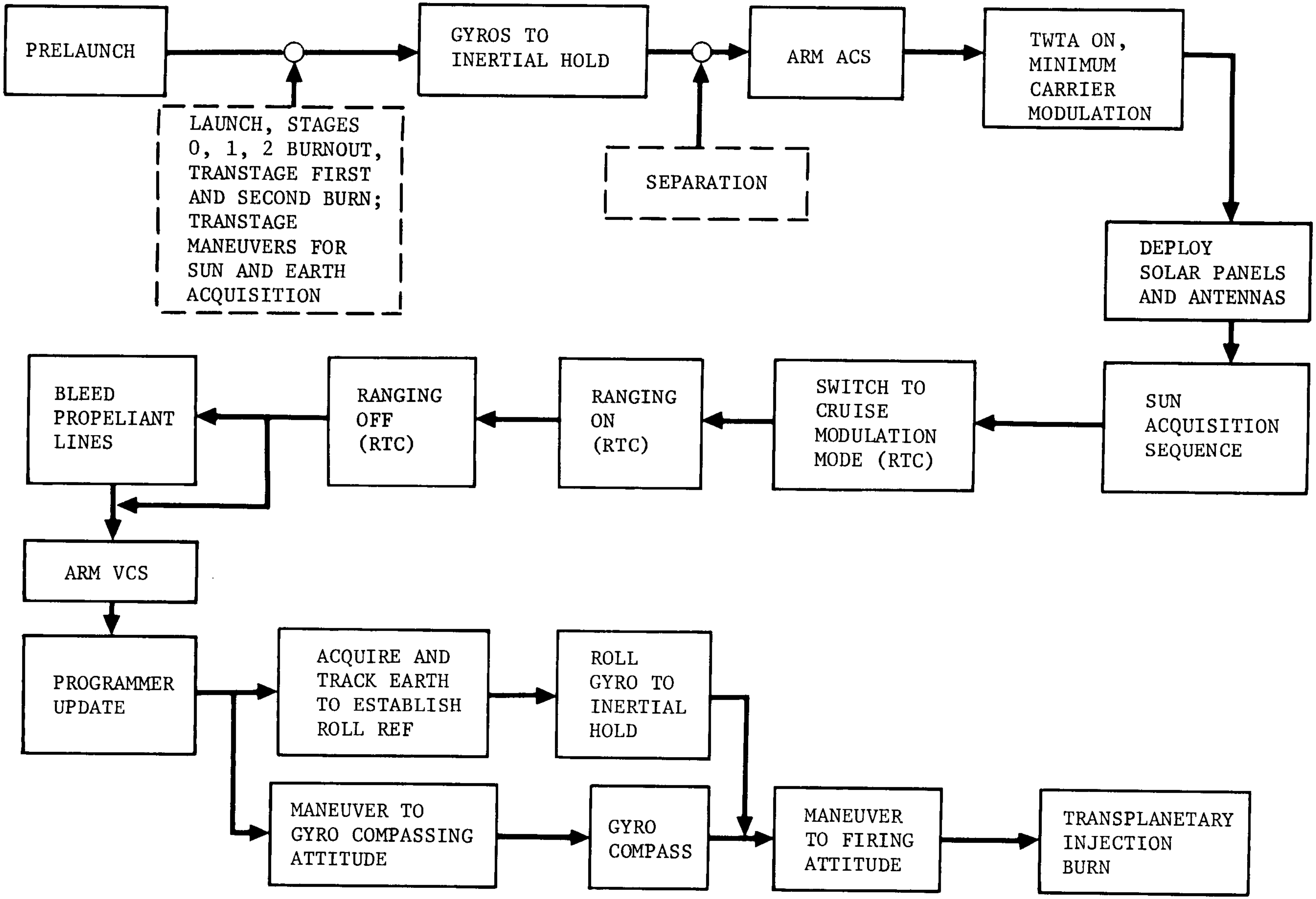
PRELAUNCH
LAUNCH, STAGES 0, 1, 2 BURNOUT, TRANSTAGE FIRST AND SECOND BURN; TRANSTAGE MANEUVERS FOR SUN AND EARTH ACQUISITION
GYROS TO INERTIAL HOLD
SEPARATION
ARM ACS
TWTA ON, MINIMUM CARRIER MODULATION
DEPLOY SOLAR PANELS AND ANTENNAS
SUN ACQUISITION SEQUENCE
SWITCH TO CRUISE MODULATION MODE (RTC)
RANGING ON (RTC)
RANGING OFF (RTC)
BLEED PROPELIANT LINES
ARM VCS
PROGRAMMER UPDATE
ACQUIRE AND TRACK EARTH TO ESTABLISH ROLL REF
ROLL GYRO TO INERTIAL HOLD
MANEUVER TO GYRO COMPASSING ATTITUDE
GYRO COMPASS
MANEUVER TO FIRING ATTITUDE
TRANSPLANETARY INJECTION BURN

Figure A5-1: LONG HOLDING ORBIT CASE EVENT SEQUENCE

with the best modulation mode for acquisition selected. Then the solar panels and antennas are deployed, and the Sun-acquisition sequence initiated. All of these spacecraft events following separation will be programmed to occur with as little delay as practical, allowing for settling, etc. It may be desirable to initiate these events by means of the staging sequence (versus the spacecraft programmer clock). The TWTA is turned on before deployment and Sun acquisition to provide a good probability that the tracking station(s) will be receiving data on these events as they occur.

The solar panels will be oriented toward the Sun before deployment, and Sun acquisition will occur rapidly after the sequence is initiated. Because the orbit period is approximately 21 hours, the solar panels must be deployed before the spacecraft velocity burn. This imposes constraints on the spacecraft boost-assist engine and/or solar panel and antenna (which would also normally be deployed) mechanical design.

Sometime during the deployment or Sun-acquisition sequence, the spacecraft signal should be acquired by one of the three prime 85-foot antennas (Goldstone, Tinbinbilla, or Madrid). As soon as practical after the Sun-acquisition sequence, the communications modulation mode will be commanded by real-time command (RTC) from the acquisition mode to the normal transplanetary cruise mode. A verification of spacecraft subsystem performance will be made at this point, and any housekeeping functions such as heater power, etc., will be commanded by RTC. A period of approximately 10 minutes should be adequate to verify subsystem performance. After completion of this activity, the spacecraft ranging unit will be commanded on by RTC, and the tracking station will turn ranging modulation on. The next several hours will be devoted to ranging, with no planned command activity and no maneuvers.

Figure A5-2 is a schedule showing the time required by flight-path analysis and command (FPAC) and spacecraft performance analysis and command (SPAC) activities involved in performing an orbit determination and updating the programmer. The injection maneuver will be programmed in the spacecraft at liftoff, requiring only a command fire time update and, possibly, maneuver attitude updates.

Spacecraft command activity and/or maneuvers will not be planned between 19 and 14 hours before the transplanetary injection burn. Ranging modulation would begin at 19 hours and be continued until data is unavailable. At 14 hours, an updated orbit determination would be started. After the tracking station has turned ranging modulation off, the spacecraft ranging unit will be commanded off by RTC. Bleeding the propellant lines, if required, and arming of the VCS will then occur. The propellant line bleed sequence could be accomplished by use of an RTC, but this is not recommended as it is a risky procedure. This is especially true due to the possible 12-minute delay in locking up the command system for a Mars spacecraft.

The later part of the orbit will be used to obtain an attitude reference. Either one of two techniques will be used: a single-axis horizon sensor to determine a roll reference, plus Sun sensors for pitch and yaw, or a two-axis horizon sensor and use of a gyro-compassing technique to obtain a three-axis reference. These techniques are described in Appendix C and are not repeated

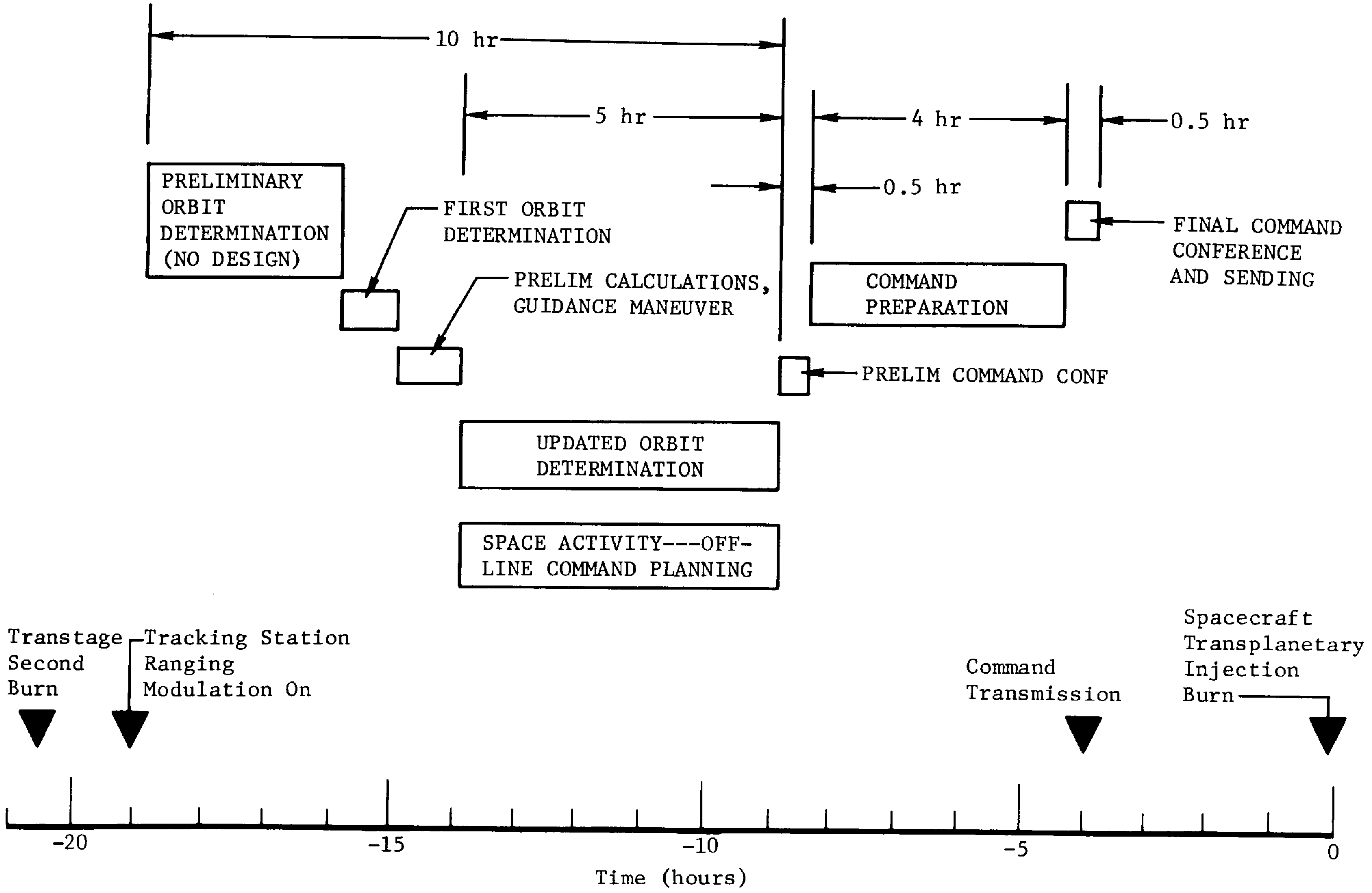
10 hr
5 hr
4 hr
0.5 hr
0.5 hr
PRELIMINARY ORBIT DETERMINATION (NO DESIGN)
FIRST ORBIT DETERMINATION
PRELIM CALCULATIONS, GUIDANCE MANEUVER
COMMAND PREPARATION
FINAL COMMAND CONFERENCE AND SENDING
PRELIM COMMAND CONF
UPDATED ORBIT DETERMINATION
SPACE ACTIVITY---OFF-LINE COMMAND PLANNING
Transtage Second Burn
Tracking Station Ranging Modulation On
Command Transmission
Spacecraft Transplanetary Injection Burn
-20
-15
-10
-5
0
Time (hours)

Figure A5-2: INJECTION MANEUVER ACTIVITY SCHEDULE

here. If the gyro-compassing technique is used, it will be performed in the last hour before injection burn. If the single-axis horizon sensor is used for the roll reference, the time of employing this technique will be a function of orbit geometry. To keep the roll gyro drift error low, the technique will have to be performed sometime in the last few hours before injection burn. Two alternate paths are shown in Figure A5-2 to include the use of either technique. Figure A5-3 shows the major operational activities occurring during the long holding orbit. The table below lists typical times for these operational events. (Note that these times are typical only and will vary as explained previously.)

Table A5-1: TYPICAL EVENT TIMES FOR LONG HOLDING ORBITS

| Time (hr:min) | Event |
|---|---|
| 00:00 | Transtage second burn |
| 00:10 | Prime station (DSS 12, 42, or 62) acquisition |
| 01:30 | Housekeeping functions complete, ranging modulation on |
| 11:30 | Ranging modulation off |
| 13:30 | Propellant line bleed sequence, arm VCS |
| 16:30 | Command transmission |
| 17:00 to 19:30 | Initiate attitude reference sequence |
| Perigee | Transplanetary injection burn |

From an operational viewpoint, the prolonged time in the Van Allen belt resulting from this long holding orbit will pose no operational problems otner than those involved in obtaining an attitude reference. No operational problems are anticipated in turning radiation sensors on or off, etc., once these constraints have been defined.

Should a serious operational or other problem occur during the long holding orbit, the injection burn could be aborted by an RTC up to a short time (20 to 30 minutes) before the burn and delayed for an orbit.

The following conclusions can be drawn for the long holding orbit case.

1) From an operational standpoint, the powered spacecraft concept is feasible for the long holding orbit case (see Appendix C, Section 2.0, *Initial Attitude Errors*). The questionable factor is obtaining an attitude reference and whetner the operational aspects of that activity are feasible. The period available to perform the operational activities required is adequate and the operational risk over a baseline mission is moderate.

2) If a problem occurs in obtaining the attitude reference, it is likely that insufficient time will be available to take corrective action and the injection maneuver will have to be aborted, at least for another orbit. The type of problem visualized here is a nonoperational problem.

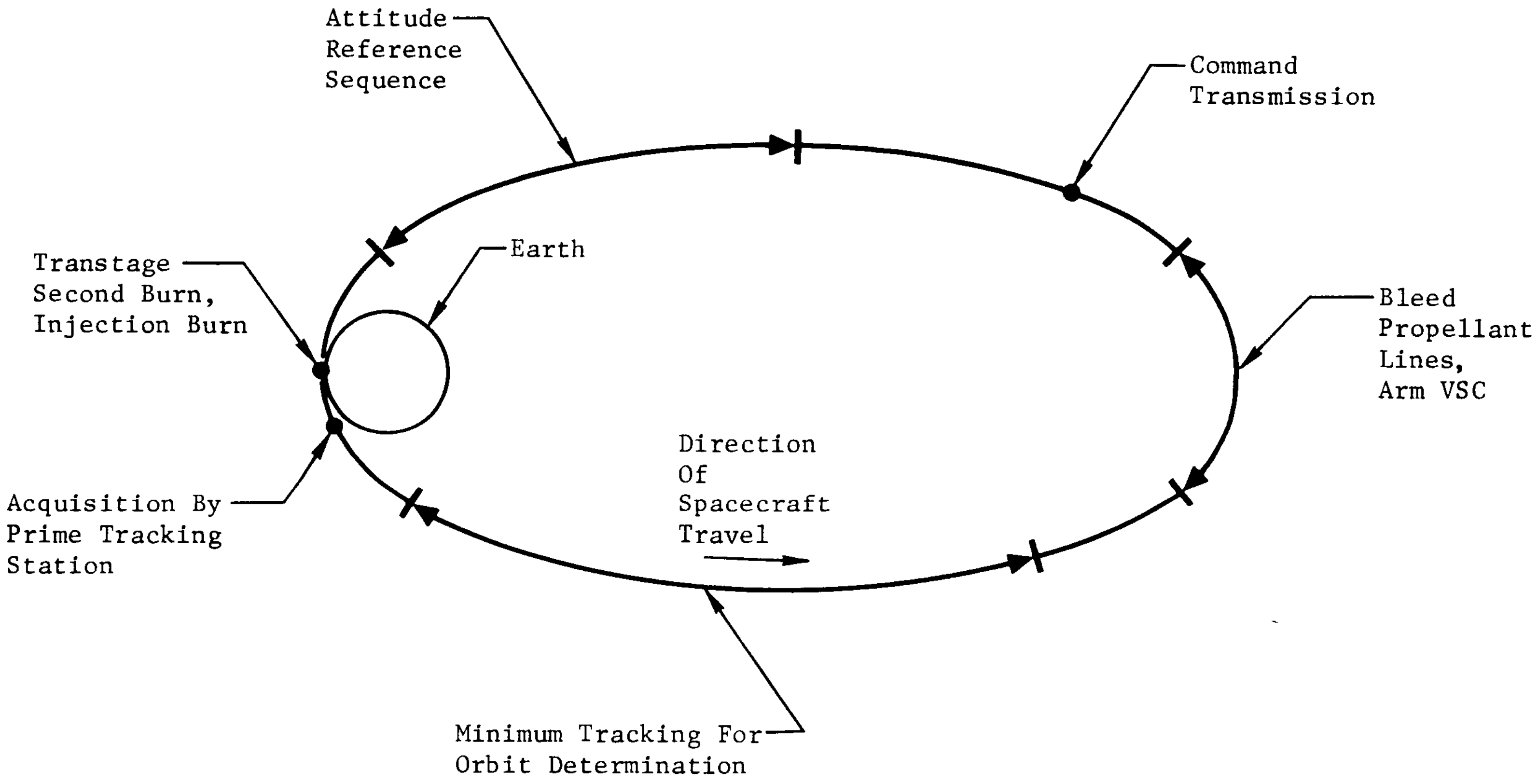
Attitude Reference Sequence
Command Transmission
Earth
Transtage Second Burn, Injection Burn
Bleed Propellant Lines, Arm VSC
Direction Of Spacecraft Travel
Acquisition By Prime Tracking Station
Minimum Tracking For Orbit Determination

Figure A5-3: MAJOR OPERATIONAL EVENTS DURING LONG HOLDING ORBIT

An operational fix to this type of problem is not likely if only one orbit is considered. If there is an abort capability (injection possible without too great a penalty on the second or later orbit), then the probability of solving a technical problem increases greatly.

3) Command capability is not available for 20 to 30 minutes before and during the spacecraft velocity burn.

4) Tracking station command capability is only required from the three prime 85-foot antenna stations.

5) It is desirable to have a spacecraft programmer capability to perform the propellant line bleed sequence independent of real-time command activity.

# APPENDIX A6
# MINIMUM VELOCITY BIT (MVB)

From the error analysis results of the Voyager Task D study (Reference 6), the second and third midcourse $\Delta V$ requirements were determined to be small, ranging from 7.2 down to 0.4 m/sec, $3\sigma$. Because the minimum $\Delta V$ bit capability of contemplated engine and attitude control subsystems is commonly within this same range of values or larger, it is expedient to investigate means to consume the balance of a minimum $\Delta V$ bit when it is larger than the individual midcourse requirement. Trade data is required to evaluate the feasibility of the concept, to allow choice of the method to be used, and to indicate the size of the minimum $\Delta V$ bit that can be allowed within an acceptable $\Delta V$ penalty. Such data is provided below, with the following discussions treating in turn three approaches to the problem:

- Adjust midcourse aim point biasing
- $\Delta V$ dumping in the noncritical direction
- Shift midcourse correction times

The general assumptions used in the analyses are as follows.

1) The trajectory is the 1973 Voyager Task D error analysis trajectory for the middle launch date of August 17, 1973.* The middle trajectory requires the lowest midcourse $\Delta V$'s, and therefore presents the largest problem concerning MVB's.
2) The spacecraft attitude and velocity control subsystem errors used are: $3\sigma$ pointing = 2.4 degrees, $3\sigma$; scale factor = 1%, $3\sigma$; shutoff = 0.05 m/sec.
3) Orbit trim will not present an MVB problem because the $\Delta V$'s in the range of interest can readily be dumped out of plane with relatively insignificant consequences. Specifically, a plane change of only 0 degrees, 27 minutes is required to consume an entire 6-m/sec $\Delta V$ bit for a bounding case of a trim at apoapsis with $h_p$ = 500 km, $h_a$ = 18,600 km.

*Adjust Midcourse Aim Point Biasing (to always require at least the MVB for each maneuver)*--The aim points for each of the three midcourse corrections are different (see Section 5.6.4 of Reference 6) because of the contamination constraint. The approach here is to make the aim points sufficiently different so that even in the presence of trajectory guidance and control dispersions, at least the MVB will always be required. The logic behind the determination of the new specific aim points is diagrammed in Figure A6-1.

Concerning Figure A6-1, an assumption was made that the larger $3\sigma$, post-third-midcourse trajectory dispersion around the new third midcourse aim point should lie outside a similar boundary determined in the Task D Voyager study. This

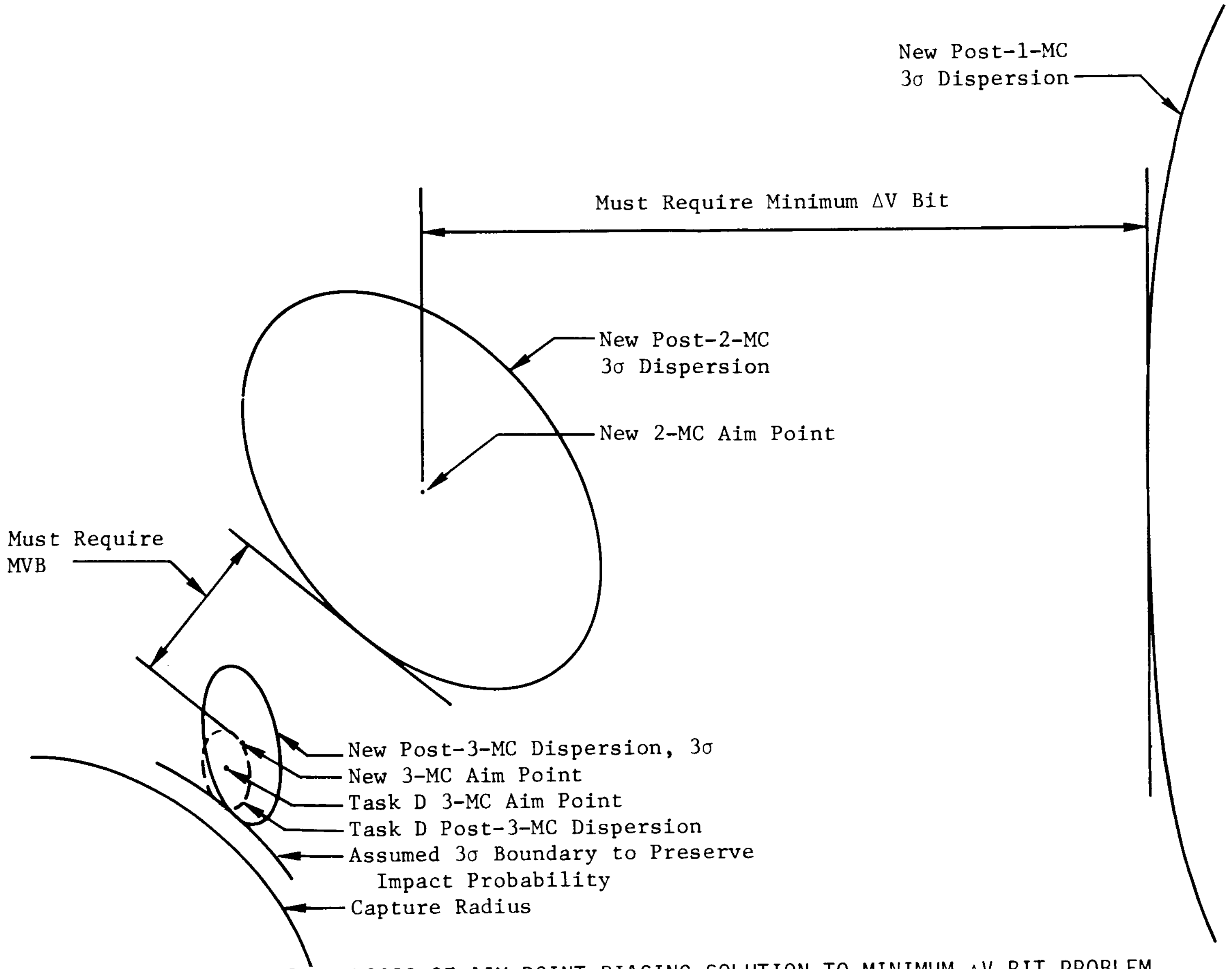
New Post-1-MC
3σ Dispersion
Must Require Minimum ΔV Bit
New Post-2-MC
3σ Dispersion
New 2-MC Aim Point
Must Require
MVB
New Post-3-MC Dispersion, 3σ
New 3-MC Aim Point
Task D 3-MC Aim Point
Task D Post-3-MC Dispersion
Assumed 3σ Boundary to Preserve
Impact Probability
Capture Radius

Figure A6-1: LOGIC OF AIM POINT BIASING SOLUTION TO MINIMUM ΔV BIT PROBLEM

preserves approximately the same impact probability without the need for rerunning probability data. Aim points for the second and third midcourses were moved radially outward from the Task D locations, and the first midcourse aim point was located relative to the second in the same direction as for Task D. Because post-midcourse dispersions are not accurately predictable until the previous maneuver has been analyzed, an iterative procedure was required.

The results of the analysis are summarized in Figures A6-2 and A6-3. The increasing miss distances of the first and second midcourse aim points for MVB's over about 3 m/sec would cause some degradation in data from a flyby mission in case of engine failure. Total midcourse $\Delta V$ increases somewhat significantly with MVB. The encounter errors accompanying the larger midcourse corrections are large (Figure A6-4). Note that the plots of Figure A6-4 are $1\sigma$ except for the $\Delta V$ curve.

Encounter errors increase significantly with increasing MVB's, but a hard constraint is not well defined. These encounter errors must be accommodated by suitable adjustments to the Mars orbit parameters, with a probable insertion $\Delta V$ penalty. Further, the Mars orbit, if intolerable for a specific mission, must be corrected by subsequent orbit trim maneuvers with additional $\Delta V$ penalties. An estimate of the total $\Delta V$ penalty of insertion plus trim for accommodating given encounter errors and correcting Mars orbit size is shown in Figure A6-6 with the total $\Delta V$ penalties of MVB's in Figure A6-7.

*$\Delta V$ Dumping in Noncritical Direction*---The direction normal to the plane formed by the gradient vectors of $\partial\vec{B}\cdot\hat{T}/\partial\dot{X}$ and $\partial\vec{B}\cdot\hat{R}/\partial\dot{X}$ is termed the noncritical direction. Midcourse velocity added in this direction affects only the final planet encounter time. It is postulated that a limited amount of variation in planet encounter time can be tolerated without significant consequences regarding the mission. Therefore, a vector component can be added or "dumped" in this direction to yield a total $\Delta V$ equal to the MVB. The logic of accomplishing a second moment error analysis employing this technique is diagrammed in Figure A6-3.

The results of the analysis are summarized in Figure A6-5. A breakpoint in the curve of $\Delta$ encounter time appears at an MVB of about 4 m/sec. One possible hard constraint on $\Delta$ encounter time is visibility of the insertion maneuver by the Goldstone DSN tracking station. For the 1973 opportunity, the visibility period above 5 degrees over the horizon is 12 hours, 54 minutes, giving a potential encounter time tolerance of ± 6 hours, 27 minutes. Variation in encounter time also affects the ground trace of the Mars orbit with time, and causes a negligible shift of the orbit relative to the terminator. No mission requirement is recognized at this time that would require holding encounter time tolerance to less than say the above discussed 6 hours.

The encounter errors accompanying the larger midcourse corrections are again significant. Total midcourse $\Delta V$ increases only slightly with increasing MVB; however, the insertion and trim $\Delta V$ penalty required in accommodating the larger B.T and B.R errors (as described in the aim point bias approach) is again significant (see Figure A6-6). The total $\Delta V$ penalties (midcourse plus insertion and trim) of both the "aim point biasing" and "$\Delta V$ dumping" approaches are shown in Figure A6-7 as a function of the MVB size.

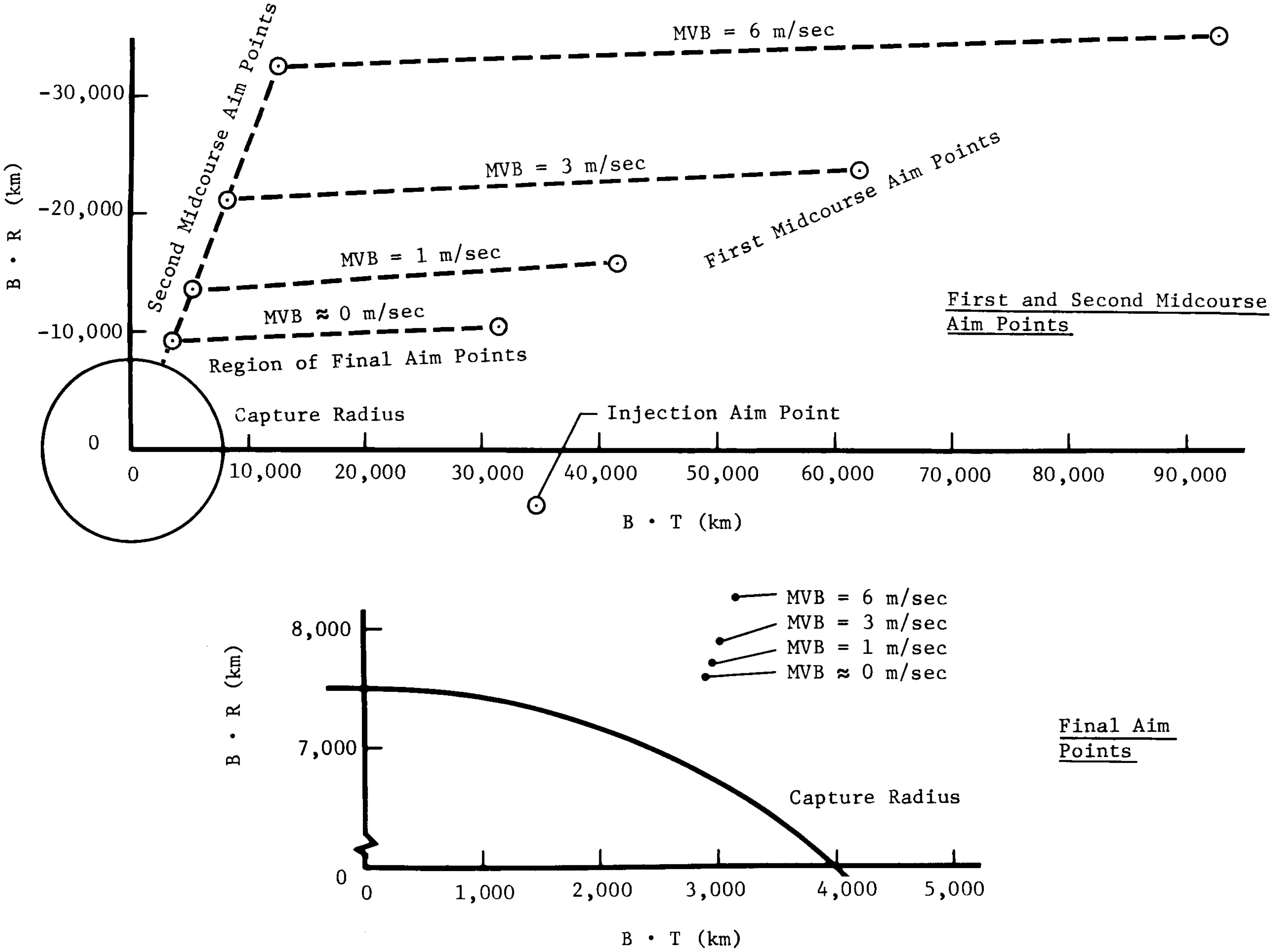

Figure A6-2: AIM POINT BIASING TO ACCOMMODATE MINIMUM ΔV BIT (MVB) SIZES

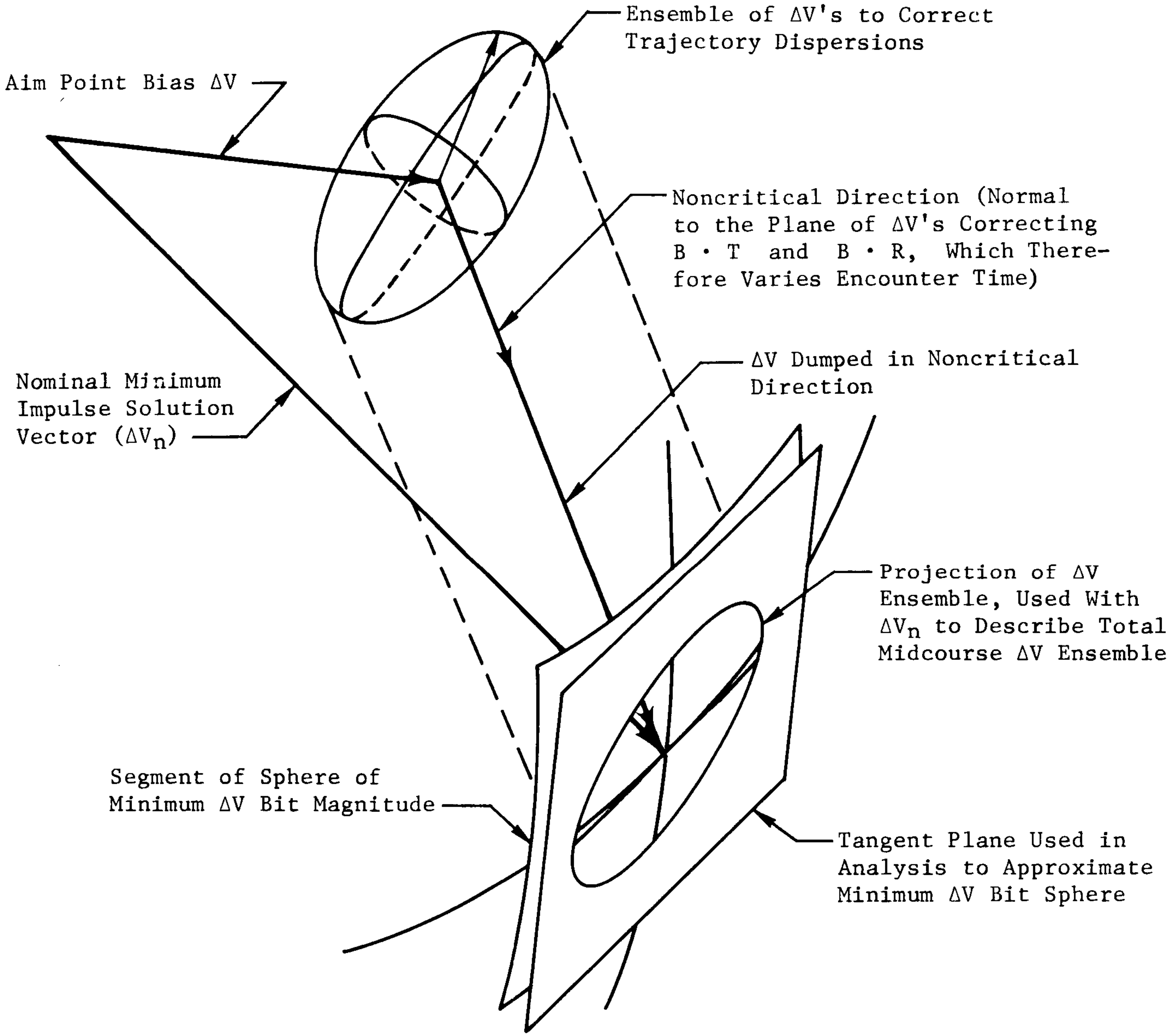
Ensemble of $\Delta V$'s to Correct Trajectory Dispersions
Aim Point Bias $\Delta V$
Noncritical Direction (Normal to the Plane of $\Delta V$'s Correcting $B \cdot T$ and $B \cdot R$, Which Therefore Varies Encounter Time)
$\Delta V$ Dumped in Noncritical Direction
Nominal Minimum Impulse Solution Vector ($\Delta V_n$)
Projection of $\Delta V$ Ensemble, Used With $\Delta V_n$ to Describe Total Midcourse $\Delta V$ Ensemble
Segment of Sphere of Minimum $\Delta V$ Bit Magnitude
Tangent Plane Used in Analysis to Approximate Minimum $\Delta V$ Bit Sphere

Figure A6-3: ENCOUNTER ERRORS ACCOMPANYING AIM POINT BIASING SOLUTION TO VARIOUS MINIMUM $\Delta V$ BIT (MVB) SIZES

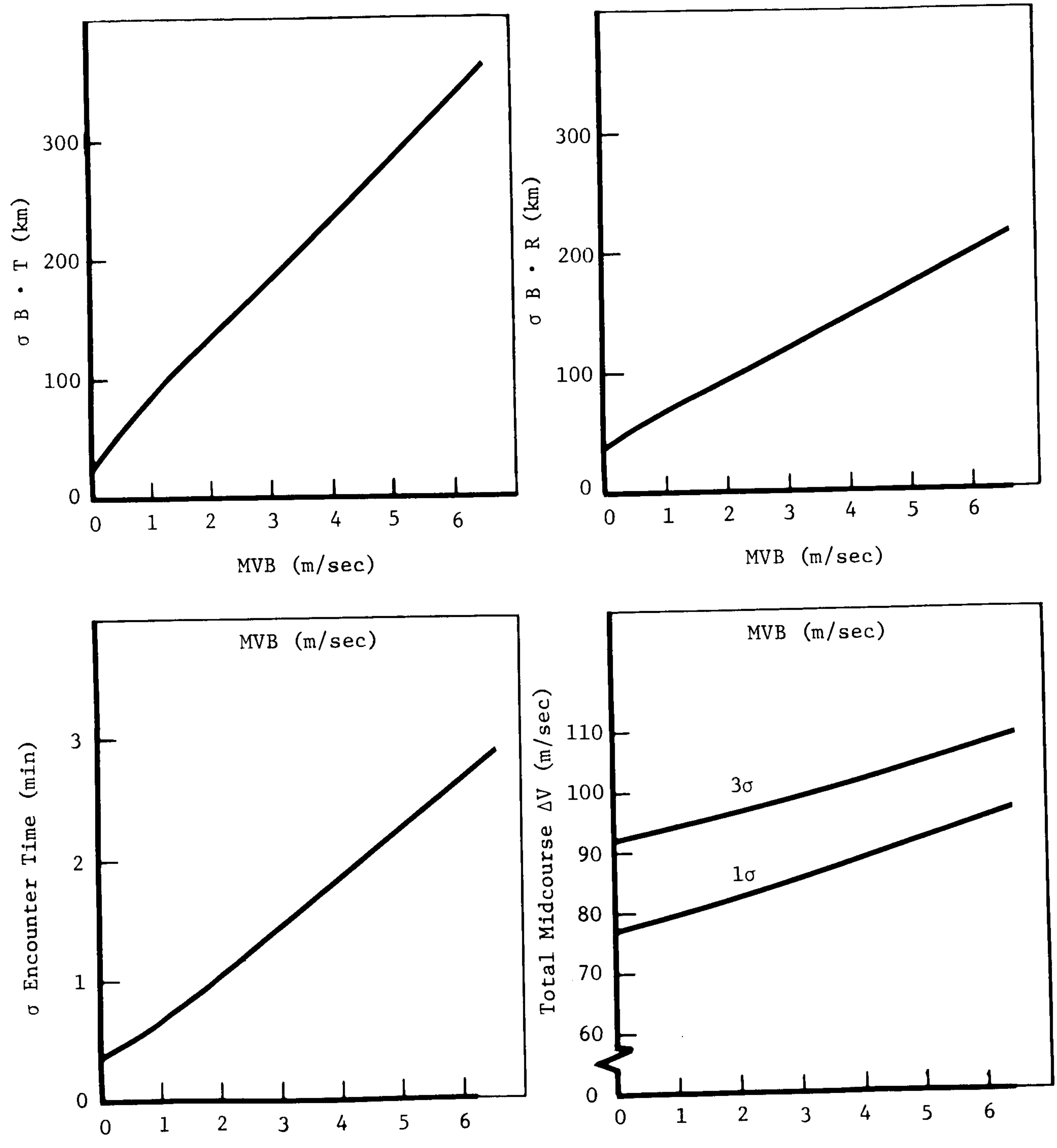

Figure A6-4: LOGIC OF ΔV DUMPING IN NONCRITICAL DIRECTION SOLUTION TO MINIMUM IMPULSE BIT PROBLEM

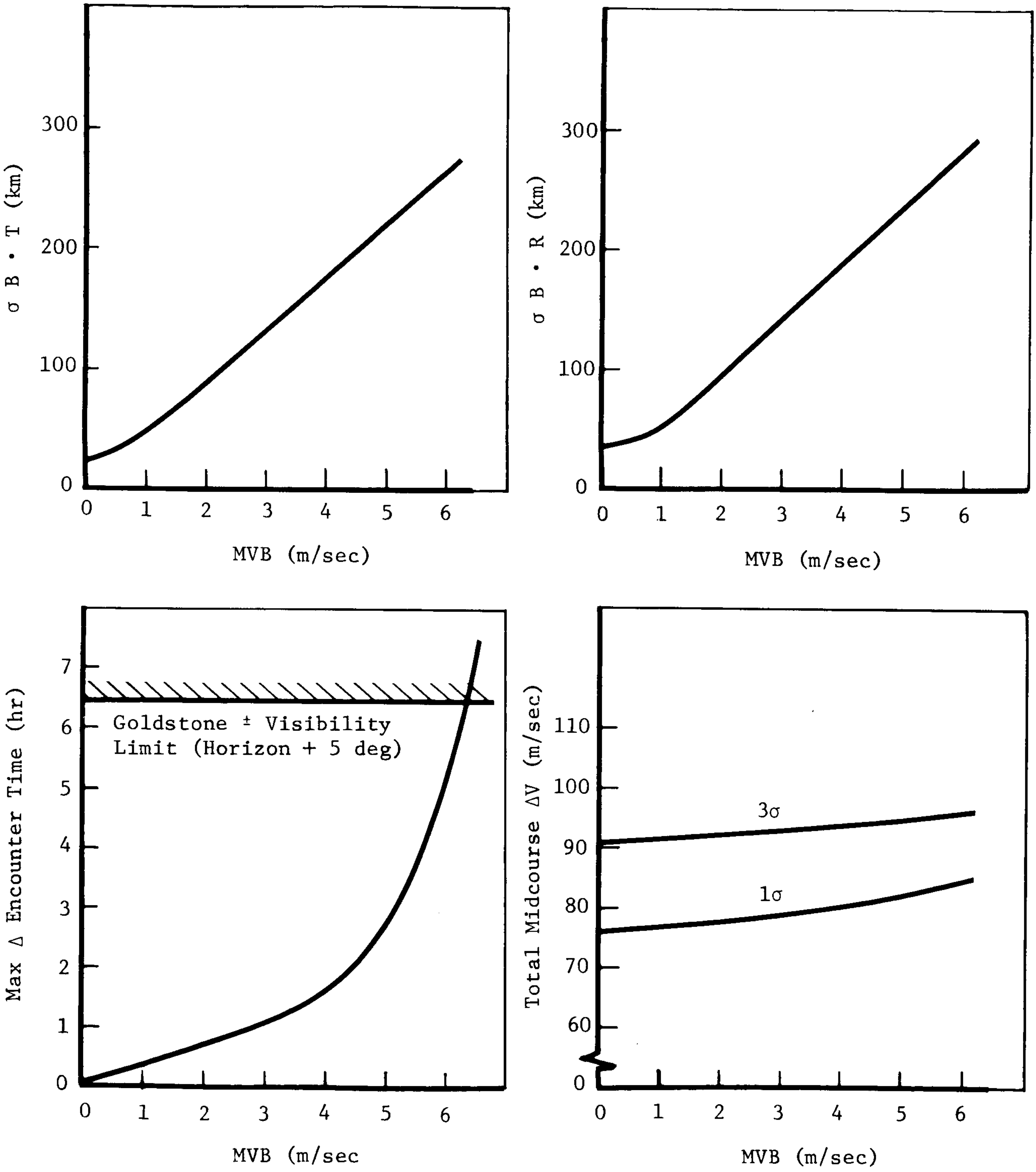

Figure A6-5: ENCOUNTER ERRORS ACCOMPANYING ΔV DUMPING IN NONCRITICAL DIRECTION SOLUTION TO VARIOUS MINIMUM ΔV BIT SIZES

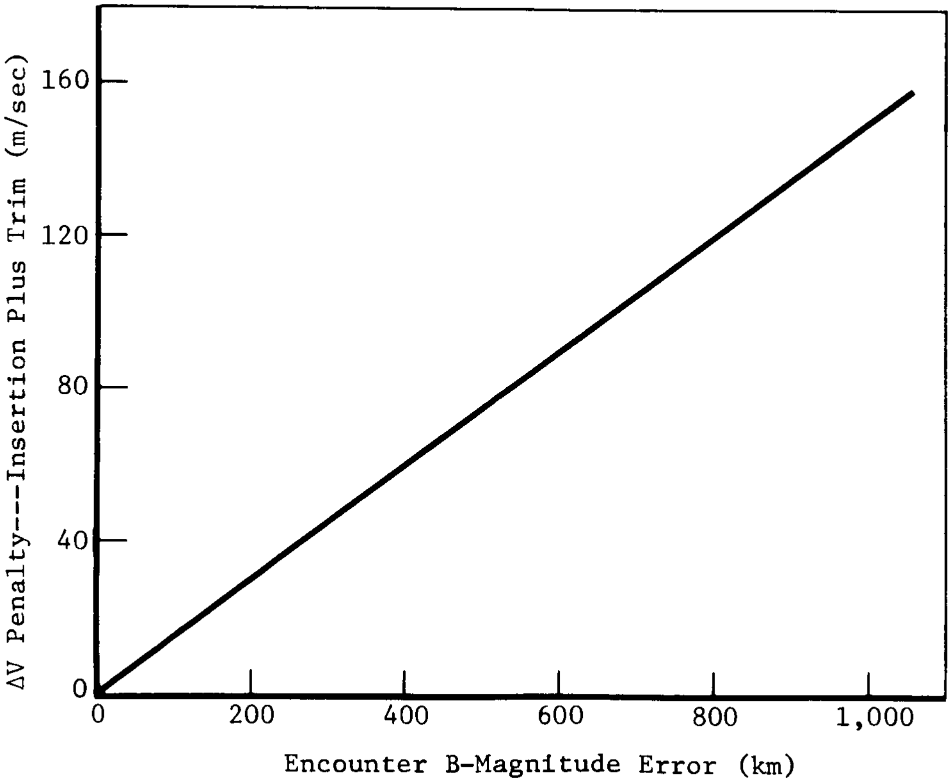

Figure A6-6: ESTIMATED MARS INSERTION AND CONSEQUENT ORBIT TRIM ΔV PENALTIES FROM PLANET ENCOUNTER ERRORS

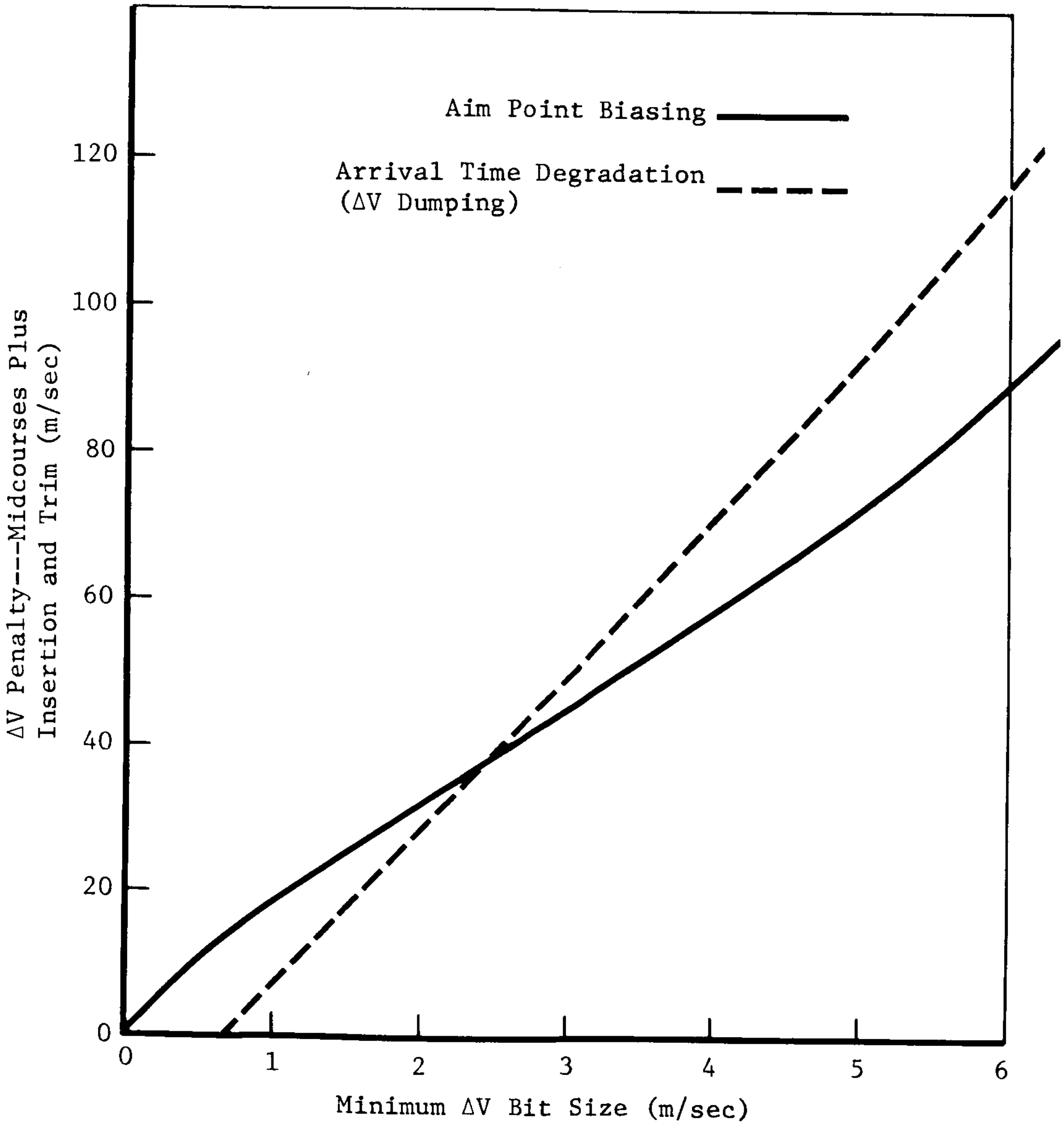

Figure A6-7: TOTAL ΔV PENALTIES

*Shift Midcourse Time*---The midcourse $\Delta V$ required to correct a given dispersion increases as the time for the midcourse is delayed (Figure A6-8). Thus, a potential solution to the MVB problem is to delay the midcourse time. However, for the Mars mission, three midcourse corrections are highly probable, each correcting about two magnitudes of error. From the third midcourse plots of Figure A6-8, it is seen that even for a second midcourse at 25 days, the third midcourse for a $1\sigma$ size error would have to be delayed from the nominal T-10 days to probably T-2 days to result in 1 m/sec. Two days is about the limit to still allow adequate tracking time for post-third-midcourse orbit determination. However, to increase the second midcourse $1\sigma$ $\Delta V$ requirement to even 1 m/sec would require delaying the second midcourse time from 25 to about 120 days, further complicating the third midcourse MVB problem. The method is therefore concluded to be impractical for MVB's in the range of 1 to 6 m/sec.

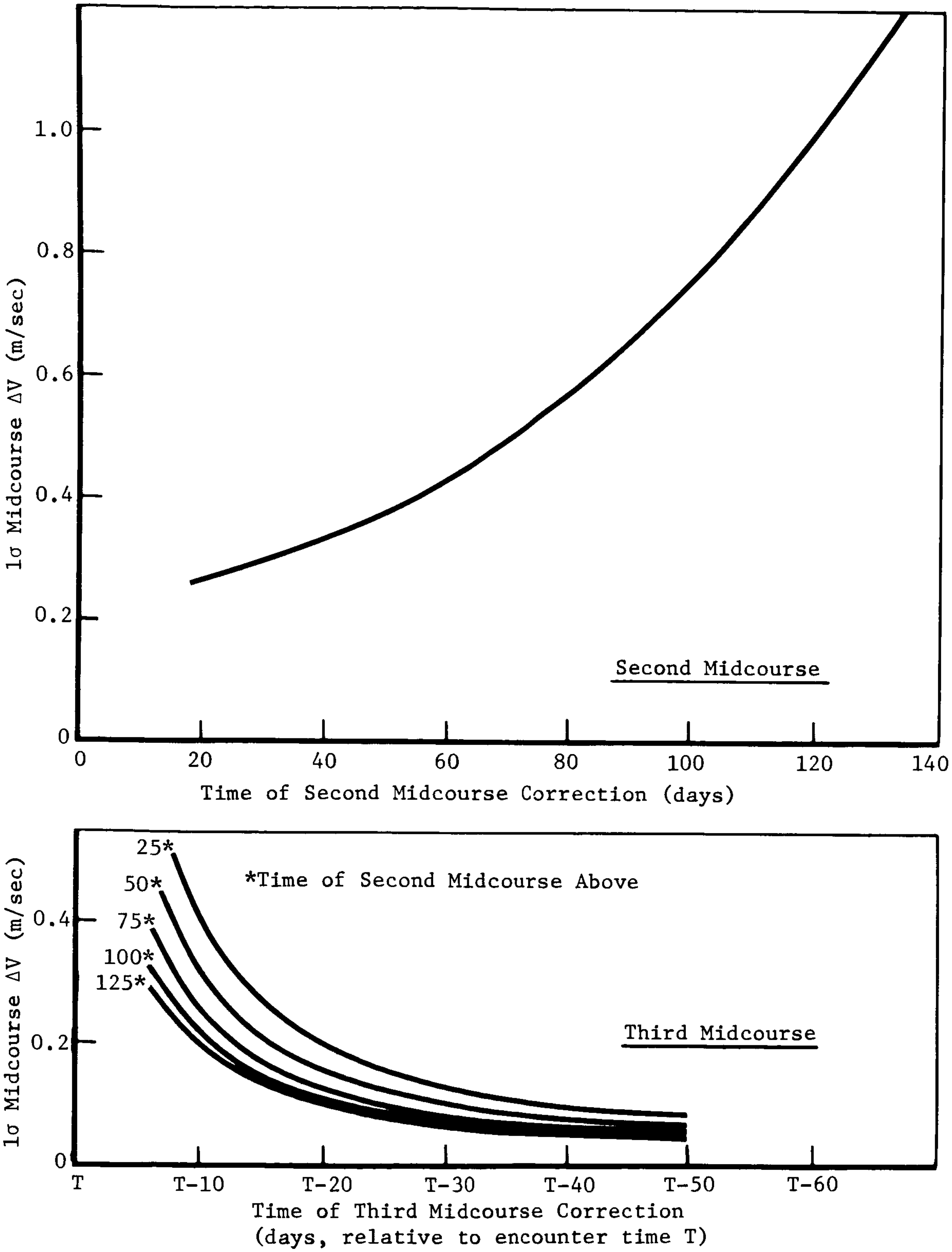

Figure A6-8: MIDCOURSE ΔV REQUIREMENTS FOR CORRECTING THE PREVIOUS DISPERSION AS FUNCTIONS OF MIDCOURSE TIME

# APPENDIX B
# PROPULSION SUBSYSTEM STUDIES

The powered spacecraft mission uses a single primary propulsion system several times in transferring from Earth orbit to a suitable orbit at Mars. This imposes requirements on the propulsion system that are not always complementary. The following sections discuss these conditions and the studies conducted to arrive at a suitable system design. Component data compiled on existing equipment in support of these studies is report in Reference 1.

Propulsion system design for the powered spacecraft mission was limited to current technology and, where possible, available hardware. Trade studies were conducted when required to make conceptual decisions and to select major components.

## 1.0 ENGINE SELECTION

The powered spacecraft mission encompasses both large and small propulsive maneuvers. Large velocity increments are associated with injection into a trans-Mars trajectory (spacecraft-assist) and with insertion into Mars orbit. Small maneuvers are required for midcourse correction and orbit trim sequences.

Conflicting requirements are imposed in engine selection when the engine must deliver both large and small velocity increments. Low-thrust engines are generally most effective in small maneuvers because they are more controllable and precise and impose fewer penalties in terms of engine weight, envelope, attitude control, power requirements, and thermal loads. However, the inverse relationship of operating duration to thrust means that small engines require more time to make a given velocity change. The spacecraft is thus out of nominal orientation for longer periods, which can penalize power, guidance, communications, and thermal control. Propellant penalties associated with prolonged maneuvers performed in gravitational environments (finite-burn penalties) are perhaps the most significant factor restricting the use of small engines. In the powered spacecraft mission, finite-burn penalties for maneuvers conducted at Earth can be significant, commonly exceeding similar penalties at Mars.

Engines considered for the powered spacecraft mission were either developed undergoing development, or were engines on which considerable development effort had been expended. Nineteen candidate engines, and their variations, were identified and evaluated in terms of their potential adaptability to the powered spacecraft mission. These engines received "good" or "fair" adaptability ratings indicating that they had adequate performance potential and considerable development. These engines encompassed a thrust range of 100 to 10,500 pounds.

Subsequent studies related spacecraft useful (i.e., nonpropulsive) weight, including Earth departure finite-burn effects, to velocity and engine thrust level. Initial studies made it apparent that a single 100-pound-thrust engine was insufficient. Consistent with the next available engine, the minimum thrust level was set at 300 pounds. Similarly, it was apparent that thrust levels above 6,000 to 7,000 pounds entailed excessive penalties in engine weight, envelope, small maneuvers, and acceleration. Finite-burn penalties were not significant beyond approximately 2,000 pounds thrust. The three engines remaining within the 300- to 3,500-pound thrust boundaries were: (1) the 316-pound-thrust Post-Boost Propulsion System (PBPS) engine; (2) the 2,200-pound-thrust Apolla subscale; and (3) the 3,500-pound Lunar Module Ascent engine. Characteristics of these engines are listed in Table B-1. The PBPS engine was evaluated at 300 pounds thrust and, in a three-engine installation, at 900 pounds thrust. Figure B-1 shows the results of this study. The 2,200- and 3,500-pound-thrust engines consistently had more useful weight above spacecraft-assist velocities of 900 m/sec. At 1,200 m/sec, there was at least a 100-pound advantage.

Table B-1: ENGINE CHARACTERISTICS

| Engine/Program | Apollo Lunar Module Ascent Engine | Apollo Subscale Engine | PBPS Velocity Engine |
|---|---|---|---|
| Thrust (lb) | 3,500 | 2,200 | 300* |
| Propellants | $N_2O_4/A_Z$-50 | $N_2O_4/A_Z$-50 | $N_2O_4$/MMH |
| Mixture Ratio (Oxid/Fuel) | 1.6 | 2.0 | 1.6 |
| Specific Impulse, Nominal (sec) | 310.4 | 309 | Classified |
| Minimum (sec) | 306.3 | 305 | Classified |
| Chamber Pressure (psia) | 120 | 100 | 117 |
| Engine Inlet Pressure | 165 | 175 | 225 |
| Nozzle Area Ratio ($A_E/A_T$) | 45.6 | 60 | 40 |
| Burn Time Capability | >500 | 750 | >1,000* |
| Minimum Impulse Bit (lb-sec) | 462** | 182** | |
| Restart Capability | ≥35 | Unlimited | Unlimited |
| TVC Capability (degrees) | ±6* | ±6* | |
| Cooling Method: Chamber | Ablative | Ablative | Boundary Layer |
| Nozzle Extension | Ablative (or Radiation)* | Radiation | Conduction and Radiation |
| Weight (Incl valves and gimbal) | 227 (174)* | 110.5* | 16.8 |

*As Modified

**To 90% Thrust

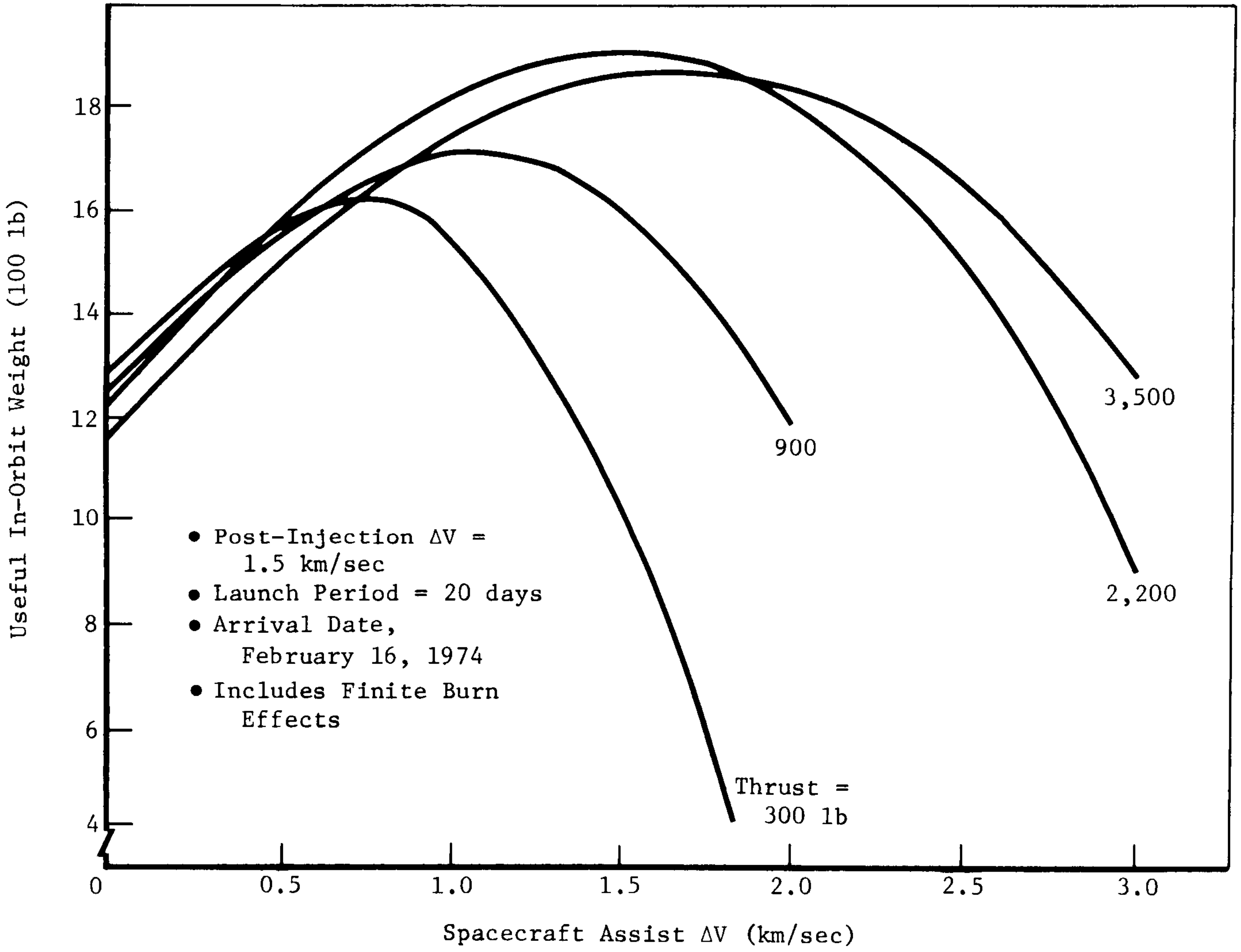

Figure B-1: TITAN IIIC SPACECRAFT THRUST EFFECTS

These engines are further compared in Table B-2. From this comparison, it is apparent that the Apollo Lunar Module Ascent Stage engine has progressed in development considerably beyond the Apollo subscale engine, and will continue to do so. The Lunar Module Ascent engine program is a viable program that must necessarily yield qualified hardware for the Apollo program. The Apollo subscale program has been concluded for some time without having reached a corresponding level of development. The three-engine PBPS cluster gives considerably less useful spacecraft weight, requires much longer maneuver periods, and requires more extensive modification for the powered spacecraft mission than does the Lunar Module Ascent engine. Significantly, the Lunar Module Ascent engine should require less extensive qualification testing for the Powered Spacecraft Mission because of its similarities in maneuver requirements and operating environment.

Based on these considerations, the 3,500-pound-thrust Lunar Module Ascent Stage engine was selected for use in the powered spacecraft propulsion systems.

Table B-2: FINAL ENGINE COMPARISON

| Engine | Apollo Lunar Module Ascent Engine | Apollo Subscale Engine | PBPS Velocity Engine |
|---|---|---|---|
| Thrust (lb) | 3,500 | 2,200 | 3 x 300 |
| Useful Spacecraft Weight (lb) (Post-Injection $\Delta V$ = 1.5 km/sec) | 1,820 | 1,880 | 1,710 |
| Mars Mission Burn Time Requirements (sec) | ~360 | ≃575 | 1,400 |
| Engine Design Burn Time (sec) | >500 | 750 | 197 |
| Present Engine Status | In-Qualification for Apollo | Program Terminated (Subscale Test Engine) | In-Qualification for PBPS |
| Modifications Required | Gimbal Assembly | Gimbal Assembly<br>Bipropellant Valves | Radiation Nozzle Recontour<br>Throat Standoff<br>Valves |
| Qualification Required for Powered Spacecraft | Mission Simulation | Qualification | Qualification |

## 2.0 PRESSURIZATION TRADES

Current practice in propellant tank pressurization involves the use of either nitrogen or helium gas. Helium pressurization systems are lighter because much less gas weight is required. Nitrogen gas, however, is more desirable for reaction control applications because it usually yields the lighter system, particularly when thruster leakage allowances are applied.

A trade study was conducted to evaluate the use of helium and nitrogen as pressurizing gases in the powered spacecraft. This study included the influence of nitrogen reaction control systems and separate versus common gas storage systems. Pressurization system transient conditions were also determined.

Pressurization system characteristics were established by iterating an incremental time-energy balance on the propellant tank until the total required gas weight equalled that withdrawn from the pressurant tank. Four 36.3-inch (ID) spherical propellant tanks were assumed, having a 2.4% ullage at 70°F and an ullage pressure of 190 psia. Oxidizer was used at a 4.43 lb/sec (70°F) flow rate, and fuel at 2.76 lb/sec (in an approximately 210-second initial engine burn, followed by a 150-second final burn). Acceleration levels varied with time from 0.50 to 1.23 g's. Pressurant bottle initial pressure and temperature were 3,500 psia and 70°F, respectively. Final bottle pressure was limited to 300 psia.

A separate study showed that gas leakage in a welded or brazed pressurization system, such as that selected for the powered spacecraft, was not large enough to influence the pressurization gas trade.

Results of the nitrogen/helium pressurization gas comparative study are shown in Figure B-2. The separate tank helium system is more than 57 pounds lighter than the separate tank nitrogen system and 46 pounds lighter than the common tank nitrogen system. Final bottle sizes were almost the same, which suggests that weight differences were due primarily to pressurizing gas weight itself.

This study did not measure the effects of pressurant tank envelope on spacecraft structure. However, significant weight penalties are involved in compact configurations because the additional envelope required for multitank installations imposes a structural weight penalty for structural stiffeners and extended plumbing. In early powered spacecraft configurations, this structural penalty virtually offset any weight advantage of the helium system. It was thus desirable to use nitrogen gas as a pressurant in installations having common gas storage with the reaction control system.

Subsequent spacecraft configuration exercises have demonstrated that this selection is configuration sensitive. Later configurations accommodated multitank installations without incurring a significant structural weight penalty, which made the lighter helium system more desirable. Consequently, helium was selected on a weight basis as the pressurizing gas for the final powered spacecraft configurations. This resulted in the spacecraft having both helium and nitrogen aboard. The resulting service, checkout, and utility disadvantages were accepted to attain the substantial indicated weight savings.

Transient characteristics of both the helium and nitrogen systems are shown in Figures B-3 and B-4 for the conditions studied.

| Pressurant Gas | Heat Transfer Rate Pressurant Tank | Heat Transfer Rate Propellant Tank | Molar Heat Capacity | Specific Heat Ratio $C_p/C_v$ |
|---|---|---|---|---|
| Helium | 27.6 Btu/hr ft$^2$ °R | 7.5 Btu/hr ft$^2$ °R | 5.0 Btu/lb mol °R | 1.65 |
| Nitrogen | 10.2 Btu/hr ft$^2$ °R | 2.62 Btu/hr ft$^2$ °R | 7.0 Btu/lb mol °R | 1.40 |

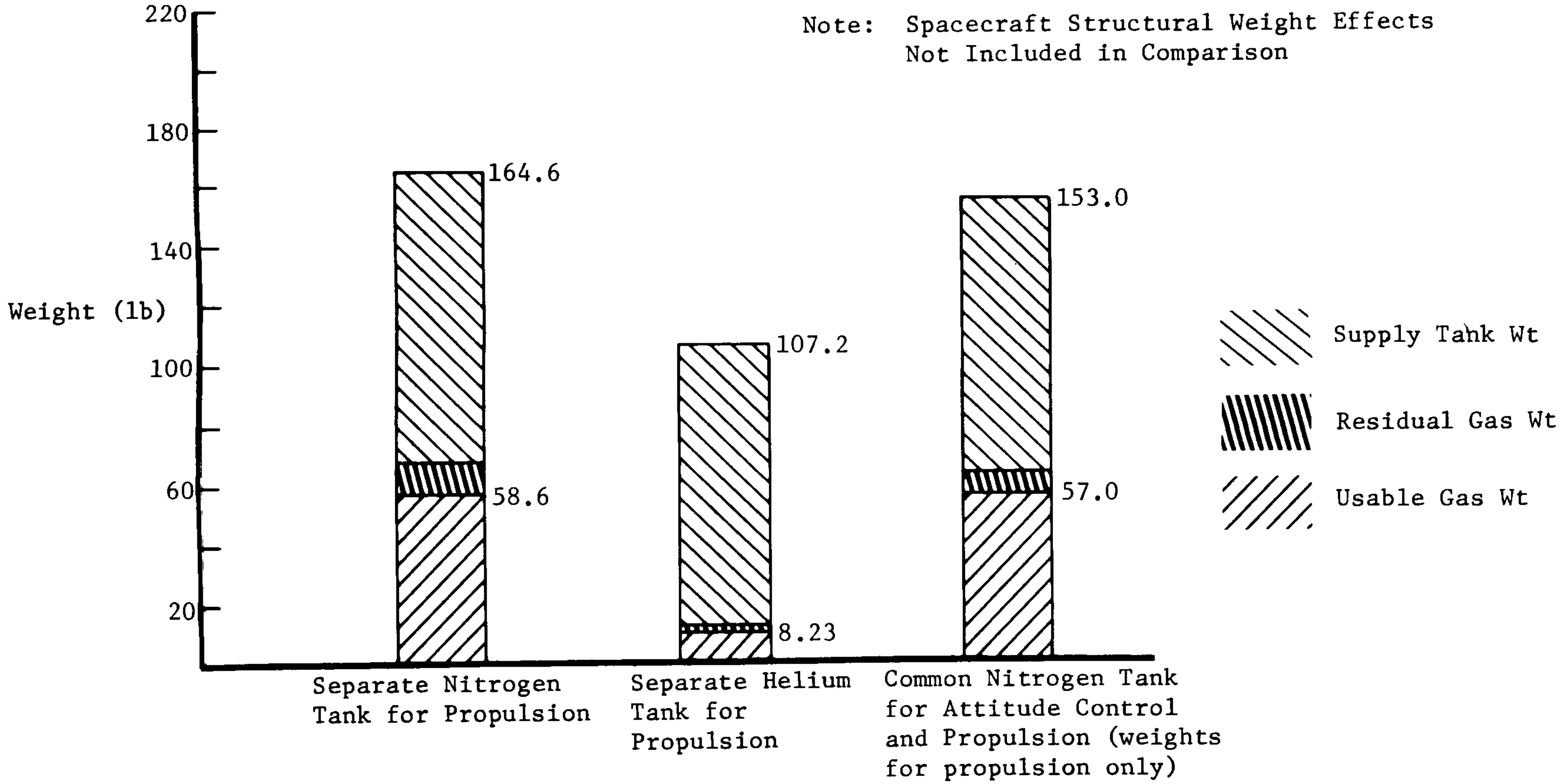

Note: Spacecraft Structural Weight Effects Not Included in Comparison

Figure B-2: PRESSURIZATION STUDY

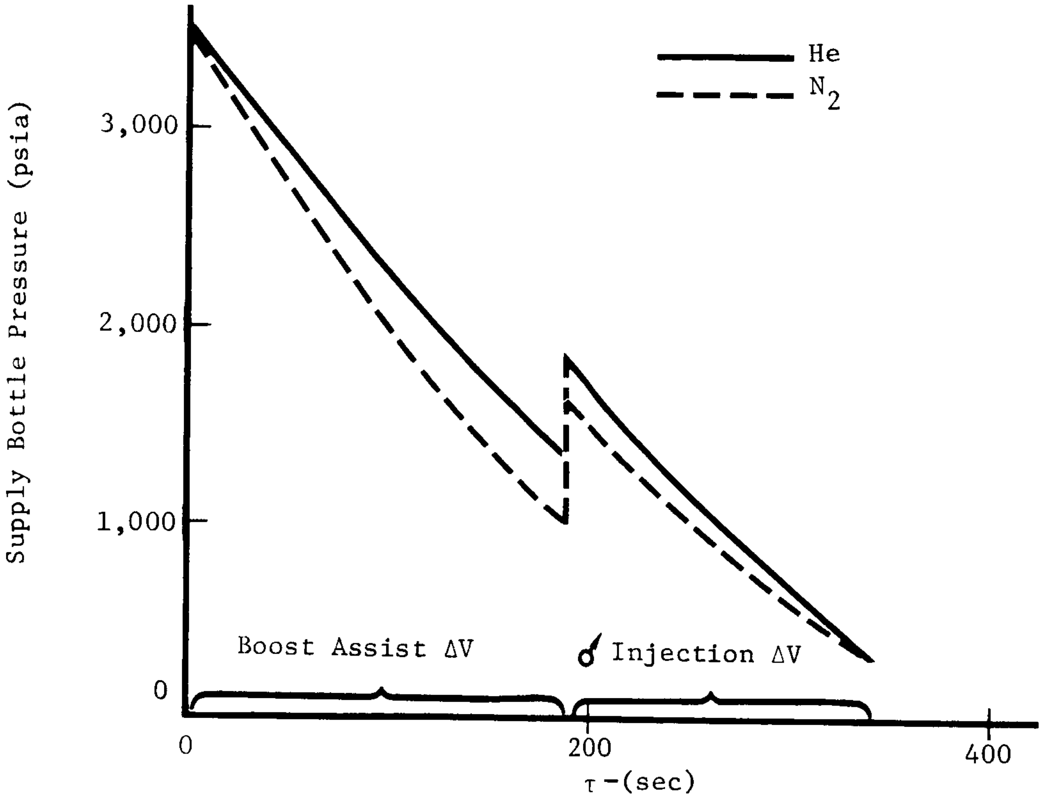

Figure B-3: TRANSIENT CHARACTERISTICS

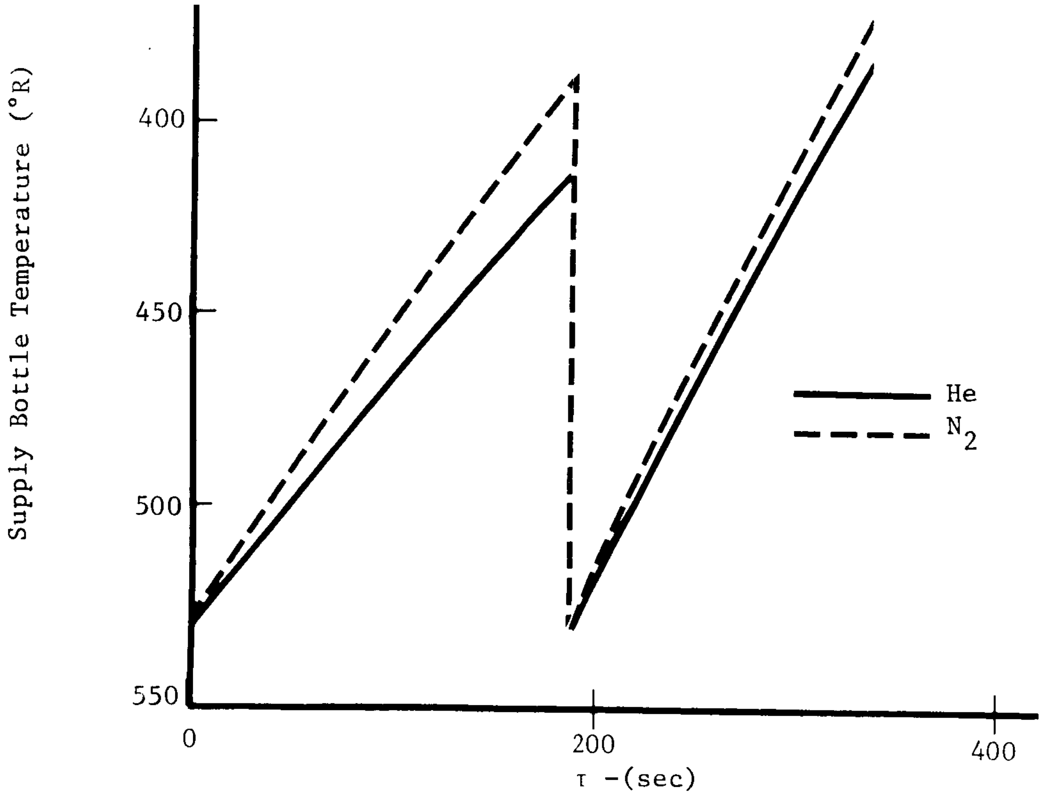

Figure B-4: TRANSIENT CHARACTERISTICS

## 3.0 PROPELLANT CONTROL

Various propellant control methods may be used to position propellants relative to the tank outlet, to exclude gas bubbles in the propellant lines, and to provide positive propellant expulsion. Methods frequently suggested for performing some or all of these functions include elastomeric bladders, metal diaphragms or bellows, expulsion screens, separate "start" tanks, or separate "ullage" propulsion systems for propellant settling.

A comparative study of propellant control methods was conducted to relate weight, dynamic sensitivity, cycle capability, and hardware availability. This study covered teflon and teflon/aluminum gladders, reversing-type spherical metal diaphragms, cylindrical metal bellows, expulsion screens, refillable start tanks, and ullage propulsion systems. A separate study of expulsion screens was conducted in which the internally contained, nonrefillable expulsion screen concept was chosen for comparison with these other concepts.

The expulsion screen study was conducted to select appropriate screen concepts and to determine their hardware characteristics for the propellant control study. Screens use propellant surface tension to localize a quantity of vapor-free liquid at the tank outlet throughout the mission. They are assigned to either contain the propellant against the total interior tank surface (full containment) or against part of the surface (partial containment). They are either of the filling or nonrefilling type, depending on the amount of propellant contained.

The screen study was conducted for a 7,000-pound Mars spacecraft having a 3,500-pound-thrust engine that could gimbal ±6 degrees. Boost-assist velocity was 1,200 m/sec, and post-injection velocity was 1,404 m/sec. Propellants were $N_2O_4$/Aerozine 50 at a mixture ratio of 1.6. Useful propellant weight was 4,063.5 pounds. Total loaded propellant weight was 4,200 pounds, consisting of 2,575 pounds of oxidizer and 1,625 pounds of fuel. Total propellant tank volume was 55.19 cubic feet contained in four 36.54-inch-diameter tanks. Engine inlet pressure and chamber pressure were 165 and 120 psia, respectively. Nitrogen gas was used at a propellant tank operating pressure of 185 psi, and regulator lockup pressure was 190 psi. Tank relief pressure was 250 psi, which provided sufficient margin over the maximum thermal recovery pressure of 220 psi.

An initial qualitative assessment of expulsion screen concepts is summarized in Figure B-5. Total screen containment configurations were ruled out by the acceleration limits because the screens could not support the hydrostatic head at 1.25 g's. Among the remaining partial containment variations, external sumps were omitted because of their excessive weight. Internally located, partial containment screens were thus selected for further study. The nonrefilling variety was chosen because it is particularly suited to the powered spacecraft propulsion duty cycle. Subsequent evaluation showed that this screen system weighed 24 pounds for all four tanks, had a volumetric efficiency of 99.5%, and an expulsion efficiency of at least 98%.

In the propellant control study, each expulsion method was quantitatively evaluated, where possible. Mission characteristics assumed for this comparison are shown in Table B-3.

| Propellant Tank/Screen Configuration | 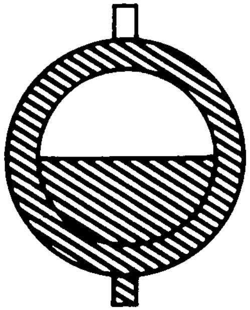 | 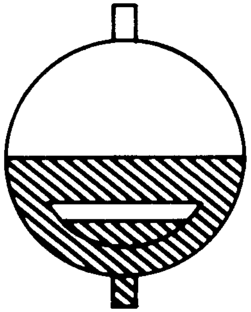 | | 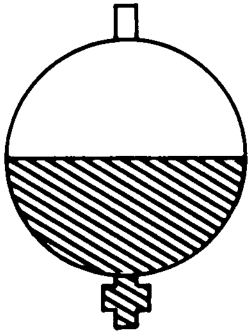 |
|---|---|---|---|---|
| Propellant Containment by Screens | Total | Partial | | |
| Screen Location | Internal | Internal | | External |
| Sump Type | | Refilling | Nonrefilling | Refilling/Nonrefilling |
| Remarks | Screen Cannot Support Hydrostatic Head at 1.25 g's | Long Screen Necessary<br>Causes Large Residuals | Particularly Suitable for Few, Predictable Starts | Extra Weight Required for Large, Pressure-Designed External Sump |
| Study Status | Discontinued | Discontinued | Continued | Discontinued |

Figure B-5: PROPELLANT CONTROL STUDY---SURFACE TENSION DEVICES

Table B-3: MISSION CHARACTERISTICS FOR PROPELLANT CONTROL STUDY

| Mission Phase | Duration (days) | Weight (lb) | | ΔV (km/sec) |
|---|---|---|---|---|
| | | Spacecraft | Propellant Remaining | |
| Launch and In-Orbit | ≈1 | 7,000 | 4,200 | 1.200 |
| Transfer to Planet | 200 | 4,680 | 1,880 | |
| Planet - Prime Mission | 30 | ≥2,920 | ≥120 | 1.404 |
| - Extended Mission | 150 | ≥2,920 | ≥120 | |

Nitrogen gas was used for tank pressurization because initial configurations favored its use. These conditions were equated to weight penalties peculiar to each propellant control method. For example, the elastomeric bladders involve expulsion equipment weight, gas and propellant lost to permeation, expulsion inefficiencies, and incremental tank penalties arising from volumetric and pressure requirements of the bladder. These items are summed to a total "expulsion sensitive weight" increment, which shows inert weight differences between concepts.

The results of this study are summarized in Table B-4. Bellows systems are shown to be significantly heavier than all other approaches. The remaining methods were approximately the same weight except for metal diaphragms, which were somewhat (±18%) heavier.

An additional weight penalty can exist in the form of reduced engine specific impulse when operating with propellants containing dissolved gases. This penalty was not assigned because it is unique to particular engines. However, when it does occur, it may additionally penalize those systems not having metal diaphragms or bellows by as much as 50 to 100 pounds of propellant.

Reversing metal diaphragms are shown to be cycle limited, which is a disadvantage in test and checkout operations. They have not progressed beyond the R&D hardware stage, which is also the case with the refillable start tank. Expulsion screen development has been limited to booster (Agena) applications. The particular expulsion device to be used in the powered spacecraft mission will require development because it is not currently available in the appropriate size.

Refillable start tanks and separate ullage propulsion systems are shown to be competitive with bladders and screens because complexity, reliability, and failure criteria were not assessed. However, these systems are more complex.

Based on these findings, bladders were selected for propellant control in the powered spacecraft. Teflon/aluminum bladders were selected in initial

Table B-4: PROPELLANT CONTROL STUDY SUMMARY

| Item | Bladders | | Reversing Metal Diaphragm | Metal Bellows | Start Tank (Refillable) | Expulsion Screens | Ullage Propulsion System |
|---|---|---|---|---|---|---|---|
| (Based on $W_P$ = 4,200 lb $N_2O_4/A_Z$-50 at MR = 1.6) | Teflon | Teflon/ Aluminum | | | | | |
| Weight Sensitivity | | | | | | | |
| o Expulsion Apparatus | (36) | (37) | (45) | (128) | (75) | (24) | (75) |
| o Expulsion Residuals, $(1-\eta_x)\ W_P$ | (84) | (84) | (84) | (84) | (53) | (84) | (50) |
| o Incremental Tank Weight, $\Delta W_T$: | (4) | (4) | (18) | (68) | (-15)** | (1) | (-8)** |
| Volumetric Efficiency | 2 | 2 | 2 | 18 | -15** | 0 | -8** |
| Tank Shape Compatibility | 0 | 0 | 0 | 45 | 0 | 0 | 0 |
| ΔP for Expulsion Efficiency | 2 | 2 | 16 | 5 | 0 | 1 | 0 |
| o Permeation Effects, ΔW: | (9) | (2) | (0) | (0) | (10) | (10) | (10) |
| Gas Loss-Dissolved Gases | 3 | 1 | 0 | 0 | 3 | 3 | 3 |
| Propellant Loss-Permeation | 6 | 1 | 0 | 0 | - | - | - |
| Propellant Loss-Vapor | * | * | 0 | 0 | 7 | 7 | 7 |
| Total Expulsion Sensitive Weight | 133 | 127 | 147 | 280 | 123 | 119 | 127 |
| Slosh Self-Damping | Limited | Limited | Yes | Yes | No | No | No |
| Cycle Life (cycles) | 25 | 25 | 1 | 200 | 200 | Unlimited | Restart Limited |
| Hardware Status | Space Qualified | Space Qualified | R&D | Space Qualified | R&D | Limited Qualification | Space Qualified |
| Hardware Availability | Dev Rqd | Dev Rqd | Dev Rqd | Dev Rqd | Dev Rqd | Dev Rqd | Dev Rqd |

*Charged as permeation loss **Adjusted for volume of auxiliary tanks configurations using nitrogen gas because the aluminum significantly inhibited gas transmission rate. Subsequent configurations, using helium as a pressurant, employ the teflon (TFE-FEP) bladder because the aluminum laminate does not affect helium gas transmission enough to offset the increased development required. There is also evidence that helium does not reduce performance when dissolved in the oxidizer.

## 4.0 THERMAL CONTROL

The Lunar Module Ascent engine with a radiation-cooled nozzle skirt extension imposes a thermal radiation load on the spacecraft and, particularly, on the solar array. It was thus necessary to evaluate this load and its sensitivity to variations in thermally related parameters.

An existing computer program was used to evaluate the solar array-nozzle skirt view factor, F. A nominal value of 0.015 was obtained. An effective solar heating rate of 40.7 watts/ft$^2$ ($S \alpha \cos \theta$) was used, which is the heating rate at Mars. This rate was used because the solar array will not be extended during the spacecraft-assist portion of the trans-Mars injection maneuver. Power withdrawal rate was 4 watts/ft$^2$, which is consistent with an approximately 10% conversion efficiency. The nozzle skirt exterior temperature was established at 2,735°R, consistent with current bipropellant engines of this type.

The peak temperature experienced along the solar array under these conditions with the solar panels oriented normal to the Sun was approximately 510°F.

This temperature will vary with changes to the major parameters. Figure B-6 shows the sensitivity of peak solar array temperature to variations in these parameters under steady-state conditions considered to exist after engine burns of 200 or more seconds. It is apparent from this figure that array temperature is most sensitive to nozzle skirt temperature; that is, a 10% change in this parameter changes peak solar array temperature by approximately 140°F. The next most significant item is the view factor. Solar heating rate and power withdrawal rate are not particularly influential. However, the solar heating rate at Earth is approximately three times as large as that at Mars, which increases the slope of this curve correspondingly.

## 5.0 SOLID-LIQUID STAGING

The powered spacecraft propulsion system furnishes a portion of the velocity increment requirement for transplanet injection. By using the spacecraft propulsion system in this manner, a net gain in useful weight (i.e., nonpropulsive) in Mars orbit is possible. The baseline propulsion system assumed for the powered spacecraft is an all-liquid bipropellant system using a single engine for all maneuvers. However, these maneuvers could also be conducted with a solid propellant system, particularly if it was augmented with a small liquid propellant system for velocity control and, possibly, thrust vector control. The solid propellant system is uniquely adapted to staging, which is, from a weight basis, a distinct advantage.

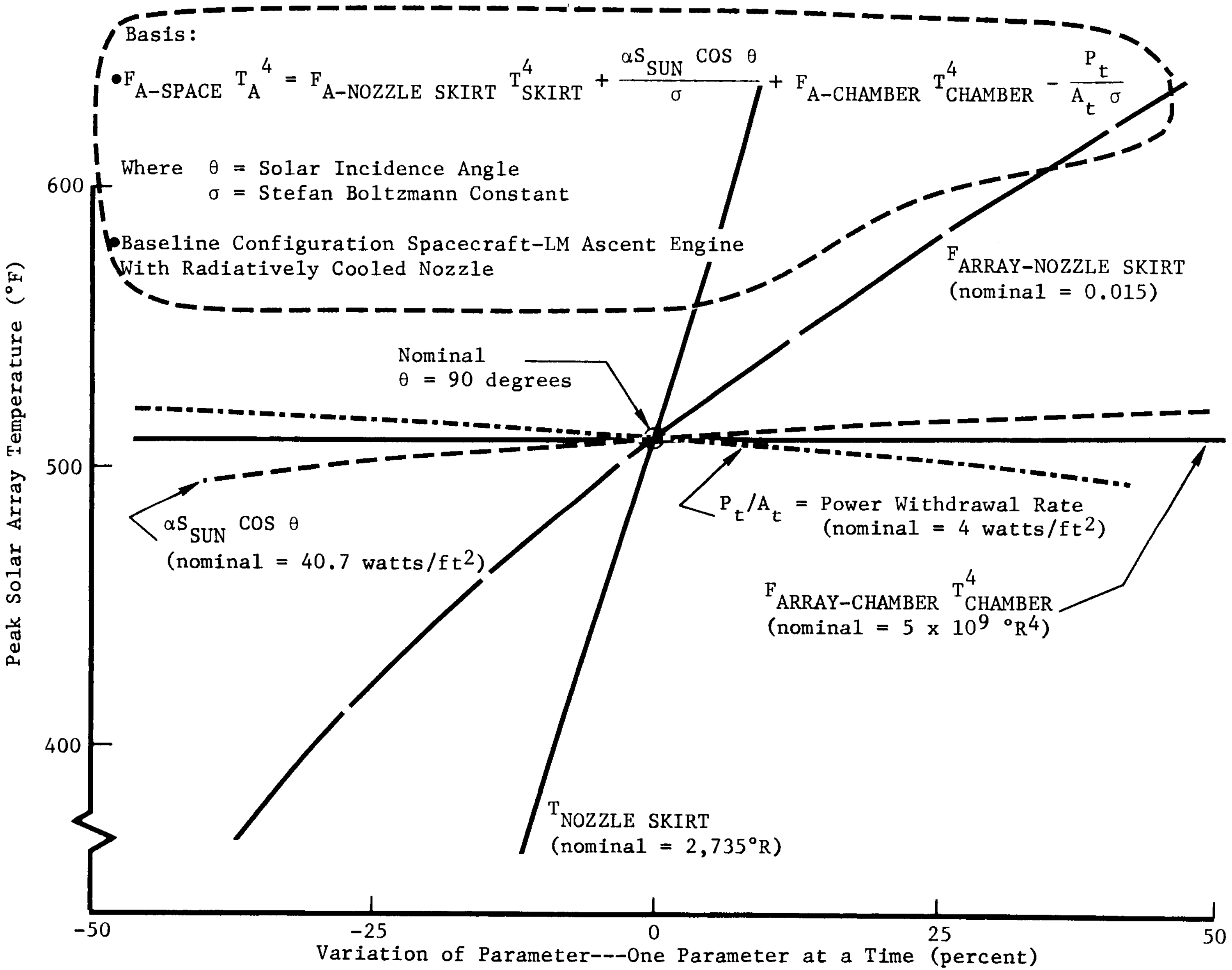

Figure B-6: SOLAR ARRAY SENSITIVITY TO RADIATIVELY COOLED ENGINE

A study was conducted to compare the solid propellant system to the baseline liquid propellant approach, including the effects of staging.

The two propulsion system configurations compared in this study used: (1) staged solid propellant motors; and (2) the baseline liquid bipropellant engine.

The staged solid motor configuration used motors selected from the Thiokol TE-M-364 series currently employed, in various configurations, in Surveyor, Burner-IV, Improved Delta, and ATS. A cross-sectional drawing of the TE-364-2 motor is shown in Figure B-7. Figure B-8 shows a cross-sectional drawing of the TE-364-4 motor. Pertinent performance characteristics of this family of solid propellant motors are summarized in Table B-5.

The powered spacecraft mission requires some impulse control, so a liquid propulsion system was also used with the staged solid propellant system. This study was conducted to the following conditions affecting this combined propulsion system.

Table B-5: THIOKOL TE-M-364 SERIES APOGEE MOTORS

| Model Designation | Program | Maximum Thrust (lb) | Specific Impulse (sec) | | Propellant Weight (lb) | | Motor Weight (lb) |
|---|---|---|---|---|---|---|---|
| | | | Nominal | Minimum | Nominal | Minimum | |
| TE-M-364-4 (04) | Improved ATS | 17,000 | 285.7 | 284 | 2,336 | NA | 2,492 |
| TE-M-364-4 (03) | Improved Delta | 18,000 | 285.7 | 284 | 2,009 | NA | 2,165 |
| TE-M-364-4 (02) | None Derated (04) | 15,500 | 285.7 | 284 | 1,896 | NA | 2,052 |
| TE-M-364-4 (01) | None Derated (04) | 18,300 | 285.7 | 284 | 1,831 | NA | 1,987 |
| TE-M-364-3 | Delta | 10,800 | 289.7 | 288 | 1,440 | 1,437 | 1,578 |
| TE-M-364-2 | Burner II | 10,800 | 289.7 | 288 | 1,440 | 1,437 | 1,580 |
| TE-M-364-1 | Surveyor | 9,760 | 289.7 | 288 | 1,230 | 1,227 | 1,368 |

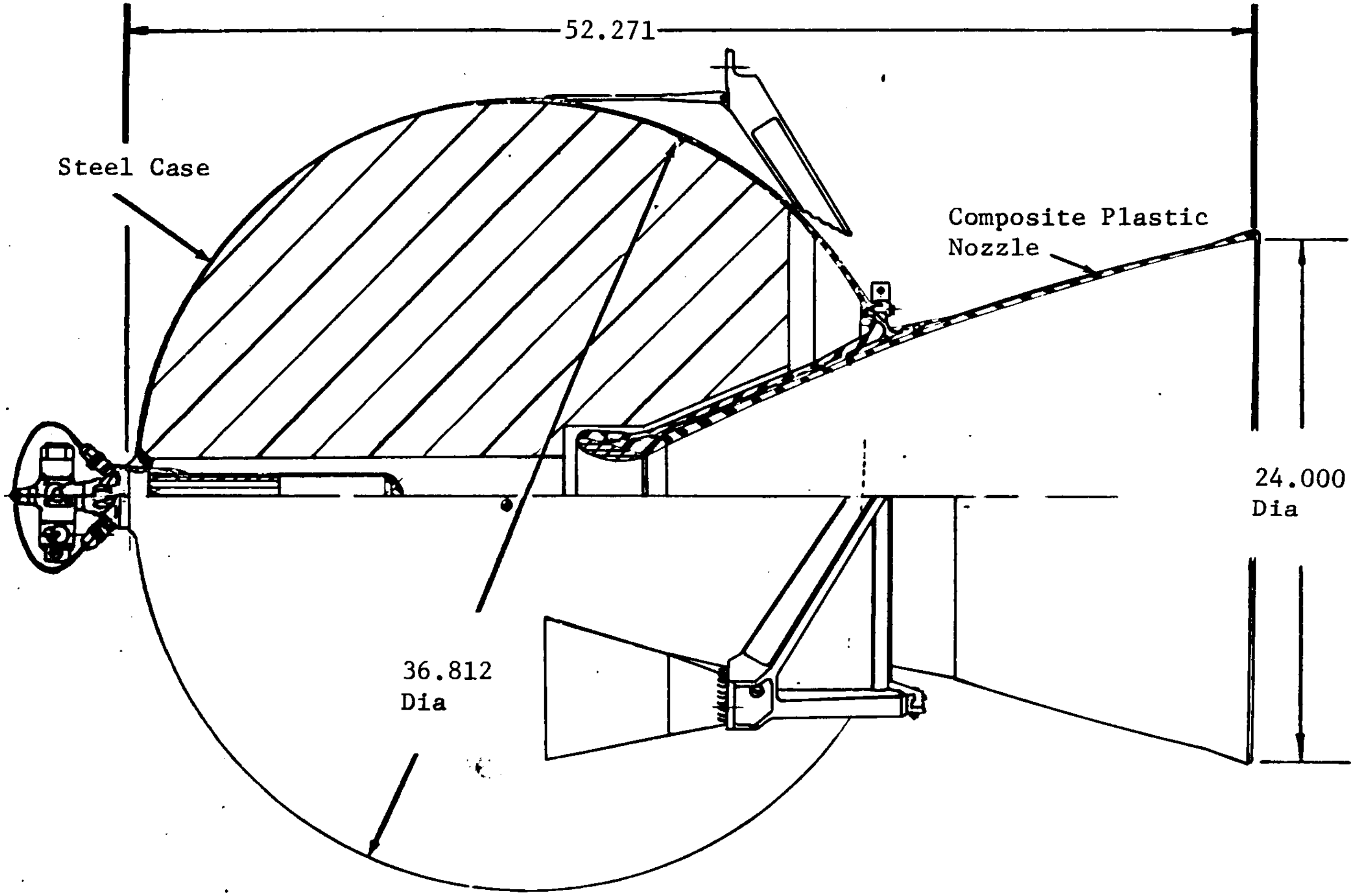
52.271
Steel Case
Composite Plastic Nozzle
24.000 Dia
36.812 Dia

Figure B-7: TE-364-2 BURNER II ROCKET MOTOR ASSEMBLY

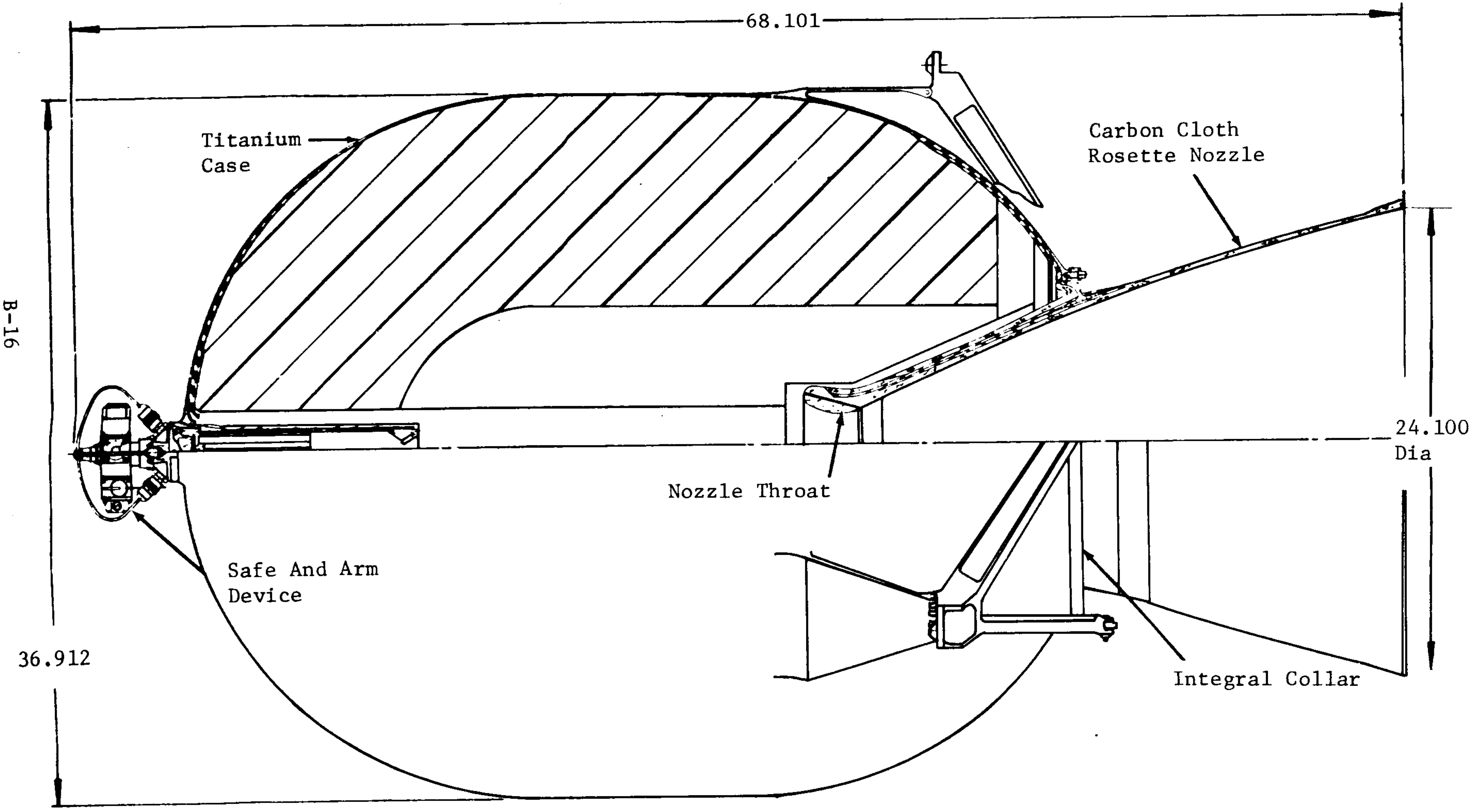
68.101
Titanium Case
Carbon Cloth Rosette Nozzle
24.100 Dia
Nozzle Throat
Safe And Arm Device
36.912
Integral Collar

Figure B-8: TE-M-364-4 ROCKET MOTOR ASSEMBLY

1) The solid propellant motor was sized for the minimum $C_3$ value associated with the Titan-IIIC launch vehicle and a 1973 Type I mission trajectory to Mars.

2) The solid propellant motor impulse was used to inject the spacecraft into the proper trans-Mars trajectory. Propulsive energy required for injection trim, midcourse maneuvers, Mars orbit insertion, and orbit trim is provided by a liquid propellant system configured around four Marquardt R-4D engines.

3) The solid propellant motor provides all or nearly all the impulse (velocity) required to inject the spacecraft into a trans-Mars trajectory.

4) The auxiliary liquid propellant system used four Marquardt R-4D-4 engines modified from the MOL configuration to a nozzle expansion ratio of 65.

5) The auxiliary liquid propellant system is used during solid propellant motor operation to provide thrust vector control by means of pulse modulation. After burnout, the solid motor is jettisoned, and all further velocity maneuvers are provided by the liquid propellant system.

6) The liquid system was sized for total mission requirements less that provided by the solid motor, plus the additional TVC requirement. Performance of the R-4D engine was 290 seconds using nitrogen tetroxide and MMH at a mixture ratio of 1.6. Lunar Orbiter propulsion component weights were employed in the calculations of fixed weights for this system.

The baseline, all-liquid configuration uses the 3,500-pound-thrust Apollo Lunar Module Ascent Stage engine to perform all maneuvers. This engine was modified to include a radiation-cooled nozzle extension and a gimbal mount for thrust vector control. Delivered engine specific impulse was assumed to be 306 seconds. Applicable Lunar Module Ascent Stage propulsion component weights are included in the calculation of thrust-dependent and flow-rate-dependent weights. The engine uses nitrogen tetroxide ($N_2O_4$) and Aerozine-50 (50% $N_2O_4$/50% UDMH) as propellants at an operating mixture ratio of 1.6. Propellant and pressurant expendables and tankage requirements were selected in accordance with total mission velocity requirements. This study was conducted on the basis of the following conditions affecting the baseline, all liquid bipropellant system.

1) The all-liquid configuration employs a single liquid propulsion system to perform all maneuvers. This propulsion system configuration uses the 3,500-pound-thrust Apollo Lunar Module Ascent engine. In this application, the engine is gimbaled for thrust vector control and includes a radiation-colled nozzle extension.

2) Liquid propulsion system propellant and pressurant tankage weights were obtained by correlating data acquired in Task I; weights of solid propellant motors and various liquid propellant components (other than tankage) were obtained from existing program data sources.

3) Specific details of this configuration are described in Section 7.3.1.2 of this report.

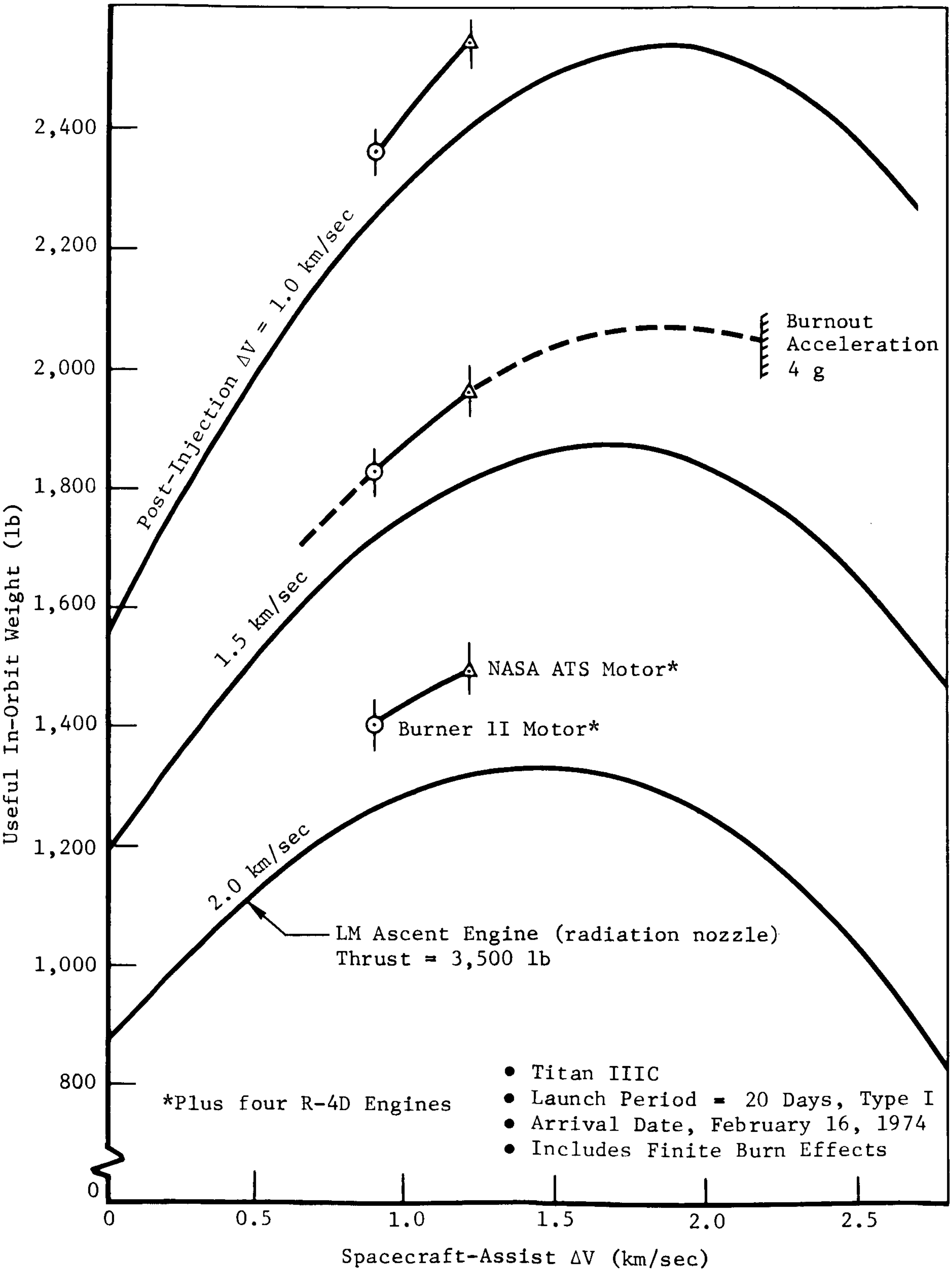

Figure B-9: COMPARISON OF STAGED SOLID PROPELLANT MOTORS WITH A NONSTAGED LIQUID SYSTEM

These configurations were evaluated on a useful in-orbit weight basis as a function of boost-assist and post-injection velocity capability. Figure B-9 summarizes the results of the study. The plots show that the jettisonable, solid-assist motor provides a greater useful in-orbit weight (about 150 pounds) than does the baseline all-liquid system.

# APPENDIX C
# GUIDANCE AND CONTROL SUBSYSTEM TRADE STUDIES

The trade studies conducted in the guidance and control area were, in a broad sense, intended to demonstrate the feasibility of the powered spacecraft concept and to provide sufficient data to establish a basis for preliminary design of a general configuration, including weight and power. The areas investigated were:

- Initial Attitude Errors
- Staging Rates
- Reaction Control Subsystem
- Thrust Vector Control Subsystem

These studies led to the conclusion that it is feasible to use a Lunar Orbiter control concept as shown in Figures 7.3-2 and 7.3-3 for the powered spacecraft concept.

## 1.0 SUMMARY AND CONCLUSIONS

The preferred method of establishing the attitude for the boost-assist velocity increment is to maneuver to the required attitude using the Titan IIIC transtage. Just before separation the powered spacecraft inertial reference unit gyros will be placed in the rate-integrating mode. As soon as the spacecraft separation sequence is completed and the spacecraft has converged to a stable limit cycle, the spacecraft engine is started. The study showed that the minimum time from transtage engine cutoff to spacecraft engine ignition is 1.5 minutes and 4 minutes for the engine-down and engine-up configurations, respectively. The attitude errors are less than 1 degree. The pitch and yaw separation rates of 0.60 degree are controlled by the reaction control system. Roll rates are near limit cycle rate and should cause no problems.

A three-axis, all-jet, cold nitrogen system is preferred to control moment gyros, reaction wheels, or hot gas reaction jet systems for the assumed transit time plus a planetary mission of 180 days. The recommended reaction control system sizing and performance parameters for a 7,000-pound spacecraft are:

| | | |
|---|---|---|
| Nitrogen | 17.25 pounds | |
| Thruster Size | Pitch | 0.29 lb |
| | Yaw | 0.29 lb |
| | Roll | 0.07 lb (2 in couple) |

Control Acceleration:

| | Start Burn | Transit | Orbit |
|---|---|---|---|
| Pitch | 0.05 deg/sec$^2$ | 0.053 deg/sec$^2$ | 0.185 deg/sec$^2$ |
| Yaw | 0.05 | 0.053 | 0.185 |
| Roll | 0.03 | 0.040 | 0.065 |

Maneuver Rate: 0.2 deg/sec (all axes)

Limit Cycle Deadband:

| | |
|---|---|
| Narrow | ±0.30 degree in all axes. At Earth the Sun sensor narrows this to ±0.135 degree in pitch and yaw; |
| Wide | Not determined by this study. |

The thrust vector control system was evaluated by linear analysis assuming a first order deflection control actuator and a second order rigid body. The results of this analysis lead to the following performance requirements:

TVC Actuator:

| | |
|---|---|
| Corner Frequency | 15 rad/sec |
| Minimum Rate | 10 deg/sec |
| Minimum Deflection | 3 deg |
| Stall Torque | Loads not defined by this study |

Closed TVC Loop System (Midcourse condition):

| | |
|---|---|
| Natural Frequency | 4.44 rad/sec |
| Damping Ratio | 0.7 |

The expected weight and power of two actuators is 18.5 pounds and 250 watts. This was determined by comparison with similar high rate electrical actuators.

Studies relating thrust vector control to the minimum allowable velocity increment showed that the controlling parameter was the center-of-gravity shift. This parameter can be held to 0.7 degree if propellant migration is eliminated.

The minimum velocity increment is therefore not limited because engine cutoff will always occur at body rates within the recovery limits of the reaction control system without loss of attitude reference.

This is the recommended approach because the alternative of allowing propellant migration would either establish a minimum 8-m/sec limit with resulting $\Delta V$ penalties, increase the TVC requirements to about 60 deg/sec and 20 degrees, plus requiring an increase in the gimbal angle of the inertial reference unit, or result in loss of attitude reference that would necessitate reacquisition search for celestial references.

## 2.0 INITIAL ATTITUDE ERRORS

After separation from the booster, the initial attitude of the spacecraft must be accurately established to provide the proper thrust vector pointing. Four modes were investigated: transtage reference, gyrocompass, single-axis horizon scanner, and Canopus tracker. The transtage reference mode uses the transtage attitude to establish the reference position at which the spacecraft gyros were uncaged, i.e., placed in the rate-integrating mode. The gyrocompass mode uses a two-axis horizon scanner to establish the roll and pitch attitudes and the roll component of orbital rate due to yaw error to establish yaw attitude. The single-axis horizon scanner mode uses a two-axis Sun sensor to establish pitch and yaw attitude and a single-axis horizon scanner to establish roll. The Canopus tracker mode uses a two-axis Sun sensor to establish pitch and yaw attitude and a Canopus tracker to establish roll attitude. Details on these modes appear in subsequent paragraphs.

The general requirement is to initiate spacecraft engine firing at perigee of the Earth orbit that corresponded to transtage engine cutoff.

The weight penalty due to engine ignition delay ranges up to 65 pounds at 4.5 minutes as shown by Figure C-1. If the engine delay time runs much over this, the penalty is not acceptable and it is better to coast one orbit to phase ignition with the epoch of perigee passage. As a result, each of the four control modes were evaluated for "off-transtage" error, "once-around" error, and earliest firing time. The comparative results are shown in Table C-1. The transtage reference mode with the engine-down configuration is preferred.

Table C-1: COMPARISON OF CONTROL MODES FOR INITIAL ATTITUDE

| | Mode of Control | | | |
|---|---|---|---|---|
| | Transtage Reference | Gyro Compass | Single-Axis Horizon Scanner | Canopus Tracker |
| Error "Off Transtage" | < 1.0 deg | 0.7 deg | 0.7-1.5 deg | Not Applicable |
| Error "Once Around" | 1.5 deg | 0.7 deg | 0.7-1.5 deg | 0.7-1.2 deg |
| Earliest Firing Time Delay | Eng down 1 min 30 sec<br>Eng up 3 min 55 sec | 8 min 30 sec | 21 min 5 sec | 2.5 hr |
| Added Weight | None | 10-22 lb | 10-17 lb | None |
| Added Power | None | 5-22 w | 5-12 w | None |
| Critical Constraints | None | ● Requires convergence time of 6 minutes<br>● Requires orbital rate program | ● Requires mechanically gimbaled scanner as function of Earth cone angle<br>● Requires scanner capable of up to 64,000-n-mi range | ● Not applicable to holding orbit with apogee below 39,000 km<br>● Tracker must not be operated below 39,000 km |

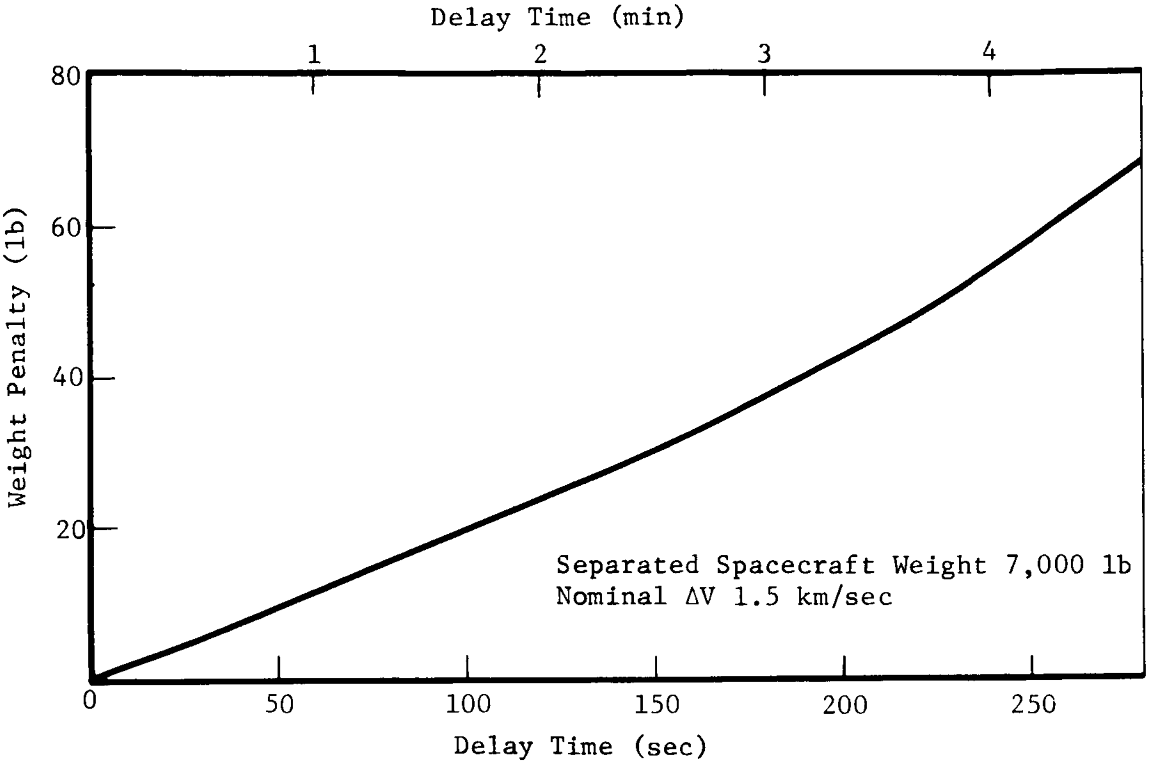

Figure C-1: WEIGHT PENALTY DUE TO ENGINE IGNITION DELAY

Each of the following sections develop comparative data on the four modes. The assumptions involved in every section are:

- Transtage maneuver rate is 2 deg/sec;
- Transtage settling time is 60 seconds maximum after main engine cutoff and 10 seconds after maneuvers;
- Transtage maneuver can be made immediately after engine cutoff without waiting for settling to occur;
- Powered spacecraft settling time after spacecraft separation is 60 seconds and after a maneuver is 30 seconds;
- Powered spacecraft maneuver rate is 0.2 deg/sec;
- Thrust vector control errors due to predictable center-of-gravity errors will be taken care of by adjusting the attitude. The unpredictable errors have been neglected.

## 2.1 Transtage Reference Mode

The transtage reference mode establishes the reference attitude for spacecraft firing by uncaging the IRU gyros during a quiescent period just before spacecraft separation from transtage. The transtage will have been maneuvered to the proper attitude for spacecraft firing before separation. In the case of the engine-up configuration (Model 971-101), it will be necessary to maneuver the transtage out of the way before firing the spacecraft.

*Performance*---Analysis of the powered spacecraft attitude errors that result from using the booster for an attitude reference is summarized in Figure C-2. The errors are shown as a function of time for several spacecraft staging times. If the spacecraft engine is to be fired as soon as possible after transtage burnout, the spacecraft attitude error will be less than 1 degree, $3\sigma$. If the spacecraft is to be fired after a one-orbit coast period of 21 hours, the error will be about 4.5 degrees, $3\sigma$ when spacecraft staging is delayed for the maximum time of 6.5 hours.

The error sources considered in this analysis are listed below.

ERROR SOURCES---BOOSTER REFERENCE MODE

| | |
|---|---|
| Transtage ($3\ \sigma$) | |
| Inertial Measurement Unit Installation | < 1 deg |
| Booster Pad Orientation | |
| IMU Acceleration Sensitive and Acceleration Insensitive Drifts (noncompensable) | |
| IMU Optisyn Quantizing | |
| MGC Computation | |
| Transtage Limit Cycle | |
| Powered Spacecraft ($3\ \sigma$) | |
| Spacecraft/Booster Alignment | 0.125 deg |
| IRU/Spacecraft Alignment | 0.18 deg |
| IRU Drift | 0.3 deg |
| Limit Cycle | 0.3 deg |

The analysis was based on the assumptions listed below.

- Transtage maneuvers to attitude for spacecraft $\Delta V$ firing no matter what the length of the coast period. This means no Sun-acquisition maneuvers for solar panel orientation can be made until after the burn. The cost of these additional maneuvers can be obtained by RSS an additional 0.42 degree, assuming the 0.3-degree deadband is not changed.

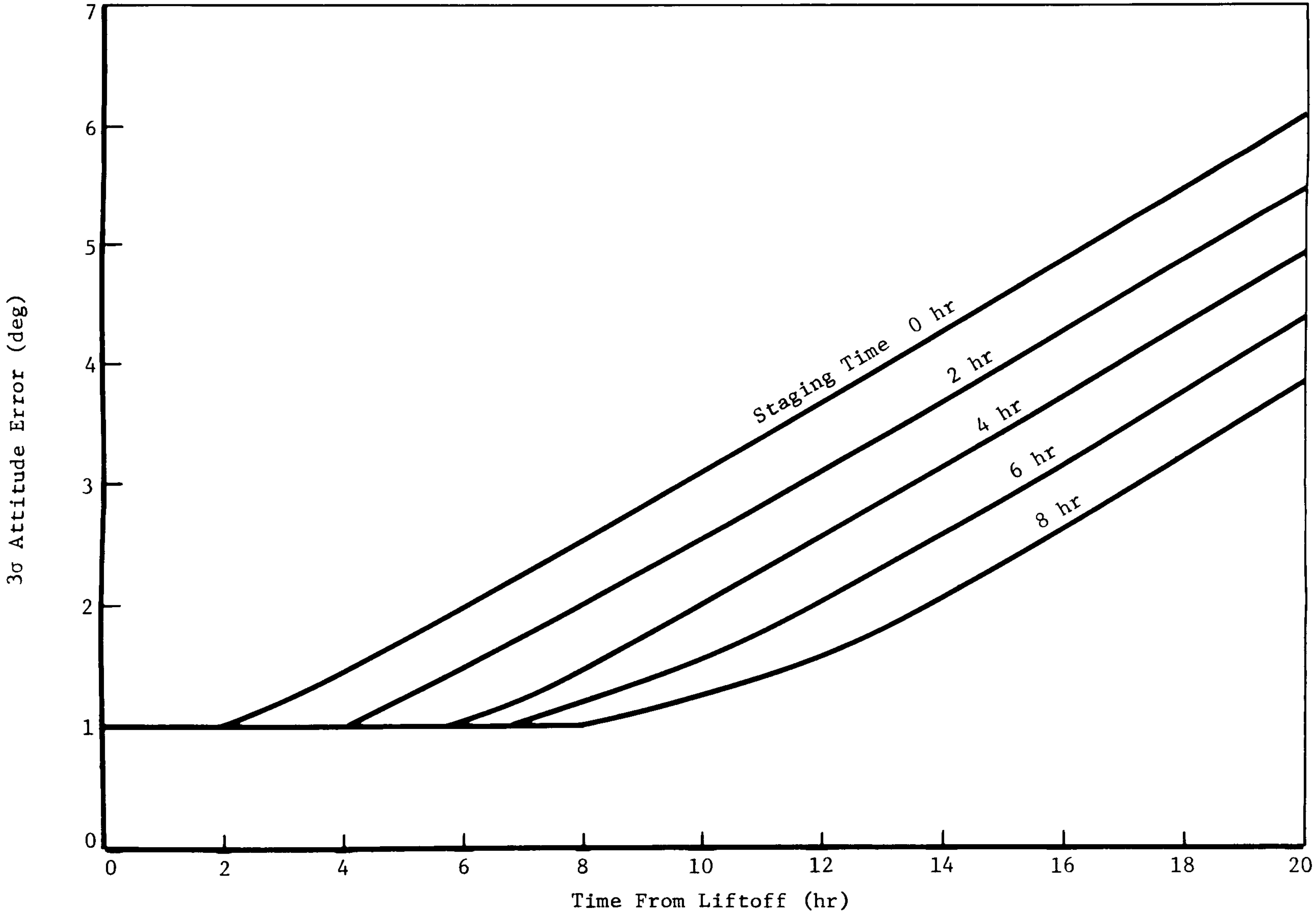

Figure C-2: SPACECRAFT ATTITUDE ERRORS---BOOSTER REFERENCE MODE

- All compensable errors in the IMU are compensated in the normal fashion in the Titan IIIC MGC software throughout the boost and coast phases.
- Center-of-gravity shift is zero. Presumably, the center of gravity will be known and can be compensated for in the attitude specification of the final transtage attitude. If not, the magnitude of this error will have to combine statistically, if random, or arithmetically, if known.
- There will be no modifications to the spacecraft to compensate for the known compensable drift rate of the IRU drift rate. This could cut the drift from 0.3 deg/hr to 0.1 deg/hr $3\sigma$.
- Strictly speaking, these calculations assume that the platform gimbal axes and spacecraft body axes are aligned. However, since the errors are assumed to be symmetrical about all axes, they can be used as body axis errors for any attitude.

*Timeline Analysis*---A timeline analysis is shown for two configurations of the powered spacecraft. Both timelines are for immediate ignition of powered spacecraft after transtage burnout. The once-around case has not been considered because the attitude errors were excessive.

### SEQUENCE OF EVENTS---BOOSTER REFERENCE MODE

Fire Powered Spacecraft at Transtage Burnout, Engine-Down Configuration

| Time (Min:Sec) | Event |
|---|---|
| 0:0 | Transtage second burn complete. |
| 0:10 | Maneuver transtage to put powered spacecraft in firing attitude. |
| 0:20 | Maneuver complete (a maximum 20-deg maneuver at 2 deg/sec). |
| 1:20 | Settling complete in 0.5-deg deadzone. Switch spacecraft gyros to inertial hold and separate spacecraft. |
| 1:30 | 20-foot separation achieved between spacecraft and transtage. |
| 1:30 | Spacecraft settling complete. Initiate powered spacecraft firing without waiting for reaction control to settle spacecraft. |

Appendage deployment must be either before or after this sequence.

Fire Powered Spacecraft at Transtage Burnout, Engine-Up Configuration

| Time (Min:Sec) | Event |
|---|---|
| 0:0 | Transtage second burn complete. |
| 0:10 | Maneuver Transtage to put powered spacecraft in firing attitude. |
| 1:40 | Maneuver complete (a maximum 180-deg maneuver at 2 deg/sec). |

| | |
|---|---|
| 2:40 | Settling complete in 0.5-degree deadzone. Switch spacecraft gyros to inertial hold and separate spacecraft. |
| 2:50 | 20 feet separation achieved. Pitch transtage 90 degrees. |
| 3:40 | Maneuver complete. Fire transtage attitude engines in propellant settling mode for 15 seconds. |
| 3:55 | 100-foot lateral separation achieved. Initiate powered spacecraft firing. |

Appendage deployment must be either before or after this sequence.

## 2.2 Gyrocompass Reference Mode

The gyrocompass reference mode of control will require the addition of a two-axis horizon scanner. The scanner will have to operate in one of the ranges shown in Figure C-3. Any of the conical scanners or edge scanners listed in the data collection can meet these requirements. The weight and power penalty will be about 10 to 22 pounds and 5 to 22 watts. Figure C-4 is a schematic of the gyrocompass system; it has been used by Agena and will be used on the Burner II SESP flight in August 1968.

*Performance*---An analysis for a system operating at an orbital rate of 0.06 deg/sec has been made. The design parameters were:

| | |
|---|---|
| Pitch Scanner Torque Gain | 0.010 deg/sec/deg |
| Yaw Scanner Torque Gain | 0.025 deg/sec/deg |
| Roll Scanner Torque Gain | 0.0074 deg/sec/deg |
| Pitch Program Rate | 0.0604 deg/sec |
| Pitch First Order Corner Frequency | 0.010 rad/sec |
| Roll/Yaw Response | 0.0052 rad/sec at 0.7 critical damping |
| System Accuracy $(1\ \sigma)$ | 0.12 deg |
| Horizon Scanner | 1.0 v/deg limited at ±5 deg |

The estimated $3\sigma$ accuracy of this system is 0.7 degree, either at the time of transtage burnout or after one orbit. A breakdown of these errors are in the following table. These are the attitude errors just before the injection burn.

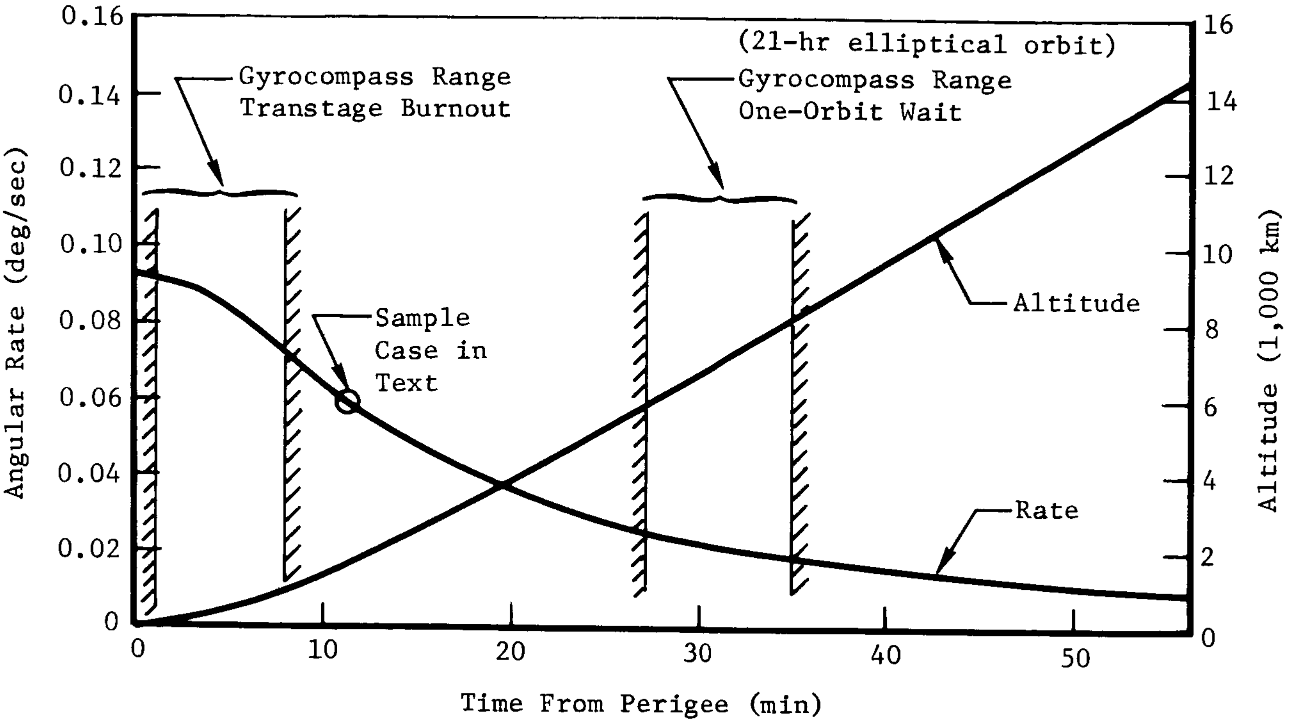

Figure C-3: GYROCOMPASS REFERENCE MODE---ORBITAL PARAMETERS

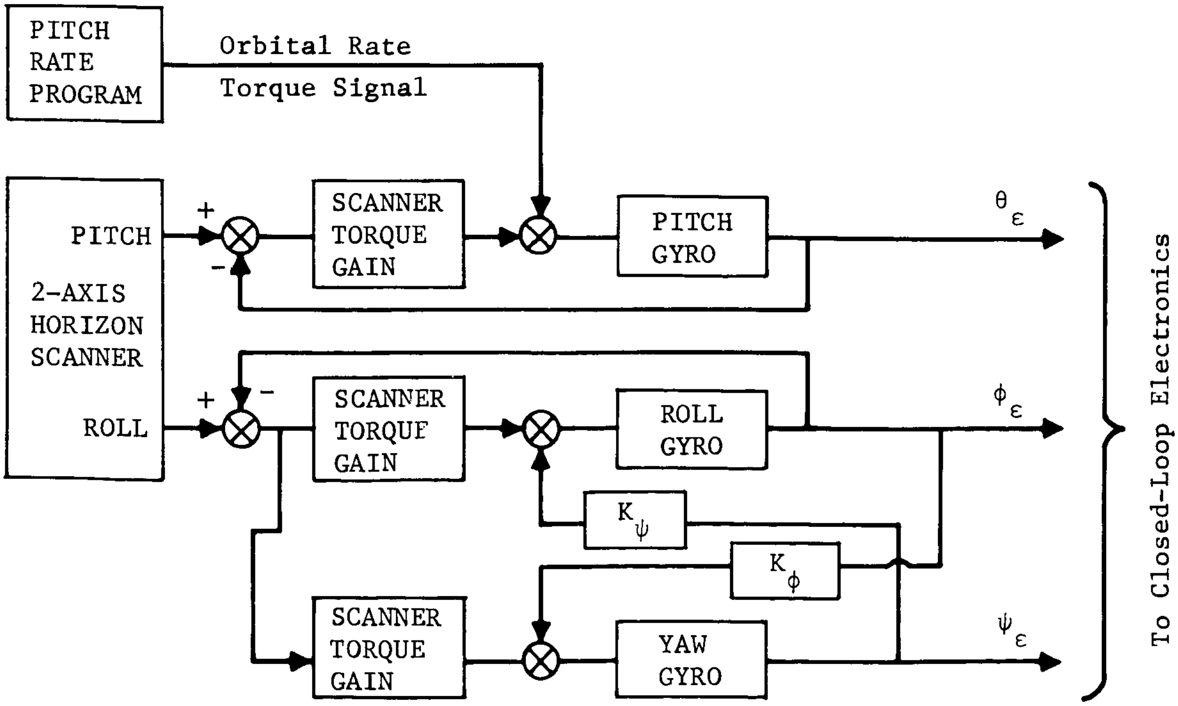
PITCH RATE PROGRAM
Orbital Rate
Torque Signal
2-AXIS HORIZON SCANNER
PITCH
ROLL
+
-
SCANNER TORQUE GAIN
PITCH GYRO
ROLL GYRO
YAW GYRO
$K_\psi$
$K_\phi$
$\theta_\varepsilon$
$\phi_\varepsilon$
$\psi_\varepsilon$
To Closed-Loop Electronics

Figure C-4: GYROCOMPASS MODE

### 3 $\sigma$ ATTITUDE ERRORS---GYROCOMPASS REFERENCE MODE

| Error Source | Transtage*** Burnout (Deg) | Once*** Around (Deg) |
|---|---|---|
| Orbit Injection | 0.08 | 0.24 |
| Horizon Scanner Gyro Compass Mode | 0.36 | 0.36 |
| Gyrocompass Convergence | 0.15 | 0.15 |
| Initial Limit Cycle | 0.3 | 0.3 |
| Maneuver* | 0.3 | 0.3 |
| Final Limit Cycle | 0.3 | 0.3 |
| Horizon Scanner Alignment** | 0.18 | 0.18 |
| RSS 3 $\sigma$ | 0.68 | 0.72 |

* 0.3%, 100 deg/axis

** Not Calibrated

*** All Axes are Approximately Symmetrical

### 2.3 Single-Axis Horizon Scanner Mode

The single-axis horizon scanner mode of control requires the addition of a horizon scanner to establish the roll attitude. This scanner will be required to operate over a wide altitude range as shown in Figure C-5; this rules out conical scanners. Either of the edge trackers listed in Reference 1 will work. The weight and power penalty will be 10 to 17 pounds and 5 to 12 watts. Figure C-6 is a schematic of the single-axis horizon scanner system.

A sequence of events is presented for gyrocompassing at either transtage burnout or at perigee after a one orbit coast.

*Performance*---The pitch and yaw axis performance is identical to that on Lunar Orbiter. The roll axis is very similar to the gyrocompassing mode pitch axis control. The critical problem involved is whether or not the desired roll attitude correction can be achieved during the sweep of the Earth. Figure C-7 summarizes the constraints on tracking time. The two S curves and the tails in the corners are the regions in which the Earth can be tracked. The assumptions for this are:

- The spacecraft X axis is locked onto the Sun;
- The scanner is oriented along the Y axis normal to the Sun line;
- The off axis, yaw, field of view of the scanner is narrow, about 2 degrees;
- The tracking period must be at least 15 minutes;

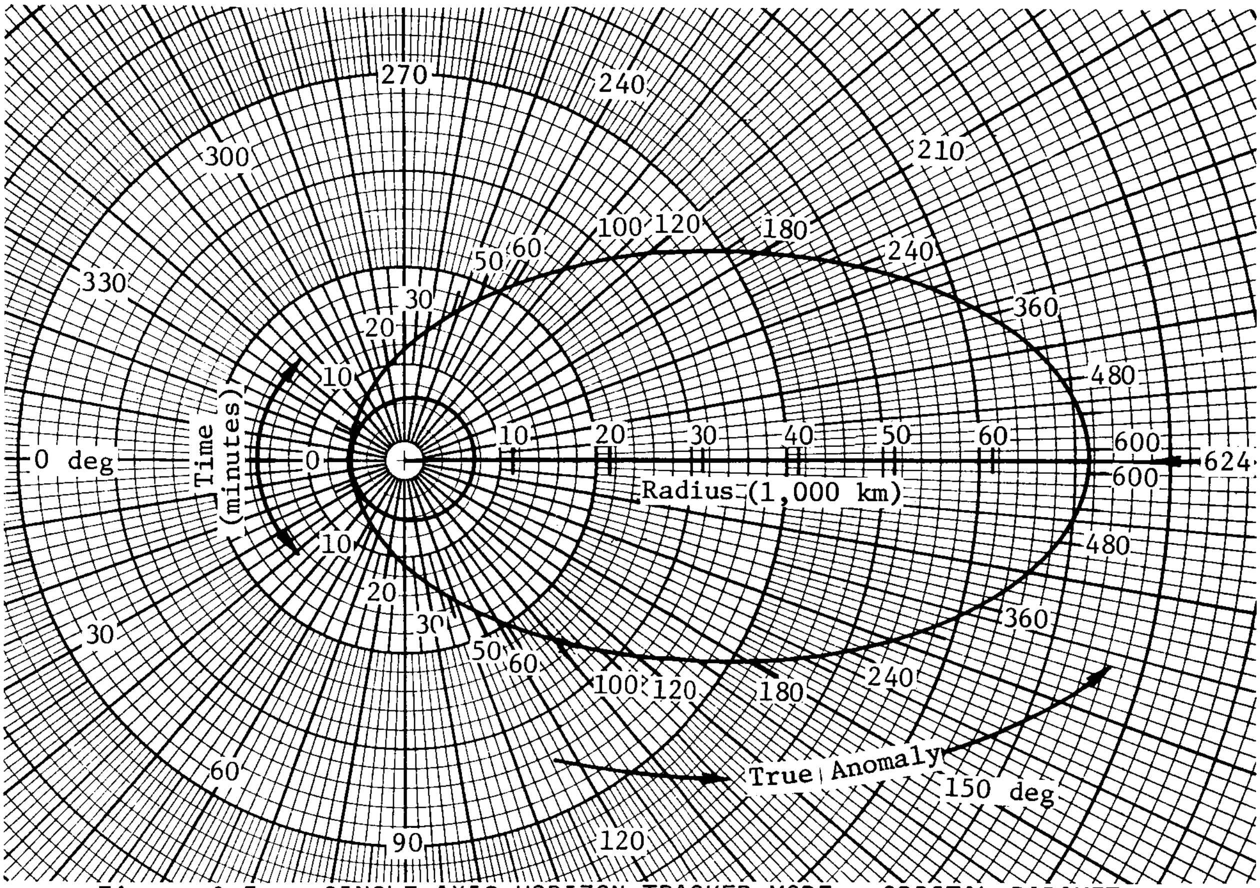

Figure C-5: SINGLE-AXIS HORIZON TRACKER MODE---ORBITAL PARAMETERS

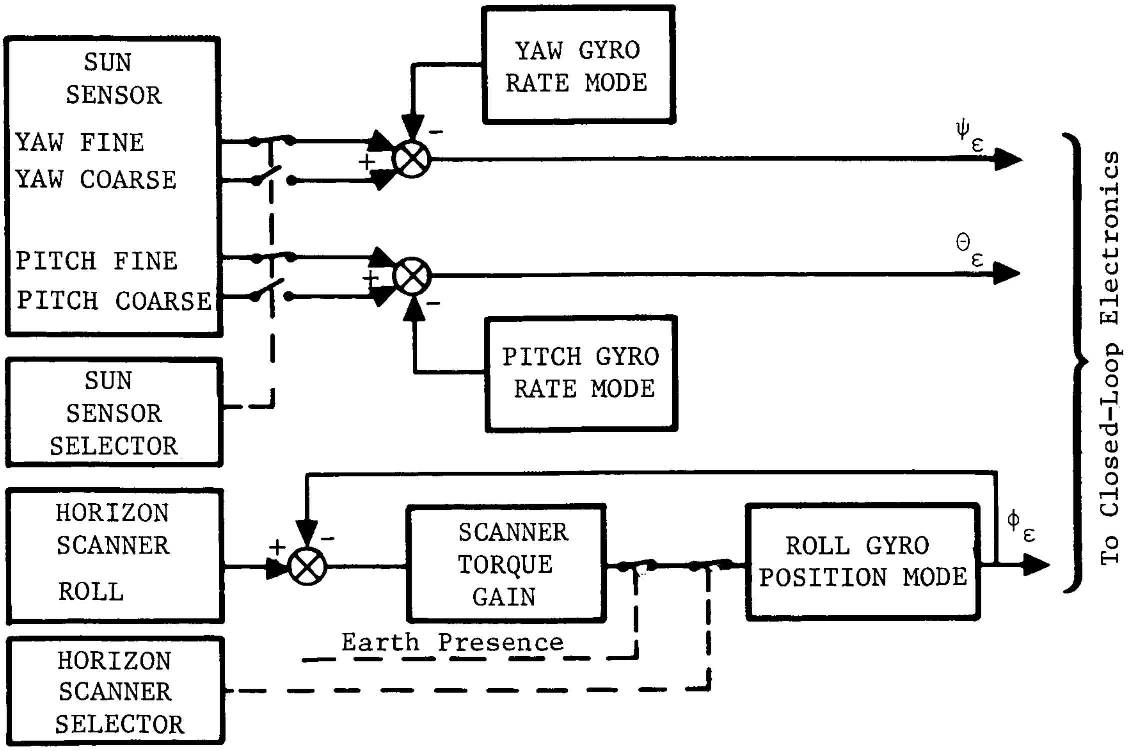
SUN SENSOR
YAW FINE
YAW COARSE
PITCH FINE
PITCH COARSE
YAW GYRO RATE MODE
-
+
$\psi_\varepsilon$
$\Theta_\varepsilon$
+
-
PITCH GYRO RATE MODE
SUN SENSOR SELECTOR
HORIZON SCANNER ROLL
+
-
SCANNER TORQUE GAIN
ROLL GYRO POSITION MODE
$\phi_\varepsilon$
Earth Presence
HORIZON SCANNER SELECTOR
To Closed-Loop Electronics

Figure C-6: SINGLE-AXIS HORIZON TRACKER MODE

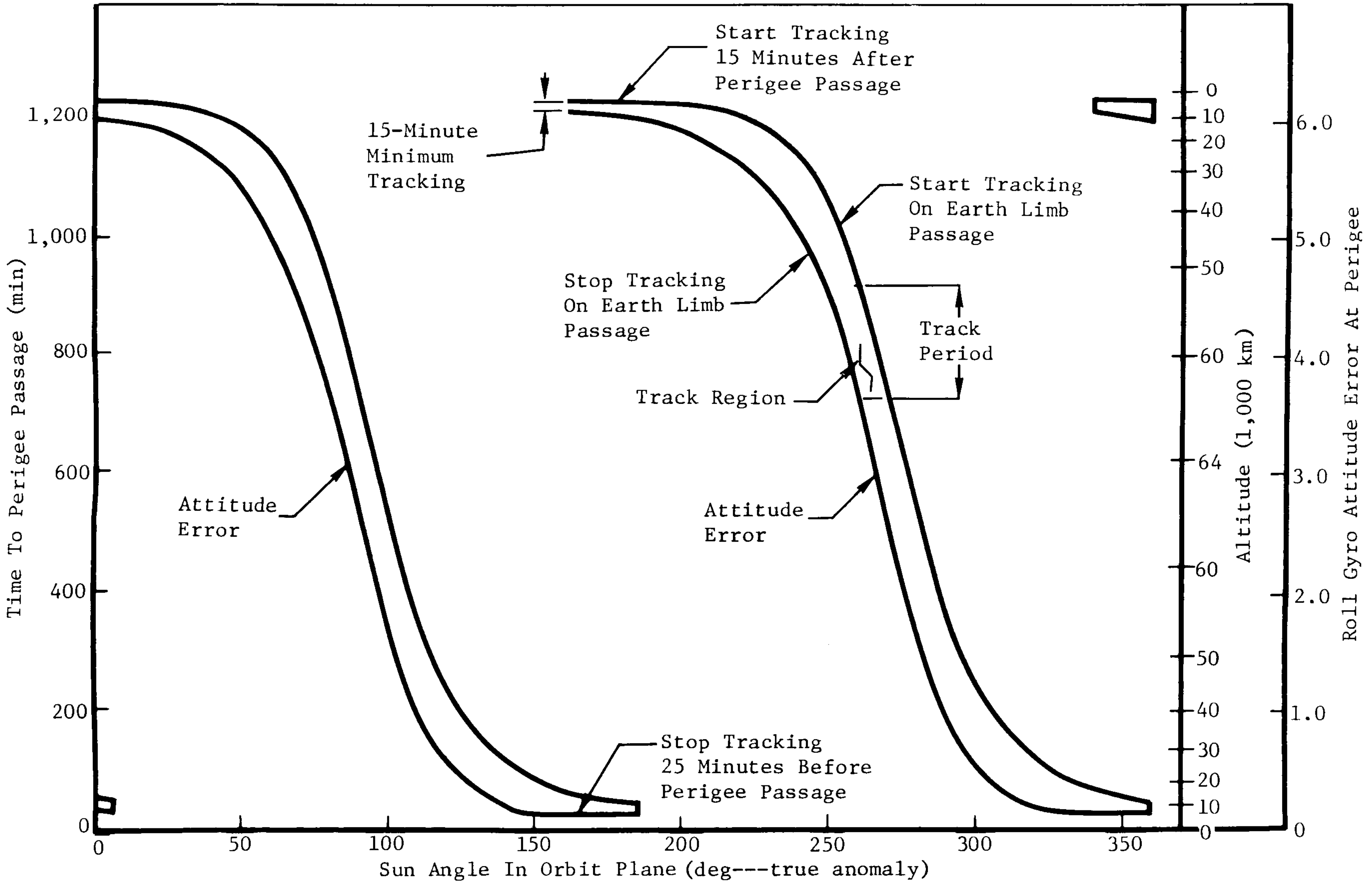

Figure C-7: SINGLE-AXIS HORIZON TRACKER MODE---TRACKING CONSTRAINTS AND DRIFT ERRORS

## SEQUENCE OF EVENTS---GYROCOMPASS REFERENCE MODE

Fire Powered Spacecraft at Transtage Burnout

| Time (Min:Sec) | Event |
|---|---|
| 0:0 | Transtage second burn complete. |
| 0:10 | Maneuver transtage to local vertical. |
| 0:30 | Maneuver complete. |
| 1:30 | Settling complete in 0.5-deg-deadzone. Switch gyros to inertial hold mode and separate spacecraft. |
| 1:40 | Separation complete. Begin gyrocompassing (3 $\sigma$ error = 1.0 deg) |
| 7:40 | Gyrocompassing complete. Pitch to attitude for spacecraft burn. (40 deg maximum single axis maneuver.) |
| 8:00 | Maneuver complete. |
| 8:30 | Initiate powered spacecraft firing. |

Appendage deployment must be either before or after this sequence.

Fire Powered Spacecraft after one Orbit Coast

| Time (Hr:Min:Sec) | Event |
|---|---|
| 0:0:0 | Transtage second burn complete. |
| 0:0:10 | Maneuver transtage to proper attitude for Sun acquisition |
| to | |
| 6:30:00 | Wait 60 sec for settling, switch gyros to inertial hold. Stage spacecraft. Acquire Sun in pitch and yaw. |
| I = Injection | |
| I-1:00:00 | Maneuver to gyro compass attitude (2-axis, 270-deg total). |
| I-00:35:00 | Maneuver complete. Begin gyrocompass at 3 $\sigma$ error-- 8 deg. |
| I-0:27:00 | Gyrocompass complete. Maneuver to firing attitude. |
| I = 0:02:00 | Maneuver complete. |
| I = 0:00:00 | Perigee---fire. |

# 3 $\sigma$ ATTITUDE ERRORS---HORIZON SCANNER REFERENCE MODE

| Error Source | | Once Around | |
|---|---|---|---|
| | | Roll (deg) | Pitch and Yaw (deg) |
| Orbit Injection | | 0.20 | 0 |
| Sun Sensor Alignment* | | -- | 0.18 |
| Sun Sensor | | -- | 0.2 |
| Horizon Scanner Alignment* | | 0.18 | -- |
| Horizon Scanner | | 0.30 | -- |
| Initial Limit Cycle | | 0.3 | 0.3 |
| Switch to Inertial Hold | | -- | 0.3 |
| Maneuver ** | | 0.3 | 0.3 |
| Final Limit Cycle | | 0.3 | 0.3 |
| Inertial Reference Unit Drift*** | | | |
| Sun Angle | 0, 180 | 0.13 | 0 |
| | 10, 190 | 6.0 | 0 |
| | 30, 210 | 5.8 | 0 |
| | 60, 240 | 5.4 | 0 |
| | 90, 270 | 2.6 | 0 |
| | 120, 300 | 0.5 | 0 |
| | 150, 330 | 0.13 | 0 |
| | 180, 360 | 0.13 | 0 |
| RSS 3 $\sigma$ *** | | | |
| Sun Angle | 0, 180 | 0.67 | 0.66 |
| | 10, 90 | 6.04 | 0.66 |
| | 30, 210 | 5.84 | 0.66 |
| | 60, 240 | 5.44 | 0.66 |
| | 90, 270 | 2.68 | 0.66 |
| | 120, 300 | 0.83 | 0.66 |
| | 150, 330 | 0.67 | 0.66 |
| | 180, 360 | 0.67 | 0.66 |

* Not Calibrated
** 0.3%, 100 deg/axis
*** Assumes scanner set at 90 deg to roll axis

- Tracking cannot be done from perigee to 15 minutes after perigee passage to allow time transtage maneuver and staging;
- Tracking cannot be done from 25 minutes from perigee passage to allow time to maneuver the spacecraft before firing spacecraft engine.

The figure shows that for all Sun orientations with respect to perigee, there is at least one period when tracking can occur. The tracker period varies from 15 minutes (at the ends of the S curves) to 200 minutes (in the center of the S curves). The acquisition time for the tracker depends on the initial error, which will be a maximum of about 6 degrees. Assuming a scanner torque gain of 0.025 deg/sec/deg acquisition should be complete in about 3 minutes.

The error at perigee depends almost exclusively on the roll gyro drift between the Earth tracking time and the time of perigee passage. It could be nearly 6 degrees for Sun angles at 20 and 200 degrees. Reduction of this possible error requires gimbaling the scanner in yaw (mechanically). This would shift the S curves by the amount of the gimbal angle.

The error analysis in the following table is based on the assumptions of Figure C-7 listed above. If the scanner is gimbaled ±60 degrees in yaw to move the tracking period as close as possible to the approaching perigee, these errors could be reduced to about 1.5 degrees. The resulting $3\sigma$ RSS error would be 1.63 degrees.

*Timeline Analysis*---A sequence of events is presented for using the horizon scanner as a single-axis roll reference. This was done for two cases: the first for firing powered spacecraft immediately after transtage burn; and the second for firing powered spacecraft after a one-orbit coast period.

## 2.4 Canopus Tracker Reference Mode

The Canopus tracker reference mode uses the baseline attitude control system, Figures 7.3.2 and 7.3.3. Sun sensors and a Canopus tracker are used to establish a celestial reference for initiating maneuvers for spacecraft velocity change.

*Performance*---The two critical performance problems to be considered are near-Earth radiation effects on tracker operation and Earth-light effects on tracker operation. The radiation effects treated in Figure C-8 are based on an average shielding of 0.14 gm/cm$^2$ and worst-case equatorial orbit. In this figure, the radiation levels above the outer Van Allen belt are derived from Lunar Orbiter flight data. The shown inner and outer Van Allen belt energy levels would surely destroy the Lunar Orbiter tracker because it has a constant voltage across the tube that results in a constant amplification factor and a very high tube current. However, the Mariner '69 tracker operates by varying the tube voltage to hold the current constant. Because of this, it is less susceptible to damage and can be operated nearer the fringes of the Van Allen belt. JPL ran tests using X rays to irradiate the Mariner tracker. They found that the tracker operated satisfactorily with little interference at radiation levels up to 50 rads/hr and that performance degradation occurred at 100 rads/hr.

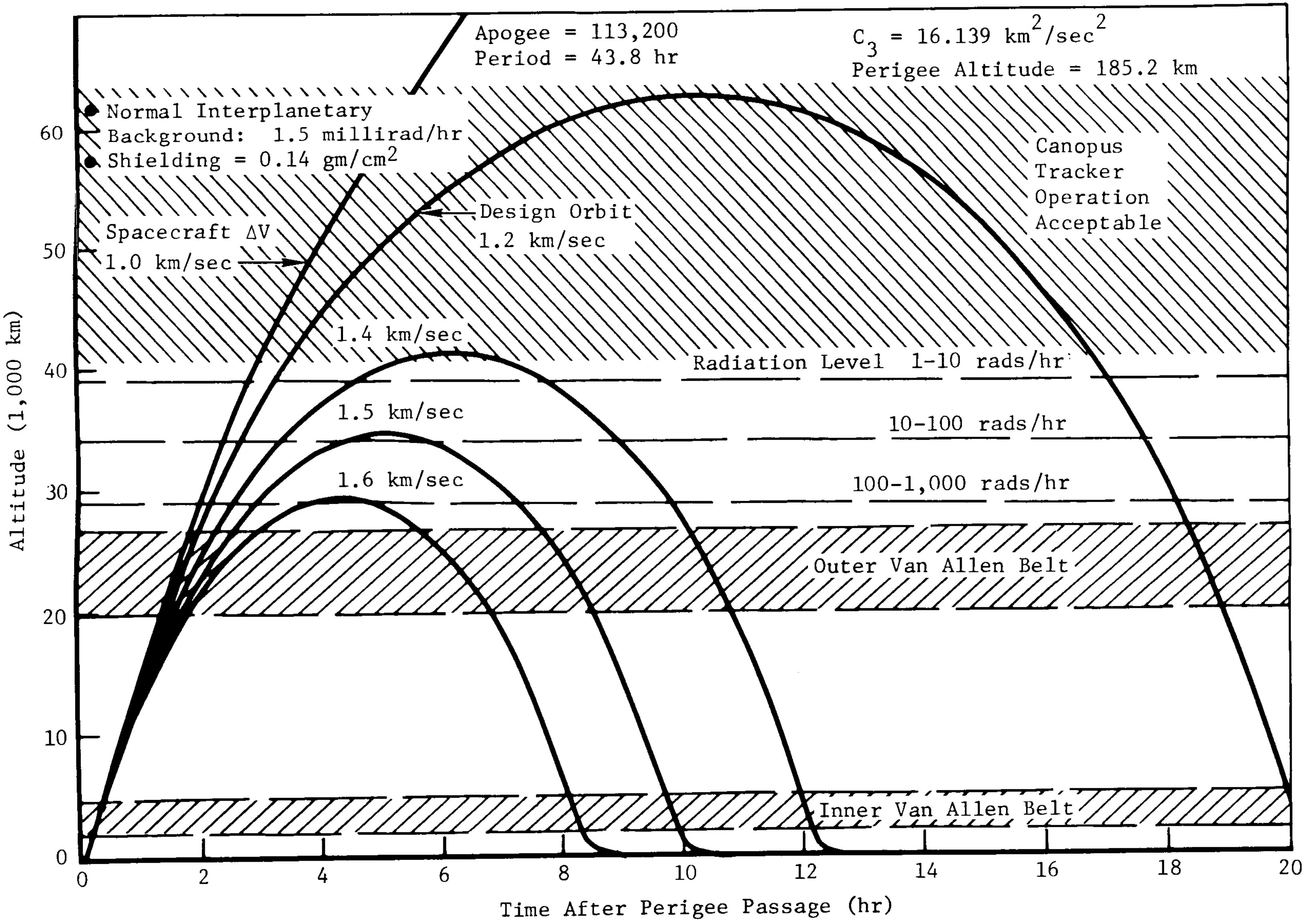

Figure C-8: RADIATION EFFECTS ON TRACKER OPERATION---CANOPUS TRACKER REFERENCE MODE

## SEQUENCE OF EVENTS---SINGLE-AXIS HORIZON SCANNER MODE

Fire-Powered Spacecraft at Transtage Burnout

| Time (Min:Sec) | Event |
|---|---|
| 0:0 | Transtage second burn complete. |
| 0:10 | Maneuver transtage to put powered spacecraft on Sun line and point scanner at Earth. |
| 1:40 | Maneuver complete. (A maximum maneuver of 180 deg was assumed at 2 deg/sec.) |
| 2:40 | Settling complete in 0.5-deg-deadzone. Switch gyros to inertial hold mode and separate spacecraft. |
| 2:50 | Separation complete. Begin Sun and Earth acquisition. |
| 3:20 | Sun acquisition complete (Initial 3 σ error = 1 deg). |
| 4:50 | Earth acquisition complete (Initial 3 σ error = 1 deg). |
| 4:50 | Maneuver to attitude for spacecraft burn. Assume maximum of 15 deg yaw and 180 deg pitch at 0.2 deg/sec. |
| 21:00 | Maneuver complete. |
| 21:05 | Initiate powered spacecraft firing. |

Appendage deployment must be either before or after this sequence.

Fire Powered Spacecraft After One Orbit Coast.

| Time (Hr:Min:Sec) | |
|---|---|
| 0:0:0 | Transtage second burn complete. |
| 0:0:10<br>to<br>6:30:00 | Maneuver transtage to put spacecraft in proper attitude for Sun and Earth acquisition. |
| | Wait 60 seconds for settling. Switch gyros to inertial hold. Stage spacecraft. Acquire Sun in pitch and yaw. |
| Earth Passage | Acquire and track Earth to establish roll attitude. The time must be compatible with the track region (Figure C-7) established by Sun location and the horizon scanner view angle in yaw. At completion of track, switch roll gyro to inertial hold. |

I = Injection

| | |
|---|---|
| I - 0:27:00 | Maneuver to firing attitude (270-deg total maneuvers at 0.2 deg/sec). |
| I - 0:02:00 | Maneuver complete. |
| I - 0:00:00 | Perigee - fire spacecraft. |

The problem of the effect of light on near-Earth operation has not been definitively analyzed. However, the Lunar Orbiter tracker was designed to track within 30 degrees of the illuminated limb of the Moon and 70 degrees from the Sun. The actual performance came very near satisfying these conditions even in the face of rather serious stray light problems, which must be corrected in future spacecraft. Power spacecraft operations at Mars will require tracker operation as near as 2,000 kilometers from Mars at about 30 degrees from the illuminated limb of Mars.

Considering the previous discussion and the data of Figure C-8, it can be concluded that a properly designed and installed tracker should have no problem operating at 30 degrees from the illuminated limb of the Earth at or above 39,000 kilometers. This altitude limit on tracker operation limits the tracking time to about 13 hours for the design orbit. Figure C-9 shows the effects of various orbits on the tracking time. It also shows the roll error that results because the spacecraft must coast in inertial hold between 39,000 feet and perigee.

The error at perigee after a one-orbit coast should be about 0.7 degree in pitch and yaw and 1.2 degrees in roll ($3\sigma$). These are estimated below.

$3\sigma$ ATTITUDE ERRORS CANOPUS TRACKER REFERENCE MODE

| | Roll | Pitch and Yaw |
|---|---|---|
| Sun Sensor Alignment* | 0 | 0.18 |
| Sun Sensor | 0 | 0.2 |
| Canopus Tracker Alignment* | 0.18 | 0 |
| Canopus Tracker | 0.3 | 0 |
| Initial Limit Cycle | 0.3 | 0.3 |
| Switch to Inertial Hold | 0.3 | 0.3 |
| Maneuver** | 0.3 | 0.3 |
| Final Limit Cycle | 0.3 | 0.3 |
| Inertial Reference Unit Drift | 0.9 | 0 |
| RSS $3\sigma$ | 1.18 deg | 0.66 deg |

* Not calibrated.

** 0.39 degree, 100 deg/axis

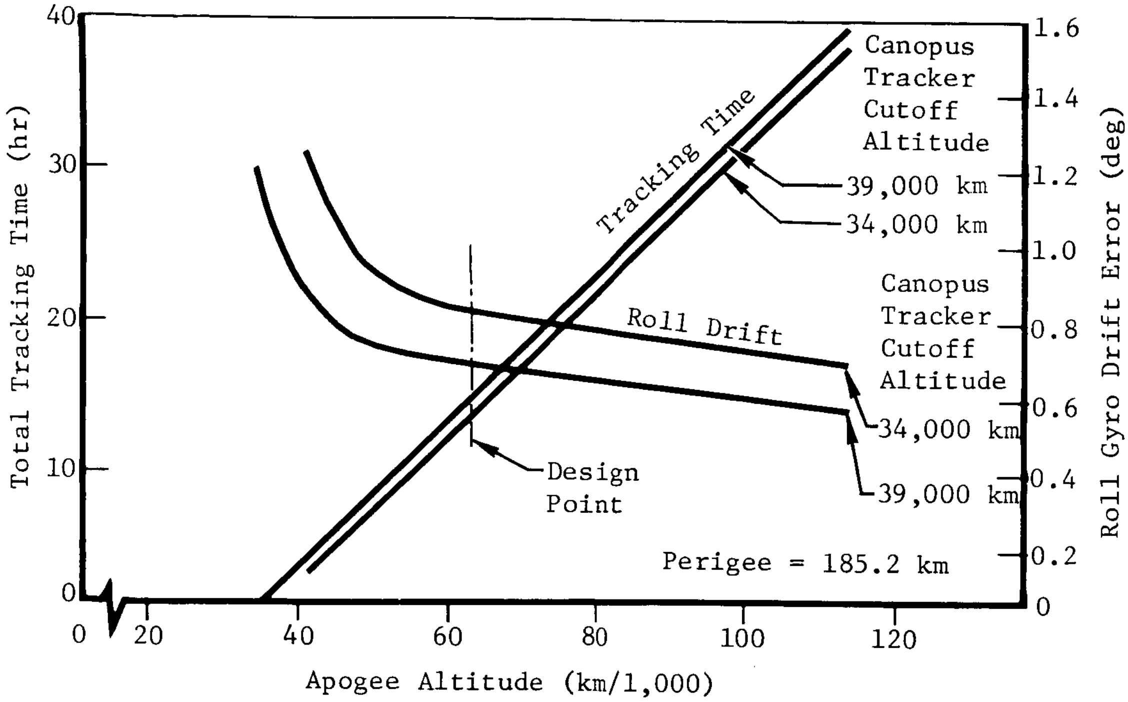

Figure C-9: CANOPUS TRACKER REFERENCE MODE---ORBIT EFFECT ON DRIFT AND TRACKING

## 3.0 STAGING RATE STUDIES

All of the methods for establishing the initial spacecraft attitude assume some prior knowledge of its attitude to a reasonable degree of accuracy. This is necessary either to establish the boost-assist thrusting attitude directly or to establish a reference attitude from which to initiate acquisition using spacecraft sensors. Therefore, it is necessary to ensure that staging rates imparted to the spacecraft are below those that the reaction control system can damp out before attitude reference is lost by hitting the IRU gyro stops.

Two methods of staging have been considered. The first is a helium-retro system designed by the Martin Company, the second is a conventional spring-separation system.

The Martin Company's helium-retro system is preferred because the separation rates should not exceed the maximum limit cycle rates of the transtage with powered spacecraft attached. Figure C-10 indicates these rates will be less than 0.2 deg/sec in roll and 0.04 deg/sec in pitch and yaw for a 7,000-pound spacecraft. The system operates by venting the remaining transtage propulsion system helium pressurant, which retards the forward velocity after redundant explosive nuts on separation bolts have been blown. This system has been designed and flown but it is not currently installed on transtage. The system will add 25 pounds to the transtage. A minimum of 20 feet separation in 10 seconds will be achieved.

An analysis of a more conventional spring-separation staging system was conducted to determine the separation rates to be expected. These rates are used for a design constraint on the reaction control system design. The

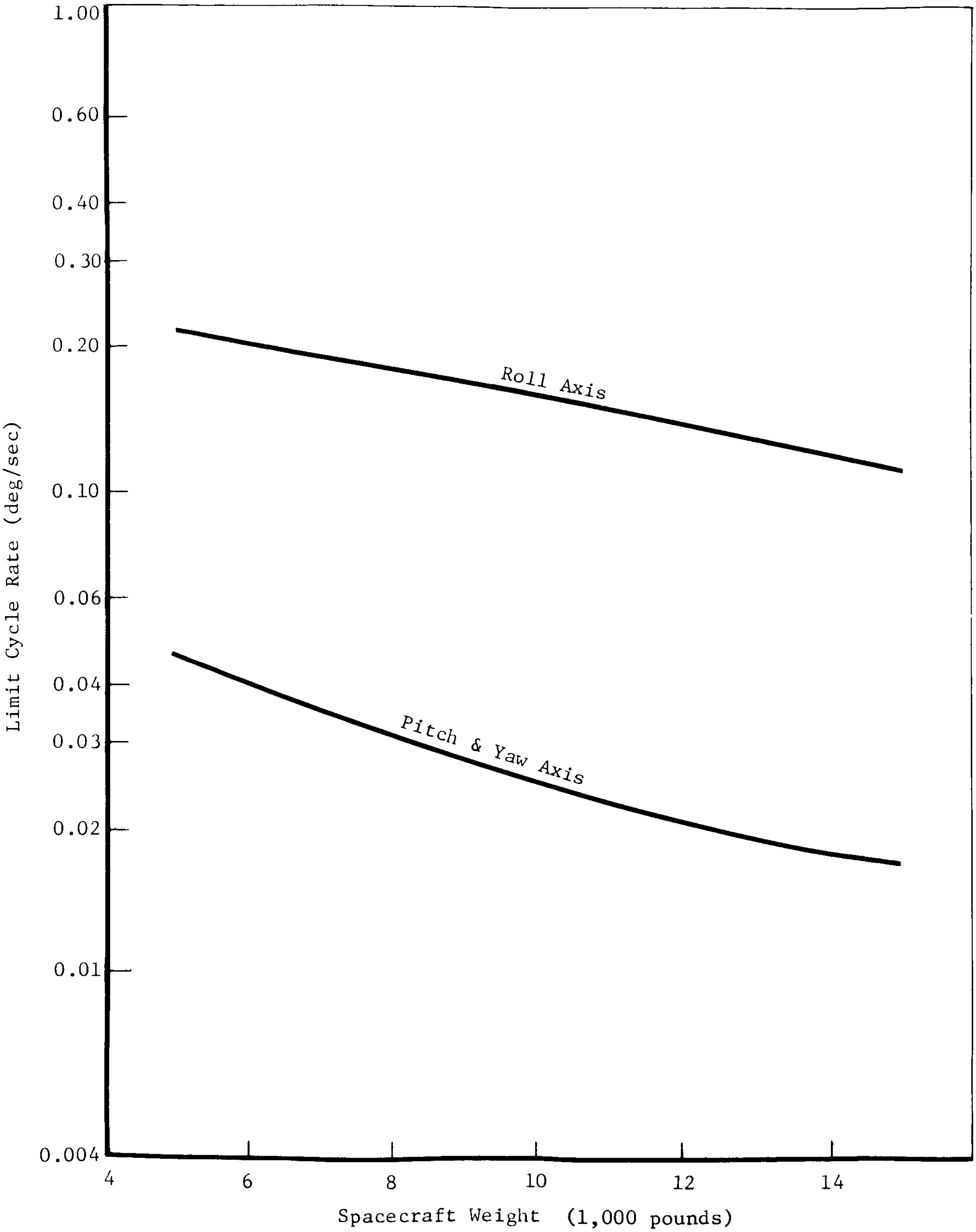

Figure C-10: LIMIT CYCLE CONTRIBUTION TO SPACECRAFT TIP-OFF RATES design requirement on the system is that 20 feet separation occurs in 10 seconds. The analogy used for the analysis is shown in Figure C-11. The pitch and yaw rate contributions of limit cycle, a 4% spring tolerance, and a 1-inch center-of-gravity offset were statistically combined. These error sources and the resulting 3σ design limit are shown in Figure C-12. Pitch and yaw rates of 0.6 deg/sec were used for the 7,000-pound spacecraft.

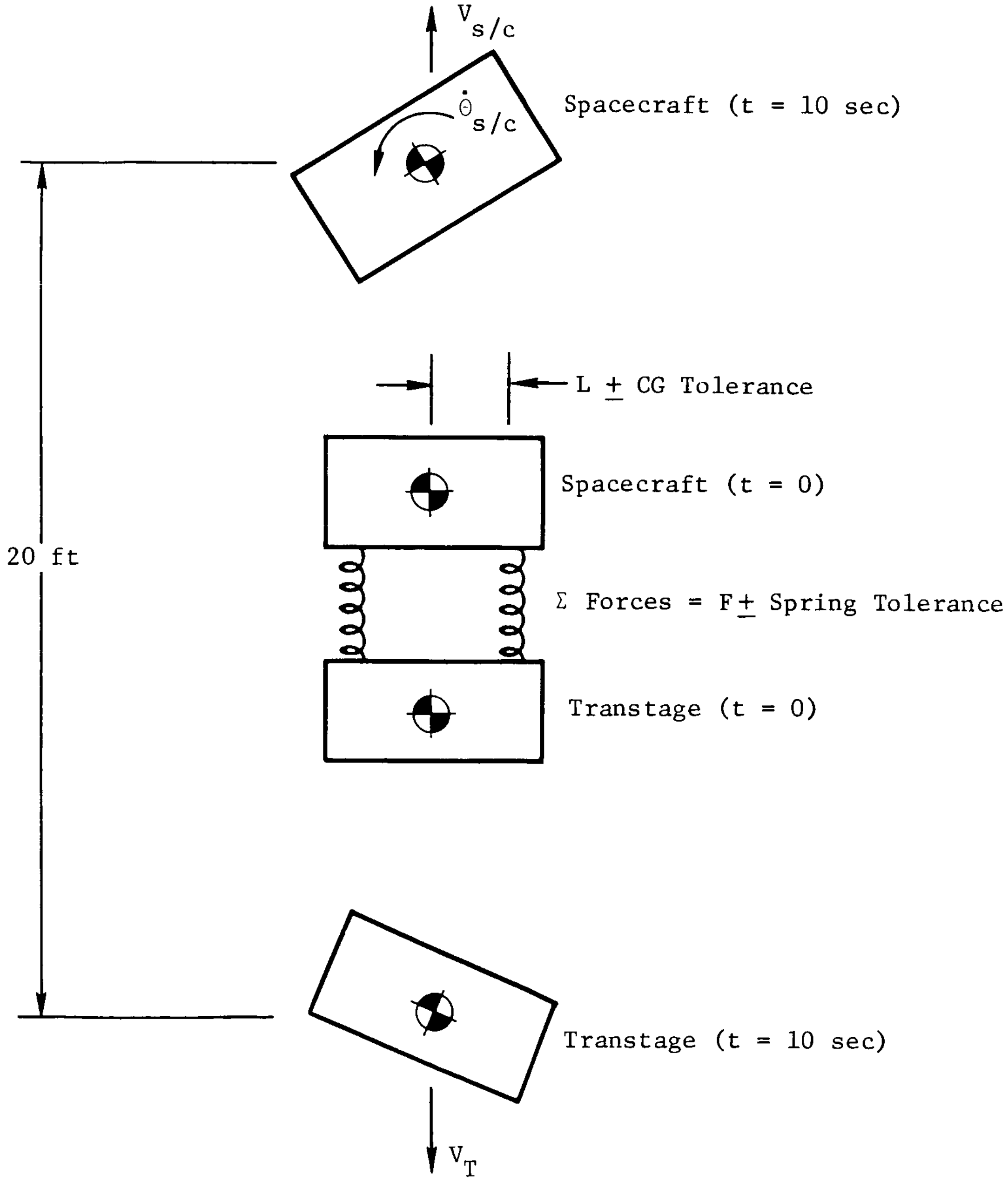
$V_{s/c}$
$\dot{\Theta}_{s/c}$
Spacecraft (t = 10 sec)
L ± CG Tolerance
Spacecraft (t = 0)
20 ft
Σ Forces = F ± Spring Tolerance
Transtage (t = 0)
Transtage (t = 10 sec)
$V_T$

Figure C-11: SPRING SEPARATION MECHANISM MODEL

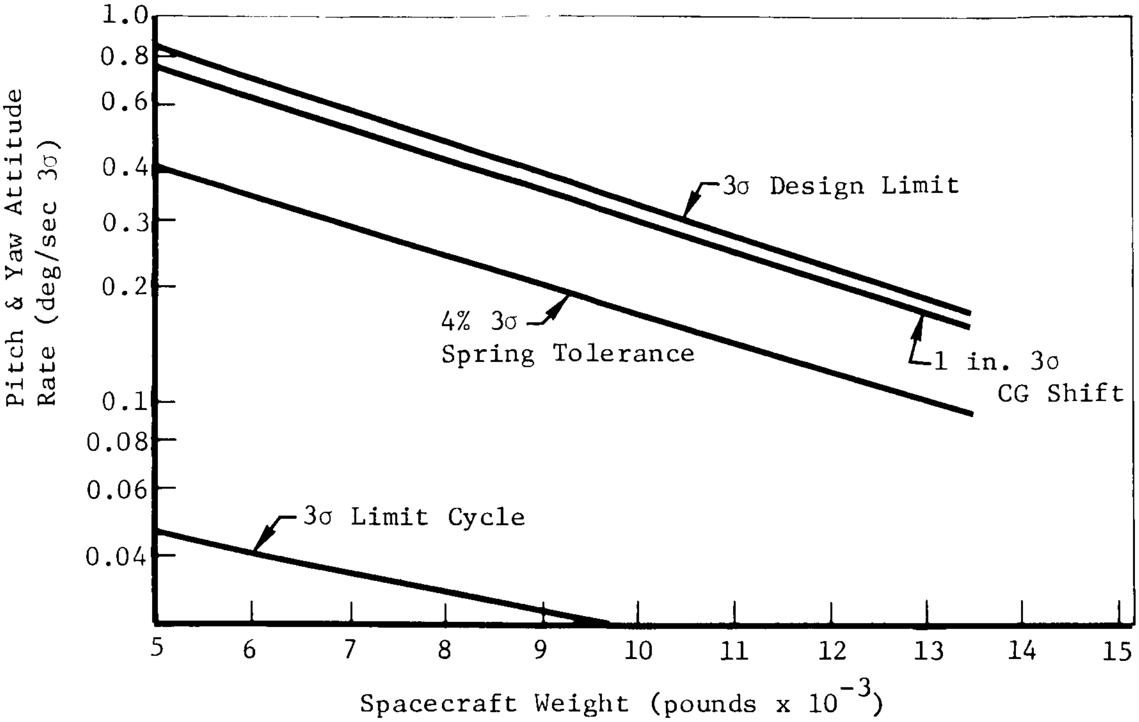

Figure C-12: ATTITUDE RATES AT SEPARATION---SPRING MECHANISM

## 4.0 REACTION CONTROL SUBSYSTEM

The purposes of the reaction control subsystem (RCS) study were to define the attitude control performance requirements, to determine the optimum torquing mechanization to meet these requirements, and to size the optimum system. A cold-nitrogen reaction control system was found to be the best system. This analysis was confined to the 7,000-pound spacecraft.

### 4.1 Attitude Control Performance Requirements

To provide a realistic evaluation of the attitude control system torquing mechanization, it will first be desirable to establish control system performance requirements that will satisfy mission operational requirements and also be compatible with known hardware and interface subsystem constraints. Control acceleration and rate constraints are convenient parameters to consider first, as they provide insight to performance requirements regardless of spacecraft size.

*Maneuver Rate and Control Acceleration*---A minimum spacecraft maneuver rate will be determined by either science pointing requirements or by the electrical power system constraint of off-Sun time related to required maneuvers. In the absence of known requirements on science pointing, it is assumed that these requirements will be satisfied by rates established for other known requirements. The longest off-Sun time (other than the boost-assist ΔV burn) is assumed to occur during the planet orbit insertion maneuver, where a two- or three-axes maneuver and approximately a 3-minute engine burn is required. For a 90-minute off-Sun constraint, as defined by the power subsystem, a maneuver rate of 0.1 deg/sec appears to be a minimum acceptable design constraint.

Maximum allowable spacecraft maneuver rates that can be used depend on operational procedures, IRU mechanization, and spacecraft control acceleration capability. If, for example, the Lunar Orbiter maneuver procedure is considered, where the gyro is switched to the inertial hold mode at completion of a maneuver, the allowable maneuver rate is dependent on gyro gimbal limits and available control acceleration. This relationship is plotted in Figure C-13 for three values of gimbal limits. This data also provides control acceleration requirements for the spacecraft attitude control system when the transtage is used as a reference for the boost-assist engine burn. Based on estimated separation rates of 0.6 deg/sec for a 7,000-pound spacecraft, the required pitch and yaw control acceleration must be 0.045 deg/sec$^2$ or greater. Because roll separation rates are only 0.2 deg/sec, a 0.03 deg/sec$^2$ control acceleration is selected to provide reasonable maneuver settling time. This level can tolerate roll separation rates up to 0.5 deg/sec.

The control impulse (reaction control nitrogen) varies directly as a function of total rate change for a given maneuver. Therefore, to minimize the maneuver nitrogen requirement and a maneuver rate of 0.2 deg/sec, which appears to be a conservative design condition, was chosen. For the required control acceleration levels (0.045 deg/sec$^2$ and 0.03 deg/sec$^2$), maneuver settling time will be about 20 seconds. If derived rate in the form of lag around the switching amplifier is included, the settling time will be approximately doubled.

By combining the known constraints, as shown in Figure C-14, an acceptable region for attitude control design conditions is defined. Selected ACS requirements for the powered spacecraft are indicated. Typical Lunar Orbiter and Voyager design points are also included for reference.

### 4.2 Reaction Control System

Having established a startburn design requirement, the reaction control system thrust levels can next be determined for any specific configuration. It is obvious that the reaction control acceleration requirements (consequently, thrust levels) are sized by the transtage separation rates when the transtage attitude reference must be retained by the powered spacecraft. For the specific case of the 7,000-pound spacecraft, the required 0.05 deg/sec$^2$ acceleration results in a reaction control thrust requirement of 0.29 pound in pitch and yaw. Note that acceleration levels will be more than three times as great for the orbit condition if a single-thrust-level system is used.

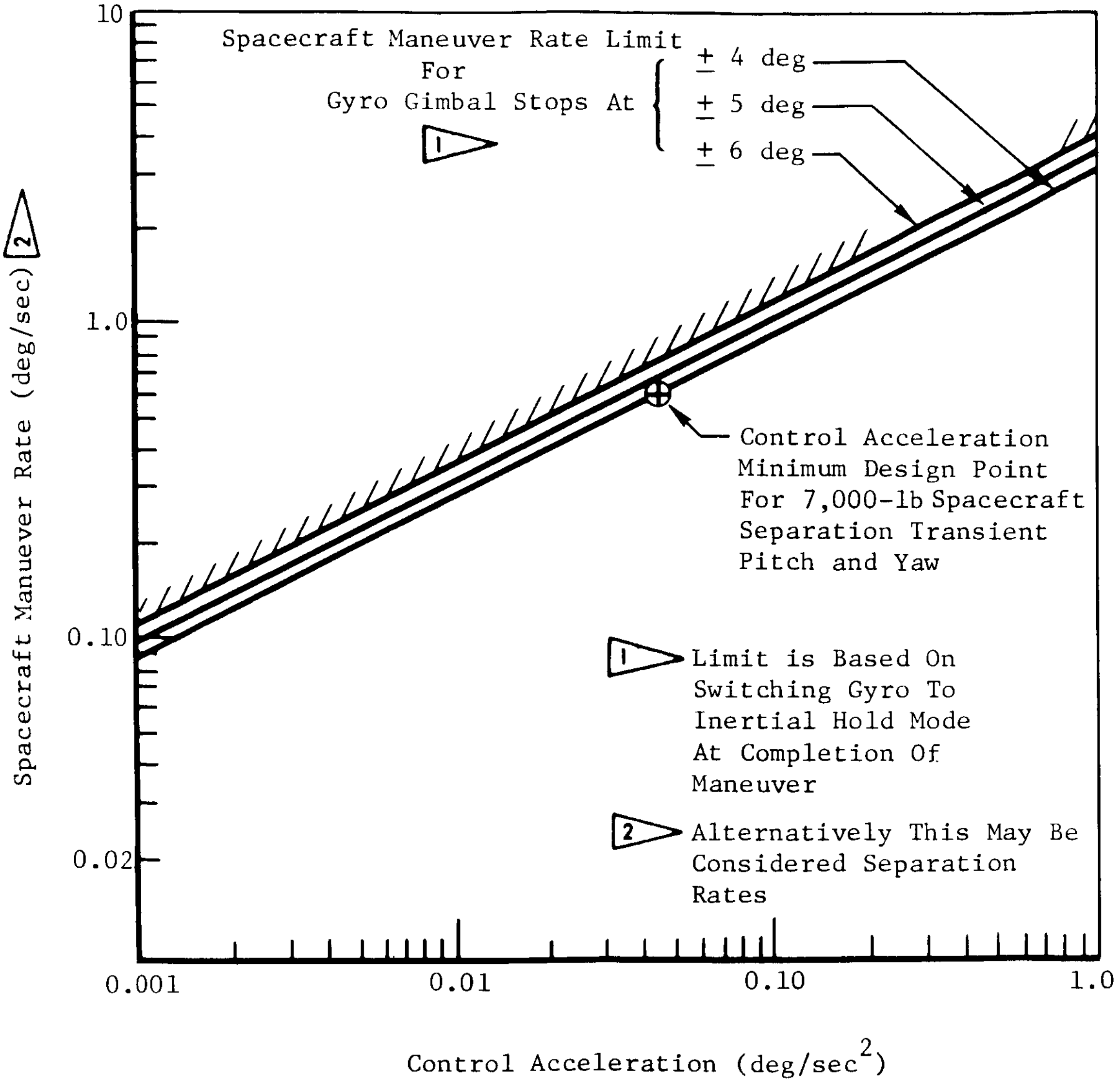

Figure C-13: SPACECRAFT CONTROL ACCELERATION AND RATE LIMITATIONS AS CONSTRAINED BY GYRO GIMBAL LIMITS

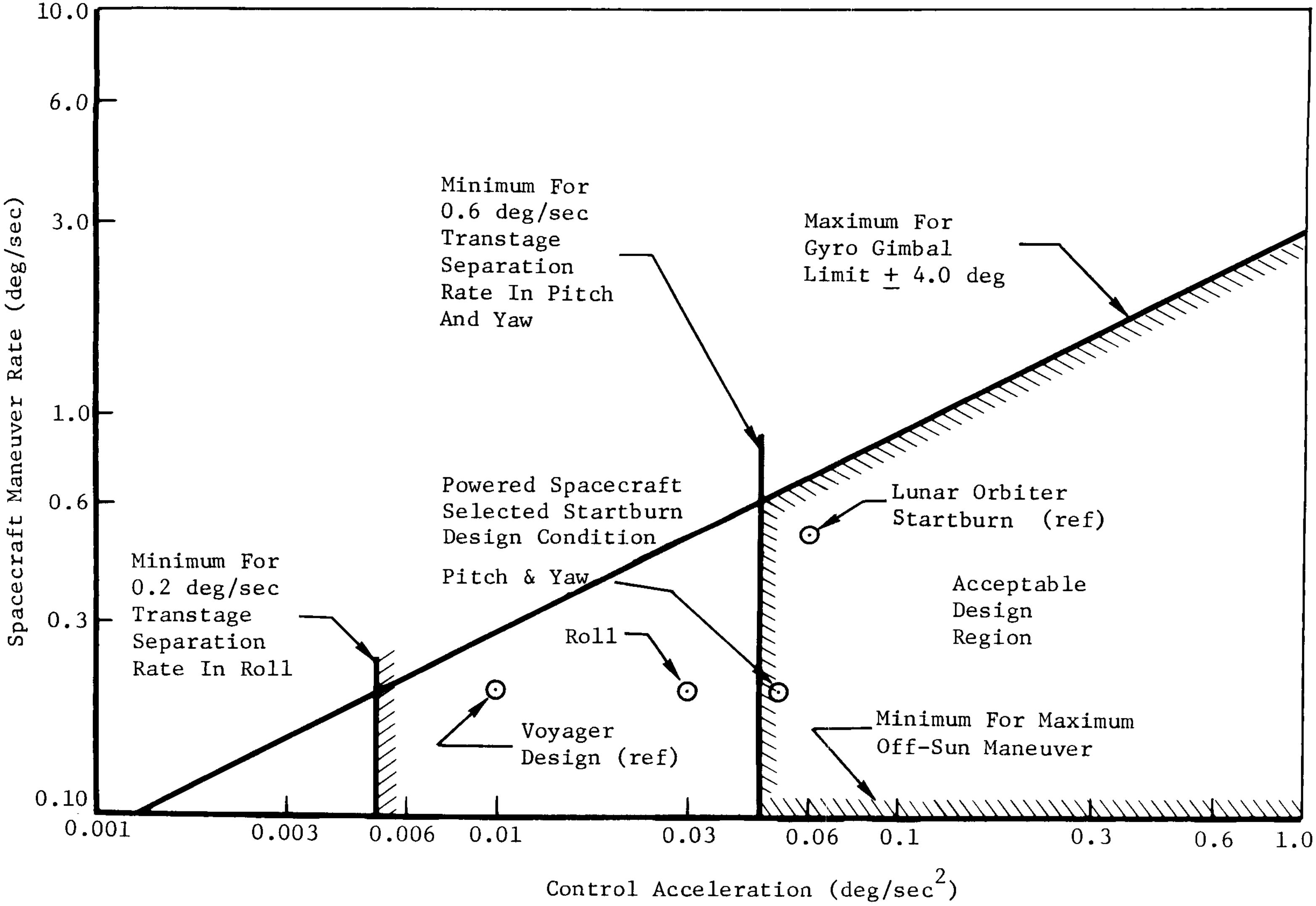

Figure C-14: POWERED SPACECRAFT ATTITUDE CONTROL SYSTEM PERFORMANCE REQUIREMENTS

The roll thruster sizing is based on 0.03 deg/sec$^2$ acceleration capability at the startburn inertia. Two thrusters in couple at 0.07 pound each will meet this requirement. The resultant control accelerations increase to a maximum of 0.065 deg/sec$^2$ for the orbit condition.

*Reaction Control Nitrogen Budget*---An estimate of the reaction control system nitrogen requirement for the 7,000-pound spacecraft can be calculated based on the following assumed control system performance parameters.

1) Maneuver Rate 0.2 deg/sec

2) Control Acceleration (deg/sec$^2$)

| | Startburn | Transit | Orbit |
|---|---|---|---|
| Pitch | 0.05 | 0.053 | 0.185 |
| Yaw | 0.05 | 0.053 | 0.185 |
| Roll | 0.03 | 0.04 | 0.065 |

3) Thrust Level (pounds)

| | |
|---|---|
| Pitch | 0.29 |
| Yaw | 0.29 |
| Roll | 0.07 (2 in couple) |

4) Limit Cycle Deadband ±0.3 deg at Mars. For an uncompensated Sun sensor, the resultant deadband would be ±135 deg at Earth. An average value of ±0.22 deg will be used for nitrogen calculation for the transplanet phase.

5) Limit cycle residual rate varies with control acceleration and thruster impulse bit as shown in Figure C-15. Rates associated with a 20-millisecond pulse time will be used for determining limit cycle nitrogen requirements. This is equivalent to double pulse operation, as a nominal 10-millisecond one shot will be included in the design.

6) Solar pressure disturbance torque is a function of antenna area, solar pressure constant (both of which vary throughout the mission), and antenna boom length. Furthermore, the antenna projected area varies differently for each mission as the area is a function of antenna cone and clock angle requirements. While maximum torques can be estimated for any configuration, a specific mission disturbance profile must be calculated to provide a realistic disturbance level and the associated reaction control system penalty. An estimated average value of $24 \times 10^{-6}$ ft/lb will be used in calculating the disturbance penalty. This is based on a projected antenna area of 35 square feet, an antenna boom length of 10 feet, and an average Earth-Mars solar constant.

Although several candidate mission procedures are being considered, a nitrogen budget will be calculated for only one, as differences reflected in the nitrogen requirement will be insignificant. Table C-2 itemizes the estimated attitude control nitrogen requirement for the transplanet phase, including the orbit insertion maneuver, for the 7,000-pound powered spacecraft.

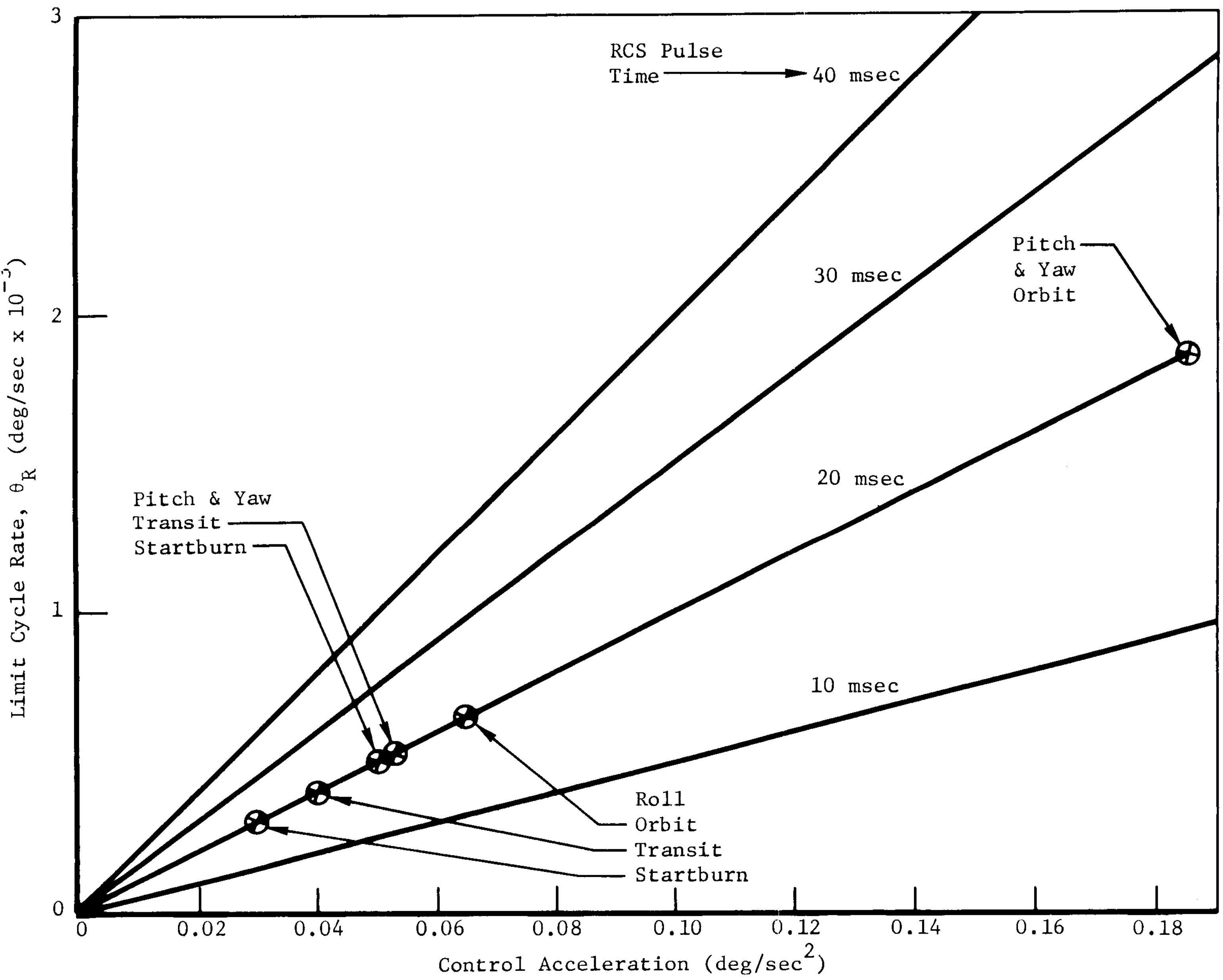

Figure C-15: LIMIT CYCLE RATE

Table C-2: POWERED SPACECRAFT RCS NITROGEN ESTIMATE---TRANSPLANET

| Item | $N_2$ Weight (lb) | |
|---|---|---|
| 1. Initial Acquisition | | |
| • Reduce Separation Rates | 0.4 | |
| • Acquire Sun | 0.1 | |
| • Acquire Canopus | 0.4 | |
| Subtotal | | 0.9 |
| 2. Maneuvers | | |
| • Boost Assist | 0.3 | |
| • 3 Midcourse | 2.3 | |
| • 1 Orbit Injection | 0.3 | |
| Subtotal | | 2.9 |
| 3. Cruise (230 days) | | |
| • Disturbance (Pitch) | 2.30 | |
| • Coupling | 0.7 | |
| • Limit Cycle (Yaw and Roll) | 1.3 | |
| • Leakage | 1.0 | |
| Subtotal | | 5.3 |
| Total Transplanet | | 9.1 |

An estimate of attitude control nitrogen requirements for a 30-day primary mission is shown in Table C-3. The largest requirement is the result of an assumed one science maneuver for each orbit. Because the use rate is constant for all items, the primary mission penalty is essentially 0.1 pound per day.

Also shown in Table C-2 is an estimate for an additional 150-day extended mission where no maneuvers are required. Sun reacquisition nitrogen is an added requirement and occurs during the first half of the extended mission. All other use rates are constant, so an average rate of 0.035 lb/day is representative.

Table C-3: POWERED SPACECRAFT RCS NITROGEN ESTIMATE---ORBIT

| Primary Mission | $N_2$ Weight (lb) |
|---|---|
| Orbit (30 days - 24-hr Orbit) | |
| 1. Science Maneuvers (30 - 3 Axes) | 2.10 |
| 2. Disturbance (Pitch) | 0.15 |
| 3. Coupling | 0.05 |
| 4. Limit Cycle (Yaw and Roll) | 0.5 |
| 5. Reacquisition | 0 |
| 6. Leakage | 0.15 |
| Total | 2.95 |
| Rate = 0.1 lb/day | |
| **Extended Mission** | |
| Orbit (150 days) | |
| 1. Maneuvers | 0 |
| 2. Disturbance | 0.75 |
| 3. Coupling | 0.25 |
| 4. Limit Cycle | 2.25 |
| 5. Reacquisition | |
| Sun (77 - 1 Axis) | 1.30 |
| Canopus | 0 |
| 6. Leakage | 0.65 |
| Total Orbit | 5.20 |
| Rate = 0.035 lb/day | |
| Total Requirement - Transplanet and Orbit | 17.25 |

The estimated total $M_2$ required from transplanet through the extended mission is 17.25 pounds. No safety factor or contingency budget is included in these values.

## 4.3 Control Torque Trade Study

Trade study results of various control torquing mechanization schemes are presented in Figure C-16. These results indicate that the guidance and control subsystem weight using a cold-nitrogen reaction control system is competitive with a hot gas system for the powered spacecraft mission. A nitrogen RCS is therefore recommended for the powered spacecraft torquing control based on past use, availability, and expected costs.

The only hot gas system considered was the monopropellant hydrazine plenum system. Other hydrazine systems could not be considered because of limitations in minimum pulse capability, small thruster development required, and excessive delays in cold thruster response. The small weight saving with this system does not appear to offset potential thermal problems, development problems, and high cost.

The reaction wheel and control moment gyro system weights represent a system in which either the wheel or gyro is used to provide maneuver control and limit cycle stabilization. A reaction control system is, however, still required for separation transient control and gyro or wheel desaturation necessitated because of unidirectional disturbances. Sizing of component is determined by the angular momentum requirement for the startburn maneuver requirement of 6.5 ft-lb/sec. Representative components to meet this requirement are:

Reaction Wheel

Bendix Reaction Wheel---Three Required

Type 1823408

H = 8.84 ft-lb/sec at 1,250 rpm

Stall Power = 43 watts

Weight = 18 pounds each

Size = 12-degree diameter x 5 inches high

Control Moment Gyro

Nortronics CMG---Three Required

Model II

H = 6.7 ft-lb/sec

Running Power = 9 watts

Weight = 23 pounds each

Size = 7-inch diameter x 10 inches long

An added weight penalty, not included in Figure C-16, is that incurred by the electrical power subsystem. Even without this penalty (typically 0.30 pound per watt), it is apparent that neither of these configurations are competitive and are not recommended.

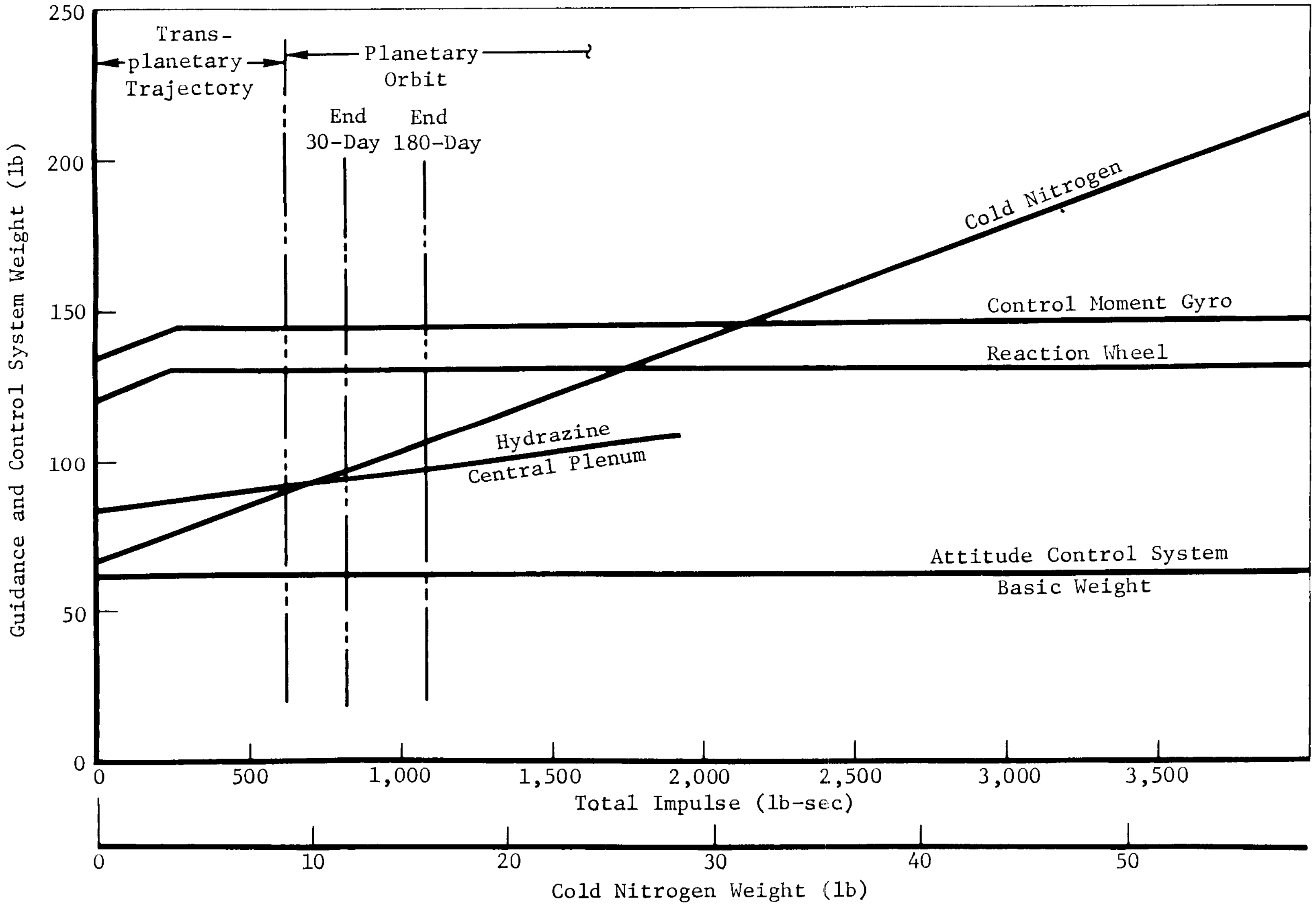

Figure C-16: GUIDANCE AND CONTROL WEIGHT TRADE---7,000-LB SPACECRAFT

## 5.0 THRUST VECTOR CONTROL

The purposes of the thrust vector control study were:

- To establish thrust vector actuator performance requirements;
- To examine the interface with the minimum velocity increment requirements;
- To define weight and power trade data for the thrust vector control actuator.

Performance data and minimum $\Delta V$ information was developed using linear analysis with a first order thrust vector control actuator and a second order rigid body. It was determined that a 15-cps actuator with rate and deflection requirements of 10 deg/sec and 3 degrees was adequate for the 7,000-pound spacecraft with a 3,500-pound-thrust engine. A closed-loop natural frequency of 4.44 rad/sec and 0.7 damping ratio was assumed to be low enough to avoid coupling with structural frequencies and high enough to provide reasonable frequency response. The minimum allowable $\Delta V$ is not limited when the center-of-gravity shift is held to the estimated 0.7 degree. The expected weight and power of two electromechanical actuators is 18.5 pounds and 250 watts.

*Linear Simulation Definition*---The performance requirements of the TVC system are established to a major extent by the dynamic behavior of the system. Hence, the third order linear digital simulation shown in Figure C-17 was used for preliminary design purposes. Table C-4 lists the variable used throughout this discussion. The normal disturbance for a TVC system is the misalignment between the thrust and the center of mass at engine startup.

Figure C-18 is the normalized rate response for this third order system for several values of $\gamma/\omega_n$. This parameter relates the time constant of the actuator to the outer loop gain. From the standpoint of hardware design, it is desirable to keep $\gamma/\omega_n$ small, because this is a lower frequency response actuator requirement. The figure shows that reasonable performance is obtained using $\gamma/\omega_n = 2$ and increasing the factor to 10 does not significantly improve the response time. Figure C-19 shows the response time to get within an arbitrary limit of 0.25 deg/sec for a step $\varepsilon_{cg}$ command. Assuming that 1 second is a desirable recovery time, the natural frequency is selected at 4.44 rad/sec. If an additional assumption is made that the actuator corner frequency $K_A K_\delta$ should be greater than three times the system natural frequency, the system parameters in Figure C-17 can be evaluated:

$K_\delta$ = 50 volts/radian
$K_A$ = 0.3 radian/second/volt
$K_{\dot\theta}$ = 47 volts/radian/second
$K_\theta$ = 109 volts/radian
$K_T$ = 5.3 at midcourse

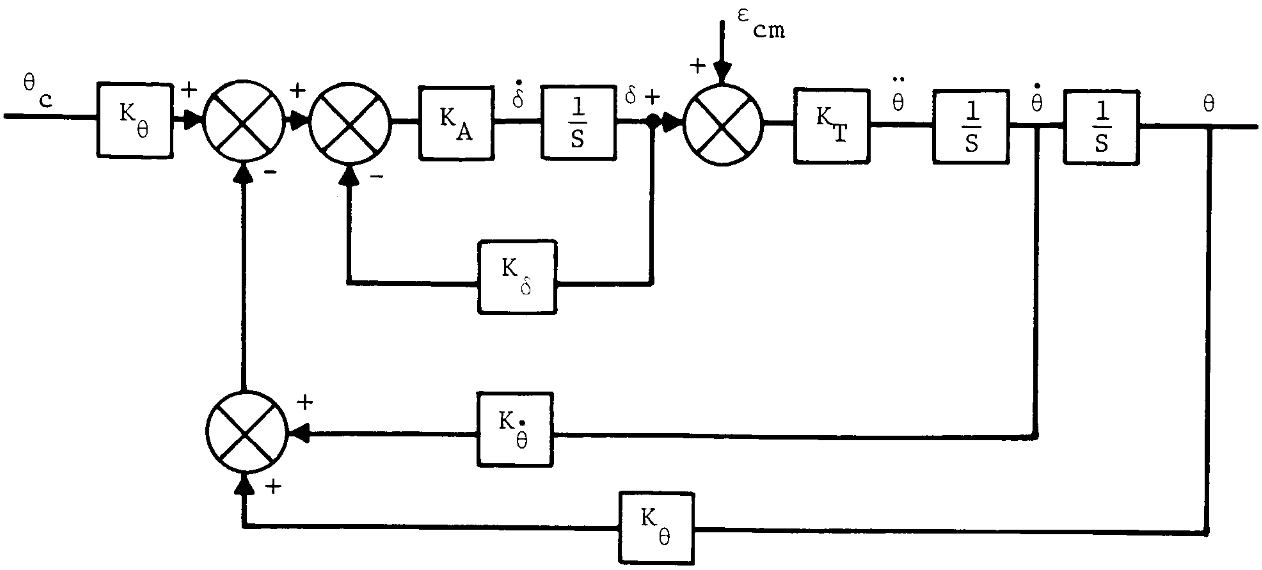
$\theta_c$
$K_\theta$
+
-
+
-
$K_A$
$\dot{\delta}$
$\frac{1}{S}$
$\delta$
+
$\varepsilon_{cm}$
+
$K_T$
$\ddot{\theta}$
$\frac{1}{S}$
$\dot{\theta}$
$\frac{1}{S}$
$\theta$
$K_\delta$
+
$K_{\dot{\theta}}$
+
$K_\theta$

Figure C-17: THRUST VECTOR CONTROL SIMULATION

Table C-4: LIST OF VARIABLES AND TVC STUDIES

$K_\Theta$ = Position gain (volts/radian)

$K_A$ = Actuator forward loop gain (radians/second/volt)

$K_T$ = Torque gain ($F\ell/I$)

$F$ = Engine thrust (pounds)

$\ell$ = Center of gravity to gimbal point (feet)

$I$ = Moment of inertia (slug-square feet)

$K_\Theta$ = Rate gain (volts/ radian/second)

$K_\delta$ = Actuator deflection gain (volts/radian)

$\gamma$ = Closed-loop root due to actuator (radians/second)

$\omega_n$ = Second order natural frequency (radians/second)

$\zeta$ = Second order damping factor

$\Theta_c$ = Position command (volts)

$\varepsilon_{cm}$ = Center-of-gravity offset (radians)

$\delta, \dot{\delta}$ = Actuator deflection, rate

$\Theta, \dot{\Theta}, \ddot{\Theta}$ = Vehicle position, rate, acceleration

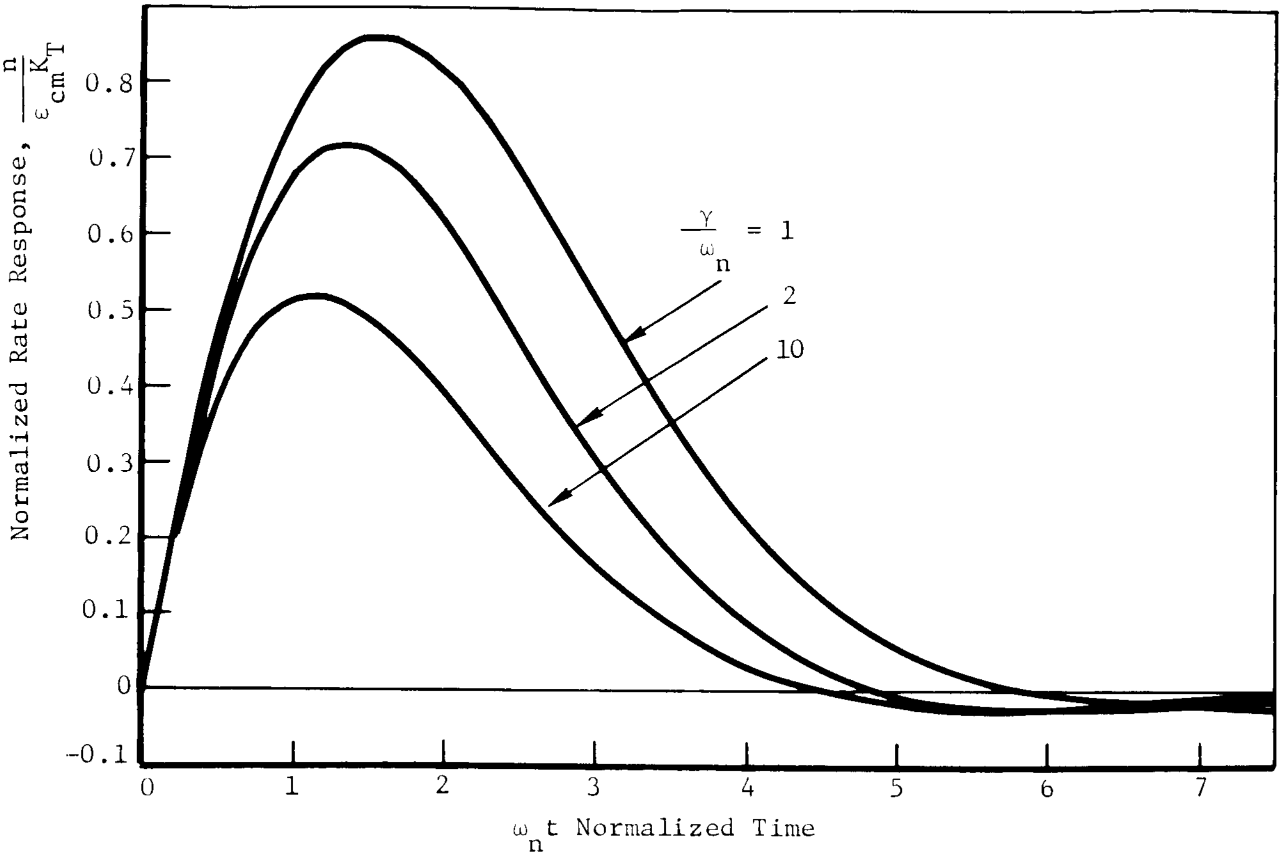

Figure C-18: RATE RESPONSE OF A THIRD ORDER SYSTEM

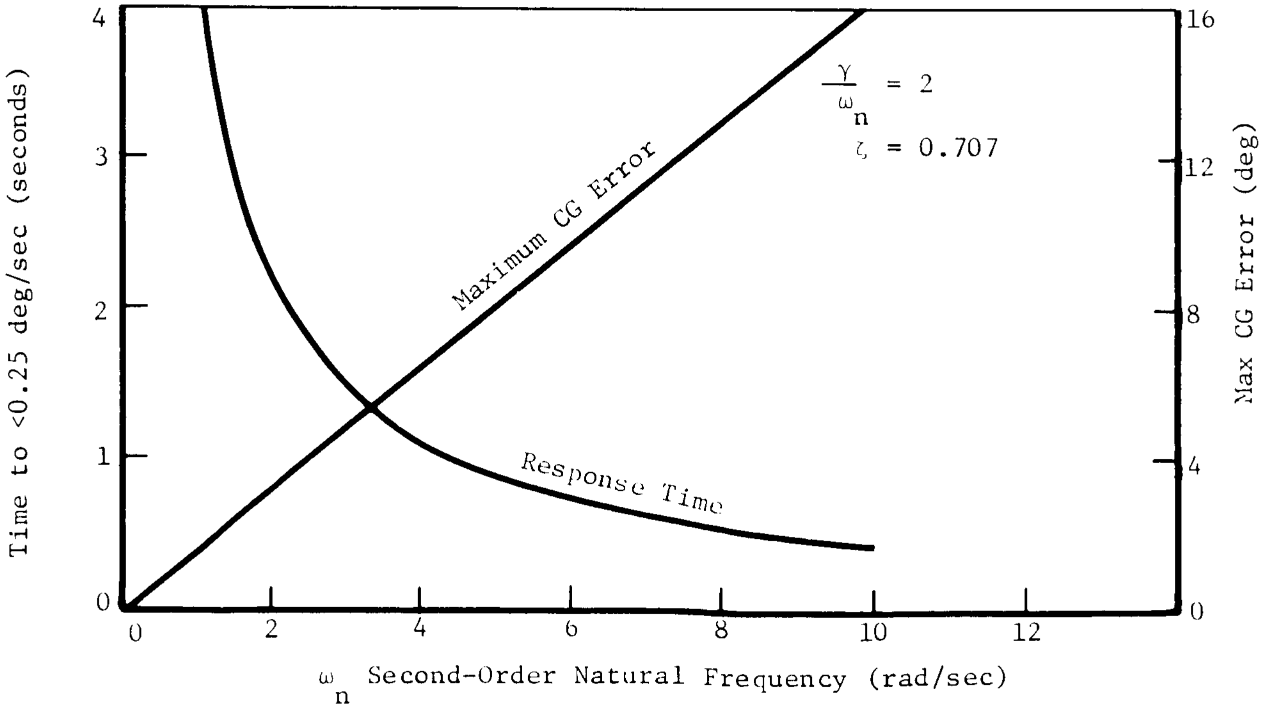

Figure C-19: RESPONSE TIME TO A STEP CG ERROR

The thrust profile shown in Figure C-20 is used in the simulation, which causes $K_T$ to be a linear function of time. The delay in buildup of the control function causes no problem in the simulation because there is no initial 0 error. However, in real life, limit cycle error could cause thrust vector motion if control authority were transferred to the TVC system before the start of thrust rise. Therefore, it is assumed that control will not be transferred to the TVC system until thrust rise begins. This could be handled either by a timed signal or by an acceleration switch.

*Short Burn Response Trade*---The digital simulation was used to investigate the effect of center-of-gravity offset from thrust line at startburn on maximum actuator deflection and rate requirements, minimum velocity impulse, and reaction control recovery capability. The phase plane shown in Figure C-21 summarizes this result. The figure is specifically for the midcourse condition during transit to Mars.

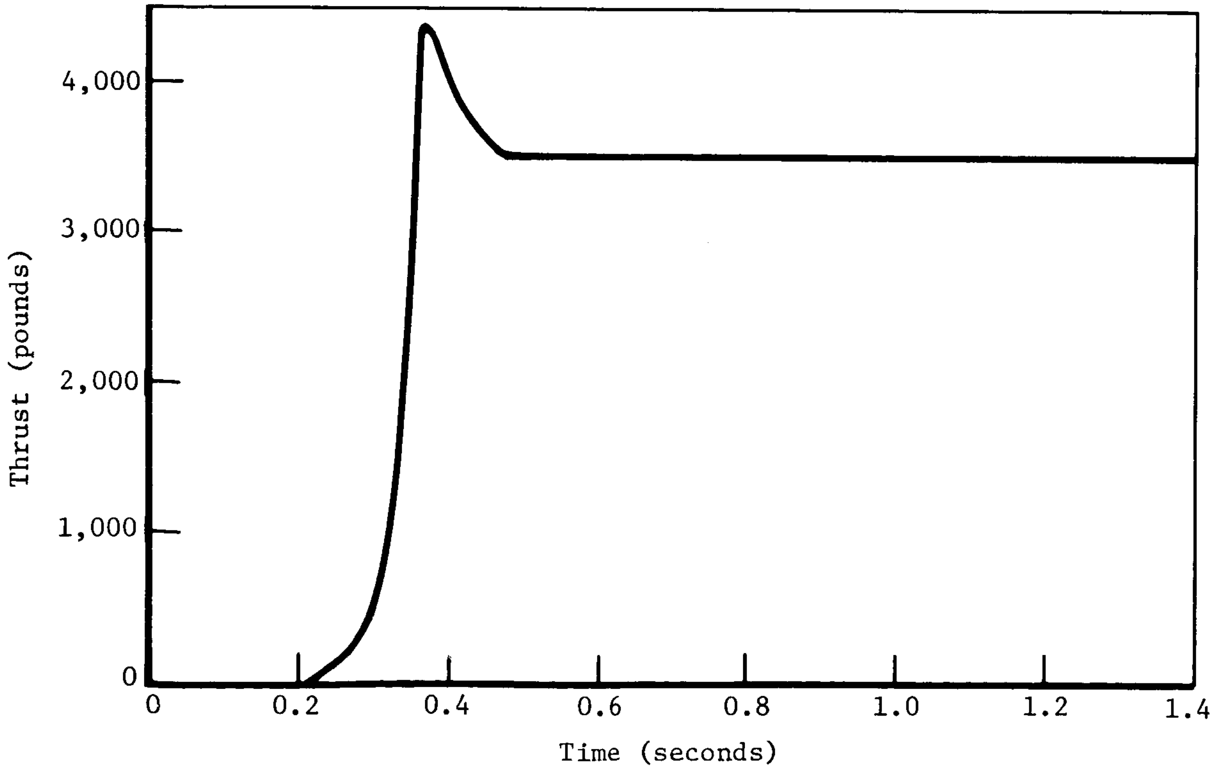

Figure C-20: THRUST RISE PROFILE

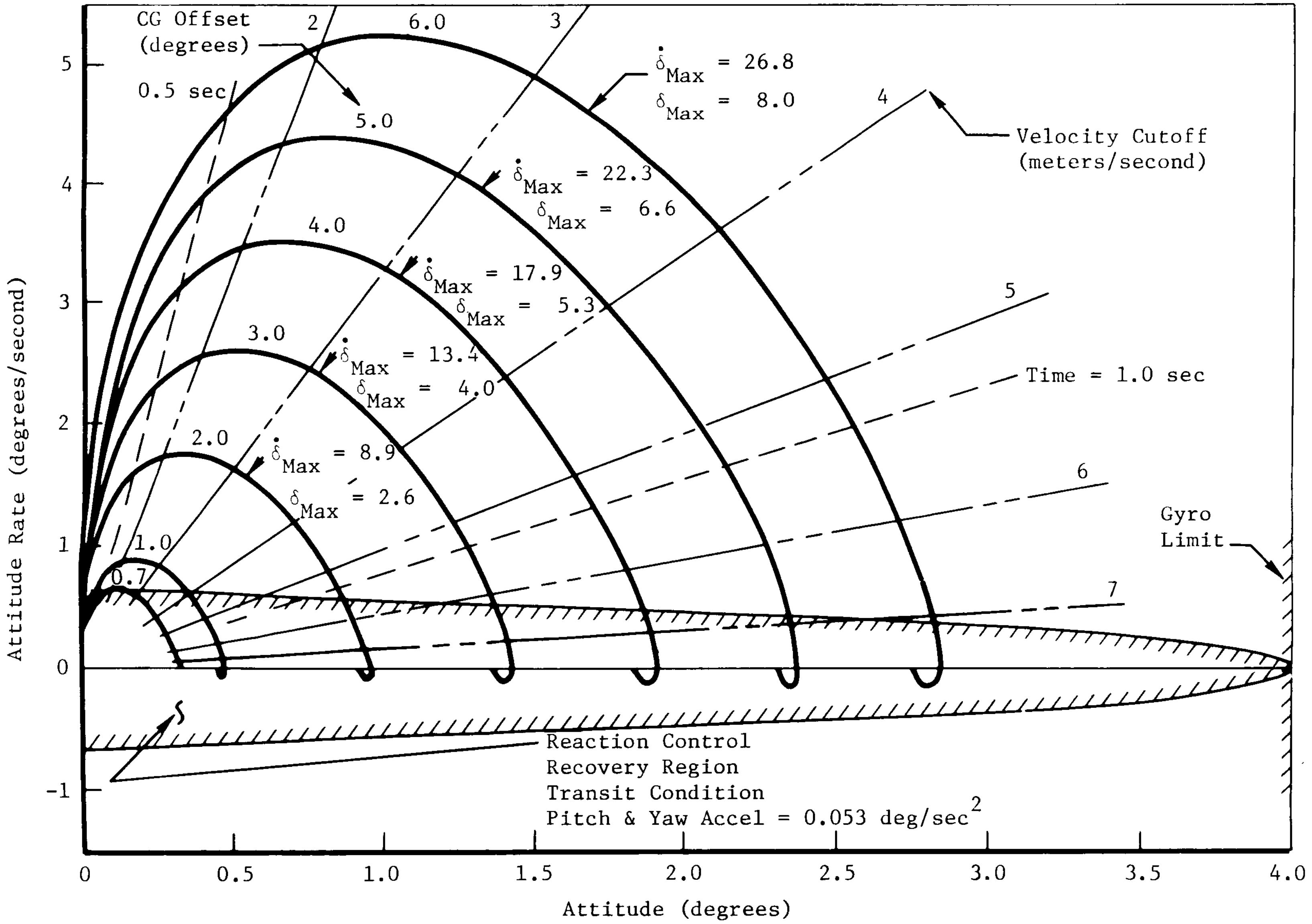

Figure C-21: THRUST VECTOR CONTROL SYSTEM---SHORT BURN RESPONSE TRADE

The solid lines are the trajectories that result while the 3,500-pound engine is firing and the TVC system is active. Trajectories are shown for center-of-gravity offsets from the thrust line from 0.7 to 6 degrees. Time increases along these curves starting at zero rate and position in a clockwise direction. The radial lines indicate the engine cutoff points for various velocity increments. The region enclosed by the cross-hatched parabola indicates the vehicle attitude and attitude rate from which the reaction control system as sized in 4.0 can stabilize the system without hitting the gyro gimbal limits. Hence, a 3-degree center-of-gravity offset trajectory which cuts off at ΔV of 4 m/sec cannot be controlled. A minimum impulse of about 6.7 m/sec is required. With the RCS sized as it is, a center-of-gravity offset of 0.7 degree can be allowed without any limitation on minimum ΔV.

*Center-of-Gravity Offset*---Because center-of-gravity offset is a powerful variable, it was explored further. First, it must be emphasized that it is the center-of-gravity offset at the start of each burn that is critical, not the total offset from the vehicle centerline. For example, at the start of the first burn, the total center-of-gravity offset might be 3 degrees. Because this is a long burn, the actuator will have time to converge and track the center of gravity and there is no short burn cutoff recovery problem. After cutoff, the actuator stays put either because it is inherently irreversible or it has a brake. Between cutoff and first midcourse, effective center-of-gravity shifts could occur due to various causes like antenna rotation, propellant migration, and TVE shutdown drift.

The worst-case center-of-gravity migration that could occur (about 10 degrees) would result if uncontrolled propellant migration were allowed. This cannot be controlled with the system as simulated. The gyro limits would have to be increased to about 5 degrees, the minimum velocity increment would be about 8 m/sec, and the TVC requirements would be 60 deg/sec and 20 degrees including design margins. Hence, propellant migration was eliminated by propulsion system hardware design.

Without propellant migration, the center-of-gravity shift will be the summation of several small tolerances:

| | Degree |
|---|---|
| Antenna Rotation | 0.25 |
| TVC Drift at Cutoff | 0.25 |
| TVC Limit Cycle | 0.10 |
| Lander Drop (After Injection) | 0.50 |
| Propellant Unbalance | 0.25 |
| RSS 3 σ | 0.67 |

Thus, it appears that 0.7-degree shift for midcourse design is reasonable.

*Minimum* $\Delta V$---Now that a 3 $\sigma$ center-of-gravity shift between burns is established at 0.7 degree maximum, it is clear from the discussions on the short burn response trades that there is no limit on the minimum velocity increment. However, if further studies should show that increased $\dot{\theta}$ is required, then the reaction control authority could be increased by increasing the thrust of the pitch and yaw thrusters during the velocity burn. As an example, if 1 degree center-of-gravity offset is demonstrated, the recovery rate requirements is 1.0 deg/sec, which can be taken care of by increasing the thrust to 0.7 to provide 0.125-second acceleration. This could be supplied by two 0.35-pound thrusters where both are used only during a velocity burn and only one is used during normal coast, or by a two step regulator where the high pressure setting is used only during velocity burn.

*Performance Requirements*---The paragraph on "Linear Simulation Definition" concluded that the closed-loop natural frequency and damping ratio ought to be 4.44 rad/sec and 0.7, respectively, and the actuator corner frequency should be 15 rad/sec. The gains required to obtain these parameters were calculated. The actuator rate and deflection requirements are yet to be determined.

Figure C-21 notes the maximum actuator rates and deflections that occurred for various center-of-gravity offsets. Realizing that the system is linear with respect to center-of-gravity offset, these numbers, which are for 4.44 rad/sec, can be extrapolated to obtain rate (Figure C-22) and deflection requirements.

| | Natural Frequency (rad/sec) | Allowable CG Shift (deg) | Actuator Rate (deg/sec) | Actuator Deflection (deg) |
|---|---|---|---|---|
| Boost Assist | 3.9 | 2.0 | 8.0 | 2.6 |
| Midcourse | 4.4 | 0.7 | 3.2 | 0.9 |
| Injection | 10.0 | 0.7 | 6.5 | 0.9 |
| Capsule Off | 13.0 | 1.0 | 7.0 | 1.3 |

A design rate of 10 deg/sec and 3 degrees is adequate to meet boost-assist, midcourse, and injection requirements.

*Actuator Weight and Power*---The use of high rate electrical actuators for spacecraft TVC servo applications has been limited to Lunar Orbiter and the Apollo service module. Consequently, it is somewhat difficult to develop weight and power parametric data. However, the Voyager Task D study provided an additional data point because an electrical actuator was proposed for TVC and a reasonable weight and power estimate was determined. An examination of these data showed that actuator weight was linear with the engine thrust, and power was a linear function of actuator weight on a log/log plot. The data are presented as Figures C-23 and C-24, respectively.

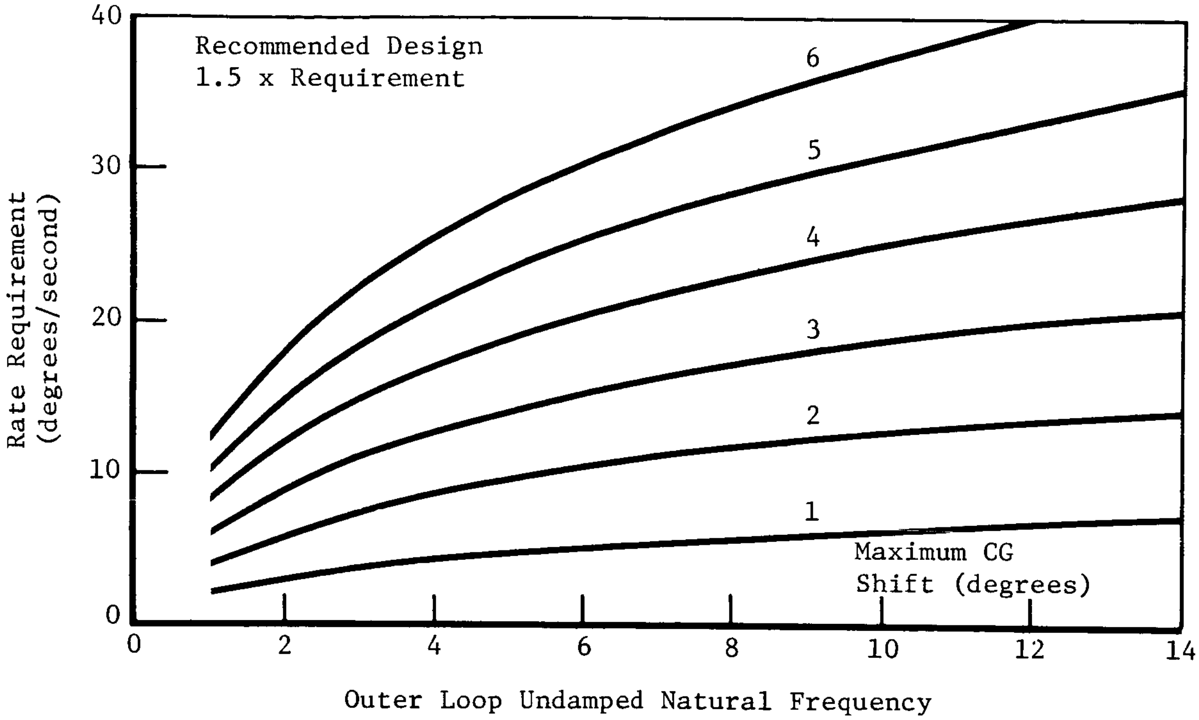

Figure C-22: THRUST VECTOR CONTROL ACTUATOR RATE CRITERIA

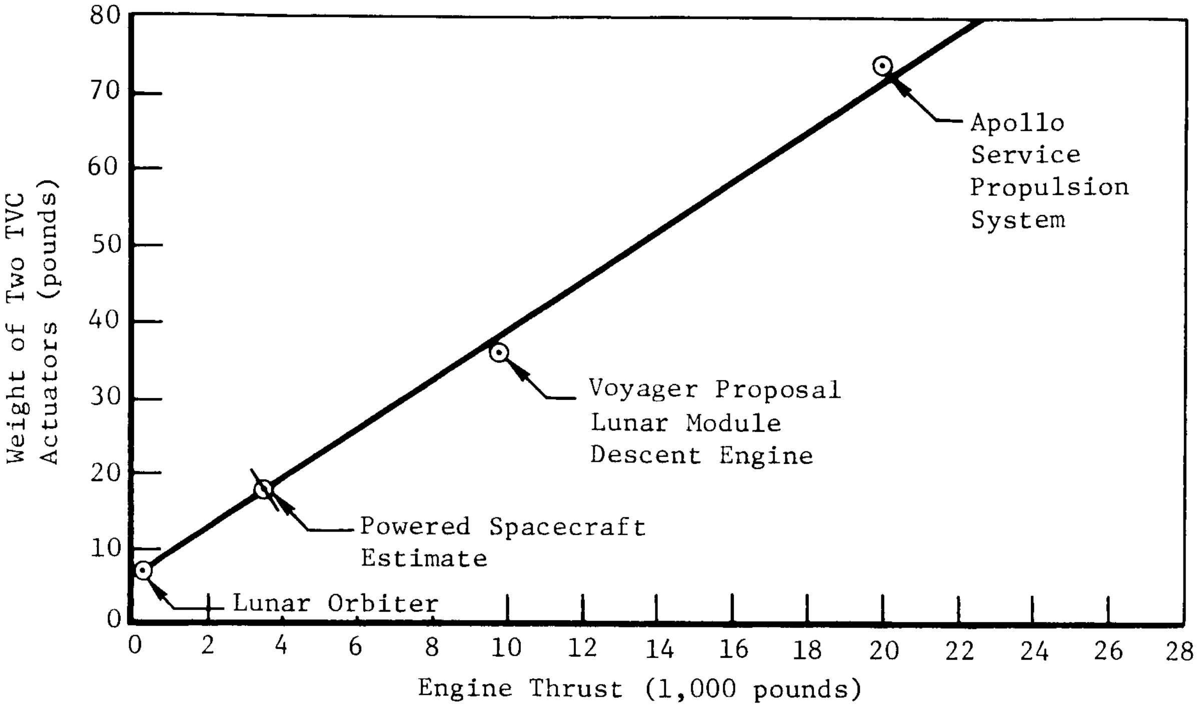

Figure C-23: THRUST VECTOR CONTROL ACTUATOR WEIGHT

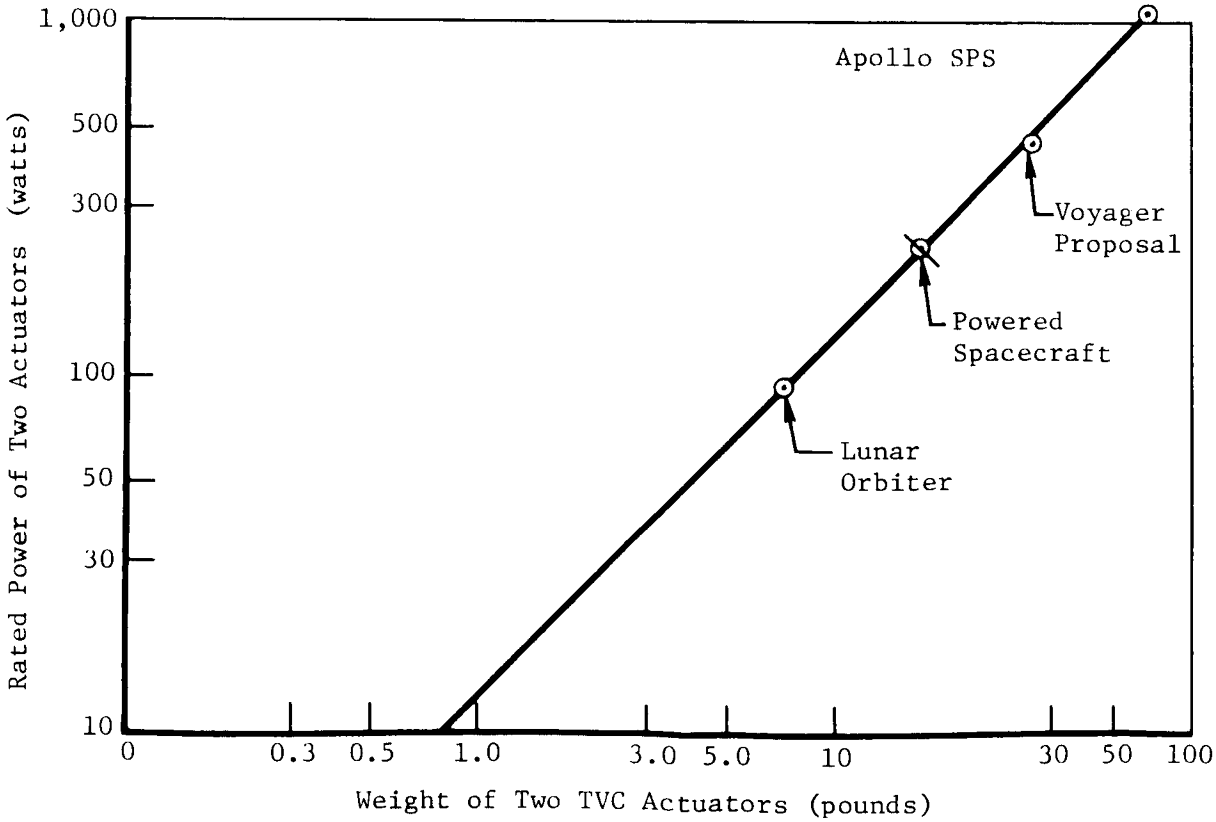

Figure C-24: THRUST VECTOR CONTROL ACTUATOR POWER

## 6.0 MASS PROPERTIES MODEL

Because most of the trade studies ran concurrently, it was necessary to develop a mass properties model for ACS studies before comparable data were available from other studies. The configuration used is shown in Figure C-25 along with pertinent data for a 7,000-pound separated spacecraft weight.

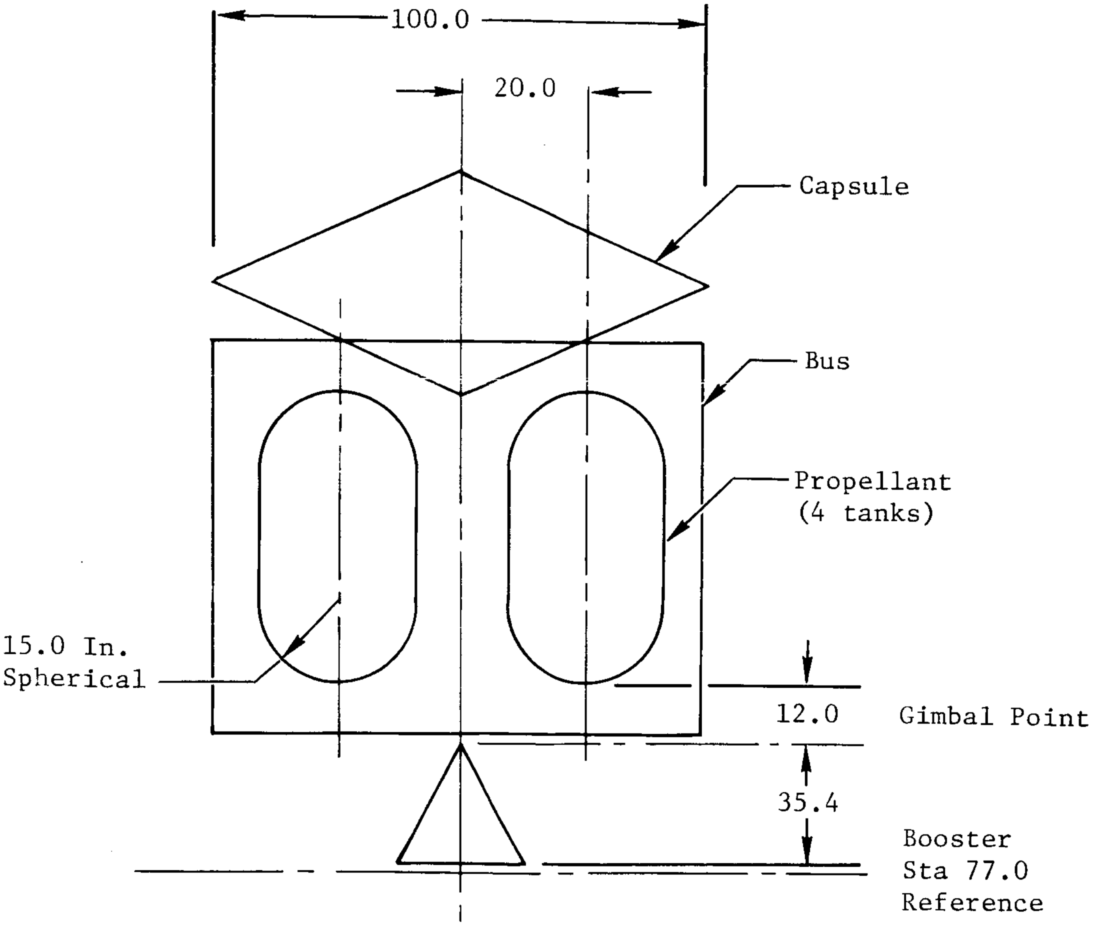
100.0
20.0
Capsule
Bus
Propellant (4 tanks)
15.0 In. Spherical
12.0
Gimbal Point
35.4
Booster Sta 77.0 Reference

7,000-lb Separated Spacecraft

| Configuration | Gimbal to CG (inches) | Roll Inertia (slug-ft$^2$) | Pitch Inertia (slug-ft$^2$) | Yaw Inertia (slug-ft$^2$) |
|---|---|---|---|---|
| Start Burn | 46.0 | 1,150 | 1,850 | 1,850 |
| Transit | 44.5 | 950 | 1,750 | 1,750 |
| End Burn Capsule On | 57.5 | 800 | 1,460 | 1,460 |
| End Burn Capsule Off | 26.5 | 560 | 450 | 450 |

Figure C-25: MASS PROPERTIES MODEL

# REFERENCES

1. *Data Collection,* D2-140028-4, The Boeing Company, July 1968
2. *Program 624A---Titan III Inertial Guidance System,* AC Electronics Division Quarterly Error Analysis Report 67-RT000-V3124, July 1967
3. *Study and Analysis of Satellite Power Systems Configurations for Maximum Utilization of Power,* NASA CR-898, October 1967
4. *Titan III Zero Characteristics Report---Range Safety Section,* Aerospace Corporation, April 1968
5. *AFETR, MSFN and DSIF Station View Periods---Lunar Orbiter, July/August 1967 Mission,* D2-100767-1, The Boeing Company, May 1967
6. *A Compilation of Flight Mechanics Analyses of Voyager Missions,* Report No. 2-7837-VTD-16, D2-90733-7 Voyager Task D Final Report, Vol. II, The Boeing Company, November 1967